ISSN 2307-8960 (online)

World Journal of *Clinical Cases*

World J Clin Cases 2023 April 6; 11(10): 2123-2362

Published by Baishideng Publishing Group Inc

World Journal of Clinical Cases

Contents

Thrice Monthly Volume 11 Number 10 April 6, 2023

EVIDENCE REVIEW

REVIEW

MINIREVIEWS

ORIGINAL ARTICLE

Retrospective Study

World Journal of Clinical Cases

Thrice Monthly Volume 11 Number 10 April 6, 2023

Contents

World Journal of Clinical Cases

Thrice Monthly Volume 11 Number 10 April 6, 2023

Contents

World Journal of Clinical Cases

Thrice Monthly Volume 11 Number 10 April 6, 2023

Contents

NAME OF JOURNAL
World Journal of Clinical Cases

ISSN
ISSN 2307-8960 (online)

LAUNCH DATE
April 16, 2013

FREQUENCY
Thrice Monthly

EDITORS-IN-CHIEF
Bao-Gan Peng, Jerzy Tadeusz Chudek, George Kontogeorgos, Maurizio Serati, Ja Hyeon Ku

EDITORIAL BOARD MEMBERS
https://www.wjgnet.com/2307-8960/editorialboard.htm

PUBLICATION DATE
April 6, 2023

INSTRUCTIONS TO AUTHORS
https://www.wjgnet.com/bpg/gerinfo/204

GUIDELINES FOR ETHICS DOCUMENTS
https://www.wjgnet.com/bpg/GerInfo/287

GUIDELINES FOR NON-NATIVE SPEAKERS OF ENGLISH
https://www.wjgnet.com/bpg/gerinfo/240

PUBLICATION ETHICS
https://www.wjgnet.com/bpg/GerInfo/288

PUBLICATION MISCONDUCT
https://www.wjgnet.com/bpg/gerinfo/208

ARTICLE PROCESSING CHARGE
https://www.wjgnet.com/bpg/gerinfo/242

STEPS FOR SUBMITTING MANUSCRIPTS
https://www.wjgnet.com/bpg/GerInfo/239

ONLINE SUBMISSION
https://www.f6publishing.com

E-mail: bpgoffice@wjgnet.com https://www.wjgnet.com

World Journal of Clinical Cases

Submit a Manuscript: https://www.f6publishing.com

World J Clin Cases 2023 April 6; 11(10): 2123-2139

DOI: 10.12998/wjcc.v11.i10.2123

ISSN 2307-8960 (online)

EVIDENCE REVIEW

Fractional flow reserve and non-hyperemic indices: Essential tools for percutaneous coronary interventions

Amine Mamoun Boutaleb, Chadi Ghafari, Claudiu Ungureanu, Stéphane Carlier

Specialty type: Cardiac and cardiovascular systems

Provenance and peer review: Invited article; Externally peer reviewed.

Peer-review model: Single blind

Peer-review report's scientific quality classification

Grade A (Excellent): 0
Grade B (Very good): 0
Grade C (Good): C
Grade D (Fair): D
Grade E (Poor): 0

P-Reviewer: Batta A, India; Hong X, China

Received: December 27, 2022
Peer-review started: December 28, 2022
First decision: February 8, 2023
Revised: February 22, 2023
Accepted: March 15, 2023
Article in press: March 15, 2023
Published online: April 6, 2023

Amine Mamoun Boutaleb, Department of Cardiology, Ibn Rochd University Hospital, Casablanca 20230, Casablanca, Morocco

Amine Mamoun Boutaleb, Stéphane Carlier, Department of Cardiology, Centre Hospitalier Universitaire Ambroise Paré, Mons 7000, Belgium

Chadi Ghafari, Claudiu Ungureanu, Stéphane Carlier, Department of Cardiology, University of Mons, Mons 7000, Belgium

Claudiu Ungureanu, Catheterization Unit, Jolimont Hospital, La Louvière 7100, Belgium, Belgium

Corresponding author: Stéphane Carlier, MD, PhD, Professor, Department of Cardiology, University of Mons, Pentagone, Aile 2, Avenue du Champ de Mars, 6, Mons 7000, Belgium. stephane.carlier@umons.ac.be

Abstract

Hemodynamical evaluation of a coronary artery lesion is an important diagnostic step to assess its functional impact. Fractional flow reserve (FFR) received a class IA recommendation from the European Society of Cardiology for the assessment of angiographically moderate stenosis. FFR evaluation of coronary artery disease offers improvement of the therapeutic strategy, deferring unnecessary procedures for lesions with a FFR > 0.8, improving patients' management and clinical outcome. Post intervention, an optimal FFR > 0.9 post stenting should be reached and > 0.8 post drug eluting balloons. Non-hyperemic pressure ratio measurements have been validated in previous studies with a common threshold of 0.89. They might overestimate the hemodynamic significance of some lesions but remain useful whenever hyperemic agents are contraindicated. FFR remains the gold standard reference for invasive assessment of ischemia. We illustrate this review with two cases introducing the possibility to estimate also non-invasively FFR from reconstructed 3-D angiograms by quantitative flow ratio. We conclude introducing a hybrid approach to intermediate lesions (DFR 0.85-0.95) potentially maximizing clinical decision from all measurements.

Key Words: Fractional flow measurements; Coronary artery physiology; Quantitative flow reserve; Non-hyperemic pressure ratios

Core Tip: Fractional flow reserve and non-hyperemic indices are the cornerstone for optimal percutaneous interventions. In this extensive review we discuss their rationale of use, indications guidelines, benefits and pitfalls. The comprehensive use of coronary artery physiology for the guidance of percutaneous interventions may be beneficial for every interventional cardiologist. Hence, we aimed to make a clear statement of physiology-guided percutaneous interventions to enhance coronary artery revascularization techniques.

Citation: Boutaleb AM, Ghafari C, Ungureanu C, Carlier S. Fractional flow reserve and non-hyperemic indices: Essential tools for percutaneous coronary interventions. *World J Clin Cases* 2023; 11(10): 2123-2139
URL: https://www.wjgnet.com/2307-8960/full/v11/i10/2123.htm
DOI: https://dx.doi.org/10.12998/wjcc.v11.i10.2123

INTRODUCTION

Coronary artery angiography remains the cornerstone for coronary artery disease (CAD) assessment confirming stenoses or occlusions of epicardial coronary arteries. These are often subjectively estimated by the operator who visually evaluates the percentage of intraluminal narrowing of the artery. Quantitative coronary angiography improves this guess work, optimizing devices sizing by accurately measuring the length and reference diameter of coronary stenoses[1]. However, this anatomic evaluation remains often insufficient requiring adjunctive information provided by a functional assessment. The presence of inducible ischemia in patients with CAD has been associated with adverse clinical outcome with risk stratification based on the extent of myocardial ischemia[2,3]. However, this was not confirmed in the more recent Ischemia trial where the severity of ischemia was not associated with an increased risk after adjustment for CAD severity[4].

Medical treatment is efficient in relieving anginal symptoms related to myocardial ischemia while revascularization improves downstream coronary blood flow and therefore relieves myocardial cells from the changes related to anaerobic metabolism[5].

Although current guidelines have implemented non-invasive stress testing prior to percutaneous interventions (PCI), the frequency of upstream testing remains low[6].

Fractional flow reserve (FFR) is used during coronary artery angiography to directly measure the pressure drop across an epicardial stenosis[7]. It is nowadays considered as the gold standard for the detection of myocardial ischemia and is recommended by the ESC 2018 myocardial revascularization guidelines[8]. This invasive diagnostic tool is the current standard of care for the functional assessment of lesion severity in patients with intermediate grade stenosis (40%-90%) without evidence of ischemia. FFR-guided PCI has been shown to be superior to angiographic guided PCI as well as its safety for PCI deferral of non-functionally significant stenosis[9-11].

With the increasing use of physiological assessment for CAD, new pressure-derived indices have emerged to guide PCI and to overcome some of the issues of FFR. Non-hyperemic pressure ratios (NHPR) are now an integral part of most current pressure wire systems and are widely used in the majority of catheterization laboratories. These indices evaluate coronary artery functional severity over either the diastolic phase or the whole cardiac cycle. A good correlation with FFR was found for the instantaneous wave free ratio (iFR), the first NHPR developed, with an 80% approximative accuracy[12-14]. Numerous NHPR are now available and are numerically equivalent with a common threshold[15].

FRACTIONAL FLOW RESERVE

Definition of FFR

Fractional flow reserve is defined as the maximal achievable blood flow in the presence of an epicardial coronary stenosis divided by the maximum flow in the same healthy vessel if there was no obstructive epicardial disease[16]. It can be estimated by the simplified ratio of the coronary artery pressure downstream an epicardial stenosis over the aortic pressure during maximal hyperemia, taking into account the central venous pressure. Hence, FFR estimates the percentage of maximal blood flow limited by the presence of an epicardial stenosis. It is expressed by the following relationship, considering a constant and minimal coronary arterial bed resistance: FFR = (Pd-Pv)/(Pa-Pv), where Pd is the pressure recorded downstream the epicardial stenosis, Pa is the aortic pressure and Pv the central venous pressure (Figure 1).

Maximal hyperemia is generally obtained by intravenous or intracoronary perfusion of adenosine [17]. Other agents such as Regadenoson or Papaverine can also be used[18,19]. The coronary vasodilator agent dose and side effects perfusion are presented in Table 1[20].

Table 1 Coronary hyperemic agents

Agent		Dose	Side effects
Adenosine	Intravenous Intracoronary	140 μg/kg/min IV; > 40 μg RCA; > 80 μg LCA	Transient AV block, chest pain, shortness of breath, hypotension, headache, flushing
Regadenoson		400 μg singe bolus central or peripheral IV	Rhythm or conduction abnormalities, rare gastrointestinal side effects, less frequent chest pain and dyspnea
Papaverine		10-12 mg in RCA; 15-20 mg in LCA	Abdominal symptoms, headache, flushing of face, increase in heart rate, QTc prolongation, ventricular tachyarrhythmias

AV bloc: Atrioventricular block; IV: Intravenous; RCA: Right coronary artery; LCA: Left coronary artery. Table 1 summarizes the hyperemic agents used for fractional flow reserve measurements and gives the dose and potential side effects of each agent. One has to choose in function of the clinical parameters of the patient.

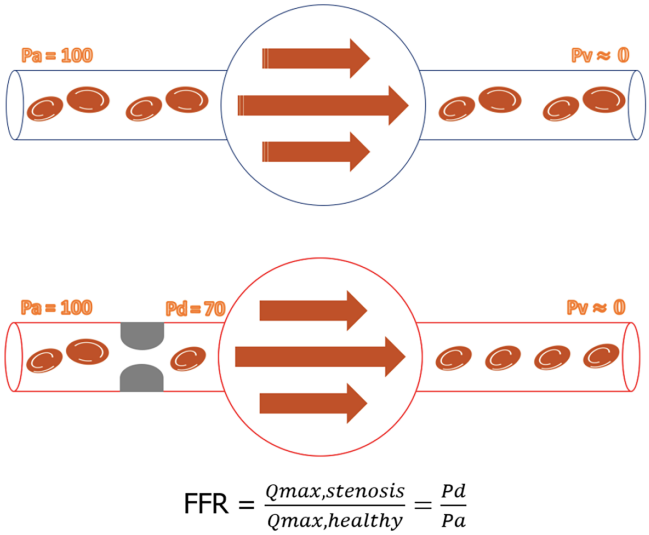

DOI: 10.12998/wjcc.v11.i10.2123

Figure 1 Invasive measurement of fractional flow reserve. FFR: Fractional flow reserve.

Intracoronary Adenosine is the preferred vasodilator agent inducing a quick (5-10 s) response to maximal hyperemia, however it may cause transient atrioventricular block, chest discomfort and shortness of breath and is contraindicated in patients presenting with chronic pulmonary obstructive disease. A more stable hyperemia is achieved using an intravenous perfusion[21]. Regadenoson (Rapiscan) is a selective agonist of the receptor A2 of adenosine with a 10-fold lower affinity for the A1 adenosine receptor. Its injection produces coronary vasodilatation and increases coronary blood flow. Given its selectivity for the A2 receptor, cardiac conduction sides effects are less frequently observed and is generally well tolerated in patients with chronic obstructive pulmonary disease (COPD)[22,23]. A good correlation between both agents has been reported in multiple trials[24,25].

The first proposed FFR threshold was 0.75. The issue of a grey-zone decision between 0.75 and 0.80 has been solved recommending now a threshold of 0.80[26]. An accuracy of 90% was reported in the FAME trial[10]. The revascularization between 0.75 and 0.80 remains debatable, but should be considered depending on the potential major adverse cardiovascular events (MACE) rates of the patients and coronary artery stenosis localization[27].

The cutoff threshold values have been validated in multiple trials comparing non-invasive measurements to FFR associated to the reversal of the presence of ischemia after PCI[7,26,28,29].

Technical aspect of FFR measurement

The majority of PCI are performed using 6 French guiding catheters (GC). All FFR systems are with a low profile allowing to use already 5 Fr GC but care must then be taken to optimize the quality of phasic pressure recordings, flushing the catheter with saline solution.

FFR systems are based either on a piezoelectrical or an optical sensor. Both types of pressure sensors generate a membrane deflection through the pressure, inducing either an electrical charge or a phase delay in a reflected light beam.

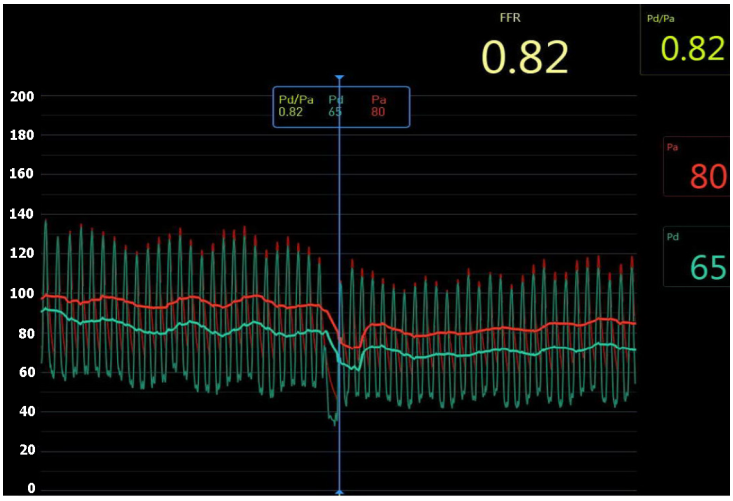

DOI: 10.12998/wjcc.v11.i10.2123

Figure 2 POLARIS display screen showing negative fractional flow reserve value.

These systems have been well validated, with a reduction in pressure drift reported with the optical method[30,31]. Moreover, the latest versions of optical pressure guidewires enable its use as a workhorse guidewire for PCI by disconnecting and reconnecting the system.

The first step consists of zeroing the fluid-filled aortic pressure and the FFR pressure system *ex vivo* to the atmospheric one, ideally at the level of the right atrium. The pressure wire is then advanced few millimeters beyond the tip of the GC. Both pressure curves are equalized with the introducer needle off the Y connector[32]. Contrast may dampen the catheter waveform pressure, hence flushing the system with saline is mandatory before pressure measurements.

After intracoronary administration of isosorbide dinitrate, FFR and NHPR can be measured with the wire advanced at least 3 vessels diameters distal to the stenosis. In case of multiple stenosis and diffuse disease, a recording of the pressure during a pull back of the wire identifies spots with significant pressure changes where a PCI might be useful. At the end, a possible drift (significant if > 3 mmHg) of the FFR system is carried out[33]. Figure 2 represents the display screen of the POLARIS monitor (Boston Scientific, Marlborough, MA, United States) using the COMET™ wire, showing a non-significant FFR value of 0.82.

Several intracoronary pressure systems are currently available on the market: WaveWire™ (Philips Inc, Eindhoven, the Netherlands), COMET™ (Boston Scientific, Marlborough, MA, USA), PressureWire™ (St. Jude/Abbott, St. Paul, MN, United States), NAVVUS RXi® (ACIST Medical Systems, Inc, Eden Prairie, MN), TruePhysio™ (Insight Lifetech) and OptoWire Deux (Opsens medical, Quebec, Canada) with fewer drift[31]. The COMET trial comparing the COMET™ and the PressureWire™ found similar results in terms of safety and performance[34]. The RIPCORD 2 trial was a large prospective, multicenter study where investigators used the COMET™ wire to evaluate a FFR-guided revascularization strategy in patients presenting with stable CAD or NSTE-ACS.

In most guidewires, the pressure sensor is usually located at the proximal part of the radiopaque tip. In the case of the NAVVUS RXi®, the pressure sensor is located 5 mm above the distal tip of the microcatheter.

Conventional pressure wires have generally less torque control, flexibility and crossing ability than workhorse or specialized guidewires. Therefore, the NAVVUS RXi® and the TruePhysio™ are microcatheters to be used with any workhorse wire to overcome these issues, with debatable opinions. In vitro assessment of the novel 0.014'' OptoWire™ showed improved pushability, steerability and torquability in comparison with regular PCI wires, offering reliable pre and post PCI hemodynamic assessment[35].

Validation of fractional flow reserve measurement

Myocardial ischemia is defined as a lack of coronary blood flow with electrical, functional, metabolic and structural consequences for the myocardium. The imbalance between oxygen supply and myocardial oxygen need is the central point of interest that should be improved with optimal medical therapy and/or coronary artery revascularization[36].

The FFR was first introduced by Pijls *et al*[7] who demonstrated the initial threshold of 0.75 demonstrating reversal of non-invasive stress tests after performing PCI.

The DEFER trial investigated the appropriateness of not stenting a functionally non-significant coronary stenosis and showed the safety to defer PCI when the FFR was > 0.75[37].

Table 2 Diagnostic performance of different non-invasive stress tests

Test	Anatomically Significant CAD		Functionally significant CAD	
	Specificity (95%CI)	Sensitivity (95%CI)	Specificity (95%CI)	Sensitivity (95%CI)
Stress ECG	62 (54-69)	58 (46-69)	73 (55-86)	68 (60-75)
Stress echo	82 (72-89)	85 (80-89)		
CCTA	78 (67-86)	97 (93-99)	53 (37-68)	93 (89-96)
SPECT	70 (63-76)	87 (83-90)	83 (71-90)	73 (62-82)
PET	85 (78-90)	90 (78-96)	85 (81-88)	89 (82-93)
Stress CMR	80 (69-88)	90 (83-94)	87 (83-91)	89 (85-92)

CAD: Coronary artery disease; CCTA: Coronary Computed Tomography Angiography; CMR: Cardiac Magnestic Resonance; ECG: Electrocardiogram; echo: echocardiography; SPECT: Single-Photon Emission Computerized Tomography; PET: Positron Emission tomography. The Table 2 summarize the multiple non-invasive stress tests available at this day for coronary artery disease screening. Each exam is characterized by its specificity and sensibility. The exam choice depends on the patient's clinical situation.

Tonino *et al*[10] showed in the FAME I trial that FFR-guided PCI is associated with fewer MACE and less resource utilization compared with angiography-guided PCI in patient with multivessel disease using a threshold of 0.80.

De Bruyne *et al*[9] proved in the FAME II trial that the addition of FFR measurements to optimal medical therapy in patients presenting stable CAD is superior to best medical therapy alone.

In the context of non ST-elevation acute coronary syndrome (NSTE-ACS) FFR guided revascularization of non-culprit lesions may be used during the index procedure to evaluate the need for further revascularization therapy[38].

The meta-analysis of Knuuti *et al*[39] evaluated the performance of non-invasive stress test to rule-in and rule-out significant CAD choosing as reference invasive coronary angiography with FFR measurements. They concluded that imaging methods are clearly superior to stress electrocardiogram. Functional imaging techniques including positron emission tomography, cardiac magnetic resonance and single-photon emission computerized tomography offer the best diagnostic performance even if the anatomical correlation is poor as shown in Table 2.

All these major trials support the class IA recommendation to assess the hemodynamic relevance of intermediate coronary artery disease by FFR and as class IIB in multivessel disease evaluation[8]. In fact, both the European and American guidelines state that patients undergoing coronary angiography without prior ischemia assessment should have invasive hemodynamic test (FFR or NHPR) to optimize the revascularization strategy[40].

FFR features and applications

The theoretical value of FFR is 1 in a normal healthy epicardial coronary artery. FFR decreases with increasing epicardial stenosis severity. This index is not influenced by systemic hemodynamics and remain stable in case of systemic pressure, heart rate and left ventricular contractility changes[41]. In addition, Johnson *et al*[42] found a 98% reproducibility rates. Among its other advantages, FFR takes into account the contribution of collaterals by reflecting both antegrade and retrograde blood flow during maximal hyperemia[43].

Considering the critical prognostic importance of left main (LM) stem disease and its difficult angiographic assessment, the revascularization of intermediate LM should be guided by FFR or intravascular imaging[44]. Generally, LM disease is frequently associated with other stenoses of the coronary artery tree. FFR could therefore stratify patients for surgical or percutaneous revascularization taking into account downstream lesion implication[45,46].

FFR can guide revascularization of non-culprit lesions in patients presenting with acute coronary syndromes (ACS). The FAME trial demonstrated that the benefits of FFR-guided PCI were similar in patients with unstable angina or NSTEMI and chronic coronary syndrome[47]. However, controversial findings were reported by Liou *et al*[48] advocating in depth assessment of FFR guided PCI in ACS context.

Tandem lesions are defined by two 50% or more stenoses separated by an angiographically normal segment. In serial lesions, FFR measurements of all stenoses is carried out, followed by a slow pull back of the FFR wire under steady state hyperemia and fluoroscopic view to determine the exact drop of pressure localization[48]. These cases remain challenging to interpret considering the interaction of downstream coronary artery stenosis: the FFR value of the proximal lesion might be overestimated and equations to predict FFR for each stenosis have been reported using the coronary wedge pressure, measured with an inflated balloon[45-46,49]. For a tandem lesion, NHPR are easier and more precise in assessing the respective significance of each stenosis. Table 3 summarizes the major trials evaluating the

Table 3 Studies that evaluated the outcomes of fractional flow reserve in intermediate coronary artery disease

Author or Study	Single or MVD CAD	Study design	FFR value defining ischemia	No. of patients	Survival %	Event-free survival %	Follow up, mo	Primary outcome rate %
DEFER[37]	Single	Randomized, prospective, multicenter	0.75	91/144	93/91	80/63	60	
FAME[10]	MVD	Randomized, prospective, multicenter	0.80	509/1005	37/509	73	12	
Hamilos *et al*[50]	LM	Prospective, single center	0.80	136/73	89.8/85.4	74.2/82.8	35	
FLOWER MI[51]	MVD	Randomized, prospective, multicenter	0.80	590/1171	5.5/4.2	98.5/98.3	12.36	
PHANTOM[52]	NR	Prospective, multicenter	0.75	39/21	100/100	97/76	12	
FAME 2[9]	Single + MVD	Randomized, prospective, multicenter	0.80	447/1220			60	8.7
FAME 3[53]	MVD	Randomized, prospective, multicenter	0.80	757/1500			12	10.6

CAD: Coronary artery disease; MVD: Multivessel disease; FFR: Fractional flow reserve; mo: Months; LM: Left main; No: Number. Table 3 represents the multiple studies that evaluated the fractional flow reserve through years. These diverse trials had different end points but generally converged to the common conclusion that fractional flow reserve guided- percutaneous interventions (PCI) has better outcomes than angiography-guided PCI. FFR clinical threshold has been chosen upon these studies.

outcomes of FFR in intermediate coronary lesions of LM and non LM lesions[9-11,50-53].

FFR post-interventions

In an otherwise healthy vessel with only a short stenosis, the FFR after stenting should theoretically revert to 1. However, atherosclerosis affects diffusely most of the coronary vessels and FFR values will therefore be affected by a mix of potential sub-optimal stenting (*e.g.* a remaining sub-expansion of the stent in a calcified lesion), issues at the edges (*e.g.* a dissection), or a remaining stenosis outside the stented segment. In the DKCRUSH VII registry the only statistically significant predictor of target vessel failure (TVF) at 3-year was a post-PCI FFR < 0.88[54]. Hwang *et al*[55] reported an optimal cut-off post-PCI FFR predicting TVF of < 0.82, associated with a 10.9% rate of events while it was only 2.5% when the post-PCI FFR was ≥ 0.82 in the left anterior descending artery (LAD). Similarly, a FFR post PCI < 0.88 was associated with 8% of TVF, but 1.9% with a FFR ≥ 0.88 in a non-LAD vessel. Conversely, Diletti *et al*[56] more recently reported among 1000 patients that a sub-optimal FFR < 0.90 was measured in 38% of the treated vessels. At 2-year follow-up, in a patient level analysis, there were no increase in major adverse cardiac events. A vessel level analysis demonstrated a significant doubling of target vessel revascularization (P = 0.030) and a trend towards a higher stent thrombosis rate [HR, 2.89 (95%CI, 0.88–9.48), P = 0.08]. After balloon angioplasty without stenting, favorable outcomes have been associated with a final FFR ranging between 0.90 and 0.75. An optimal FFR cut-off of 0.80 was reported for drug eluting balloon angioplasty without stenting[57].

NON-HYPEREMIC PRESSURE RATIOS

Rational of instantaneous wave-free ratio

FFR has become the gold standard invasive diagnostic tool to guide coronary artery revascularization. Understanding the mechanisms of fractional flow measurement is essential before performing any physiological assessment of CAD. Coronary resistance fluctuates during the cardiac cycle in a phasic pattern, due to the compression and decompression of the myocardium. A specific period, not affected by forward and backward effects, named instantaneous wave free period, has been identified[58]. The iFR concept relies on the theory that intracoronary resistance is naturally low and constant during this wave free period allowing to compute a reliable pressure index. This particular cardiac window has been defined in the ADVISE (Adenosine vasodilator independent stenosis evaluation) trial to start 25%

Table 4 Summary of main instantaneous wave free ratio trials

Trial	Study population	Mean FFR value +/-SD	Mean iFR-value +/-SD	iFR cut-off	*P* value for non-inferiority	Correlation	Sensitivity %	Specificity %
DEFINE-FLAIR[13]	2492	0.83 +/-0.09	0.91+/- 0.09	0.89	< 0.001			
iFR SWEDEHEART [12]	2037	0.82 +/-0.10	0.91+/- 0.10	0.89	0.007			
ADVISE study[59]	131	0.72+/- 0.2		0.83		0.9 (P < 0.001)	85	91
VERIFY[65]	206			0.83		0.67	54 (49-60)	96 (95-99)
JUSTIFY-CFR[61]	186	0.74+/- 0.17	0.81+/- 0.21	0.89		0.68 0.60-0.76	73	74

FFR: Fractional flow reserve; SD: Standard deviation. Table 4 summarize the primary studies evaluating the instantaneous wave free ratio (iFR). These trials have evaluated the correlation rate between iFR and FFR value and showed that iFR guided- percutaneous interventions (PCI) could be an alternative to FFR guided-PCI.

after the start of the diastolic phase and ends 5 ms before the systolic phase start. iFR is measured without the need of hyperemia/adenosine and the 0.89 threshold corresponding to ischemia has been validated *vs* FFR measurements[59].

Validation studies

The ADVISE study assessed the accuracy of iFR compared with FFR. A close correlation was found between both indices with good diagnostic performance (receiver-operating characteristic (ROC) area of 93%, at FFR< 0.8) with specificity, sensitivity, negative and positive predictive values respectively at 91%, 85%, 85% and 91%[59]. In the CLARIFY study, an agreement of 92% between iFR and FFR values was found. In the four lesions with mismatch between the two indices, the hyperemic stenosis resistance was correlated either to FFR or iFR[60]. In addition, the SWEDEHEART trial highlighted the noninferiority of iFR-guided PCI compared with a FFR-guided PCI[12]. The same finding were reported in the DEFINE FLAIR trial with a reduction in adverse procedural symptoms related to adenosine infusion and shorter time of procedures[13]. A better agreement between iFR than FFR and coronary flow velocity reserve was reported in JUSTIFY-CFR. In 4% of their non-significant iFR values (> 0.90) a significant drop in FFR value (< 0.75) was noted[61]. Multiple trials have reported an approximative 80% accuracy between iFR and FFR[14,59,62].

The ADIVSE II trial reported a strong correlation between iFR and FFR and identified 0.89 as the optimal iFR threshold with an area under the ROC curve of 0.90. This cut-off correctly classified 82.5% of coronary artery stenoses with a sensitivity and specificity of respectively 73% and 87.8%. The hybrid iFR-FFR approach based on a iFR treatment value below 0.85 and deferral above 0.94 showed a better correlation rate of 94.2%[63].

Using respectively 0.89 and 0.80 as cutoffs for iFR and FFR, Modi reported a 25% discordance rate, which is in line with the previous studies. This discrepancy can be lowered to 11% using respectively 0.86 and 0.75 cutoffs[64]. Table 4 presents these different studies.

In contrast, the VERIFY trial revealed only a moderate overall correlation between iFR and FFR with a weak correlation in the clinically important range for decision making, between 0.60 and 0.90. The authors do not recommend the use of iFR for clinical decision making for PCI[65]. We will also personally guide our clinical decisions to revascularize or defer an intervention in our patients using the results of their FFR that we will always assess in any doubtful result of a NHPR in a grey zone between 0.84 and 0.94.

New NHPR

With the increasing use of invasive hemodynamic assessment of CAD severity, novel NHPR have been proposed by different manufacturers. These indices have been compared to iFR and are summarized in Table 5.

Figure 3 shows the different periods used for NHPR calculation over the cardiac cycle. These indices can be separated into two groups, the ones using the whole cycle and the others using calculating diastolic indices.

The retrospective VALIDATE study showed the diagnostic comparability between resting full-cycle ratio (RFR) and iFR. It is important to note that 12.2% of RFR were measured outside the diastolic phase with a predominant discrepancy rate between both measurements when iFR was > 0.93. This difference was found to be more important in waveforms acquired in right coronary arteries (6.5%)[66]. The REVALIDATE RFR study had the same purpose using a prospective analysis methodology showing a 97.8% overall diagnostic accuracy, sensitivity and specificity. Thus, RFR is an alternative diagnostic tool for the guidance of PCI reducing time and cost procedures by avoiding hyperemic agents need[67].

Table 5 Non-hyperemic pressure ratio indices

Acronym	Full name	Manufacturer	Method	Threshold	Evidence
iFR	Instantaneous wave-free ratio	Philips Heathcare	Mean five Pd/Pa during the WFP	0.89	DEFINE FLAIR[13], SWEDEHAEART TRIAL[12]
RFR	Resting full-cycle ratio	Abbott	Lowest value of Pd/Pa across the whole cardiac cycle	0.89	VALIDATE RFR[68], RE-VALIDATE RFR[69]
DFR	Diastolic hyperemia-free ratio	Boston Scientific	Average 5 consecutive cardiac cycles Pd/Pa ratio over the approximated[a] diastolic period	0.89	Comparison of different diastolic resting indexes to iFR [15]
dPR	Diastolic pressure ratio	ACIST/Opsens Medical	Average 5 beats Pd/Pa ratio at the pressure peak-to-peak midpoint	0.89	Diastolic pressure ratio: New approach and validation *vs* the iFR[69]
Resting Pd/Pa		Not proprietary technology	Pd/Pa averaged over the entire cardiac cycle	0.91	

[a]Diastole approximated as negatively sloped segment of tracing where Pa falls below mean Pa. Pd: Distal coronary artery pressure; Pa: Aortic pressure; WFP: Wave Free Period. This table represents the multiple non-hyperemic pressure ratios available at this day. Each manufacturer has led its trial to support the use of its non-hyperemic pressure ratios (NHPR) indices. These studies compared the new calculations methods to the instantaneous wave free ratio (iFR) and showed good correlation between NHPR. These indices have the same cut-off value of 0.89 below which a coronary artery stenosis is considered functionally significant.

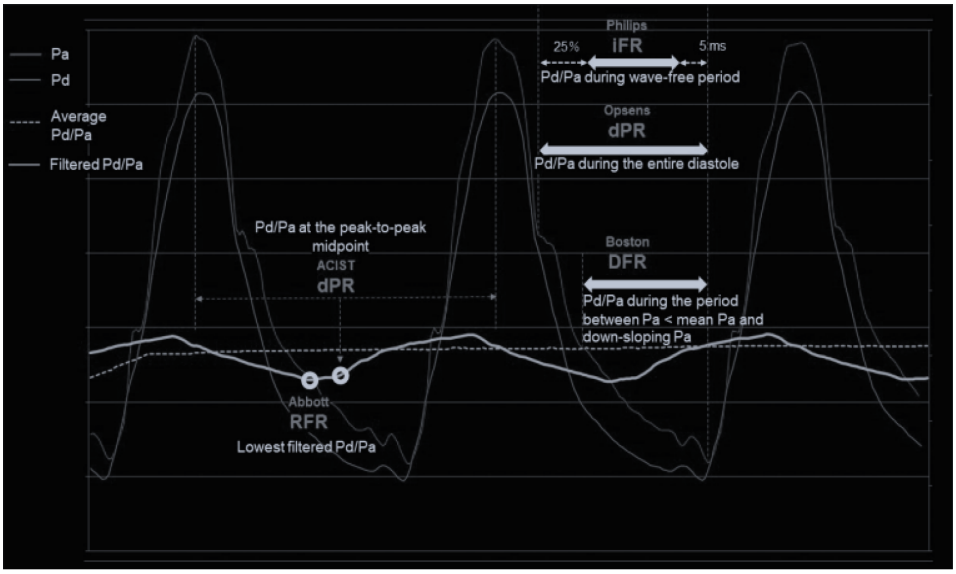

DOI: 10.12998/wjcc.v11.i10.2123

Figure 3 Non-Hyperemic pressure ratios calculation over cardiac cycle. RFR: Resting full-cycle ratio; DFR: Diastolic hyperemia-free ratio; dPR: Diastolic pressure ratio.

The diastolic Pressure Ratio study found a strong linear correlation between the diastolic pressure ratio and iFR (r = 0,997, P < 0.001) on one hand and FFR (r = 0.77, P < 0.001) on the other[68,69]. The dPR measured with the Optowire (Opsens, Quebec City, Quebec, Canada) showed strong correlation with other NHPR (RFR, iFR) in the RPG study with an r = 0.84[70].

A novel Opsens dPR algorithm using the mean of 4 consecutive beats Pd/Pa ratio at diastole was highly correlated to iFR (R^2 = 0.99) with high accuracy to predict iFR at 95.6%, with a sensitivity of 93.5% and specificity of 96.7%[71]. As reviewed by De Maria *et al*[72] among the major advantages of the resting indices is the hyperemia drug free evaluation.

The cut-off for these non-hyperemic indices is 0.89 with a proportion of discordance ranging between 15% to 20% particularly in proximal vessel subtending large myocardial areas[58]. Theses resting indices were not evaluated in randomized controlled trials but have only been compared in studies to support their clinical use[15,73].

Indications for the use of non-hyperemic pressure ratios

Following the validation studies described above, NHPR share similar indications than FFR but

additional specific clinical scenario's have been investigated. For example, a retrospective study reported how to decide to perform a PCI with iFR in non-culprit lesions of patients presenting with ACS [74].

The iLITRO study found an agreement of 80% between iFR and FFR in left main intermediate stenosis. Intravascular ultrasound imaging (IVUS) was used in cases with discrepancy, using the threshold of 6 mm^2 as a cut-off for revascularization. In discordant FFR/iFR measurements, IVUS showed an MLA < 6 mm^2 in 69% of the cases of FFR+/iFR-, while in FFR-/iFR+ cases, 40% only had an MLA< 6 mm^2. The patients deferred from revascularization with discordant hemodynamic measurements and a negative IVUS evaluation had a low incidence of MACE at follow-up, leading to an iFR-guided LMCA revascularization strategy combined with IVUS in the discordant cases (hybrid approach)[44].

An iFR pullback enables the operator to predict an iFR value after the treatment of a selected stenosis [75]. The comparison of functional PCI results using NHPR in the REFINE-RPG study showed comparable results between RFR, dPR and iFR while reducing the total length of treated lesions using NHPR pullback PCI-guided strategy compared to angiography-guided PCI. The correlation between predicted and actual post PCI NHPR was high (r = 0.73) with no difference among NHPR groups[70].

THE HYBRID APPROACH

In multiple scenarios, the use of FFR or iFR alone may not suffice to take the proper therapeutic decision. Hence, a hybrid approach is useful in some clinical scenarios. Using FFR as the gold standard, NHPR has an average accuracy of 80% resulting in stenoses misclassifications. A combined physiological assessment without adenosine in the first line demonstrated a reduction of the need of intracoronary vasodilator in more than half of the CAD patients in need of functional assessment. Furthermore, the use a 0.86-0.93 cut-off range for iFR improve its positive and negative predictive value to respectively 92% and 91%[61].

The technical aspect of PCI optimization involves proper use of diagnostic and guidance imaging, equipment, techniques, and antithrombotic therapy to achieve optimal patient outcomes. Recently, the value of low post PCI FFR has been linked to poor outcomes related to suboptimal stent placement or remaining disease[76]. In this specific setting, intravascular imaging may be helpful to understand the mechanisms behind inadequate functional improvement. The FFR REACT trial used a post PCI threshold of 0.90 and randomized 291 patients for IVUS or traditional standard of care. This strategy resulted in the improvement of post PCI FFR in 20% of the vessels with a trend for lower target vessel revascularization in the IVUS guided arm (P = 0.06)[77].

Intermediate left main coronary artery lesions can be evaluated more thoroughly with either intracoronary imaging (using IVUS) or physiological assessment (using FFR pressure wire). These invasive tools can provide more detailed information on the anatomical severity and hemodynamic significance of the lesions to be discussed in the heart team to improve the decision of the revascularization strategy and its optimization. Park has reviewed in detail the role of pre and post PCI IVUS and FFR[78]. The ILITRO-EPIC07 study showed that FFR and iFR had an average agreement of 80%, while IVUS was more likely to match FFR's classification of stenosis significance in discrepant cases. Therefore, from a clinician's viewpoint, the best approach for determining if revascularization can be safely deferred in intermediate left main coronary artery lesions is a combination of IVUS and physiology[44].

QUANTITATIVE FLOW RATIO AND FRACTIONAL FLOW RESERVE COMPUTED TOMOGRAPHY

More recently, physiological coronary assessment has been evaluated with virtual tools computing the flow ratio. Quantitative flow ratio (QFR) is based on the analysis of two angiography views 25° apart at least with minimal superposition between the main and side branches. The QFR uses a mathematical model, the three-dimensional reconstruction and coronary contrast product progression in order to determine the coronary flow. The FAVOR trial was the first to assess this technique, and showed significant correlation with FFR (r = 0.77; P < 0.001) with an 80% accuracy using an FFR threshold of 0.80 [79]. Along with these promising results, the FAVOR II Europe-Japan Study found that QFR is superior to angiographic assessment of intermediate coronary artery stenosis using FFR as standard reference [80]. Kasinadhuni *et al*[81] showed that QFR has a superior diagnostic performance compared to the benchmark FFR in evaluating intermediate lesions physiologically outperforming the anatomical percentage diameter stenosis with a significant difference (P < 0.001).

QFR and FFR have excellent consistency and alignment. The ability of QFR to determine the functional impact of coronary disease has been demonstrated in the meta-analysis and systematic review of Cortés *et al*[82]. This new tool, and a similar one, vFFR implemented in the CAAS Worstation

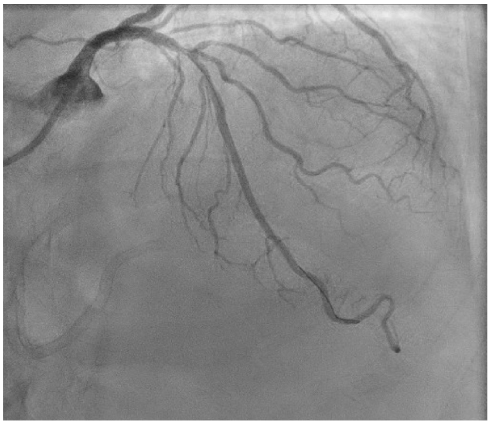

DOI: 10.12998/wjcc.v11.i10.2123 **Copyright** ©The Author(s) 2023.

Figure 4 Left anterior oblique cranial view demonstrating a moderate proximal left anterior descending stenosis.

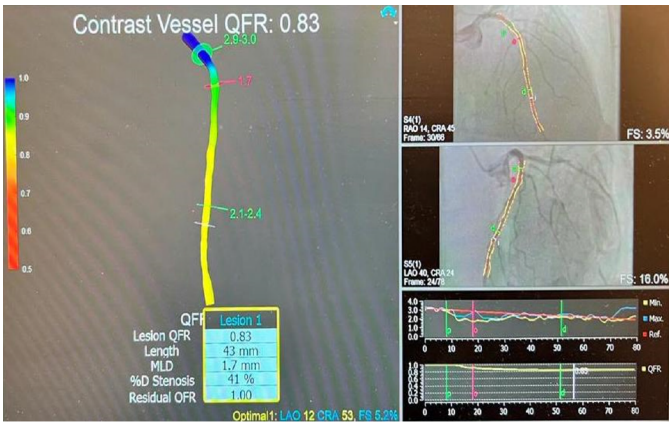

DOI: 10.12998/wjcc.v11.i10.2123 **Copyright** ©The Author(s) 2023.

Figure 5 Quantitative flow ratio of the left anterior descending. QFR: Quantitative flow ratio.

(Pie Medical Imaging, Maastricht, the Netherlands) are independent predictors for MACE with beneficial effect of PCI for low QFR/vFFR values[83,84].

Finally non-invasively, The SYNTAX III REVOLUTION study showed that using computed coronary tomography angiography to decide between CABG and PCI for coronary artery disease, based on the predicted four-year mortality as indicated by the SYNTAX score II, resulted in high agreement (93%) in treatment decisions, with an "almost perfect kappa" of 0.82, compared to decisions made using ICA[85,86].

FFR-Computed Tomography (FFR-CT) allows for the measurement of flow across the entire coronary artery bed unlike the usual method which assess the functional significance of a specific coronary stenosis and its upstream segments[20,87].

These new concepts open new tracks for a better risk stratification and prognosis prediction of patients presenting with coronary artery disease. Their use is increasing in the context of stable CAD for the guidance of percutaneous interventions, but some authors have demonstrated the prognostic implication of a post interventional pan-coronary-QFR evaluation in patients with ACS[88].

We hypothesize that further improvement of these techniques might help the physicians to discriminate atherosclerotic NSTE-ACS from type II Myocardial infarction and myocardial infarction with non-obstructive coronary disease.

A hybrid approach, with a combined use of both anatomical (IVUS) and functional methods to determine the significance of coronary stenosis, could provide a more comprehensive and accurate assessment enabling the operators to take more targeted and individualized decisions. However, the hybrid approach does require additional imaging and testing, which can increase the cost and complexity of the evaluation. Using QFR and IVUS simultaneously, or FFR-CT before, seems appealing as they combine an invasive evaluation with a noninvasive one, lowering the cost.

We will illustrate this concept in two recent clinical cases we performed. A stable patient with suspected myocardial ischemia after dobutamine stress test had a coronary angiogram demonstrating a LAD with a moderate long lesion in the proximal and mid part (Figure 4) that was evaluated by QFR at 0.83 (Figure 5). Regarding these intermediate values, a complementary IVUS evaluation was performed

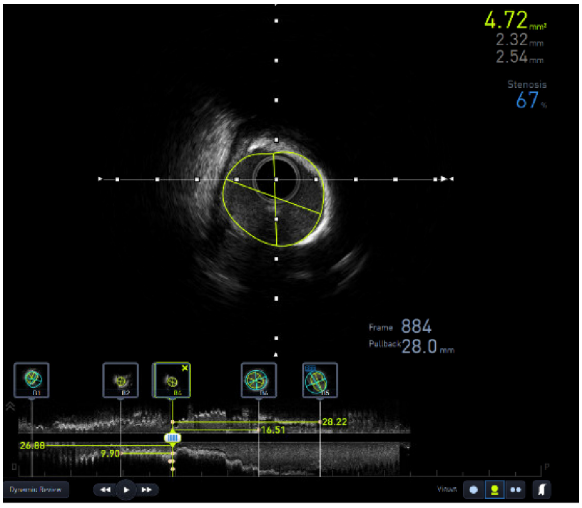

DOI: 10.12998/wjcc.v11.i10.2123 **Copyright** ©The Author(s) 2023.

Figure 6 Intravascular ultrasound imaging showing the minimal luminal area of 4.72 mm², diameters and percentage stenosis of the left anterior descending.

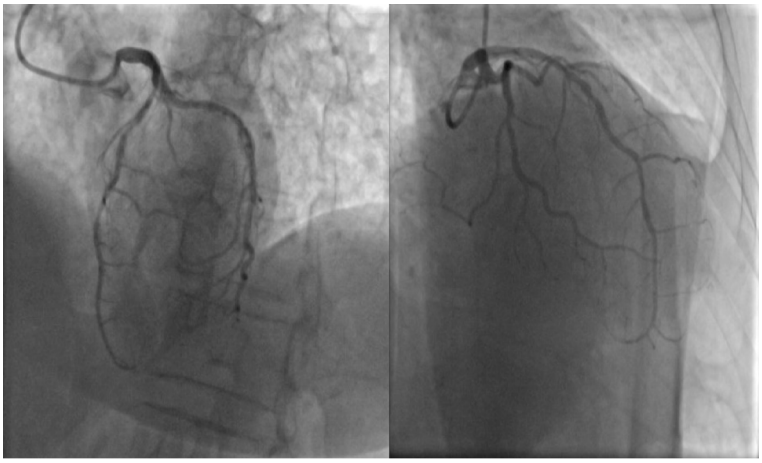

DOI: 10.12998/wjcc.v11.i10.2123 **Copyright** ©The Author(s) 2023.

Figure 7 Cranial left and right anterior oblique view demonstrating serial stenoses of the left anterior descending.

(Figure 6) showing a non-significant lesion with a minimal lumen area of was 4.7 mm².

The good agreement between QFR and FFR is illustrated in another case summarized on Figures 7 to 9. On the coronary angiogram of a patient with recurrent clinical symptoms, we noticed multiple intermediate lesions in the proximal, mid, and distal LAD (Figure 7).

The FFR was positive in the distal LAD at 0.78 and also the DFR was 0.86 (Figure 8). The QFR of 0.75 was well aligned with these measurements (Figure 9). The relationship between QFR and clinical outcomes, and its cost-effectiveness, requires further prospective validation.

CONCLUSION

Invasive hemodynamic assessment of coronary artery disease is a critical component of a patient evaluation. Today, fractional flow reserve and non-hyperemic pressure ratios guide the physician in optimizing coronary artery tree revascularization therapy. Their development has been backed up by extensive validation studies and physiology and they obtained a class I indication during PCI. The possibility to assess the spatial distribution of epicardial resistances and determine the focal or diffuse characteristics of coronary artery disease is crucial for revascularization therapy decisions. In the case of a difference between the measured fractional flow reserve and any non-hyperemic pressure ratio, we recommend following the results of the FFR and defer an intervention when its value is superior to 0.80.

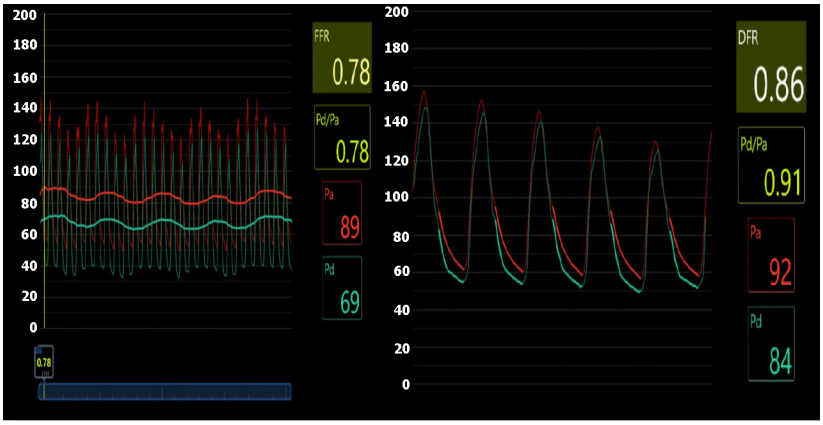

DOI: 10.12998/wjcc.v11.i10.2123 **Copyright** ©The Author(s) 2023.

Figure 8 Distal left anterior descending diastolic flow ratio and fractional flow reserve. FFR: Fractional flow reserve; DFR: Diastolic hyperemia-free ratio.

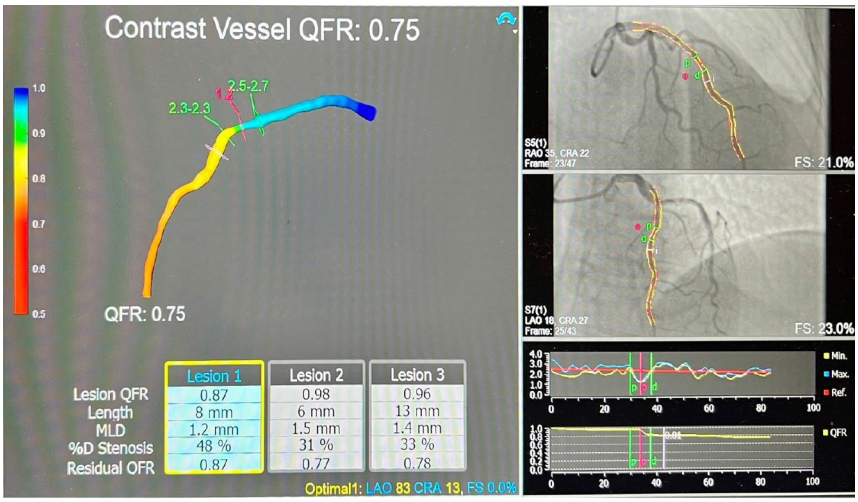

DOI: 10.12998/wjcc.v11.i10.2123 **Copyright** ©The Author(s) 2023.

Figure 9 Quantitative flow ratio of left anterior descending evaluating each stenosis residual quantitative flow ratio and final result. QFR: Quantitative flow ratio.

FOOTNOTES

Author contributions: All authors equally contributed to this paper with conception and design of the study, literature review and analysis, drafting and critical revision and editing, and final approval of the final version.

Conflict-of-interest statement: No potential conflicts of interest. No financial support.

Country/Territory of origin: Belgium

ORCID number: Amine Mamoun Boutaleb 0000-0002-1892-0070; Chadi Ghafari 0000-0002-5971-5073; Claudiu Ungureanu 0000-0002-1583-5882; Stéphane Carlier 0000-0001-7787-1937.

S-Editor: Liu JH
L-Editor: A
P-Editor: Liu JH

REFERENCES

1 **Suzuki N**, Asano T, Nakazawa G, Aoki J, Tanabe K, Hibi K, Ikari Y, Kozuma K. Clinical expert consensus document on quantitative coronary angiography from the Japanese Association of Cardiovascular Intervention and Therapeutics. *Cardiovasc Interv Ther* 2020; **35**: 105-116 [PMID: 32125622 DOI: 10.1007/s12928-020-00653-7]

2 **Beller GA**, Zaret BL. Contributions of nuclear cardiology to diagnosis and prognosis of patients with coronary artery disease. *Circulation* 2000; **101**: 1465-1478 [PMID: 10736294 DOI: 10.1161/01.CIR.101.12.1465]

3 **Hachamovitch R**, Berman DS, Shaw LJ, Kiat H, Cohen I, Cabico JA, Friedman J, Diamond GA. Incremental prognostic value of myocardial perfusion single photon emission computed tomography for the prediction of cardiac death: differential stratification for risk of cardiac death and myocardial infarction. *Circulation* 1998; **97**: 535-543 [PMID: 9494023 DOI: 10.1161/01.CIR.97.6.535]

4 **Reynolds HR**, Shaw LJ, Min JK, Page CB, Berman DS, Chaitman BR, Picard MH, Kwong RY, O'Brien SM, Huang Z, Mark DB, Nath RK, Dwivedi SK, Smanio PEP, Stone PH, Held C, Keltai M, Bangalore S, Newman JD, Spertus JA, Stone GW, Maron DJ, Hochman JS. Outcomes in the ISCHEMIA Trial Based on Coronary Artery Disease and Ischemia Severity. *Circulation* 2021; **144**: 1024-1038 [PMID: 34496632 DOI: 10.1161/CIRCULATIONAHA.120.049755]

5 **Jennings RB**, Reimer KA. The cell biology of acute myocardial ischemia. *Annu Rev Med* 1991; **42**: 225-246 [PMID: 2035969 DOI: 10.1146/annurev.me.42.020191.001301]

6 **Knuuti J**, Wijns W, Saraste A, Capodanno D, Barbato E, Funck-Brentano C, Prescott E, Storey RF, Deaton C, Cuisset T, Agewall S, Dickstein K, Edvardsen T, Escaned J, Gersh BJ, Svitil P, Gilard M, Hasdai D, Hatala R, Mahfoud F, Masip J, Muneretto C, Valgimigli M, Achenbach S, Bax JJ; ESC Scientific Document Group. 2019 ESC Guidelines for the diagnosis and management of chronic coronary syndromes. *Eur Heart J* 2020; **41**: 407-477 [PMID: 31504439 DOI: 10.1093/eurheartj/ehz425]

7 **Pijls NH**, De Bruyne B, Peels K, Van Der Voort PH, Bonnier HJ, Bartunek J Koolen JJ, Koolen JJ. Measurement of fractional flow reserve to assess the functional severity of coronary-artery stenoses. *N Engl J Med* 1996; **334**: 1703-1708 [PMID: 8637515 DOI: 10.1056/NEJM199606273342604]

8 **Neumann FJ**, Sousa-Uva M. 'Ten commandments' for the 2018 ESC/EACTS Guidelines on Myocardial Revascularization. *Eur Heart J* 2019; **40**: 79-80 [PMID: 30615155 DOI: 10.1093/eurheartj/ehy855]

9 **De Bruyne B**, Pijls NH, Kalesan B, Barbato E, Tonino PA, Piroth Z, Jagic N, Möbius-Winkler S, Rioufol G, Witt N, Kala P, MacCarthy P, Engström T, Oldroyd KG, Mavromatis K, Manoharan G, Verlee P, Frobert O, Curzen N, Johnson JB, Jüni P, Fearon WF; FAME 2 Trial Investigators. Fractional flow reserve-guided PCI versus medical therapy in stable coronary disease. *N Engl J Med* 2012; **367**: 991-1001 [PMID: 22924638 DOI: 10.1056/NEJMoa1205361]

10 **Tonino PA**, De Bruyne B, Pijls NH, Siebert U, Ikeno F, van' t Veer M, Klauss V, Manoharan G, Engstrøm T, Oldroyd KG, Ver Lee PN, MacCarthy PA, Fearon WF; FAME Study Investigators. Fractional flow reserve versus angiography for guiding percutaneous coronary intervention. *N Engl J Med* 2009; **360**: 213-224 [PMID: 19144937 DOI: 10.1056/NEJMoa0807611]

11 **Zimmermann FM**, Ferrara A, Johnson NP, van Nunen LX, Escaned J, Albertsson P, Erbel R, Legrand V, Gwon HC, Remkes WS, Stella PR, van Schaardenburgh P, Bech GJ, De Bruyne B, Pijls NH. Deferral vs. performance of percutaneous coronary intervention of functionally non-significant coronary stenosis: 15-year follow-up of the DEFER trial. *Eur Heart J* 2015; **36**: 3182-3188 [PMID: 26400825 DOI: 10.1093/eurheartj/ehv452]

12 **Götberg M**, Christiansen EH, Gudmundsdottir IJ, Sandhall L, Danielewicz M, Jakobsen L, Olsson SE, Öhagen P, Olsson H, Omerovic E, Calais F, Lindroos P, Maeng M, Tödt T, Venetsanos D, James SK, Kåregren A, Nilsson M, Carlsson J, Hauer D, Jensen J, Karlsson AC, Panayi G, Erlinge D, Fröbert O; iFR-SWEDEHEART Investigators. Instantaneous Wave-free Ratio versus Fractional Flow Reserve to Guide PCI. *N Engl J Med* 2017; **376**: 1813-1823 [PMID: 28317438 DOI: 10.1056/NEJMoa1616540]

13 **Davies JE**, Sen S, Dehbi HM, Al-Lamee R, Petraco R, Nijjer SS, Bhindi R, Lehman SJ, Walters D, Sapontis J, Janssens L, Vrints CJ, Khashaba A, Laine M, Van Belle E, Krackhardt F, Bojara W, Going O, Härle T, Indolfi C, Niccoli G, Ribichini F, Tanaka N, Yokoi H, Takashima H, Kikuta Y, Erglis A, Vinhas H, Canas Silva P, Baptista SB, Alghamdi A, Hellig F, Koo BK, Nam CW, Shin ES, Doh JH, Brugaletta S, Alegria-Barrero E, Meuwissen M, Piek JJ, van Royen N, Sezer M, Di Mario C, Gerber RT, Malik IS, Sharp ASP, Talwar S, Tang K, Samady H, Altman J, Seto AH, Singh J, Jeremias A, Matsuo H, Kharbanda RK, Patel MR, Serruys P, Escaned J. Use of the Instantaneous Wave-free Ratio or Fractional Flow Reserve in PCI. *N Engl J Med* 2017; **376**: 1824-1834 [PMID: 28317458 DOI: 10.1056/NEJMoa1700445]

14 **Jeremias A**, Maehara A, Généreux P, Asrress KN, Berry C, De Bruyne B, Davies JE, Escaned J, Fearon WF, Gould KL, Johnson NP, Kirtane AJ, Koo BK, Marques KM, Nijjer S, Oldroyd KG, Petraco R, Piek JJ, Pijls NH, Redwood S, Siebes M, Spaan JAE, van 't Veer M, Mintz GS, Stone GW. Multicenter core laboratory comparison of the instantaneous wave-free ratio and resting Pd/Pa with fractional flow reserve: the RESOLVE study. *J Am Coll Cardiol* 2014; **63**: 1253-1261 [PMID: 24211503 DOI: 10.1016/j.jacc.2013.09.060]

15 **Van't Veer M**, Pijls NHJ, Hennigan B, Watkins S, Ali ZA, De Bruyne B, Zimmermann FM, van Nunen LX, Barbato E, Berry C, Oldroyd KG. Comparison of Different Diastolic Resting Indexes to iFR: Are They All Equal? *J Am Coll Cardiol* 2017; **70**: 3088-3096 [PMID: 29268922 DOI: 10.1016/j.jacc.2017.10.066]

16 **Pijls NH**, van Son JA, Kirkeeide RL, De Bruyne B, Gould KL. Experimental basis of determining maximum coronary, myocardial, and collateral blood flow by pressure measurements for assessing functional stenosis severity before and after percutaneous transluminal coronary angioplasty. *Circulation* 1993; **87**: 1354-1367 [PMID: 8462157 DOI: 10.1161/01.CIR.87.4.1354]

17 **Mohdnazri SR**, Keeble TR, Sharp AS. Fractional Flow Reserve: Does a Cut-off Value add Value? *Interv Cardiol* 2016; **11**: 17-26 [PMID: 29588700 DOI: 10.15420/icr.2016:7:2]

18 **Warisawa T**, Cook CM, Akashi YJ, Davies JE. Past, Present and Future of Coronary Physiology. *Rev Esp Cardiol (Engl Ed)* 2018; **71**: 656-667 [PMID: 29551700 DOI: 10.1016/j.rec.2018.02.003]

19 **van Nunen LX**, Lenders GD, Schampaert S, van 't Veer M, Wijnbergen I, Brueren GR, Tonino PA, Pijls NH. Single bolus intravenous regadenoson injection versus central venous infusion of adenosine for maximum coronary hyperaemia in

fractional flow reserve measurement. *EuroIntervention* 2015; **11**: 905-913 [PMID: 25136887 DOI: 10.4244/EIJY14M08_10]

20 **Shantouf RS**, Mehra A. Coronary fractional flow reserve. *AJR Am J Roentgenol* 2015; **204**: W261-W265 [PMID: 25714310 DOI: 10.2214/AJR.14.13933]

21 **Layland J**, Carrick D, Lee M, Oldroyd K, Berry C. Adenosine: physiology, pharmacology, and clinical applications. *JACC Cardiovasc Interv* 2014; **7**: 581-591 [PMID: 24835328 DOI: 10.1016/j.jcin.2014.02.009]

22 **Andrikopoulou E**, Hage FG. Adverse effects associated with regadenoson myocardial perfusion imaging. *J Nucl Cardiol* 2018; **25**: 1724-1731 [PMID: 29468467 DOI: 10.1007/s12350-018-1218-7]

23 **Thomas GS**, Tammelin BR, Schiffman GL, Marquez R, Rice DL, Milikien D, Mathur V. Safety of regadenoson, a selective adenosine A2A agonist, in patients with chronic obstructive pulmonary disease: A randomized, double-blind, placebo-controlled trial (RegCOPD trial). *J Nucl Cardiol* 2008; **15**: 319-328 [PMID: 18513638 DOI: 10.1016/j.nuclcard.2008.02.013]

24 **Arumugham P**, Figueredo VM, Patel PB, Morris DL. Comparison of intravenous adenosine and intravenous regadenoson for the measurement of pressure-derived coronary fractional flow reserve. *EuroIntervention* 2013; **8**: 1166-1171 [PMID: 23164748 DOI: 10.4244/EIJV8I10A180]

25 **Nair PK**, Marroquin OC, Mulukutla SR, Khandhar S, Gulati V, Schindler JT, Lee JS. Clinical utility of regadenoson for assessing fractional flow reserve. *JACC Cardiovasc Interv* 2011; **4**: 1085-1092 [PMID: 22017933 DOI: 10.1016/j.jcin.2011.07.011]

26 **Pijls NH**, Van Gelder B, Van der Voort P, Peels K, Bracke FA, Bonnier HJ, el Gamal MI. Fractional flow reserve. A useful index to evaluate the influence of an epicardial coronary stenosis on myocardial blood flow. *Circulation* 1995; **92**: 3183-3193 [PMID: 7586302 DOI: 10.1161/01.CIR.92.11.3183]

27 **Adjedj J**, Flore V, Gioia GD, Ferrara A, Pellicano M, Toth G, Wijns W, de Bruyne B, Barbato E. 0043: FFR Gray zone and clinical outcome. *Arch Cardiovasc Dis Suppl* 2016; **8**: 8-9 [DOI: 10.1016/S1878-6480(16)30026-X]

28 **Watkins S**, McGeoch R, Lyne J, Steedman T, Good R, McLaughlin MJ, Cunningham T, Bezlyak V, Ford I, Dargie HJ, Oldroyd KG. Validation of magnetic resonance myocardial perfusion imaging with fractional flow reserve for the detection of significant coronary heart disease. *Circulation* 2009; **120**: 2207-2213 [PMID: 19917885 DOI: 10.1161/CIRCULATIONAHA.109.872358]

29 **Bartunek J**, Van Schuerbeeck E, de Bruyne B. Comparison of exercise electrocardiography and dobutamine echocardiography with invasively assessed myocardial fractional flow reserve in evaluation of severity of coronary arterial narrowing. *Am J Cardiol* 1997; **79**: 478-481 [PMID: 9052353 DOI: 10.1016/S0002-9149(96)00788-6]

30 **Fearon WF**, Chambers JW, Seto AH, Sarembock IJ, Raveendran G, Sakarovitch C, Yang L, Desai M, Jeremias A, Price MJ; ACIST-FFR Study Investigators. ACIST-FFR Study (Assessment of Catheter-Based Interrogation and Standard Techniques for Fractional Flow Reserve Measurement). *Circ Cardiovasc Interv* 2017; **10**: e005905 [PMID: 29246917 DOI: 10.1161/CIRCINTERVENTIONS.117.005905]

31 **Cottens D**, Ferdinande B, Polad J, Vrolix M, Ameloot K, Hendrickx I, Poels E, Maeremans J, Dens J. FFR pressure wire comparative study for drift: piezo resistive versus optical sensor. *Am J Cardiovasc Dis* 2022; **12**: 42-52 [PMID: 35291508]

32 **Vranckx P**, Cutlip DE, McFadden EP, Kern MJ, Mehran R, Muller O. Coronary pressure-derived fractional flow reserve measurements: recommendations for standardization, recording, and reporting as a core laboratory technique. Proposals for integration in clinical trials. *Circ Cardiovasc Interv* 2012; **5**: 312-317 [PMID: 22511740 DOI: 10.1161/CIRCINTERVENTIONS.112.968511]

33 **Pijls NH**, Bruyne BD. Fractional Flow Reserve, Coronary Pressure Wires, and Drift. *Circ J* 2016; **80**: 1704-1706 [PMID: 27430249 DOI: 10.1253/circj.CJ-16-0623]

34 **Stables RH**, Elguindy M, Kemp I, Nicholas Z, Mars C, Mullen L, Curzen N. A randomised controlled trial to compare two coronary pressure wires using simultaneous measurements in human coronary arteries: the COMET trial. *EuroIntervention* 2019; **14**: e1578-e1584 [PMID: 30375339 DOI: 10.4244/EIJ-D-18-00786]

35 **Ulacia P**, Rimac G, Lalancette S, Belleville C, Mongrain R, Plante S, Rusza Z, Matsuo H, Bertrand OF. A novel fiber-optic based 0.014″ pressure wire: Designs of the OptoWire™, development phases, and the O(2) first-in-man results. *Catheter Cardiovasc Interv* 2020 [PMID: 33090670 DOI: 10.1002/ccd.29321]

36 **Heusch G**. Myocardial Ischemia: Lack of Coronary Blood Flow or Myocardial Oxygen Supply/Demand Imbalance? *Circ Res* 2016; **119**: 194-196 [PMID: 27390331 DOI: 10.1161/CIRCRESAHA.116.308925]

37 **Pijls NH**, van Schaardenburgh P, Manoharan G, Boersma E, Bech JW, van't Veer M, Bär F, Hoorntje J, Koolen J, Wijns W, de Bruyne B. Percutaneous coronary intervention of functionally nonsignificant stenosis: 5-year follow-up of the DEFER Study. *J Am Coll Cardiol* 2007; **49**: 2105-2111 [PMID: 17531660 DOI: 10.1016/j.jacc.2007.01.087]

38 **Collet JP**, Thiele H, Barbato E, Barthélémy O, Bauersachs J, Bhatt DL, Dendale P, Dorobantu M, Edvardsen T, Folliguet T, Gale CP, Gilard M, Jobs A, Jüni P, Lambrinou E, Lewis BS, Mehilli J, Meliga E, Merkely B, Mueller C, Roffi M, Rutten FH, Sibbing D, Siontis GCM; ESC Scientific Document Group. 2020 ESC Guidelines for the management of acute coronary syndromes in patients presenting without persistent ST-segment elevation. *Eur Heart J* 2021; **42**: 1289-1367 [PMID: 32860058 DOI: 10.1093/eurheartj/ehaa575]

39 **Knuuti J**, Ballo H, Juarez-Orozco LE, Saraste A, Kolh P, Rutjes AWS, Jüni P, Windecker S, Bax JJ, Wijns W. The performance of non-invasive tests to rule-in and rule-out significant coronary artery stenosis in patients with stable angina: a meta-analysis focused on post-test disease probability. *Eur Heart J* 2018; **39**: 3322-3330 [PMID: 29850808 DOI: 10.1093/eurheartj/ehy267]

40 **Fezzi S**, Huang J, Lunardi M, Ding D, Ribichini FL, Tu S, Wijns W. Coronary physiology in the catheterisation laboratory: an A to Z practical guide. *AsiaIntervention* 2022; **8**: 86-109 [PMID: 36798834 DOI: 10.4244/AIJ-D-22-00022]

41 **de Bruyne B**, Bartunek J, Sys SU, Pijls NH, Heyndrickx GR, Wijns W. Simultaneous coronary pressure and flow velocity measurements in humans. Feasibility, reproducibility, and hemodynamic dependence of coronary flow velocity reserve, hyperemic flow versus pressure slope index, and fractional flow reserve. *Circulation* 1996; **94**: 1842-1849 [PMID: 8873658 DOI: 10.1161/01.CIR.94.8.1842]

42 **Johnson NP**, Johnson DT, Kirkeeide RL, Berry C, De Bruyne B, Fearon WF, Oldroyd KG, Pijls NHJ, Gould KL.

Repeatability of Fractional Flow Reserve Despite Variations in Systemic and Coronary Hemodynamics. *JACC Cardiovasc Interv* 2015; **8**: 1018-1027 [PMID: 26205441 DOI: 10.1016/j.jcin.2015.01.039]

43 **De Bruyne B**, Sarma J. Fractional flow reserve: a review: invasive imaging. *Heart* 2008; **94**: 949-959 [PMID: 18552231 DOI: 10.1136/hrt.2007.122838]

44 **Rodriguez-Leor O**, de la Torre Hernández JM, García-Camarero T, García Del Blanco B, López-Palop R, Fernández-Nofrerías E, Cuellas Ramón C, Jiménez-Kockar M, Jiménez-Mazuecos J, Fernández Salinas F, Gómez-Lara J, Brugaletta S, Alfonso F, Palma R, Gómez-Menchero AE, Millán R, Tejada Ponce D, Linares Vicente JA, Ojeda S, Pinar E, Fernández-Pelegrina E, Morales-Ponce FJ, Cid-Álvarez AB, Rama-Merchan JC, Molina Navarro E, Escaned J, Pérez de Prado A. Instantaneous Wave-Free Ratio for the Assessment of Intermediate Left Main Coronary Artery Stenosis: Correlations With Fractional Flow Reserve/Intravascular Ultrasound and Prognostic Implications: The iLITRO-EPIC07 Study. *Circ Cardiovasc Interv* 2022; **15**: 861-871 [PMID: 36111801 DOI: 10.1161/CIRCINTERVENTIONS.122.012328]

45 **Yong AS**, Daniels D, De Bruyne B, Kim HS, Ikeno F, Lyons J, Pijls NH, Fearon WF. Fractional flow reserve assessment of left main stenosis in the presence of downstream coronary stenoses. *Circ Cardiovasc Interv* 2013; **6**: 161-165 [PMID: 23549643 DOI: 10.1161/CIRCINTERVENTIONS.112.000104]

46 **De Bruyne B**, Pijls NH, Heyndrickx GR, Hodeige D, Kirkeeide R, Gould KL. Pressure-derived fractional flow reserve to assess serial epicardial stenoses: theoretical basis and animal validation. *Circulation* 2000; **101**: 1840-1847 [PMID: 10769286 DOI: 10.1161/01.cir.101.15.1840]

47 **Sels JW**, Tonino PA, Siebert U, Fearon WF, Van't Veer M, De Bruyne B, Pijls NH. Fractional flow reserve in unstable angina and non-ST-segment elevation myocardial infarction experience from the FAME (Fractional flow reserve versus Angiography for Multivessel Evaluation) study. *JACC Cardiovasc Interv* 2011; **4**: 1183-1189 [PMID: 22115657 DOI: 10.1016/j.jcin.2011.08.008]

48 **Liou KP**, Ooi SM, Hoole SP, West NEJ. Fractional flow reserve in acute coronary syndrome: a meta-analysis and systematic review. *Open Heart* 2019; **6**: e000934 [PMID: 30774965 DOI: 10.1136/openhrt-2018-000934]

49 **Liu LY**, Wu HP, Lin PL. Fractional Flow Reserve Assessment of a Significant Coronary Stenosis Masked by a Downstream Serial Lesion. *Case Rep Cardiol* 2016; **2016**: 1987238 [PMID: 27529035 DOI: 10.1155/2016/1987238]

50 **Hamilos M**, Muller O, Cuisset T, Ntalianis A, Chlouverakis G, Sarno G, Nelis O, Bartunek J, Vanderheyden M, Wyffels E, Barbato E, Heyndrickx GR, Wijns W, De Bruyne B. Long-term clinical outcome after fractional flow reserve-guided treatment in patients with angiographically equivocal left main coronary artery stenosis. *Circulation* 2009; **120**: 1505-1512 [PMID: 19786633 DOI: 10.1161/CIRCULATIONAHA.109.850073]

51 **Puymirat E**, Cayla G, Simon T, Steg PG, Montalescot G, Durand-Zaleski I, le Bras A, Gallet R, Khalife K, Morelle JF, Motreff P, Lemesle G, Dillinger JG, Lhermusier T, Silvain J, Roule V, Labèque JN, Rangé G, Ducrocq G, Cottin Y, Blanchard D, Charles Nelson A, De Bruyne B, Chatellier G, Danchin N; FLOWER-MI Study Investigators. Multivessel PCI Guided by FFR or Angiography for Myocardial Infarction. *N Engl J Med* 2021; **385**: 297-308 [PMID: 33999545 DOI: 10.1056/NEJMoa2104650]

52 **Costa MA**, Sabate M, Staico R, Alfonso F, Seixas AC, Albertal M, Crossman A, Angiolillo DJ, Zenni M, Sousa JE, Macaya C, Bass TA. Anatomical and physiologic assessments in patients with small coronary artery disease: final results of the Physiologic and Anatomical Evaluation Prior to and After Stent Implantation in Small Coronary Vessels (PHANTOM) trial. *Am Heart J* 2007; **153**: 296.e1-296.e7 [PMID: 17239692 DOI: 10.1016/j.ahj.2006.10.036]

53 **Fearon WF**, Zimmermann FM, De Bruyne B, Piroth Z, van Straten AHM, Szekely L, Davidavičius G, Kalinauskas G, Mansour S, Kharbanda R, Östlund-Papadogeorgos N, Aminian A, Oldroyd KG, Al-Attar N, Jagic N, Dambrink JE, Kala P, Angerås O, MacCarthy P, Wendler O, Casselman F, Witt N, Mavromatis K, Miner SES, Sarma J, Engstrøm T, Christiansen EH, Tonino PAL, Reardon MJ, Lu D, Ding VY, Kobayashi Y, Hlatky MA, Mahaffey KW, Desai M, Woo YJ, Yeung AC, Pijls NHJ; FAME 3 Investigators. Fractional Flow Reserve-Guided PCI as Compared with Coronary Bypass Surgery. *N Engl J Med* 2022; **386**: 128-137 [PMID: 34735046 DOI: 10.1056/NEJMoa2112299]

54 **Li SJ**, Ge Z, Kan J, Zhang JJ, Ye F, Kwan TW, Santoso T, Yang S, Sheiban I, Qian XS, Tian NL, Rab TS, Tao L, Chen SL. Cutoff Value and Long-Term Prediction of Clinical Events by FFR Measured Immediately After Implantation of a Drug-Eluting Stent in Patients With Coronary Artery Disease: 1- to 3-Year Results From the DKCRUSH VII Registry Study. *JACC Cardiovasc Interv* 2017; **10**: 986-995 [PMID: 28456699 DOI: 10.1016/j.jcin.2017.02.012]

55 **Hwang D**, Lee JM, Lee HJ, Kim SH, Nam CW, Hahn JY, Shin ES, Matsuo A, Tanaka N, Matsuo H, Lee SY, Doh JH, Koo BK. Influence of target vessel on prognostic relevance of fractional flow reserve after coronary stenting. *EuroIntervention* 2019; **15**: 457-464 [PMID: 30561367 DOI: 10.4244/EIJ-D-18-00913]

56 **Diletti R**, Masdjedi K, Daemen J, van Zandvoort LJC, Neleman T, Wilschut J, Den Dekker WK, van Bommel RJ, Lemmert M, Kardys I, Cummins P, de Jaegere P, Zijlstra F, Van Mieghem NM. Impact of Poststenting Fractional Flow Reserve on Long-Term Clinical Outcomes: The FFR-SEARCH Study. *Circ Cardiovasc Interv* 2021; **14**: e009681 [PMID: 33685214 DOI: 10.1161/CIRCINTERVENTIONS.120.009681]

57 **Jeger RV**, Eccleshall S, Wan Ahmad WA, Ge J, Poerner TC, Shin ES, Alfonso F, Latib A, Ong PJ, Rissanen TT, Saucedo J, Scheller B, Kleber FX; International DCB Consensus Group. Drug-Coated Balloons for Coronary Artery Disease: Third Report of the International DCB Consensus Group. *JACC Cardiovasc Interv* 2020; **13**: 1391-1402 [PMID: 32473887 DOI: 10.1016/j.jcin.2020.02.043]

58 **Michail M**, Thakur U, Mehta O, Ramzy JM, Comella A, Ihdayhid AR, Cameron JD, Nicholls SJ, Hoole SP, Brown AJ. Non-hyperaemic pressure ratios to guide percutaneous coronary intervention. *Open Heart* 2020; **7** [PMID: 33004619 DOI: 10.1136/openhrt-2020-001308]

59 **Sen S**, Escaned J, Malik IS, Mikhail GW, Foale RA, Mila R, Tarkin J, Petraco R, Broyd C, Jabbour R, Sethi A, Baker CS, Bellamy M, Al-Bustami M, Hackett D, Khan M, Lefroy D, Parker KH, Hughes AD, Francis DP, Di Mario C, Mayet J, Davies JE. Development and validation of a new adenosine-independent index of stenosis severity from coronary wave-intensity analysis: results of the ADVISE (ADenosine Vasodilator Independent Stenosis Evaluation) study. *J Am Coll Cardiol* 2012; **59**: 1392-1402 [PMID: 22154731 DOI: 10.1016/j.jacc.2011.11.003]

60 **Sen S**, Asrress KN, Nijjer S, Petraco R, Malik IS, Foale RA, Mikhail GW, Foin N, Broyd C, Hadjiloizou N, Sethi A, Al-Bustami M, Hackett D, Khan MA, Khawaja MZ, Baker CS, Bellamy M, Parker KH, Hughes AD, Francis DP, Mayet J, Di

Mario C, Escaned J, Redwood S, Davies JE. Diagnostic classification of the instantaneous wave-free ratio is equivalent to fractional flow reserve and is not improved with adenosine administration. Results of CLARIFY (Classification Accuracy of Pressure-Only Ratios Against Indices Using Flow Study). *J Am Coll Cardiol* 2013; **61**: 1409-1420 [PMID: 23500218 DOI: 10.1016/j.jacc.2013.01.034]

61 **Petraco R**, van de Hoef TP, Nijjer S, Sen S, van Lavieren MA, Foale RA, Meuwissen M, Broyd C, Echavarria-Pinto M, Foin N, Malik IS, Mikhail GW, Hughes AD, Francis DP, Mayet J, Di Mario C, Escaned J, Piek JJ, Davies JE. Baseline instantaneous wave-free ratio as a pressure-only estimation of underlying coronary flow reserve: results of the JUSTIFY-CFR Study (Joined Coronary Pressure and Flow Analysis to Determine Diagnostic Characteristics of Basal and Hyperemic Indices of Functional Lesion Severity-Coronary Flow Reserve). *Circ Cardiovasc Interv* 2014; **7**: 492-502 [PMID: 24987048 DOI: 10.1161/CIRCINTERVENTIONS.113.000926]

62 **Park JJ**, Petraco R, Nam CW, Doh JH, Davies J, Escaned J, Koo BK. Clinical validation of the resting pressure parameters in the assessment of functionally significant coronary stenosis; results of an independent, blinded comparison with fractional flow reserve. *Int J Cardiol* 2013; **168**: 4070-4075 [PMID: 23890849 DOI: 10.1016/j.ijcard.2013.07.030]

63 **Escaned J**, Echavarría-Pinto M, Garcia-Garcia HM, van de Hoef TP, de Vries T, Kaul P, Raveendran G, Altman JD, Kurz HI, Brechtken J, Tulli M, Von Birgelen C, Schneider JE, Khashaba AA, Jeremias A, Baucum J, Moreno R, Meuwissen M, Mishkel G, van Geuns RJ, Levite H, Lopez-Palop R, Mayhew M, Serruys PW, Samady H, Piek JJ, Lerman A; ADVISE II Study Group. Prospective Assessment of the Diagnostic Accuracy of Instantaneous Wave-Free Ratio to Assess Coronary Stenosis Relevance: Results of ADVISE II International, Multicenter Study (ADenosine Vasodilator Independent Stenosis Evaluation II). *JACC Cardiovasc Interv* 2015; **8**: 824-833 [PMID: 25999106 DOI: 10.1016/j.jcin.2015.01.029]

64 **Modi BN**, Rahman H, Kaier T, Ryan M, Williams R, Briceno N, Ellis H, Pavlidis A, Redwood S, Clapp B, Perera D. Revisiting the Optimal Fractional Flow Reserve and Instantaneous Wave-Free Ratio Thresholds for Predicting the Physiological Significance of Coronary Artery Disease. *Circ Cardiovasc Interv* 2018; **11**: e007041 [PMID: 30562079 DOI: 10.1161/CIRCINTERVENTIONS.118.007041]

65 **Berry C**, van 't Veer M, Witt N, Kala P, Bocek O, Pyxaras SA, McClure JD, Fearon WF, Barbato E, Tonino PA, De Bruyne B, Pijls NH, Oldroyd KG. VERIFY (VERification of Instantaneous Wave-Free Ratio and Fractional Flow Reserve for the Assessment of Coronary Artery Stenosis Severity in EverydaY Practice): a multicenter study in consecutive patients. *J Am Coll Cardiol* 2013; **61**: 1421-1427 [PMID: 23395076 DOI: 10.1016/j.jacc.2012.09.065]

66 **Svanerud J**, Ahn JM, Jeremias A, van 't Veer M, Gore A, Maehara A, Crowley A, Pijls NHJ, De Bruyne B, Johnson NP, Hennigan B, Watkins S, Berry C, Oldroyd KG, Park SJ, Ali ZA. Validation of a novel non-hyperaemic index of coronary artery stenosis severity: the Resting Full-cycle Ratio (VALIDATE RFR) study. *EuroIntervention* 2018; **14**: 806-814 [PMID: 29790478 DOI: 10.4244/EIJ-D-18-00342]

67 **Kumar G**, Desai R, Gore A, Rahim H, Maehara A, Matsumura M, Kirtane A, Jeremias A, Ali Z. Real world validation of the nonhyperemic index of coronary artery stenosis severity-Resting full-cycle ratio-RE-VALIDATE. *Catheter Cardiovasc Interv* 2020; **96**: E53-E58 [PMID: 31631521 DOI: 10.1002/ccd.28523]

68 **Ligthart J**, Masdjedi K, Witberg K, Mastik F, van Zandvoort L, Lemmert ME, Wilschut J, Diletti R, de Jaegere P, Zijlstra F, Kardys I, Van Mieghem NM, Daemen J. Validation of Resting Diastolic Pressure Ratio Calculated by a Novel Algorithm and Its Correlation With Distal Coronary Artery Pressure to Aortic Pressure, Instantaneous Wave-Free Ratio, and Fractional Flow Reserve. *Circ Cardiovasc Interv* 2018; **11**: e006911 [PMID: 30562091 DOI: 10.1161/CIRCINTERVENTIONS.118.006911]

69 **Johnson NP**, Li W, Chen X, Hennigan B, Watkins S, Berry C, Fearon WF, Oldroyd KG. Diastolic pressure ratio: new approach and validation vs. the instantaneous wave-free ratio. *Eur Heart J* 2019; **40**: 2585-2594 [PMID: 31329863 DOI: 10.1093/eurheartj/ehz230]

70 **Omori H**, Kawase Y, Mizukami T, Tanigaki T, Hirata T, Kikuchi J, Ota H, Sobue Y, Miyake T, Kawamura I, Okubo M, Kamiya H, Hirakawa A, Kawasaki M, Nakagawa M, Tsuchiya K, Suzuki Y, Ito T, Terashima M, Kondo T, Suzuki T, Escaned J, Matsuo H. Comparisons of Nonhyperemic Pressure Ratios: Predicting Functional Results of Coronary Revascularization Using Longitudinal Vessel Interrogation. *JACC Cardiovasc Interv* 2020; **13**: 2688-2698 [PMID: 33129819 DOI: 10.1016/j.jcin.2020.06.060]

71 **Versaci F**, Conte M, Van't Veer M, Lalancette S, Oldroyd K, Calcagno S, Biondi Zoccai G. A novel algorithm for the computation of the diastolic pressure ratio in the invasive assessment of the functional significance of coronary artery disease. *Panminerva Med* 2021; **63**: 206-213 [PMID: 34154320 DOI: 10.23736/S0031-0808.20.04202-0]

72 **De Maria GL**, Garcia-Garcia HM, Scarsini R, Hideo-Kajita A, Gonzalo López N, Leone AM, Sarno G, Daemen J, Shlofmitz E, Jeremias A, Tebaldi M, Bezerra HG, Tu S, Lemos PA, Ozaki Y, Dan K, Collet C, Banning AP, Barbato E, Johnson NP, Waksman R. Novel Indices of Coronary Physiology: Do We Need Alternatives to Fractional Flow Reserve? *Circ Cardiovasc Interv* 2020; **13**: e008487 [PMID: 32295416 DOI: 10.1161/CIRCINTERVENTIONS.119.008487]

73 **Lee JM**, Choi KH, Park J, Hwang D, Rhee TM, Kim J, Kim HY, Jung HW, Cho YK, Yoon HJ, Song YB, Hahn JY, Nam CW, Shin ES, Doh JH, Hur SH, Koo BK. Physiological and Clinical Assessment of Resting Physiological Indexes. *Circulation* 2019; **139**: 889-900 [PMID: 30586749 DOI: 10.1161/CIRCULATIONAHA.118.037021]

74 **Hidalgo F**, Gonzalez-Manzanares R, Ojeda S, Benito-González T, Gutiérrez-Barrios A, De la Torre Hernández JM, Minguito-Carazo C, Izaga-Torralba E, Cabrera-Rubio I, Flores-Vergara G, de Lezo JS, Romero-Moreno M, de Prado AP, Pan M. Instantaneous wave-free ratio for guiding treatment of nonculprit lesions in patients with acute coronary syndrome: A retrospective study. *Catheter Cardiovasc Interv* 2022; **99**: 489-496 [PMID: 34862839 DOI: 10.1002/ccd.30025]

75 **Nijjer SS**, Sen S, Petraco R, Mayet J, Francis DP, Davies JE. The Instantaneous wave-Free Ratio (iFR) pullback: a novel innovation using baseline physiology to optimise coronary angioplasty in tandem lesions. *Cardiovasc Revasc Med* 2015; **16**: 167-171 [PMID: 25977227 DOI: 10.1016/j.carrev.2015.01.006]

76 **Wolfrum M**, Fahrni G, de Maria GL, Knapp G, Curzen N, Kharbanda RK, Fröhlich GM, Banning AP. Impact of impaired fractional flow reserve after coronary interventions on outcomes: a systematic review and meta-analysis. *BMC Cardiovasc Disord* 2016; **16**: 177 [PMID: 27608682 DOI: 10.1186/s12872-016-0355-7]

77 **Neleman T**, van Zandvoort LJC, Tovar Forero MN, Masdjedi K, Ligthart JMR, Witberg KT, Groenland FTW, Cummins P, Lenzen MJ, Boersma E, Nuis RJ, den Dekker WK, Diletti R, Wilschut J, Zijlstra F, Van Mieghem NM, Daemen J. FFR-

Guided PCI Optimization Directed by High-Definition IVUS Versus Standard of Care: The FFR REACT Trial. *JACC Cardiovasc Interv* 2022; **15**: 1595-1607 [PMID: 35981832 DOI: 10.1016/j.jcin.2022.06.018]

78 **Park S**, Park SJ, Park DW. Percutaneous Coronary Intervention for Left Main Coronary Artery Disease: Present Status and Future Perspectives. *JACC Asia* 2022; **2**: 119-138 [PMID: 36339118 DOI: 10.1016/j.jacasi.2021.12.011]

79 **Tu S**, Westra J, Yang J, von Birgelen C, Ferrara A, Pellicano M, Nef H, Tebaldi M, Murasato Y, Lansky A, Barbato E, van der Heijden LC, Reiber JHC, Holm NR, Wijns W; FAVOR Pilot Trial Study Group. Diagnostic Accuracy of Fast Computational Approaches to Derive Fractional Flow Reserve From Diagnostic Coronary Angiography: The International Multicenter FAVOR Pilot Study. *JACC Cardiovasc Interv* 2016; **9**: 2024-2035 [PMID: 27712739 DOI: 10.1016/j.jcin.2016.07.013]

80 **Westra J**, Andersen BK, Campo G, Matsuo H, Koltowski L, Eftekhari A, Liu T, Di Serafino L, Di Girolamo D, Escaned J, Nef H, Naber C, Barbierato M, Tu S, Neghabat O, Madsen M, Tebaldi M, Tanigaki T, Kochman J, Somi S, Esposito G, Mercone G, Mejia-Renteria H, Ronco F, Bøtker HE, Wijns W, Christiansen EH, Holm NR. Diagnostic Performance of In-Procedure Angiography-Derived Quantitative Flow Reserve Compared to Pressure-Derived Fractional Flow Reserve: The FAVOR II Europe-Japan Study. *J Am Heart Assoc* 2018; **7** [PMID: 29980523 DOI: 10.1161/JAHA.118.009603]

81 **Kasinadhuni G**, Batta A, Gawalkar AA, Budakoty S, Gupta A, Vijayvergiya R. Validity and correlation of quantitative flow ratio with fractional flow reserve for assessment of intermediate coronary lesions. *Acta Cardiol* 2023; **78**: 91-98 [PMID: 35382706 DOI: 10.1080/00015385.2022.2059857]

82 **Cortés C**, Carrasco-Moraleja M, Aparisi A, Rodriguez-Gabella T, Campo A, Gutiérrez H, Julca F, Gómez I, San Román JA, Amat-Santos IJ. Quantitative flow ratio-Meta-analysis and systematic review. *Catheter Cardiovasc Interv* 2021; **97**: 807-814 [PMID: 32196932 DOI: 10.1002/ccd.28857]

83 **Hamaya R**, Hoshino M, Kanno Y, Yamaguchi M, Ohya H, Sumino Y, Kanaji Y, Usui E, Murai T, Lee T, Yonetsu T, Hirao K, Kakuta T. Prognostic implication of three-vessel contrast-flow quantitative flow ratio in patients with stable coronary artery disease. *EuroIntervention* 2019; **15**: 180-188 [PMID: 30686781 DOI: 10.4244/EIJ-D-18-00896]

84 **Masdjedi K**, van Zandvoort LJC, Balbi MM, Gijsen FJH, Ligthart JMR, Rutten MCM, Lemmert ME, Wilschut JM, Diletti R, de Jaegere P, Zijlstra F, Van Mieghem NM, Daemen J. Validation of a three-dimensional quantitative coronary angiography-based software to calculate fractional flow reserve: the FAST study. *EuroIntervention* 2020; **16**: 591-599 [PMID: 31085504 DOI: 10.4244/EIJ-D-19-00466]

85 **Andreini D**, Modolo R, Katagiri Y, Mushtaq S, Sonck J, Collet C, De Martini S, Roberto M, Tanaka K, Miyazaki Y, Czapla J, Schoors D, Plass A, Maisano F, Kaufmann P, Orry X, Metzdorf PA, Folliguet T, Färber G, Diamantis I, Schönweiß M, Bonalumi G, Guglielmo M, Ferrari C, Olivares P, Cavallotti L, Leal I, Lindeboom W, Onuma Y, Serruys PW, Bartorelli AL; SYNTAX III REVOLUTION Investigators. Impact of Fractional Flow Reserve Derived From Coronary Computed Tomography Angiography on Heart Team Treatment Decision-Making in Patients With Multivessel Coronary Artery Disease: Insights From the SYNTAX III REVOLUTION Trial. *Circ Cardiovasc Interv* 2019; **12**: e007607 [PMID: 31833413 DOI: 10.1161/CIRCINTERVENTIONS.118.007607]

86 **Serruys PW**, Hara H, Garg S, Kawashima H, Nørgaard BL, Dweck MR, Bax JJ, Knuuti J, Nieman K, Leipsic JA, Mushtaq S, Andreini D, Onuma Y. Coronary Computed Tomographic Angiography for Complete Assessment of Coronary Artery Disease: JACC State-of-the-Art Review. *J Am Coll Cardiol* 2021; **78**: 713-736 [PMID: 34384554 DOI: 10.1016/j.jacc.2021.06.019]

87 **Nørgaard BL**, Fairbairn TA, Safian RD, Rabbat MG, Ko B, Jensen JM, Nieman K, Chinnaiyan KM, Sand NP, Matsuo H, Leipsic J, Raff G. Coronary CT Angiography-derived Fractional Flow Reserve Testing in Patients with Stable Coronary Artery Disease: Recommendations on Interpretation and Reporting. *Radiol Cardiothorac Imaging* 2019; **1**: e190050 [PMID: 33778528 DOI: 10.1148/ryct.2019190050]

88 **Erbay A**, Penzel L, Abdelwahed YS, Klotsche J, Heuberger A, Schatz AS, Steiner J, Haghikia A, Sinning D, Fröhlich GM, Landmesser U, Stähli BE, Leistner DM. Prognostic Impact of Pancoronary Quantitative Flow Ratio Assessment in Patients Undergoing Percutaneous Coronary Intervention for Acute Coronary Syndromes. *Circ Cardiovasc Interv* 2021; **14**: e010698 [PMID: 34674555 DOI: 10.1161/CIRCINTERVENTIONS.121.010698]

World Journal of Clinical Cases

Submit a Manuscript: https://www.f6publishing.com

World J Clin Cases 2023 April 6; 11(10): 2140-2159

DOI: 10.12998/wjcc.v11.i10.2140

ISSN 2307-8960 (online)

REVIEW

Diagnosis, treatment protocols, and outcomes of liver transplant recipients infected with COVID-19

Mai Hashem, Mohamed El-Kassas

Specialty type: Medicine, research and experimental

Provenance and peer review: Invited article; Externally peer reviewed.

Peer-review model: Single blind

Peer-review report's scientific quality classification

Grade A (Excellent): 0
Grade B (Very good): 0
Grade C (Good): C, C
Grade D (Fair): 0
Grade E (Poor): 0

P-Reviewer: Koganti SB, United States; Swanson KJ, United States

Received: September 2, 2022
Peer-review started: September 2, 2022
First decision: January 5, 2023
Revised: January 20, 2023
Accepted: March 9, 2023
Article in press: March 9, 2023
Published online: April 6, 2023

Mai Hashem, Fellow of Tropical Medicine and Gastroenterology, Assiut University Hospital, Assiut 71515, Egypt

Mohamed El-Kassas, Department of Endemic Medicine, Faculty of Medicine, Helwan University, Cairo 11795, Egypt

Corresponding author: Mohamed El-Kassas, MD, Professor, Department of Endemic Medicine, Faculty of Medicine, Helwan University, Ain Helwan, Cairo 11795, Egypt.
m_elkassas@hq.helwan.edu.eg

Abstract

Several cases of fatal pneumonia during November 2019 were linked initially to severe acute respiratory syndrome coronavirus 2, which the World Health Organization later designated as coronavirus disease 2019 (COVID-19). The World Health Organization declared COVID-19 as a pandemic on March 11, 2020. In the general population, COVID-19 severity can range from asymptomatic/mild symptoms to seriously ill. Its mortality rate could be as high as 49%. The Centers for Disease Control and Prevention have acknowledged that people with specific underlying medical conditions, among those who need immunosuppression after solid organ transplantation (SOT), are at an increased risk of developing severe illness from COVID-19. Liver transplantation is the second most prevalent SOT globally. Due to their immunosuppressed state, liver transplant (LT) recipients are more susceptible to serious infections. Therefore, comorbidities and prolonged immunosuppression among SOT recipients enhance the likelihood of severe COVID-19. It is crucial to comprehend the clinical picture, immunosuppressive management, prognosis, and prophylaxis of COVID-19 infection because it may pose a danger to transplant recipients. This review described the clinical and laboratory findings of COVID-19 in LT recipients and the risk factors for severe disease in this population group. In the following sections, we discussed current COVID-19 therapy choices, reviewed standard practice in modifying immunosuppressant regimens, and outlined the safety and efficacy of currently licensed drugs for inpatient and outpatient management. Additionally, we explored the clinical outcomes of COVID-19 in LT recipients and mentioned the efficacy and safety of vaccination use.

Key Words: COVID-19; Liver transplantation; Recipient; Protocols; Outcomes

Core Tip: Liver transplant (LT) patients infected with severe acute respiratory syndrome coronavirus 2 have clinical, biochemical, and radiological features highly comparable to those of immunocompetent patients, except for a higher incidence of gastrointestinal symptoms. The prognosis of LT recipients is similar to non-LT patients and is not significantly affected by immunosuppression but rather by comorbidities. Considering the risk of organ rejection, it may not be wise to stop all immunosuppression after a coronavirus disease 2019 diagnosis. All LT recipients should be vaccinated, considering booster doses augment vaccination immunogenicity. Still, a considerable proportion of patients remain at risk for coronavirus disease 2019. Therefore, social isolation and other precautions must be maintained.

Citation: Hashem M, El-Kassas M. Diagnosis, treatment protocols, and outcomes of liver transplant recipients infected with COVID-19. *World J Clin Cases* 2023; 11(10): 2140-2159
URL: https://www.wjgnet.com/2307-8960/full/v11/i10/2140.htm
DOI: https://dx.doi.org/10.12998/wjcc.v11.i10.2140

INTRODUCTION

Several cases of serious pneumonia in November 2019 were initially linked to severe acute respiratory syndrome coronavirus 2 (SARS-CoV-2), which the World Health Organization later designated as coronavirus disease 2019 (COVID-19)[1]. The infection was first discovered in Wuhan, Hubei Province, China[2]. The World Health Organization declared COVID-19 as a pandemic on March 11, 2020[3]. As of July 2022, COVID-19 has caused more than 6.3 million fatalities and over 560 million documented cases worldwide[4]. In the general population, COVID-19 severity can range from asymptomatic/mild symptoms to seriously ill[3]. The mortality rate in some patient populations has been reported to be as high as 49%[5].

The Centers for Disease Control and Prevention (CDC) have acknowledged that people with specific underlying medical conditions such as cancer, chronic kidney disease, liver disease, chronic obstructive pulmonary disease, obesity, type 2 diabetes mellitus, serious heart conditions, respiratory diseases, and immunocompromised status, including those who need immunosuppression after solid organ transplantation (SOT), are at an increased risk for developing severe illness from COVID-19[6]. With a reported rate of 3.7 *per* million people, liver transplantation is the second most prevalent SOT globally, following kidney transplantation[7]. Due to their immunosuppressed state, recipients of SOT, especially liver transplant (LT) recipients, are more susceptible to serious infections[1]. Therefore, comorbidities and prolonged immunosuppression among SOT recipients may enhance the likelihood of severe COVID-19[8,9]. Additionally, LT cannot be postponed due to a greater waitlist mortality risk since SARS-CoV-2 can aggravate liver illness[10,11]. As a result, transplant centers have resumed SOT worldwide[11,12].

SARS-CoV-2, like other RNA respiratory viruses, can cause atypical and attenuated infection symptoms in immunosuppressed patients, frequently resulting in delayed presentations and missed diagnoses[13]. It is crucial to recognize COVID-19 infection in this population to guide immunosuppressive management, prognosis, and prophylaxis in this disease associated with high morbidity/mortality[14].

This review described the clinical and laboratory findings of COVID-19 in LT recipients and the risk factors for SARS-CoV-2 infection in those patients. We discussed current COVID-19 therapy choices, including a review of standard practice in modifying immunosuppressant regimens. Additionally, we outlined the safety and efficacy of the currently licensed drugs for inpatient and outpatient management of COVID-19 in LT recipients and the efficacy and safety of vaccination.

DIAGNOSIS OF SARS-COV-2

Reverse transcription PCR analysis of upper respiratory secretions, taken *via* nasopharyngeal swabs, is the current diagnostic test for COVID-19[15]. However, it exhibits substantial false negative rates[16]. In addition to identifying prior asymptomatic infection, serological assays for SARS-CoV-2 immunoglobulin G (IgG) and IgM antibodies can diagnose individuals with a negative reverse transcription PCR despite having COVID-like symptoms[17]. Staff performing COVID-19 testing should be aware of the various essential steps and protocols that help confirm a diagnosis of COVID-19. The best available kits are 75% sensitive and 95% specific, which is attributed to various factors, including collection method of collection, duration of illness, collection site, illness severity, and sampling skill. False-negative results from viral mutations cause new infection outbreaks due to insufficient identification of positive cases. These can be avoided by amplifying several regions of the virus genome to minimize the possibility of the probe and primer mismatch[18,19]. The highest positive results are in bronchoalveolar

lavage samples, sputum, nasopharyngeal swabs, and nasal swabs. The Cepheid GeneXpert platform, which qualitatively detects E and N protein genes in 45 min, can be used in emergency scenarios, such as liver transplantation for acute liver failure, where prompt viral detection results are required[18-20].

CLINICAL PICTURE

According to the CDC, clinical symptoms of COVID-19 include cough and dyspnea, along with at least two of the following: Fever, chills, muscle pain, headache, sore throat, and new loss of taste (dysgeusia) or smell (anosmia). There are also reports of diarrhea[8]. Most LT recipients have radiological evidence of COVID-19 on chest computed tomography (contrast or non-contrast) or X-rays and are symptomatic, with a possible impact of immunosuppressants[21-24]. Fever, cough, dyspnea, fatigue, and myalgia were the most frequently reported symptoms at the time of diagnosis, just like in the general population, with fever and cough being the two most frequently reported symptoms[25-29] and anosmia and dysgeusia the least reported[14]. A significant variation in the incidence of gastrointestinal symptoms in COVID-19 (ranging from 3% to 79%) has been reported[30], with rates between 5% and 15% in two large-scale studies[31,32]. Notably, gastrointestinal symptoms such as abdominal discomfort, diarrhea, nausea, and/or vomiting were more common in COVID-19 LT recipients[22,25,27,28,33], a piece of information that should be kept in mind when assessing LT patients at risk for SARS-CoV-2[21]. Table 1 reports the prevalence of COVID-19 symptoms among LT recipients, as reported in the literature.

LABORATORY

Although laboratory testing cannot confirm COVID-19 infection, it can help evaluate the severity and progression of the illness. Typically, severe systemic inflammation is manifested by lymphopenia, the neutrophil-to-lymphocyte ratio of ≥ 3.13, thrombocytopenia, elevated C-reactive protein (CRP), ferritin, D-dimer, and interleukin (IL)-6, and elevated liver enzymes in more severe disease, indicating liver affections[34-36]. Studies have shown that patients who needed mechanical ventilation had higher levels of procalcitonin and CRP and that procalcitonin levels were identified as a predictor of poor outcomes[37,38].

RISK FACTORS FOR SEVERE DISEASE IN LT RECIPIENTS WITH COVID-19

Comorbidities

The probability of more severe COVID-19 disease in SOT, including LT patients, is increased by their long-term immunosuppression and comorbidities[9,39]. Still, the outcomes after LTs at a transplant center in India were the same during the COVID-19 era and before its emergence[40]. Webb *et al*[33] showed in their multinational registry study that the mortality risk of COVID-19 participants was not significantly increased by LT (absolute risk difference: 1.4%, 95%CI: 7.7-10.4). The likelihood of developing severe COVID-19 and having a high mortality rate in the general population[31,41,42] and LT recipients[33] rises significantly with increasing age and comorbidities, including hypertension, type 2 diabetes, and obesity. Fraser *et al*[21] showed that LT recipient patients 60 years or older with COVID-19 had a 3-fold higher risk for COVID-19-related death than those younger than 60 and a 2-fold higher risk of mortality if diabetic. In contrast, a recent systematic review and meta-analysis showed that LT recipients with COVID-19 who were on immunosuppression drugs and had comorbidities were not significantly associated with severity and mortality. These comorbidities included diabetes, hypertension, cardiovascular diseases, chronic kidney disease, age > 60, the length of LT prior to the detection of COVID-19, and obesity. This was explained by the higher proportion of patients with mild illness in the included studies or the potential protective effects of immunosuppression in LT patients [43].

Cancer

A higher incidence of COVID-19 infection and a worse outcome were associated with having undergone a transplant for hepatocellular carcinoma or having an active malignancy at the time of COVID-19 diagnosis[22]. Chinese national reports, including more than 2000 confirmed cases of COVID-19 with a history of cancer, confirmed this finding[44,45].

Time from LT to the diagnosis of COVID-19

Data on the effect of the interval between LT and COVID-19 diagnosis on the disease severity and mortality are conflicting. As LT recipients are on higher doses of immunosuppression in the 1st year, which is slowly tapered as a maintenance dosage, it may contribute to an increase in viral load and a

Table 1 The prevalence of coronavirus disease 2019 symptoms among liver transplantation recipients, as reported in the literature, *n* (%)

Ref.	Country	Design	Number of LT	Fever	Cough	Dyspnea	GIT symptoms	Fatigue or myalgia	Anosmia or dysgeusia
Becchetti *et al* [22], 2020	Switzerland	Prospective, multicenter	57	44 (79)	31 (55)	26 (46)	18 (33)	32 (56)	4 (7)
Loinaz *et al* [27], 2020	Spain	Retrospective, single center	19	(57.9)	(84.2)	(47.4)	(31.0)	NA	NA
Lee *et al*[28], 2020	United States	Retrospective, single center	38	23 (61)	21 (55)	13 (34)	16 (42)	11 (29) or 9 (24)	1 (3)
Webb *et al* [33], 2020	United Kingdom	Retrospective, multinational registry study, multicenter	151	NA	114 (77) respiratory symptoms	NA	45 (30)	NA	NA
Belli *et al*[23], 2021	Europe	Retrospective, European registry, multicenter	243	190 (78)	143 (59)	82 (34)	55 (23)	90 (37)	21 (9)
Colmenero *et al*[24], 2021	Spain	Prospective, multicenter	111	83 (75)	78 (70)	46 (41)	38 (34)	NA	NA
Dumortier *et al*[25], 2021	France	Retrospective, nationwide registry, multicenter	91	55 (60)	51 (56)	45 (50)	25 (27)	28 (31)	9 (10)
Becchetti *et al* [2], 2021		Meta-analysis	1076	(61.4)	(58.6)	(36.2)	(27.9)	NA	NA
Kulkarni *et al* [11], 2021		Meta-analysis	994	494 (49.70)	435 (43.86)	291 (29.27)	271 (27.26)	NA	NA
Guarino *et al* [26], 2022	Italy	Prospective, double center	30	14 (46.66)	11 (36.66)	8 (26.66)	5 (16.66)	11 (36.66)	11 (36.66) or 10 (33.33)
Jadaun *et al* [29], 2022	India	Prospective, single center	81	52 (76.5)	35 (52.2)	17 (25.8)	7 (10.6)	NA	NA

Data expressed as *n* (%). GIT: Gastrointestinal tract; LT: Liver transplantation; NA: Not available.

delayed recovery from COVID-19 in the 1st year after LT. Secondly, the outcomes of LT recipients with COVID-19 can be adversely impacted by the increasing frequencies of comorbidities brought on by chronic immunosuppression[43].

Guarino *et al*[26] found that the asymptomatic group had a significantly shorter time from LT to COVID-19 diagnosis (8.62 years compared to 16.81 years in symptomatic patients) (P = 0.031). Several studies showed that the time between LT until SARS-CoV-2 infection does not affect the probability of developing severe COVID-19 or fatality[33,43,46]. On the contrary, data from the European Liver and Intestine Transplant Association/European LT Registry COVID-19 registry suggests that mortality increases in long-term LT recipients[47]. They have more frequent comorbidities such as hypertension and cardiovascular disease[2,48] and present more frequently with fever and dyspnea than short-term LT recipients. Risk factors for severe COVID-19 disease in LT recipients is shown in Figure 1.

COVID-19 TREATMENT IN LT RECIPIENTS

During the current pandemic, major international liver societies advised restricting LTs to patients with advanced hepatocellular carcinoma or high Model for End-Stage Liver Disease scores. According to the American Association for the Study of Liver Diseases, transplantation is not advised for LT candidates with active COVID-19 infection[49]. Treatment of COVID-19 relies on the understanding of its pathophysiology. In the early phase of COVID-19 infection, viral clearance occurs due to the immunological response. In the second phase, dysregulation of CD4+ T cells and activation of CD8+ T cells and macrophages may ensue, accompanied by a cytokine storm[50]. Immunomodulatory drugs could reduce this detrimental immune response, but this could increase the viral load and slow disease recovery.

Two approaches have been prioritized for the management of LT recipients infected with COVID-19: (1) Reducing or discontinuing immunosuppressive medications used to prevent allograft rejection; and (2) Using antiviral (such as remdesivir), anti-inflammatory (such as high-dose corticosteroids), and immunomodulatory therapies (such as tocilizumab), as indicated in general populations[14]. Immunosuppression management and its effect on COVID-19 outcomes present significant challenges

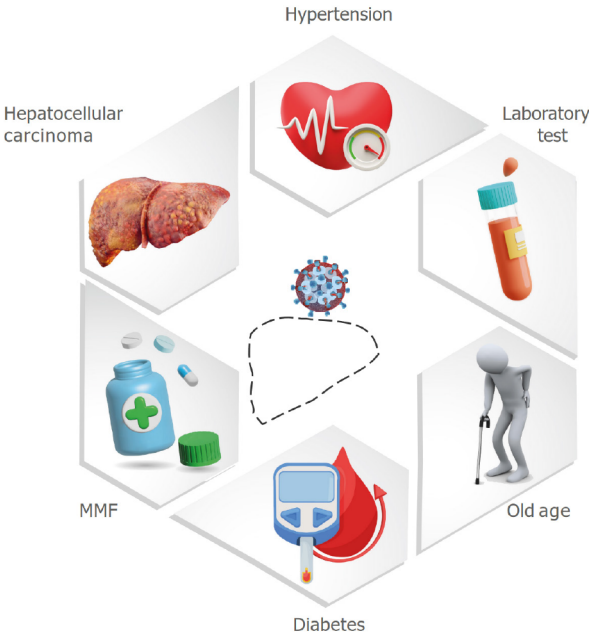

DOI: 10.12998/wjcc.v11.i10.2140

Figure 1 Risk factors for severe disease in liver transplantation recipients with coronavirus disease 2019. MMF: Mycophenolate mofetil.

[51]. Excessive immunosuppression might increase the viral load and postpone recovery, whereas a healthy immune system can worsen the condition[52]. The standard treatment for COVID-19 infection of different severity can be administered to LT recipients, albeit cautiously[53,54]. In most cases, it is advised to maintain immunosuppression, preferably the minimum effective regimen, to prevent rejection and aid recovery from COVID-19[55]. Systematic reviews and meta-analyses showed that the most commonly used immunosuppressant in LT recipients with COVID-19 were calcineurin inhibitors (CNI), followed by antimetabolites like mycophenolate mofetil (MMF), and finally corticosteroids. Unless there is a severe, progressing illness, the immunosuppression dosage should not be changed[11,21,56]. Management of liver transplantation recipients infected with COVID-19 is summarized in Figure 2.

CNIs

Tacrolimus-containing immunosuppression improved survival in LT patients with COVID-19[47]. Tacrolimus, and CNIs in general, can reduce human coronavirus replication *in vitro* by acting on the cyclophilin pathway[57]. By moderating T cell activation, CNIs may also reduce the harmful effects of the late COVID-19 inflammatory phase[52]. It is recommended to decrease but not stop CNI in LT recipients with COVID-19-related lymphopenia, fever, or deteriorating pulmonary status[58]. In patients with renal impairment, it is recommended to use a higher corticosteroid dose while reducing or stopping CNI until kidney functions are normalized[55].

Antimetabolites

MMF and SARS-CoV-2 may have a negative synergistic effect on reducing peripheral lymphocytes since both have a cytostatic effect on activated lymphocytes[59,60]. MMF therapy was an independent, dose-dependent predictor of a severe infection outcome. Until complete recovery from COVID-19, a dose reduction or momentary switch to everolimus or CNIs may be contemplated[46]. Lowering the dosage of azathioprine or mycophenolate should be considered when COVID-19-induced lymphopenia, fever, or worsening pneumonia are present[58].

Corticosteroids

Since most patients with severe COVID-19 have elevated levels of inflammatory mediators, corticosteroids have been advocated as an anti-inflammatory medication to prevent or reduce a systemic inflammatory response[61]. The National Institutes of Health discourages the routine use of systemic corticosteroids for the treatment of COVID-19 in hospitalized patients with COVID-19 who have undergone a transplant unless they are in the intensive care unit (ICU)[62]. Proper prednisone dose adjustment is required to prevent adrenal insufficiency[58]. Critically ill patients with COVID-19 who require oxygen therapy have better outcomes after receiving corticosteroids[63]. During active infection with COVID-19, reducing or discontinuing immunosuppressive medicines has not been shown to enhance the risk of rejection in LT recipients, as long as liver functions are followed up[48,64-66].

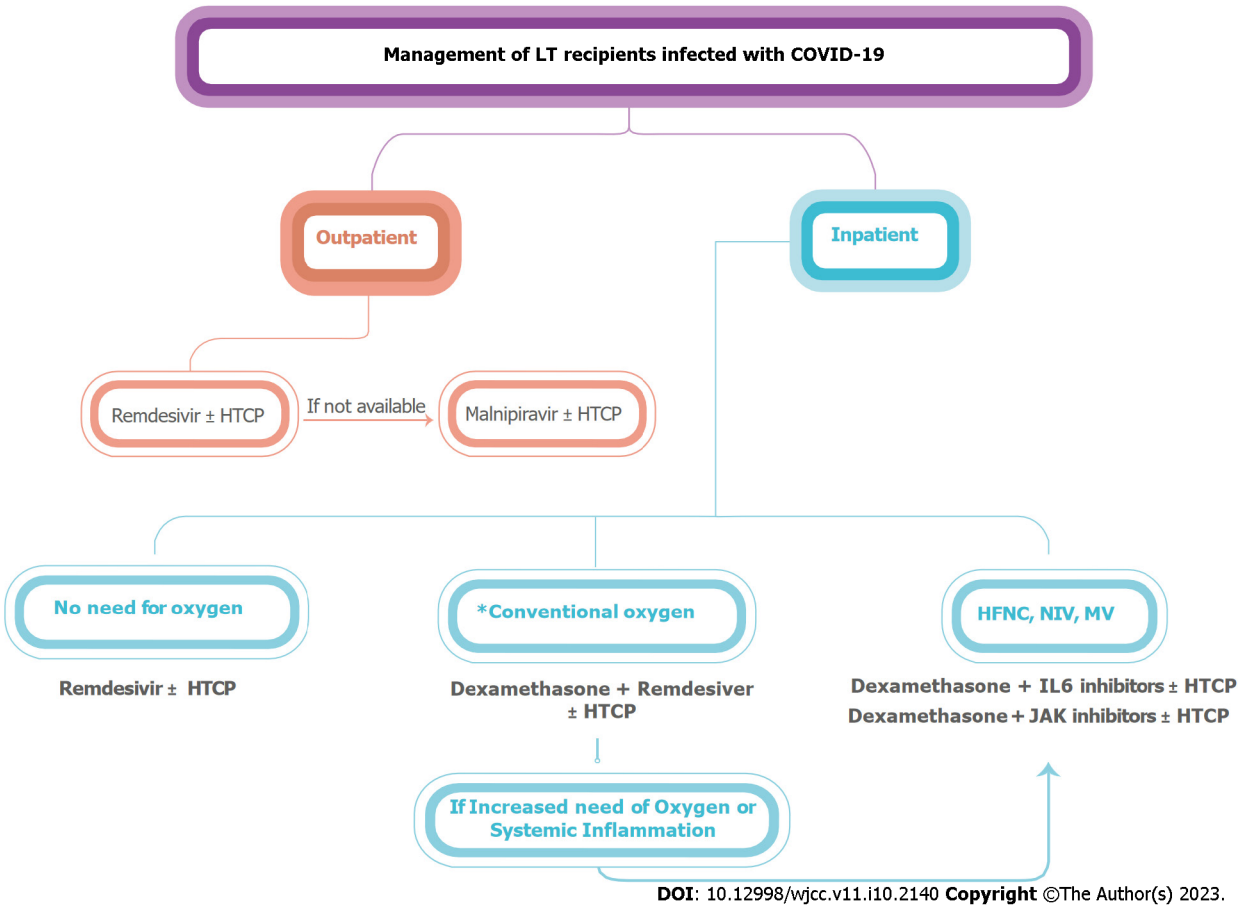

Figure 2 Management of liver transplantation recipients infected with coronavirus disease 2019. COVID-19: Coronavirus disease 2019; LT: Liver transplantation; HFNC: High flow nasal canula; HTCP: High-titer convalescent plasma; IL-6: Interleukin 6; JAK: Janus kinase; LT: Liver transplant; MV: Mechanical ventilation; NIV: Noninvasive ventilation.

OUTPATIENT MANAGEMENT OF COVID-19 IN LT PATIENTS

Hydroxychloroquine (HCQ) (with or without azithromycin), azithromycin alone, and lopinavir/ritonavir are treatments that have been proven ineffective or even hazardous[67].

Lopinavir/ritonavir

Protease inhibitors, mainly lopinavir/ritonavir, were considered effective against other coronaviruses, but no benefit was seen in a recently published clinical trial involving individuals with severe COVID-19[68].

Antimalarial agents

Chloroquine and HCQ were the cornerstones of treatment throughout the early days of the pandemic. They have antiviral activity against SARS-CoV-2 *in vitro*, and their immunomodulatory properties may decrease the host's inflammatory response[69]. Early observational data revealed that azithromycin might be helpful when added to HCQ[70]. However, HCQ with or without azithromycin did not improve clinical outcomes; instead, it increased adverse events, according to research including nearly 500 patients randomly assigned to receive either HCQ, HCQ with azithromycin, or the standard treatment[71]. In June 2020, the Food and Drug Administration (FDA) canceled its emergency use authorization (EUA) because of the significant number of controlled trials that failed to demonstrate any advantage from HCQ[71-75].

Ritonavir-boosted nirmatrelvir (paxlovid)

Nirmatrelvir is an orally administered protease inhibitor that blocks MPRO, a viral protease crucial to viral replication[76]. For optimal pharmacokinetic performance, nirmatrelvir is combined with ritonavir (in the form of paxlovid), a potent inhibitor of cytochrome P450 3A4. To achieve therapeutic concentrations of nirmatrelvir, coadministration of ritonavir is necessary. On December 22, 2021, the FDA approved nirmatrelvir with ritonavir as an emergency therapy for COVID-19[77].

All human-infecting coronaviruses have been shown to be susceptible to its antiviral effects[78]. Despite the absence of clinical efficacy data, it is anticipated that ritonavir-boosted nirmatrelvir will be efficacious against all omicron subvariants[79-81].

A 5-d regimen of ritonavir-boosted nirmatrelvir is one of the preferred treatments for mild to moderate COVID-19 among outpatients at risk of disease progression. During treatment and for ≥ 3 d after ritonavir is ended, ritonavir may raise concentrations of some concurrent medicines, including CNIs and the mammalian target of rapamycin (mTOR) inhibitors. Significant elevations in the concentrations of these medications may result in severe and occasionally fatal drug toxicity[82]. Anti-SARS-CoV-2 monoclonal antibodies or remdesivir are recommended as first-line therapy for nonhospitalized transplant patients who are also on CNIs or mTOR inhibitors for antirejection. If these medications are unavailable, ritonavir-boosted nirmatrelvir may be administered cautiously, with thorough patient monitoring and transplant specialist consultation[83].

Until sufficient data are available to determine the optimum dose, the EUA advises against ritonavir-boosted nirmatrelvir for patients with an estimated glomerular filtration rate of < 30 mL/min[77] and those with significant hepatic impairment (Child-Pugh Class C) and to be taken with caution in patients with pre-existing liver disorders, liver enzyme abnormalities, or hepatitis[82].

Compared to a placebo in the EPIC-HR study, ritonavir-boosted nirmatrelvir significantly decreased the risk of hospitalization or mortality by 88% in unvaccinated, nonhospitalized persons with laboratory-confirmed SARS-CoV-2 infection[77,84]. This outcome is similar to that seen in similar patient populations for remdesivir (87% relative reduction)[85] and better than that seen for molnupiravir (31% relative reduction)[86].

Molnupiravir

Molnupiravir is the oral prodrug of beta-D-N4-deoxycytidine, a ribonucleoside with antiviral activity *in vitro* and clinical trials against SARS-CoV-2[87,88]. When viral RNA-dependent RNA polymerases integrate beta-D-N4-deoxycytidine, it leads to mutations in the virus and lethal mutagenesis[89,90]. The FDA approved an EUA for molnupiravir on December 23, 2021 to treat adults with mild to moderate COVID-19 within 5 d of symptom onset, who are at high risk of progressing to severe disease and for whom alternative antiviral treatments are not available or clinically acceptable[91,92]. Molnupiravir is effective against omicron subvariants, as shown by *in vitro* and animal trials[81,88,93,94].

In the pre-omicron era, the MOVe-OUT trial found that compared to a placebo, molnupiravir reduced the rate of hospitalization or death by 31% among nonhospitalized adults who were unvaccinated and at high risk of progression to severe disease[77,86]. A subset of patients who received molnupiravir in the MOVe-OUT trial and subsequently required hospitalization had a lower likelihood of requiring respiratory interventions than those who got a placebo[95]. When ritonavir-boosted nirmatrelvir and remdesivir are not accessible, feasible, or clinically acceptable, the COVID-19 Treatment Guidelines recommend using molnupiravir orally for 5 d as an alternate therapy in nonhospitalized adult patients with mild to moderate COVID-19 who are at high risk of disease progression. After the onset of symptoms, treatment should begin as soon as feasible and no later than 5 d[82]. Molnupiravir therapy should be continued for the entire 5 d. Whether a shorter course of treatment results in poorer efficacy or is linked to the development of molnupiravir-resistant mutations remains unanswered. The whole course of molnupiravir treatment can be completed even if hospitalization is necessary during treatment [82].

Anti-SARS-CoV-2 monoclonal antibodies

Monoclonal antibodies (MABs), one of the weapons in the arsenal against COVID-19, block the virus' ability to attach to the angiotensin-converting enzyme receptor on host cells and impede internalization [96]. The FDA has granted EUAs for several anti-SARS-CoV-2 MABs for the treatment of COVID-19 and post-exposure prophylaxis[97-99].

Treatment of mild to moderate COVID-19

Antibodies against SARS-CoV-2 are now approved for treating mild to moderate COVID-19 and post-exposure prophylaxis, and SOT recipients are included[100]. As of October 2021, the FDA EUA has authorized casirivimab-imdevimab, bamlanivimab-etesevimab, and sotrovimab for the treatment of outpatients diagnosed with mild to moderate COVID-19 and are at high risk of developing a severe illness or requiring hospitalization. Once positive results of the SARS-CoV-2 antigen or nucleic acid amplification test are obtained, and no later than 10 d after the onset of symptoms, treatment with MABs should be initiated[100]. When administered early in the course of COVID-19 (median 4 d after the beginning of symptoms), MABs reduce hospitalization and mortality by 70% as well as the viral load[101-103]. MABs appear more effective in patients with high viral loads[103] but ineffective in hospitalized patients with severe COVID-19[104].

The use of MABs in SOT recipients was related to a low incidence of emergency department visits, hospitalizations, mechanical breathing, and the need for intensive care, and fatality was observed over a 28-30-d post-infusion follow-up period. A further decreased incidence of subsequent emergency department visits or hospitalization was linked to early MAB delivery (4 d *vs* 6 d)[105]. Casirivimab-imdevimab was used to treat COVID-19 in 25 SOT recipients; none suffered worsening symptoms or

needed to be hospitalized[105]. The use of MAB (75.3% bamlanivimab) for the treatment of COVID-19 in 73 SOT recipients was described in a retrospective analysis by Yetmar *et al*[106]. Of these patients, 12.3% were hospitalized, although none required intubation, died, or had rejection. Since the appearance of the omicron variant in December 2021, most of the previously available MABs have shown drastically reduced activity, except for sotrovimab, which is effective against omicron BA.1 and BA.1.1 subvariants, in addition to previous variants. However, it is less effective against the BA.2 subvariant[107].

Bebtelovimab, which was found to be effective against omicron BA.1, BA.1.1, and BA.2 subvariants, was granted an EUA by the United States FDA in February 2022[108] and revoked in November 2022 because it was not expected to neutralize omicron subvariants BQ.1 and BQ.1.1[109].

Post-exposure prophylaxis

FDA EUA permits the utilization of casirivimab-imdevimab and bamlanivimab-etesevimab for post-exposure prophylaxis as of October 2021. In high-risk exposure, an incomplete vaccination schedule or an insufficient immunological response to complete vaccination, as observed in immunocompromised persons, are indicators for post-exposure prophylaxis administration. For optimum response, the administration should be within 7 d[100]. No major transfusion-related adverse events were observed after the administration of MABs in SOT recipients. This includes no cases of acute allograft rejection, overreactions to the immune system, or anaphylaxis. Preliminary findings suggest promising outcomes, such as a reduction in COVID-19-related hospitalizations and deaths[100]. The likelihood of emerging resistant strains may increase in immunocompromised people with a higher viral burden. This danger may be reduced with the timely and appropriate administration of these MABs[100].

INPATIENT MANAGEMENT OF COVID-19 IN LT PATIENTS

Remdesivir

Remdesivir is a nucleoside analog that showed anti-SARS-CoV-2 activity in human cell lines[110]. On October 22, 2020, the FDA approved remdesivir for treatment in adult and pediatric patients with COVID-19 who require hospitalization and are > 12-years-old and > 40 kg[58]. It appears to be most efficient when administered to individuals on oxygen within 10 d of the onset of symptoms, even if no mortality advantage has been shown. It also tends to minimize the length of illness and hospitalization [111]. Hospitalized patients with liver illnesses or LT recipients who need supplemental oxygen and have COVID-19 should get remdesivir for 5 d. However, if their condition worsens and they require mechanical ventilation, it should not be given[58]. Both patients and healthy volunteers who were given remdesivir showed increased levels of amino transaminases after taking the drug. Liver biochemistry should be checked before starting remdesivir and then regularly throughout treatment; if any tests show elevations > 10 × upper limit of normal or indicate liver inflammation, the medicine should be stopped [58].

Dexamethasone

Hospitalized COVID-19 patients who need supplemental oxygen have a lower death rate when dexamethasone is administered at a dose of 6 mg *per* day for up to 10 d[63]. People who needed mechanical ventilation benefited the most, patients who did not need supplemental oxygen had a deteriorating tendency, and patients who had been experiencing their symptoms for longer than 7 d did not benefit. In the absence of dexamethasone, an alternate corticosteroid in a comparable dosage may be used[58]. Besides oxygenation, particular biochemical markers may be relevant in evaluating who may benefit from corticosteroids. Although Keller *et al*[112] found no association between steroid use and overall mortality benefit, they found a substantial reduction in mortality risk in individuals whose baseline CRP was greater than 20 mg/dL (odds ratio: 0.23; 95%CI: 0.08-0.70).

IL-6 inhibitors (tocilizumab, sarilumab)

The FDA has authorized the use of the IL-6 inhibitors tocilizumab and sarilumab to treat autoimmune disorders and chimeric antigen receptor T cell driven cytokine release syndrome. Evidence from case series published during the early stages of the COVID-19 pandemic revealed that suppressing the inflammatory state experienced by some COVID-19 patients by blocking IL-6 could improve their prognoses[113]. Contradictory results were reported in randomized studies. In general, patients with recent (within 24 h) or imminent requirements for mechanical ventilation and raised inflammatory markers (CRP levels > 75 mg/L) may benefit from the addition of tocilizumab to dexamethasone (limited data available for sarilumab)[114,115]. Tocilizumab may help certain patients whose conditions are rapidly deteriorating and who are already receiving corticosteroids, but there is insufficient data to make any recommendations regarding its usage in patients with liver disease or SOT at this time[58].

Baricitinab

Baricitinab is an FDA-approved Janus kinase inhibitor for treating refractory rheumatoid arthritis. In

patients with COVID-19, kinase inhibitors reduce inflammation, which may aggravate organ dysfunction, and may have direct antiviral activities[58]. In the ACTT-2 trial, hospitalized COVID-19 patients received baricitinib + remdesivir or remdesivir alone. Baricitinib-treated patients recovered faster, especially those on high-flow oxygen or noninvasive ventilation. No mortality benefit was observed, and total mortality was low[116]. Baricitinib may be an option for individuals with liver disease or transplant recipients who are intolerant to corticosteroids and yet fulfill their requirements [58].

Convalescent plasma

Neutralizing antibodies are detectable in the sera of people who have recovered from the infection, as evidenced by earlier coronavirus outbreaks[117]. Passive antibody therapy using convalescent plasma is another potential treatment for COVID-19, acting by viral neutralization[118]. Recent evidence showed that individuals who received plasma early in their illness had a much lower 30-d mortality rate[119]. In addition, the mortality rate was lower for patients who were given plasma with higher antibody levels than those who were given plasma with lower antibody levels. Accordingly, the FDA issued an EUA for convalescent plasma for hospitalized COVID-19 patients on August 23, 2020 and updated it on February 3, 2021 to exclude low-titer plasma[58]. Subsequently, the EUA was updated. The present EUA restricts convalescent plasma products containing high levels of anti-SARS-CoV-2 antibodies to patients with COVID-19 who have an immunosuppressive condition or are receiving immunosuppressive therapy. This restriction applies to both inpatients and outpatients[82].

A Chinese randomized trial found a trend toward clinical improvement with plasma therapy (51.9% *vs* 43.1%) but failed to reach statistical significance ($P = 0.26$), presumably because of underpowering as the study was terminated early due to a decline in COVID-19 cases in China[120]. Data from 804 patients with COVID-19 from randomized controlled trials, matched control studies, and case series were combined and analyzed. Results demonstrated that patients who received plasma had a significantly lower risk of death than those who received standard care (13% *vs* 25%; $P < 0.001$)[121].

Nonetheless, despite these optimistic preliminary results, a recent randomized trial of 464 patients with moderate COVID-19 and given convalescent plasma showed no improvement in mortality or illness progression[122]. Hospitalized patients with liver illness or LT recipients rarely benefit from receiving convalescent plasma[58]. Using high-titer plasma in patients with recent symptoms, mild disease, and risk factors for a progressive disease may be beneficial[122-124].

CLINICAL OUTCOMES IN LT RECIPIENTS WITH COVID-19

Infection rate

SARS-CoV-2 infection rates are lower among LT patients than among other solid organ recipients. Heart and lung transplant recipients tend to have the highest risk of infection, while LT recipients appear to have the lowest risk[125,126].

Hospitalization rate

Despite having a similar need for ICU care, ventilatory support, and severe COVID-19 infection, when compared to the general population, LT patients infected with COVID-19 were reportedly more frequently hospitalized (at a rate ranging from 71.0% to 86.5%)[28,33,46,125], which may be ascribed to safety precautions[127,128], especially if they have additional risk factors for a more severe COVID-19 course like hypertension, diabetes, or obesity[129]. Guarino *et al*[26], on the other side, reported a significantly lower rate of hospitalization, 16.66%, attributing this discrepancy to the period of COVID-19 infection during which the study was enrolled. This was during the second pandemic wave (from September 2020 to January 2021), when expertise and skills in managing infections in immunosuppressed patients improved, indicating a better understanding of patients and less worry among clinicians about the potential effects of the COVID-19 disease course on LT recipients.

Mortality rates

In the general population of Wuhan, China, the COVID-19 mortality rate was first reported to be 1.4% [130]. Mortality increased considerably among hospitalized patients (10.0%)[38] and ICU patients (26.0%)[131]. The mortality rate of SARS-CoV-2 infection in the LT cohort reported by literature ranges from 12.0% to 22.3%. Webb *et al*[33] and Colmenero *et al*[24] reported 19% and 18% mortality rates, respectively, which were lower than matched control groups. The estimated mortality rate reported on 57 LT recipients in a European cohort was 12% (95%CI: 5%-24%), which increased to 17% (95%CI: 7%-32%) among hospitalized patients[22].

Ravanan *et al*[126] conducted a comparative study between patients waitlisted for transplants and SOT recipients and described a mortality rate of 20.3% among LT recipients, which was lower than reported by other SOT. The highest mortality rates were reported in heart and lung transplant recipients. Heart transplant recipients reported an overall mortality rate of 15%-33% and a rate of 25%-41% among hospitalized patients, according to data from four studies with small sample sizes (13-28

patients)[132-135]. This was supported by Trapani *et al*[125], who found that the liver is more resistant to COVID-19 infection than other organs and has a lower mortality rate (15.7%) with mortality rates of 35.8% and 40.0% for heart and lung transplant recipients, respectively. They hypothesized that immunosuppressive therapy of LT recipients was milder than usual, and they had a higher immune tolerance than other SOT recipients[125]. Data from an Italian transplant center in Lombardy showed a remarkably low mortality rate among LT recipients with COVID-19, primarily related to metabolic syndrome comorbidities[48].

Kidney transplant recipients infected with COVID-19 have higher hospitalization rates and mortality rates when compared to LT recipients. This is attributed to chronic immunosuppression together with associated comorbidities[136,137]. Estimated mortality rates in liver transplantation recipients with COVID-19 in the literature are shown in Table 2.

IMMUNIZATION

Since the COVID-19 pandemic started, an excellent program of vaccine research, testing, approval, and wide-scale dissemination has been implemented using a variety of platforms, including mRNA (Pfizer/BioNTech BNT162B1/2 and Moderna mRNA-1273), replication-deficient adenovirus (Oxford AstraZeneca ChAdOx1-S-nCoV and Janssen, Ad26.COV2.S), recombinant adenovirus (Gamaleya, GamCOVIDVac), and inactivated virus (Sinovac, CoronaVac/PiCoVac)[138]. Vaccination is a crucial way to avoid getting SARS-CoV-2 and a severe illness. Early vaccine trials for COVID-19 in the general population were very effective, with reported response rates of 95% for BNT162b2 and 94% for mRNA-1273. However, these trials did not include people taking immunosuppressant drugs[39,139,140]. On the other hand, Ad26.COV2.S recombinant adenovirus vaccine prevented moderate to severe-critical COVID-19 in the general population by 66.1%, excluding people on immunosuppression[141].

The health authorities of numerous countries have prioritized SOT recipients for vaccination with mRNA vaccines. Antirejection drugs inhibit T cell activation, interact with antigen-presenting cells, and reduce B cell memory responses in SOT recipients, making SARS-CoV-2 vaccines less effective in this population[142-144]. In addition to diminished vaccine efficiency, considerably lower anti-spike IgG antibodies have been found in completely vaccinated liver, kidney, heart, and lung transplant recipients following mRNA vaccination[145-148]. While measuring humoral immune response as a surrogate marker for vaccine effectiveness has received significant attention, the clinical endpoints, such as immunity to SARS-CoV-2 infection and severe/acute disease, are the most critical outcomes. Outcomes were explicitly examined in COVID-19 vaccine studies in the general population but not in immunosuppressed patients[139-141].

Ignoring cellular immunity is one way in which antibody measurements alone may not fully predict clinical protection from SARS-CoV-2 vaccination. Studies showed that SOT recipients had worse cellular immunity after SARS-CoV-2 immunization than healthy controls[120,121]. In the same studies, cellular and humoral immune responses did not correlate; some patients had a solid cellular response but no humoral response. The role of T cells in vaccinations is poorly understood due to a paucity of commercially available tests[149].

Furian *et al*[150] identified a link between anti-SARS-CoV-2 antibody production and T cell responses in kidney and LT recipients after SARS-CoV-2 vaccination. Patients with antibody seroconversion had more significant amounts of interferon (IFN)-producing T cells. These findings support earlier research [151,152]. However, they found serological converts who did not have anti-SARS-CoV-2 IFN-γ T cell responses[150]. This supports the concept that anti-SARS-CoV-2 antibody production is at least partially independent of T cells[153]. Oddly, immunosuppression impacted anti-SARS-CoV-2 IFN-γ T cell responses more negatively than antibody production[150]. Severe cases of COVID-19 have also been reported in transplant recipients who had received two doses of the vaccine[154]. Due to concerns regarding insufficient protection with a two-dose series, extra vaccination doses have been observed to improve antibody response for SOT recipients[155,156]. Based on these findings, the FDA allowed a third vaccination dosage for immunocompromised people on August 12, 2021, and the CDC revised their recommendations consequently[157].

Moreover, the CDC proposed a fourth booster dose 3 mo after the original series, but only some real-world data support this. In comparison to the placebo, the third dosage of the mRNA vaccine was considered safe among 60/120 adult SOT recipients and was linked to higher levels of specific T cells (432 *vs* 67 cells *per* 106 CD4+ T cells), median virus neutralization (71% *vs* 13%), and anti-receptor-binding domain antibodies of at least 100 U/mL in more patients (55% *vs* 18%)[158]. These results suggest that even a third vaccination dose is insufficient to protect SOT recipients from COVID-19. Therefore, further measures will be required to safeguard these vulnerable patients against COVID-19. This can entail passive immunization and/or reducing immunosuppression in some patients[100].

Tu *et al*[159] attempted to assess the effectiveness and safety of COVID-19-inactivated vaccinations in LT patients. The immunological response to the inactivated COVID-19 vaccination is markedly suboptimal. The predictors of negative antibody response were a shorter duration post-LT, the usage of a mycophenolate acid derivative, and IL-2R activation during LT. However, no serious adverse

Table 2 Estimated mortality rates in liver transplantation recipients with coronavirus disease 2019 in the literature, *n* (%)

Ref.	Design	Origin	LT recipients with COVID-19	Mortality rate
Becchetti *et al*[22], 2020	Prospective, multicenter	Europe	57	7 (12.0)
Lee *et al*[28], 2020	Retrospective, single center	United States	38	7 (18.0)
Bhoori *et al*[48], 2020	Single center cohort study	Italy	111	3 (3.0)
Rabiee *et al*[66], 2020	Retrospective, multicenter	United States	112	25 (22.3)
Webb *et al*[33], 2020	Retrospective, multinational registry study, multicenter	International	151	28 (19.0)
Agnes *et al*[136], 2020	National survey, multicenter	Italy	24	5 (21.0)
Fraser *et al*[21], 2020	Systematic review and quantitative analysis	Europe	233	43 (19.3)
Ravanan *et al*[126], 2020	Multicenter national cohort study	United Kingdom	64	13 (20.3)
Loinaz *et al*[27], 2020	Retrospective, single center	Spain	19	2 (10.5)
Trapani *et al*[125], 2021	Nationwide population-based study	Italy	89	14 (15.7)
Belli *et al*[23], 2021	Retrospective, European registry, multicenter	Europe	243	49 (20.1)
Colmenero *et al*[24], 2021	Prospective, multicenter	Spain	111	20 (18.0)
Dumortier *et al*[25], 2021	Retrospective, nationwide registry, multicenter	France	91	19 (20.0)
Raszeja-Wyszomirska *et al*[137], 2021	Prospective, single center	Poland	81	2 (2.5)
Guarino *et al*[26], 2022	Prospective, double center	Italy	30	2 (6.7)

COVID-19: Coronavirus disease 2019; LT: Liver transplantation; NA: Not available.

reactions to the inactivated vaccination or graft rejection were reported. Therefore, they concluded that LT recipients need booster vaccination[159]. Despite limited evidence, the American Association for the Study of Liver Diseases and European Association for the Study of the Liver advise vaccinating LT patients 3 mo after transplantation[160,161].

PRE-EXPOSURE PROPHYLAXIS

The FDA has authorized the long-acting combination MABs tixagevimab-cilgavimab (EVUSHELD™) for pre-exposure prophylaxis to prevent COVID-19 in December 2021. In the United States, this agent is the only one to have received an EUA for this use[107]. Those who are not likely to produce an effective immune response to vaccination may nevertheless benefit from this medication's protective effects, such as those who are immunocompromised due to a medical condition or immunosuppressive medication, as well as those for whom COVID-19 vaccination is not recommended due to a history of severe adverse reaction to COVID-19 vaccine[162].

However, it is currently unknown whether tixagevimab/cilgavimab is effective in preventing COVID-19 in SOT recipients. The combination is more effective than either tixagevimab or cilgavimab alone against omicron, and it appears to be more effective *in vitro* against BA.2 than against BA.1 or BA.1.1 subvariants[163].

CONCLUSION

LT patients with SARS-CoV-2 infection have clinical, biochemical, and radiological features that are highly comparable to those of immunocompetent patients, except for a higher incidence of gastrointestinal symptoms. Particular focus should be given to gastrointestinal symptoms as a diagnostic indicator for COVID-19 among LT patients, even in the absence of fever or respiratory symptoms. Even if the risk of infection appears to be considered after an LT, alterations in innate and adaptive immunity induced by immunosuppressants cause the severity of COVID-19 to remain low. The prognosis of LT recipients is similar to non-LT patients and is not affected by immunosuppression but rather by comorbidities. Considering the risk of organ rejection, it may not be wise to stop all

immunosuppression after a COVID-19 diagnosis. However, depending on the severity of the disease, MMF may be withdrawn or substituted from an immunosuppressive regimen with CNIs or mTOR inhibitors in some selected LT patients with COVID-19. All LT recipients should be vaccinated. The administration of a booster dose considerably enhances the vaccine's immunogenicity. However, many patients continue to be at risk for COVID-19. Consequently, social isolation and other protective measures must be maintained for these individuals.

FOOTNOTES

Author contributions: Hashem M, and El-Kassas M contributed to the conception and design of the work, literature review, drafting and critical revision, editing, and approval of the final version of the manuscript.

Conflict-of-interest statement: The authors report no relevant conflicts of interest for this article.

Country/Territory of origin: Egypt

ORCID number: Mohamed El-Kassas 0000-0002-3396-6894.

S-Editor: Liu GL
L-Editor: Filipodia
P-Editor: Liu GL

REFERENCES

1 **Gagliotti C**, Morsillo F, Moro ML, Masiero L, Procaccio F, Vespasiano F, Pantosti A, Monaco M, Errico G, Ricci A, Grossi P, Nanni Costa A; SInT Collaborative Study Group. Infections in liver and lung transplant recipients: a national prospective cohort. *Eur J Clin Microbiol Infect Dis* 2018; **37**: 399-407 [PMID: 29380226 DOI: 10.1007/s10096-018-3183-0]
2 **Becchetti C**, Gschwend SG, Dufour JF, Banz V. COVID-19 in Liver Transplant Recipients: A Systematic Review. *J Clin Med* 2021; **10** [PMID: 34501463 DOI: 10.3390/jcm10174015]
3 **World Health Organization**. WHO Director-General's opening remarks at the media briefing on COVID-19. [Internet] [cited 11 March 2020]. Available from: https:// www.who.int/director-general/speeches/detail/who-director-general-sopening-remarks-at-the-media-briefing-on-covid-19---11-march-2020
4 COVID Live - Coronavirus Statistics - Worldometer. [Internet] [cited 29 January 2020]. Available from: https:// www.worldometers.info/coronavirus/
5 **Onder G**, Rezza G, Brusaferro S. Case-Fatality Rate and Characteristics of Patients Dying in Relation to COVID-19 in Italy. *JAMA* 2020; **323**: 1775-1776 [PMID: 32203977 DOI: 10.1001/jama.2020.4683]
6 **Centers for Disease Control and Prevention**. People with certain medical conditions. Available from: https:// www.cdc.gov/coronavirus/2019-ncov/need-extra-precautions/people-with-medical-conditions.html
7 **Carmona M**, Álvarez M, Marco J, Mahíllo B, Domínguez-Gil B, Núñez JR, Matesanz R. Global Organ Transplant Activities in 2015. Data from the Global Observatory on Donation and Transplantation (GODT). *Transplantation* 2017; **101**: S29 [DOI: 10.1097/01.tp.0000525015.43613.75]
8 **Azzi Y**, Bartash R, Scalea J, Loarte-Campos P, Akalin E. COVID-19 and Solid Organ Transplantation: A Review Article. *Transplantation* 2021; **105**: 37-55 [PMID: 33148977 DOI: 10.1097/TP.0000000000003523]
9 **Elias M**, Pievani D, Randoux C, Louis K, Denis B, Delion A, Le Goff O, Antoine C, Greze C, Pillebout E, Abboud I, Glotz D, Daugas E, Lefaucheur C. COVID-19 Infection in Kidney Transplant Recipients: Disease Incidence and Clinical Outcomes. *J Am Soc Nephrol* 2020; **31**: 2413-2423 [PMID: 32847984 DOI: 10.1681/ASN.2020050639]
10 **Kumar P**, Sharma M, Sulthana SF, Kulkarni A, Rao PN, Reddy DN. Severe Acute Respiratory Syndrome Coronavirus 2-related Acute-on-chronic Liver Failure. *J Clin Exp Hepatol* 2021; **11**: 404-406 [PMID: 33398222 DOI: 10.1016/j.jceh.2020.12.007]
11 **Kulkarni AV**, Tevethia HV, Premkumar M, Arab JP, Candia R, Kumar K, Kumar P, Sharma M, Rao PN, Reddy DN. Impact of COVID-19 on liver transplant recipients-A systematic review and meta-analysis. *EClinicalMedicine* 2021; **38**: 101025 [PMID: 34278287 DOI: 10.1016/j.eclinm.2021.101025]
12 **Thorburn D**, Taylor R, Whitney J, Adair A, Attia M, Gibbs P, Grammatikopoulos T, Isaac JR, Masson S, Marshall A, Mirza DF, Prachalias A, Watson S, Manas DM, Forsythe J. Resuming liver transplantation amid the COVID-19 pandemic. *Lancet Gastroenterol Hepatol* 2021; **6**: 12-13 [PMID: 33308431 DOI: 10.1016/S2468-1253(20)30360-5]
13 **Manuel O**, Estabrook M; AST Infectious Diseases Community of Practice. RNA respiratory viruses in solid organ transplantation. *Am J Transplant* 2013; **13** Suppl 4: 212-219 [PMID: 23465014 DOI: 10.1111/ajt.12113]

14 **Piedade J**, Pereira G. COVID-19 in liver transplant recipients. *Journal of Liver Transplantation* 2021; **3**: 100026 [DOI: 10.1016/j.liver.2021.100026]

15 **Hanson KE**, Caliendo AM, Arias CA, Englund JA, Hayden MK, Lee MJ, Loeb M, Patel R, Altayar O, El Alayli A, Sultan S, Falck-Ytter Y, Lavergne V, Morgan RL, Murad MH, Bhimraj A, Mustafa RA. Infectious Diseases Society of America Guidelines on the Diagnosis of COVID-19:Serologic Testing. *Clin Infect Dis* 2020 [PMID: 32918466 DOI: 10.1093/cid/ciaa1343]

16 **Liu R**, Han H, Liu F, Lv Z, Wu K, Liu Y, Feng Y, Zhu C. Positive rate of RT-PCR detection of SARS-CoV-2 infection in 4880 cases from one hospital in Wuhan, China, from Jan to Feb 2020. *Clin Chim Acta* 2020; **505**: 172-175 [PMID: 32156607 DOI: 10.1016/j.cca.2020.03.009]

17 **Xie J**, Ding C, Li J, Wang Y, Guo H, Lu Z, Wang J, Zheng C, Jin T, Gao Y, He H. Characteristics of patients with coronavirus disease (COVID-19) confirmed using an IgM-IgG antibody test. *J Med Virol* 2020; **92**: 2004-2010 [PMID: 32330303 DOI: 10.1002/jmv.25930]

18 **Tahamtan A**, Ardebili A. Real-time RT-PCR in COVID-19 detection: issues affecting the results. *Expert Rev Mol Diagn* 2020; **20**: 453-454 [PMID: 32297805 DOI: 10.1080/14737159.2020.1757437]

19 **Burki TK**. Testing for COVID-19. *Lancet Respir Med* 2020; **8**: e63-e64 [PMID: 32479792 DOI: 10.1016/S2213-2600(20)30247-2]

20 **Dinnes J**, Deeks JJ, Adriano A, Berhane S, Davenport C, Dittrich S, Emperador D, Takwoingi Y, Cunningham J, Beese S, Dretzke J, Ferrante di Ruffano L, Harris IM, Price MJ, Taylor-Phillips S, Hooft L, Leeflang MM, Spijker R, Van den Bruel A; Cochrane COVID-19 Diagnostic Test Accuracy Group. Rapid, point-of-care antigen and molecular-based tests for diagnosis of SARS-CoV-2 infection. *Cochrane Database Syst Rev* 2020; **8**: CD013705 [PMID: 32845525 DOI: 10.1002/14651858.CD013705]

21 **Fraser J**, Mousley J, Testro A, Smibert OC, Koshy AN. Clinical Presentation, Treatment, and Mortality Rate in Liver Transplant Recipients With Coronavirus Disease 2019: A Systematic Review and Quantitative Analysis. *Transplant Proc* 2020; **52**: 2676-2683 [PMID: 32891405 DOI: 10.1016/j.transproceed.2020.07.012]

22 **Becchetti C**, Zambelli MF, Pasulo L, Donato MF, Invernizzi F, Detry O, Dahlqvist G, Ciccarelli O, Morelli MC, Fraga M, Svegliati-Baroni G, van Vlierberghe H, Coenraad MJ, Romero MC, de Gottardi A, Toniutto P, Del Prete L, Abbati C, Samuel D, Pirenne J, Nevens F, Dufour JF; COVID-LT group. COVID-19 in an international European liver transplant recipient cohort. *Gut* 2020; **69**: 1832-1840 [PMID: 32571972 DOI: 10.1136/gutjnl-2020-321923]

23 **Belli LS**, Fondevila C, Cortesi PA, Conti S, Karam V, Adam R, Coilly A, Ericzon BG, Loinaz C, Cuervas-Mons V, Zambelli M, Llado L, Diaz-Fontenla F, Invernizzi F, Patrono D, Faitot F, Bhooori S, Pirenne J, Perricone G, Magini G, Castells L, Detry O, Cruchaga PM, Colmenero J, Berrevoet F, Rodriguez G, Ysebaert D, Radenne S, Metselaar H, Morelli C, De Carlis LG, Polak WG, Duvoux C; ELITA-ELTR COVID-19 Registry. Protective Role of Tacrolimus, Deleterious Role of Age and Comorbidities in Liver Transplant Recipients With Covid-19: Results From the ELITA/ELTR Multi-center European Study. *Gastroenterology* 2021; **160**: 1151-1163.e3 [PMID: 33307029 DOI: 10.1053/j.gastro.2020.11.045]

24 **Colmenero J**, Rodríguez-Perálvarez M, Salcedo M, Arias-Milla A, Muñoz-Serrano A, Graus J, Nuño J, Gastaca M, Bustamante-Schneider J, Cachero A, Lladó L, Caballero A, Fernández-Yunquera A, Loinaz C, Fernández I, Fondevila C, Navasa M, Iñarrairaegui M, Castells L, Pascual S, Ramírez P, Vinaixa C, González-Dieguez ML, González-Grande R, Hierro L, Nogueras F, Otero A, Álamo JM, Blanco-Fernández G, Fábrega E, García-Pajares F, Montero JL, Tomé S, De la Rosa G, Pons JA. Epidemiological pattern, incidence, and outcomes of COVID-19 in liver transplant patients. *J Hepatol* 2021; **74**: 148-155 [PMID: 32750442 DOI: 10.1016/j.jhep.2020.07.040]

25 **Dumortier J**, Duvoux C, Roux O, Altieri M, Barraud H, Besch C, Caillard S, Coilly A, Conti F, Dharancy S, Durand F, Francoz C, Garaix F, Houssel-Debry P, Kounis I, Lassailly G, Laverdure N, Leroy V, Mallet M, Mazzola A, Meunier L, Radenne S, Richardet JP, Vanlemmens C, Hazzan M, Saliba F; French Solid Organ Transplant COVID Registry; Groupe de Recherche Français en Greffe de Foie (GReF²). Covid-19 in liver transplant recipients: the French SOT COVID registry. *Clin Res Hepatol Gastroenterol* 2021; **45**: 101639 [PMID: 33636654 DOI: 10.1016/j.clinre.2021.101639]

26 **Guarino M**, Cossiga V, Loperto I, Esposito I, Ortolani R, Fiorentino A, Pontillo G, De Coppi L, Cozza V, Galeota Lanza A, Di Costanzo GG, Picciotto FP, Morisco F. COVID-19 in liver transplant recipients: incidence, hospitalization and outcome in an Italian prospective double-centre study. *Sci Rep* 2022; **12**: 4831 [PMID: 35318432 DOI: 10.1038/s41598-022-08947-x]

27 **Loinaz C**, Marcacuzco A, Fernández-Ruiz M, Caso O, Cambra F, San Juan R, Justo I, Calvo J, García-Sesma A, Manrique A, Pérez-Jacoiste Asín MA, Folgueira MD, Aguado JM, Lumbreras C. Varied clinical presentation and outcome of SARS-CoV-2 infection in liver transplant recipients: Initial experience at a single center in Madrid, Spain. *Transpl Infect Dis* 2020; **22**: e13372 [PMID: 32562561 DOI: 10.1111/tid.13372]

28 **Lee BT**, Perumalswami PV, Im GY, Florman S, Schiano TD; COBE Study Group. COVID-19 in Liver Transplant Recipients: An Initial Experience From the US Epicenter. *Gastroenterology* 2020; **159**: 1176-1178.e2 [PMID: 32442561 DOI: 10.1053/j.gastro.2020.05.050]

29 **Jadaun SS**, Singh SA, Madan K, Gupta S. "SARS-CoV-2 Infection in Liver Transplant Recipients - Immunosuppression is the Silver Lining? *J Clin Exp Hepatol* 2022; **12**: 384-389 [PMID: 34305351 DOI: 10.1016/j.jceh.2021.07.005]

30 **Tian Y**, Rong L, Nian W, He Y. Review article: gastrointestinal features in COVID-19 and the possibility of faecal transmission. *Aliment Pharmacol Ther* 2020; **51**: 843-851 [PMID: 32222988 DOI: 10.1111/apt.15731]

31 **Li X**, Xu S, Yu M, Wang K, Tao Y, Zhou Y, Shi J, Zhou M, Wu B, Yang Z, Zhang C, Yue J, Zhang Z, Renz H, Liu X, Xie J, Xie M, Zhao J. Risk factors for severity and mortality in adult COVID-19 inpatients in Wuhan. *J Allergy Clin Immunol* 2020; **146**: 110-118 [PMID: 32294485 DOI: 10.1016/j.jaci.2020.04.006]

32 **Mao R**, Qiu Y, He JS, Tan JY, Li XH, Liang J, Shen J, Zhu LR, Chen Y, Iacucci M, Ng SC, Ghosh S, Chen MH. Manifestations and prognosis of gastrointestinal and liver involvement in patients with COVID-19: a systematic review and meta-analysis. *Lancet Gastroenterol Hepatol* 2020; **5**: 667-678 [PMID: 32405603 DOI: 10.1016/S2468-1253(20)30126-6]

33 **Webb GJ**, Marjot T, Cook JA, Aloman C, Armstrong MJ, Brenner EJ, Catana MA, Cargill T, Dhanasekaran R, García-

Juárez I, Hagström H, Kennedy JM, Marshall A, Masson S, Mercer CJ, Perumalswami PV, Ruiz I, Thaker S, Ufere NN, Barnes E, Barritt AS 4th, Moon AM. Outcomes following SARS-CoV-2 infection in liver transplant recipients: an international registry study. *Lancet Gastroenterol Hepatol* 2020; **5**: 1008-1016 [PMID: 32866433 DOI: 10.1016/S2468-1253(20)30271-5]

34 **Moutchia J**, Pokharel P, Kerri A, McGaw K, Uchai S, Nji M, Goodman M. Clinical laboratory parameters associated with severe or critical novel coronavirus disease 2019 (COVID-19): A systematic review and meta-analysis. *PLoS One* 2020; **15**: e0239802 [PMID: 33002041 DOI: 10.1371/journal.pone.0239802]

35 **Ghahramani S**, Tabrizi R, Lankarani KB, Kashani SMA, Rezaei S, Zeidi N, Akbari M, Heydari ST, Akbari H, Nowrouzi-Sohrabi P, Ahmadizar F. Laboratory features of severe vs. non-severe COVID-19 patients in Asian populations: a systematic review and meta-analysis. *Eur J Med Res* 2020; **25**: 30 [PMID: 32746929 DOI: 10.1186/s40001-020-00432-3]

36 **Elshazli RM**, Toraih EA, Elgamal A, El-Mowafy M, El-Mesery M, Amin MN, Hussein MH, Killackey MT, Fawzy MS, Kandil E. Diagnostic and prognostic value of hematological and immunological markers in COVID-19 infection: A meta-analysis of 6320 patients. *PLoS One* 2020; **15**: e0238160 [PMID: 32822430 DOI: 10.1371/journal.pone.0238160]

37 **Zhou F**, Yu T, Du R, Fan G, Liu Y, Liu Z, Xiang J, Wang Y, Song B, Gu X, Guan L, Wei Y, Li H, Wu X, Xu J, Tu S, Zhang Y, Chen H, Cao B. Clinical course and risk factors for mortality of adult inpatients with COVID-19 in Wuhan, China: a retrospective cohort study. *Lancet* 2020; **395**: 1054-1062 [PMID: 32171076 DOI: 10.1016/S0140-6736(20)30566-3]

38 **Goyal P**, Choi JJ, Pinheiro LC, Schenck EJ, Chen R, Jabri A, Satlin MJ, Campion TR Jr, Nahid M, Ringel JB, Hoffman KL, Alshak MN, Li HA, Wehmeyer GT, Rajan M, Reshetnyak E, Hupert N, Horn EM, Martinez FJ, Gulick RM, Safford MM. Clinical Characteristics of Covid-19 in New York City. *N Engl J Med* 2020; **382**: 2372-2374 [PMID: 32302078 DOI: 10.1056/NEJMc2010419]

39 **El Kassas M**, Alboraie M, Al Balakosy A, Abdeen N, Afify S, Abdalgaber M, Sherief AF, Madkour A, Abdellah Ahmed M, Eltabbakh M, Salaheldin M, Wifi MN. Liver transplantation in the era of COVID-19. *Arab J Gastroenterol* 2020; **21**: 69-75 [PMID: 32439237 DOI: 10.1016/j.ajg.2020.04.019]

40 **Soin AS**, Choudhary NS, Yadav SK, Saigal S, Saraf N, Rastogi A, Bhangui P, Srinivasan T, Mohan N, Saha SK, Gupta A, Chaudhary RJ, Yadav K, Dhampalwar S, Govil D, Gupta N, Vohra V. Restructuring Living-Donor Liver Transplantation at a High-Volume Center During the COVID-19 Pandemic. *J Clin Exp Hepatol* 2021; **11**: 418-423 [PMID: 33052181 DOI: 10.1016/j.jceh.2020.09.009]

41 **Hussain A**, Mahawar K, Xia Z, Yang W, El-Hasani S. Obesity and mortality of COVID-19. Meta-analysis. *Obes Res Clin Pract* 2020; **14**: 295-300 [PMID: 32660813 DOI: 10.1016/j.orcp.2020.07.002]

42 **Kumar A**, Arora A, Sharma P, Anikhindi SA, Bansal N, Singla V, Khare S, Srivastava A. Is diabetes mellitus associated with mortality and severity of COVID-19? *Diabetes Metab Syndr* 2020; **14**: 535-545 [PMID: 32408118 DOI: 10.1016/j.dsx.2020.04.044]

43 **Yadav DK**, Adhikari VP, Ling Q, Liang T. Immunosuppressants in Liver Transplant Recipients With Coronavirus Disease 2019: Capability or Catastrophe? *Front Med (Lausanne)* 2021; **8**: 756922 [PMID: 34859012 DOI: 10.3389/fmed.2021.756922]

44 **Liang W**, Guan W, Chen R, Wang W, Li J, Xu K, Li C, Ai Q, Lu W, Liang H, Li S, He J. Cancer patients in SARS-CoV-2 infection: a nationwide analysis in China. *Lancet Oncol* 2020; **21**: 335-337 [PMID: 32066541 DOI: 10.1016/S1470-2045(20)30096-6]

45 **Desai A**, Sachdeva S, Parekh T, Desai R. COVID-19 and Cancer: Lessons From a Pooled Meta-Analysis. *JCO Glob Oncol* 2020; **6**: 557-559 [PMID: 32250659 DOI: 10.1200/GO.20.00097]

46 **Başkıran A**, Akbulut S, Şahin TT, Tunçer A, Kaplan K, Bayındır Y, Yılmaz S. Coronavirus Precautions: Experience of High Volume Liver Transplant Institute. *Turk J Gastroenterol* 2022; **33**: 145-152 [PMID: 35115295 DOI: 10.5152/tjg.2022.21748]

47 **Belli LS**, Duvoux C, Karam V, Adam R, Cuervas-Mons V, Pasulo L, Loinaz C, Invernizzi F, Patrono D, Bhoori S, Ciccarelli O, Morelli MC, Castells L, Lopez-Lopez V, Conti S, Fondevila C, Polak W. COVID-19 in liver transplant recipients: preliminary data from the ELITA/ELTR registry. *Lancet Gastroenterol Hepatol* 2020; **5**: 724-725 [PMID: 32505228 DOI: 10.1016/S2468-1253(20)30183-7]

48 **Bhoori S**, Rossi RE, Citterio D, Mazzaferro V. COVID-19 in long-term liver transplant patients: preliminary experience from an Italian transplant centre in Lombardy. *Lancet Gastroenterol Hepatol* 2020; **5**: 532-533 [PMID: 32278366 DOI: 10.1016/S2468-1253(20)30116-3]

49 **Mohammed A**, Paranji N, Chen PH, Niu B. COVID-19 in Chronic Liver Disease and Liver Transplantation: A Clinical Review. *J Clin Gastroenterol* 2021; **55**: 187-194 [PMID: 33394628 DOI: 10.1097/MCG.0000000000001481]

50 **Mehta P**, McAuley DF, Brown M, Sanchez E, Tattersall RS, Manson JJ; HLH Across Speciality Collaboration, UK. COVID-19: consider cytokine storm syndromes and immunosuppression. *Lancet* 2020; **395**: 1033-1034 [PMID: 32192578 DOI: 10.1016/S0140-6736(20)30628-0]

51 **Ritchie AI**, Singanayagam A. Immunosuppression for hyperinflammation in COVID-19: a double-edged sword? *Lancet* 2020; **395**: 1111 [PMID: 32220278 DOI: 10.1016/S0140-6736(20)30691-7]

52 **Willicombe M**, Thomas D, McAdoo S. COVID-19 and Calcineurin Inhibitors: Should They Get Left Out in the Storm? *J Am Soc Nephrol* 2020; **31**: 1145-1146 [PMID: 32312797 DOI: 10.1681/ASN.2020030348]

53 **Contributors to the C4 article**. C4 article: Implications of COVID-19 in transplantation. *Am J Transplant* 2021; **21**: 1801-1815 [PMID: 33040483 DOI: 10.1111/ajt.16346]

54 **Schoot TS**, Kerckhoffs APM, Hilbrands LB, van Marum RJ. Immunosuppressive Drugs and COVID-19: A Review. *Front Pharmacol* 2020; **11**: 1333 [PMID: 32982743 DOI: 10.3389/fphar.2020.01333]

55 **Philips CA**, Rela M, Soin AS, Gupta S, Surendran S, Augustine P. Critical Update on the Diagnosis and Management of COVID-19 in Advanced Cirrhosis and Liver Transplant Recipients. *J Clin Transl Hepatol* 2021; **9**: 947-959 [PMID: 34966658 DOI: 10.14218/JCTH.2021.00228]

56 **Kullar R**, Patel AP, Saab S. COVID-19 in Liver Transplant Recipients. *J Clin Transl Hepatol* 2021; **9**: 545-550 [PMID:

34447684 DOI: 10.14218/JCTH.2020.00098]
57 **Ma-Lauer Y**, Zheng Y, Malešević M, von Brunn B, Fischer G, von Brunn A. Influences of cyclosporin A and non-immunosuppressive derivatives on cellular cyclophilins and viral nucleocapsid protein during human coronavirus 229E replication. *Antiviral Res* 2020; **173**: 104620 [PMID: 31634494 DOI: 10.1016/j.antiviral.2019.104620]
58 **Fix OK**, Hameed B, Fontana RJ, Kwok RM, McGuire BM, Mulligan DC, Pratt DS, Russo MW, Schilsky ML, Verna EC, Loomba R, Cohen DE, Bezerra JA, Reddy KR, Chung RT. Clinical Best Practice Advice for Hepatology and Liver Transplant Providers During the COVID-19 Pandemic: AASLD Expert Panel Consensus Statement. *Hepatology* 2020; **72**: 287-304 [PMID: 32298473 DOI: 10.1002/hep.31281]
59 **Allison AC**, Eugui EM. Mycophenolate mofetil and its mechanisms of action. *Immunopharmacology* 2000; **47**: 85-118 [PMID: 10878285 DOI: 10.1016/s0162-3109(00)00188-0]
60 **Brennan DC**, Legendre C, Patel D, Mange K, Wiland A, McCague K, Shihab FS. Cytomegalovirus incidence between everolimus *vs* mycophenolate in de novo renal transplants: pooled analysis of three clinical trials. *Am J Transplant* 2011; **11**: 2453-2462 [PMID: 21812923 DOI: 10.1111/j.1600-6143.2011.03674.x]
61 **Lu X**, Chen T, Wang Y, Wang J, Yan F. Adjuvant corticosteroid therapy for critically ill patients with COVID-19. *Crit Care* 2020; **24**: 241 [PMID: 32430057 DOI: 10.1186/s13054-020-02964-w]
62 **Fix OK**, Serper M. Telemedicine and Telehepatology During the COVID-19 Pandemic. *Clin Liver Dis (Hoboken)* 2020; **15**: 187-190 [PMID: 32537134 DOI: 10.1002/cld.971]
63 **RECOVERY Collaborative Group**, Horby P, Lim WS, Emberson JR, Mafham M, Bell JL, Linsell L, Staplin N, Brightling C, Ustianowski A, Elmahi E, Prudon B, Green C, Felton T, Chadwick D, Rege K, Fegan C, Chappell LC, Faust SN, Jaki T, Jeffery K, Montgomery A, Rowan K, Juszczak E, Baillie JK, Haynes R, Landray MJ. Dexamethasone in Hospitalized Patients with Covid-19. *N Engl J Med* 2021; **384**: 693-704 [PMID: 32678530 DOI: 10.1056/NEJMoa2021436]
64 **Pereira MR**, Mohan S, Cohen DJ, Husain SA, Dube GK, Ratner LE, Arcasoy S, Aversa MM, Benvenuto LJ, Dadhania DM, Kapur S, Dove LM, Brown RS Jr, Rosenblatt RE, Samstein B, Uriel N, Farr MA, Satlin M, Small CB, Walsh TJ, Kodiyanplakkal RP, Miko BA, Aaron JG, Tsapepas DS, Emond JC, Verna EC. COVID-19 in solid organ transplant recipients: Initial report from the US epicenter. *Am J Transplant* 2020; **20**: 1800-1808 [PMID: 32330343 DOI: 10.1111/ajt.15941]
65 **Gerussi A**, Rigamonti C, Elia C, Cazzagon N, Floreani A, Pozzi R, Pozzoni P, Claar E, Pasulo L, Fagiuoli S, Cristoferi L, Carbone M, Invernizzi P. Coronavirus Disease 2019 in Autoimmune Hepatitis: A Lesson From Immunosuppressed Patients. *Hepatol Commun* 2020; **4**: 1257-1262 [PMID: 32838102 DOI: 10.1002/hep4.1557]
66 **Rabiee A**, Sadowski B, Adeniji N, Perumalswami PV, Nguyen V, Moghe A, Latt NL, Kumar S, Aloman C, Catana AM, Bloom PP, Chavin KD, Carr RM, Dunn W, Chen VL, Aby ES, Debes JD, Dhanasekaran R; COLD Consortium. Liver Injury in Liver Transplant Recipients With Coronavirus Disease 2019 (COVID-19): U.S. Multicenter Experience. *Hepatology* 2020; **72**: 1900-1911 [PMID: 32964510 DOI: 10.1002/hep.31574]
67 **Bhimraj A**, Morgan RL, Shumaker AH, Baden L, Cheng VC, Edwards KM, Gallagher JC, Gandhi RT, Muller WJ, Nakamura MM, O'Horo JC, Shafer RW, Shoham S, Murad MH, Mustafa RA, Sultan S, Falck-Ytter Y. IDSA Guidelines on the Treatment and Management of Patients with COVID-19. [Internet] [cited 27 May 2021]. Available from: https://www.idsociety.org/practice-guideline/covid-19-guideline-treatment-and-management/
68 **Cao B**, Wang Y, Wen D, Liu W, Wang J, Fan G, Ruan L, Song B, Cai Y, Wei M, Li X, Xia J, Chen N, Xiang J, Yu T, Bai T, Xie X, Zhang L, Li C, Yuan Y, Chen H, Li H, Huang H, Tu S, Gong F, Liu Y, Wei Y, Dong C, Zhou F, Gu X, Xu J, Liu Z, Zhang Y, Shang L, Wang K, Li K, Zhou X, Dong X, Qu Z, Lu S, Hu X, Ruan S, Luo S, Wu J, Peng L, Cheng F, Pan L, Zou J, Jia C, Liu X, Wang S, Wu X, Ge Q, He J, Zhan H, Qiu F, Guo L, Huang C, Jaki T, Hayden FG, Horby PW, Zhang D, Wang C. A Trial of Lopinavir-Ritonavir in Adults Hospitalized with Severe Covid-19. *N Engl J Med* 2020; **382**: 1787-1799 [PMID: 32187464 DOI: 10.1056/NEJMoa2001282]
69 **Yao X**, Ye F, Zhang M, Cui C, Huang B, Niu P, Liu X, Zhao L, Dong E, Song C, Zhan S, Lu R, Li H, Tan W, Liu D. In Vitro Antiviral Activity and Projection of Optimized Dosing Design of Hydroxychloroquine for the Treatment of Severe Acute Respiratory Syndrome Coronavirus 2 (SARS-CoV-2). *Clin Infect Dis* 2020; **71**: 732-739 [PMID: 32150618 DOI: 10.1093/cid/ciaa237]
70 **Gautret P**, Lagier JC, Parola P, Hoang VT, Meddeb L, Mailhe M, Doudier B, Courjon J, Giordanengo V, Vieira VE, Tissot Dupont H, Honoré S, Colson P, Chabrière E, La Scola B, Rolain JM, Brouqui P, Raoult D. Hydroxychloroquine and azithromycin as a treatment of COVID-19: results of an open-label non-randomized clinical trial. *Int J Antimicrob Agents* 2020; **56**: 105949 [PMID: 32205204 DOI: 10.1016/j.ijantimicag.2020.105949]
71 **Cavalcanti AB**, Zampieri FG, Rosa RG, Azevedo LCP, Veiga VC, Avezum A, Damiani LP, Marcadenti A, Kawano-Dourado L, Lisboa T, Junqueira DLM, de Barros E Silva PGM, Tramujas L, Abreu-Silva EO, Laranjeira LN, Soares AT, Echenique LS, Pereira AJ, Freitas FGR, Gebara OCE, Dantas VCS, Furtado RHM, Milan EP, Golin NA, Cardoso FF, Maia IS, Hoffmann Filho CR, Kormann APM, Amazonas RB, Bocchi de Oliveira MF, Serpa-Neto A, Falavigna M, Lopes RD, Machado FR, Berwanger O; Coalition Covid-19 Brazil I Investigators. Hydroxychloroquine with or without Azithromycin in Mild-to-Moderate Covid-19. *N Engl J Med* 2020; **383**: 2041-2052 [PMID: 32706953 DOI: 10.1056/NEJMoa2019014]
72 **Boulware DR**, Pullen MF, Bangdiwala AS, Pastick KA, Lofgren SM, Okafor EC, Skipper CP, Nascene AA, Nicol MR, Abassi M, Engen NW, Cheng MP, LaBar D, Lother SA, MacKenzie LJ, Drobot G, Marten N, Zarychanski R, Kelly LE, Schwartz IS, McDonald EG, Rajasingham R, Lee TC, Hullsiek KH. A Randomized Trial of Hydroxychloroquine as Postexposure Prophylaxis for Covid-19. *N Engl J Med* 2020; **383**: 517-525 [PMID: 32492293 DOI: 10.1056/NEJMoa2016638]
73 **Mitjà O**, Corbacho-Monné M, Ubals M, Tebé C, Peñafiel J, Tobias A, Ballana E, Alemany A, Riera-Martí N, Pérez CA, Suñer C, Laporte P, Admella P, Mitjà J, Clua M, Bertran L, Sarquella M, Gavilán S, Ara J, Argimon JM, Casabona J, Cuatrecasas G, Cañadas P, Elizalde-Torrent A, Fabregat R, Farré M, Forcada A, Flores-Mateo G, Muntada E, Nadal N, Narejos S, Nieto A, Prat N, Puig J, Quiñones C, Reyes-Ureña J, Ramírez-Viaplana F, Ruiz L, Riveira-Muñoz E, Sierra A, Velasco C, Vivanco-Hidalgo RM, Sentís A, G-Beiras C, Clotet B, Vall-Mayans M. Hydroxychloroquine for Early

Treatment of Adults With Mild Coronavirus Disease 2019: A Randomized, Controlled Trial. *Clin Infect Dis* 2021; **73**: e4073-e4081 [PMID: 32674126 DOI: 10.1093/cid/ciaa1009]

74 **Skipper CP**, Pastick KA, Engen NW, Bangdiwala AS, Abassi M, Lofgren SM, Williams DA, Okafor EC, Pullen MF, Nicol MR, Nascene AA, Hullsiek KH, Cheng MP, Luke D, Lother SA, MacKenzie LJ, Drobot G, Kelly LE, Schwartz IS, Zarychanski R, McDonald EG, Lee TC, Rajasingham R, Boulware DR. Hydroxychloroquine in Nonhospitalized Adults With Early COVID-19 : A Randomized Trial. *Ann Intern Med* 2020; **173**: 623-631 [PMID: 32673060 DOI: 10.7326/M20-4207]

75 **Tang W**, Cao Z, Han M, Wang Z, Chen J, Sun W, Wu Y, Xiao W, Liu S, Chen E, Chen W, Wang X, Yang J, Lin J, Zhao Q, Yan Y, Xie Z, Li D, Yang Y, Liu L, Qu J, Ning G, Shi G, Xie Q. Hydroxychloroquine in patients with mainly mild to moderate coronavirus disease 2019: open label, randomised controlled trial. *BMJ* 2020; **369**: m1849 [PMID: 32409561 DOI: 10.1136/bmj.m1849]

76 **Pillaiyar T**, Manickam M, Namasivayam V, Hayashi Y, Jung SH. An Overview of Severe Acute Respiratory Syndrome-Coronavirus (SARS-CoV) 3CL Protease Inhibitors: Peptidomimetics and Small Molecule Chemotherapy. *J Med Chem* 2016; **59**: 6595-6628 [PMID: 26878082 DOI: 10.1021/acs.jmedchem.5b01461]

77 Fact sheet for healthcare providers: Emergency use authorization for paxlovidtm. Available from: chrome-extension://efaidnbmnnnibpcajpcglclefindmkaj/https://www.fda.gov/media/155050/download

78 **Owen DR**, Allerton CMN, Anderson AS, Aschenbrenner L, Avery M, Berritt S, Boras B, Cardin RD, Carlo A, Coffman KJ, Dantonio A, Di L, Eng H, Ferre R, Gajiwala KS, Gibson SA, Greasley SE, Hurst BL, Kadar EP, Kalgutkar AS, Lee JC, Lee J, Liu W, Mason SW, Noell S, Novak JJ, Obach RS, Ogilvie K, Patel NC, Pettersson M, Rai DK, Reese MR, Sammons MF, Sathish JG, Singh RSP, Steppan CM, Stewart AE, Tuttle JB, Updyke L, Verhoest PR, Wei L, Yang Q, Zhu Y. An oral SARS-CoV-2 M(pro) inhibitor clinical candidate for the treatment of COVID-19. *Science* 2021; **374**: 1586-1593 [PMID: 34726479 DOI: 10.1126/science.abl4784]

79 **Greasley SE**, Noell S, Plotnikova O, Ferre R, Liu W, Bolanos B, Fennell K, Nicki J, Craig T, Zhu Y, Stewart AE, Steppan CM. Structural basis for the in vitro efficacy of nirmatrelvir against SARS-CoV-2 variants. *J Biol Chem* 2022; **298**: 101972 [PMID: 35461811 DOI: 10.1016/j.jbc.2022.101972]

80 **Rai DK**, Yurgelonis I, McMonagle P, Rothan HA, Hao L, Gribenko A, Titova E, Kreiswirth B, White KM, Zhu Y, Anderson AS, Cardin RD. Nirmatrelvir, an orally active Mpro inhibitor, is a potent inhibitor of SARS-CoV-2 Variants of Concern. *bioRxiv* 2022 [DOI: 10.1101/2022.01.17.476644]

81 **Vangeel L**, Chiu W, De Jonghe S, Maes P, Slechten B, Raymenants J, André E, Leyssen P, Neyts J, Jochmans D. Remdesivir, Molnupiravir and Nirmatrelvir remain active against SARS-CoV-2 Omicron and other variants of concern. *Antiviral Res* 2022; **198**: 105252 [PMID: 35085683 DOI: 10.1016/j.antiviral.2022.105252]

82 COVID-19 Treatment Guidelines. Available from: https://www.covid19treatmentguidelines.nih.gov/

83 **Malinis M**, Koff A. Mycobacterium tuberculosis in solid organ transplant donors and recipients. *Curr Opin Organ Transplant* 2021; **26**: 432-439 [PMID: 34074939 DOI: 10.1097/MOT.0000000000000885]

84 **Hammond J**, Leister-Tebbe H, Gardner A, Abreu P, Bao W, Wisemandle W, Baniecki M, Hendrick VM, Damle B, Simón-Campos A, Pypstra R, Rusnak JM; EPIC-HR Investigators. Oral Nirmatrelvir for High-Risk, Nonhospitalized Adults with Covid-19. *N Engl J Med* 2022; **386**: 1397-1408 [PMID: 35172054 DOI: 10.1056/NEJMoa2118542]

85 **Gottlieb RL**, Vaca CE, Paredes R, Mera J, Webb BJ, Perez G, Oguchi G, Ryan P, Nielsen BU, Brown M, Hidalgo A, Sachdeva Y, Mittal S, Osiyemi O, Skarbinski J, Juneja K, Hyland RH, Osinusi A, Chen S, Camus G, Abdelghany M, Davies S, Behenna-Renton N, Duff F, Marty FM, Katz MJ, Ginde AA, Brown SM, Schiffer JT, Hill JA; GS-US-540-9012 (PINETREE) Investigators. Early Remdesivir to Prevent Progression to Severe Covid-19 in Outpatients. *N Engl J Med* 2022; **386**: 305-315 [PMID: 34937145 DOI: 10.1056/NEJMoa2116846]

86 **Jayk Bernal A**, Gomes da Silva MM, Musungaie DB, Kovalchuk E, Gonzalez A, Delos Reyes V, Martín-Quirós A, Caraco Y, Williams-Diaz A, Brown ML, Du J, Pedley A, Assaid C, Strizki J, Grobler JA, Shamsuddin HH, Tipping R, Wan H, Paschke A, Butterton JR, Johnson MG, De Anda C; MOVe-OUT Study Group. Molnupiravir for Oral Treatment of Covid-19 in Nonhospitalized Patients. *N Engl J Med* 2022; **386**: 509-520 [PMID: 34914868 DOI: 10.1056/NEJMoa2116044]

87 **Fischer WA 2nd**, Eron JJ Jr, Holman W, Cohen MS, Fang L, Szewczyk LJ, Sheahan TP, Baric R, Mollan KR, Wolfe CR, Duke ER, Azizad MM, Borroto-Esoda K, Wohl DA, Coombs RW, James Loftis A, Alabanza P, Lipansky F, Painter WP. A phase 2a clinical trial of molnupiravir in patients with COVID-19 shows accelerated SARS-CoV-2 RNA clearance and elimination of infectious virus. *Sci Transl Med* 2022; **14**: eabl7430 [PMID: 34941423 DOI: 10.1126/scitranslmed.abl7430]

88 **Zou R**, Peng L, Shu D, Zhao L, Lan J, Tan G, Peng J, Yang X, Liu M, Zhang C, Yuan J, Wang H, Li S, Lu H, Zhong W, Liu Y. Antiviral Efficacy and Safety of Molnupiravir Against Omicron Variant Infection: A Randomized Controlled Clinical Trial. *Front Pharmacol* 2022; **13**: 939573 [PMID: 35784723 DOI: 10.3389/fphar.2022.939573]

89 **Kabinger F**, Stiller C, Schmitzová J, Dienemann C, Kokic G, Hillen HS, Höbartner C, Cramer P. Mechanism of molnupiravir-induced SARS-CoV-2 mutagenesis. *Nat Struct Mol Biol* 2021; **28**: 740-746 [PMID: 34381216 DOI: 10.1038/s41594-021-00651-0]

90 **Zhou S**, Hill CS, Sarkar S, Tse LV, Woodburn BMD, Schinazi RF, Sheahan TP, Baric RS, Heise MT, Swanstrom R. β-d-N4-hydroxycytidine Inhibits SARS-CoV-2 Through Lethal Mutagenesis But Is Also Mutagenic To Mammalian Cells. *J Infect Dis* 2021; **224**: 415-419 [PMID: 33961695 DOI: 10.1093/infdis/jiab247]

91 Fact sheet for healthcare providers: emergency use authorization for lagevrio™ (molnupiravir) capsules. Available from: chrome-extension://efaidnbmnnnibpcajpcglclefindmkaj/https://www.fda.gov/media/155054/download

92 People with Certain Medical Conditions | CDC. Available from: https://www.cdc.gov/coronavirus/2019-ncov/need-extra-precautions/people-with-medical-conditions.html

93 **Takashita E**, Yamayoshi S, Simon V, van Bakel H, Sordillo EM, Pekosz A, Fukushi S, Suzuki T, Maeda K, Halfmann P, Sakai-Tagawa Y, Ito M, Watanabe S, Imai M, Hasegawa H, Kawaoka Y. Efficacy of Antibodies and Antiviral Drugs against Omicron BA.2.12.1, BA.4, and BA.5 Subvariants. *N Engl J Med* 2022; **387**: 468-470 [PMID: 35857646 DOI: 10.1056/NEJMc2207519]

94 **Uraki R**, Kiso M, Iida S, Imai M, Takashita E, Kuroda M, Halfmann PJ, Loeber S, Maemura T, Yamayoshi S, Fujisaki S,

Wang Z, Ito M, Ujie M, Iwatsuki-Horimoto K, Furusawa Y, Wright R, Chong Z, Ozono S, Yasuhara A, Ueki H, Sakai-Tagawa Y, Li R, Liu Y, Larson D, Koga M, Tsutsumi T, Adachi E, Saito M, Yamamoto S, Hagihara M, Mitamura K, Sato T, Hojo M, Hattori SI, Maeda K, Valdez R; IASO study team, Okuda M, Murakami J, Duong C, Godbole S, Douek DC, Maeda K, Watanabe S, Gordon A, Ohmagari N, Yotsuyanagi H, Diamond MS, Hasegawa H, Mitsuya H, Suzuki T, Kawaoka Y. Characterization and antiviral susceptibility of SARS-CoV-2 Omicron BA.2. *Nature* 2022; **607**: 119-127 [PMID: 35576972 DOI: 10.1038/s41586-022-04856-1]

95 **Johnson MG**, Puenpatom A, Moncada PA, Burgess L, Duke ER, Ohmagari N, Wolf T, Bassetti M, Bhagani S, Ghosn J, Zhang Y, Wan H, Williams-Diaz A, Brown ML, Paschke A, De Anda C. Effect of Molnupiravir on Biomarkers, Respiratory Interventions, and Medical Services in COVID-19 : A Randomized, Placebo-Controlled Trial. *Ann Intern Med* 2022; **175**: 1126-1134 [PMID: 35667065 DOI: 10.7326/M22-0729]

96 **Sarrell BA**, Bloch K, El Chediak A, Kumm K, Tracy K, Forbes RC, Langone A, Thomas L, Schlendorf K, Trindade AJ, Perri R, Wright P, Concepcion BP. Monoclonal antibody treatment for COVID-19 in solid organ transplant recipients. *Transpl Infect Dis* 2022; **24**: e13759 [PMID: 34787345 DOI: 10.1111/tid.13759]

97 Fact sheet for healthcare providers emergency use authorization (EUA) of sotrovimab authorized use. Available from: chrome-extension://efaidnbmnnnibpcajpcglclefindmkaj/https://www.fda.gov/media/149534/download

98 Fact sheet for health care providers emergency use authorization (EUA) of regen-cov ® (casirivimab and imdevimab). Available from: chrome-extension://efaidnbmnnnibpcajpcglclefindmkaj/https://www.fda.gov/media/145611/download

99 Fact sheet for health care providers emergency use authorization (EUA) of bamlanivimab and etesevimab authorized use treatment. Available from: chrome-extension://efaidnbmnnnibpcajpcglclefindmkaj/https://www.fda.gov/media/145802/download

100 **Dhand A**, Razonable RR. COVID-19 and Solid Organ Transplantation: Role of Anti-SARS-CoV-2 Monoclonal Antibodies. *Curr Transplant Rep* 2022; **9**: 26-34 [PMID: 35070639 DOI: 10.1007/s40472-022-00357-2]

101 **Chen P**, Nirula A, Heller B, Gottlieb RL, Boscia J, Morris J, Huhn G, Cardona J, Mocherla B, Stosor V, Shawa I, Adams AC, Van Naarden J, Custer KL, Shen L, Durante M, Oakley G, Schade AE, Sabo J, Patel DR, Klekotka P, Skovronsky DM; BLAZE-1 Investigators. SARS-CoV-2 Neutralizing Antibody LY-CoV555 in Outpatients with Covid-19. *N Engl J Med* 2021; **384**: 229-237 [PMID: 33113295 DOI: 10.1056/NEJMoa2029849]

102 **Weinreich DM**, Sivapalasingam S, Norton T, Ali S, Gao H, Bhore R, Musser BJ, Soo Y, Rofail D, Im J, Perry C, Pan C, Hosain R, Mahmood A, Davis JD, Turner KC, Hooper AT, Hamilton JD, Baum A, Kyratsous CA, Kim Y, Cook A, Kampman W, Kohli A, Sachdeva Y, Graber X, Kowal B, DiCioccio T, Stahl N, Lipsich L, Braunstein N, Herman G, Yancopoulos GD; Trial Investigators. REGN-COV2, a Neutralizing Antibody Cocktail, in Outpatients with Covid-19. *N Engl J Med* 2021; **384**: 238-251 [PMID: 33332778 DOI: 10.1056/NEJMoa2035002]

103 **Gottlieb RL**, Nirula A, Chen P, Boscia J, Heller B, Morris J, Huhn G, Cardona J, Mocherla B, Stosor V, Shawa I, Kumar P, Adams AC, Van Naarden J, Custer KL, Durante M, Oakley G, Schade AE, Holzer TR, Ebert PJ, Higgs RE, Kallewaard NL, Sabo J, Patel DR, Klekotka P, Shen L, Skovronsky DM. Effect of Bamlanivimab as Monotherapy or in Combination With Etesevimab on Viral Load in Patients With Mild to Moderate COVID-19: A Randomized Clinical Trial. *JAMA* 2021; **325**: 632-644 [PMID: 33475701 DOI: 10.1001/jama.2021.0202]

104 **ACTIV-3/TICO LY-CoV555 Study Group**, Lundgren JD, Grund B, Barkauskas CE, Holland TL, Gottlieb RL, Sandkovsky U, Brown SM, Knowlton KU, Self WH, Files DC, Jain MK, Benfield T, Bowdish ME, Leshnower BG, Baker JV, Jensen JU, Gardner EM, Ginde AA, Harris ES, Johansen IS, Markowitz N, Matthay MA, Østergaard L, Chang CC, Davey VJ, Goodman A, Higgs ES, Murray DD, Murray TA, Paredes R, Parmar MKB, Phillips AN, Reilly C, Sharma S, Dewar RL, Teitelbaum M, Wentworth D, Cao H, Klekotka P, Babiker AG, Gelijns AC, Kan VL, Polizzotto MN, Thompson BT, Lane HC, Neaton JD. A Neutralizing Monoclonal Antibody for Hospitalized Patients with Covid-19. *N Engl J Med* 2021; **384**: 905-914 [PMID: 33356051 DOI: 10.1056/NEJMoa2033130]

105 **Dhand A**, Lobo SA, Wolfe K, Feola N, Lee L, Nog R, Chen D, Glicklich D, Diflo T, Nabors C. Casirivimab-imdevimab for Treatment of COVID-19 in Solid Organ Transplant Recipients: An Early Experience. *Transplantation* 2021; **105**: e68-e69 [PMID: 33724242 DOI: 10.1097/TP.0000000000003737]

106 **Yetmar ZA**, Beam E, O'Horo JC, Ganesh R, Bierle DM, Brumble L, Seville MT, Razonable RR. Monoclonal Antibody Therapy for COVID-19 in Solid Organ Transplant Recipients. *Open Forum Infect Dis* 2021; **8**: ofab255 [PMID: 34631921 DOI: 10.1093/ofid/ofab255]

107 **Avery RK**. Update on COVID-19 Therapeutics for Solid Organ Transplant Recipients, Including the Omicron Surge. *Transplantation* 2022; **106**: 1528-1537 [PMID: 35700481 DOI: 10.1097/TP.0000000000004200]

108 **Food and Drug Administration**. Coronavirus (COVID-19) Update: FDA Authorizes New Monoclonal Antibody for Treatment of COVID-19 that Retains Activity Against Omicron Variant. Available from: https://www.fda.gov/news-events/press-announcements/coronavirus-covid-19-update-fda-authorizes-new-monoclonal-antibody-treatment-covid-19-retains

109 **Crosby TC**, Kittel EC, Gieseker CM. Phish-Pharm: A Searchable Database of Pharmacokinetics and Drug Residue Literature in Fish - 2022 Update. *AAPS J* 2022; **24**: 105 [PMID: 36195686 DOI: 10.1208/s12248-022-00750-w]

110 **Wang M**, Cao R, Zhang L, Yang X, Liu J, Xu M, Shi Z, Hu Z, Zhong W, Xiao G. Remdesivir and chloroquine effectively inhibit the recently emerged novel coronavirus (2019-nCoV) in vitro. *Cell Res* 2020; **30**: 269-271 [PMID: 32020029 DOI: 10.1038/s41422-020-0282-0]

111 **Beigel JH**, Tomashek KM, Dodd LE, Mehta AK, Zingman BS, Kalil AC, Hohmann E, Chu HY, Luetkemeyer A, Kline S, Lopez de Castilla D, Finberg RW, Dierberg K, Tapson V, Hsieh L, Patterson TF, Paredes R, Sweeney DA, Short WR, Touloumi G, Lye DC, Ohmagari N, Oh MD, Ruiz-Palacios GM, Benfield T, Fätkenheuer G, Kortepeter MG, Atmar RL, Creech CB, Lundgren J, Babiker AG, Pett S, Neaton JD, Burgess TH, Bonnett T, Green M, Makowski M, Osinusi A, Nayak S, Lane HC; ACTT-1 Study Group Members. Remdesivir for the Treatment of Covid-19 - Final Report. *N Engl J Med* 2020; **383**: 1813-1826 [PMID: 32445440 DOI: 10.1056/NEJMoa2007764]

112 **Keller MJ**, Kitsis EA, Arora S, Chen JT, Agarwal S, Ross MJ, Tomer Y, Southern W. Effect of Systemic Glucocorticoids on Mortality or Mechanical Ventilation in Patients With COVID-19. *J Hosp Med* 2020; **15**: 489-493 [PMID: 32804611 DOI: 10.12788/jhm.3497]

113 **Xu X**, Han M, Li T, Sun W, Wang D, Fu B, Zhou Y, Zheng X, Yang Y, Li X, Zhang X, Pan A, Wei H. Effective treatment of severe COVID-19 patients with tocilizumab. *Proc Natl Acad Sci U S A* 2020; **117**: 10970-10975 [PMID: 32350134 DOI: 10.1073/pnas.2005615117]

114 **RECOVERY Trial**. Tocilizumab reduces deaths in patients hospitalised with COVID-19. Available from: https://www.recoverytrial.net/news/tocilizumab-reduces-deaths-in-patients-hospitalised-with-covid-19

115 **REMAP-CAP Investigators**, Gordon AC, Mouncey PR, Al-Beidh F, Rowan KM, Nichol AD, Arabi YM, Annane D, Beane A, van Bentum-Puijk W, Berry LR, Bhimani Z, Bonten MJM, Bradbury CA, Brunkhorst FM, Buzgau A, Cheng AC, Detry MA, Duffy EJ, Estcourt LJ, Fitzgerald M, Goossens H, Haniffa R, Higgins AM, Hills TE, Horvat CM, Lamontagne F, Lawler PR, Leavis HL, Linstrum KM, Litton E, Lorenzi E, Marshall JC, Mayr FB, McAuley DF, McGlothlin A, McGuinness SP, McVerry BJ, Montgomery SK, Morpeth SC, Murthy S, Orr K, Parke RL, Parker JC, Patanwala AE, Pettilä V, Rademaker E, Santos MS, Saunders CT, Seymour CW, Shankar-Hari M, Sligl WI, Turgeon AF, Turner AM, van de Veerdonk FL, Zarychanski R, Green C, Lewis RJ, Angus DC, McArthur CJ, Berry S, Webb SA, Derde LPG. Interleukin-6 Receptor Antagonists in Critically Ill Patients with Covid-19. *N Engl J Med* 2021; **384**: 1491-1502 [PMID: 33631065 DOI: 10.1056/NEJMoa2100433]

116 **Kalil AC**, Patterson TF, Mehta AK, Tomashek KM, Wolfe CR, Ghazaryan V, Marconi VC, Ruiz-Palacios GM, Hsieh L, Kline S, Tapson V, Iovine NM, Jain MK, Sweeney DA, El Sahly HM, Branche AR, Regalado Pineda J, Lye DC, Sandkovsky U, Luetkemeyer AF, Cohen SH, Finberg RW, Jackson PEH, Taiwo B, Paules CI, Arguinchona H, Erdmann N, Ahuja N, Frank M, Oh MD, Kim ES, Tan SY, Mularski RA, Nielsen H, Ponce PO, Taylor BS, Larson L, Rouphael NG, Saklawi Y, Cantos VD, Ko ER, Engemann JJ, Amin AN, Watanabe M, Billings J, Elie MC, Davey RT, Burgess TH, Ferreira J, Green M, Makowski M, Cardoso A, de Bono S, Bonnett T, Proschan M, Deye GA, Dempsey W, Nayak SU, Dodd LE, Beigel JH; ACTT-2 Study Group Members. Baricitinib plus Remdesivir for Hospitalized Adults with Covid-19. *N Engl J Med* 2021; **384**: 795-807 [PMID: 33306283 DOI: 10.1056/NEJMoa2031994]

117 **Zhang JS**, Chen JT, Liu YX, Zhang ZS, Gao H, Liu Y, Wang X, Ning Y, Liu YF, Gao Q, Xu JG, Qin C, Dong XP, Yin WD. A serological survey on neutralizing antibody titer of SARS convalescent sera. *J Med Virol* 2005; **77**: 147-150 [PMID: 16121363 DOI: 10.1002/jmv.20431]

118 **Casadevall A**, Pirofski LA. The convalescent sera option for containing COVID-19. *J Clin Invest* 2020; **130**: 1545-1548 [PMID: 32167489 DOI: 10.1172/JCI138003]

119 **Joyner MJ**, Senefeld JW, Klassen SA, Mills JR, Johnson PW, Theel ES, Wiggins CC, Bruno KA, Klompas AM, Lesser ER, Kunze KL, Sexton MA, Diaz Soto JC, Baker SE, Shepherd JRA, van Helmond N, van Buskirk CM, Winters JL, Stubbs JR, Rea RF, Hodge DO, Herasevich V, Whelan ER, Clayburn AJ, Larson KF, Ripoll JG, Andersen KJ, Buras MR, Vogt MNP, Dennis JJ, Regimbal RJ, Bauer PR, Blair JE, Paneth NS, Fairweather D, Wright RS, Carter RE, Casadevall A. Effect of Convalescent Plasma on Mortality among Hospitalized Patients with COVID-19: Initial Three-Month Experience. *medRxiv* 2020 [PMID: 32817978 DOI: 10.1101/2020.08.12.20169359]

120 **Li L**, Zhang W, Hu Y, Tong X, Zheng S, Yang J, Kong Y, Ren L, Wei Q, Mei H, Hu C, Tao C, Yang R, Wang J, Yu Y, Guo Y, Wu X, Xu Z, Zeng L, Xiong N, Chen L, Man N, Liu Y, Xu H, Deng E, Zhang X, Li C, Wang C, Su S, Zhang L, Wu Y, Liu Z. Effect of Convalescent Plasma Therapy on Time to Clinical Improvement in Patients With Severe and Life-threatening COVID-19: A Randomized Clinical Trial. *JAMA* 2020; **324**: 460-470 [PMID: 32492084 DOI: 10.1001/jama.2020.10044]

121 **Joyner MJ**, Klassen SA, Senefeld JW, Johnson PW, Carter RE, Wiggins CC, Shoham S, Grossman BJ, Henderson JP, Musser JM, Salazar E, Hartman WR, Bouvier NM, Liu STH, Pirofski L, Baker SE, van Helmond N, Wright RS, Fairweather D, Bruno KA, Paneth NS, Casadevall A. Evidence favouring the efficacy of convalescent plasma for COVID-19 therapy. *medRxiv* 2020 [DOI: 10.1101/2020.07.29.20162917]

122 **Agarwal A**, Mukherjee A, Kumar G, Chatterjee P, Bhatnagar T, Malhotra P; PLACID Trial Collaborators. Convalescent plasma in the management of moderate covid-19 in adults in India: open label phase II multicentre randomised controlled trial (PLACID Trial). *BMJ* 2020; **371**: m3939 [PMID: 33093056 DOI: 10.1136/bmj.m3939]

123 **Libster R**, Pérez Marc G, Wappner D, Coviello S, Bianchi A, Braem V, Esteban I, Caballero MT, Wood C, Berrueta M, Rondan A, Lescano G, Cruz P, Ritou Y, Fernández Viña V, Álvarez Paggi D, Esperante S, Ferreti A, Ofman G, Ciganda Á, Rodriguez R, Lantos J, Valentini R, Itcovici N, Hintze A, Oyarvide ML, Etchegaray C, Neira A, Name I, Alfonso J, López Castelo R, Caruso G, Rapelius S, Alvez F, Etchenique F, Dimase F, Alvarez D, Aranda SS, Sánchez Yanotti C, De Luca J, Jares Baglivo S, Laudanno S, Nowogrodzki F, Larrea R, Silveyra M, Leberzstein G, Debonis A, Molinos J, González M, Perez E, Kreplak N, Pastor Argüello S, Gibbons L, Althabe F, Bergel E, Polack FP; Fundación INFANT–COVID-19 Group. Early High-Titer Plasma Therapy to Prevent Severe Covid-19 in Older Adults. *N Engl J Med* 2021; **384**: 610-618 [PMID: 33406353 DOI: 10.1056/NEJMoa2033700]

124 **Simonovich VA**, Burgos Pratx LD, Scibona P, Beruto MV, Vallone MG, Vázquez C, Savoy N, Giunta DH, Pérez LG, Sánchez MDL, Gamarnik AV, Ojeda DS, Santoro DM, Camino PJ, Antelo S, Rainero K, Vidiella GP, Miyazaki EA, Cornistein W, Trabadelo OA, Ross FM, Spotti M, Funtowicz G, Scordo WE, Losso MH, Ferniot I, Pardo PE, Rodriguez E, Rucci P, Pasquali J, Fuentes NA, Esperatti M, Speroni GA, Nannini EC, Matteaccio A, Michelangelo HG, Follmann D, Lane HC, Belloso WH; PlasmAr Study Group. A Randomized Trial of Convalescent Plasma in Covid-19 Severe Pneumonia. *N Engl J Med* 2021; **384**: 619-629 [PMID: 33232588 DOI: 10.1056/NEJMoa2031304]

125 **Trapani S**, Masiero L, Puoti F, Rota MC, Del Manso M, Lombardini L, Riccardo F, Amoroso A, Pezzotti P, Grossi PA, Brusaferro S, Cardillo M; Italian Network of Regional Transplant Coordinating Centers Collaborating group; Italian Surveillance System of Covid-19, Italian Society for Organ Transplantation (SITO), The Italian Board of Experts in Liver Transplantation (I-BELT) Study Group, Italian Association for the Study of the Liver (AISF), Italian Society of Nephrology (SIN), SIN-SITO Study Group. Incidence and outcome of SARS-CoV-2 infection on solid organ transplantation recipients: A nationwide population-based study. *Am J Transplant* 2021; **21**: 2509-2521 [PMID: 33278850 DOI: 10.1111/ajt.16428]

126 **Ravanan R**, Callaghan CJ, Mumford L, Ushiro-Lumb I, Thorburn D, Casey J, Friend P, Parameshwar J, Currie I, Burnapp L, Baker R, Dudley J, Oniscu GC, Berman M, Asher J, Harvey D, Manara A, Manas D, Gardiner D, Forsythe JLR. SARS-CoV-2 infection and early mortality of waitlisted and solid organ transplant recipients in England: A national

cohort study. *Am J Transplant* 2020; **20**: 3008-3018 [PMID: 32780493 DOI: 10.1111/ajt.16247]

127 **Mansoor E**, Perez A, Abou-Saleh M, Sclair SN, Cohen S, Cooper GS, Mills A, Schlick K, Khan A. Clinical Characteristics, Hospitalization, and Mortality Rates of Coronavirus Disease 2019 Among Liver Transplant Patients in the United States: A Multicenter Research Network Study. *Gastroenterology* 2021; **160**: 459-462.e1 [PMID: 33010251 DOI: 10.1053/j.gastro.2020.09.033]

128 **Li J**, Huang DQ, Zou B, Yang H, Hui WZ, Rui F, Yee NTS, Liu C, Nerurkar SN, Kai JCY, Teng MLP, Li X, Zeng H, Borghi JA, Henry L, Cheung R, Nguyen MH. Epidemiology of COVID-19: A systematic review and meta-analysis of clinical characteristics, risk factors, and outcomes. *J Med Virol* 2021; **93**: 1449-1458 [PMID: 32790106 DOI: 10.1002/jmv.26424]

129 **Boettler T**, Newsome PN, Mondelli MU, Maticic M, Cordero E, Cornberg M, Berg T. Care of patients with liver disease during the COVID-19 pandemic: EASL-ESCMID position paper. *JHEP Rep* 2020; **2**: 100113 [PMID: 32289115 DOI: 10.1016/j.jhepr.2020.100113]

130 **Guan WJ**, Ni ZY, Hu Y, Liang WH, Ou CQ, He JX, Liu L, Shan H, Lei CL, Hui DSC, Du B, Li LJ, Zeng G, Yuen KY, Chen RC, Tang CL, Wang T, Chen PY, Xiang J, Li SY, Wang JL, Liang ZJ, Peng YX, Wei L, Liu Y, Hu YH, Peng P, Wang JM, Liu JY, Chen Z, Li G, Zheng ZJ, Qiu SQ, Luo J, Ye CJ, Zhu SY, Zhong NS; China Medical Treatment Expert Group for Covid-19. Clinical Characteristics of Coronavirus Disease 2019 in China. *N Engl J Med* 2020; **382**: 1708-1720 [PMID: 32109013 DOI: 10.1056/NEJMoa2002032]

131 **Grasselli G**, Zangrillo A, Zanella A, Antonelli M, Cabrini L, Castelli A, Cereda D, Coluccello A, Foti G, Fumagalli R, Iotti G, Latronico N, Lorini L, Merler S, Natalini G, Piatti A, Ranieri MV, Scandroglio AM, Storti E, Cecconi M, Pesenti A; COVID-19 Lombardy ICU Network. Baseline Characteristics and Outcomes of 1591 Patients Infected With SARS-CoV-2 Admitted to ICUs of the Lombardy Region, Italy. *JAMA* 2020; **323**: 1574-1581 [PMID: 32250385 DOI: 10.1001/jama.2020.5394]

132 **Ketcham SW**, Adie SK, Malliett A, Abdul-Aziz AA, Bitar A, Grafton G, Konerman MC. Coronavirus Disease-2019 in Heart Transplant Recipients in Southeastern Michigan: A Case Series. *J Card Fail* 2020; **26**: 457-461 [PMID: 32417380 DOI: 10.1016/j.cardfail.2020.05.008]

133 **Iacovoni A**, Boffini M, Pidello S, Simonato E, Barbero C, Sebastiani R, Vittori C, Fontana A, Terzi A, De Ferrari GM, Rinaldi M. A case series of novel coronavirus infection in heart transplantation from 2 centers in the pandemic area in the North of Italy. *J Heart Lung Transplant* 2020; **39**: 1081-1088 [PMID: 32709482 DOI: 10.1016/j.healun.2020.06.016]

134 **Rivinius R**, Kaya Z, Schramm R, Boeken U, Provaznik Z, Heim C, Knosalla C, Schoenrath F, Rieth A, Berchtold-Herz M, Barten MJ, Rauschning D, Mücke VT, Heyl S, Pistulli R, Grinninger C, Hagl C, Gummert JF, Warnecke G, Schulze PC, Katus HA, Kreusser MM, Raake PW. COVID-19 among heart transplant recipients in Germany: a multicenter survey. *Clin Res Cardiol* 2020; **109**: 1531-1539 [PMID: 32783099 DOI: 10.1007/s00392-020-01722-w]

135 **Latif F**, Farr MA, Clerkin KJ, Habal MV, Takeda K, Naka Y, Restaino S, Sayer G, Uriel N. Characteristics and Outcomes of Recipients of Heart Transplant With Coronavirus Disease 2019. *JAMA Cardiol* 2020; **5**: 1165-1169 [PMID: 32402056 DOI: 10.1001/jamacardio.2020.2159]

136 **Gruttadauria S**; Italian Board of Experts in Liver Transplantation (I-BELT) Study Group, The Italian Society of Organ Transplantation (SITO). Preliminary Analysis of the Impact of the Coronavirus Disease 2019 Outbreak on Italian Liver Transplant Programs. *Liver Transpl* 2020; **26**: 941-944 [PMID: 32378325 DOI: 10.1002/lt.25790]

137 **Raszeja-Wyszomirska J**, Wójcicki M, Milkiewicz P. Outcomes of COVID19 in patients after liver transplantation: a singlecenter experience. *Pol Arch Intern Med* 2021; **131** [PMID: 34664491 DOI: 10.20452/pamw.16090]

138 **McDonald I**, Murray SM, Reynolds CJ, Altmann DM, Boyton RJ. Comparative systematic review and meta-analysis of reactogenicity, immunogenicity and efficacy of vaccines against SARS-CoV-2. *NPJ Vaccines* 2021; **6**: 74 [PMID: 33986272 DOI: 10.1038/s41541-021-00336-1]

139 **Polack FP**, Thomas SJ, Kitchin N, Absalon J, Gurtman A, Lockhart S, Perez JL, Pérez Marc G, Moreira ED, Zerbini C, Bailey R, Swanson KA, Roychoudhury S, Koury K, Li P, Kalina WV, Cooper D, Frenck RW Jr, Hammitt LL, Türeci Ö, Nell H, Schaefer A, Ünal S, Tresnan DB, Mather S, Dormitzer PR, Şahin U, Jansen KU, Gruber WC; C4591001 Clinical Trial Group. Safety and Efficacy of the BNT162b2 mRNA Covid-19 Vaccine. *N Engl J Med* 2020; **383**: 2603-2615 [PMID: 33301246 DOI: 10.1056/NEJMoa2034577]

140 **Baden LR**, El Sahly HM, Essink B, Kotloff K, Frey S, Novak R, Diemert D, Spector SA, Rouphael N, Creech CB, McGettigan J, Khetan S, Segall N, Solis J, Brosz A, Fierro C, Schwartz H, Neuzil K, Corey L, Gilbert P, Janes H, Follmann D, Marovich M, Mascola J, Polakowski L, Ledgerwood J, Graham BS, Bennett H, Pajon R, Knightly C, Leav B, Deng W, Zhou H, Han S, Ivarsson M, Miller J, Zaks T; COVE Study Group. Efficacy and Safety of the mRNA-1273 SARS-CoV-2 Vaccine. *N Engl J Med* 2021; **384**: 403-416 [PMID: 33378609 DOI: 10.1056/NEJMoa2035389]

141 **Sadoff J**, Gray G, Vandebosch A, Cárdenas V, Shukarev G, Grinsztejn B, Goepfert PA, Truyers C, Fennema H, Spiessens B, Offergeld K, Scheper G, Taylor KL, Robb ML, Treanor J, Barouch DH, Stoddard J, Ryser MF, Marovich MA, Neuzil KM, Corey L, Cauwenberghs N, Tanner T, Hardt K, Ruiz-Guiñazú J, Le Gars M, Schuitemaker H, Van Hoof J, Struyf F, Douoguih M; ENSEMBLE Study Group. Safety and Efficacy of Single-Dose Ad26.COV2.S Vaccine against Covid-19. *N Engl J Med* 2021; **384**: 2187-2201 [PMID: 33882225 DOI: 10.1056/NEJMoa2101544]

142 **Kumar D**, Blumberg EA, Danziger-Isakov L, Kotton CN, Halasa NB, Ison MG, Avery RK, Green M, Allen UD, Edwards KM, Miller G, Michaels MG; AST Infectious Diseases Community of Practice. Influenza vaccination in the organ transplant recipient: review and summary recommendations. *Am J Transplant* 2011; **11**: 2020-2030 [PMID: 21957936 DOI: 10.1111/j.1600-6143.2011.03753.x]

143 **Lindemann M**, Zaslavskaya M, Fiedler M, Wilde B, Heinemann FM, Heinold A, Horn PA, Witzke O. Humoral and Cellular Responses to a Single Dose of Fendrix in Renal Transplant Recipients with Non-response to Previous Hepatitis B Vaccination. *Scand J Immunol* 2017; **85**: 51-57 [PMID: 27763680 DOI: 10.1111/sji.12497]

144 **Friedrich P**, Sattler A, Müller K, Nienen M, Reinke P, Babel N. Comparing Humoral and Cellular Immune Response Against HBV Vaccine in Kidney Transplant Patients. *Am J Transplant* 2015; **15**: 3157-3165 [PMID: 26137874 DOI: 10.1111/ajt.13380]

145 **Rabinowich L**, Grupper A, Baruch R, Ben-Yehoyada M, Halperin T, Turner D, Katchman E, Levi S, Houri I, Lubezky N,

Shibolet O, Katchman H. Low immunogenicity to SARS-CoV-2 vaccination among liver transplant recipients. *J Hepatol* 2021; **75**: 435-438 [PMID: 33892006 DOI: 10.1016/j.jhep.2021.04.020]

146 **Grupper A**, Rabinowich L, Schwartz D, Schwartz IF, Ben-Yehoyada M, Shashar M, Katchman E, Halperin T, Turner D, Goykhman Y, Shibolet O, Levy S, Houri I, Baruch R, Katchman H. Reduced humoral response to mRNA SARS-CoV-2 BNT162b2 vaccine in kidney transplant recipients without prior exposure to the virus. *Am J Transplant* 2021; **21**: 2719-2726 [PMID: 33866672 DOI: 10.1111/ajt.16615]

147 **Itzhaki Ben Zadok O**, Shaul AA, Ben-Avraham B, Yaari V, Ben Zvi H, Shostak Y, Pertzov B, Eliakim-Raz N, Abed G, Abuhazira M, Barac YD, Mats I, Kramer MR, Aravot D, Kornowski R, Ben-Gal T. Immunogenicity of the BNT162b2 mRNA vaccine in heart transplant recipients - a prospective cohort study. *Eur J Heart Fail* 2021; **23**: 1555-1559 [PMID: 33963635 DOI: 10.1002/ejhf.2199]

148 **Havlin J**, Svorcova M, Dvorackova E, Lastovicka J, Lischke R, Kalina T, Hubacek P. Immunogenicity of BNT162b2 mRNA COVID-19 vaccine and SARS-CoV-2 infection in lung transplant recipients. *J Heart Lung Transplant* 2021; **40**: 754-758 [PMID: 34120839 DOI: 10.1016/j.healun.2021.05.004]

149 **Pollard AJ**, Bijker EM. A guide to vaccinology: from basic principles to new developments. *Nat Rev Immunol* 2021; **21**: 83-100 [PMID: 33353987 DOI: 10.1038/s41577-020-00479-7]

150 **Furian L**, Russo FP, Zaza G, Burra P, Hartzell S, Bizzaro D, Di Bello M, Di Bella C, Nuzzolese E, Agnolon C, Florman S, Rana M, Lee JH, Kim Y, Maggiore U, Maltzman JS, Cravedi P. Differences in Humoral and Cellular Vaccine Responses to SARS-CoV-2 in Kidney and Liver Transplant Recipients. *Front Immunol* 2022; **13**: 853682 [PMID: 35493446 DOI: 10.3389/fimmu.2022.853682]

151 **Angyal A**, Longet S, Moore SC, Payne RP, Harding A, Tipton T, Rongkard P, Ali M, Hering LM, Meardon N, Austin J, Brown R, Skelly D, Gillson N, Dobson SL, Cross A, Sandhar G, Kilby JA, Tyerman JK, Nicols AR, Spegarova JS, Mehta H, Hornsby H, Whitham R, Conlon CP, Jeffery K, Goulder P, Frater J, Dold C, Pace M, Ogbe A, Brown H, Ansari MA, Adland E, Brown A, Chand M, Shields A, Matthews PC, Hopkins S, Hall V, James W, Rowland-Jones SL, Klenerman P, Dunachie S, Richter A, Duncan CJA, Barnes E, Carroll M, Turtle L, de Silva TI; PITCH Consortium. T-cell and antibody responses to first BNT162b2 vaccine dose in previously infected and SARS-CoV-2-naive UK health-care workers: a multicentre prospective cohort study. *Lancet Microbe* 2022; **3**: e21-e31 [PMID: 34778853 DOI: 10.1016/S2666-5247(21)00275-5]

152 **Mak WA**, Koeleman JGM, van der Vliet M, Keuren F, Ong DSY. SARS-CoV-2 antibody and T cell responses one year after COVID-19 and the booster effect of vaccination: A prospective cohort study. *J Infect* 2022; **84**: 171-178 [PMID: 34896516 DOI: 10.1016/j.jinf.2021.12.003]

153 **Woodruff MC**, Ramonell RP, Nguyen DC, Cashman KS, Saini AS, Haddad NS, Ley AM, Kyu S, Howell JC, Ozturk T, Lee S, Suryadevara N, Case JB, Bugrovsky R, Chen W, Estrada J, Morrison-Porter A, Derrico A, Anam FA, Sharma M, Wu HM, Le SN, Jenks SA, Tipton CM, Staitieh B, Daiss JL, Ghosn E, Diamond MS, Carnahan RH, Crowe JE Jr, Hu WT, Lee FE, Sanz I. Extrafollicular B cell responses correlate with neutralizing antibodies and morbidity in COVID-19. *Nat Immunol* 2020; **21**: 1506-1516 [PMID: 33028979 DOI: 10.1038/s41590-020-00814-z]

154 **Wadei HM**, Gonwa TA, Leoni JC, Shah SZ, Aslam N, Speicher LL. COVID-19 infection in solid organ transplant recipients after SARS-CoV-2 vaccination. *Am J Transplant* 2021; **21**: 3496-3499 [PMID: 33890410 DOI: 10.1111/ajt.16618]

155 **Del Bello A**, Abravanel F, Marion O, Couat C, Esposito L, Lavayssière L, Izopet J, Kamar N. Efficiency of a boost with a third dose of anti-SARS-CoV-2 messenger RNA-based vaccines in solid organ transplant recipients. *Am J Transplant* 2022; **22**: 322-323 [PMID: 34331842 DOI: 10.1111/ajt.16775]

156 **Hall VG**, Ferreira VH, Ku T, Ierullo M, Majchrzak-Kita B, Chaparro C, Selzner N, Schiff J, McDonald M, Tomlinson G, Kulasingam V, Kumar D, Humar A. Randomized Trial of a Third Dose of mRNA-1273 Vaccine in Transplant Recipients. *N Engl J Med* 2021; **385**: 1244-1246 [PMID: 34379917 DOI: 10.1056/NEJMc2111462]

157 **Food and Drug Administration**. Coronavirus (COVID-19) Update: FDA Authorizes Additional Vaccine Dose for Certain Immunocompromised Individuals. Available from: https://www.fda.gov/news-events/press-announcements/coronavirus-covid-19-update-fda-authorizes-additional-vaccine-dose-certain-immunocompromised

158 **Buchwald UK**, Pirofski L. Immune therapy for infectious diseases at the dawn of the 21st century: the past, present and future role of antibody therapy, therapeutic vaccination and biological response modifiers. *Curr Pharm Des* 2003; **9**: 945-968 [PMID: 12678861 DOI: 10.2174/1381612033455189]

159 **Tu ZH**, Jin PB, Chen DY, Chen ZY, Li ZW, Wu J, Lou B, Zhang BS, Zhang L, Zhang W, Liang TB. Evaluating the Response and Safety of Inactivated COVID-19 Vaccines in Liver Transplant Recipients. *Infect Drug Resist* 2022; **15**: 2469-2474 [PMID: 35592105 DOI: 10.2147/IDR.S359919]

160 **Cornberg M**, Buti M, Eberhardt CS, Grossi PA, Shouval D. EASL position paper on the use of COVID-19 vaccines in patients with chronic liver diseases, hepatobiliary cancer and liver transplant recipients. *J Hepatol* 2021; **74**: 944-951 [PMID: 33563499 DOI: 10.1016/j.jhep.2021.01.032]

161 **Fix OK**, Blumberg EA, Chang KM, Chu J, Chung RT, Goacher EK, Hameed B, Kaul DR, Kulik LM, Kwok RM, McGuire BM, Mulligan DC, Price JC, Reau NS, Reddy KR, Reynolds A, Rosen HR, Russo MW, Schilsky ML, Verna EC, Ward JW, Fontana RJ; AASLD COVID-19 Vaccine Working Group. American Association for the Study of Liver Diseases Expert Panel Consensus Statement: Vaccines to Prevent Coronavirus Disease 2019 Infection in Patients With Liver Disease. *Hepatology* 2021; **74**: 1049-1064 [PMID: 33577086 DOI: 10.1002/hep.31751]

162 **Centers for Disease Control and Prevention**. Coronavirus Disease 2019 (COVID-19). Available from: https://www.cdc.gov/coronavirus/2019-ncov/index.html

163 **Case JB**, Mackin S, Errico JM, Chong Z, Madden EA, Whitener B, Guarino B, Schmid MA, Rosenthal K, Ren K, Dang HV, Snell G, Jung A, Droit L, Handley SA, Halfmann PJ, Kawaoka Y, Crowe JE Jr, Fremont DH, Virgin HW, Loo YM, Esser MT, Purcell LA, Corti D, Diamond MS. Resilience of S309 and AZD7442 monoclonal antibody treatments against infection by SARS-CoV-2 Omicron lineage strains. *Nat Commun* 2022; **13**: 3824 [PMID: 35780162 DOI: 10.1038/s41467-022-31615-7]

World Journal of Clinical Cases

Submit a Manuscript: https://www.f6publishing.com

World J Clin Cases 2023 April 6; 11(10): 2160-2167

DOI: 10.12998/wjcc.v11.i10.2160

ISSN 2307-8960 (online)

MINIREVIEWS

Treatment of stellate ganglion block in diseases: Its role and application prospect

Jing-Jing Deng, Cai-Ling Zhang, Dian-Wen Liu, Tao Huang, Jian Xu, Qing-Yan Liu, Yue-Nong Zhang

Specialty type: Medicine, research and experimental

Provenance and peer review: Invited article; Externally peer reviewed.

Peer-review model: Single blind

Peer-review report's scientific quality classification

Grade A (Excellent): 0
Grade B (Very good): B
Grade C (Good): C
Grade D (Fair): 0
Grade E (Poor): 0

P-Reviewer: Ait Addi R, Morocco; Shirini K, Iran

Received: November 14, 2022
Peer-review started: November 14, 2022
First decision: February 17, 2023
Revised: February 24, 2023
Accepted: March 14, 2023
Article in press: March 14, 2023
Published online: April 6, 2023

Jing-Jing Deng, Jian Xu, Qing-Yan Liu, Yue-Nong Zhang, Department of Surgery and Anesthesia, The Third Affiliated Hospital of Sun Yat-sen University Yuedong Hospital, Meizhou 514700, Guangdong Province, China

Cai-Ling Zhang, Department of Anesthesiology, Meizhou Hospital of Traditional Chinese Medicine, Meizhou 514700, Guangdong Province, China

Dian-Wen Liu, Department of Anesthesiology, Shangqiu Maternal and Children Health Care Hospital, Shangqiu 476000, Henan Province, China

Tao Huang, Department of Anesthesiology, Fengshun Hospital of Traditional Chinese Medicine, Meizhou 514700, Guangdong Province, China

Corresponding author: Yue-Nong Zhang, MD, Chief Doctor, Doctor, Department of Surgery and Anesthesia, The Third Affiliated Hospital of Sun Yat-sen University Yuedong Hospital, No. 124 Park North Road, Xinxian Town, Meizhou, 514700, Guangdong Province, China. 36856665@qq.com

Abstract

The stellate ganglion (SG), as a type of sympathetic ganglion, consists of the sixth and seventh cervical vertebrae and the first thoracic sympathetic ganglia. SG block (SGB) is a minimally invasive injection that aims to inject low-concentration local anesthetics to induce a broad sympathetic blocking effect near the SG. There have been no changes and progress in the clinical application of SGB since the 1830s due to several potential risks, including hematoma from blood vessel injury, hoarseness from recurrent laryngeal nerve injury, and cardiopulmonary arrest. The feasibility and safety of SGB have greatly improved since the appearance of ultrasound-guided SGB. In recent years, SGB has been widely applied in the field of non-anesthesiology sedation, with significant therapeutic effects on pain, immunological diseases, somnipathy, psychological disorders, arrhythmias, and endocrine diseases. The present study reviews the present application of SGB in clinical practice.

Key Words: Echocardiography; Pain; Immunological diseases; Somnipathy; Psychological disorders; Arrhythmias; Endocrine diseases

Core Tip: Several reviews in the literature have contributed to the therapeutic effect of stellate ganglion block (SGB). The present study reviews the anatomical structure and mechanism of SGB, the advantages of ultrasound localization, and the application of SGB in the treatment of painful diseases, immunological diseases, somnipathy, psychological diseases, arrhythmias, and endocrine diseases.

Citation: Deng JJ, Zhang CL, Liu DW, Huang T, Xu J, Liu QY, Zhang YN. Treatment of stellate ganglion block in diseases: Its role and application prospect. *World J Clin Cases* 2023; 11(10): 2160-2167
URL: https://www.wjgnet.com/2307-8960/full/v11/i10/2160.htm
DOI: https://dx.doi.org/10.12998/wjcc.v11.i10.2160

INTRODUCTION

Development of the stellate ganglion block

Stellate ganglion block (SGB) has been applied in clinical practice for nearly a century to relieve pain-related syndromes, and treat vascular defects of the upper extremities. Since the 1940s, SGB has been performed to treat sympathetic pain conditions[1]. Over these years, through further exploration and investigation, the technique of blocking the cervical sympathetic nerve has been gradually established as a clinical treatment for certain diseases.

Anatomy of the stellate ganglion and stellate ganglion block

The stellate ganglion (SG), which is also known as the cervical and thoracic sympathetic ganglion, is a part of the cervical sympathetic trunk. The SG consists of the sixth (C6) and seventh (C7) cervical vertebrae, and the first thoracic sympathetic ganglia, which lies in front of the first costal neck, and extends to the inferior of the transverse process of C7. The preganglionic fiber of the SG crosses over the sympathetic chain of the neck, and the postganglionic fiber locates in the medial of the scalenus, outside of the longus cervicalis, esophagus and trachea, and the anterior aspect of the transverse process[2]. The SG provides sympathetic inputs to the ipsilateral upper limbs, chest, face and head. SGB aims to inject low-concentration local anesthetics near the SG, which can reversibly block the preganglionic and postganglionic fibers, and innervated area. Furthermore, SGB blocks the sympathetic nerves in the head, neck and upper limbs by acting on both pre-and post-ganglionic fibers[3]. The SGB procedure is described, as follows:

Before the procedure, patients who underwent SGB were instructed to relax and take the supine position, and the patient's neck was extended. Then, local anesthetics were injected between C6 and C7 to the surface of the long muscle of the neck, and the syringe was pulled out. The duration of the whole procedure was not more than 30 min. The success of the SGB was based on the following: Appearance of Horner's syndrome, elevated facial temperature, eardrum congestion, and nasal congestion. The efficacy of the SGB was traditionally evaluated by the emergence of Horner's findings, which included unilateral pupil reduction, ptosis, and the absence of sweat on the face. The perfusion index (PI) is the ratio of pulsating and non-pulsating signals. This was automatically and non-invasively measured to assess the pulse oxygen saturation. The use of the PI in regional anesthesia can improve the success rate of SGB, because this is a rapid, non-invasive and simple method that can provide early measurable data, when compared to Horner's sign and other similar clinical signs[4,5]. Therefore, the PI can be used as an indicator to evaluate the therapeutic efficacy of SGB. Previous studies have revealed that ultrasound-guided SGB can increase blood flow and reduce the vascular resistance of the arm. The decrease in vascular resistance and increase in blood flow of the arm may be significant indicators for a successful SGB. Thus, pulsed-wave Doppler can be used to monitor the success of SGB[6]. Doytchinova *et al*[7] reported that the sympathetic nerve activity of the skin can reflect the sympathetic nerve activity emitted by the SG, and that the sympathetic nerve activity on the skin surface can be measured by high-filtered electrocardiography. Compared to the subjective judgment of Horner's syndrome, the PI and cutaneous sympathetic nerve activity are more objective indicators to assess the success of SGB, which are presently hot research topics. However, the presence of Horner's syndrome is still more commonly used as an indicator of success of SGB in clinical practice.

Mechanism of the stellate ganglion block

SGB inhibits cardiovascular movement, glandular secretion, muscle tension, bronchial contraction, and pain conduction innervated by sympathetic nerve fibers from the SG distribution area. These can be taken as an advantage when treating some relative diseases involved in the head, neck, upper limb, shoulder and heart. The SG has extensive connections to the cerebral cortex, hypothalamus, amygdala and hippocampus[8]. Furthermore, SGB can regulate the autonomic nervous system, cardiovascular system, endocrine system, and immune system through the hypothalamic mechanism.

Ultrasound-guided stellate ganglion block

The SG is small in size, has a complex anatomical location, is adjacent to several important organs, and has more vessels and nerves. In addition, there is a certain proportion of anatomical variation in the population. Blind puncture of the SGB may easily lead to several severe complications, including hematoma caused by blood vessel injury and hoarseness caused by laryngeal recurrent nerve injury, which may lead to permanent Horner's syndrome. With the development of visualization technology, the positioning technology for SGB guided by X-ray, computed tomography, or ultrasound has become more accurate, greatly reducing complications. Compared to blind puncture, ultrasound-guided SGB greatly reduces the risk of SG puncture, and improves the success rate of the puncture. To date, ultrasound guidance has become the preferred method for SGB, when compared to blind and fluoroscopic guidance. The ideal position of the puncture during ultrasound-guided SGB should be anterolateral to the longus cervical muscle, and extend to the prevertebral fascia (in order to prevent diffusion along the carotid sheath), but should be shallow to the fascia that covers the longus cervical muscle (in order to prevent the injection of muscle material) (Figure 1). Thus, ultrasound-guided SGB improves the quality of the block, and requires fewer local anesthetics, when compared to traditional blind techniques [9]. In addition, ultrasound-guided SGB can improve surgical safety by allowing for the direct observation of vascular structures (inferior thyroid artery, common carotid artery, internal jugular vein) and soft tissue (thyroid, esophagus and nerve roots). The success rate of ultrasound-guided SGB can presently reach as high as 98%, and this can successfully prevent the involvement of the common carotid artery, internal jugular vein, and vagus nerve[10]. Therefore, ultrasound-guided SGB technology is bound to be rapidly popularized.

Stellate ganglion block and pain disorders

Although the mechanism of pain remains unclear, the application of SGB in the treatment of various types of pain remains feasible. Studies have revealed that the application of SGB to alleviate most of the symptoms of migraine in the treatment of migraine[11,12] and cluster headache[13] may be attributed to the inhibition of sympathetic overactivity or weakening of vascular inflammatory response. Furthermore, a previous study reported that ultrasound-guided SGB can effectively relieve cervical headache[14]. A successful case of SGB in the treatment of refractory tension headache was reported in 2019[15]. Furthermore, early SGB combined with antiviral drugs is a very effective treatment approach for herpes zoster or postherpetic neuralgia in the head, face and neck[16,17]. This significantly reduced the intensity and duration of acute pain, and reduced the incidence of postherpetic neuralgia. The therapeutic mechanism of SGB may be involved in improving the blood supply to the head and neck, inhibiting the hyperexcitability of sympathetic nerves, and reducing the synthesis and release of vasoconstricting substances, such as nitric oxide and prostaglandin. Similar cases on the treatment of SGB have also been reported for postoperative pain in head and neck cancer[18], peripheral arterial pain (Raynaud's disease[19], Burger's disease, diabetic vascular disease, arterial embolism, *etc.*), and neoplastic pain (pain after breast cancer resection)[20,21]. In pathophysiology, a part of the complex regional pain syndrome (CRPS) is considered to be correlated to autonomic disorders in the affected limb and the overreaction to catecholamines, which can lead to pain. SGB has been traditionally regarded as an important means for the diagnosis and treatment of CRPS-type I and -type II[22]. In the fourth edition of the American guidelines for the diagnosis and treatment of CRPS, the sympathetic block represented by SGB is listed as the first-line diagnosis and treatment. In a review of the results for CRPS, interventional pain physicians often performed SGB to relieve pain in the upper extremity of CRPS patients[23]. Therefore, SGB can be used as an effective treatment for pain diseases, which may provide underestimated clinical results.

Stellate ganglion block and Immune diseases

The immune system is the main defender of the body, and is involved in regulating the stability of the internal environment. The neurotransmitter released from the nerve terminus can diffuse and act on immune cells. For example, norepinephrine (NE) suppresses the immune response, acetylcholine and enkephalin enhances the immune response, and beta-endorphin sometimes promotes or suppresses the immune response. Furthermore, nerves can produce immune factors in certain circumstances. SGB can inhibit hyperactive sympathetic nerve activity, reduce levels of catecholamine and cortisol, weaken the stress response of the body, promote the recovery of human immune function, and further inhibit inflammation. A study[24] reported that ultrasound-guided SGB reduced the fluctuation of circulation, the concentration of peripheral adrenaline and cortisol, and the postoperative gastrointestinal dysfunction and stress response of patients who underwent radical resection of colorectal cancer. In addition, the anxiety during the perioperative period was relieved, and the recovery of gastrointestinal function after the operation was promoted. Furthermore, SGB can improve splenic $CD4^+$ T cell function after hemorrhagic shock, indicating its therapeutic effect on immunological diseases[25]. By blocking the sympathetic nerves that innervate the gastrointestinal system, SGB can expand gastrointestinal vessels, increase the blood supply, enhance gastrointestinal motility, and significantly relieve the symptoms of chronic ulcerative colitis[26].

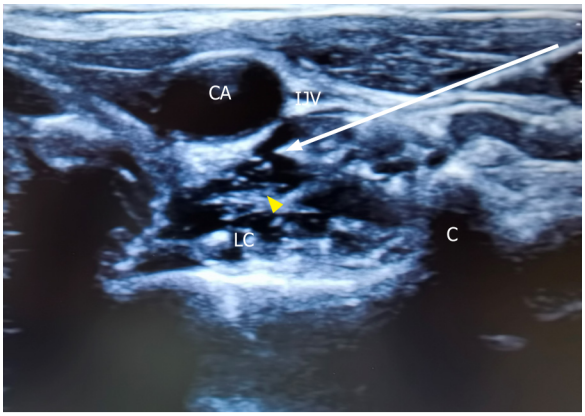

DOI: 10.12998/wjcc.v11.i10.2160

Figure 1 Ultrasound-guided stellate ganglion block at cervical 6 Level. CA: Carotid artery; LC: Longus colli; IJV: Vena jugularis interna; C: Cervical 6 anterior tubercle of the transverse process; Yellow triangle: Stellate ganglion; White arrow: Needle for piercing.

Stellate ganglion block and sleep disorders

Somnipathy is closely correlated to melatonin, which is periodically secreted by the pineal gland throughout the day and night, affecting the body's sleep and awakening. In a study on sleep deprivation in rats with SGB, right SGB improved the dysfunction of spatial learning and memory in sleep-deprived rats. The mechanism may be attributed to the reduction in hippocampal apoptosis and inflammation in sleep deprived rats. Sleep deprivation is associated with decreased cognitive function mediated by melatonin, which inhibits the hypothalamic-pituitary-gonadal axis, reduces gonadotropin-releasing hormone levels, and reduces the levels of androgens, estrogens and progesterone by directly acting on the gonads. The various effects of SGB may exhibit similar effects on the therapeutic intervention mediated by melatonin[27]. A report on the application of SGB in a patient with excessive daytime sleepiness (EDS) revealed[28] that SGB produced obvious and desirable effects on EDS, which may be attributed to the stabilization of the autonomic nervous system by reversing the imbalance of the autonomic nervous system. Somnipathy is generally treated with drugs in clinical practice, which has certain disadvantages. Therefore, SGB treatment can be applied as an alternative treatment for patients.

Stellate ganglion block and psychological diseases

At present, more treatments, such as drugs and psychotherapy, are being performed for psychological diseases. However, there are still some difficulties. Therefore, more therapeutic measures are urgently needed to make up for the shortage. Kerzner *et al*[29] were the first to present a case on SGB in the treatment of depression in 1947 through a systematic review of prospects for clinical research on SGB for psychiatric disorders. These authors noted that the SGB improved the mood and occasional feelings of euphoria of the patients. In addition, the first case reported on the treatment of posttraumatic stress disorder (PTSD) by SGB in 1990 entailed the application of SGB in the treatment of a 15-year-old female with reflex sympathetic dystrophy and PTSD. SGB reduced the pain, and significantly improved the PTSD-related symptoms. These early studies are crucial, because these paves the way for subsequent researches on SGB as a treatment approach for mental illness. PTSD is defined by the Diagnostic and Statistical Manual of Mental Disorders (DSM-V) as pathological trauma and stress disorders that occur in individuals following severe trauma. The lifetime prevalence of PTSD is approximately 3.9%. There are four types of symptoms: Re-experiencing the traumatic event, avoidance, persistent negative thoughts or feelings, and arousal and response associated with trauma[30]. In a multicentre randomized clinical trial of SGB for the treatment of PTSD[31], the incidence for active-duty military personnel with PTSD significantly decreased after eight weeks of SGB treatment. Therefore, SGB has been used to treat this disorder, providing long-term relief of sympathetic overactivity, and relieving the anxiety symptoms associated with PTSD.

Stellate ganglion block and arrhythmias

For the treatment of ventricular arrhythmias (VAs; such as congenital long QT syndrome, catecholamine-dependent polymorphous ventricular tachycardia, atrial fibrillation, and sinus tachycardia) and ischemic cardiomyopathy, SGB has frequently been taken as an adjuvant therapy. However, this is only carefully selected when adverse drug reactions could not be tolerated by the patient[32]. Refractory VAs are often exacerbated by increased sympathetic nerve tone in patients. Multiple studies[33-37] have revealed that SGB is associated with the dramatic decrease in VA burden, and these studies strongly recommend the use of SGB in refractory VA, offering potential promise for its wider use in high-risk populations. A randomized controlled trial observed the effect of SGB treatment to perioperative atrial fibrillation in patients undergoing lobectomy before surgery, and the results

revealed that right SGB before surgery can significantly reduce the incidence of intraoperative and postoperative atrial fibrillation[38]. Furthermore, in a case where a patient with myocardial infarction failed to recover the autonomic rhythm after cardiopulmonary resuscitation in a hospital, the autonomic rhythm was recovered, and sufficient neural activity and hemodynamic recovery were observed after using SGB[39]. This may have been due to the inhibition of the release of NE, reduction in content of catecholamine, prolonged atrial effective refractory period, and increased in stability of cardiac electrophysiology induced by SGB. In addition, SGB can restrain the stress reaction, reduce the production of inflammatory markers, expand the blood flow of the coronary artery, and improve the oxygen supply of cardiomyocytes. Therefore, SGB, as the ending treatment for arrhythmia, provides a basis for the treatment of patients with malignant arrhythmia.

Stellate ganglion block and endocrine diseases

The nervous system is closely correlated to the endocrine system, and the extension of sympathetic nerve tension can affect the secretion of various endocrine glands. SGB can reverse the autonomic imbalance caused by the increase in sympathetic tone, and affect the neuroendocrine system. Vasomotor symptoms (VMS), which are also known as hot flashes and night sweats, are common symptoms of menopause. These are associated with reduced quality of life in perimenopausal and postmenopausal women. SGB is a safe and effective treatment for women who are unable to use or choose not to use hormone therapy. Furthermore, SGB reduces and lengthens the nerve growth factor (NGF), and reduces the synthesis and release of NE in the brain, and content of NGF in the brain, thereby alleviating the hot flashes, CRPS and PTSD symptoms. Moreover, SGB inhibits the secretion of sweat glands and regulates body temperature, thereby alleviating symptoms. Rahimzadeh *et al*[40] reported that SGB is as effective as paroxetine in reducing the frequency of hot flashes in breast cancer survivors, and improving sleep quality, with minimal side effects and acceptable tolerance in patients. Several clinical cases have also reported that SGB can be used to treat hyperhidrosis, and the mechanism was considered to be mainly correlated to the decrease in sweating function due to the vasodilation and sympathetic nerve block in the dominant part of the SG[41]. Lee *et al*[42] also support the use of SGB for VMS in perimenopausal and postmenopausal women, especially for patients with severe symptoms and difficulty in receiving more conservative treatment.

The occurrence of diabetes mellitus (DM) is not only correlated to primary insulin dysfunction and metabolic syndrome, but also correlated to mental stress, dietary factors, and other factors that reduce insulin secretion, and/or increase the secretion of glucagon and other glucose-raising hormones through the neuroendocrine system. Diabetic cardiovascular autonomic neuropathy (DCAN) is a common complication of type 1 and type 2 DM, with high morbidity and mortality. SG neurons are usually surrounded by satellite glial cells (SGC). Axotomy, inflammation, and other injuries can activate SGC in the primary sensory ganglia. The P2Y12 receptor is expressed in SGC, and may be involved in the bidirectional communication with neuron-glial cells. Furthermore, the P2Y12 receptor may play an important role in the occurrence of diabetic cardiovascular complications, while the P2Y12 receptor in the SG plays a crucial role in DCAN. SGB can significantly improve the autonomic nervous regulation function in diabetic patients[43]. Furthermore, it has also been shown that SGB can reduce inflammation and improve nerve function during ischemic stroke in diabetic rats[44]. Therefore, SGB can increase perioperative safety, and reduce the risk of cardiac events in patients with type 2 DM.

Stellate ganglion block and refractory diseases

Medically unexplained symptoms (MUS) are defined as somatic symptoms that cannot be reasonably explained by any organic disease. A patient with MUS would have a good therapeutic effect after SGB [45], suggesting that repeated SGB may be effective for modulating nerves and reducing sympathetic activity. When Xu and Zhang[46] performed SGB on a patient who suffered from hypothyroidism, Hashimoto's encephalopathy, cerebral infarction, and frequent premature ventricular beats, the patient presented with significantly improved sleep quality and a restored sinus rhythm after treatment. This may be correlated to the improvement in central and peripheral nerve functions induced by SGB, which maintains the body's autonomic nervous activity, endocrine potency, and immune function. After recovering from coronavirus disease 2019 (COVID-19), a large proportion of symptomatic and asymptomatic patients would develop long-term COVID syndromes, which are also known as the acute sequelae of severe acute respiratory syndrome coronavirus 2 infection. According to the clinical case definition of the World Health Organization, long-term COVID-19 symptoms may include fatigue, orthostatic intolerance, rapid resting heart rate, shortness of breath, brain fog, sleep disturbances, fever, gastrointestinal symptoms, loss of smell, taste disorders, anxiety, and depression. In a latest medical report[47], long-term COVID-19 symptoms, including taste, smell and fatigue, were significantly improved in two patients after planetary ganglion block. This may be due to the involvement of SGB in the central sympathetic nerve adjustment, which increases cerebral blood flow, and re-balances the interaction between the nervous system and immune system. Therefore, SGB can be considered when conventional treatment is ineffective, or when there is no better treatment plan.

CONCLUSION

The present review reported the clinical application of SGB in the field of pain disease, autoimmune disease, somnipathy, psychological disease, arrhythmia and endocrine diseases, which is minimally invasive, and can easily be accepted by patients. This can provide an effective treatment plan for disease treatment, which is not widely recognized by relevant specialists at present. Therefore, it was considered that SGB has a broad application prospect, and that it is necessary to carry out more multidisciplinary cooperation to promote the use of SGB. The mechanism of action of SGB needs to be further studied for its application to a wider range of fields, providing more theoretical bases for its safety and effectiveness.

FOOTNOTES

Author contributions: Deng JJ and Zhang CL composed the manuscript; Liu DW and Huang T collected and sorted out the literature; Xu J and Liu QY edited and polished the manuscript; Zhang YN designed the outline and edited the manuscript; All authors have read and approved the final manuscript.

Conflict-of-interest statement: All the authors report no relevant conflicts of interest for this article.

Country/Territory of origin: China

ORCID number: Yue-Nong Zhang 0000-0002-2318-3204.

S-Editor: Li L
L-Editor: A
P-Editor: Li L

REFERENCES

1 **New Progress in Stellate Ganglion Block**. Foreign Language Science and Technology Journal Database Medicine and Health 2021. [DOI: 10.47939/mh.v2i12.136]
2 **Gunduz OH**, Kenis-Coskun O. Ganglion blocks as a treatment of pain: current perspectives. *J Pain Res* 2017; **10**: 2815-2826 [PMID: 29276402 DOI: 10.2147/JPR.S134775]
3 **Piraccini E**, Munakomi S, Chang KV. Stellate Ganglion Blocks. 2022 Aug 9. In: StatPearls [Internet]. Treasure Island (FL): StatPearls Publishing; 2022 Jan- [PMID: 29939575]
4 **Şahin ÖF**, Tarıkçı Kılıç E, Aksoy Y, Kaydu A, Gökçek E. The importance of perfusion index monitoring in evaluating the efficacy of stellate ganglion blockage treatment in Raynaud's disease. *Libyan J Med* 2018; **13**: 1422666 [PMID: 29350104 DOI: 10.1080/19932820.2017.1422666]
5 **Buono RD**, Pascarella G, Costa F, Agrò FE. The perfusion index could early predict a nerve block success: A preliminary report. *Saudi J Anaesth* 2020; **14**: 442-445 [PMID: 33447184 DOI: 10.4103/sja.SJA_171_20]
6 **Kim MK**, Yi MS, Park PG, Kang H, Lee JS, Shin HY. Effect of Stellate Ganglion Block on the Regional Hemodynamics of the Upper Extremity: A Randomized Controlled Trial. *Anesth Analg* 2018; **126**: 1705-1711 [PMID: 29049072 DOI: 10.1213/ANE.0000000000002528]
7 **Doytchinova A**, Hassel JL, Yuan Y, Lin H, Yin D, Adams D, Straka S, Wright K, Smith K, Wagner D, Shen C, Salanova V, Meshberger C, Chen LS, Kincaid JC, Coffey AC, Wu G, Li Y, Kovacs RJ, Everett TH 4th, Victor R, Cha YM, Lin SF, Chen PS. Simultaneous noninvasive recording of skin sympathetic nerve activity and electrocardiogram. *Heart Rhythm* 2017; **14**: 25-33 [PMID: 27670627 DOI: 10.1016/j.hrthm.2016.09.019]
8 **Lipov E**, Gluncic V, Lukić IK, Candido K. How does stellate ganglion block alleviate immunologically-linked disorders? *Med Hypotheses* 2020; **144**: 110000 [PMID: 32758866 DOI: 10.1016/j.mehy.2020.110000]
9 **Li J**, Pu S, Liu Z, Jiang L, Zheng Y. Visualizing stellate ganglion with US imaging for guided SGB treatment: A feasibility study with healthy adults. *Front Neurosci* 2022; **16**: 998937 [PMID: 36161183 DOI: 10.3389/fnins.2022.998937]
10 **Zhang L**, Li X, Yao J, Wulan N. Ultrasound-guided stellate ganglion block: A visual teaching method. *Asian J Surg* 2022; **45**: 1596-1597 [PMID: 35361549 DOI: 10.1016/j.asjsur.2022.03.034]
11 **Moon S**, Lee J, Jeon Y. Bilateral stellate ganglion block for migraine: A case report. *Medicine (Baltimore)* 2020; **99**: e20023 [PMID: 32358380 DOI: 10.1097/MD.0000000000020023]
12 **Hou J**, Pu S, Xu X, Lu Z, Wu J. Real-time ultrasound-guided stellate ganglion block for migraine: an observational study. *BMC Anesthesiol* 2022; **22**: 78 [PMID: 35331152 DOI: 10.1186/s12871-022-01622-8]
13 **Zacharias NA**, Karri J, Garcia C, Lachman LK, Abd-Elsayed A. Interventional Radiofrequency Treatment for the

Sympathetic Nervous System: A Review Article. *Pain Ther* 2021; **10**: 115-141 [PMID: 33433856 DOI: 10.1007/s40122-020-00227-8]

14 **Yu Q**, Zheng E, Li X, Ding X. Ultrasound image guided lateral cervical approach to stellate ganglion block for cervical headache. *Neurosci Lett* 2020; **735**: 135139 [PMID: 32522602 DOI: 10.1016/j.neulet.2020.135139]

15 **Ueshima H**. A successful case of stellate ganglion block for difficult therapy of refractory tension headache. *J Clin Anesth* 2019; **54**: 149 [PMID: 30553218 DOI: 10.1016/j.jclinane.2018.12.007]

16 **Wang C**, Yuan F, Cai L, Lu H, Chen G, Zhou J. Ultrasound-Guided Stellate Ganglion Block Combined with Extracorporeal Shock Wave Therapy on Postherpetic Neuralgia. *J Healthc Eng* 2022; **2022**: 9808994 [PMID: 35035867 DOI: 10.1155/2022/9808994]

17 **Lin CS**, Lin YC, Lao HC, Chen CC. Interventional Treatments for Postherpetic Neuralgia: A Systematic Review. *Pain Physician* 2019; **22**: 209-228 [PMID: 31151330]

18 **Sharbel D**, Singh P, Blumenthal D, Sullivan J, Dua A, Albergotti WG, Groves M, Byrd JK. Preoperative Stellate Ganglion Block for Perioperative Pain in Lateralized Head and Neck Cancer: Preliminary Results. *Otolaryngol Head Neck Surg* 2020; **162**: 87-90 [PMID: 31791223 DOI: 10.1177/0194599819889688]

19 **Punj J**, Garg H, Gomez G, Bagri NK, Thakur JP, Singh LD, Jain D, Darlong V, Pandey R. Sympathetic Blocks for Raynaud's Phenomena in Pediatric Rheumatological Disorders. *Pain Med* 2022; **23**: 1211-1216 [PMID: 35135008 DOI: 10.1093/pm/pnac015]

20 **Abbas DN**, Reyad RM. Thermal Versus Super Voltage Pulsed Radiofrequency of Stellate Ganglion in Post-Mastectomy Neuropathic Pain Syndrome: A Prospective Randomized Trial. *Pain Physician* 2018; **21**: 351-362 [PMID: 30045592]

21 **Salman AS**, Abbas DN, Elrawas MM, Kamel MA, Mohammed AM, Abouel Soud AH, Abdelgalil AS. Postmastectomy pain syndrome after preoperative stellate ganglion block: a randomized controlled trial. *Minerva Anestesiol* 2021; **87**: 786-793 [PMID: 33938674 DOI: 10.23736/S0375-9393.21.15112-0]

22 **Yalamuru B**, Weisbein J, Pearson ACS, Kandil ES. Minimally-invasive pain management techniques in palliative care. *Ann Palliat Med* 2022; **11**: 947-957 [PMID: 34412500 DOI: 10.21037/apm-20-2386]

23 **Shim H**, Rose J, Halle S, Shekane P. Complex regional pain syndrome: a narrative review for the practising clinician. *Br J Anaesth* 2019; **123**: e424-e433 [PMID: 31056241 DOI: 10.1016/j.bja.2019.03.030]

24 **Xie A**, Zhang X, Ju F, Li W, Zhou Y, Wu D. Effects of the Ultrasound-Guided Stellate Ganglion Block on Hemodynamics, Stress Response, and Gastrointestinal Function in Postoperative Patients with Colorectal Cancer. *Comput Intell Neurosci* 2022; **2022**: 2056969 [PMID: 35875745 DOI: 10.1155/2022/2056969]

25 **Li Y**, Du HB, Jiang LN, Wang C, Yin M, Zhang LM, Zhang H, Zhao ZA, Liu ZK, Niu CY, Zhao ZG. Stellate Ganglion Block Improves the Proliferation and Function of Splenic CD4 + T Cells Through Inhibition of Posthemorrhagic Shock Mesenteric Lymph-Mediated Autophagy. *Inflammation* 2021; **44**: 2543-2553 [PMID: 34533673 DOI: 10.1007/s10753-021-01523-x]

26 **Lipov E**, Candido K. Efficacy and safety of stellate ganglion block in chronic ulcerative colitis. *World J Gastroenterol* 2017; **23**: 3193-3194 [PMID: 28533676 DOI: 10.3748/wjg.v23.i17.3193]

27 **Dai D**, Zheng B, Yu Z, Lin S, Tang Y, Chen M, Ke P, Zheng C, Chen Y, Wu X. Right stellate ganglion block improves learning and memory dysfunction and hippocampal injury in rats with sleep deprivation. *BMC Anesthesiol* 2021; **21**: 272 [PMID: 34749669 DOI: 10.1186/s12871-021-01486-4]

28 **Xu J**, Liu Q, Huang T, Zhong R, Zhang Y. Stellate ganglion block rectifies excessive daytime sleepiness: a case report. *J Int Med Res* 2022; **50**: 3000605221118681 [PMID: 35983675 DOI: 10.1177/03000605221118681]

29 **Kerzner J**, Liu H, Demchenko I, Sussman D, Wijeysundera DN, Kennedy SH, Ladha KS, Bhat V. Stellate Ganglion Block for Psychiatric Disorders: A Systematic Review of the Clinical Research Landscape. *Chronic Stress (Thousand Oaks)* 2021; **5**: 24705470211055176 [PMID: 34901677 DOI: 10.1177/24705470211055176]

30 **Antonelli-Salgado T**, Ramos-Lima LF, Machado CDS, Cassidy RM, Cardoso TA, Kapczinski F, Passos IC. Neuroprogression in post-traumatic stress disorder: a systematic review. *Trends Psychiatry Psychother* 2021; **43**: 167-176 [PMID: 33872477 DOI: 10.47626/2237-6089-2020-0099]

31 **Rae Olmsted KL**, Bartoszek M, Mulvaney S, McLean B, Turabi A, Young R, Kim E, Vandermaas-Peeler R, Morgan JK, Constantinescu O, Kane S, Nguyen C, Hirsch S, Munoz B, Wallace D, Croxford J, Lynch JH, White R, Walters BB. Effect of Stellate Ganglion Block Treatment on Posttraumatic Stress Disorder Symptoms: A Randomized Clinical Trial. *JAMA Psychiatry* 2020; **77**: 130-138 [PMID: 31693083 DOI: 10.1001/jamapsychiatry.2019.3474]

32 **Witt CM**, Bolona L, Kinney MO, Moir C, Ackerman MJ, Kapa S, Asirvatham SJ, McLeod CJ. Denervation of the extrinsic cardiac sympathetic nervous system as a treatment modality for arrhythmia. *Europace* 2017; **19**: 1075-1083 [PMID: 28340164 DOI: 10.1093/europace/eux011]

33 **Fudim M**, Boortz-Marx R, Ganesh A, Waldron NH, Qadri YJ, Patel CB, Milano CA, Sun AY, Mathew JP, Piccini JP. Stellate ganglion blockade for the treatment of refractory ventricular arrhythmias: A systematic review and meta-analysis. *J Cardiovasc Electrophysiol* 2017; **28**: 1460-1467 [PMID: 28833780 DOI: 10.1111/jce.13324]

34 **Ganesh A**, Qadri YJ, Boortz-Marx RL, Al-Khatib SM, Harpole DH Jr, Katz JN, Koontz JI, Mathew JP, Ray ND, Sun AY, Tong BC, Ulloa L, Piccini JP, Fudim M. Stellate Ganglion Blockade: an Intervention for the Management of Ventricular Arrhythmias. *Curr Hypertens Rep* 2020; **22**: 100 [PMID: 33097982 DOI: 10.1007/s11906-020-01111-8]

35 **Wittwer ED**, Radosevich MA, Ritter M, Cha YM. Stellate Ganglion Blockade for Refractory Ventricular Arrhythmias: Implications of Ultrasound-Guided Technique and Review of the Evidence. *J Cardiothorac Vasc Anesth* 2020; **34**: 2245-2252 [PMID: 31919004 DOI: 10.1053/j.jvca.2019.12.015]

36 **Tian Y**, Wittwer ED, Kapa S, McLeod CJ, Xiao P, Noseworthy PA, Mulpuru SK, Deshmukh AJ, Lee HC, Ackerman MJ, Asirvatham SJ, Munger TM, Liu XP, Friedman PA, Cha YM. Effective Use of Percutaneous Stellate Ganglion Blockade in Patients With Electrical Storm. *Circ Arrhythm Electrophysiol* 2019; **12**: e007118 [PMID: 31514529 DOI: 10.1161/CIRCEP.118.007118]

37 **Fudim M**, Qadri YJ, Waldron NH, Boortz-Marx RL, Ganesh A, Patel CB, Podgoreanu MV, Sun AY, Milano CA, Tong BC, Harpole DH Jr, Mathew JP, Piccini JP. Stellate Ganglion Blockade for the Treatment of Refractory Ventricular Arrhythmias. *JACC Clin Electrophysiol* 2020; **6**: 562-571 [PMID: 32439042 DOI: 10.1016/j.jacep.2019.12.017]

38 **Ouyang R**, Li X, Wang R, Zhou Q, Sun Y, Lei E. [Effect of ultrasound-guided right stellate ganglion block on perioperative atrial fibrillation in patients undergoing lung lobectomy: a randomized controlled trial]. *Braz J Anesthesiol* 2020; **70**: 256-261 [PMID: 32532550 DOI: 10.1016/j.bjan.2020.03.007]

39 **Margus C**, Correa A, Cheung W, Blaikie E, Kuo K, Hockensmith A, Kinas D, She T. Stellate Ganglion Nerve Block by Point-of-Care Ultrasonography for Treatment of Refractory Infarction-Induced Ventricular Fibrillation. *Ann Emerg Med* 2020; **75**: 257-260 [PMID: 31564380 DOI: 10.1016/j.annemergmed.2019.07.026]

40 **Rahimzadeh P**, Imani F, Nafissi N, Ebrahimi B, Faiz SHR. Comparison of the effects of stellate ganglion block and paroxetine on hot flashes and sleep disturbance in breast cancer survivors. *Cancer Manag Res* 2018; **10**: 4831-4837 [PMID: 30464591 DOI: 10.2147/CMAR.S173511]

41 **Park JH**, Kim R, Na SH, Kwon SY. Effect of botulinum toxin in stellate ganglion for craniofacial hyperhidrosis: a case report. *J Int Med Res* 2021; **49**: 3000605211004213 [PMID: 33788638 DOI: 10.1177/03000605211004213]

42 **Lee YS**, Wie C, Pew S, Kling JM. Stellate ganglion block as a treatment for vasomotor symptoms: Clinical application. *Cleve Clin J Med* 2022; **89**: 147-153 [PMID: 35232827 DOI: 10.3949/ccjm.89a.21032]

43 **Guo J**, Sheng X, Dan Y, Xu Y, Zhang Y, Ji H, Wang J, Xu Z, Che H, Li G, Liang S. Involvement of P2Y(12) receptor of stellate ganglion in diabetic cardiovascular autonomic neuropathy. *Purinergic Signal* 2018; **14**: 345-357 [PMID: 30084083 DOI: 10.1007/s11302-018-9616-5]

44 **Li TT**, Wan Q, Zhang X, Xiao Y, Sun LY, Zhang YR, Liu XN, Yang WC. Stellate ganglion block reduces inflammation and improves neurological function in diabetic rats during ischemic stroke. *Neural Regen Res* 2022; **17**: 1991-1997 [PMID: 35142688 DOI: 10.4103/1673-5374.335162]

45 **Huang Y**, Xu J, Liu Q, Zeng Z, Zhang Y. Stellate ganglion block successfully relieved medically unexplained chronic pain: a case report. *J Int Med Res* 2022; **50**: 3000605221086735 [PMID: 35301893 DOI: 10.1177/03000605221086735]

46 **Xu Y**, Zhang Y. Treatment of multiple physiological and psychological disorders in one patient with stellate ganglion block: a case report. *J Int Med Res* 2021; **49**: 300060520985645 [PMID: 33472461 DOI: 10.1177/0300060520985645]

47 **Liu LD**, Duricka DL. Stellate ganglion block reduces symptoms of Long COVID: A case series. *J Neuroimmunol* 2022; **362**: 577784 [PMID: 34922127 DOI: 10.1016/j.jneuroim.2021.577784]

World Journal of Clinical Cases

Submit a Manuscript: https://www.f6publishing.com

World J Clin Cases 2023 April 6; 11(10): 2168-2180

DOI: 10.12998/wjcc.v11.i10.2168

ISSN 2307-8960 (online)

MINIREVIEWS

Clinical application of SARS-CoV-2 antibody detection and monoclonal antibody therapies against COVID-19

Jin Sun, Zhen-Dong Yang, Xiong Xie, Li Li, Hua-Song Zeng, Bo Gong, Jian-Qiang Xu, Ji-Hong Wu, Bei-Bei Qu, Guo-Wei Song

Specialty type: Medicine, research and experimental

Provenance and peer review: Unsolicited article; Externally peer reviewed.

Peer-review model: Single blind

Peer-review report's scientific quality classification

Grade A (Excellent): 0
Grade B (Very good): B
Grade C (Good): C
Grade D (Fair): 0
Grade E (Poor): E

P-Reviewer: Kumar I, India; Nassar G, France; Wijaya JH, Indonesia

Received: December 7, 2022
Peer-review started: December 7, 2022
First decision: January 5, 2023
Revised: January 17, 2023
Accepted: March 10, 2023
Article in press: March 10, 2023
Published online: April 6, 2023

Jin Sun, Bei-Bei Qu, Medical Innovation Research Office, Sinopharm Gezhouba Central Hospital, Third Clinical Medical College of Three Gorges University, Yichang 443002, Hubei Province, China

Zhen-Dong Yang, Department of Respiratory, Beijing Jindu Children Hospital, Beijing 102208, China

Zhen-Dong Yang, Innovative Medicine Working Committee of the Chinese Society of Water Resources and Electric Power Medical Science and Technology, Beijing 100053, China

Zhen-Dong Yang, Xiong Xie, Department of Pediatrics, Sinopharm Gezhouba Central Hospital, Third Clinical Medical College of Three Gorges University, Yichang 443002, Hubei Province, China

Li Li, Department of Intensive Care, First Clinical Medical College of Three Gorges University, Yichang 443000, Hubei Province, China

Hua-Song Zeng, Department of Allergy Immunology and Rheumatology, Guangzhou Children's Hospital, Women's and Children's Medical Center Affiliated with Guangzhou Medical University, Guangzhou 510000, Guangdong Province, China

Bo Gong, Central Laboratory, Shanghai Changning District Maternal and Child Health, Maternal and Child Health Hospital Affiliated with Shanghai East China Normal University, Shanghai 210000, China

Jian-Qiang Xu, Department of Respiratory and Critical Care Medicine, Sinopharm Gezhouba Central Hospital, Third Clinical Medical College of Three Gorges University, Yichang 443002, Hubei Province, China

Ji-Hong Wu, School of Clinical Medicine, Beijing Tsinghua Chang Gung Hospital Affiliated to Tsinghua University, Beijing 102218, China

Guo-Wei Song, Department of Emergency, Children's Hospital Affiliated with Beijing Capital Institute of Pediatrics, Beijing 100020, China

Corresponding author: Zhen-Dong Yang, Chief Physician, Professor, Department of Respiratory, Beijing Jindu Children Hospital, No. 308 Huilongguan East Street, Changping district, Beijing 102208, China. yzd886@sina.com

Abstract

The purpose of this study was to investigate the clinical application of severe acute respiratory distress syndrome coronavirus-2 (SARS-CoV-2) specific antibody detection and anti-SARS-CoV-2 specific monoclonal antibodies (mAbs) in the treatment of coronavirus infectious disease 2019 (COVID-19). The dynamic changes of SARS-CoV-2 specific antibodies during COVID-19 were studied. Immunoglobulin M (IgM) appeared earlier and lasted for a short time, while immunoglobulin G (IgG) appeared later and lasted longer. IgM tests can be used for early diagnosis of COVID-19, and IgG tests can be used for late diagnosis of COVID-19 and identification of asymptomatic infected persons. The combination of antibody testing and nucleic acid testing, which complement each other, can improve the diagnosis rate of COVID-19. Monoclonal anti-SARS-CoV-2 specific antibodies can be used to treat hospitalized severe and critically ill patients and non-hospitalized mild to moderate COVID-19 patients. COVID-19 convalescent plasma, highly concentrated immunoglobulin, and anti-SARS-CoV-2 specific mAbs are examples of anti-SARS-CoV-2 antibody products. Due to the continuous emergence of mutated strains of the novel coronavirus, especially omicron, its immune escape ability and infectivity are enhanced, making the effects of authorized products reduced or invalid. Therefore, the optimal application of anti-SARS-CoV-2 antibody products (especially anti-SARS-CoV-2 specific mAbs) is more effective in the treatment of COVID-19 and more conducive to patient recovery.

Key Words: SARS-CoV-2 antibody; Detection; COVID-19; Monoclonal antibody; Clinical application

Core Tip: Immunoglobulin M testing can be used for early diagnosis of coronavirus infectious disease 2019 (COVID-19). Immunoglobulin G testing can be used for the late diagnosis of COVID-19 and the identification of asymptomatic patients. The combination of antibody and nucleic acid testing has improved the diagnosis rate of COVID-19. The continuous emergence of mutated strains of the novel coronavirus, especially omicron, enhances its immune escape ability and infectivity, making the effects of authorized products reduced or invalid. The specific monoclonal antibodies against severe acute respiratory distress syndrome coronavirus-2 authorized by the United States Food and Drug Administration are more beneficial for the treatment of COVID-19 and patient recovery.

Citation: Sun J, Yang ZD, Xie X, Li L, Zeng HS, Gong B, Xu JQ, Wu JH, Qu BB, Song GW. Clinical application of SARS-CoV-2 antibody detection and monoclonal antibody therapies against COVID-19. *World J Clin Cases* 2023; 11(10): 2168-2180
URL: https://www.wjgnet.com/2307-8960/full/v11/i10/2168.htm
DOI: https://dx.doi.org/10.12998/wjcc.v11.i10.2168

INTRODUCTION

Since the coronavirus infectious disease 2019 (COVID-19) pandemic began in 2019, it has had a devastating impact on communities across the globe. So far, severe acute respiratory distress syndrome coronavirus-2 (SARS-CoV-2) has mutated several times with the identification of the following variant strains: Alpha (B.1.1.7) was first discovered in the United Kingdom in late December 2020; Beta (B.1.351) was first reported in South Africa in December 2020; Gamma was first reported in Brazil in early January 2021; Delta (B.1.617.2) was first reported in India in December 2020; Omicron (B.1.1.529) was first reported in South Africa in November 2021 and quickly spread to countries around the world due to its increased infectivity. Omicron's spike protein has exhibited more than 30 changes that enhanced viral capacity for immune escape. Studies have shown that Omicron shows a 13-fold increase in viral infectivity, and is 2.8 times more infectious than the delta variant, and previously approved monoclonal antibodies (mAbs) against SARS-CoV-2 are less effective against this variant. Furthermore, vaccines against SARS-CoV-2 are less effective in prevention of Omicron infection, and treatment is more challenging[1]. For these reasons, Omicron has become a major variant of concern in many countries, and many mutants of this strain have been identified (*e.g.*, BA.1, BA.2, BA.3, BA.4, BA.5, and XBB.1.5). The XBB1.5 mutant is becoming increasingly frequent in the United States, and is still defined as an Omicron lineage variant[2]. It remains to be seen whether this specific mutant strain will worsen the ongoing COVID-19 pandemic.

As of January 13, 2023, there have been over 660 million confirmed COVID-19 cases and over 6.7 million deaths reported to the World Health Organization (WHO)[3]. The timely and accurate diagnosis of COVID-19 is necessary for controlling the spread of the virus, initiating prompt treatment, and rehabilitating patients. The primary method for diagnosing COVID-19 is *via* detection of SARS-CoV-2 RNA using polymerase chain reaction (PCR). However, the accuracy of PCR analysis depends on many factors, such as the quality of the reagents, the quality and method of sample collection (oropharynx, nasopharynx, lower respiratory tract, and swabs), and the skill level of the operator. Changes in the above factors may lead to either false negative or false positive results. PCR has many additional limitations: long testing time (average 2–3 h); complex technology; easy contamination of samples; high cost; and requirement for a laboratory with strict biosafety certification and trained technicians. These issues pose serious challenges in screening for COVID-19, achieving early diagnosis, implementing isolation of infected patients, and starting treatment. As such, new diagnostic tools are urgently needed to help compensate for the shortcomings of PCR[4].

The detection of SARS-CoV-2 specific antibodies (SSAs) can aid in the diagnosis of COVID-19. Additionally, asymptomatic infected people and those with milder symptoms can also be identified, helping to calculate the population infection rate more accurately. Large scale serological maps of a population can also be used in epidemiological investigations to provide a better understanding of the pandemic status, help to control the spread of the virus, and aid in treating patients efficiently. Antibody detection and nucleic acid detection can complement each other and improve the rate of accurate COVID-19 diagnosis. Indeed, serological detection technology has been widely used in the clinic[4].

SARS-CoV-2 induces an excessive and prolonged cytokine/chemokine response, known as a cytokine storm, in some infected individuals, particularly those with severe COVID-19 disease. Cytokine storm can cause acute respiratory distress syndrome or multiple organ dysfunction, which can lead to deterioration or death. Timely control of early cytokine storm with administration of immunomodulators and cytokine antagonists can reduce inflammatory cell infiltration into the lung and limit the disease. Suppressing cytokine storm effectively is important to prevent deterioration in COVID-19 patients and key to preventing death associated with this disease[5].

mAbs are immunoglobulins that are produced from single-cell lineages and have a high affinity for their target cells. When used as antiviral therapy, neutralizing Abs (Nabs) aid in the development of passive antiviral immunity. The viral genome is susceptible to mutation, resulting in the emergence of viral escape variants that render the virus resistant to specific mAbs. Several mAbs were combined into cocktails to improve efficacy and overcome the phenomenon of viral escape. The United States Food and Drug Administration (FDA) has granted emergency use authorization (EUA) for 4 mAbs. As new SARS-CoV-2 variants emerge, the clinical efficacy of previously approved mAbs is being called into question, prompting clinicians and scientists to reconsider and pursue the development of new drugs to treat COVID-19. The FDA has also made numerous updates to previously authorized recommended drugs, rendering them unavailable or making conditional recommendations.

Convalescent plasma (CP), highly concentrated immunoglobulin (HIG), and anti-SSA (ASSA) products have been recommended or conditionally recommended for use in clinical research and healthcare facilities. For patients with mild to moderate COVID-19 who are at risk of progressing to critical illness, the FDA has approved the use of single or combined mAbs. Two mAbs can be combined in some cases to interfere with SARS-CoV-2 for post-exposure prophylaxis. Tocilizumab, an anti-interleukin-6 inhibitor, and baricitinib, a Janus kinase inhibitor, have received EUA from the FDA and are recommended for patients with severe COVID-19 who are receiving corticosteroids[6]. Tocilizumab reduces mortality in critically ill patients and also the number of days without need for artificial organ support; the recommended dose is 8 mg tocilizumab per kg body weight (up to 800 mg) in 1 h intravenous infusion, with a second dose repeated 12 to 24 h later if needed[7]. The combination of interleukin-6 blockers in particular may be more beneficial[8]. Baricitinib, an antiviral drug, is used to treat severe or critical COVID-19 and has been shown to reduce mortality, hospitalization, and the need for mechanical ventilation[9,10]. Corticosteroids are usually only used as a last resort in COVID-19 patients who are critically ill; routine use is generally not advised.

The purpose of this article is to discuss the clinical value of SSA detection technologies and ASSA in the treatment of COVID-19.

DYNAMIC CHANGES IN SARS-COV-2 SPECIC ANTIBODIES

Antibodies are reactive substances (immunoglobulins) produced by the immune system to combat invading pathogenic microorganisms and can bind to specific pathogens. SSAs are mainly composed of immunoglobulin M (IgM) and immunoglobulin G (IgG) Abs. IgM Abs are produced during the early stages of infection and can enhance the ability of the innate immune system to phagocytose, agglutinate, and kill pathogens. IgG is the main type of Ab in plasma (approximately 75%) and is involved in Ab-dependent cellular phagocytosis and complement-mediated cytotoxicity against bacterial and viral infections. Abs positivity is indirect evidence of infection caused by pathogenic microorganisms.

Detecting the levels of IgM and IgG can also reveal the immune function of the body, which is an important factor contributing to public health and has great clinical significance.

After infection by a pathogen, certain steps associated with the production of Abs can be used to diagnose and treat disease. In a COVID-19 study involving 34 adults, Abs were assessed starting at 2 wk after disease onset. After 3 wk, the Ab tests of all patients were positive. The average levels of IgG and IgM were 112.40 AU/mL and 322.80 AU/mL (reference range < 10 AU/mL), respectively. After 4 wk, the level of IgM began to decline, and an average value of 147.92 AU/mL was recorded; the average level of IgG increased to 157.01 AU/mL. After 5 wk, the average level of IgM continued to fall, reaching 78.03 AU/mL, and 2 patients were negative for IgM; the IgG levels of all patients increased, reaching an average of 163.56 AU/mL. At the end of week 7, the study was terminated. Two patients were negative for IgM, and the average IgM level dropped to 21.83 AU/mL; all patients were positive for IgG, and their average titer increased to 167.16 AU/mL. A high level of IgM indicates that the infection is in the acute phase, and relatively high IgM levels lasting longer than 1 mo indicate a longer viral replication time. IgG Abs appear later than IgM Abs, persist longer, and are present at a higher level, indicating that the humoral immune response acts to defend the host against SARS-CoV-2 infection[11].

A study by Lee *et al*[12] showed that IgM was detected on the day 5 of infection, and the longest duration of detection was 42 d after the onset of disease. In another patient, IgG was also detected by day 5 after the onset of disease. In most cases, once positive, IgG remains positive. The duration of PCR positivity is related to the Abs response and clinical manifestations. In patients with detectable symptoms and IgM Abs positivity, nucleic acid-based tests can quickly become negative[12]. Another study analyzed 38 cases of COVID-19 and found the highest level of viral RNA in sputum samples (92.3%) in the early stage of the disease (7 d after disease onset); the next highest viral RNA level was detected in pharyngeal swabs (69.2%). In this study, Abs were detected in fewer positive cases (IgM 23.0% and IgG 53.8%). Abs titers increased to 50.0% (IgM) and 87.5% (IgG) after 8 d, and Abs detection was found to be easier than viral RNA detection. After 15 d, the detection rate of viral RNA was 52.2%, indicating that Abs detection could be useful for auxiliary diagnosis. For patients who have achieved clearance of the virus, PCR testing is not suitable. The initial immune response is marked by an increase in the IgM level and the detection of IgM indicates that the infection is recent; as such, IgM can be used for the early diagnosis of COVID-19. IgG is produced after IgM and persists longer; it is a diagnostic indicator of a secondary infection or previous exposure[13].

Timilsina *et al*[14], described an electrochemical device that can rapidly and quantitatively detect Abs against SARS-CoV-2 in clinic. This method was shown to be simple to use, economic, sensitive (100% sensitivity and specificity), and fast (10 min). Furthermore, it required blood samples of only 1.5 μL, and Abs could even be detected in dry blood spots. This test can be operated on-site and *via* remote application, and may have great promise in the future of COVID-19 testing[14].

The monumental achievement in creating an effective vaccine against SARS-CoV-2 presents a new challenge for Abs testing: can Abs produced by vaccination be distinguished from those produced by the real virus? How long do the Abs from the vaccine last? The answers to these questions are key to preparing for any future wave of the COVID-19 pandemic[15]. A schematic diagram of the dynamic changes in human antibody production after the initial infection (Figure 1).

Zamani *et al*[16] studied the kinetics of seroconversion in 118 hospitalized patients with COVID-19 (Table 1). The authors demonstrated the kinetics of seroconversion in COVID-19 patients, and showed that 83.5% of IgM and 36.8% of IgG patients who were originally positive were found to be negative within 3 mo after the onset of symptoms. These findings suggest that the retention time of anti-SARS-CoV-2 Abs could be used as a reference for SARS-CoV-2 prevention, control, and vaccine administration. No correlation was found between Abs titers and patient age at any time point. In addition, mean Abs levels at different times after the onset of clinical symptoms also did not exhibit a predilection for either sex.

ROLE OF SARS-COV-2 SPECIFIC ANTIBODIES IN COVID-19 SCREENING AND DIGNOSIS

Wu *et al*[17] performed COVID-19 screening on 1021 workers in the Recovery Work Group (RG) and 381 patients in the COVID-19 Non-Hospital Group (NHG), totaling 1402 subjects. Screening included nasopharyngeal swab nucleic acid detection, chest computed tomography (CT), and IgM and IgG Abs detection. In NHG, one case of nucleic acid was positive, as were IgM and IgG. Other patients' CT chest radiographs were normal, and the nucleic acid tests were negative. After being diagnosed with COVID-19, the positive patient was "cured." He was transferred to a hospital specializing in COVID-19 treatment after testing positive again. In RG, 98 (98/1021, 9.60%) patients were IgG positive, IgM negative, and nasopharyngeal swab PCR negative. In NHG, 39 cases (39/380, 10.3%) of nasopharyngeal swab samples were positive for IgG, negative for IgM, and negative by PCR. These findings suggest that 137 (98 + 39) patients had previously been infected with SARS-CoV-2. The IgG-positive patients had no suspicious symptoms and no history of COVID-19. None of these cases had previously been tested by PCR. In other words, the patients had recovered from asymptomatic infections discovered only through Abs screening[17].

Table 1 Seropositive rates of severe acute respiratory distress syndrome coronavirus-2-specific immunoglobulin G and immunoglobulin M at various time points after symptom onset

Days after symptom onset	IgM positivity rate (%)	IgG positivity rate (%)
0–5	44/118 (37.3)	71/118 (60.2)
6–15	36/55 (65.5)	44/55 (80.0)
16–25	48/70 (68.6)	56/70 (80.0)
26–35	26/56 (46.4)	2/56 (75.0)
36–95	17/95 (17.9)	56/95 (58.9)

IgG: Immunoglobulin G; IgM: Immunoglobulin M.

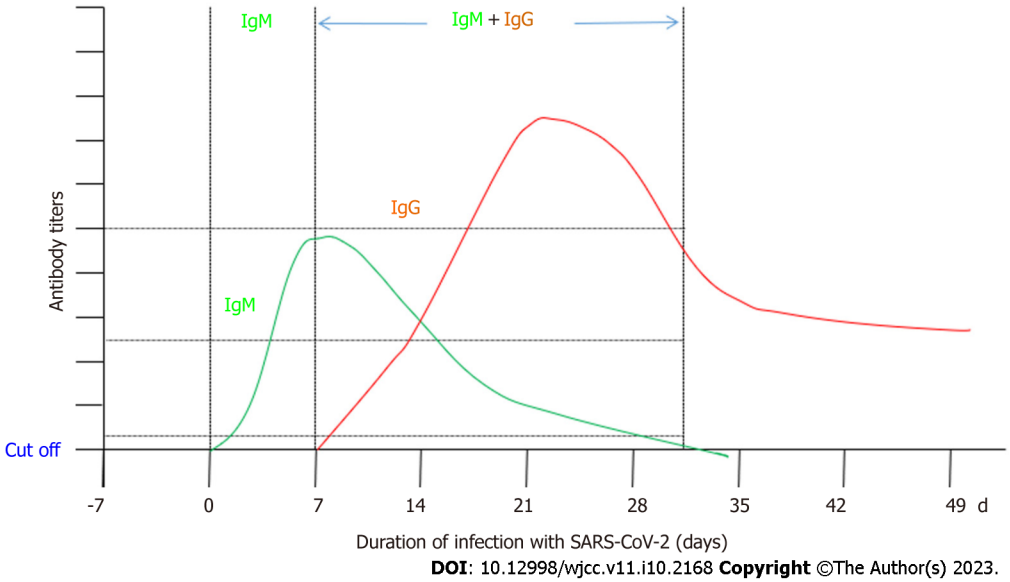

DOI: 10.12998/wjcc.v11.i10.2168

Figure 1 Schematic diagram of the dynamic changes in antibody production after initial infection with severe acute respiratory virus-2. Due to differences in data from analytical studies, these data are considered approximations only.

To determine the diagnostic efficacy of IgM and IgG Abs in suspected cases, Abs tests were conducted in 52 patients whose symptoms or CT imaging characteristics met the COVID-19 criteria but who had multiple consecutive negative PCR results. IgG or IgM Abs were positive in 4 patients. Reasonable speculation led to a diagnosis of COVID-19. Similarly, to determine the diagnostic efficacy of IgG and IgM tests for asymptomatic infections, the team conducted Ab screening in 164 close contacts, 16 of whom were positive for IgM or IgG. Among the 148 patients excluded by PCR 1 mo before the screening process, 7 were also positive for the Abs. These individuals had never experienced any symptoms, indicating that they were asymptomatic carriers who could not have been diagnosed by nucleic acid detection. Thus, increasing the frequency of IgM and IgG Abs testing could help to confirm the diagnosis of suspected cases and screen for asymptomatic individuals[18].

A comprehensive study found that the earliest IgM Abs appear within 5–7 d after infection with SARS-CoV-2[13]. Abs testing can provide results within 15 min, and the technique is simple and convenient, which is helpful for the rapid screening of febrile patients. In infected individuals, during the incubation period of the virus before the development of the disease, IgM is not produced and cannot be detected. Hence, the detection of Abs alone is not suitable for early screening. Abs testing can only play an auxiliary diagnostic role; the maintenance time of IgM is short, and IgM disappears by the end of the infection. IgM positivity is the only basis for the early diagnosis of an infection. IgG is produced 10–15 d after infection and is present for a long period after the disease course has ended. Furthermore, IgG can persist in the body, even in the blood, for a lifetime. A positive IgG Ab test can indicate a pathogenic infection. When the same pathogen is encountered, the specific IgG binds to the pathogen, reducing its activity and preventing it from binding to human cells. IgG can also rapidly activate the innate immune system, shortening immune response time and avoiding or reducing the recurrence of the disease. Abs detection is a practical method for conducting an epidemiological survey after an outbreak, despite the reported 10%–15% deviation. It has high sensitivity and can serve as a

valid metric for a long time after a disease is no longer present in an individual. Moreover, Abs detection can very accurately identify asymptomatic infected individuals and thereby helps determine the actual scale of the pandemic[17,18].

In a study of 173 patients, plasma samples (n = 535) were collected for the detection of total anti-SARS-CoV-2 Abs, IgG, and IgM. The dynamics of the antibody levels during disease progression were also analyzed. The seroconversion rates of IgG, IgM, and Abs were 64.7%, 82.7%, and 93.1%, respectively. The median seroconversion times of IgM, IgG, and Abs were 14 d, 12 d, and 11 d, respectively. One week after disease onset, the prevalence of antibodies in studied patients was less than 40%. From 15 d after onset, the prevalence increased starkly to 79.8% (IgG), 94.3% (IgM), and 100.0% (Abs). The detectability of RNA decreased from 66.7% (58/87) at day 7 to 45.5% (25/55) between 15 d and 39 d after the disease onset. Even in the early stages, the combined application of RNA and Abs detection can significantly improve the diagnosis rate of COVID-19 ($p < 0.001$)[19]. When rapid PCR testing for SARS-CoV-2 was not available, another study concluded that using rapid antigen-Abs combined testing improved detection accuracy, with a sensitivity of 91.2% and a specificity of 98.9%. The results of antigen and Abs testing can be used as a reliable substitute for PCR testing[20]. Clinical significance of the combined detection of SSA and SARS-CoV-2 RNA (Table 2).

ROLE OF ANTI-SARS-COV-2 SPECIFIC ANTIBODIES IN THE TREATMENT OF COVID-19

Therapeutic effect of convalescent plasma on COVID-19

Immunological studies have shown that Abs in CP can recognize antigenic determinants of pathogens, including those of viruses. These Abs can neutralize the virus, reduce the viral load, and prevent or cure disease. In other words, Abs can trigger and participate in a self-repairing process in the body. By providing Nabs, CP is a form of passive immunotherapy. The benefits of CP infusion in related diseases were first studied in the 20th century[21]. In the absence of specific treatments for emerging infectious diseases, CP therapy remains an important treatment method[22]. CP has been shown to be effective in treating patients with influenza A (H1N1)[23], severe acute respiratory syndrome[24], and Middle East respiratory syndrome[25].

On August 23, 2020, the United States FDA approved the emergency use of CP as a potential COVID-19 treatment. Plasma therapy, according to the FDA, can effectively reduce the severity or the duration of COVID-19 disease in some hospitalized patients, and the known potential benefits far outweigh the product's risks[26]. With the continuous emergence of SARS-CoV-2 variants, previously effective treatment methods have been called into question. Several other observational studies and randomized controlled trials have recently been reviewed by experts from the National Institutes of Health (NIH) in the United States[27-29]. In these studies, the efficacy of CP against COVID-19 was investigated in both outpatient and inpatient settings. The FDA updated the EUA of CP to treat COVID-19[30] on November 28, 2021. Only CP with high titers of SARS-CoV-2 Abs is thought to be effective in patients with COVID-19 who are immunocompromised (*i.e.* those who have recently received radiation, chemotherapy, or who have immunodeficiency disease) or have received immunosuppressive therapy[29], and the potential benefits to patients may outweigh the known potential risks. However, infusion of CP in immunocompetent COVID-19 patients is unlikely to be clinically beneficial, and its use in these patients is not advised.

The WHO treatment guidelines only recommend the use of CP in the research and clinical trial settings[31]. However, based on subgroup data analysis from several observational studies and randomized controlled trials[27-29], the NIH treatment guidelines still recommend that CP be used for COVID-19 patients with secondary or primary humoral immunodeficiency (*e.g.*, with agammaglobulinemia, hematological malignancies, solid organ transplant, or other immunodeficiency)[32,33]. In a subset of immunocompromised patients, some findings suggest that CP may provide benefits such as improved survival and/or more days without organ support when compared to placebo [odds ratio 1.51; 95 percent confidence interval(CI): 0.80–2.92][29].

In clinical practice, a high titer CP with a volume of 200 mL can be considered first, and the need to increase the dose can be determined based on the individual patient scenario. Past and current studies have demonstrated real-world clinical efficacy for the treatment of COVID-19 with CP[34-36] This suggests that high-level randomized controlled trials (RCTs) should be designed in the future to investigate the potential therapeutic effects of CP in the treatment of COVID-19.

The Infectious Diseases Society of America and the FDA have also re-evaluated CP for use in outpatients at risk of progression due to the lack of antiviral drugs, as the polyclonal nature of CP can render SARS-CoV-2 variants less able to escape immune defenses[37,38].

Therapeutic effect of highly concentrated immunoglobulin on COVID-19

HIG is a high-titer Abs preparation made up of anti-SARS-CoV-2 mAbs from multiple CP donors that is more concentrated than anti-SARS-CoV-2 Specific antibodies (ASSAs) from a single donor (the SARS-CoV-2 Abs titer is several times higher)[39].The preparation may work by inhibiting the virus and altering inflammation. Varicella zoster immunoglobulin has been used for varicella post-exposure

Table 2 Clinical significance of combined detection of severe acute respiratory distress syndrome coronavirus-2-specific antibodies and RNA

No.	Antibody assay		Nucleic acid detection	Clinical significance
	IgM	IgG		
1	+	+	+	During the active infection period, the body has a certain resistance to COVID-19 (persistent IgG has been produced)
2	+	-	+	The patient may be in the middle of the SARS-CoV-2 infection. The body's immune response produces IgM antibodies early in the disease course. IgG has not yet been produced, or the IgG level has not reached the limit of detection
3	-	+	+	The patient may be in the middle or late phase of the disease or may have a recurrent infection of SARS-CoV-2
4	-	-	+	This is the COVID-19 "window period", which usually lasts 2 wk
5	+	+	-	The patient is in the recovery phase of COVID-19. The virus has been cleared from the body, and IgM and IgG are positive. Alternatively, this may indicate that the nucleic acid test result was a false negative, and the patient is in the active phase of infection
6	+	-	-	IgM positivity indicates that the patient may be in the early stage of infection. Suspicious nucleic acid test results require repeated sampling and verification
7	±	-	-	This indicates that the patient is in the early stage of viral infection, and the viral load is very low. The patient is in the acute stage of COVID-19, and the body has not yet produced IgG. Alternatively, the result for IgM may have been an error caused by the presence of rheumatoid factor. One week later, the examination and diagnosis must be repeated based to evaluate for changes in IgM and IgG
8	-	+	-	The patient may have been infected with the virus in the past and has recovered; the virus has been cleared from the body. IgG can last for a long time, possibly even for life
9	-	-	-	The individual is healthy or in the incubation period of infection

IgM: Immunoglobulin M; IgG: Immunoglobulin G; COVID-19: Coronavirus infectious disease 2019; SARS-CoV-2: Severe acute respiratory distress syndrome coronavirus-2.

prophylaxis (PEP) in high-risk individuals, and cytomegalovirus immunoglobulin has been shown to be effective and safe for the prevention of post-transplant cytomegalovirus infection. However, clinical data on the treatment of COVID-19 with HIG are currently lacking[40].

Therapeutic effect of anti-SARS-CoV-2 specific antibodies against COVID-19

Spike protein (S), nucleocapsid protein, membrane protein, envelope protein, and auxiliary and nonstructural proteins are all encoded by the SARS-CoV-2 genome. S1 and S2 are thorn protein subtypes. S1 is binds to angiotensin-converting enzyme 2 receptors on host cells. It causes S2 to change conformation, fuses the viral and host cell membranes, and allows the virus to enter human cells[41]. Binding of spike protein by mAbs decreases SARS-CoV-2 infectivity, resulting in a therapeutic effect. Indeed, ASSAs have shown clinical efficacy in the treatment of SARS-CoV-2 infection[42].

Anti-SARS-CoV-2 monoclonal antibody for pre-exposure prophylaxis of SARS-CoV-2 infection

Experts recommend intramuscular tixagevimab plus cilgavimab (Evusheld) as SARS-CoV-2 pre-exposure prophylaxis (PrEP) for adults and adolescents (age ≥ 12 years and weight ≥ 40 kg) who have not been exposed to COVID-19. In patients with moderate to severe immunocompromise, the immune response to the COVID-19 vaccine may be insufficient, or vaccination with any available COVID-19 vaccine may not be complete[43]. Omicron mutant sensitivity to tixagevimab plus cilgavimab has been shown to be moderately reduced, but the regimen was still beneficial for PrEP prevention of infection by Omicron strains.

Anti-SARS-CoV-2 monoclonal antibodies for post-exposure prophylaxis of SARS-CoV-2 infection

Casirivimab plus imdevimab and bamlanivimab plus elesevimab are not recommended for PEP of SARS-CoV-2[42] in countries and regions where Omicron variant strains are prevalent as these strains are not susceptible to these drugs. Prior to Omicron, the FDA issued a EUA for this regimen, allowing PEP in people who are at high risk of SARS-CoV-2 infection and have a high risk of developing severe COVID-19 disease. This protocol should be made available for PEP of the individuals listed above in non-Omicron endemic countries and regions.

Anti-SARS-CoV-2 monoclonal antibodies for outpatient COVID-19 patients

To treat outpatients (age ≥ 12 years and weight ≥ 40 kg) with mild to moderate COVID-19 and high risk of clinical progression, the use of sotrovimab 500 mg as a single intravenous infusion within 10 d of symptom onset is recommended. Sotrovimab retains *in vitro* activity against Omicron variants and is

believed to benefit Omicron-infected patients clinically[44].

Experts do not recommend casirivimab plus imdevimab or bamlanivimab plus etesevimab because Omicron is not susceptible to these drugs. However, because the FDA issued EUA prior to the Omicron epidemic, these regimens can be used in countries and regions where Omicron is not endemic. The use of cascilimab plus imdevimab has also been halted in the United States due to Omicron variant insensitivity[45]. Cascilimab 600 mg plus imdevimab 600 mg administered as a single intravenous infusion were approved by the FDA prior to the spread of Omicron and is approved for the treatment of patients with mild to moderate COVID-19. The use of this protocol is supported by results from a phase 3 double-blind, randomized, placebo-controlled trial in outpatients with mild to moderate COVID-19[46]. This regimen can still be used in places where non-Omicron variants are prevalent.

Anti-SARS-CoV-2 monoclonal antibodies for COVID-19 hospitalized patients

In one study, 583 outpatients with mild to moderate COVID-19 were studied. Two hundred ninety-one subjects were randomly assigned to receive sotrovimab (500 mg IV) and 292 subjects received placebo. On day 29, the primary endpoint was the proportion of hospital stays longer than 24 h or death from any cause. Three patients (1%) in the sotrovimab group and 21 patients (7%) in the placebo group required hospitalization or died as a result of disease progression (relative risk reduction, 85%; 97.24%CI: 44-96; P = 0.002). On day 29, 1 patient in the placebo group died after being admitted to the intensive care unit. Adverse events were reported in 17% of patients in the sotrovimab group and 19% of patients in the placebo group during the safety assessment; the incidence of serious adverse events was lower in the sotrovimab group than in the placebo group (2% and 6%, respectively). Sostovizumab reduced the risk of COVID-19 exacerbations in high-risk patients with mild to moderate COVID-19[47].

The use of bamlanivimab plus etesevimab to treat COVID-19 has been halted in the United States because the Omicron variant has poor susceptibility to this mAb *in vitro*[45]. Prior to the emergence of the Omicron variant, the BLAZE-1 phase 3 clinical trial demonstrated that bamlanivimab plus etesevimab benefits patients with mild to moderate COVID-19 at risk of progression to severe disease with or without hospitalization[46]. The main SARS-CoV-2 strain currently introduced to China from abroad is Omicron BA.2. Pfizer's antiviral drug Paxlovid (nimatovir plus ritonavir) is recommended for adults and adolescents aged 12–17 years old, weight ≥ 40 kg. Paxlovid is given in cases of mild disease within 5 d of onset according to China's Protocol for Prevention and Control of Novel Coronavirus Infection (10th Ed)[48].

Anti-SARS-CoV-2 monoclonal antibodies for hospitalized patients with severe or critical COVID-19

ASSA are not currently approved for use in hospitalized patients with severe COVID-19; however, these products may see use in such patients through an expanded access plan. Casirivimab plus imdevimab is conditionally recommended for COVID-19 patients with severe or critical illness, and may also benefit seronegative patients. According to the RECOVERY trial, a credible subgroup effect suggests that casirivimab plus imdevimab may reduce mortality and days requiring mechanical ventilation in patients with seronegative status[31].

Relevant literature is summarized in Table 3[49-54]. Many therapeutic mAbs that were previously effective became ineffective in the face of the Omicron variant; studies of these are not included.

Safety of monoclonal antibodies in clinical application

In most studies, adverse events with the use of therapeutic mAbs were not serious (*e.g.*, nausea, diarrhea) and were mostly self-limiting. The most common adverse events were mild reactions, chills, headache, injection site pain, and bronchospasm. Serious adverse events were rare, and observed instances of shortness of breath may be associated with exacerbations of COVID-19 itself[37].

Limitations of this article

SARS-CoV-2 has been raging for nearly 3 years. In the past 2 years, the mutation of SARS-CoV-2 has become more and more frequent, and transmission speed is also faster, especially with the Omicron variant. Fortunately, Omicron is becoming less toxic. The mutation of the virus reduces the efficacy of existing therapeutic drugs, which can now only be applied in some special circumstances. This is the case of the use of CP or mAbs in the treatment of COVID-19. The FDA's EUAs for many drugs are require constant updates. As human efforts cannot keep up with the speed of Omicron mutation, we should redouble our efforts to proactively discover the pattern of SARS-CoV-2 mutation and finally defeat the novel coronavirus.

CONCLUSION

SSA detection technology is widely used in clinical practice. It can assist PCR nucleic acid in the diagnosis, screening, and tracking of infection in patients with COVID-19 (including mild and asymptomatic infections). Thus, it is valuable for public health and has many potential clinical applications[55].

Table 3 Sensitivity of Omicron variants to therapeutic monoclonal antibodies

mAb (s)	FDA EUA	Target on S	Omicron variant			
			BA.1	IC_{50}	BA.2	IC_{50}
Bamla/Etese	Yes	BRD or S	Reduction in activity *vs* control approximately 1000-fold (highly resistant)	> 10000 ng/mL	Reduction in activity *vs* control approximately 1000-fold (highly resistant)	> 10000 ng/mL
Casir/Imdev	Yes	BRD	Reduction in activity *vs* control approximately 1000-fold (highly resistant)	> 10000 ng/mL	Reduction in activity *vs* control approximately 1000-fold (highly resistant)	> 10000 ng/mL
Sotro	Yes	BRD	Median fold reduction in susceptibility 4.0 (IQR: 2.6 to 6.9)	Median 276 ng/mL (IQR: 163 to 423)	Median fold reduction in susceptibility 17 (IQR: 13 to 30)	Median 1250 ng/mL (IQR: 567 to 1456)
Cilag/Tixag	Yes	BRD	Median fold reduction in susceptibility 86 (IQR:27 to 151). The FDA recommended that the dosage for each mAb in this combination be increased 300 mg and administered intramus-cularly	Median 256 ng/mL (IQR: 170 to 750)	Median fold reduction in susceptibility 5.4 (IQR: 3.7 to 6.9). Nearly complete restoration BA.2 suscept-ibility to cilgavimab	Median 44 ng/mL (IQR: 27 to 73)
Bebte	Yes	BRD	Median fold reduction in susceptibility 1.0 (IQR: 0.7 to 1.4) Bebtelovimab is the only mAb active against the current dominant circulating Omicron variant; in non- hospitalized adults, bebtelovimab may be used as an alternative therapy when no preferred therapy (*e.g.*, nirmatrelvir/ritonavir, remdesivir) available	Median 2.6 ng/mL (IQR: 1.8 to 5.0)	Median fold reduction in susceptibility 1.0 (IQR: 0.7 to 1)	Median 4.0 ng/mL (IQR: 0.8 to 5.0)
Regda	No	BRD	Displayed little residual activity	NA	Displayed little residual activity	NA
Amuba	No	BRD	Displayed little residual activity	NA	Displayed little residual activity	NA
Romlu	No	BRD	Retained partial activity	NA	Displayed little residual activity	NA
Adint	No	BRD	Retained partial activity	NA		NA

Adint: Adintrevimab; Amuba: Amubarvimab; Bamla/Etese: Bamlanivimab/Etesevimab; Bebte: Bebtelovimab; BRD: Spike receptor binding domain; Casir/Imdev: Casirivimab/Imdevimab; Cilag/Tixa: Cilgavimab/Tixagevimab; EUA: Emergency use authorization; FDA: United States Food and Drug Administration; IC_{50}: 50% inhibitory concentration; IQR: Interquartile range; mAbs: Monoclonal antibodies; NA: Not available; Regda: Regdanvimab; Romlu: Romlusevimab; S: Spike protein; Sotro: Sotrovimab.

Because of the emergence of Delta and Omicron variants, the use of CP is severely limited. It is only recommended for use in COVID-19 patients with impaired immune function, immunodeficiency, or who are taking immunosuppressants. HIG could theoretically treat COVID-19, but there is currently insufficient data to guide its use. Treatment with ASSAs has made significant progress, and outpatient outcomes are promising. Several clinical trials[27-29] have assessed ASSA's efficacy and safety in the treatment of non-hospitalized COVID-19 patients. Sotrovimab was evaluated in the Phase 3 trial COMET-ICE for the treatment of COVID-19. This mAb treatment is thought to be more effective, and has proven effective in preventing COVID-19[47]. The United States FDA granted a EUA for the use of sotrovimab[56] in May 2021. The BLAZE-1 study investigated the efficacy of intravenous bamlanimab in the early treatment of COVID-19[57]. Bebtelovimab is the only anti-SARS-CoV-2 mAb active against the current dominant circulating Omicron variant[50]. Monoclonal antibodies can protect unvaccinated people or people exposed to high-risk environments in a prophylactic manner. The effectiveness of mAbs targeting the SARS-CoV-2 spike protein is also promising; however, research must continue to actively pursue new drugs and methods for the accurate and rapid diagnosis and treatment of COVID-19.

FOOTNOTES

Author contributions: Yang ZD and Sun J contributed to conception and design, these authors have contributed equally to this work and share first authorship; Yang ZD, Qu BB, Song GW, Xu JQ and Gong B contributed to administrative support; Song GW and Li L contributed to provision of study materials; Yang ZD, Song GW , Xie X, Li L, Zeng HS and Wu JH contributed to collection and assembly of data; Yang ZD, Sun J, Zeng HS, Gong B, Xu JQ, Qu BB and Xie X contributed to data analysis and interpretation; All authors contributed to manuscript revision and approved the submitted version.

Conflict-of-interest statement: All the authors report having no relevant conflicts of interest for this article.

Country/Territory of origin: China

ORCID number: Jin Sun 0000-0002-6308-1958; Zhen-Dong Yang 0000-0003-0719-7400; Xiong Xie 0000-0003-4990-6703; Li Li 0000-0003-0928-1796; Hua-Song Zeng 0000-0002-7166-0941; Bo Gong 0000-0002-4793-7699; Jian-Qiang Xu 0000-0002-6990-3289; Ji-Hong Wu 0000-0002-6232-0187; Bei-Bei Qu 0000-0003-2113-8968; Guo-Wei Song 0000-0002-9356-9145.

S-Editor: Li L
L-Editor: Filipodia
P-Editor: Li L

REFERENCES

1 **Aleem A**, Akbar Samad AB, Slenker AK. Emerging Variants of SARS-CoV-2 And Novel Therapeutics Against Coronavirus (COVID-19). 2022 Oct 10. In: StatPearls [Internet]. Treasure Island (FL): StatPearls Publishing; 2022 Jan- [PMID: 34033342]
2 **Callaway E**. Coronavirus variant XBB.1.5 rises in the United States - is it a global threat? *Nature* 2023; **613**: 222-223 [PMID: 36624320 DOI: 10.1038/d41586-023-00014-3]
3 **World Health Organization**. Coronavirus Disease (COVID-19) Dashboard. [cited 13 January 2023]. Available from: https://covid19.who.int/
4 **Infantino M**, Damiani A, Gobbi FL, Grossi V, Lari B, Macchia D, Casprini P, Veneziani F, Villalta D, Bizzaro N, Cappelletti P, Fabris M, Quartuccio L, Benucci M, Manfredi M. Serological Assays for SARS-CoV-2 Infectious Disease: Benefits, Limitations and Perspectives. *Isr Med Assoc J* 2020; **22**: 203-210 [PMID: 32286019]
5 **Ye Q**, Wang B, Mao J. The pathogenesis and treatment of the `Cytokine Storm' in COVID-19. *J Infect* 2020; **80**: 607-613 [PMID: 32283152 DOI: 10.1016/j.jinf.2020.03.037]
6 **National Institutes of Health**. Coronavirus disease 2019 (COVID-19) treatment guidelines. 2021. [cited 15 February 2022]. Available from: www.covid19treatmentguidelines.nih.gov
7 **Bartoletti M**, Azap O, Barac A, Bussini L, Ergonul O, Krause R, Paño-Pardo JR, Power NR, Sibani M, Szabo BG, Tsiodras S, Verweij PE, Zollner-Schwetz I, Rodríguez-Baño J. ESCMID COVID-19 living guidelines: drug treatment and clinical management. *Clin Microbiol Infect* 2022; **28**: 222-238 [PMID: 34823008 DOI: 10.1016/j.cmi.2021.11.007]
8 **Shankar-Hari M**, Vale CL, Godolphin PJ, Fisher D, Higgins JPT, Spiga F, Savovic J, Tierney J, Baron G, Benbenishty JS, Berry LR, Broman N, Cavalcanti AB, Colman R, De Buyser SL, Derde LPG, Domingo P, Omar SF, Fernandez-Cruz A, Feuth T, Garcia F, Garcia-Vicuna R, Gonzalez-Alvaro I, Gordon AC, Haynes R, Hermine O, Horby PW, Horick NK, Kumar K, Lambrecht BN, Landray MJ, Leal L, Lederer DJ, Lorenzi E, Mariette X, Merchante N, Misnan NA, Mohan SV, Nivens MC, Oksi J, Perez-Molina JA, Pizov R, Porcher R, Postma S, Rajasuriar R, Ramanan AV, Ravaud P, Reid PD, Rutgers A, Sancho-Lopez A, Seto TB, Sivapalasingam S, Soin AS, Staplin N, Stone JH, Strohbehn GW, Sunden-Cullberg J, Torre-Cisneros J, Tsai LW, van Hoogstraten H, van Meerten T, Veiga VC, Westerweel PE, Murthy S, Diaz JV, Marshall JC, Sterne JAC; WHO Rapid Evidence Appraisal for COVID-19 Therapies (REACT) Working Group. Association Between Administration of IL-6 Antagonists and Mortality Among Patients Hospitalized for COVID-19: A Meta-analysis. *JAMA* 2021; **326**: 499-518 [PMID: 34228774 DOI: 10.1001/jama.2021.11330]
9 **Kalil AC**, Patterson TF, Mehta AK, Tomashek KM, Wolfe CR, Ghazaryan V, Marconi VC, Ruiz-Palacios GM, Hsieh L, Kline S, Tapson V, Iovine NM, Jain MK, Sweeney DA, El Sahly HM, Branche AR, Regalado Pineda J, Lye DC, Sandkovsky U, Luetkemeyer AF, Cohen SH, Finberg RW, Jackson PEH, Taiwo B, Paules CI, Arguinchona H, Erdmann N, Ahuja N, Frank M, Oh MD, Kim ES, Tan SY, Mularski RA, Nielsen H, Ponce PO, Taylor BS, Larson L, Rouphael NG, Saklawi Y, Cantos VD, Ko ER, Engemann JJ, Amin AN, Watanabe M, Billings J, Elie MC, Davey RT, Burgess TH, Ferreira J, Green M, Makowski M, Cardoso A, de Bono S, Bonnett T, Proschan M, Deye GA, Dempsey W, Nayak SU, Dodd LE, Beigel JH; ACTT-2 Study Group Members. Baricitinib plus Remdesivir for Hospitalized Adults with Covid-19. *N Engl J Med* 2021; **384**: 795-807 [PMID: 33306283 DOI: 10.1056/NEJMoa2031994]
10 **Marconi VC**, Ramanan AV, de Bono S, Kartman CE, Krishnan V, Liao R, Piruzeli MLB, Goldman JD, Alatorre-Alexander J, de Cassia Pellegrini R, Estrada V, Som M, Cardoso A, Chakladar S, Crowe B, Reis P, Zhang X, Adams DH, Ely EW; COV-BARRIER Study Group. Efficacy and safety of baricitinib for the treatment of hospitalised adults with COVID-19 (COV-BARRIER): a randomised, double-blind, parallel-group, placebo-controlled phase 3 trial. *Lancet Respir Med* 2021; **9**: 1407-1418 [PMID: 34480861 DOI: 10.1016/S2213-2600(21)00331-3]
11 **Xiao AT**, Gao C, Zhang S. Profile of specific antibodies to SARS-CoV-2: The first report. *J Infect* 2020; **81**: 147-178 [PMID: 32209385 DOI: 10.1016/j.jinf.2020.03.012]
12 **Lee YL**, Liao CH, Liu PY, Cheng CY, Chung MY, Liu CE, Chang SY, Hsueh PR. Dynamics of anti-SARS-Cov-2 IgM and IgG antibodies among COVID-19 patients. *J Infect* 2020; **81**: e55-e58 [PMID: 32335168 DOI: 10.1016/j.jinf.2020.04.019]
13 **Yong G**, Yi Y, Tuantuan L, Xiaowu W, Xiuyong L, Ang L, Mingfeng H. Evaluation of the auxiliary diagnostic value of

antibody assays for the detection of novel coronavirus (SARS-CoV-2). *J Med Virol* 2020; **92**: 1975-1979 [PMID: 32320064 DOI: 10.1002/jmv.25919]

14 **Timilsina SS**, Durr N, Jolly P, Ingber DE. Rapid quantitation of SARS-CoV-2 antibodies in clinical samples with an electrochemical sensor. *Biosens Bioelectron* 2023; **223**: 115037 [PMID: 36584477 DOI: 10.1016/j.bios.2022.115037]

15 **Hajissa K**, Mussa A, Karobari MI, Abbas MA, Ibrahim IK, Assiry AA, Iqbal A, Alhumaid S, Mutair AA, Rabaan AA, Messina P, Scardina GA. The SARS-CoV-2 Antibodies, Their Diagnostic Utility, and Their Potential for Vaccine Development. *Vaccines (Basel)* 2022; **10** [PMID: 36016233 DOI: 10.3390/vaccines10081346]

16 **Zamani M**, Ghasemi A, Shamshirgaran M, Ahmadpour S, Hormati A, Khodadadi J, Varnasseri M, Amini F, Shayanrad A, Younesi V, Poustchi H, Shabani M. Investigation of Durability of SARS-CoV-2-specific IgG and IgM Antibodies in Recovered COVID-19 Patients: A Prospective Study. *Avicenna J Med Biotechnol* 2022; **14**: 233-238 [PMID: 36061129 DOI: 10.18502/ajmb.v14i3.9830]

17 **Wu X**, Fu B, Chen L, Feng Y. Serological tests facilitate identification of asymptomatic SARS-CoV-2 infection in Wuhan, China. *J Med Virol* 2020; **92**: 1795-1796 [PMID: 32311142 DOI: 10.1002/jmv.25904]

18 **Long QX**, Liu BZ, Deng HJ, Wu GC, Deng K, Chen YK, Liao P, Qiu JF, Lin Y, Cai XF, Wang DQ, Hu Y, Ren JH, Tang N, Xu YY, Yu LH, Mo Z, Gong F, Zhang XL, Tian WG, Hu L, Zhang XX, Xiang JL, Du HX, Liu HW, Lang CH, Luo XH, Wu SB, Cui XP, Zhou Z, Zhu MM, Wang J, Xue CJ, Li XF, Wang L, Li ZJ, Wang K, Niu CC, Yang QJ, Tang XJ, Zhang Y, Liu XM, Li JJ, Zhang DC, Zhang F, Liu P, Yuan J, Li Q, Hu JL, Chen J, Huang AL. Antibody responses to SARS-CoV-2 in patients with COVID-19. *Nat Med* 2020; **26**: 845-848 [PMID: 32350462 DOI: 10.1038/s41591-020-0897-1]

19 **Zhao J**, Yuan Q, Wang H, Liu W, Liao X, Su Y, Wang X, Yuan J, Li T, Li J, Qian S, Hong C, Wang F, Liu Y, Wang Z, He Q, Li Z, He B, Zhang T, Fu Y, Ge S, Liu L, Zhang J, Xia N, Zhang Z. Antibody Responses to SARS-CoV-2 in Patients With Novel Coronavirus Disease 2019. *Clin Infect Dis* 2020; **71**: 2027-2034 [PMID: 32221519 DOI: 10.1093/cid/ciaa344]

20 **Mori K**, Imaki S, Ohyama Y, Satoh K, Abe T, Takeuchi I. Rapid screening for severe acute respiratory syndrome coronavirus 2 infection with a combined point-of-care antigen test and an immunoglobulin G antibody test. *PLoS One* 2022; **17**: e0263327 [PMID: 35104281 DOI: 10.1371/journal.pone.0263327]

21 **Marano G**, Vaglio S, Pupella S, Facco G, Catalano L, Liumbruno GM, Grazzini G. Convalescent plasma: new evidence for an old therapeutic tool? *Blood Transfus* 2016; **14**: 152-157 [PMID: 26674811 DOI: 10.2450/2015.0131-15]

22 **Burnouf T**, Seghatchian J. Ebola virus convalescent blood products: where we are now and where we may need to go. *Transfus Apher Sci* 2014; **51**: 120-125 [PMID: 25457751 DOI: 10.1016/j.transci.2014.10.003]

23 **Hung IF**, To KK, Lee CK, Lee KL, Chan K, Yan WW, Liu R, Watt CL, Chan WM, Lai KY, Koo CK, Buckley T, Chow FL, Wong KK, Chan HS, Ching CK, Tang BS, Lau CC, Li IW, Liu SH, Chan KH, Lin CK, Yuen KY. Convalescent plasma treatment reduced mortality in patients with severe pandemic influenza A (H1N1) 2009 virus infection. *Clin Infect Dis* 2011; **52**: 447-456 [PMID: 21248066 DOI: 10.1093/cid/ciq106]

24 **Soo YO**, Cheng Y, Wong R, Hui DS, Lee CK, Tsang KK, Ng MH, Chan P, Cheng G, Sung JJ. Retrospective comparison of convalescent plasma with continuing high-dose methylprednisolone treatment in SARS patients. *Clin Microbiol Infect* 2004; **10**: 676-678 [PMID: 15214887 DOI: 10.1111/j.1469-0691.2004.00956.x]

25 **Arabi YM**, Hajeer AH, Luke T, Raviprakash K, Balkhy H, Johani S, Al-Dawood A, Al-Qahtani S, Al-Omari A, Al-Hameed F, Hayden FG, Fowler R, Bouchama A, Shindo N, Al-Khairy K, Carson G, Taha Y, Sadat M, Alahmadi M. Feasibility of Using Convalescent Plasma Immunotherapy for MERS-CoV Infection, Saudi Arabia. *Emerg Infect Dis* 2016; **22**: 1554-1561 [PMID: 27532807 DOI: 10.3201/eid2209.151164]

26 **United States Food and Drug Administration**. Recommendations for Investigational COVID-19 Convalescent Plasma. [cited 8 February 2023]. Available from: www.fda.gov/vaccines-blood-biologics/investigational-new-drug-applications-inds-cber-regulated-products/recommendations-investigational-covid-19-convalescent-plasma

27 **RECOVERY Collaborative Group**. Convalescent plasma in patients admitted to hospital with COVID-19 (RECOVERY): a randomised controlled, open-label, platform trial. *Lancet* 2021; **397**: 2049-2059 [PMID: 34000257 DOI: 10.1016/S0140-6736(21)00897-7]

28 **Bégin P**, Callum J, Jamula E, Cook R, Heddle NM, Tinmouth A, Zeller MP, Beaudoin-Bussières G, Amorim L, Bazin R, Loftsgard KC, Carl R, Chassé M, Cushing MM, Daneman N, Devine DV, Dumaresq J, Fergusson DA, Gabe C, Glesby MJ, Li N, Liu Y, McGeer A, Robitaille N, Sachais BS, Scales DC, Schwartz L, Shehata N, Turgeon AF, Wood H, Zarychanski R, Finzi A; CONCOR-1 Study Group, Arnold DM. Convalescent plasma for hospitalized patients with COVID-19: an open-label, randomized controlled trial. *Nat Med* 2021; **27**: 2012-2024 [PMID: 34504336 DOI: 10.1038/s41591-021-01488-2]

29 **Estcourt LJ**, Turgeon AF, McQuilten ZK, McVerry BJ, Al-Beidh F, Annane D, Arabi YM, Arnold DM, Beane A, Bégin P, van Bentum-Puijk W, Berry LR, Bhimani Z, Birchall JE, Bonten MJM, Bradbury CA, Brunkhorst FM, Buxton M, Callum JL, Chassé M, Cheng AC, Cove ME, Daly J, Derde L, Detry MA, De Jong M, Evans A, Fergusson DA, Fish M, Fitzgerald M, Foley C, Goossens H, Gordon AC, Gosbell IB, Green C, Haniffa R, Harvala H, Higgins AM, Hills TE, Hoad VC, Horvat C, Huang DT, Hudson CL, Ichihara N, Laing E, Lamikanra AA, Lamontagne F, Lawler PR, Linstrum K, Litton E, Lorenzi E, MacLennan S, Marshall J, McAuley DF, McDyer JF, McGlothlin A, McGuinness S, Miflin G, Montgomery S, Mouncey PR, Murthy S, Nichol A, Parke R, Parker JC, Priddee N, Purcell DFJ, Reyes LF, Richardson P, Robitaille N, Rowan KM, Rynne J, Saito H, Santos M, Saunders CT, Serpa Neto A, Seymour CW, Silversides JA, Tinmouth AA, Triulzi DJ, Turner AM, van de Veerdonk F, Walsh TS, Wood EM, Berry S, Lewis RJ, Menon DK, McArthur C, Zarychanski R, Angus DC, Webb SA, Roberts DJ, Shankar-Hari M; Writing Committee for the REMAP-CAP Investigators. Effect of Convalescent Plasma on Organ Support-Free Days in Critically Ill Patients With COVID-19: A Randomized Clinical Trial. *JAMA* 2021; **326**: 1690-1702 [PMID: 34606578 DOI: 10.1001/jama.2021.18178]

30 **Food and Drug Administration**. EUA of COVID-19 convalescent plasma for the treatment of COVID-19 in hospitalized patients: fact sheet for health care providers. 2021. [sited 15 February 2023]. Available from: https://www.fda.gov/media/141478/download

31 **Lamontagne F**, Agarwal A, Rochwerg B, Siemieniuk RA, Agoritsas T, Askie L, Lytvyn L, Leo YS, Macdonald H, Zeng L, Amin W, da Silva ARA, Aryal D, Barragan FAJ, Bausch FJ, Burhan E, Calfee CS, Cecconi M, Chacko B, Chanda D, Dat VQ, De Sutter A, Du B, Freedman S, Geduld H, Gee P, Gotte M, Harley N, Hashimi M, Hunt B, Jehan F, Kabra SK,

Kanda S, Kim YJ, Kissoon N, Krishna S, Kuppalli K, Kwizera A, Lado Castro-Rial M, Lisboa T, Lodha R, Mahaka I, Manai H, Mendelson M, Migliori GB, Mino G, Nsutebu E, Preller J, Pshenichnaya N, Qadir N, Relan P, Sabzwari S, Sarin R, Shankar-Hari M, Sharland M, Shen Y, Ranganathan SS, Souza JP, Stegemann M, Swanstrom R, Ugarte S, Uyeki T, Venkatapuram S, Vuyiseka D, Wijewickrama A, Tran L, Zeraatkar D, Bartoszko JJ, Ge L, Brignardello-Petersen R, Owen A, Guyatt G, Diaz J, Kawano-Dourado L, Jacobs M, Vandvik PO. A living WHO guideline on drugs for covid-19. *BMJ* 2020; **370**: m3379 [PMID: 32887691 DOI: 10.1136/bmj.m3379]

32 **Ferrari S**, Caprioli C, Weber A, Rambaldi A, Lussana F. Convalescent hyperimmune plasma for chemo-immunotherapy induced immunodeficiency in COVID-19 patients with hematological malignancies. *Leuk Lymphoma* 2021; **62**: 1490-1496 [PMID: 33461387 DOI: 10.1080/10428194.2021.1872070]

33 **Senefeld JW**, Klassen SA, Ford SK, Senese KA, Wiggins CC, Bostrom BC, Thompson MA, Baker SE, Nicholson WT, Johnson PW, Carter RE, Henderson JP, Hartman WR, Pirofski LA, Wright RS, Fairweather L, Bruno KA, Paneth NS, Casadevall A, Joyner MJ. Use of convalescent plasma in COVID-19 patients with immunosuppression. *Transfusion* 2021; **61**: 2503-2511 [PMID: 34036587 DOI: 10.1111/trf.16525]

34 **Kanj S**, Al-Omari B. Convalescent Plasma Transfusion for the Treatment of COVID-19 in Adults: A Global Perspective. *Viruses* 2021; **13** [PMID: 34066932 DOI: 10.3390/v13050849]

35 **O'Donnell MR**, Grinsztejn B, Cummings MJ, Justman JE, Lamb MR, Eckhardt CM, Philip NM, Cheung YK, Gupta V, João E, Pilotto JH, Diniz MP, Cardoso SW, Abrams D, Rajagopalan KN, Borden SE, Wolf A, Sidi LC, Vizzoni A, Veloso VG, Bitan ZC, Scotto DE, Meyer BJ, Jacobson SD, Kantor A, Mishra N, Chauhan LV, Stone EF, Dei Zotti F, La Carpia F, Hudson KE, Ferrara SA, Schwartz J, Stotler BA, Lin WW, Wontakal SN, Shaz B, Briese T, Hod EA, Spitalnik SL, Eisenberger A, Lipkin WI. A randomized double-blind controlled trial of convalescent plasma in adults with severe COVID-19. *J Clin Invest* 2021; **131** [PMID: 33974559 DOI: 10.1172/JCI150646]

36 **Kloypan C**, Saesong M, Sangsuemoon J, Chantharit P, Mongkhon P. CONVALESCENT plasma for COVID-19: A meta-analysis of clinical trials and real-world evidence. *Eur J Clin Invest* 2021; **51**: e13663 [PMID: 34375445 DOI: 10.1111/eci.13663]

37 **Focosi D**, McConnell S, Casadevall A, Cappello E, Valdiserra G, Tuccori M. Monoclonal antibody therapies against SARS-CoV-2. *Lancet Infect Dis* 2022; **22**: e311-e326 [PMID: 35803289 DOI: 10.1016/S1473-3099(22)00311-5]

38 **Infectious Diseases Society of America**. Infectious Diseases Society of America IDSA guidelines on the treatment and management of patients with COVID-19.2022. [sited 8 January 2023]. Available from: https://www.idsociety.org/practice-guideline/covid-19-guideline-treatment-and-management/

39 **Vandeberg P**, Cruz M, Diez JM, Merritt WK, Santos B, Trukawinski S, Wellhouse A, Jose M, Willis T. Production of anti-SARS-CoV-2 hyperimmune globulin from convalescent plasma. *Transfusion* 2021; **61**: 1705-1709 [PMID: 33715160 DOI: 10.1111/trf.16378]

40 **National Institutes of Health**. Immunoglobulins: SARS-CoV-2 Specific. [sited 26 September 2022]. Available from: https://www.covid19treatmentguidelines.nih.gov/search/?q=Immunoglobulins%3A%20SARS-CoV-2%20Specific

41 **Jiang S**, Hillyer C, Du L. Neutralizing Antibodies against SARS-CoV-2 and Other Human Coronaviruses. *Trends Immunol* 2020; **41**: 355-359 [PMID: 32249063 DOI: 10.1016/j.it.2020.03.007]

42 **National Institutes of Health**. Anti-SARS-CoV-2 Monoclonal Antibodies. [sited 24 September 2022] Available from: https://www.covid19treatmentguidelines.nih.gov/search/?q=Anti-SARS-CoV-2%20Monoclonal%20Antibodies

43 **Food and Drug Administration**. Fact sheet for healthcare providers: emergency use authorization for Evusheld (tixagevimab co-packaged with cilgavimab). 2021. [sited 8 January 2023]. Available from: https://www.fda.gov/media/154701/download

44 **Food and Drug Administration**. Fact sheet for healthcare providers: emergency use authorization (EUA) of sotrovimab. 2021. [sited 8 January 2023]. Available from: https://www.fda.gov/media/149534/download

45 **Food and Drug Administration**. Coronavirus (COVID-19) | Drugs. Dec 22, 2022. [sited 8 January 2023]. Available from: https://www.fda.gov/drugs/emergency-preparedness-drugs/coronavirus-covid-19-drugs#:~:text=Sars-Cov-2-Targeting%20Monoclonal%20Antibodies

46 **Dougan M**, Azizad M, Mocherla B, Gottlieb RL, Chen P, Hebert C, Perry R, Boscia J, Heller B, Morris J, Crystal C, Igbinadolor A, Huhn G, Cardona J, Shawa I, Kumar P, Blomkalns A, Adams AC, Van Naarden J, Custer KL, Knorr J, Oakley G, Schade AE, Holzer TR, Ebert PJ, Higgs RE, Sabo J, Patel DR, Dabora MC, Williams M, Klekotka P, Shen L, Skovronsky DM, Nirula A. A Randomized, Placebo-Controlled Clinical Trial of Bamlanivimab and Etesevimab Together in High-Risk Ambulatory Patients With COVID-19 and Validation of the Prognostic Value of Persistently High Viral Load. *Clin Infect Dis* 2022; **75**: e440-e449 [PMID: 34718468 DOI: 10.1093/cid/ciab912]

47 **Gupta A**, Gonzalez-Rojas Y, Juarez E, Crespo Casal M, Moya J, Falci DR, Sarkis E, Solis J, Zheng H, Scott N, Cathcart AL, Hebner CM, Sager J, Mogalian E, Tipple C, Peppercorn A, Alexander E, Pang PS, Free A, Brinson C, Aldinger M, Shapiro AE; COMET-ICE Investigators. Early Treatment for Covid-19 with SARS-CoV-2 Neutralizing Antibody Sotrovimab. *N Engl J Med* 2021; **385**: 1941-1950 [PMID: 34706189 DOI: 10.1056/NEJMoa2107934]

48 **National Health Commission of China**. Novel Coronavirus Pneumonia Diagnosis and Treatment Plan (Trial Version 9). Mar 3, 2022. [cited 2 April 2022]. Available from: http://www.gov.cn/zhengce/zhengceku/2022-03/15/5679257/files/49854a49c7004f4ea9e622f3f2c568d8.pdf

49 **Tao K**, Tzou PL, Kosakovsky Pond SL, Ioannidis JPA, Shafer RW. Susceptibility of SARS-CoV-2 Omicron Variants to Therapeutic Monoclonal Antibodies: Systematic Review and Meta-analysis. *Microbiol Spectr* 2022; **10**: e0092622 [PMID: 35700134 DOI: 10.1128/spectrum.00926-22]

50 **National Institutes of Health**. Coronavirus Disease 2019 (COVID-19) Treatment Guidelines. [sited: 28 September 2022]. Available from: https://www.covid19treatmentguidelines.nih.gov/

51 **United States Food and Drug Administration**. Fact sheet for healthcare providers: emergency use authorization for bebtelovimab. 2022. [sited 8 January 2023]. Available from: https://www.fda.gov/media/156152/download

52 **United States Food and Drug Administration**. Fact sheet for healthcare providers: emergency use authorization (EUA) of sotrovimab. 2022. [sited 8 January 2023] Available from: https://www.fda.gov/media/149534/download

53 **United States Food and Drug Administration**. Fact sheet for healthcare providers: emergency use authorization for Evusheld (tixagevimab co-packaged with cilgavimab). 2022. [sited 8 January 2023]. Available from: https://www.fda.gov/media/154701/download

54 **Dong J**, Zost SJ, Greaney AJ, Starr TN, Dingens AS, Chen EC, Chen RE, Case JB, Sutton RE, Gilchuk P, Rodriguez J, Armstrong E, Gainza C, Nargi RS, Binshtein E, Xie X, Zhang X, Shi PY, Logue J, Weston S, McGrath ME, Frieman MB, Brady T, Tuffy KM, Bright H, Loo YM, McTamney PM, Esser MT, Carnahan RH, Diamond MS, Bloom JD, Crowe JE Jr. Genetic and structural basis for SARS-CoV-2 variant neutralization by a two-antibody cocktail. *Nat Microbiol* 2021; **6**: 1233-1244 [PMID: 34548634 DOI: 10.1038/s41564-021-00972-2]

55 **Zhen-Dong Y**, Gao-Jun Z, Run-Ming J, Zhi-Sheng L, Zong-Qi D, Xiong X, Guo-Wei S. Clinical and transmission dynamics characteristics of 406 children with coronavirus disease 2019 in China: A review. *J Infect* 2020; **81**: e11-e15 [PMID: 32360500 DOI: 10.1016/j.jinf.2020.04.030]

56 **United States Food and Drug Administration**. Coronavirus (COVID-19) Update: FDA Authorizes New Monoclonal Antibody for Treatment of COVID-19 that Retains Activity Against Omicron Variant. Feb 11, 2022. [stied 12 February 2023]. Accessed from: https://www.fda.gov/news-events/press-announcements/coronavirus-covid-19-update-fda-authorizes-new-monoclonal-antibody-treatment-covid-19-retains

57 **Chen P**, Nirula A, Heller B, Gottlieb RL, Boscia J, Morris J, Huhn G, Cardona J, Mocherla B, Stosor V, Shawa I, Adams AC, Van Naarden J, Custer KL, Shen L, Durante M, Oakley G, Schade AE, Sabo J, Patel DR, Klekotka P, Skovronsky DM; BLAZE-1 Investigators. SARS-CoV-2 Neutralizing Antibody LY-CoV555 in Outpatients with Covid-19. *N Engl J Med* 2021; **384**: 229-237 [PMID: 33113295 DOI: 10.1056/NEJMoa2029849]

World Journal of Clinical Cases

Submit a Manuscript: https://www.f6publishing.com

World J Clin Cases 2023 April 6; 11(10): 2181-2188

DOI: 10.12998/wjcc.v11.i10.2181

ISSN 2307-8960 (online)

MINIREVIEWS

Cheesy material on macroscopic on-site evaluation after endoscopic ultrasound-guided fine-needle biopsy: Don't miss the tuberculosis

Hanane Delsa, Khadija Bellahammou, Hussein Hassan Okasha, Fahd Ghalim

Specialty type: Gastroenterology and hepatology

Provenance and peer review: Invited article; Externally peer reviewed.

Peer-review model: Single blind

Peer-review report's scientific quality classification

Grade A (Excellent): 0
Grade B (Very good): B
Grade C (Good): C
Grade D (Fair): 0
Grade E (Poor): 0

P-Reviewer: Chai NL, China; Thandassery RB, United States

Received: December 27, 2022
Peer-review started: December 27, 2022
First decision: January 22, 2023
Revised: January 28, 2023
Accepted: March 14, 2023
Article in press: March 14, 2023
Published online: April 6, 2023

Hanane Delsa, Fahd Ghalim, Department of Gastroenterology and Hepatology, Cheikh Khalifa International University Hospital, Mohammed VI University of Sciences and Health, Casablanca 82403, Morocco

Khadija Bellahammou, Department of Oncology, Tetouan Hospital, Tetouan 93000, Morocco

Hussein Hassan Okasha, Department of Internal Medicine, Division of Gastroenterology, Hepatology and Endoscopy, Kasr Al-Ainy School of Medicine, Cairo university, Cairo 11562, Egypt

Corresponding author: Hanane Delsa, MD, Assistant Professor, Department of Gastroenterology and Hepatology, Cheikh Khalifa International University Hospital, Mohammed VI University of Sciences and Health, Avenue Mohamed Taieb Naciri, Casablanca 82403, Morocco. dr.delsa.hanane@gmail.com

Abstract

Endoscopic ultrasound-guided fine-needle biopsy (EUS-FNB) is an excellent investigation to diagnose pancreatic lesions and has shown high accuracy for its use in pathologic diagnosis. Recently, macroscopic on-site evaluation (MOSE) performed by an endoscopist was introduced as an alternative to rapid on-site cytologic evaluation to increase the diagnostic yield of EUS-FNB. The MOSE of the biopsy can estimate the adequacy of the sample directly by the macroscopic evaluation of the core tissue obtained from EUS-FNB. Isolated pancreatic tuberculosis is extremely rare and difficult to diagnose because of its non-specific signs and symptoms. Therefore, this challenging diagnosis is based on endoscopy, imaging, and the bacteriological and histological examination of tissue biopsies. This uncommon presentation of tuberculosis can be revealed as pancreatic mass mimicking cancer. EUS-FNB can be very useful in providing a valuable histopathological diagnosis. A calcified lesion with a cheesy core in MOSE must be suggestive of tuberculosis, leading to the request of the GeneXpert, which can detect *Mycobacterium tuberculosis* deoxyribonucleic acid and resistance to rifampicin. A decent diagnostic strategy is crucial to prevent unnecessary surgical resection and to supply conservative management with antitubercular therapy.

Key Words: Pancreatic tuberculosis; Endoscopic ultrasound; Fine-needle biopsy; Macroscopic on-site evaluation; Cheesy material; GeneXpert

Core Tip: In this article, we discussed the role of endoscopic ultrasound with fine-needle biopsy as a diagnostic tool in patients with suspicious pancreatic tuberculosis. This review aims to provide knowledge on the utility of fine-needle biopsy and macroscopic on-site evaluation of the core to suspect pancreatic tuberculosis, in addition to diverting the attention of the endoscopists to consider tuberculosis when the core is cheesy.

Citation: Delsa H, Bellahammou K, Okasha HH, Ghalim F. Cheesy material on macroscopic on-site evaluation after endoscopic ultrasound-guided fine-needle biopsy: Don't miss the tuberculosis. *World J Clin Cases* 2023; 11(10): 2181-2188
URL: https://www.wjgnet.com/2307-8960/full/v11/i10/2181.htm
DOI: https://dx.doi.org/10.12998/wjcc.v11.i10.2181

INTRODUCTION

Tuberculosis (TB) is a transmissible disease caused by *Mycobacterium tuberculosis* (MT). TB was the first cause of death worldwide from infectious diseases until the coronavirus disease 2019 (COVID-19) pandemic[1]. In 2020, approximately 10 million people developed TB, and almost 25% of the world's population has been infected with MT[1].

The most common site of TB is the lungs; however, in approximately 12.5% of cases, it can affect other sites (extrapulmonary TB), with abdominal localization in 11%-16%[2]. The diagnosis of extrapulmonary TB can be very challenging because the usual method based on the detection of MT is insufficiently sensitive, and other tools based on immune responses cannot always differentiate a latent infection from an active disease[3].

Pancreatic TB remains a rare site of abdominal TB, often misdiagnosed as pancreatic carcinoma. Nevertheless, endoscopic ultrasound (EUS) with pancreatic fine needle aspiration or biopsy (FNA/FNB) and a polymerase chain reaction (PCR) are important tools to make the definitive diagnosis and to initiate adequate treatment[4,5].

Recently, macroscopic on-site evaluation (MOSE) performed by an endoscopist was introduced as an alternative to rapid on-site cytologic evaluation (ROSE) to increase the diagnostic yield of EUS-FNB. The MOSE of the biopsy can estimate the adequacy of the sample directly by the macroscopic evaluation of the core tissue obtained from EUS-FNB[6]. In our practice, a cheesy core was found in all patients with isolated pancreatic TB, which led us to perform GeneXpert, which can detect MT DNA and resistance to rifampicin. This diagnostic strategy is critical for avoiding unnecessary surgical resection and for providing conservative management with antitubercular therapy.

In the present article, we reviewed pancreatic TB, discussed the role of EUS with FNA/FNB in diagnosis, and reported the correlation between cheesy core and tuberculosis. Based on this, we also discussed the usefulness of MOSE in avoiding misdiagnosing this rare disease.

PANCREATIC TB

Isolated pancreatic TB is an extremely rare disease, even in countries where tuberculosis is widespread. However, due to the development of new techniques like EUS, diagnosing pancreatic TB is becoming easier. EUS-FNB allows obtaining pancreatic specimens with cytopathology. Many cases have been published worldwide in the last few years with different and non-specific clinical manifestations (Table 1)[5,7-10].

The systematic review conducted by Panic, including 116 studies reporting data on 166 patients, revealed multiple symptoms dominated by abdominal pain in 74.8% of patients, followed by weight loss and fever in almost half of patients (51.6% and 46.5%, respectively). However, jaundice was found in 20.0% of cases. The most common presentations of pancreatic TB were pancreatic mass mimicking cancer (79.5%), pancreatic head (59.0%), body (18.2%), tail (13.4%), and neck (1.8%). Nonetheless, other pancreatic lesions were reported, like abscesses in 12.1% of patients and chronic or acute pancreatitis in 6.6% and 6.0%, respectively. As an extra-pancreatic localization of TB, peripancreatic lymph nodes were observed in 47.3% of cases. The other sites were rarely described: the spleen (8.3%), intestines (8.2%), liver (6.9%), and lungs (6.3%)[2].

In a study conducted by Ray, 16 pancreatic TB were identified, and the main symptoms were epigastric pain (81%), weight loss (75%), and anorexia (69%). Half of the patients had a fever, and 31% had jaundice[9].

As in pulmonary tuberculosis, immunocompromised individuals are the most affected, particularly in cases of advanced-stage malignant diseases and acquired immunodeficiency syndrome (AIDS), with a high rate of a pancreatic abscess (70%) and mortality (10.8%). In cases of delayed diagnosis and

Table 1 Clinical presentation and endoscopic ultrasound finding of pancreatic tuberculosis patients

Ref.	No. of patients	Age	Sex	Clinical presentation	EUS finding	Microbiological and histological findings
Diaconu *et al* [5], 2022	1	55	F	Fever, jaundice, and asthenia	Cephalic pancreatic lesion with changes suggestive of chronic pancreatitis	Positive culture
Miyamoto *et al*[7], 2022	1	19	F	Abdominal pain and weight loss		Positive PCR for MT, granulomas with caseous necrosis and acid-fast bacilli
Hoilat *et al* [8], 2020	1	26	M	Abdominal pain, increased nausea and vomiting	Hypoechoic lesion	FNA: Abundant fibrinopurulent exudate and necrotizing suppurative granulomatous inflammation
Ray *et al*[9], 2021	16	13-59	12 M, 4 F	Epigastric pain, weight loss, anorexia, fever, and jaundice		5 EUS-FNA; 5 CT-FNA; 6 Surgery
Chang-Xin *et al*[10], 2022	1	24	F	Jaundice		Granulomatous inflammation infiltrated by multinucleated giant cells in FNA; Positive tuberculin skin test and tuberculous infection of T cells spot test

CT: Computed tomography, MT: *Mycobacterium tuberculosis*, FNA: Fine needle aspiration; PCR: Polymerase chain reaction.

without proper treatment, pancreatic TB can be deadly, and the prognosis is grave due to the underlying disease[11,12].

EUS

EUS is considered the main tool for evaluating pancreatic masses and a valuable diagnostic modality for pancreatic TB. It can precisely determine the characteristics of pancreatic lesions (size, vascular invasion, and calcifications) and the aspect of peripancreatic lymph nodes. Combined with EUS-FNB, it has become an excellent investigation to diagnose pancreatic lesions and has established a high accuracy for its use in pathologic diagnosing[13,14].

However, few studies have been published about EUS in pancreatic TB compared to other sites of TB [14]. In the EUS, it can appear as a solid mass or mixed solid cystic lesions, usually with hypoechoic or anechoic echotexture without vascular invasion[14]. Although vascular invasion has been reported in some cases of pancreatic TB, it cannot be used to confirm malignancy[9].

In addition, EUS can demonstrate pancreatic calcifications, reported in 56% of patients, and also detect extra-pancreatic localizations like abdominal or mediastinal lymphadenopathy[15,16]. In our cases, we observed pancreatic mass with central calcification, respecting all vessels (Figure 1).

In the brief communication of Rana *et al*[17] comparing 25 patients with pancreatic adenocarcinoma to 6 patients with pancreatic tuberculosis, the EUS appearances were similar between the two groups. However, in patients with pancreatic TB, EUS typically revealed hypoechoic lesions. However, the group with adenocarcinoma had some specific aspects compared to patients with TB: advanced age, high bilirubin levels, significant dilatation of the common bile duct, and sometimes a dilated pancreatic duct.

EUS elastography can help to characterize the pancreatic mass better and differentiate pancreatic TB from adenocarcinoma through the demarcated lesion characteristics. In TB, it showed stiffer tissue than the healthy pancreatic parenchyma. Nevertheless, pancreatic TB and autoimmune pancreatitis have a similar appearance in elastography. Therefore, EUS elastography has a limited contribution to diagnosing pancreatic TB[18].

In addition, EUS allows tissue acquisition by FNB or aspiration by FNA to exclude another diagnosis like adenocarcinoma or autoimmune pancreatitis. At the same time, the endoscopist can perform multiple biopsies of the abdominal or mediastinal lymphadenopathy and the suspicious pancreatic masses, even the smaller ones (less than 1 cm) located in the body and tail regions[19]. With these samples, histopathology can be performed; however, pancreatic fluid culture microbiology (Ziehl–Neelsen staining and acid-fast bacilli culture) and PCR assay (to detect mycobacterial DNA) are required to improve the diagnostic yield (up to 76% for TB *vs* 95% for cancer)[20]. The EUS-FNA has a good sensitivity (from 85% to 90%) and excellent specificity up to 100%[21].

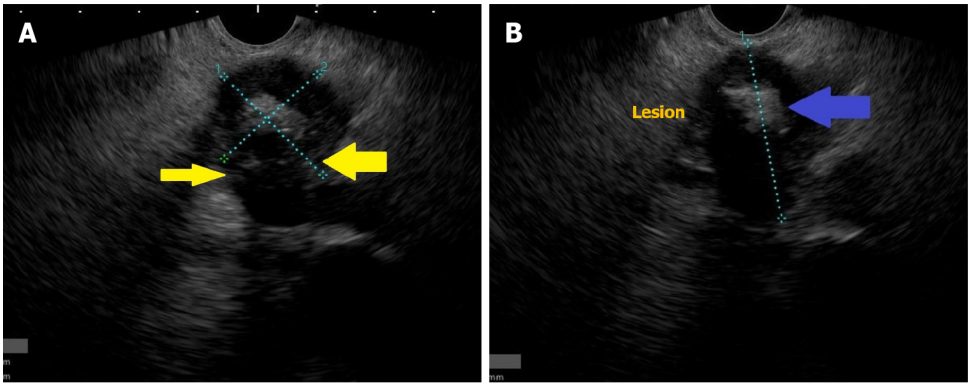

DOI: 10.12998/wjcc.v11.i10.2181

Figure 1 Endoscopic ultrasound of pancreatic tuberculosis. A: Image showing a pancreatic lesion respecting vessels (yellow arrow), B: Pancreatic lesion with central calcification (blue arrow).

MOSE AND HISTOLOGY

In the past century, surgical procedures were the main tool to obtain tissue or liquid specimens from pancreatic masses. The development of the EUS with FNA/FNB as a less invasive method has become the procedure of choice for confirming the diagnosis of pancreatic TB[2].

First, after performing EUS-FNA/FNB, every endoscopist must observe the samples. This MOSE will assess the adequacy of histologic cores obtained during EUS-FNA/FNB. This evaluation of the quality and quantity of the core by the operator may help potentially decide the number of passes[22].

Iwashita introduced this concept of MOSE in 2015 when he published his cohort of patients that underwent EUS-FNA with a 19G needle. In this pilot study, the authors observed better diagnostic yield when the macroscopically visible core on MOSE was superior to 4 mm[23].

Nowadays, some authors have proposed performing MOSE of the core as an alternative to ROSE, which requires a cytopathologist's presence[22]. Gaia proposed a classification in his study published in 2022, which included 76 patients performing EUS-FNB for pancreatic and extra-pancreatic solid masses (Table 2)[24].

However, no studies described the sample's aspect based on the final diagnosis. Diaconu reported a case of pancreatic TB with a cephalic pancreatic lesion and changes suggesting chronic pancreatitis; the EUS-FNB revealed purulent material with a positive culture for TB[5]. Therefore, when the EUS-FNA/FNB shows purulent material, a cytological and bacteriological examination must be performed to exclude pancreatic TB.

Caseous material was described in tuberculosis as a unique type of tissue aspirate. The gross appearance can be soft, white, or cheesy-looking (caseating) material[25]. In many studies, cheesy material was noted as an aspect of tuberculosis at different sites (Table 3)[26-30].

This cheesy-looking appearance was initially reported intraoperatively. However, in the study of Lakhey, which included 122 patients with tubercular lymphadenitis, the acid-fast bacilli (AFB) positivity rate of fine needle aspiration cytology was higher when cheesy material was aspirated (82.3%)[29].

In our series, a young patient was presented with a pancreatic mass with central calcification. Respecting all vessels, EUS-FNB was performed with 3 passes. The core of the first two passes was cheesy, and the third one was also cheesy but a little bloody (Figure 2). This cheesy appearance leads us to perform GeneXpert, which can detect MT DNA and resistance to rifampicin. Positive GeneXpert results and benign-looking histopathology confirmed the diagnosis of pancreatic TB.

A definitive diagnosis of pancreatic TB is commonly based on the microbiological and histopathological examination of a core obtained directly from the pancreas or the peripancreatic lymphadenopathy.

The most common histopathological finding of pancreatic TB on specimens is necrotizing granuloma, reported in more than 50% of cases[15,31]. It is not specific to pancreatic TB as it occurs in other diseases such as Crohn's, sarcoidosis, and autoimmune pancreatitis. Contrary to caseous necrosis, multinucleated giant cells and the identification of AFB are more specific[12].

GENXPERT MT OR XPERT MTB/RIF ASSAY

The diagnosis of pancreatic TB is challenging, and histopathology is not always specific. To have a definitive diagnosis, scientists promoted the development of more sensitive and quick tests such as interferon-gamma release assays, Xpert Ultra, and Xpert MTB/RIF[32].

Table 2 Macroscopic on-site evaluation score and sample classification[24]

Score	Aspects of the core	Classification of the biopsy
0	No material	Negative
1	Haematic or necrotic material	Acceptable
2	≥ 1 core tissue with ≤ 2 mm yellowish-white	Positive
3	≥ 1 core tissue with > 2 mm yellowish-white	Positive

Table 3 Sites of tuberculosis with cheesy material

Ref.	No. of patients	Presentation	Site of tuberculosis	Procedure
Yeat *et al*[26]	1	Pontomedullary junction, ring-enhancing lobulated lesion	Brainstem	Suboccipital craniotomy
Gopakumar *et al*[27]	1	Retropharyngeal cold abscess	Cervical lymphad-enitis	Surgical exploration of the parapharyngeal space by needle aspiration
Ng *et al*[28]	1	Right adnexal mass	Abdominopelvic	Exploratory laparotomy
Lakhey *et al*[29]	122		Lymphadenopathy	Fine-needle aspiration cytology
Sahoo *et al*[30]	1	Pain in the left foot	Talus bone	Debridement and curettage of the lesion

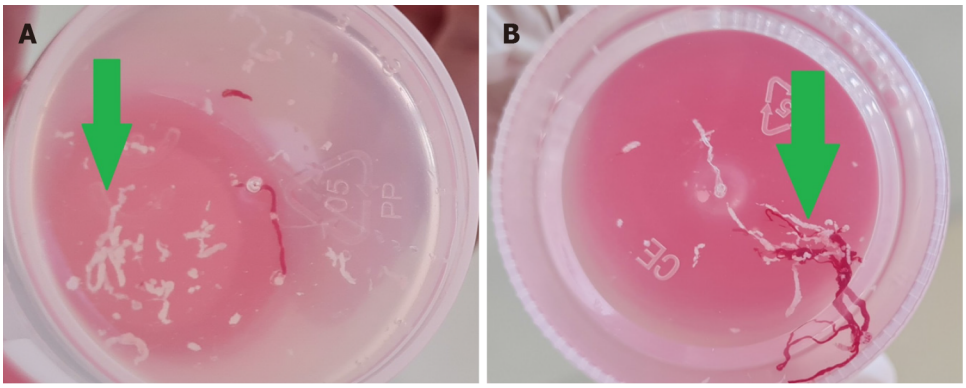

DOI: 10.12998/wjcc.v11.i10.2181

Figure 2 Cheesy macroscopic on-site evaluation (green arrow). A: The core of the first two passes was cheesy; B: The third one was also cheesy but a little bloody.

Worldwide, the most commonly used molecular test for the diagnosis of TB is Xpert MTB/RIF, approved by the World Health Organization in 2013. When performed directly in specimens, it can detect the DNA of the MT complex in biopsies and the rifampicin (RIF) resistance conferred by the *rpoB* gene mutation detected by nested real-time PCR within 2 h. This test is generally available in less than 24 h[3,9]. Thus, over the last decade, these molecular tests have played an essential role in controlling TB [3].

Even if these tools are more commonly performed, their use for the diagnosis of extrapulmonary TB, especially pancreatic, has not been well studied. In the Panic review, including 166 patients, PCR confirmed the diagnosis in only 9.6% *vs* 59.6% for histology[2]. However, in recent studies, PCR is increasingly used to detect TB rapidly with a higher positive rate (43%-67%)[4,33].

In cases of the human immunodeficiency virus (HIV)- positive patients with AIDS, TB is an extremely common opportunistic infection[12]. The success rate of FNA under computed tomography scan or ultrasound guidance in diagnosing pancreatic TB was 50.0% in the Jenney review for non-HIV-infected patients (37 cases). However, this reported success rate was much lower than the 85.7% rate in HIV-infected cases in the systemic review of Meesir, which reflects the operator-dependent nature of the procedure[11,12].

In Morocco, the correct diagnosis of TB is based on histopathology, whereas bacteriology testing is uncommonly used to confirm TB. In a Moroccan cross-sectional study including 262 patients with cervical lymph nodes, Xpert tests confirmed the diagnosis of TB in 47.3%[34].

Table 4 Doses of antitubercular therapy

Drugs	Doses (mg/kg/d)	Duration (mo)
Rifampin	10 (8-12)	6
Isoniazid	5 (4-6)	6
Pyrazinamide	25 (20-30)	2
Ethambutol	15 (15-20)	2

The study of Mechal, including 714 patients with pulmonary or extrapulmonary TB, analyzed all the samples using GeneXpert MTB/RIF. Its sensitivity and specificity were almost the same in both groups: 79.3% and 90.3% for pulmonary TB *vs* 78.2% and 90.4% for extrapulmonary TB, respectively[35]. Therefore, GeneXpert MTB/RIF can be considered the test of choice for diagnosing extrapulmonary TB because of its high sensitivity and specificity[35].

TREATMENT

Treatment of pancreatic TB, as the other localization, is based on antitubercular therapy (ATT) using 3 or 4 drugs given for 6–12 mo: isoniazid, rifampin, pyrazinamide, and ethambutol (Table 4)[15].

According to the initial finding, follow-up is based on clinical improvement, weight, radiology, or endoscopy. Moreover, performing the liver function test is crucial for detecting the hepatotoxicity of ATT. In pancreatic TB, EUS may also be a good modality for follow-up[33]. These tools allow us to decide the duration of ATT, even for pancreatic TB, which is usually 6 or 9 mo, depending on the country. Otherwise, it is suggested to search for other immunosuppression like diabetes and HIV in these patients[15].

In the presence of a pancreatic abscess, percutaneous or EUS-aspiration should be performed to make the correct diagnosis and avoid unnecessary surgery. Some patients, even under ATT, can develop pruritus with cholestatic symptoms or severe cholangitis, and a biliary stent will be placed[10].

CONCLUSION

Isolated pancreatic tuberculosis is an extremely rare site of abdominal TB, often misdiagnosed as pancreatic carcinoma. Nevertheless, a EUS with pancreatic FNA/FNB is important to confirm the diagnosis. A calcified lesion with a cheesy core in MOSE must be suggestive of tuberculosis and leads to the request of the GeneXpert, which can detect MT deoxyribonucleic acid and resistance to rifampicin. A decent diagnostic strategy is crucial to prevent unnecessary surgical resection and provide conservative management with antitubercular therapy.

To our knowledge, this is the first review relating the correlation between cheesy core and tuberculosis and the importance of MOSE in diagnosing this rare disease, a subject to which the authors wish to draw attention.

FOOTNOTES

Author contributions: Delsa H collected the literature; Delsa H and Bellahammou K wrote the manuscript, and Okasha HH and Ghalim F revised the paper; All authors read and validated the final version of the manuscript.

Conflict-of-interest statement: All authors declare that they have no conflicts of interest.

Country/Territory of origin: Morocco

ORCID number: Hanane Delsa 0000-0001-7008-8552; Khadija Bellahammou 0000-0001-9487-3942; Hussein Hassan Okasha 0000-0002-0815-1394; Fahd Ghalim 0000-0002-9081-239X.

S-Editor: Liu JH
L-Editor: A
P-Editor: Liu JH

REFERENCES

1 **World Health Organization (WHO)**. Global Tuberculosis Report 2021; WHO: Geneva, Switzerland, 2021. (accessed on 1 November 2022). Available from: https://www.who.int/publications/i/item/9789240037021
2 **Panic N**, Maetzel H, Bulajic M, Radovanovic M, Löhr JM. Pancreatic tuberculosis: A systematic review of symptoms, diagnosis and treatment. *United European Gastroenterol J* 2020; **8**: 396-402 [PMID: 32213022 DOI: 10.1177/2050640620902353]
3 **Huang Y**, Ai L, Wang X, Sun Z, Wang F. Review and Updates on the Diagnosis of Tuberculosis. *J Clin Med* 2022; **11** [PMID: 36233689 DOI: 10.3390/jcm11195826]
4 **Song TJ**, Lee SS, Park DH, Lee TY, Lee SO, Seo DW, Lee SK, Kim MH. Yield of EUS-guided FNA on the diagnosis of pancreatic/peripancreatic tuberculosis. *Gastrointest Endosc* 2009; **69**: 484-491 [PMID: 19231490 DOI: 10.1016/j.gie.2008.10.007]
5 **Diaconu CC**, Gheorghe G, Hortopan A, Enache V, Ceobanu G, Jinga V, Adrian C, Ionescu VA. Pancreatic Tuberculosis-A Condition That Mimics Pancreatic Cancer. *Medicina (Kaunas)* 2022; **58** [PMID: 36143842 DOI: 10.3390/medicina58091165]
6 **So H**, Seo DW, Hwang JS, Ko SW, Oh D, Song TJ, Park DH, Lee SK, Kim MH. Macroscopic on-site evaluation after EUS-guided fine needle biopsy may replace rapid on-site evaluation. *Endosc Ultrasound* 2021; **10**: 111-115 [PMID: 33885006 DOI: 10.4103/EUS-D-20-00113]
7 **Miyamoto T**, Tone K, Inaki S, Saito R, Maeda M, Nagano Y, Akutsu T, Furube A, Gochi M, Motohashi K, Koido S, Takagi M, Kuwano K. Pancreatic tuberculosis in an immunocompetent young female mimicking a malignant tumor: A case report and diagnostic radiological investigation. *Clin Imaging* 2022; **81**: 114-117 [PMID: 34700173 DOI: 10.1016/j.clinimag.2021.09.021]
8 **Hoilat GJ**, Abdu M, Hoilat J, Gitto L, Bhutta AQ. A Rare Case of Pancreatic Tuberculosis Diagnosed *via* Endoscopic Ultrasound-Guided Fine Needle Aspiration and Polymerase Chain Reaction. *Cureus* 2020; **12**: e8795 [PMID: 32724744 DOI: 10.7759/cureus.8795]
9 **Ray S**, Das K, Ghosh R. Isolated pancreatic and peripancreatic nodal tuberculosis: A single-centre experience. *Trop Doct* 2021; **51**: 203-209 [PMID: 33104450 DOI: 10.1177/0049475520962941]
10 **Wu CX**, Xiao LB, Luo ZF, Shi SH. Diagnostic approaches for pancreatic tuberculosis. *Hepatobiliary Pancreat Dis Int* 2023; **22**: 107-110 [PMID: 35168872 DOI: 10.1016/j.hbpd.2022.01.004]
11 **Jenney AW**, Pickles RW, Hellard ME, Spelman DW, Fuller AJ, Spicer WJ. Tuberculous pancreatic abscess in an HIV antibody-negative patient: case report and review. *Scand J Infect Dis* 1998; **30**: 99-104 [PMID: 9730291 DOI: 10.1080/003655498750003438]
12 **Meesiri S**. Pancreatic tuberculosis with acquired immunodeficiency syndrome: a case report and systematic review. *World J Gastroenterol* 2012; **18**: 720-726 [PMID: 22363146 DOI: 10.3748/wjg.v18.i7.720]
13 **Gonzalo-Marin J**, Vila JJ, Perez-Miranda M. Role of endoscopic ultrasound in the diagnosis of pancreatic cancer. *World J Gastrointest Oncol* 2014; **6**: 360-368 [PMID: 25232461 DOI: 10.4251/wjgo.v6.i9.360]
14 **Maulahela H**, Fauzi A, Renaldi K, Srisantoso QP, Jasmine A. Current role of endoscopic ultrasound for gastrointestinal and abdominal tuberculosis. *JGH Open* 2022; **6**: 745-753 [PMID: 36406654 DOI: 10.1002/jgh3.12823]
15 **Sharma V**, Rana SS, Kumar A, Bhasin DK. Pancreatic tuberculosis. *J Gastroenterol Hepatol* 2016; **31**: 310-318 [PMID: 26414325 DOI: 10.1111/jgh.13174]
16 **Gupta D**, Patel J, Rathi C, Ingle M, Sawant P. Primary Pancreatic Head Tuberculosis: Great Masquerader of Pancreatic Adenocarcinoma. *Gastroenterology Res* 2015; **8**: 193-196 [PMID: 27785295 DOI: 10.14740/gr650w]
17 **Rana SS**, Bhasin DK, Srinivasan R, Sampath S, Mittal BR, Singh K. Distinctive endoscopic ultrasound features of isolated pancreatic tuberculosis and requirements for biliary stenting. *Clin Gastroenterol Hepatol* 2012; **10**: 323-325 [PMID: 22037426 DOI: 10.1016/j.cgh.2011.10.018]
18 **Dong Y**, Jürgensen C, Puri R, D'Onofrio M, Hocke M, Wang WP, Atkinson N, Sharma M, Dietrich CF. Ultrasound imaging features of isolated pancreatic tuberculosis. *Endosc Ultrasound* 2018; **7**: 119-127 [PMID: 28721972 DOI: 10.4103/2303-9027.210901]
19 **Sharma V (ed)**. Tuberculosis of the Gastrointestinal system. Singapore: Springer Nature Singapore [DOI: 10.1007/978-981-16-9053-2]
20 **Patel D**, Loren D, Kowalski T, Siddiqui AA. Pancreatic tuberculosis mimicking malignancy diagnosed with endoscopic ultrasound-guided fine needle aspiration. *Endosc Ultrasound* 2013; **2**: 38-40 [PMID: 24949364 DOI: 10.7178/eus.04.007]
21 **Varadarajulu S**, Wallace MB. Applications of endoscopic ultrasonography in pancreatic cancer. *Cancer Control* 2004; **11**: 15-22 [PMID: 14749619 DOI: 10.1177/107327480401100103]
22 **Mangiavillano B**, Frazzoni L, Togliani T, Fabbri C, Tarantino I, De Luca L, Staiano T, Binda C, Signoretti M, Eusebi LH, Auriemma F, Lamonaca L, Paduano D, Di Leo M, Carrara S, Fuccio L, Repici A. Macroscopic on-site evaluation (MOSE) of specimens from solid lesions acquired during EUS-FNB: multicenter study and comparison between needle gauges. *Endosc Int Open* 2021; **9**: E901-E906 [PMID: 34079874 DOI: 10.1055/a-1395-7129]
23 **Iwashita T**, Yasuda I, Mukai T, Doi S, Nakashima M, Uemura S, Mabuchi M, Shimizu M, Hatano Y, Hara A, Moriwaki H. Macroscopic on-site quality evaluation of biopsy specimens to improve the diagnostic accuracy during EUS-guided FNA using a 19-gauge needle for solid lesions: a single-center prospective pilot study (MOSE study). *Gastrointest Endosc* 2015; **81**: 177-185 [PMID: 25440688 DOI: 10.1016/j.gie.2014.08.040]

24 **Gaia S**, Rizza S, Bruno M, Ribaldone DG, Maletta F, Sacco M, Pacchioni D, Rizzi F, Saracco GM, Fagoonee S, De Angelis CG. Impact of Macroscopic On-Site Evaluation (MOSE) on Accuracy of Endoscopic Ultrasound-Guided Fine-Needle Biopsy (EUS-FNB) of Pancreatic and Extrapancreatic Solid Lesions: A Prospective Study. *Diagnostics (Basel)* 2022; **12** [PMID: 35204519 DOI: 10.3390/diagnostics12020428]

25 **Adigun R**, Basit H, Murray J. Cell Liquefactive Necrosis. 2022 Aug 8. In: StatPearls [Internet]. Treasure Island (FL): StatPearls Publishing; 2022 Jan- [PMID: 28613685]

26 **Yeat CM**, Achmad Sankala H, Mohd Zaki F, Mohamed Mukari SA. Tumour-like presentation of brainstem tuberculoma: a lesson learnt. *BMJ Case Rep* 2022; **15** [PMID: 36109096 DOI: 10.1136/bcr-2022-251672]

27 **Gopakumar KG**, Mohan N, Prasanth VR, Ajayakumar MK. Isolated parapharyngeal cold abscess in a 9-year-old boy. *Paediatr Int Child Health* 2019; **39**: 139-141 [PMID: 29493439 DOI: 10.1080/20469047.2018.1430666]

28 **Ng BK**, Yakob KA, Ng WYL, Lim PS, Abd Rahman R, Abdul Karim AK, Zainuddin AA, Mahdy ZA. Abdominopelvic Tuberculosis Secondary to a Nontuberculous Mycobacterium in an Immunocompetent Patient. *Case Rep Med* 2017; **2017**: 9016782 [PMID: 29259630 DOI: 10.1155/2017/9016782]

29 **Lakhey M**, Bhatta CP, Mishra S. Diagnosis of tubercular lymphadenopathy by fine needle aspiration cytology, acid-fast staining and mantoux test. *JNMA J Nepal Med Assoc* 2009; **48**: 230-233 [PMID: 20795463]

30 **Sahoo SS**, Tiwari V, Velagada S. A Rare Case of Tuberculosis as a Cause of Lytic Lesion of Talus Without Adjacent Bone Involvement in a Four-Year-Old Child. *Cureus* 2021; **13**: e16909 [PMID: 34513482 DOI: 10.7759/cureus.16909]

31 **Vafa H**, Arvanitakis M, Matos C, Demetter P, Eisendrath P, Toussaint E, Hittelet AB, Deviere J, Delhaye M. Pancreatic tuberculosis diagnosed by EUS: one disease, many faces. *JOP* 2013; **14**: 256-260 [PMID: 23669474 DOI: 10.6092/1590-8577/1355]

32 **Park M**, Kon OM. Use of Xpert MTB/RIF and Xpert Ultra in extrapulmonary tuberculosis. *Expert Rev Anti Infect Ther* 2021; **19**: 65-77 [PMID: 32806986 DOI: 10.1080/14787210.2020.1810565]

33 **Kim JB**, Lee SS, Kim SH, Byun JH, Park DH, Lee TY, Lee BU, Jeong SU, Seo DW, Lee SK, Kim MH. Peripancreatic tuberculous lymphadenopathy masquerading as pancreatic malignancy: a single-center experience. *J Gastroenterol Hepatol* 2014; **29**: 409-416 [PMID: 24303923 DOI: 10.1111/jgh.12410]

34 **Bennani K**, Khattabi A, Akrim M, Mahtar M, Benmansour N, Essakalli Hossyni L, Karkouri M, Cherradi N, El Messaoudi MD, Lahlou O, Cherkaoui I, Khader Y, Maaroufi A, Ottmani SE. Evaluation of the Yield of Histopathology in the Diagnosis of Lymph Node Tuberculosis in Morocco, 2017: Cross-Sectional Study. *JMIR Public Health Surveill* 2019; **5**: e14252 [PMID: 31599732 DOI: 10.2196/14252]

35 **Mechal Y**, Benaissa E, El Mrimar N, Benlahlou Y, Bssaibis F, Zegmout A, Chadli M, Malik YS, Touil N, Abid A, Maleb A, Elouennass M. Evaluation of GeneXpert MTB/RIF system performances in the diagnosis of extrapulmonary tuberculosis. *BMC Infect Dis* 2019; **19**: 1069 [PMID: 31856744 DOI: 10.1186/s12879-019-4687-7]

World Journal of Clinical Cases

Submit a Manuscript: https://www.f6publishing.com

World J Clin Cases 2023 April 6; 11(10): 2189-2200

DOI: 10.12998/wjcc.v11.i10.2189

ISSN 2307-8960 (online)

MINIREVIEWS

Liver manifestations in COVID-19 patients: A review article

Mariana Helou, Janane Nasr, Nour El Osta, Elsy Jabbour, Rola Husni

Specialty type: Medicine, research and experimental

Provenance and peer review: Invited article; Externally peer reviewed.

Peer-review model: Single blind

Peer-review report's scientific quality classification

Grade A (Excellent): 0
Grade B (Very good): B
Grade C (Good): C, C
Grade D (Fair): 0
Grade E (Poor): 0

P-Reviewer: Al-Ani RM, Iraq; He YH, China; Omar BJ, India

Received: December 27, 2022
Peer-review started: December 27, 2022
First decision: January 30, 2023
Revised: February 9, 2023
Accepted: March 10, 2023
Article in press: March 10, 2023
Published online: April 6, 2023

Mariana Helou, Division of Emergency Medicine, Department of Internal Medicine, Lebanese American University Medical Center, Lebanese American University School of Medicine, Beirut 1102-2801, Lebanon

Janane Nasr, Rola Husni, Division of Infectious Diseases, Department of Internal Medicine, Lebanese American University, School of Medicine, Beirut 1102-2801, Lebanon

Nour El Osta, Elsy Jabbour, Division of Emergency, Department of Internal Medicine, Lebanese American University, School of Medicine, Beirut 1102-2801, Lebanon

Corresponding author: Rola Husni, MD, Professor, Division of Infectious Diseases, Department of Internal Medicine, Lebanese American University, School of Medicine, Zahar Street, Beirut 1102-2801, Lebanon. roula.husni@lau.edu.lb

Abstract

The coronavirus disease 2019 (COVID-19) initially presented as a disease that affected the lungs. Then, studies revealed that it intricately affected disparate organs in the human body, with the liver being one of the most affected organs. This review aimed to assess the association between COVID-19 and liver function, shedding light on its clinical implication. However, its exact pathophysiology remains unclear, involving many factors, such as active viral replication in the liver cells, direct cytotoxic effects of the virus on the liver or adverse reactions to viral antigens. Liver symptoms are mild-to-moderate transaminase elevation. In some patients, with underlying liver disease, more serious outcomes are observed. Thus, liver function should be meticulously considered in patients with COVID-19.

Key Words: COVID-19; Liver injury; Liver disease; Liver manifestations

Core Tip: Coronavirus disease or coronavirus disease 2019 (COVID-19) is not only a respiratory illness but it can also affect the gastrointestinal system particularly the liver. Although the exact pathophysiology is unknown, more serious outcomes are seen when there is an underlying liver disease. Meticulous attention should be given to liver function in patients with COVID-19 infection.

Citation: Helou M, Nasr J, El Osta N, Jabbour E, Husni R. Liver manifestations in COVID-19 patients: A review article. *World J Clin Cases* 2023; 11(10): 2189-2200
URL: https://www.wjgnet.com/2307-8960/full/v11/i10/2189.htm
DOI: https://dx.doi.org/10.12998/wjcc.v11.i10.2189

INTRODUCTION

In December 2019, several cases of virus-induced respiratory pneumonia were reported in Wuhan, China. By March 2020, the virus severe acute respiratory syndrome coronavirus 2 (SARS-CoV-2) had already spread to other countries and infected thousands of individuals worldwide, which made the World Health Organization to declare a global pandemic. The disease initially presented with symptoms affecting the pulmonary system. Although some infected individuals could remain asymptomatic, most individuals with coronavirus disease 2019 (COVID-19) had reported fever, cough, fatigue, headache, and anosmia as the most common symptoms. However, approximately 15% of people suffered from severe COVID-19, including pneumonia with respiratory compromise, coagulopathies, strokes, multi-organ failure, and death[1]. Severe COVID-19 was most commonly reported in elderly people, men, and those with preexisting comorbidities, such as hypertension, diabetes, and coronary artery disease[2].

Studies showed that the impact of COVID-19 can extend from the pulmonary to other systems in the body and can affect disparate organs. Extrapulmonary manifestations involved cardiovascular, renal, gastrointestinal tract, reproductive, nervous, hematologic, and immune system symptoms[3]. The liver was found to be one of the affected organs following a COVID-19 infection. Several studies of liver dysfunction and elevated liver function tests such as alanine aminotransferase (ALT) and/or aspartate aminotransferase (AST) in patients without previous liver disease were reported shortly after the declaration of the COVID-19 pandemic[4]. For instance, one Chinese study demonstrated that nearly half of patients manifest liver dysfunction during their illness.

Researchers tried to investigate the possible causes of liver involvement during the COVID-19 infection. Direct hepatotoxicity resulting from the natural evolution of the disease, liver damage from the medication used for COVID-19 treatment, or the potential role of other comorbidities could be considered as factors causing liver dysfunction during the COVID-19 infection. Others reported that ongoing inflammatory processes and hypoxia following the COVID-19 infection may cause liver injury [5]. Nevertheless, the exact reasons behind liver damage remain unclear. Hence, multiple possible mechanisms contribute to these manifestations[6].

This review aimed to assess the association between SARS-CoV-2 and liver function, shedding light on its clinical implication. It also presents a perspective on the appropriate management of patients with COVID-19 with liver injury.

This narrative review was conducted following the Preferred Reporting Items for Systematic Reviews and Meta-Analyses (PRISMA) guidelines (Figure 1). Electronic databases and online sources were searched up to August 2022 using The Cochrane Library, the *Reference Citation Analysis* (https://www.referencecitationanalysis.com/) database, Medline, Embase, and Google Scholar. The following keywords were combined and used to identify relevant studies: "COVID-19" and "liver" and "liver injury" and "liver manifestations" and "liver tests." The articles were reviewed, and duplicates were excluded. An initial scan for titles and abstracts was performed, and then, full papers were kept for assessment. We included all articles written in the English language, published within the last 2 years after the COVID-19 pandemic, and where full texts were available. We excluded gray literature and studies not written in English.

The results of the literature search are summarized in a PRISMA flowchart (Figure 1). A total of 58 manuscripts were included in this review.

LIVER INJURY DUE TO COVID-19

COVID-19 manifestations are variable, with different clinical presentations, such as myalgia, fever, fatigue, headache, nausea vomiting, diarrhea, sore throat, nasal congestion, taste and smell abnormalities, confusion, chest pain, and abdominal pain[7].

The gastro-intestinal gastrointestinal (GI) tract is a prominent extrapulmonary site for COVID-19 involvement. Many patients complain of GI symptoms, such as nausea, diarrhea, and abdominal pain at the early stages of COVID-19, with studies estimating that number between 10% and 15%[8]. A meta-analysis of 12797 patients from 11 countries found that diarrhea is the most common GI presentation in patients with COVID-19 (12%), followed by nausea (9%), vomiting (9%), and abdominal pain (6%)[9, 10]. In critical patients, GI symptoms tend to be more severe, ranging from ileal (55.8%) to bowel ischemia (3.8%) among other serious complications[10].

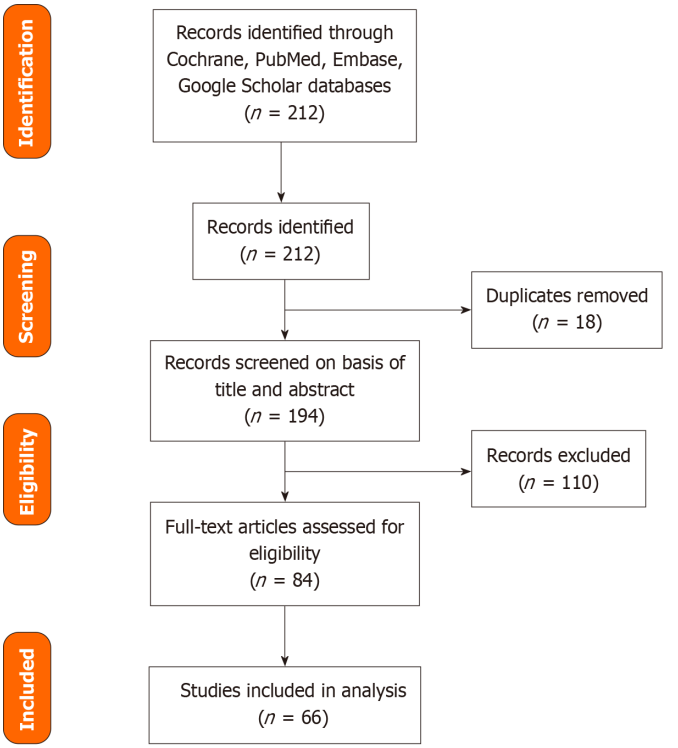

DOI: 10.12998/wjcc.v11.i10.2189

Figure 1 Prisma flowchart.

Symptoms may persist throughout the disease course and even after its finished, indicating a possible direct involvement and viral invasion of the GI tract. Stool samples of up to 50% of hospitalized patients infected with COVID-19 had the virus detectable in their stool samples, and some of them can still test positive for the viral for up to 1 wk after viral clearance from the lungs[11]. Histologically, biopsies taken from the esophagus, stomach, duodenum, and rectum of patients with COVID-19 revealed the presence of viral ribonucleic acid RNAs[8,11]. As for the liver in infected patients, a polymerase chain reaction of the liver tissue confirmed the presence of viral deoxyribonucleic acid DNAs[12-14]. COVID-19 was detected in the cytoplasm of hepatocytes, resulting in mitochondrial swelling, endoplasmic reticulum system dilatation, and cell membrane impairment[15].

The incidence rate of liver injuries in patients with COVID-19 varies greatly. An abnormal liver function was defined as an elevation of any parameter (ALT, AST, alkaline phosphatase, gamma-glutamyl transferase, and total bilirubin). Liver injury is defined as mild (< 2 times upper level of normal), moderate (2-5 times upper level of normal), and severe (> 5 times upper level of normal)[16,17]. Studies found that liver injury in patients with SARS-CoV-2 infection is between 14%-53%[16,17]. In a retrospective cohort study conducted by Phipps *et al*[18] on 2273 COVID-19 patients in the United States, 45% had mild, 21% had moderate, and 6.4% had a severe liver injury[18]. The severity of liver injury was significantly associated with the severity of the COVID-19 disease[19]. Moderate and severe liver injury was found to be more common in patients who required admission to the Intensive Care Unit[18]. However, even asymptomatic infected patients with COVID-19 have the same viral load, and consequently, liver damage can happen with elevation of liver enzymes, but to a lesser extended than the severe symptomatic patients[19]. Liver injury is more common in patients with high viral load. Thus, the risk of initial liver injury may be increased in patients infected with Delta mutations and having relatively large viral loads[19]. A study by Deng *et al*[20] compared liver injury in patients with Delta and Omicron variant-infected patients. The extended of inflammation and liver injury was similar among the two groups. However, male gender and high peak viral load were independent factors associated with liver injury[20]. A study conducted in young children with COVID-19 and liver injury showed that these patients have a milder course with less radiological and laboratory changes compared to adults[21].

A Chinese study of 1100 patients reported that AST and ALT levels were elevated in 18% and 20% of patients with non-severe COVID-19, as compared with 56% and 28% of patients with severe COVID-19, respectively, which can promote AST and ALT elevation of reaching up to 7590 and 1445 U/L, respectively, in some severe cases[22,23]. In patients with fatal COVID-19, the incidence of liver damage could range between 58.06% and 78%[24]. ALT elevation tends to peak between days 4 and 17 of hospitalization[25,26]. Other symptoms of liver dysfunction are hypoalbuminemia, increased prothrombin time, elevated serum bilirubin levels, hypoglycemia, and hyperammonemia[16].

Table 1 summarizes the different types of liver injury seen in COVID-19 patient[22-24,27-35].

PATHOPHYSIOLOGY

The pathophysiology of COVID-19's impact on the liver remains unclear. Several potential theories could explain the COVID-19 method affecting the liver.

One theory is that COVID-19 might contribute to liver damage through active viral replication in liver cells. A suggested mechanism for direct injury is hepatocytes apoptosis. This happens through viral proteins in specific protein 7a that can trigger cellular apoptosis in the liver but also in different organs, such as the lungs and kidneys. This cellular destruction is described by Tan *et al*[25]. Another possible entry of the virus is through receptors. Three receptors are the most commonly involved in this: Transmembrane serine protease 2 (TMPRSS2), Furin, and angiotensin converting enzyme 2 (ACE2) proteins. ACE2 receptors are present abundantly in the liver and the gastrointestinal mucosa. The virus binds to ACE2 receptors, abundantly present in the liver cells and GI mucosa[26]. The COVID-19 was detected inside the cytoplasm of the hepatocytes, leading to dilatation of the endoplasmic reticulum system, mitochondrial swelling, and cell membrane impairment. These receptors are more prevalent in the bile duct cells (53%) than in the liver cells (2.6%)[36,37]. Liver dysfunction can happen through bile duct damage more than a direct cytotoxic effect of the virus on the liver[26]. However, even though the ACE2 receptors are more commonly present in cholangiocytes than hepatocytes, a cholestatic pattern is less likely observed, and serum aminotransferase elevation is usually the common presentation. A possible reason for this is that other contributing factors are in cause and can raise the serum aminotransferase levels in liver injury. As example, a study discusses the possibility of the presence of co-receptors on the liver or an increase of the ACE2 receptors on liver cell surfaces[15]. This could explain the damage detected in the livers of patients with COVID-19, who showed signs of microvascular steatosis on post-mortem biopsies[38].

Another pathway for viral entry is TMPRSS2 found on hepatocytes, cholangiocytes, erythroid cells, and sinusoidal endothelial cells in the liver. Furin is another transmembrane serine protease that is present in all cell types[14,15,39]. Viral receptors expression on cell membranes is dynamic, upregulated by viral entry or even preexisting liver diseases[40].

Liver damage could also be caused by the adverse reactions to viral antigens. Respiratory viruses such the influenza virus, parvovirus, and respiratory syncytial virus bronchiolitis can all induce liver dysfunction with mild elevation of the liver enzyme levels to acute liver failure[16]. SARS-CoV-2 is speculated to affect the liver by SARS-CoV-2 viral antigens, in the form of nucleocapsids and spike proteins[12].

Immune dysregulation caused by COVID-19 plays a role in liver damage. COVID-19 leads to an inflammation in the lungs with elevation in serum inflammatory markers and production of pro-inflammatory cytokines, such as tumor necrosis factors (TNF-α), procalcitonin, C-reactive protein (CRP) and interleukins (IL-1, IL-2, IL-6, IL-8, IL-10, IL-17). Interferons are released, initiating a cascade that induces the expression of genes responsible for antiviral activity and viral replication disruption[41]. However, the consequence of rapid viral proliferation is a generalized inflammatory reaction with elevated inflammatory markers[26,42,43]. This can indirectly contribute to liver damage[26,42,43]. Research conducted on severe cases of COVID-19 have demonstrated the involvement of granulocyte-colony stimulating factor, TNF-α, interferon-inducible protein-10, monocyte chemotactic protein 1, and macrophage inflammatory protein 1 alpha, T helper 17, CD8 T cells, and IL-2, IL-6, IL-7, IL-10 in the immune response[44]. Moreover, inflammatory reaction and activation of the coagulation cascade resulting in a prothrombotic state in the blood can disrupt the gut vascular barrier and exacerbate liver injury[45].

Hypoxemia can also be a cause of liver injury. Cases of severe COVID-19 generally ends in sepsis state particularly when patients have gut microbiota imbalance and pre-existing liver disease[44]. Hepatic damage post sepsis is usually associated with shock, cholestasis, drug toxicity, and inflammation[44]. Severe infection with hemodynamic instability and shock compromises blood supply to vital organs, including the liver. The result is hypoxic ischemia of the liver, characterized by centrilobular hepatocellular necrosis that can progress to irreversible hypoxic injury[16]. Hypoxemia is one cause of liver injury with bad prognosis[44]. Recent data shows that hypoxic liver injury in COVID-19 patients is caused by metabolic acidosis with calcium overloading and abnormality in the mitochondrial permeability transition pore protein[44].

Hepatotoxic drugs are a common cause of liver injury in COVID-19 patients. Combinations of antiviral, steroid, and antibiotic drugs were all used to decrease symptom severity and prevent potentially fatal complications. Since most of these drugs were metabolized in the liver, medications used for the treatment of COVID-19 can induce liver dysfunction[46]. The rate of drug-induced liver injury was found to be approximately 25% in a meta-analysis of 20874 patients with COVID-19[47,48]. Remdesivir, tocilizumab, lopinavir/ritonavir, ribavirin, hydroxychloroquine, steroids, and macrolides, all used for the treatment of COVID-19, can cause hepatotoxicity[49].

Antiviral treatments for COVID-19 are prescribed to approximately 50% of critical patients, and these drugs cause hepatotoxicity. Evidence suggests that the use of lopinavir or ritonavir can contribute to

Table 1 Liver injury in coronavirus disease 2019 patients in different trials

Ref.	Number of patients infected with COVID-19	Patients with liver injury (percentage)	Patients with preexisting liver damage (percentage)	Elevated indicators	Mortality
Chen *et al*[23]	99	43 (43.4)	-	43 patients had differing degrees of liver function abnormality. Prothrombin time increased by 5%, one patient had severe liver function damage (ALT: 7590 U/L, AST: 1445 U/L)	11% (day 24)
Wang *et al*[27]	69	42 (60.9)	1 (1)	Abnormal ALT: 33%; abnormal AST: 28%	7.5% (day 19)
Cai *et al* [28]	298	44 (14.8)	8 (2.7)	Abnormal ALT: 13.1%; abnormal AST: 8.4%	1% (day 55)
Zhang *et al*[29]	82 death cases	64 (78.0)	2 (2.4)	Abnormal ALT: 30.6%; abnormal AST: 61.1%; abnormal total bilirubin 30.6%	ALT (> 40 U/L), AST (> 40 U/L), and TBIL (> 20.5 mmol/L) increased in 30.6%, 61.1%, and 30.6% cases
Wang *et al*[30]	138	55 (39.9)	4 (29)	Abnormal ALT: 17.4%; abnormal AST: 22.5%	4.3% (day 33)
Li *et al* [31]	85	33 (38.8)	6 (7)	Abnormal ALT: 38.8%	-
Yang *et al*[32]	52	15 (28.9)	15 (29)	-	62% (day 28)
Fan *et al* [33]	148	75 (50.7)	6 (8)	Abnormal ALT: 18.2%; abnormal AST: 21.6%	0.67% (day 11)
Huang *et al*[24]	41	15 (36.6)	1 (2)	Abnormal AST: 37%	15% (day 17)
Guan *et al*[22]	67	22 (32)	Hepatitis B: 2.1%	Abnormal ALT: 21.3%; abnormal AST: 22.2%	22% (day 51)
Shi *et al* [34]	81	42 (53)	Hepatitis or liver cirrhosis in 9% of cases	Abnormal AST: 53%	5% (day 50)
Xu *et al* [35]	62	4 (12)	7 (11)	Levels of AST increased in 10 (16%) patients	0% (day 34)

COVID-19: Coronavirus disease 2019; AST: Aspartate aminotransferase; ALT: Alanine aminotransferase; TBIL: Total bilirubin.

liver injury in patients with COVID-19, as those with liver injury were found to have higher usage rates of these medications compared with those with normal livers[33]. Patients treated with lopinavir/ritonavir show commonly liver damage, and liver injury is 3.58 times greater in patients receiving treatment compared with patients who did not receive treatment[50]. Liver damage is increased by 12.1% after drug treatment[50]. Ribavirin-induced hemolysis could exacerbate tissue hypoxia and further liver ischemia and injury. The National Health Commission of the People's Republic of China had to stipulate that treatment for long term with these drugs, especially in high doses, can lead to hepatotoxicity[26]. Remdesivir was approved in May 2020 for the treatment of COVID-19. Remdesivir is metabolized by Cytochromes P450. The treatment with remdesivir reduces the hospitalization time for COVID-19 patients and accelerates recovery[44]. In COVID-19 patients treated by remdesivir, reversible elevations of ALT and AST were found with 6% of patients having a marked increase in AST and ALT while only 2% having a life-threatening situation[44].

Chinese drugs used by individuals to treat their infections may also induce liver injury[7]. Further, many patients infected with COVID-19 firstly present with fever, cough, and fatigue; and many of them self-medicate using antipyretics, such as acetaminophen, a known hepatotoxic medication. Moreover, herbal products, used for cough or pain, may have a deleterious effect on liver function[7]. Patients with preexisting liver diseases or chronic hepatitis are more susceptible to drug-induced liver damage, and thereby, special consideration must be given before prescribing any drug[7].

Figure 2 shows different mechanisms of liver injury in COVID-19.

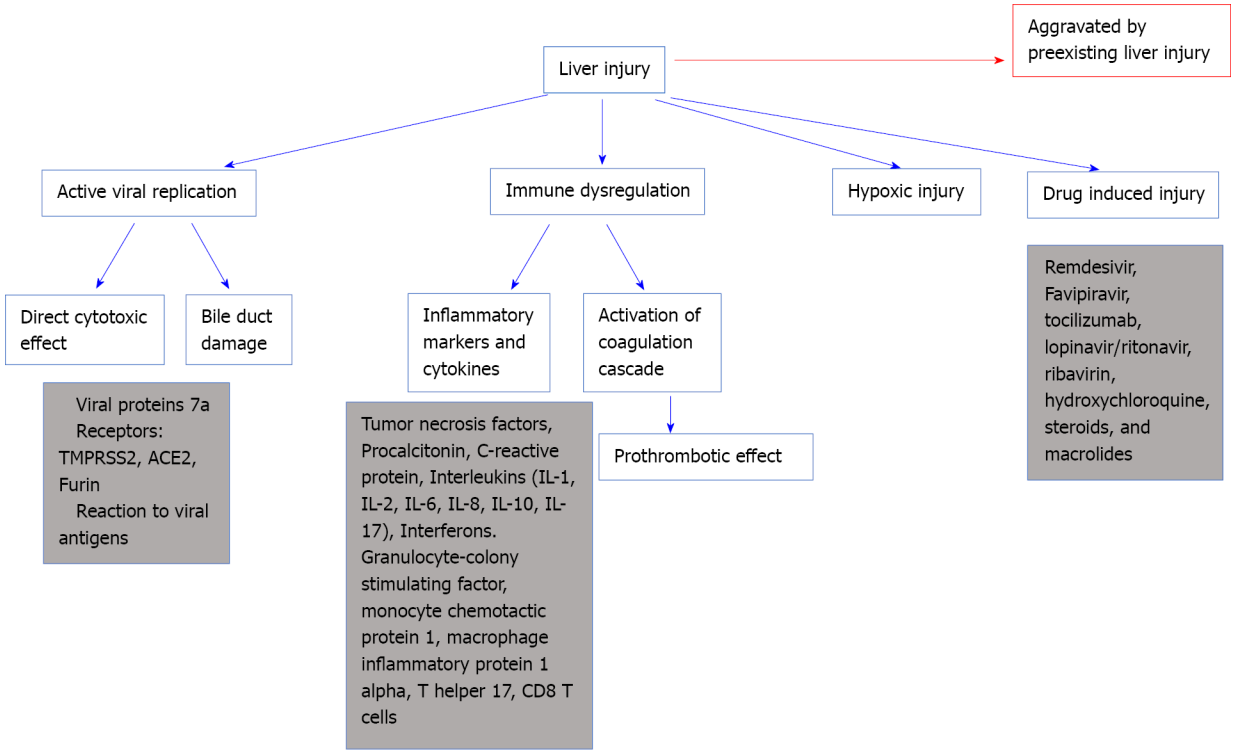

DOI: 10.12998/wjcc.v11.i10.2189

Figure 2 Mechanisms of liver injury from coronavirus disease 2019 infection. IL: Interleukin; ACE2: Angiotensin converting enzyme 2; TMPRSS2: Transmembrane serine protease 2.

COVID-19 IN PATIENTS WITH CHRONIC LIVER DISEASE

Early evidence denied the likelihood of increased risk of COVID-19 infection in patients with chronic yet well-managed hepatitis B or C. However, COVID-19 could still affect liver function in these patients through hepatic decompensation of the already depleted hepatic reserves, and reactivation of hepatitis viral replication following the immunocompromised state that SARS-CoV-2 induces in these patients [51]. Furthermore, patients with preexisting liver diseases tend to have co-existing comorbidities, such as diabetes, hypertension, and cardiovascular disease that also confer higher chances of severe diseases to these patients. To date, no studies confirmed that patients with liver disorders are at increased risk of being infected; however, these patients may have other risk factors that may complicate the course of infection, making it more severe, such as diabetes, anemia, and cardiovascular disorders[49].

Chen *et al*[52] found that chronic hepatitis B patients are more prone to COVID-19 infection[52]; however, other studies showed that chronic viral hepatitis is not proportional to the severity of COVID-19 infection[22,53]. Regarding viral hepatitis treatment in patients co-infected with COVID-19, the American Association for the Study of Liver Diseases (AASLD) recommends to continue the treatment for hepatitis B and C if already started before the COVID-19 infection and considers initiating hepatitis B treatment in patients suspected of hepatitis B flare; however, studies are still lacking. Starting the treatment for hepatitis C in a patient with COVID-19 is not yet routinely warranted.

COVID-19 AND NONALCOHOLIC STEATOHEPATITIS

Nonalcoholic fatty liver disease (NAFLD) was found to be associated with a more severe COVID-19 disease course and protracted viral shedding time[54]. Patients with NAFLD had a higher probability of disease progression and higher risk of elevating liver tests upon admission to discharge[47]. This could be caused by hepatic macrophage dysfunction and imbalance between M1 macrophages, promoters of inflammation and M2 macrophages, suppressers of inflammation observed in patients with NAFLD and by excessive production of cytokines, such as TNF-α by the adipose and Kupffer cells[38,54].

Obesity was found to increase mortality risks in patients with COVID-19 and was associated with a higher likelihood of needing invasive ventilation. ACE2 receptors are predominantly found in the adipose tissues, which might facilitate COVID-19 invasion in the fat tissues. Patients with nonalcoholic steatohepatitis (NASH) generally have disrupted inflammatory mechanisms, making them more vulnerable. Thus, close monitoring is advisable in these patients. These deleterious effects are

compounded when considering that obese patients are also highly at higher risk for NASH[6].

Some studies reportedly undermined NAFLD's role in COVID-19-associated liver damage. A series of 155 patients hospitalized for COVID-19 infection showed that steatosis (present in 43% of the cases) was not associated with mortality[55]. A larger study conducted on 745 patients from 29 countries having chronic liver disease and cirrhosis found that the odds ratio for death in patients with NAFLD was 1.01 (95% confidence interval: 0.57–1.79)[56].

Mushtaq *et al*[57] studied 589 symptomatic COVID-19 patients with who were hospitalized in the state of Qatar. They found that NAFLD predicts mild to moderate liver injury while it does not predicts mortality, disease severity or disease progression[57].

These inconsistent findings require more, larger studies to assess the presence of increased mortality risk in patients with NAFLD and NASH infected with COVID-19.

COVID-19 AND PREEXISTING CHRONIC LIVER DISEASE

Patients with chronic liver disease and cirrhosis would be more prone to COVID-19 induced liver injury than those without preexisting liver damage. A meta-analysis of 5595 patients infected with COVID-19 showed that 3% of patients with preexisting liver disease had higher rates of severe complications (57.335) and mortality (17.65%) than those without the chronic liver disease[58].

Patients with cirrhosis are known to be a high-risk population and prone to higher rates of mortality when infected with COVID-19[59]. In a national registry study, Marjot *et al*[56] found that patients with cirrhosis had a mortality rate of 32% while patients with no cirrhosis had a rate of 8%, with higher rates of liver decompensation observed in the former group[56]. Lung injury is the primary cause of death in patients with COVID-19, and liver dysfunction helps exacerbate this injury[60]. Cirrhosis have been associated with inflammation and dysregulation of the immune system. This dysregulation may explain the increased severity and mortality due to COVID-19. Additionally, in cirrhosis, coagulation disorders, cirrhotic decompensation, cytokine release, and exacerbation of ascites or encephalopathy all strain the already depleted liver reserves and increase mortality rates[59].

Studies on the impact of COVID-19 on patients with alcohol-associated liver disease (ALD) are limited[39]. Nevertheless, data show that patients with COVID-19 and alcohol-related cirrhosis also exhibited increased mortality, a finding consistent with other patients with liver cirrhosis[61]. Kim *et al*[62] supported these findings through their study of 867 patients with chronic liver disease having a COVID-19 infection, demonstrating that patients with ALD had an increased risk of poor survival and higher risk of mortality rate[62]. ALD is associated with danger-associated molecular patterns that induce an inflammatory state with cytokine release[63]. In patients with ALD, the superimposed cytokine storm caused by COVID-19 could increases the inflammatory process and results in worse outcomes[39].

Hepatocellular carcinoma (HCC) and COVID-19 infection are also associated with poor outcomes. Chinese patients with underlying malignancies infected with COVID-19 were found to have higher odds of being infected with SARS-CoV-2 and progressing to more severe disease forms. As in any other malignancy, HCC is associated with poor immunity and hypoproteinemia, in addition to chemotherapy that promotes further immunosuppression, leading to the recommendation of deferring locoregional treatments wherever possible and gradually phasing out immunological anticancer therapies when at risk of COVID-19 disease[64].

PATIENTS WHO UNDERWENT A LIVER TRANSPLANT

Many centers for liver transplantation had to cut down their procedures because of the COVID-19 crisis. Yet, current evidence suggests that liver transplant recipients who are on immunosuppressants have the same fatality rate as the rest of the population[39].

Management of liver transplant recipients infected with COVID-19 is challenging because of drug-drug interactions and the right immunosuppressant levels. Current evidence supports continuing immunosuppressive treatment in liver transplant recipients and preventing dose reduction. It remains unclear whether steroids help liver transplant patients with COVID-19, as it was proven to help hospitalized COVID-19 patients[56].

The benefit of vaccination should be heightened in patients with chronic liver disease due to their imbalanced immune system, from their disease, and immunosuppressive treatment.

TREATMENT OF LIVER DISEASE

The advancement of developing the best therapy for COVID-19 evolves at a high pace. Yet, little is known about the ideal treatment for liver injury. AASLD recommends continuing treatment of viral

hepatitis in patients with co-infection with COVID-19 and prevention of hepatitis flare. If steroids are to be prescribed, the risk of hepatitis flare should be evaluated. Most liver damages caused by COVID-19 infection are temporary and rarely result in liver failure. However, when severe liver dysfunction increases, prompt assessment, and screening for underlying diseases and previous history of liver diseases are warranted. Exposure to hepatotoxic agents such as alcohol and drug chemicals should be examined, as should the circulation and ventilation statuses of the patient.

Liver function tests should be routinely measured to preclude further liver damage. Furthermore, other etiologies for liver injury should be considered. If AST and lactate dehydrogenase are elevated but ALT levels are normal, the skeletal muscle or cardiac origin of elevation should be considered. L-ornithine-L-aspartate could be effective in hepatic encephalopathy with elevated ammonia levels[44]. However this is only used as a complimentary treatment. Probiotics can also be considered, they restore gut microbiota dysbiosis and prevent any infections. Ursodeoxycholic acid 500 mg/d protect hepatic function from injury due to its anti-inflammatory and immunomodulating activities. Nevertheless, further studies are needed to confirm this benefit[5,44]. N-acetylcysteine could be used in COVID-19 patients, it causes obvious drop in inflammatory markers in particular CRP and ferritin levels. In addition, NAC blocked hemolysis and liver enzyme elevation. Further studies for this treatment are needed[44].

The treatment of COVID-19-induced liver injury is dependent on the severity of the damage and the identification and treatment of underlying causes if present. Patients with mildly elevated liver enzymes do not need hepatoprotective drugs. Patients with severe liver dysfunction require treatment with hepatoprotective, jaundice-reducing, and anti-inflammatory drugs, such as polyene phosphatidylcholine, glycyzic acid, bicyclol, and vitamin E. In critically ill patients, special consideration should be taken for the extent of liver injury and the number of medications used. This minimizes the risk of drug-drug interactions and eschews the risk of aggravating the liver injury by selecting an antiviral drug with minimal hepatotoxicity. One group of antivirals could be glycyrrhizic acid derivatives as shown by[65]. Glycyrrhizin has been used for several years as an anti-inflammatory of choice for liver disease protection.

Inconsistent findings have been reported in the literature on whether anticoagulation increases the risk of bleeding in cirrhotic patients with COVID-19 since they are excluded from the majority of published studies related to thromboprophylaxis. However, an Italian multicenter study conducted on 40 patients reassured no increased hemorrhagic risk among cirrhotic patients admitted with COVID-19.

Effects of the COVID-19 vaccine on specific organs, such as the liver and GI tract remain unknown. Further study is required to evaluate the long-term effects of the vaccine based on the GI tract.

PROGNOSIS

Liver injury in patients with mild COVID-19 is usually transient and does not require treatment. Liver failure is also rarely reported.

Despite using elevated serum aminotransferases as indicators of liver injury during COVID-19 infection, a direct correlation between elevated liver enzymes and COVID-19 severity could not be demonstrated. However, patients with severe COVID-19 disease tend to have more elevated liver function tests than those with mild disease. After recovery, liver enzymes gradually return to their normal levels. Further noteworthy consequences of COVID-19-induced liver injury, especially for elderly individuals, include the activation of fibrinolytic and clothing pathways and innate immune system dysregulation.

The prognostic correlation with elevated liver enzymes remains debatable. No evidence showed that higher liver enzymes are associated with higher mortality risk. Age, associated comorbidities, and preexisting alcohol-related liver disease are the main risk factors for poor outcomes[66].

Fan *et al*[33] concluded in their trial on 148 hospitalized patients that abnormal liver functions are associated with prolonged hospitalization[33].

Comparable results were drawn from other studies. Wang *et al*[27] also concluded that the male sex predisposes to more liver damage[27].

CONCLUSION

Despite the lack of evidence to elucidate the mechanisms of liver injury induced by COVID-19 infection, this review provides a comprehensive approach to several theories investigated. Further research is needed to clarify the factors in cause and determine factors that might exacerbate liver injury in COVID-19 infected patients. Meticulous attention should be kept on the liver of patients with COVID-19 infection, especially during hospitalization. It is not clear yet on how to treat liver damage in patients with COVID-19 infection. There are no clear guidelines for proper treatment of liver injury in COVID-19 patients. Comparative studies might be needed for better evidence.

FOOTNOTES

Author contributions: Authors have contributed equally in the writing; All authors had full access to all of the data in the study and can take responsibility for the integrity and accuracy of the data.

Conflict-of-interest statement: All the authors report no relevant conflicts of interest for this article.

Country/Territory of origin: Lebanon

ORCID number: Mariana Helou 0000-0001-8626-8988; Rola Husni 0000-0001-5892-7608.

S-Editor: Fan JR
L-Editor: A
P-Editor: Fan JR

REFERENCES

1 **Berlin DA**, Gulick RM, Martinez FJ. Severe Covid-19. *N Engl J Med* 2020; **383**: 2451-2460 [PMID: 32412710 DOI: 10.1056/NEJMcp2009575]
2 **Williamson EJ**, Walker AJ, Bhaskaran K, Bacon S, Bates C, Morton CE, Curtis HJ, Mehrkar A, Evans D, Inglesby P, Cockburn J, McDonald HI, MacKenna B, Tomlinson L, Douglas IJ, Rentsch CT, Mathur R, Wong AYS, Grieve R, Harrison D, Forbes H, Schultze A, Croker R, Parry J, Hester F, Harper S, Perera R, Evans SJW, Smeeth L, Goldacre B. Factors associated with COVID-19-related death using OpenSAFELY. *Nature* 2020; **584**: 430-436 [PMID: 32640463 DOI: 10.1038/s41586-020-2521-4]
3 **Zheng KI**, Feng G, Liu WY, Targher G, Byrne CD, Zheng MH. Extrapulmonary complications of COVID-19: A multisystem disease? *J Med Virol* 2021; **93**: 323-335 [PMID: 32648973 DOI: 10.1002/jmv.26294]
4 **Cai Q**, Huang D, Yu H, Zhu Z, Xia Z, Su Y, Li Z, Zhou G, Gou J, Qu J, Sun Y, Liu Y, He Q, Chen J, Liu L, Xu L. COVID-19: Abnormal liver function tests. *J Hepatol* 2020; **73**: 566-574 [PMID: 32298767 DOI: 10.1016/j.jhep.2020.04.006]
5 **Cichoż-Lach H**, Michalak A. Liver injury in the era of COVID-19. *World J Gastroenterol* 2021; **27**: 377-390 [PMID: 33584070 DOI: 10.3748/wjg.v27.i5.377]
6 **Metawea MI**, Yousif WI, Moheb I. COVID 19 and liver: An A-Z literature review. *Dig Liver Dis* 2021; **53**: 146-152 [PMID: 32988758 DOI: 10.1016/j.dld.2020.09.010]
7 **Yang RX**, Zheng RD, Fan JG. Etiology and management of liver injury in patients with COVID-19. *World J Gastroenterol* 2020; **26**: 4753-4762 [PMID: 32921955 DOI: 10.3748/wjg.v26.i32.4753]
8 **Lin L**, Jiang X, Zhang Z, Huang S, Fang Z, Gu Z, Gao L, Shi H, Mai L, Liu Y, Lin X, Lai R, Yan Z, Li X, Shan H. Gastrointestinal symptoms of 95 cases with SARS-CoV-2 infection. *Gut* 2020; **69**: 997-1001 [PMID: 32241899 DOI: 10.1136/gutjnl-2020-321013]
9 **Tariq R**, Saha S, Furqan F, Hassett L, Pardi D, Khanna S. Prevalence and Mortality of COVID-19 Patients With Gastrointestinal Symptoms: A Systematic Review and Meta-analysis. *Mayo Clin Proc* 2020; **95**: 1632-1648 [PMID: 32753138 DOI: 10.1016/j.mayocp.2020.06.003]
10 **Bhurwal A**, Minacapelli CD, Orosz E, Gupta K, Tait C, Dalal I, Zhang C, Zhao E, Rustgi VK. COVID-19 status quo: Emphasis on gastrointestinal and liver manifestations. *World J Gastroenterol* 2021; **27**: 7969-7981 [PMID: 35046624 DOI: 10.3748/wjg.v27.i46.7969]
11 **Xiao F**, Tang M, Zheng X, Liu Y, Li X, Shan H. Evidence for Gastrointestinal Infection of SARS-CoV-2. *Gastroenterology* 2020; **158**: 1831-1833.e3 [PMID: 32142773 DOI: 10.1053/j.gastro.2020.02.055]
12 **Cheung CCL**, Goh D, Lim X, Tien TZ, Lim JCT, Lee JN, Tan B, Tay ZEA, Wan WY, Chen EX, Nerurkar SN, Loong S, Cheow PC, Chan CY, Koh YX, Tan TT, Kalimuddin S, Tai WMD, Ng JL, Low JG, Yeong J, Lim KH. Residual SARS-CoV-2 viral antigens detected in GI and hepatic tissues from five recovered patients with COVID-19. *Gut* 2022; **71**: 226-229 [PMID: 34083386 DOI: 10.1136/gutjnl-2021-324280]
13 **Tian D**, Ye Q. Hepatic complications of COVID-19 and its treatment. *J Med Virol* 2020; **92**: 1818-1824 [PMID: 32437004 DOI: 10.1002/jmv.26036]
14 **Song M**, Li ZL, Zhou YJ, Tian G, Ye T, Zeng ZR, Deng J, Wan H, Li Q, Liu JB. Gastrointestinal involvement of COVID-19 and potential faecal transmission of SARS-CoV-2. *J Zhejiang Univ Sci B* 2020; **21**: 749-751 [PMID: 32893532 DOI: 10.1631/jzus.B2000253]
15 **Wang Y**, Liu S, Liu H, Li W, Lin F, Jiang L, Li X, Xu P, Zhang L, Zhao L, Cao Y, Kang J, Yang J, Li L, Liu X, Li Y, Nie R, Mu J, Lu F, Zhao S, Lu J, Zhao J. SARS-CoV-2 infection of the liver directly contributes to hepatic impairment in patients with COVID-19. *J Hepatol* 2020; **73**: 807-816 [PMID: 32437830 DOI: 10.1016/j.jhep.2020.05.002]
16 **Vargas-Mendoza N**, García-Machorro J, Angeles-Valencia M, Martínez-Archundia M, Madrigal-Santillán EO, Morales-González Á, Anguiano-Robledo L, Morales-González JA. Liver disorders in COVID-19, nutritional approaches and the use of phytochemicals. *World J Gastroenterol* 2021; **27**: 5630-5665 [PMID: 34629792 DOI: 10.3748/wjg.v27.i34.5630]

17 **Zhou F**, Xia J, Yuan HX, Sun Y, Zhang Y. Liver injury in COVID-19: Known and unknown. *World J Clin Cases* 2021; **9**: 4980-4989 [PMID: 34307548 DOI: 10.12998/wjcc.v9.i19.4980]

18 **Phipps MM**, Barraza LH, LaSota ED, Sobieszczyk ME, Pereira MR, Zheng EX, Fox AN, Zucker J, Verna EC. Acute Liver Injury in COVID-19: Prevalence and Association with Clinical Outcomes in a Large U.S. Cohort. *Hepatology* 2020; **72**: 807-817 [PMID: 32473607 DOI: 10.1002/hep.31404]

19 **Choi CW**, Sung HK, Jeong JY, Lim DH, Choi J, Kwon HC, Nam S, Kim Y, Chin B. Changing Features of Liver Injury in COVID-19 Patients: Impact of Infection with the SARS-CoV-2 Delta (B.1.617.2) Variants. *Infect Chemother* 2022; **54**: 744-756 [PMID: 36596683 DOI: 10.3947/ic.2022.0122]

20 **Deng H**, Lin H, Mai Y, Liu H, Chen W. Clinical features and predictive factors related to liver injury in SARS-CoV-2 Delta and Omicron variant-infected patients. *Eur J Gastroenterol Hepatol* 2022; **34**: 933-939 [PMID: 35482929 DOI: 10.1097/MEG.0000000000002381]

21 **Xu Y**, Li X, Zhu B, Liang H, Fang C, Gong Y, Guo Q, Sun X, Zhao D, Shen J, Zhang H, Liu H, Xia H, Tang J, Zhang K, Gong S. Characteristics of pediatric SARS-CoV-2 infection and potential evidence for persistent fecal viral shedding. *Nat Med* 2020; **26**: 502-505 [PMID: 32284613 DOI: 10.1038/s41591-020-0817-4]

22 **Guan WJ**, Ni ZY, Hu Y, Liang WH, Ou CQ, He JX, Liu L, Shan H, Lei CL, Hui DSC, Du B, Li LJ, Zeng G, Yuen KY, Chen RC, Tang CL, Wang T, Chen PY, Xiang J, Li SY, Wang JL, Liang ZJ, Peng YX, Wei L, Liu Y, Hu YH, Peng P, Wang JM, Liu JY, Chen Z, Li G, Zheng ZJ, Qiu SQ, Luo J, Ye CJ, Zhu SY, Zhong NS; China Medical Treatment Expert Group for Covid-19. Clinical Characteristics of Coronavirus Disease 2019 in China. *N Engl J Med* 2020; **382**: 1708-1720 [PMID: 32109013 DOI: 10.1056/NEJMoa2002032]

23 **Chen N**, Zhou M, Dong X, Qu J, Gong F, Han Y, Qiu Y, Wang J, Liu Y, Wei Y, Xia J, Yu T, Zhang X, Zhang L. Epidemiological and clinical characteristics of 99 cases of 2019 novel coronavirus pneumonia in Wuhan, China: a descriptive study. *Lancet* 2020; **395**: 507-513 [PMID: 32007143 DOI: 10.1016/S0140-6736(20)30211-7]

24 **Huang C**, Wang Y, Li X, Ren L, Zhao J, Hu Y, Zhang L, Fan G, Xu J, Gu X, Cheng Z, Yu T, Xia J, Wei Y, Wu W, Xie X, Yin W, Li H, Liu M, Xiao Y, Gao H, Guo L, Xie J, Wang G, Jiang R, Gao Z, Jin Q, Wang J, Cao B. Clinical features of patients infected with 2019 novel coronavirus in Wuhan, China. *Lancet* 2020; **395**: 497-506 [PMID: 31986264 DOI: 10.1016/S0140-6736(20)30183-5]

25 **Tan YJ**, Fielding BC, Goh PY, Shen S, Tan TH, Lim SG, Hong W. Overexpression of 7a, a protein specifically encoded by the severe acute respiratory syndrome coronavirus, induces apoptosis *via* a caspase-dependent pathway. *J Virol* 2004; **78**: 14043-14047 [PMID: 15564512 DOI: 10.1128/JVI.78.24.14043-14047.2004]

26 **Wu J**, Song S, Cao HC, Li LJ. Liver diseases in COVID-19: Etiology, treatment and prognosis. *World J Gastroenterol* 2020; **26**: 2286-2293 [PMID: 32476793 DOI: 10.3748/wjg.v26.i19.2286]

27 **Wang Z**, Yang B, Li Q, Wen L, Zhang R. Clinical Features of 69 Cases With Coronavirus Disease 2019 in Wuhan, China. *Clin Infect Dis* 2020; **71**: 769-777 [PMID: 32176772 DOI: 10.1093/cid/ciaa272]

28 **Cai Q**, Huang D, Ou P, Yu H, Zhu Z, Xia Z, Su Y, Ma Z, Zhang Y, Li Z, He Q, Liu L, Fu Y, Chen J. COVID-19 in a designated infectious diseases hospital outside Hubei Province, China. *Allergy* 2020; **75**: 1742-1752 [PMID: 32239761 DOI: 10.1111/all.14309]

29 **Zhang B**, Zhou X, Qiu Y, Song Y, Feng F, Feng J, Song Q, Jia Q, Wang J. Clinical characteristics of 82 cases of death from COVID-19. *PLoS One* 2020; **15**: e0235458 [PMID: 32645044 DOI: 10.1371/journal.pone.0235458]

30 **Wang D**, Hu B, Hu C, Zhu F, Liu X, Zhang J, Wang B, Xiang H, Cheng Z, Xiong Y, Zhao Y, Li Y, Wang X, Peng Z. Clinical Characteristics of 138 Hospitalized Patients With 2019 Novel Coronavirus-Infected Pneumonia in Wuhan, China. *JAMA* 2020; **323**: 1061-1069 [PMID: 32031570 DOI: 10.1001/jama.2020.1585]

31 **Li L**, Li S, Xu MM, Yu PF, Zheng SJ, Duan ZP, Liu J, Chen Y, Li JF. Risk factors related to hepatic injury in patients with corona virus disease 2019. 2020 Preprint. Available from: medRxiv:2020.02.28.20028514 [DOI: 10.1101/2020.02.28.20028514]

32 **Yang X**, Yu Y, Xu J, Shu H, Xia J, Liu H, Wu Y, Zhang L, Yu Z, Fang M, Yu T, Wang Y, Pan S, Zou X, Yuan S, Shang Y. Clinical course and outcomes of critically ill patients with SARS-CoV-2 pneumonia in Wuhan, China: a single-centered, retrospective, observational study. *Lancet Respir Med* 2020; **8**: 475-481 [PMID: 32105632 DOI: 10.1016/S2213-2600(20)30079-5]

33 **Fan Z**, Chen L, Li J, Cheng X, Yang J, Tian C, Zhang Y, Huang S, Liu Z, Cheng J. Clinical Features of COVID-19-Related Liver Functional Abnormality. *Clin Gastroenterol Hepatol* 2020; **18**: 1561-1566 [PMID: 32283325 DOI: 10.1016/j.cgh.2020.04.002]

34 **Shi H**, Han X, Jiang N, Cao Y, Alwalid O, Gu J, Fan Y, Zheng C. Radiological findings from 81 patients with COVID-19 pneumonia in Wuhan, China: a descriptive study. *Lancet Infect Dis* 2020; **20**: 425-434 [PMID: 32105637 DOI: 10.1016/S1473-3099(20)30086-4]

35 **Xu XW**, Wu XX, Jiang XG, Xu KJ, Ying LJ, Ma CL, Li SB, Wang HY, Zhang S, Gao HN, Sheng JF, Cai HL, Qiu YQ, Li LJ. Clinical findings in a group of patients infected with the 2019 novel coronavirus (SARS-Cov-2) outside of Wuhan, China: retrospective case series. *BMJ* 2020; **368**: m606 [PMID: 32075786 DOI: 10.1136/bmj.m606]

36 **Zhao Y**, Zhao Z, Wang Y, Zhou Y, Ma Y, Zuo W. Single-Cell RNA Expression Profiling of ACE2, the Receptor of SARS-CoV-2. *Am J Respir Crit Care Med* 2020; **202**: 756-759 [PMID: 32663409 DOI: 10.1164/rccm.202001-0179LE]

37 **Zhang H**, Kang Z, Gong H, Xu D, Wang J, Li Z, Cui X, Xiao J, Meng T, Zhou W, Liu J, Xu H. The digestive system is a potential route of 2019-nCov infection: a bioinformatics analysis based on single-cell transcriptomes. 2020 Preprint. Available from: BioRxiv:2020.01.30.927806 [DOI: 10.1101/2020.01.30.927806]

38 **Xu Z**, Shi L, Wang Y, Zhang J, Huang L, Zhang C, Liu S, Zhao P, Liu H, Zhu L, Tai Y, Bai C, Gao T, Song J, Xia P, Dong J, Zhao J, Wang FS. Pathological findings of COVID-19 associated with acute respiratory distress syndrome. *Lancet Respir Med* 2020; **8**: 420-422 [PMID: 32085846 DOI: 10.1016/S2213-2600(20)30076-X]

39 **Dawood DRM**, Salum GM, El-Meguid MA. The Impact of COVID-19 on Liver Injury. *Am J Med Sci* 2022; **363**: 94-103 [PMID: 34752738 DOI: 10.1016/j.amjms.2021.11.001]

40 **Paizis G**, Tikellis C, Cooper ME, Schembri JM, Lew RA, Smith AI, Shaw T, Warner FJ, Zuilli A, Burrell LM, Angus PW. Chronic liver injury in rats and humans upregulates the novel enzyme angiotensin converting enzyme 2. *Gut* 2005; **54**:

1790-1796 [PMID: 16166274 DOI: 10.1136/gut.2004.062398]
41 **Bouayad A**. Innate immune evasion by SARS-CoV-2: Comparison with SARS-CoV. *Rev Med Virol* 2020; **30**: 1-9 [PMID: 32734714 DOI: 10.1002/rmv.2135]
42 **Pedersen SF**, Ho YC. SARS-CoV-2: a storm is raging. *J Clin Invest* 2020; **130**: 2202-2205 [PMID: 32217834 DOI: 10.1172/JCI137647]
43 **McGonagle D**, Sharif K, O'Regan A, Bridgewood C. The Role of Cytokines including Interleukin-6 in COVID-19 induced Pneumonia and Macrophage Activation Syndrome-Like Disease. *Autoimmun Rev* 2020; **19**: 102537 [PMID: 32251717 DOI: 10.1016/j.autrev.2020.102537]
44 **Sivandzadeh GR**, Askari H, Safarpour AR, Ejtehadi F, Raeis-Abdollahi E, Vaez Lari A, Abazari MF, Tarkesh F, Bagheri Lankarani K. COVID-19 infection and liver injury: Clinical features, biomarkers, potential mechanisms, treatment, and management challenges. *World J Clin Cases* 2021; **9**: 6178-6200 [PMID: 34434987 DOI: 10.12998/wjcc.v9.i22.6178]
45 **de Lucena TMC**, da Silva Santos AF, de Lima BR, de Albuquerque Borborema ME, de Azevêdo Silva J. Mechanism of inflammatory response in associated comorbidities in COVID-19. *Diabetes Metab Syndr* 2020; **14**: 597-600 [PMID: 32417709 DOI: 10.1016/j.dsx.2020.05.025]
46 **Rismanbaf A**, Zarei S. Liver and Kidney Injuries in COVID-19 and Their Effects on Drug Therapy; a Letter to Editor. *Arch Acad Emerg Med* 2020; **8**: e17 [PMID: 32185369]
47 **Kulkarni AV**, Kumar P, Tevethia HV, Premkumar M, Arab JP, Candia R, Talukdar R, Sharma M, Qi X, Rao PN, Reddy DN. Systematic review with meta-analysis: liver manifestations and outcomes in COVID-19. *Aliment Pharmacol Ther* 2020; **52**: 584-599 [PMID: 32638436 DOI: 10.1111/apt.15916]
48 **Yang Z**, Xu M, Yi JQ, Jia WD. Clinical characteristics and mechanism of liver damage in patients with severe acute respiratory syndrome. *Hepatobiliary Pancreat Dis Int* 2005; **4**: 60-63 [PMID: 15730921]
49 **Amin M**. COVID-19 and the liver: overview. *Eur J Gastroenterol Hepatol* 2021; **33**: 309-311 [PMID: 32558697 DOI: 10.1097/MEG.0000000000001808]
50 **Jiang S**, Wang R, Li L, Hong D, Ru R, Rao Y, Miao J, Chen N, Wu X, Ye Z, Hu Y, Xie M, Zuo M, Lu X, Qiu Y, Liang T. Liver Injury in Critically Ill and Non-critically Ill COVID-19 Patients: A Multicenter, Retrospective, Observational Study. *Front Med (Lausanne)* 2020; **7**: 347 [PMID: 32656222 DOI: 10.3389/fmed.2020.00347]
51 **Zhou F**, Yu T, Du R, Fan G, Liu Y, Liu Z, Xiang J, Wang Y, Song B, Gu X, Guan L, Wei Y, Li H, Wu X, Xu J, Tu S, Zhang Y, Chen H, Cao B. Clinical course and risk factors for mortality of adult inpatients with COVID-19 in Wuhan, China: a retrospective cohort study. *Lancet* 2020; **395**: 1054-1062 [PMID: 32171076 DOI: 10.1016/S0140-6736(20)30566-3]
52 **Chen X**, Jiang Q, Ma Z, Ling J, Hu W, Cao Q, Mo P, Yao L, Yang R, Gao S, Gui X, Hou W, Xiong Y, Li J, Zhang Y. Clinical Characteristics of Hospitalized Patients with SARS-CoV-2 and Hepatitis B Virus Co-infection. *Virol Sin* 2020; **35**: 842-845 [PMID: 32839868 DOI: 10.1007/s12250-020-00276-5]
53 **Zhang C**, Shi L, Wang FS. Liver injury in COVID-19: management and challenges. *Lancet Gastroenterol Hepatol* 2020; **5**: 428-430 [PMID: 32145190 DOI: 10.1016/S2468-1253(20)30057-1]
54 **Ji D**, Qin E, Xu J, Zhang D, Cheng G, Wang Y, Lau G. Non-alcoholic fatty liver diseases in patients with COVID-19: A retrospective study. *J Hepatol* 2020; **73**: 451-453 [PMID: 32278005 DOI: 10.1016/j.jhep.2020.03.044]
55 **Lopez-Mendez I**, Aquino-Matus J, Gall SM, Prieto-Nava JD, Juarez-Hernandez E, Uribe M, Castro-Narro G. Association of liver steatosis and fibrosis with clinical outcomes in patients with SARS-CoV-2 infection (COVID-19). *Ann Hepatol* 2021; **20**: 100271 [PMID: 33099028 DOI: 10.1016/j.aohep.2020.09.015]
56 **Marjot T**, Webb GJ, Barritt AS 4th, Moon AM, Stamataki Z, Wong VW, Barnes E. COVID-19 and liver disease: mechanistic and clinical perspectives. *Nat Rev Gastroenterol Hepatol* 2021; **18**: 348-364 [PMID: 33692570 DOI: 10.1038/s41575-021-00426-4]
57 **Mushtaq K**, Khan MU, Iqbal F, Alsoub DH, Chaudhry HS, Ata F, Iqbal P, Elfert K, Balaraju G, Almaslamani M, Al-Ejji K, AlKaabi S, Kamel YM. NAFLD is a predictor of liver injury in COVID-19 hospitalized patients but not of mortality, disease severity on the presentation or progression - The debate continues. *J Hepatol* 2021; **74**: 482-484 [PMID: 33223215 DOI: 10.1016/j.jhep.2020.09.006]
58 **Oyelade T**, Alqahtani J, Canciani G. Prognosis of COVID-19 in Patients with Liver and Kidney Diseases: An Early Systematic Review and Meta-Analysis. *Trop Med Infect Dis* 2020; **5** [PMID: 32429038 DOI: 10.3390/tropicalmed5020080]
59 **Qi X**, Liu Y, Wang J, Fallowfield JA, Li X, Shi J, Pan H, Zou S, Zhang H, Chen Z, Li F, Luo Y, Mei M, Liu H, Wang Z, Li J, Yang H, Xiang H, Liu T, Zheng MH, Liu C, Huang Y, Xu D, Kang N, He Q, Gu Y, Zhang G, Shao C, Liu D, Zhang L, Kawada N, Jiang Z, Wang F, Xiong B, Takehara T, Rockey DC; COVID-Cirrhosis-CHESS Group. Clinical course and risk factors for mortality of COVID-19 patients with pre-existing cirrhosis: a multicentre cohort study. *Gut* 2021; **70**: 433-436 [PMID: 32434831 DOI: 10.1136/gutjnl-2020-321666]
60 **Shah BA**, Ahmed W, Dhobi GN, Shah NN, Khursheed SQ, Haq I. Validity of pneumonia severity index and CURB-65 severity scoring systems in community acquired pneumonia in an Indian setting. *Indian J Chest Dis Allied Sci* 2010; **52**: 9-17 [PMID: 20364609]
61 **Kushner T**, Cafardi J. Chronic Liver Disease and COVID-19: Alcohol Use Disorder/Alcohol-Associated Liver Disease, Nonalcoholic Fatty Liver Disease/Nonalcoholic Steatohepatitis, Autoimmune Liver Disease, and Compensated Cirrhosis. *Clin Liver Dis (Hoboken)* 2020; **15**: 195-199 [PMID: 32537135 DOI: 10.1002/cld.974]
62 **Kim D**, Adeniji N, Latt N, Kumar S, Bloom PP, Aby ES, Perumalswami P, Roytman M, Li M, Vogel AS, Catana AM, Wegermann K, Carr RM, Aloman C, Chen VL, Rabiee A, Sadowski B, Nguyen V, Dunn W, Chavin KD, Zhou K, Lizaola-Mayo B, Moghe A, Debes J, Lee TH, Branch AD, Viveiros K, Chan W, Chascsa DM, Kwo P, Dhanasekaran R. Predictors of Outcomes of COVID-19 in Patients With Chronic Liver Disease: US Multi-center Study. *Clin Gastroenterol Hepatol* 2021; **19**: 1469-1479.e19 [PMID: 32950749 DOI: 10.1016/j.cgh.2020.09.027]
63 **Sarin SK**, Choudhury A, Lau GK, Zheng MH, Ji D, Abd-Elsalam S, Hwang J, Qi X, Cua IH, Suh JI, Park JG, Putcharoen O, Kaewdech A, Piratvisuth T, Treeprasertsuk S, Park S, Wejnaruemarn S, Payawal DA, Baatarkhuu O, Ahn SH, Yeo CD, Alonzo UR, Chinbayar T, Loho IM, Yokosuka O, Jafri W, Tan S, Soo LI, Tanwandee T, Gani R, Anand L, Esmail ES,

Khalaf M, Alam S, Lin CY, Chuang WL, Soin AS, Garg HK, Kalista K, Batsukh B, Purnomo HD, Dara VP, Rathi P, Al Mahtab M, Shukla A, Sharma MK, Omata M; APASL COVID Task Force, APASL COVID Liver Injury Spectrum Study (APCOLIS Study-NCT 04345640). Pre-existing liver disease is associated with poor outcome in patients with SARS CoV2 infection; The APCOLIS Study (APASL COVID-19 Liver Injury Spectrum Study). *Hepatol Int* 2020; **14**: 690-700 [PMID: 32623632 DOI: 10.1007/s12072-020-10072-8]

64 **Boettler T**, Newsome PN, Mondelli MU, Maticic M, Cordero E, Cornberg M, Berg T. Care of patients with liver disease during the COVID-19 pandemic: EASL-ESCMID position paper. *JHEP Rep* 2020; **2**: 100113 [PMID: 32289115 DOI: 10.1016/j.jhepr.2020.100113]

65 **Li JY**, Cao HY, Liu P, Cheng GH, Sun MY. Glycyrrhizic acid in the treatment of liver diseases: literature review. *Biomed Res Int* 2014; **2014**: 872139 [PMID: 24963489 DOI: 10.1155/2014/872139]

66 **Spearman CW**, Aghemo A, Valenti L, Sonderup MW. COVID-19 and the liver: A 2021 update. *Liver Int* 2021; **41**: 1988-1998 [PMID: 34152690 DOI: 10.1111/liv.14984]

World Journal of Clinical Cases

Submit a Manuscript: https://www.f6publishing.com

World J Clin Cases 2023 April 6; 11(10): 2201-2212

DOI: 10.12998/wjcc.v11.i10.2201

ISSN 2307-8960 (online)

MINIREVIEWS

Breast reconstruction: Review of current autologous and implant-based techniques and long-term oncologic outcome

Mahdi Malekpour, Fatemeh Malekpour, Howard Tz-Ho Wang

Specialty type: Medicine, research and experimental

Provenance and peer review: Invited article; Externally peer reviewed.

Peer-review model: Single blind

Peer-review report's scientific quality classification

Grade A (Excellent): 0
Grade B (Very good): B, B
Grade C (Good): 0
Grade D (Fair): 0
Grade E (Poor): 0

P-Reviewer: Wang Z, China; Wang SY, China

Received: December 28, 2022
Peer-review started: December 28, 2022
First decision: January 30, 2023
Revised: February 13, 2023
Accepted: March 15, 2023
Article in press: March 15, 2023
Published online: April 6, 2023

Mahdi Malekpour, Fatemeh Malekpour, Howard Tz-Ho Wang, Department of Plastic and Reconstructive Surgery, University of Texas Health San Antonio, San Antonio, TX 78229, United States

Corresponding author: Mahdi Malekpour, MD, Surgeon, Department of Plastic and Reconstructive Surgery, University of Texas Health San Antonio, 7703 Floyd Curl Drive, San Antonio, TX 78229, United States. ma_malekpour@yahoo.com

Abstract

Implant-based reconstruction is the most common method of breast reconstruction. Autologous breast reconstruction is an indispensable option for breast reconstruction demanding keen microsurgical skills and robust anatomical understanding. The reconstructive choice is made by the patient after a discussion with the plastic surgeon covering all the available options. Advantages and disadvantages of each technique along with long-term oncologic outcome are reviewed.

Key Words: Breast Reconstruction; Mammaplasty; Breast Implant; Autologous Reconstruction; Oncologic Outcome; Breast Neoplasms

Core Tip: Breast reconstruction can be achieved using autologous and implant-based techniques. Each method has its indications and contraindications accompanied by advantages and disadvantages. An astute plastic surgeon should have deep understanding of the nuances for each technique when consulting patients about reconstructive breast options.

Citation: Malekpour M, Malekpour F, Wang HTH. Breast reconstruction: Review of current autologous and implant-based techniques and long-term oncologic outcome. *World J Clin Cases* 2023; 11(10): 2201-2212

URL: https://www.wjgnet.com/2307-8960/full/v11/i10/2201.htm

DOI: https://dx.doi.org/10.12998/wjcc.v11.i10.2201

INTRODUCTION

Breast reconstruction aims to recreate the breast mound in postmastectomy patients. This can be achieved using autologous and implant-based techniques. Each method has its indications and contraindications along with advantages and disadvantages. The ultimate decision is made by the patient through an informed decision when all the options are fully explained. Here, we review implant-based and autologous reconstructive techniques along with oncologic outcomes.

IMPLANT-BASED RECONSTRUCTION

The most common breast reconstruction method used by plastic surgeons is implant-based reconstruction which outpaced autologous techniques in early 21st century[1]. General advantages of implant-based reconstruction are shorter operative time, faster patient recovery and elimination of donor site morbidity. Disadvantages are capsular contracture, higher rate of infection, implant malposition, less natural feel, and breast implant illness. Complication rate and failure of implant-based reconstruction is significantly increased in patients undergoing adjuvant radiation therapy. Autologous techniques usually remain an option after implant-based reconstruction.

Prosthetic reconstructions can be performed in one or two stages and in immediate or delayed fashion. Single-stage reconstruction is favored in healthy patients with smaller breasts. A useful adjunct is use of acellular dermal matrix (ADM) which both provides better definition of the implant and maintains its position. Important risk factors for complications of prosthetic techniques are smoking, diabetes, obesity, and large breasts[2-4].

Immediate vs delayed reconstruction

Immediate breast reconstruction preserves native skin envelop and breast borders. It minimizes trips to the operating room and improves aesthetic outcome and patient satisfaction by minimizing negative psychological impacts and improving the self-image[5]. On the other hand, delayed reconstruction is associated with fewer complications such as flap necrosis, capsular contracture, and need for prosthetic removal. As a rule, immediate reconstruction is better for patients with less comorbidity, early-stage cancer, and lower body mass index. It is common practice to delay reconstruction in patients with questionable mastectomy flaps, when close tumor surveillance is needed, and in the setting of planned adjuvant therapy[6].

Single- vs two-stage reconstruction

Prosthetic reconstruction can be achieved *via* direct placement of permanent implant after mastectomy (single-stage) or placement of tissue expander and later exchange for a permanent implant (two-stage). Single-stage, a.k.a. direct-to-implant, approach has the advantage of eliminating the need for a second operation, reducing the risk of infection, and eliminating multiple office visits for device expansion. Smoking, diabetes, need for adjuvant radiation, and larger breast size are associated with increased risk of complications after single-stage reconstruction[7]. It is shown that two-stage reconstruction is associated with an overall decreased absolute rate of implant loss compared to one-stage reconstruction [8].

ADM is used as an adjunct to prostatic reconstruction to help with defining the mastectomy space, support the soft tissue, and stabilize the implant[9]. It should be noted that ADM is not yet cleared by the United States Food and Drug Administration (FDA) for use in implant-based breast reconstruction and currently wide use of ADM is off-label[10]. ADM is shown to improve aesthetic outcome in both single- and two-stage reconstruction[11]. ADM use is associated with reduced rate of capsular contracture[12]. The downside of using ADM is increased risk of postoperative complications especially infection and seroma formation[13].

Implant selection

There are many options for size, texture, and shape for both expander and implants selection. Expander options are relatively more limited, and they are available in different heights, base widths, projections, and capacities. Base width is the most important parameter which should match the width of the breast footprint on the chest wall. Implants, on the other hand, have more variety to choose from. They can be saline *vs* silicone, smooth *vs* texture, and round *vs* anatomic.

Although saline implants have a less rigorous surveillance protocol and are easier to detect when they are ruptured, they are associated with a higher rate of implant visibility and rippling. Silicone implants more closely resemble the native breast issue, but their rupture is harder to detect and can lead to capsular contracture. There are data suggesting that the rate of rupture and capsular contracture is slightly higher in silicone implants compared to saline implants[14]. On the other hand, it is shown that patients with silicone implants have higher satisfaction, and better psychological and sexual function compared to saline implants[15].

Although it might be difficult to clinically differentiate between round and anatomic-shape implants, shaped implants may result in an improved upper pole shape and better volume[16]. One should keep in mind that most shaped implants are textured which should be part of the discussion with the patient.

Implant placement

Selection of the plane to place the implant is usually surgeon-dependent. Subpectoral position places the implant between the pectoralis major muscle and the chest wall, whereas the prepectoral position places the implant between the skin flap and the pectoralis major muscle[17]. Historically, prepectoral position was associated with higher complications including capsular contracture and implant exposure but with improvement in surgical techniques and use of ADM (currently off-label use), these complications are significantly reduced leading to regaining popularity of the prepectoral implant placement[18]. With subpectoral positioning of the implant, it is a common practice to create an ADM sling (currently off-label use) for the exposed part of the implant below the pectoralis major muscle (dual-plane or partial subpectoral)[19]. Subpectoral implant placement has outpaced the historically higher rate of capsular contracture with prepectoral implant placement and it is also associated with a higher rate of animation deformity[17].

Quality of mastectomy flaps is the most important factor in the success of prepectoral implant placement[20,21]. Although it reduces the morbidity of subpectoral placement and animation deformity, it should never be performed in questionable mastectomy flaps[22]. In these situations, intraoperative Indocyanine Green (ICG) imaging can verify adequate blood supply to the mastectomy flaps. Active smoking, radiation to the field, and medical comorbidities also make prepectoral implant placement a less desirable option[23]. Tumor characteristics and location should be taken into account when choosing the appropriate plane for implant placement[24,25].

Special considerations

Need for adjuvant radiation complicates decision-making for prosthetic reconstruction techniques. Radiation is associated with increased rate of infection, flap necrosis, seroma, capsular contracture, and reconstructive failure[26,27]. Although some studies have shown no difference in the rate of complications between radiation of the expander *vs* the permanent implant in a two-stage reconstruction, the majority of available data have shown an increased rate of reconstructive failure following radiation of the permanent implant. Therefore, most plastic surgeons tend to increase the interval between completion of radiation and exchange to the permanent implant at about six-month interval[28-30].

Timing for radiation in the two-stage reconstruction is usually around 8 wk after tissue expander placement[28,29]. Rapid expansion starts in about 2 wk after placement of the expander and expansion is usually completed by the 6th week to have the patient ready for radiation at the 8th week[31]. Variations in timing of radiation is described with acceptable outcomes[32,33].

Complication rates of prostatic reconstruction of previously radiated breast can reach up to 50%[34,35]. Fibrosis and decreased vascularity does not respond well to expansion following radiation leading to three times increased risk of capsular contracture and reconstructive failure[36]. These risks appear to be slightly higher in post mastectomy radiation cases. Chemotherapy and hormonal therapy do not appear to increase the risk of complications following prosthetic reconstruction[37,38].

Complications

Acute hematoma occurs in the first 24-48 h after surgery in up to 3% of implant-base reconstructions [39]. Surgical drains are not useful for evacuation of blood clots and any hematoma can increase the risk of mastectomy skin flap necrosis and lead to poor aesthetic outcome. Infection rate can reach up to 8% following prosthetic reconstruction[40]. Capsular contracture can reach up to 13% in 3 years after prosthetic reconstruction and risk factors include radiation, hematoma, infection, and silicon rupture. The best way to prevent capsular contraction is targeting the risk factors at the index operation[41]. Wound dehiscence is another complication (Figure 1). Although data supports the use of preoperative antibiotic use, there is not sufficient evidence supporting outpatient use of antibiotics to prevent infection[42].

Oncologic outcome

In a 10-year follow-up study of patients who underwent nipple-sparing mastectomy, of whom about 75% had implant-based reconstruction, not only the overall recurrence rate was low (3.33%) but also no demographic, tumor-specific or operative factor was found to be associated with increase recurrence [43]. This is a significant improvement from an earlier study on implant-based reconstruction after nipple-sparing mastectomy which showed a recurrence rate of 24%[44]. This is in part due to advancement in cancer treatment and better neoadjuvant and adjuvant treatments.

In a recent systematic review, locoregional recurrence was found to be 0%-7.4% after a median 5-year follow-up and no increased risk of recurrence with reconstructive method[45]. In a 7-year median follow-up study, locoregional recurrence in patients with immediate breast reconstruction was found to be 3.5% and independent from the reconstructive method[46]. In another study of at least 60-mo follow-up comparing smooth and textures implants, no significant difference was found between the two in

DOI: 10.12998/wjcc.v11.i10.2201

Figure 1 Wound dehiscence after implant-based breast reconstruction.

terms of locoregional recurrence[47].

Textured implants were historically used to reduce the rate of capsular contracture and provide a more stable implant position, but studies have shown a small increased risk of breast-implant-associated anaplastic large-cell lymphoma (BIA-ALCL) with the use of textured devices[48-50]. Companies such as Allergan voluntarily recalled some textured implants (no new cases)[51]. This led to FDA scrutiny of implants and in October 2021, patient decision checklist was mandated as a condition for the sale of breast implants[52]. More recently, rare cases of breast implant capsule-associated squamous cell carcinoma (BICA-SCC) are reported which has a worse prognosis[53]. BICA-SCC can mimic BIA-ALCL but a similar diagnostic approach can be applied to distinguish between the two[54]. These should be discussed with the patient at the time of consult and during informed decision making for breast reconstruction. FDA recommends magnetic resonance imaging to detect rupture at 5 to 6 years after implant placement and then every 2 to 3 years[55]. More cohesive implants are now approved which are at an increased cohesion level compared to prior gel implants[56].

AUTOLOGOUS RECONSTRUCTION

Despite the fact that the majority of patients undergo implant-base breast construction after mastectomy, autologous breast reconstruction is the only choice for certain patients and undoubtedly an option after failure of implant-based reconstruction[57,58]. Patient-related and surgeon-related factors each play a role in the choice of reconstruction. Using autologous tissue reduces postoperative risk of infection, implant rupture, capsular contractor, and malposition. Furthermore, autologous technique is the preferred method in patients expecting to receive radiation therapy or with prior irradiated breast [59-61].

Preoperative evaluation

Thorough history and physical examination are essential parts of the preoperative evaluation. Patient's goals in terms of the reconstruction, and limitation of reconstructive options should be discussed in detail. Oncologic plan should be elucidated including neoadjuvant and adjuvant chemoradiation. Special attention should be paid to the tentative future donor site including prior surgeries, scars, skin quality, and infection. Although majority of patients prefer immediate reconstruction, when postmastectomy radiation is anticipated, delayed reconstruction is favored. Some microsurgeons elect to do preoperative imaging to elucidate vascular anatomy, yet many surgeons do not implement preoperative imaging and instead use pencil Doppler intraoperatively to identify the location of the perforators[62,63].

Pedicled flaps

Latissimus dorsi flap: The latissimus dorsi (LD) myocutaneous flap is a well-establish pedicled flap for breast reconstruction. This flap is based on the thoracodorsal vessels, which arise from subscapular vessels that are branches of the axillary vessels (Figure 2). Medial and lateral branching of the vessels allows for muscle-sparing procedures. LD is a broad muscle that allows for a wide coverage with or without a skin paddle. The downside of using LD is that it does not typically providing sufficient volume which requires combination with prostheses. LD can also be used as a salvage option once other breast reconstruction options have failed.

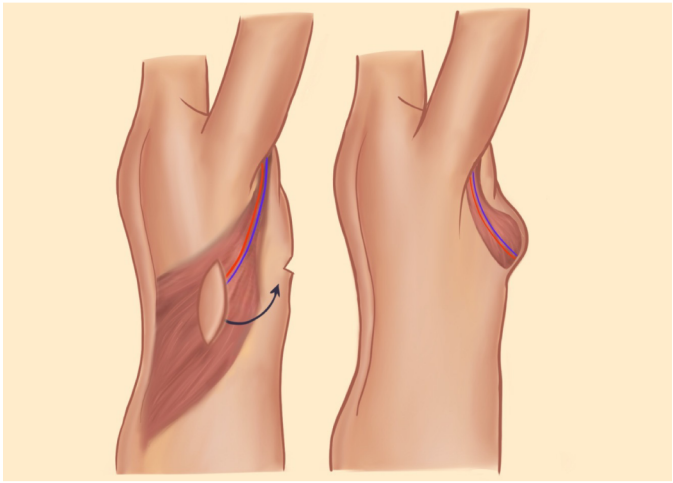

DOI: 10.12998/wjcc.v11.i10.2201 **Copyright** ©The Author(s) 2023.

Figure 2 Latissimus dorsi myocutaneous flap based on the thoracodorsal vessels.

Pedicled transverse rectus abdominis myocutaneous flap: The pedicled transverse rectus abdominis myocutaneous (TRAM) flap uses lower abdominal fat and is based on the superior epigastric artery which is a continuation of the internal mammary artery (Figure 3). It is elevated with the ipsilateral rectus muscle and tunneled into the mastectomy site. At times, delayed procedures should be performed by ligating the deep inferior epigastric artery so that choke vessels are recruited and superior epigastric vessels take over the perfusion of the pedicled TRAM flap[64]. Since harvesting this flap includes removal of the fascial coverage, closure requires implementation of mesh and there is an associated increased risk of incisional hernia in this patient population[65].

Free flaps

Commonly used free flaps are discussed below. Recipient vessels are usually internal mammary vessels, and as an alternative, thoracodorsal vessels can be used. End-to-end venous anastomosis are performed using vein couplers and end-to-end arterial anastomosis is typically handsewn using 8-0 to 10-0 nylon sutures.

Abdomen-based flaps: Abdomen-based free flaps are the most common free autologous flaps for breast construction. Besides extensive clinical experience, these flaps commonly have reliable vascular anatomy, long pedicles, reduced donor site morbidity, and sufficient soft tissue for breast reconstruction. Free flaps based on the deep inferior epigastric vessels (branches of external iliac artery) include free transverse rectus abdominis myocutaneous (TRAM), free muscle-sparing TRAM (ms-TRAM), and deep inferior epigastric perforator (DIEP). Free flap based on the superficial inferior epigastric vessels (branches of the femoral vessels) is the superficial inferior epigastric artery (SIEA) perforator flap (Figure 4). Less than 10% of abdominal-based flaps are superficially dominant[66].

For patients undergoing immediate breast reconstruction, flap harvest can be performed at the same time of the mastectomy surgery. Flap design is usually inferior to the umbilicus in a lenticular fashion. Superficial inferior epigastric vessels are isolated at the inferior aspect of the flap during flap elevation [67]. Most of the perforators needed for DIEP flap are within 10 cm from the umbilicus. Zones of perforation vary depending on the selected row of perforators[68,69]. For unilateral reconstruction, midline could be crossed to include the zone immediately adjacent to the midline, whereas this option is not available when using SIEA flaps.

The dominant perforator can be identified by temporarily clamping other perforators and assessing the flap while using ICG perfusion imaging. Once the appropriate perforators are selected, anterior rectus facia is opened, and intramuscular dissection of perforators is carried down to the level of deep inferior epigastric vessels. If a segment of muscle between the two rows of the perforators is also harvested, then ms-TRAM flap is created and with complete transaction of the rectus muscle without preserving continuity, a free TRAM flap is created. The vessels, which typically consist of two veins and one artery are ligated distal to takeoff from external iliac vessels.

Robotic-assisted DIEP flap breast reconstruction is drawing attention as a new and alternative way to harvest DIEP flaps due to reduced risk of abdominal wall herniation, bulging, motor weakness and chronic pain[70]. It is associated with improved visualization, dexterity, ergonomics, and more importantly decreased size of facial incision[71]. If the length of the intra-muscular section of the pedicle is more than 5 cm, then it is unclear if robotic-assisted DIEP would reduce the rate of complications compared to the conventional DIEP approach[72]. This method requires pre-operative vascular imaging for appropriate planning and the microsurgeon needs to be additionally trained for robotic surgery.

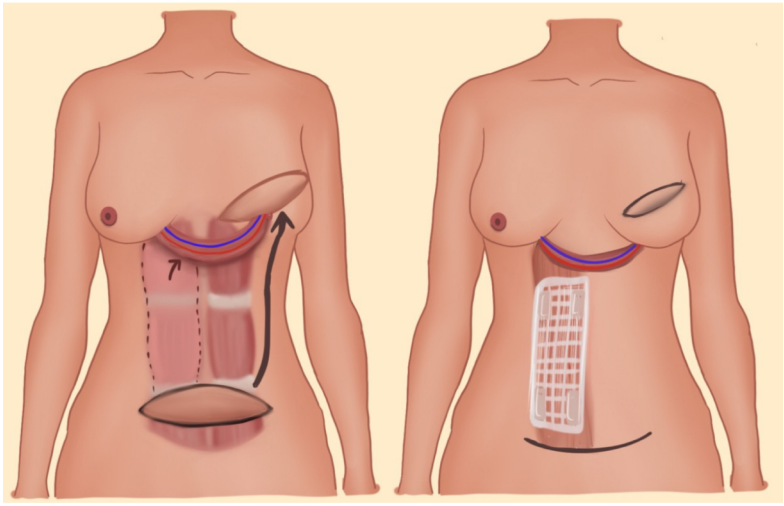

DOI: 10.12998/wjcc.v11.i10.2201 **Copyright** ©The Author(s) 2023.

Figure 3 Pedicled transverse rectus abdominis myocutaneous flap uses lower abdominal adipose tissue and is based on the superior epigastric artery.

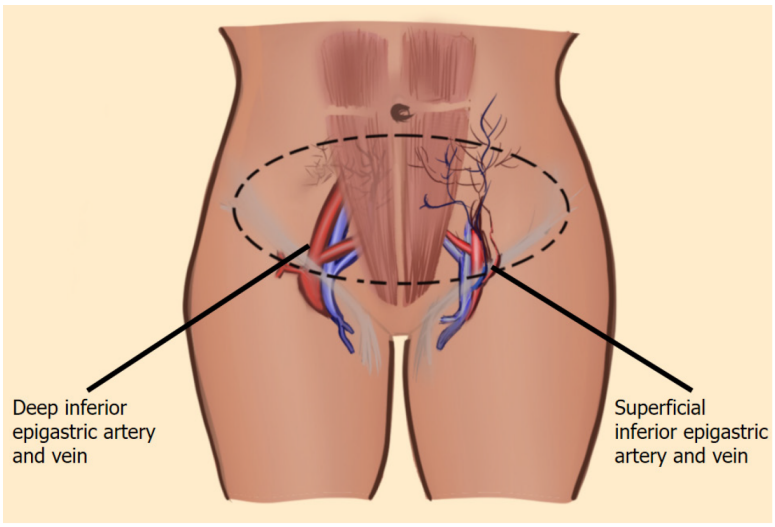

DOI: 10.12998/wjcc.v11.i10.2201 **Copyright** ©The Author(s) 2023.

Figure 4 Abdomen-based free flaps are based on superficial or deep inferior epigastric vessels.

Medial thigh flaps: Medial thigh flaps incorporate gracilis muscle and is an option for construction in patients with prior abdominoplasty or those with insufficient abdominal tissue[73]. This flap is based on the medial circumflex femoral artery which is a branch of the profunda femoris artery (Figure 5). The skin paddle can be oriented transversely in transverse upper gracilis flap, vertically in vertical upper gracilis flap or as a combination of both. This flap is better for patients with small- to moderate-sized breasts and the flap artery is usually smaller than the recipient artery.

Posterior thigh flaps: Posterior thigh skin and adipose tissue can be used for breast reconstruction based on the profunda artery perforator (PAP) flap (Figure 6). PAP flaps provide longer pedicles compared to medial thigh flaps[74]. This flap is designed as a horizontal ellipse with the superior incision below the gluteal crease. PAP flap can be harvested in prone position, though, to facilitate two-team approach, PAP flap is elevated in the lithotomy position.

Gluteal artery perforator flaps: Another option for patients who cannot have abdomen-based flaps is superior or inferior gluteal artery perforator flaps (SGAP or IGAP). The superior gluteal artery exists the pelvis above the piriformis muscle and inferior gluteal artery exits the pelvis below the piriformis muscle[75]. Patients are either positioned laterally or prone which requires positional change intraoperatively to inset the flap. Although gluteal artery perforator flaps provide adequate amount of adipose tissue for breast reconstruction, they often have relatively short pedicle lengths.

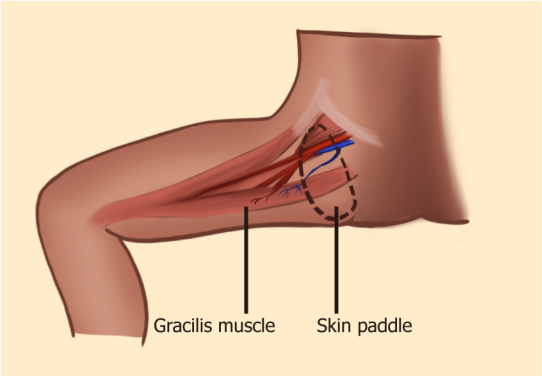

DOI: 10.12998/wjcc.v11.i10.2201 **Copyright** ©The Author(s) 2023.

Figure 5 Transverse upper gracilis flap is based on the medial circumflex femoral artery which is a branch of the profunda femoris artery.

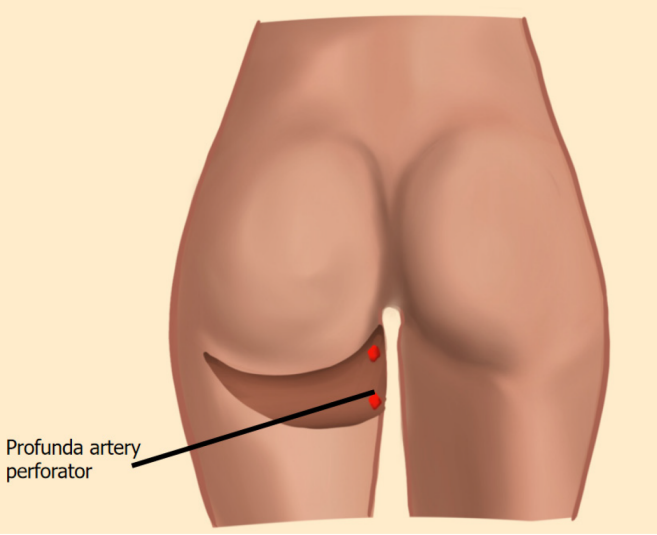

DOI: 10.12998/wjcc.v11.i10.2201 **Copyright** ©The Author(s) 2023.

Figure 6 Profunda artery perforator flap carries posterior thigh skin and adipose tissue.

The decision making about the choice of the autologous flap is based on several factors. First and foremost is the patient's choice after providing adequate information so that the patient can make an informed decision[76]. Anatomical considerations are critical in the decision making about the choice of the flap. DIEP flaps are harvested in the same position and can allow two teams to work at the same time[77]. It also provides a reliable pedicle of enough length closely matching the recipient vessels[78]. Donor site comorbidities are acceptable for DIEP flaps. Other choices of free flaps, that are discussed above, have shortcomings in one or more of these factors such as providing short length of pedicle, need for repositioning in the OR and increased donor site comorbidities[79]. This is why currently DIEP flaps are the most favorable free flaps for breast reconstruction[80].

Postoperative care and complications

Post operative protocol can differ from surgeon-to-surgeon and institution-to-institution. Typically, postoperatively, flaps are kept warm and are evaluated every hour for at least the first 24-48 h. Examination consists of clinical exam, capillary refill, warmth, color, and pencil Doppler exam if no implantable Doppler is used. It is common practice to prescribe aspirin as an anti-platelet agent and to place the patients on venous thromboembolism prophylaxis. During the first 48 h, vascular compromise due to vessel positioning, hematoma, thrombus formation and compression can be devastating leading to flap loss. Early vascular compromise equals reoperation for flap salvage.

Other postoperative complications include partial flap loss (Figure 7), fat necrosis, infections (Figure 8), wound dehiscence, hematoma (Figure 9), and seroma formation. Donor site complications include infections, seroma, hematoma, wound dehiscence, necrosis, and hernia formation. It is shown that frailty is a reliable predictor of postoperative complications in autologous reconstruction[81].

DOI: 10.12998/wjcc.v11.i10.2201

Figure 7 Partial flap loss with free deep inferior epigastric perforator flap in evolution.

DOI: 10.12998/wjcc.v11.i10.2201

Figure 8 Infected pedicled latissimus dorsi flap with implant.

DOI: 10.12998/wjcc.v11.i10.2201

Figure 9 Hematoma of the mastectomy flap following deep inferior epigastric perforator flap breast reconstruction.

Oncologic outcome

Boyed *et al*[43] performed a 10-year follow-up study on a cohort of patients of whom about 25% had autologous breast reconstruction and found no association between increased recurrence and operation [43]. No significant difference is found in terms of locoregional recurrence of cancer between implant-based and autologous reconstruction[82,83]. Low locoregional recurrence rate (3.5%) after immediate

autologous breast reconstruction is shown in another study by Wu *et al*[46] with a median follow-up of 7 years[46].

CONCLUSION

Plastic surgeons have an armamentarium of implant-based and autologous reconstructive options to manage patients with breast cancer which should be tailormade for each individual patient. Both options have favorable long-term oncologic outcomes.

FOOTNOTES

Author contributions: Malekpour M, Malekpour F, Wang HTH analyzed the data and wrote the manuscript; All authors have read and approve the final manuscript.

Conflict-of-interest statement: All the authors report no relevant conflicts of interest for this article.

Country/Territory of origin: United States

ORCID number: Mahdi Malekpour 0000-0002-7337-3479.

S-Editor: Li L
L-Editor: A
P-Editor: Li L

REFERENCES

1 **Albornoz CR**, Bach PB, Mehrara BJ, Disa JJ, Pusic AL, McCarthy CM, Cordeiro PG, Matros E. A paradigm shift in U.S. Breast reconstruction: increasing implant rates. *Plast Reconstr Surg* 2013; **131**: 15-23 [PMID: 23271515 DOI: 10.1097/PRS.0b013e3182729cde]
2 **Fischer JP**, Nelson JA, Serletti JM, Wu LC. Peri-operative risk factors associated with early tissue expander (TE) loss following immediate breast reconstruction (IBR): a review of 9305 patients from the 2005-2010 ACS-NSQIP datasets. *J Plast Reconstr Aesthet Surg* 2013; **66**: 1504-1512 [PMID: 23845908 DOI: 10.1016/j.bjps.2013.06.030]
3 **Fischer JP**, Nelson JA, Kovach SJ, Serletti JM, Wu LC, Kanchwala S. Impact of obesity on outcomes in breast reconstruction: analysis of 15,937 patients from the ACS-NSQIP datasets. *J Am Coll Surg* 2013; **217**: 656-664 [PMID: 23891077 DOI: 10.1016/j.jamcollsurg.2013.03.031]
4 **Hart A**, Funderburk CD, Chu CK, Pinell-White X, Halgopian T, Manning-Geist B, Carlson G, Losken A. The Impact of Diabetes Mellitus on Wound Healing in Breast Reconstruction. *Ann Plast Surg* 2017; **78**: 260-263 [PMID: 27505449 DOI: 10.1097/SAP.0000000000000881]
5 **Drucker-Zertuche M**, Robles-Vidal C. A 7 year experience with immediate breast reconstruction after skin sparing mastectomy for cancer. *Eur J Surg Oncol* 2007; **33**: 140-146 [PMID: 17112698 DOI: 10.1016/j.ejso.2006.10.010]
6 **Nahabedian MY**. Implant-based breast reconstruction: Strategies to achieve optimal outcomes and minimize complications. *J Surg Oncol* 2016; **113**: 895-905 [PMID: 26919072 DOI: 10.1002/jso.24210]
7 **Gdalevitch P**, Ho A, Genoway K, Alvrtsyan H, Bovill E, Lennox P, Van Laeken N, Macadam S. Direct-to-implant single-stage immediate breast reconstruction with acellular dermal matrix: predictors of failure. *Plast Reconstr Surg* 2014; **133**: 738e-747e [PMID: 24867734 DOI: 10.1097/PRS.0000000000000171]
8 **Basta MN**, Gerety PA, Serletti JM, Kovach SJ, Fischer JP. A Systematic Review and Head-to-Head Meta-Analysis of Outcomes following Direct-to-Implant versus Conventional Two-Stage Implant Reconstruction. *Plast Reconstr Surg* 2015; **136**: 1135-1144 [PMID: 26595013 DOI: 10.1097/PRS.0000000000001749]
9 **Colwell AS**, Damjanovic B, Zahedi B, Medford-Davis L, Hertl C, Austen WG Jr. Retrospective review of 331 consecutive immediate single-stage implant reconstructions with acellular dermal matrix: indications, complications, trends, and costs. *Plast Reconstr Surg* 2011; **128**: 1170-1178 [PMID: 22094736 DOI: 10.1097/PRS.0b013e318230c2f6]
10 **Ganesh Kumar N**, Berlin NL, Kim HM, Hamill JB, Kozlow JH, Wilkins EG. Development of an evidence-based approach to the use of acellular dermal matrix in immediate expander-implant-based breast reconstruction. *J Plast Reconstr Aesthet Surg* 2021; **74**: 30-40 [PMID: 33172826 DOI: 10.1016/j.bjps.2020.10.005]
11 **Forsberg CG**, Kelly DA, Wood BC, Mastrangelo SL, DeFranzo AJ, Thompson JT, David LR, Marks MW. Aesthetic outcomes of acellular dermal matrix in tissue expander/implant-based breast reconstruction. *Ann Plast Surg* 2014; **72**: S116-S120 [PMID: 24374398 DOI: 10.1097/SAP.0000000000000098]

12 **Salzberg CA**, Ashikari AY, Berry C, Hunsicker LM. Acellular Dermal Matrix-Assisted Direct-to-Implant Breast Reconstruction and Capsular Contracture: A 13-Year Experience. *Plast Reconstr Surg* 2016; **138**: 329-337 [PMID: 27064232 DOI: 10.1097/PRS.0000000000002331]

13 **Lanier ST**, Wang ED, Chen JJ, Arora BP, Katz SM, Gelfand MA, Khan SU, Dagum AB, Bui DT. The effect of acellular dermal matrix use on complication rates in tissue expander/implant breast reconstruction. *Ann Plast Surg* 2010; **64**: 674-678 [PMID: 20395795 DOI: 10.1097/SAP.0b013e3181dba892]

14 **Rohrich RJ**, Reece EM. Breast augmentation today: saline versus silicone--what are the facts? *Plast Reconstr Surg* 2008; **121**: 669-672 [PMID: 18300988 DOI: 10.1097/01.prs.0000298115.96337.72]

15 **Macadam SA**, Ho AL, Cook EF Jr, Lennox PA, Pusic AL. Patient satisfaction and health-related quality of life following breast reconstruction: patient-reported outcomes among saline and silicone implant recipients. *Plast Reconstr Surg* 2010; **125**: 761-771 [PMID: 20009795 DOI: 10.1097/PRS.0b013e3181cb5cf8]

16 **Gahm J**, Edsander-Nord Å, Jurell G, Wickman M. No differences in aesthetic outcome or patient satisfaction between anatomically shaped and round expandable implants in bilateral breast reconstructions: a randomized study. *Plast Reconstr Surg* 2010; **126**: 1419-1427 [PMID: 20639801 DOI: 10.1097/PRS.0b013e3181ef8b01]

17 **Ostapenko E**, Nixdorf L, Devyatko Y, Exner R, Wimmer K, Fitzal F. Prepectoral Versus Subpectoral Implant-Based Breast Reconstruction: A Systemic Review and Meta-analysis. *Ann Surg Oncol* 2023; **30**: 126-136 [PMID: 36245049 DOI: 10.1245/s10434-022-12567-0]

18 **Woo A**, Harless C, Jacobson SR. Revisiting an Old Place: Single-Surgeon Experience on Post-Mastectomy Subcutaneous Implant-Based Breast Reconstruction. *Breast J* 2017; **23**: 545-553 [PMID: 28295975 DOI: 10.1111/tbj.12790]

19 **Escandón JM**, Sweitzer K, Christiano JG, Gooch JC, Olzinski AT, Prieto PA, Skinner KA, Langstein HN, Manrique OJ. Subpectoral versus prepectoral two-stage breast reconstruction: A propensity score-matched analysis of 30-day morbidity and long-term outcomes. *J Plast Reconstr Aesthet Surg* 2023; **76**: 76-87 [PMID: 36513014 DOI: 10.1016/j.bjps.2022.10.028]

20 **Frey JD**, Salibian AA, Choi M, Karp NS. Mastectomy Flap Thickness and Complications in Nipple-Sparing Mastectomy: Objective Evaluation using Magnetic Resonance Imaging. *Plast Reconstr Surg Glob Open* 2017; **5**: e1439 [PMID: 28894660 DOI: 10.1097/GOX.0000000000001439]

21 **Highton L**, Johnson R, Kirwan C, Murphy J. Prepectoral Implant-Based Breast Reconstruction. *Plast Reconstr Surg Glob Open* 2017; **5**: e1488 [PMID: 29062655 DOI: 10.1097/GOX.0000000000001488]

22 **Sbitany H**. Important Considerations for Performing Prepectoral Breast Reconstruction. *Plast Reconstr Surg* 2017; **140**: 7S-13S [PMID: 29166342 DOI: 10.1097/PRS.0000000000004045]

23 **Sbitany H**, Piper M, Lentz R. Prepectoral Breast Reconstruction: A Safe Alternative to Submuscular Prosthetic Reconstruction following Nipple-Sparing Mastectomy. *Plast Reconstr Surg* 2017; **140**: 432-443 [PMID: 28574950 DOI: 10.1097/PRS.0000000000003627]

24 **Nahabedian MY**, Cocilovo C. Two-Stage Prosthetic Breast Reconstruction: A Comparison Between Prepectoral and Partial Subpectoral Techniques. *Plast Reconstr Surg* 2017; **140**: 22S-30S [PMID: 29166344 DOI: 10.1097/PRS.0000000000004047]

25 **Larson DL**, Basir Z, Bruce T. Is oncologic safety compatible with a predictably viable mastectomy skin flap? *Plast Reconstr Surg* 2011; **127**: 27-33 [PMID: 21200196 DOI: 10.1097/PRS.0b013e3181f9589a]

26 **Lam TC**, Hsieh F, Boyages J. The effects of postmastectomy adjuvant radiotherapy on immediate two-stage prosthetic breast reconstruction: a systematic review. *Plast Reconstr Surg* 2013; **132**: 511-518 [PMID: 23676964 DOI: 10.1097/PRS.0b013e31829acc41]

27 **Barry M**, Kell MR. Radiotherapy and breast reconstruction: a meta-analysis. *Breast Cancer Res Treat* 2011; **127**: 15-22 [PMID: 21336948 DOI: 10.1007/s10549-011-1401-x]

28 **Santosa KB**, Chen X, Qi J, Ballard TNS, Kim HM, Hamill JB, Bensenhaver JM, Pusic AL, Wilkins EG. Postmastectomy Radiation Therapy and Two-Stage Implant-Based Breast Reconstruction: Is There a Better Time to Irradiate? *Plast Reconstr Surg* 2016; **138**: 761-769 [PMID: 27673513 DOI: 10.1097/PRS.0000000000002534]

29 **Cordeiro PG**, Albornoz CR, McCormick B, Hudis CA, Hu Q, Heerdt A, Matros E. What Is the Optimum Timing of Postmastectomy Radiotherapy in Two-Stage Prosthetic Reconstruction: Radiation to the Tissue Expander or Permanent Implant? *Plast Reconstr Surg* 2015; **135**: 1509-1517 [PMID: 25742523 DOI: 10.1097/PRS.0000000000001278]

30 **Lentz R**, Ng R, Higgins SA, Fusi S, Matthew M, Kwei SL. Radiation therapy and expander-implant breast reconstruction: an analysis of timing and comparison of complications. *Ann Plast Surg* 2013; **71**: 269-273 [PMID: 23788143 DOI: 10.1097/SAP.0b013e3182834b63]

31 **Ricci JA**, Epstein S, Momoh AO, Lin SJ, Singhal D, Lee BT. A meta-analysis of implant-based breast reconstruction and timing of adjuvant radiation therapy. *J Surg Res* 2017; **218**: 108-116 [PMID: 28985836 DOI: 10.1016/j.jss.2017.05.072]

32 **Kronowitz SJ**, Lam C, Terefe W, Hunt KK, Kuerer HM, Valero V, Lance S, Robb GL, Feng L, Buchholz TA. A multidisciplinary protocol for planned skin-preserving delayed breast reconstruction for patients with locally advanced breast cancer requiring postmastectomy radiation therapy: 3-year follow-up. *Plast Reconstr Surg* 2011; **127**: 2154-2166 [PMID: 21311392 DOI: 10.1097/PRS.0b013e3182131b8e]

33 **Nava MB**, Pennati AE, Lozza L, Spano A, Zambetti M, Catanuto G. Outcome of different timings of radiotherapy in implant-based breast reconstructions. *Plast Reconstr Surg* 2011; **128**: 353-359 [PMID: 21788827 DOI: 10.1097/PRS.0b013e31821e6c10]

34 **Sbitany H**, Wang F, Peled AW, Lentz R, Alvarado M, Ewing CA, Esserman LJ, Fowble B, Foster RD. Immediate implant-based breast reconstruction following total skin-sparing mastectomy: defining the risk of preoperative and postoperative radiation therapy for surgical outcomes. *Plast Reconstr Surg* 2014; **134**: 396-404 [PMID: 25158699 DOI: 10.1097/PRS.0000000000000466]

35 **Momoh AO**, Ahmed R, Kelley BP, Aliu O, Kidwell KM, Kozlow JH, Chung KC. A systematic review of complications of implant-based breast reconstruction with prereconstruction and postreconstruction radiotherapy. *Ann Surg Oncol* 2014; **21**: 118-124 [PMID: 24081801 DOI: 10.1245/s10434-013-3284-z]

36 **Lee KT**, Mun GH. Prosthetic breast reconstruction in previously irradiated breasts: A meta-analysis. *J Surg Oncol* 2015;

112: 468-475 [PMID: 26374273 DOI: 10.1002/jso.24032]
37 **Wang F**, Peled AW, Chin R, Fowble B, Alvarado M, Ewing C, Esserman L, Foster R, Sbitany H. The Impact of Radiation Therapy, Lymph Node Dissection, and Hormonal Therapy on Outcomes of Tissue Expander-Implant Exchange in Prosthetic Breast Reconstruction. *Plast Reconstr Surg* 2016; **137**: 1-9 [PMID: 26368331 DOI: 10.1097/PRS.0000000000001866]
38 **Donker M**, Hage JJ, Woerdeman LA, Rutgers EJ, Sonke GS, Vrancken Peeters MJ. Surgical complications of skin sparing mastectomy and immediate prosthetic reconstruction after neoadjuvant chemotherapy for invasive breast cancer. *Eur J Surg Oncol* 2012; **38**: 25-30 [PMID: 21963981 DOI: 10.1016/j.ejso.2011.09.005]
39 **Vardanian AJ**, Clayton JL, Roostaeian J, Shirvanian V, Da Lio A, Lipa JE, Crisera C, Festekjian JH. Comparison of implant-based immediate breast reconstruction with and without acellular dermal matrix. *Plast Reconstr Surg* 2011; **128**: 403e-410e [PMID: 22030500 DOI: 10.1097/PRS.0b013e31822b6637]
40 **Zhao X**, Wu X, Dong J, Liu Y, Zheng L, Zhang L. A Meta-analysis of Postoperative Complications of Tissue Expander/Implant Breast Reconstruction Using Acellular Dermal Matrix. *Aesthetic Plast Surg* 2015; **39**: 892-901 [PMID: 26377821 DOI: 10.1007/s00266-015-0555-z]
41 **Wan D**, Rohrich RJ. Revisiting the Management of Capsular Contracture in Breast Augmentation: A Systematic Review. *Plast Reconstr Surg* 2016; **137**: 826-841 [PMID: 26910663 DOI: 10.1097/01.prs.0000480095.23356.ae]
42 **Phillips BT**, Halvorson EG. Antibiotic Prophylaxis following Implant-Based Breast Reconstruction: What Is the Evidence? *Plast Reconstr Surg* 2016; **138**: 751-757 [PMID: 27307337 DOI: 10.1097/PRS.0000000000002530]
43 **Boyd CJ**, Salibian AA, Bekisz JM, Axelrod DM, Guth AA, Shapiro RL, Schnabel FR, Karp NS, Choi M. Long-Term Cancer Recurrence Rates following Nipple-Sparing Mastectomy: A 10-Year Follow-Up Study. *Plast Reconstr Surg* 2022; **150**: 13S-19S [PMID: 35943969 DOI: 10.1097/PRS.0000000000009495]
44 **Benediktsson KP**, Perbeck L. Survival in breast cancer after nipple-sparing subcutaneous mastectomy and immediate reconstruction with implants: a prospective trial with 13 years median follow-up in 216 patients. *Eur J Surg Oncol* 2008; **34**: 143-148 [PMID: 17709228 DOI: 10.1016/j.ejso.2007.06.010]
45 **Blanckaert M**, Vranckx J. Oncological safety of therapeutic 'nipple-sparing mastectomy' followed by reconstruction: a systematic review. *Acta Chir Belg* 2021; **121**: 155-163 [PMID: 33929924 DOI: 10.1080/00015458.2021.1922829]
46 **Wu ZY**, Kim HJ, Lee JW, Chung IY, Kim JS, Lee SB, Son BH, Eom JS, Kim SB, Gong GY, Kim HH, Ahn SH, Ko B. Breast Cancer Recurrence in the Nipple-Areola Complex After Nipple-Sparing Mastectomy With Immediate Breast Reconstruction for Invasive Breast Cancer. *JAMA Surg* 2019; **154**: 1030-1037 [PMID: 31461141 DOI: 10.1001/jamasurg.2019.2959]
47 **Wu ZY**, Han HH, Han J, Son BH, Eom JS, Kim SB, Gong G, Kim HH, Ahn SH, Ko B. Breast Cancer Recurrence after Smooth versus Textured Implant-Based Breast Reconstruction: A Matched Cohort Study. *Plast Reconstr Surg* 2022; **150**: 30S-37S [PMID: 35943962 DOI: 10.1097/PRS.0000000000009491]
48 **Cordeiro PG**, Ghione P, Ni A, Hu Q, Ganesan N, Galasso N, Dogan A, Horwitz SM. Risk of breast implant associated anaplastic large cell lymphoma (BIA-ALCL) in a cohort of 3546 women prospectively followed long term after reconstruction with textured breast implants. *J Plast Reconstr Aesthet Surg* 2020; **73**: 841-846 [PMID: 32008941 DOI: 10.1016/j.bjps.2019.11.064]
49 **Collett DJ**, Rakhorst H, Lennox P, Magnusson M, Cooter R, Deva AK. Current Risk Estimate of Breast Implant-Associated Anaplastic Large Cell Lymphoma in Textured Breast Implants. *Plast Reconstr Surg* 2019; **143**: 30S-40S [PMID: 30817554 DOI: 10.1097/PRS.0000000000005567]
50 **Calobrace MB**, Schwartz MR, Zeidler KR, Pittman TA, Cohen R, Stevens WG. Long-Term Safety of Textured and Smooth Breast Implants. *Aesthet Surg J* 2017; **38**: 38-48 [PMID: 29040370 DOI: 10.1093/asj/sjx157]
51 **McGuire PA**, Deva AK, Glicksman CA, Adams WP Jr, Haws MJ. Management of Asymptomatic Patients With Textured Surface Breast Implants. *Aesthet Surg J Open Forum* 2019; **1**: ojz025 [PMID: 33791616 DOI: 10.1093/asjof/ojz025]
52 **Karp N**, McGuire P, Adams WP, Jewell ML. US FDA Patient Decision Checklist for Breast Implants: Results of a Survey to Members of The Aesthetic Society, April 2022. *Aesthet Surg J* 2023; **43**: 150-156 [PMID: 36073650 DOI: 10.1093/asj/sjac245]
53 **Goldberg MT**, Llaneras J, Willson TD, Boyd JB, Venegas RJ, Dauphine C, Kalantari BN. Squamous Cell Carcinoma Arising in Breast Implant Capsules. *Ann Plast Surg* 2021; **86**: 268-272 [PMID: 32804719 DOI: 10.1097/SAP.0000000000002524]
54 **Soni SE**, Laun JC, Beard AS, Kuykendall LV. Breast Implant Capsule-Associated Squamous Cell Carcinoma during Pregnancy: A Mimicker of Breast Implant-Associated Anaplastic Large-Cell Lymphoma. *Plast Reconstr Surg* 2022; **150**: 926e-928e [PMID: 35960919 DOI: 10.1097/PRS.0000000000009506]
55 **Nichter LS**, Hardesty RA, Anigian GM. IDEAL IMPLANT Structured Breast Implants: Core Study Results at 6 Years. *Plast Reconstr Surg* 2018; **142**: 66-75 [PMID: 29489559 DOI: 10.1097/PRS.0000000000004460]
56 **Gabriel A**, Maxwell GP. The Science of Cohesivity and Elements of Form Stability. *Plast Reconstr Surg* 2019; **144**: 7S-12S [PMID: 31246755 DOI: 10.1097/PRS.0000000000005959]
57 **Barnow A**, Canfield T, Liao R, Yadalam S, Kalsekar I, Khanna R. Breast Reconstruction Among Commercially Insured Women With Breast Cancer in the United States. *Ann Plast Surg* 2018; **81**: 220-227 [PMID: 29781849 DOI: 10.1097/SAP.0000000000001454]
58 **Sheckter CC**, Panchal HJ, Razdan SN, Rubin D, Yi D, Disa JJ, Mehrara B, Matros E. The Influence of Physician Payments on the Method of Breast Reconstruction: A National Claims Analysis. *Plast Reconstr Surg* 2018; **142**: 434e-442e [PMID: 29979366 DOI: 10.1097/PRS.0000000000004727]
59 **Sheckter CC**, Yi D, Panchal HJ, Razdan SN, Pusic AL, McCarthy CM, Cordeiro PG, Disa JJ, Mehrara B, Matros E. Trends in Physician Payments for Breast Reconstruction. *Plast Reconstr Surg* 2018; **141**: 493e-499e [PMID: 29595721 DOI: 10.1097/PRS.0000000000004205]
60 **Jagsi R**, Momoh AO, Qi J, Hamill JB, Billig J, Kim HM, Pusic AL, Wilkins EG. Impact of Radiotherapy on Complications and Patient-Reported Outcomes After Breast Reconstruction. *J Natl Cancer Inst* 2018; **110**: 157-165 [PMID: 28954300 DOI: 10.1093/jnci/djx148]

61 **Chetta MD**, Aliu O, Zhong L, Sears ED, Waljee JF, Chung KC, Momoh AO. Reconstruction of the Irradiated Breast: A National Claims-Based Assessment of Postoperative Morbidity. *Plast Reconstr Surg* 2017; **139**: 783-792 [PMID: 28002254 DOI: 10.1097/PRS.0000000000003168]

62 **Agarwal S**, Talia J, Liu PS, Momoh AO, Kozlow JH. Determining the Cost of Incidental Findings for Patients Undergoing Preoperative Planning for Abdominally Based Perforator Free Flap Breast Reconstruction with Computed Tomographic Angiography. *Plast Reconstr Surg* 2016; **138**: 804e-810e [PMID: 27782984 DOI: 10.1097/PRS.0000000000002621]

63 **Teunis T**, Heerma van Voss MR, Kon M, van Maurik JF. CT-angiography prior to DIEP flap breast reconstruction: a systematic review and meta-analysis. *Microsurgery* 2013; **33**: 496-502 [PMID: 23836386 DOI: 10.1002/micr.22119]

64 **Atisha D**, Alderman AK, Janiga T, Singal B, Wilkins EG. The efficacy of the surgical delay procedure in pedicle TRAM breast reconstruction. *Ann Plast Surg* 2009; **63**: 383-388 [PMID: 19770703 DOI: 10.1097/SAP.0b013e31819516ba]

65 **Vyas RM**, Dickinson BP, Fastekjian JH, Watson JP, DaLio AL, Crisera CA. Risk factors for abdominal donor-site morbidity in free flap breast reconstruction. *Plast Reconstr Surg* 2008; **121**: 1519-1526 [PMID: 18453973 DOI: 10.1097/PRS.0b013e31816b1458]

66 **Sbitany H**, Mirzabeigi MN, Kovach SJ, Wu LC, Serletti JM. Strategies for recognizing and managing intraoperative venous congestion in abdominally based autologous breast reconstruction. *Plast Reconstr Surg* 2012; **129**: 809-815 [PMID: 22456352 DOI: 10.1097/PRS.0b013e318244222d]

67 **Spiegel AJ**, Khan FN. An Intraoperative algorithm for use of the SIEA flap for breast reconstruction. *Plast Reconstr Surg* 2007; **120**: 1450-1459 [PMID: 18040173 DOI: 10.1097/01.prs.0000270282.92038.3f]

68 **Schaverien M**, Saint-Cyr M, Arbique G, Brown SA. Arterial and venous anatomies of the deep inferior epigastric perforator and superficial inferior epigastric artery flaps. *Plast Reconstr Surg* 2008; **121**: 1909-1919 [PMID: 18520876 DOI: 10.1097/PRS.0b013e31817151f8]

69 **Holm C**, Mayr M, Höfter E, Ninkovic M. Perfusion zones of the DIEP flap revisited: a clinical study. *Plast Reconstr Surg* 2006; **117**: 37-43 [PMID: 16404245 DOI: 10.1097/01.prs.0000185867.84172.c0]

70 **Chang EI**, Chang EI, Soto-Miranda MA, Zhang H, Nosrati N, Robb GL, Chang DW. Comprehensive analysis of donor-site morbidity in abdominally based free flap breast reconstruction. *Plast Reconstr Surg* 2013; **132**: 1383-1391 [PMID: 24005365 DOI: 10.1097/PRS.0b013e3182a805a3]

71 **Selber JC**. The Robotic DIEP Flap. *Plast Reconstr Surg* 2020; **145**: 340-343 [PMID: 31985617 DOI: 10.1097/PRS.0000000000006529]

72 **Choi JH**, Song SY, Park HS, Kim CH, Kim JY, Lew DH, Roh TS, Lee DW. Robotic DIEP Flap Harvest through a Totally Extraperitoneal Approach Using a Single-Port Surgical Robotic System. *Plast Reconstr Surg* 2021; **148**: 304-307 [PMID: 34398082 DOI: 10.1097/PRS.0000000000008181]

73 **Park JE**, Alkureishi LWT, Song DH. TUGs into VUGs and Friendly BUGs: Transforming the Gracilis Territory into the Best Secondary Breast Reconstructive Option. *Plast Reconstr Surg* 2015; **136**: 447-454 [PMID: 26057023 DOI: 10.1097/PRS.0000000000001557]

74 **DeLong MR**, Hughes DB, Bond JE, Thomas SM, Boll DT, Zenn MR. A detailed evaluation of the anatomical variations of the profunda artery perforator flap using computed tomographic angiograms. *Plast Reconstr Surg* 2014; **134**: 186e-192e [PMID: 25068339 DOI: 10.1097/PRS.0000000000000320]

75 **LoTempio MM**, Allen RJ. Breast reconstruction with SGAP and IGAP flaps. *Plast Reconstr Surg* 2010; **126**: 393-401 [PMID: 20679825 DOI: 10.1097/PRS.0b013e3181de236a]

76 **Nahabedian MY**, Momen B, Galdino G, Manson PN. Breast Reconstruction with the free TRAM or DIEP flap: patient selection, choice of flap, and outcome. *Plast Reconstr Surg* 2002; **110**: 466-475; discussion 476 [PMID: 12142662 DOI: 10.1097/00006534-200208000-00015]

77 **Patel NG**, Ramakrishnan V. Microsurgical Tissue Transfer in Breast Reconstruction. *Clin Plast Surg* 2017; **44**: 345-359 [PMID: 28340667 DOI: 10.1016/j.cps.2016.12.002]

78 **Healy C**, Allen RJ Sr. The evolution of perforator flap breast reconstruction: twenty years after the first DIEP flap. *J Reconstr Microsurg* 2014; **30**: 121-125 [PMID: 24163223 DOI: 10.1055/s-0033-1357272]

79 **Allen RJ Jr**, Lee ZH, Mayo JL, Levine J, Ahn C, Allen RJ Sr. The Profunda Artery Perforator Flap Experience for Breast Reconstruction. *Plast Reconstr Surg* 2016; **138**: 968-975 [PMID: 27391834 DOI: 10.1097/PRS.0000000000002619]

80 **Leyngold MM**. Is Unipedicled Transverse Rectus Abdominis Myocutaneous Flap Obsolete Owing to Superiority of DIEP Flap? *Ann Plast Surg* 2018; **80**: S418-S420 [PMID: 29369109 DOI: 10.1097/SAP.0000000000001319]

81 **Joo A**, Giatsidis G. In Autologous Breast Reconstruction, Frailty Is a More Accurate Predictor of Postoperative Complications: A Retrospective Cohort Analysis. *Plast Reconstr Surg* 2022; **150**: 82S-94S [PMID: 35943961 DOI: 10.1097/PRS.0000000000009531]

82 **Kim S**, Lee S, Bae Y. Nipple-sparing mastectomy for breast cancer close to the nipple: a single institution's 11-year experience. *Breast Cancer* 2020; **27**: 999-1006 [PMID: 32372321 DOI: 10.1007/s12282-020-01104-0]

83 **Stanec Z**, Žic R, Budi S, Stanec S, Milanović R, Vlajčić Z, Roje Z, Rudman F, Martić K, Held R, Božo G. Skin and nipple-areola complex sparing mastectomy in breast cancer patients: 15-year experience. *Ann Plast Surg* 2014; **73**: 485-491 [PMID: 24378808 DOI: 10.1097/SAP.0b013e31827a30e6]

World Journal of Clinical Cases

Submit a Manuscript: https://www.f6publishing.com

World J Clin Cases 2023 April 6; 11(10): 2213-2225

DOI: 10.12998/wjcc.v11.i10.2213

ISSN 2307-8960 (online)

MINIREVIEWS

Update on the current management of persistent and recurrent primary hyperparathyroidism after parathyroidectomy

Efstathios T Pavlidis, Theodoros E Pavlidis

Specialty type: Surgery

Provenance and peer review: Invited article; Externally peer reviewed.

Peer-review model: Single blind

Peer-review report's scientific quality classification

Grade A (Excellent): 0
Grade B (Very good): B
Grade C (Good): C
Grade D (Fair): 0
Grade E (Poor): 0

P-Reviewer: Gorbacheva AM, Russia; Moshref RH, Saudi Arabia

Received: January 18, 2023
Peer-review started: January 18, 2023
First decision: January 31, 2023
Revised: February 1, 2023
Accepted: March 15, 2023
Article in press: March 15, 2023
Published online: April 6, 2023

Efstathios T Pavlidis, Theodoros E Pavlidis, The Second Propedeutic Department of Surgery, Hippocration Hospital, School of Medicine, Aristotle University, Thessaloniki 54642, Greece

Corresponding author: Theodoros E Pavlidis, PhD, Full Professor, Surgeon, The Second Propedeutic Department of Surgery, Hippocration Hospital, School of Medicine, Aristotle University, Konstantinoupoleos 49, Thessaloniki 54642, Greece. pavlidth@auth.gr

Abstract

Primary hyperparathyroidism (pHPT) is the third most common endocrine disease. The surgical procedure aims for permanent cure, but recurrence has been reported in 4%-10% of pHPT patients. Preoperative localization imaging is highly valuable. It includes ultrasound, computed tomography (CT), single-photon-emission CT, sestamibi scintigraphy and magnetic resonance imaging. The operation has been defined as successful when postoperative continuous eucalcemia exists for more than the first six months. Ongoing hypercalcemia during this period is defined as persistence, and recurrence is defined as hypercalcemia after six months of normocalcemia. Vitamin D is a crucial factor for a good outcome. Intraoperative parathyroid hormone (PTH) monitoring can safely predict the outcomes and should be suggested. PTH ≤ 40 pg/mL or the traditional decrease ≥ 50% from baseline minimizes the likelihood of persistence. Risk factors for persistence are hyperplasia and normal parathyroid tissue on histopathology. Risk factors for recurrence are cardiac history, obesity, endoscopic approach and low-volume center (at least 31 cases/year). Cases with double adenomas or four-gland hyperplasia have a greater likelihood of persistence/recurrence. A 6-mo calcium > 9.7 mg/dL and eucalcemic parathyroid hormone elevation at 6 mo may be associated with recurrence necessitating long-term follow-up. 18F-fluorocholine positron emission tomography and 4-dimensional CT in persistent and recurrent cases can be valuable before reoperation. With these novel advances in preoperative imaging and localization as well as intraoperative PTH measurement, the recurrence rate has dropped to 2.5%-5%. Six-month serum calcium ≥ 9.8 mg/dL and parathyroid hormone ≥ 80 pg/mL indicate a risk of recurrence. Negative sestamibi scintigraphy, diabetes and elevated osteocalcin levels are predictors of multiglandular disease, which brings an increased risk of persistence and recurrence. Bilateral neck exploration was considered the gold-standard diagnostic method. Minimally invasive parathyroidectomy and neck exploration are both effective surgical techniques. Multidisciplinary diagnostic and surgical management is required to prevent persistence and recurrence. Long-term follow-up, even up to 10 years, is

necessary.

Key Words: Parathyroid hormone; Minimally invasive parathyreoidectomy; Hyperparathyroidism; Primary; Reoperation; Persistent; Recurrent hypercalcemia

Core Tip: Surgical intervention can permanently cure primary hyperparathyroidism. Advances in preoperative imaging and localization as well as intraoperative parathormone monitoring have significantly reduced the rates of persistence and recurrence. The criteria for reoperation must be stricter and based on biochemical confirmation of the diagnosis, review of preexisting data, and positive imaging findings. However, diagnosis and treatment are multidisciplinary tasks. The final decision about reoperation and its procedure should be made by an experienced endocrine surgeon. In any case, preoperative assessment of recurrent laryngeal nerve function and intraoperative measurement of parathyroid hormone are necessary.

Citation: Pavlidis ET, Pavlidis TE. Update on the current management of persistent and recurrent primary hyperparathyroidism after parathyroidectomy. *World J Clin Cases* 2023; 11(10): 2213-2225
URL: https://www.wjgnet.com/2307-8960/full/v11/i10/2213.htm
DOI: https://dx.doi.org/10.12998/wjcc.v11.i10.2213

INTRODUCTION

Basic prerequisites in parathyroid surgery are the ability to identify the parathyroids, the deep knowledge of their anatomical location and its wide spectrum of variations, and the ability to distinguish between a normal and pathological gland. The superior parathyroids in 85% of cases are located within a radius of 1 cm from the inferior angle of the thyroid, while inferior parathyroids in more than 50% of cases are located in the lower third of the junction between the posterior end of the thyroid gland and the anterior part of the thymus gland or within it, within the mediastinum, or even within the thyroid parenchyma. The exact anatomical location of the parathyroid glands comes in six recognized types, as shown in Table 1[1]. The anatomical location of the supernumerary parathyroid is located below the thyroid in the remnants of the thymus (two-thirds of cases) or near the thyroid, usually between the other two parathyroids (one-third)[1,2].

Primary hyperparathyroidism (pHPT) is the third most common endocrine disease[3], with ongoing incidence and 100000 new cases annually in the United States[4]. It is sporadic (90%-95%) and hereditary (5%-10%) and is associated with multiple endocrine neoplasia (MEN) syndromes. Its causes include mainly single parathyroid adenoma (PA) (80%-85%), double adenoma (4%-5%), diffuse hyperplasia (10%-15%) and parathyroid cancer (< 1%), as shown schematically in Figure 1[5]. Cure has been defined as the restoration of calcium levels (normal homeostasis) lasting six months at a minimum [3].

Cure rates currently range between 95% and 99%[3,6,7]. However, normocalcemia before the initial operation exists in 10% of pHPT[8,9]. Patients with pHPT with normal calcium levels but persistently high PTH values after parathyroidectomy should be evaluated for possible secondary HPT or recurrent disease[7].

Persistent hyperparathyroidism (P-HPT) is defined as the condition where calcium either does not return to normal values or rises again within 6 mo of the initial parathyroidectomy for pHPT[8]. It is mainly due to failure to remove an overactive parathyroid (adenoma or unrecognized parathyroid hyperplasia)[8,10,11]. Recurrent hyperparathyroidism (R-HPT) occurs when calcium increases beyond normal limits after at least 6 mo of normal values after the initial parathyroidectomy for pHPT. It is due to untreated parathyroid hyperplasia, parathyroid carcinoma (PC) or metastasis, autograft hyperplasia or parathyromatosis[3,6,12]. The latter (benign diffused multiple nodules of hyperfunctioning parathyroid tissue in the neck and superior mediastinum) is a very rare cause of R-HPT[13,14].

The causes of P-HPT/R-HPT are adenoma (68%), parathyroid hyperplasia (28%), PC (3%), and other causes (1%, parathyromatosis, autograft relapse), as shown schematically in Figure 2[9]. Cases with double adenomas or four-gland hyperplasia have a higher likelihood of P-HPT/R-HPT[15]. The ectopic locations of PA (approximately 0.3%-8%) include the hypoglossal nerve, the posterior triangle of the neck, the axilla, the mediastinum, the pericardium[16], the thymus gland[2] and thyroid gland[17].

Risk for persistence constitutes hyperplasia and normal parathyroid tissue on the histopathological report[3]. Additionally, measuring parathyroid hormone and calcium in the early postoperative period (after two weeks) may better predict later recurrent pHPT[18]. However, a postoperative increase in

Table 1 Anatomical location of the parathyroid glands

Type	Location
A1	Attached to the thyroid capsule
A2	Partially or completely embedded in the thyroid gland but outside the capsule
A3	Within the thyroid parenchyma
B1	Peripheral, existence of a natural gap space between parathyroid and thyroid gland
B2	Within the thymus gland
B3	Blood supply from thymic or mediastinal vessels

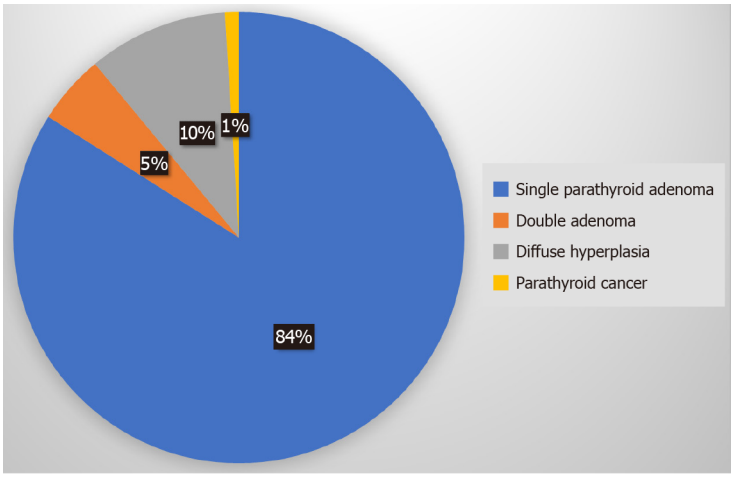

DOI: 10.12998/wjcc.v11.i10.2213 **Copyright** ©The Author(s) 2023.

Figure 1 Causes of primary hyperparathyroidism. Single parathyroid adenoma (80%-85%), double adenoma (4%-5%), diffuse hyperplasia (10%-15%), parathyroid cancer (< 1%).

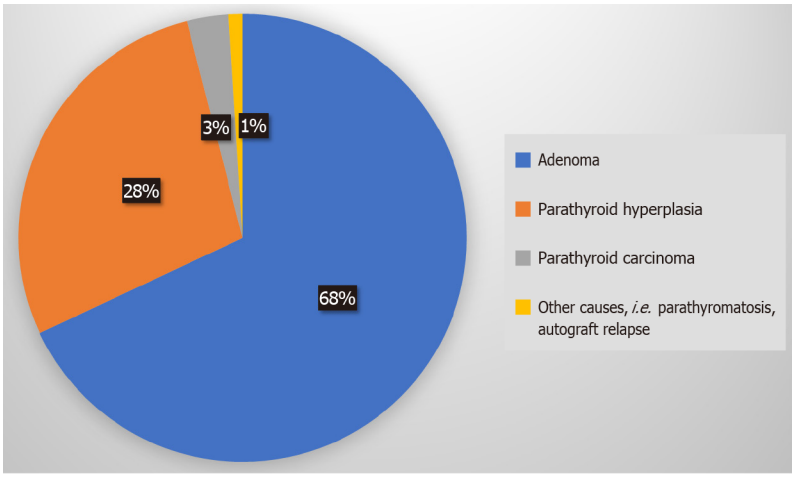

DOI: 10.12998/wjcc.v11.i10.2213 **Copyright** ©The Author(s) 2023.

Figure 2 Causes of persistent-recurrent primary hyperparathyroidism. Adenoma (68%), parathyroid hyperplasia (28%), parathyroid carcinoma (3%), other causes: *i.e.* parathyromatosis, autograft relapse (1%).

PTH does not always indicate P-HPT/R-HPT; rather, it may be due to vitamin D insufficiency, mild renal failure, hyperfunction of previously suppressed parathyroid glands, unrecognized familial hypercalciuric hypocalcemia, and increased bone redistribution of calcium[18]. Subsequently, preoperative 25-hydroxyvitamin D level must be assessed especially in patients without severe hypercalcemia, and must be corrected if low for a good outcome[19].

The incidence of P-HPT/R-HPT was approximately 30% in 1990. Today, with the ongoing advances in preoperative parathyroid imaging, implementation of intraoperative PTH monitoring (IPM), and avoidance of bilateral neck exploration (BNE) to locate the parathyroids, this percentage ranges between 2.5%-5%[12]; however, in recent reports, it was higher than traditionally described, reaching up to 10% or even 14%[8]. The predictors of P-HPT/R-HPT occurrence are shown in Table 2[12]. Transient hypercalcemia in the early postoperative period does not predict persistent pHPT, since it exists at a rate of almost 10% after successful parathyroidectomy, which in most cases is normalized within two weeks [20].

In this minireview, we evaluate the current management options for failure after surgery for pHPT, highlighting the updated knowledge by selecting and focusing on the most relevant articles from PubMed.

DIAGNOSIS

Multidisciplinary diagnostic and surgical management is required to prevent persistence and recurrence. The preoperative localization imaging of the initial operation is of great importance. It can include ultrasound (US), computed tomography (CT), single-photon emission CT (SPECT) and sestamibi scintigraphy[21].

The preoperative evaluation of P-HPT/R-HPT includes confirmation of the diagnosis, review of preexisting data, stricter indications for reintervention, and diagnostic imaging[7]. Confirmation of the diagnosis can be made by the following: (1) All biochemical data before and after the initial operation should be rechecked; (2) checking for medications that affect calcium metabolism (*e.g.*, lithium, thiazide diuretics); (3) detailed checks for elevated PTH from another cause, as mentioned above (*e.g.*, renal failure, vitamin D deficiency); (4) taking a detailed family history for MEN (MEN1, MEN2A); and (5) investigation of possible parathyroid cancer and/or parathyromatosis[7].

The review of preexisting data is based on previous imaging scans, details of the operative report, histopathological findings and even re-evaluation of paraffin blocks[12].

Diagnostic imaging

Diagnostic imaging includes US, sestamibi scintigraphy +/- SPECT, 4-dimensional (4D) CT or magnetic resonance imaging (MRI) and elective venous catheterization. The introduction of an iodine-containing contrast is contraindicated in cases where there is a decrease in the filtration function of the kidneys[12].

Normal parathyroid glands are typically not visible on US due to their small size (2-3 mm). The advantages of US include no exposure to radiation, low cost, easy availability and simultaneous checking of the thyroid gland. Its disadvantages are decreased resolution with high body mass index, which depends on the sonographer's experience, limited visibility in parathyroid hyperplasia and low-lying upper or inferior glands[7]. A meta-analysis has shown a sensitivity of up to 79%[22]. This falls to 35% in cases of parathyroid hyperplasia[23]. Specificity in some centers reaches 96%[24]. In combination with sestamibi or 4D-CT, US has the optimal cost benefit ratio[25]. The combination of US and sestamibi significantly increases the sensitivity for identifying an adenoma compared to each method alone; however, it remains low in cases of parathyroid hyperplasia, at 30%-60%[7].

Sestamibi scintigraphy is based on the differential uptake and retention of the radiotracer in mitochondria-rich cells. Its advantages include assessment of deep-neck-located or ectopic parathyroid even in the mediastinum, low radiation exposure and ability to assess parathyroid tissue autografts. Its disadvantages are weaker assessment of the thyroid gland, possible false-positive results from thyroid nodules and reduced effectiveness in parathyroid hyperplasia[7]. There are several protocols that use sestamibi (dual-phase, I^{131} subtraction, SPECT, and 4-D SPECT-CT imaging) with various strengths and weaknesses[26].

SPECT imaging provides 4-D imaging with a sensitivity of 79% (range 45%-92%). It is useful for detecting posteriorly located adenomas of superior parathyroids that are usually obscured by thyroid uptake. According to a meta-analysis, its sensitivity is reduced significantly in cases of parathyroid hyperplasia (44%) or double adenoma (33%)[23]. Additionally, the sensitivity of SPECT depends on the weight of the affected gland. If it is more than 500 mg, the sensitivity will be 93%, whereas if it is less than 500 mg, it will fall to 51%[27]. Typically, a PA is characterized by the rapid uptake of contrast medium and thus the relative elimination of its distribution to the thyroid and surrounding tissues. The advantages of 4D-CT include the accurate anatomical detail and functional condition of the parathyroid whether it has a normal or ectopic position, its being the only method that can identify normal parathyroids and its greater sensitivity for parathyroid hyperplasia compared to other methods (62.5%-85.7%). Its disadvantages are the cost, greater exposure to radiation, limited availability and accessibility, and the requirement of specialized personnel to interpret the results[7]. According to another meta-analysis, it has a sensitivity of 89%[22]. In a direct comparison, the sensitivity of 4D-CT (88%) is superior to that of US (57%) and sestamibi (65%)[28].

Table 2 Predictors of persistent/recurrent hyperparathyroidism occurrence

No.	Predictor
1	Age > 70
2	Obesity
3	ASA score 3
4	Low hospital case volume (n < 50/yr)
5	Inadequate surgeon's experience
6	Ambiguous scintigraphy results with Sestamibi
7	Primary disease (single adenoma < double adenoma < parathyroid hyperplasia)
8	Surgical strategy (not recognizing the pathological gland, not applying bilateral cervical exploration in case of inadequate PTH reduction intraoperatively)

P-HPT: Persistent hyperparathyroidism; R-HPT: Recurrent hyperparathyroidism; PTH: Parathyroid hormone.

Initial imaging

For the initial imaging of parathyroids, US of the neck is recommended to identify parathyroid disease and assess possible coexisting thyroid pathology. An experienced clinician should decide which other imaging modality to use, depending on the capabilities available in each center or region[7]. In reoperative parathyroid imaging, at least one positive preoperative imaging is necessary to plan the reoperation, as abnormal glands may also be ectopic. Otherwise, there is a fourfold greater likelihood of failure. Some surgeons require one positive imaging test, while others require two positive imaging tests before reoperation[29]. 4D-CT has a higher sensitivity (88%) than Sestamibi scintigraphy (54%) in reintervention[30]. In a study of 90 patients with reoperation, there was 90% concordance between 4D-CT and surgical findings, while the concordance between other imaging and surgical findings was only 63%, with a shorter operating time (76 min *vs* 114 min). Its efficiency in reoperations, especially in difficult undiagnosed-by-sestamibi cases and hyperplasia, along with its growing use in recent years, makes it the first choice imaging method for P-pHPT and R-pHPT[31].

Imaging before reoperation

The two most commonly used preoperative diagnostic tools are neck US and scintigraphy. The latter is typically performed using the radiotracer technetium-99m-sestamibi in combination with SPECT plus 4D-CT if needed, which may be more cost-effective[25]. In cases of P-pHPT/R-pHPT, positron emission tomography (PET)/CT can detect a hyperfunctioning parathyroid with accuracy and has been proven to be better than 4D-CT. Therefore, 18F-fluorocholine PET/CT has been recently advocated before reoperation[32-34].

A recent study demonstrated that in addition to US and myocardial perfusion imaging (MIBI), noncontrast 3-Tesla MRI further increased the preoperative localization of pHPT (sensitivity of 92.0%)[35].

A scheme of the diagnostic approach is shown in Figure 3.

Despite the above, although it can be risky, no preoperative routine imaging protocols to reduce the cost, only intraoperative PTH measurement, have been advocated for pHPT with a skilled surgeon and without previous neck surgery[36].

Invasive imaging

While noninvasive imaging methods are preferred, invasive methods play a selective role. In contrast to what happens in the initial surgery, in reoperation, US-guided fine needle aspiration of the suspected parathyroid gland preoperatively may be useful by providing cytology and PTH levels. Its potential complications are hematoma, parathyromatosis and the spread of cancer cells. Thus, it is only recommended in selected cases[7,9].

Selective venous catheterization is rarely used and is impossible if there has been ligation of the thyroid and parathyroid vessels. Catheterization of the femoral vein and assessment of PTH in venous blood drained from the cervix and mediastinum can identify the side where the pathological gland is located. Its sensitivity in P-HPT/R-HPT is 83.3% for solitary adenomas and 91.6% for parathyroid hyperplasia. However, it is expensive, requires expertise and is associated with inguinal hematoma and vascular injuries[7].

Genetic diagnosis

There are rare cases of atypical tumors[37] or atypical PA (APA) with an ambiguous potential for malignancy that have a good prognosis in the vast majority, but mutations in the CDC73 gene are

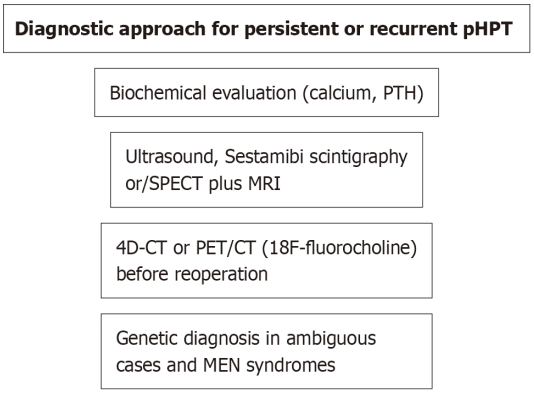

DOI: 10.12998/wjcc.v11.i10.2213

Figure 3 Scheme of diagnostic approach for persistent or recurrent primary hyperparathyroidism. pHPT: Primary hyperparathyroidism; PTH: Parathyroid hormone; SPECT: Single-photon emission computed tomography; MRI: Magnetic resonance imaging; CT: Computed tomography; PET: Positron emission tomography.

related to high P-HPT/R-HPT[38,39]. Flow-cytometric DNA analysis has been recommended in such cases[40], especially in the context of MEN syndromes[41]. *CDC73* gene mutations are not involved in the tumorigenesis of sporadic APA[38]. *KMT2D* might be a novel candidate driver gene that can be used as a diagnostic biomarker for PA. However, *CDC73* mutations can be an early developmental event from PA to PC[42]. Germline mutations in *CDKIs* (the *CDKN1B* gene and *CDKN2C* gene) should be included in the genetic testing of patients with pHPT[43].

Other diagnostic tools

In resected specimen biopsy, hypercellularity of an otherwise normal parathyroid does not indicate multiglandular disease related to hyperfunction[44].

In a multicenter study, two preoperative mathematical models predicted adenoma, atypical adenoma and PC with reliability, thus determining the choice of surgical plan[45].

MANAGEMENT

The surgical operation aims for permanent cure[21,46]. However, recurrence has been reported in 4%-10% of surgery patients[8]. The extent of surgical resection in pHPT depends on its cause. Removal of the enlarged gland is the indicated surgical technique in adenoma, the most common case. The surgical strategy in diffuse hyperplasia includes either subtotal parathyroidectomy (removal of 3.5 glands) or total parathyroidectomy and autotransplantation of thin pieces (n = 10-15) of parathyroid tissue in the forearm. The operative strategy in carcinoma includes the unblock removal of the affected gland with the corresponding thyroid lobe and surrounding tissues[9]. A scheme of the treatment approach is shown in Figures 4 and 5.

Ipsilateral cervical exploration has been recommended because the majority of cases are due to an adenoma, there is a possibility of preoperative identification of the responsible gland, and it is possible to quickly determine the parathyroid hormone levels. Its advantages ensure a limited extent of the surgical wound, shorter operation and reoperation on the contralateral intact side if needed. Its disadvantages include the limited effectiveness in the presence of supernumerary glands and the possibility of double adenoma[4,9]. With the current advancements in diagnostic adjuncts for accurate abnormal parathyroid localization, surgery has moved from BNE to a focused open parathyroidectomy or unilateral neck exploration as well as to a minimally invasive parathyroidectomy (MIP) that necessitates even more accurate preoperative localization[22,25,47-49].

Outcomes

The success rate of surgical treatment is more than 95% in experienced hands[4,10]. The causes of its failure are shown in Table 3[9,12]. In the following studies, the recurrences occurred a long time after the first intervention. This means that the tumors probably developed de novo during the follow-up period and were not missed during the first operation.

A study from the United States including 345 patients who underwent surgical intervention for pHPT, either single-gland resection (79%) or bilateral cervical exploration (38%), found that persistent hypercalcemia (9%) and recurrent hypercalcemia (14%) were transient mainly for other reasons, while only 3.2% of them required reoperation (median time to recurrence 12.2 years)[8]. Likewise, a more recent study from the United Kingdom including 404 patients with pHPT who underwent successful

Table 3 Causes of operative treatment failure for primary hyperparathyroidism

No.	Cause
1	Failure to recognize histopathological lesion
2	Supernumerary (5th) parathyroid
3	Ectopic site of responsible parathyroid gland
4	Carcinoma or spread of adenoma parts
5	Inadequate experience of the surgeon
6	Insufficient cooperation with pathologist

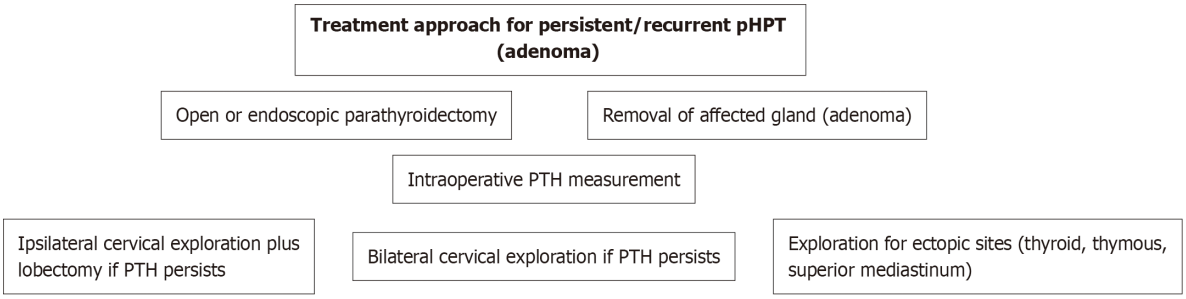

DOI: 10.12998/wjcc.v11.i10.2213

Figure 4 Scheme of treatment approach for persistent or recurrent primary hyperparathyroidism (adenoma). pHPT: Primary hyperparathyroidism; PTH: Parathyroid hormone.

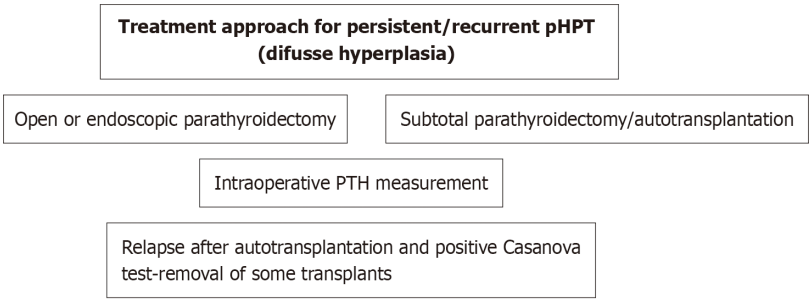

DOI: 10.12998/wjcc.v11.i10.2213

Figure 5 Scheme of treatment approach for persistent or recurrent primary hyperparathyroidism (diffuse hyperplasia). pHPT: Primary hyperparathyroidism; PTH: Parathyroid hormone.

MIP had a long-term follow-up (median 6.5 years) with normocalcemia in 96% of cases; 3.85% had biochemical recurrence after 5 years (median 7.7 years), and only one patient had persistent hypercalcemia[50]. Another recent study from the United States including 261 patients after successful parathyroidectomy for pHPT reported a 10.7% late recurrence rate (up to 17 years, median time 6.5 years) and an 89.3% cure rate of recurrences. Multivariate analysis found calcium ≥ 9.7 mg/dL and normocalcemic PTH increase as independent risk factors for late recurrence at six months[4]. Another retrospective trial including 196 patients found recurrence of 14.8% (median time 6.3 years), but 34.5% of recurrences occurred later (> 10 years), without a difference between open parathyroidectomy and MIP[51]. The above findings necessitate a long-term postoperative follow-up. Additionally, concerns about the efficacy of preoperative US and sestamibi scintigraphy alone provide more argument in favor of additional BNE again.

A recent large study from Taiwan including 522 patients after parathyroidectomy (mostly MIP) with a median follow-up of 2.5 years found, by multivariate analysis, that age > 66.5 years, serum calcium ≥ 9.8 mg/dL and parathyroid hormone ≥ 80 pg/mL at 6 mo were risk factors for recurrence (rate of 2.5%); after MIP, the discrepancy of at least one preoperative imaging study with intraoperative findings was a risk factor[47].

A recent nationwide French study including 13247 patients after focused parathyroidectomy by either open surgery (88.7%) or MIP (11.3%) found that the cure rate was 97.3% for the former and 96.5% for the latter; the need for reoperation was 2.8% at two years. The predictive risk factors for failure of the initial

parathyroidectomy and the need for reoperation shown by the multivariate analysis were cardiac history (congestive heart failure, arrhythmias, and valvular disease), obesity, endoscopic approach, and surgery at a low-volume center (at most 31 cases per year)[46].

A meta-analysis of 70 studies with 9643 patients undergoing MIP and 38 studies with 2471 patients undergoing open BNE confirmed the effectiveness of both operative methods for the management of pHPT. Comparing BNE *vs* MIP, the cure rates were 98% *vs* 97%, bleeding rates were 0.9% *vs* 0.1% [statistically significant (SS)], postoperative (short-term and long-term) hypocalcemia 13.6% *vs* 2.3% (SS), laryngeal nerve injury 0.9% *vs* 0.3% (SS), infection 0.5% *vs* 0.5% and mortality 0.5% *vs* 0.1%, respectively [52].

Useful recommendations

In patients with histologically large normal parathyroid and pHPT, a controversial issue, excision exhibits a beneficial effect on PTH levels despite the higher risk of P-HPT/R-HPT than in adenoma or hyperplasia; thus, these patients need stricter biochemical postoperative follow-up[53].

Stricter indications for reoperation for P-HPT/R-HPT have been recommended because it may cause fibrosis, alteration of normal anatomy and complications. These indications are determined by the presence of severe features, *i.e.*, persistent clinical musculoskeletal or neuropsychiatric symptoms, nephrolithiasis, nephrocalcinosis and osteoporosis[8,9,17,47]. According to the guidelines of the American Association of Endocrine Surgeons, in the above indications are added to serum calcium > 1 mg/dL above the normal upper value and young age (< 50 years)[47].

It has been reported that reoperation is linked with significantly lower cure rates (82%-98%) and higher rates of hypoparathyroidism (5%-8%) and recurrent laryngeal nerve palsy (15%) than initial parathyroidectomy[7]. Thus, rechecking nerve function preoperatively is mandatory. Intraoperative neuromonitoring is also a useful tool[9].

The cervical endoscopic approach for adenoma located at the posterior mediastinum is a current preferable safe choice[54].

A normocalcemic PTH increase may occur after parathyroidectomy for pHPT. This may be caused by higher preoperative PTH, vitamin D deficiency, and lower creatinine clearance. Postoperative calcium and vitamin D administration have been recommended in such cases[55].

The size of an adenoma (dwarf < 300 mg or giant > 3000 mg) does not affect the outcomes of parathyroidectomy, which is indicated for all dwarf adenomas, while giant adenomas do not have malignant behavior[56].

It has been postulated that the success of parathyroidectomy is reflected in a decrease in the neutrophil-to-lymphocyte ratio and platelet-to-lymphocyte ratio by its modulatory effect on systemic inflammation[57].

Multiglandular disease (its predictors by multivariable analysis are negative sestamibi scintigraphy, diabetes and elevated osteocalcin) is associated with a higher risk of intraoperative complications and P-pHPT/R-pHPT. The parathyroid glands are associated with glucose metabolism. PTH, insulin and osteocalcin interact by modulating insulin secretion and peripheral lipolysis[58].

After parathyroid tissue autotransplantation, usually in the forearm for diffuse hyperplasia and pHPT, graft recurrence indicates reoperation that is difficult, requiring much caution, but first, a recurrence in the neck or mediastinum must be excluded[12]. For this, the Casanova diagnostic test is useful. A tourniquet is applied to the arm, causing ischemia for 15 min, and PTH is measured. The test is positive when the PTH level is decreased to > 50% of the preischemic value at 10 min after the end of ischemia. A decrease of < 20% indicates a negative test[59].

The use of cinacalcet reduces PTH production and is limited in persistent-recurrent pHPT. It is mostly used in patients with high surgical risk or as short-term operative preparation in patients with high calcium levels (≥ 12 mg/dL). Antiresorptive drugs can also be used in the conservative management of patients with P-pHPT/R-pHPT[60]. Other than surgery, which is the gold standard for P-pHPT/R-pHPT, microwave ablation or ethanol ablation has been reported, but they might have a place mainly in parathyroid cancer spread or parathyromatosis[12]. In a recent comparative study, microwave ablation had comparable results with parathyroidectomy but a shorter procedure time and smaller incision[61]. Likewise, radiofrequency ablation was safe and effective, ensuring a cure rate of 98% and a recurrent HPT rate of 2%[62].

INTRAOPERATIVE TOOLS FOR PARATHYROID IDENTIFICATION

Several useful intraoperative tools facilitate accurate parathyroid assessment, but no tool can replace the surgeon's judgment and experience. The following constitute the available choices[7-9].

The confirmation of parathyroid tissue removal is achieved either by IPM, which is preferable, or by frozen section histopathological examination or *ex vivo* aspiration of the resected parathyroid tissue to confirm the presumed parathyroid tissue intraoperatively[7]. IPM is considered to indicate successful parathyroidectomy when 10 min after excision it is decreased by ≥ 50% from its highest value before excision (Miami sole criterion, often used) or the latter plus a drop to a normal value (dual criteria)[63,

64]. IPM ≤ 40 pg/mL minimizes persistence as the final PTH will fall ≤ 65 pg/mL[65]. Intraoperative PTH monitoring can safely predict the outcome (accuracy at six months 98% at least), even in patients with normohormonal HPT (8%)[6]. In a comparative study, patients who underwent reoperation with the use of IPM and without it showed normal calcium levels postoperatively in 94% and 74%, respectively[66]. A recent meta-analysis of 28 studies with a total of 13323 patients documented that IPM reduces both persistent and recurrent pHPT and so must be used[67]. However, IPM in MIP in patients with positive and concordant preoperative ultrasonography and sestamibi scintigraphy is still under debate because, on the one hand, it costs more and increases the operating time and conversion rate; on the other hand, IPM may contribute to an increase in the cure rate to 97.6% from 93.3%[68].

Visual identification of parathyroid can be achieved by near-infrared autofluorescence angiography (infrared spectroscopy)[69,70] or indocyanine green (ICG) angiography[70-72], both with high sensitivity of up to 82% and 81%, respectively[70].

The anatomical localization of the parathyroids by intraoperative US, bilateral jugular venous sampling, or radioprobe guidance is another available choice[73]. Identification using trackers is based on carbon nanoparticles (when they are collected and deposited in the lymph nodes, the thyroid, and the drainage area of the lymph node will be painted black)[74] or radioprobe guidance[9,75]. It is based on the use of technetium-99m sestamibi for intraoperative identification of hyperactive parathyroids[9]. The tracer is injected 1-2 h before surgery. The surgeon with a handheld gamma camera detects the gamma radiation. Confirmation of resection of parathyroid tissue is indicated by high radioisotope concentrations. However, it has low specificity because the radioisotope is also taken up by the thyroid and cardiac tissue.

Recurrent laryngeal nerve monitoring is valuable for identification and preservation, thus avoiding injury and palsy[76,77].

Autotransplantation and cryopreservation should be considered when hypoparathyroidism occurs after parathyroidectomy or when the target parathyroid in reoperation is the only viable parathyroid tissue remaining[78].

CONCLUSION

Much progress has been made in the management of pHPT over the last few years. Parathyroidectomy for pHPT can offer a permanent cure, and its success depends on accurate preoperative localization. Preoperative ultrasonography and technetium-99m sestamibi scintigraphy-SPECT in addition to 4D-CT or PET/CT should be done if needed. This in combination with intraoperative parathyroid hormone monitoring and other novel localization adjuncts has contributed greatly to accurate parathyroid assessment, leading to a significant decrease in persistent and recurrent hyperparathyroidism and providing the best outcomes. Multidisciplinary diagnostic and therapeutic management is highly valuable to prevent persistence and recurrence. Surgery may be either open or endoscopic. Long-term follow-up, even up to 10 years, is imperative to detect late recurrence.

FOOTNOTES

Author contributions: Pavlidis TE designed research, contributed new analytic tools, analyzed data and review; Pavlidis ET performed research, analyzed data review and wrote the paper.

Conflict-of-interest statement: There is no conflict of interest associated with any of the senior author or other coauthors contributed their efforts in this manuscript.

Country/Territory of origin: Greece

ORCID number: Efstathios T Pavlidis 0000-0002-7282-8101; Theodoros E Pavlidis 0000-0002-8141-1412.

S-Editor: Zhang H
L-Editor: A
P-Editor: Zhang H

REFERENCES

1 **Zhu J**, Tian W, Xu Z, Jiang K, Sun H, Wang P, Huang T, Guo Z, Zhang H, Liu S, Zhang Y, Cheng R, Zhao D, Fan Y, Li X, Qin J, Zhao W, Su A. Expert consensus statement on parathyroid protection in thyroidectomy. *Ann Transl Med* 2015; **3**: 230 [PMID: 26539447 DOI: 10.3978/j.issn.2305-5839.2015.08.20]

2 **Reitz RJ 3rd**, Dreimiller A, Khil A, Horwitz E, McHenry CR. Ectopic and supernumerary parathyroid glands in patients with refractory renal hyperparathyroidism. *Surgery* 2021; **169**: 513-518 [PMID: 32919783 DOI: 10.1016/j.surg.2020.08.007]

3 **Olguvn Joseau S**, Arias A, Garzσn A, Peretti E, Guzmαn L, Ruggieri M. Risk factors for surgical failure in patients undergoing surgery for primary hyperparathyroidism. *Cir Esp (Engl Ed)* 2022; **100**: 569-572 [PMID: 35504549 DOI: 10.1016/j.cireng.2022.04.008]

4 **Mallick R**, Nicholson KJ, Yip L, Carty SE, McCoy KL. Factors associated with late recurrence after parathyroidectomy for primary hyperparathyroidism. *Surgery* 2020; **167**: 160-165 [PMID: 31606193 DOI: 10.1016/j.surg.2019.05.076]

5 **Aygón N**, Uludaπ M. Surgical Treatment of Primary Hyperparathyroidism: Which Therapy to Whom? *Sisli Etfal Hastan Tip Bul* 2019; **53**: 201-214 [PMID: 32377085 DOI: 10.14744/SEMB.2019.56873]

6 **Stuart H**, Azab B, Roque OP, Pasieka J, Lew JI. Intraoperative parathormone monitoring to predict operative success in patients with normohormonal hyperparathyroidism. *Can J Surg* 2022; **65**: E468-E473 [PMID: 35902104 DOI: 10.1503/cjs.013220]

7 **Wilhelm SM**, Wang TS, Ruan DT, Lee JA, Asa SL, Duh QY, Doherty GM, Herrera MF, Pasieka JL, Perrier ND, Silverberg SJ, Solσrzano CC, Sturgeon C, Tublin ME, Udelsman R, Carty SE. The American Association of Endocrine Surgeons Guidelines for Definitive Management of Primary Hyperparathyroidism. *JAMA Surg* 2016; **151**: 959-968 [PMID: 27532368 DOI: 10.1001/jamasurg.2016.2310]

8 **Szabo Yamashita T**, Mirande M, Huang CT, Kearns A, Fyffe-Freil R, Singh R, Foster T, Thompson G, Lyden M, McKenzie T, Wermers RA, Dy B. Persistence and Recurrence of Hypercalcemia after Parathyroidectomy Over Five Decades (1965-2010) in a Community-based Cohort. *Ann Surg* 2022 [PMID: 36017920 DOI: 10.1097/SLA.0000000000005688]

9 **Nawrot I**, Chudziρski W, CïHζka T, Barczypski M, Szmidt J. Reoperations for persistent or recurrent primary hyperparathyroidism: results of a retrospective cohort study at a tertiary referral center. *Med Sci Monit* 2014; **20**: 1604-1612 [PMID: 25201515 DOI: 10.12659/MSM.890983]

10 **Erinjeri NJ**, Udelsman R. Volume-outcome relationship in parathyroid surgery. *Best Pract Res Clin Endocrinol Metab* 2019; **33**: 101287 [PMID: 31285151 DOI: 10.1016/j.beem.2019.06.003]

11 **Kota SK**, Kota SK, Jammula S, Bhargav PRK, Sahoo AK, Das S, Talluri SC, Kongara S, S Krishna SV, Modi KD. Persistent Elevation of Parathormone Levels after Surgery for Primary Hyperparathyroidism. *Indian J Endocrinol Metab* 2020; **24**: 366-372 [PMID: 33088762 DOI: 10.4103/ijem.IJEM_212_20]

12 **Guerin C**, Paladino NC, Lowery A, Castinetti F, Taieb D, Sebag F. Persistent and recurrent hyperparathyroidism. *Updates Surg* 2017; **69**: 161-169 [PMID: 28434176 DOI: 10.1007/s13304-017-0447-7]

13 **Haciyanli M**, Karaisli S, Gucek Haciyanli S, Atasever A, Arikan Etit D, Gur EO, Acar T. Parathyromatosis: a very rare cause of recurrent primary hyperparathyroidism - case report and review of the literature. *Ann R Coll Surg Engl* 2019; **101**: e178-e183 [PMID: 31509000 DOI: 10.1308/rcsann.2019.0105]

14 **Jain M**, Krasne DL, Singer FR, Giuliano AE. Recurrent primary hyperparathyroidism due to Type 1 parathyromatosis. *Endocrine* 2017; **55**: 643-650 [PMID: 27743301 DOI: 10.1007/s12020-016-1139-7]

15 **Mazotas IG**, Yen TWF, Doffek K, Shaker JL, Carr AA, Evans DB, Wang TS. Persistent/Recurrent Primary Hyperparathyroidism: Does the Number of Abnormal Glands Play a Role? *J Surg Res* 2020; **246**: 335-341 [PMID: 31635835 DOI: 10.1016/j.jss.2019.08.007]

16 **Ademiluyi A**, Jackson N, Betty S, Ademiluyi A, Appiah-Pippim J, Bonhomme K. Missing in action. *J Community Hosp Intern Med Perspect* 2021; **11**: 856-858 [PMID: 34804406 DOI: 10.1080/20009666.2021.1981531]

17 **McIntyre CJ**, Allen JL, Constantinides VA, Jackson JE, Tolley NS, Palazzo FF. Patterns of disease in patients at a tertiary referral centre requiring reoperative parathyroidectomy. *Ann R Coll Surg Engl* 2015; **97**: 598-602 [PMID: 26444799 DOI: 10.1308/rcsann.2015.0039]

18 **Ryder CY**, Jarocki A, McNeely MM, Currey E, Miller BS, Cohen MS, Gauger PG, Hughes DT. Early biochemical response to parathyroidectomy for primary hyperparathyroidism and its predictive value for recurrent hypercalcemia and recurrent primary hyperparathyroidism. *Surgery* 2021; **169**: 120-125 [PMID: 32768241 DOI: 10.1016/j.surg.2020.05.049]

19 **Carsote M**, Paduraru DN, Nica AE, Valea A. Parathyroidectomy: is vitamin D a player for a good outcome? *J Med Life* 2016; **9**: 348-352 [PMID: 27928436]

20 **Lai V**, Yen TW, Doffek K, Carr AA, Carroll TB, Fareau GG, Evans DB, Wang TS. Delayed Calcium Normalization After Presumed Curative Parathyroidectomy is Not Associated with the Development of Persistent or Recurrent Primary Hyperparathyroidism. *Ann Surg Oncol* 2016; **23**: 2310-2314 [PMID: 27006125 DOI: 10.1245/s10434-016-5190-7]

21 **Van Den Heede K**, Bonheure A, Brusselaers N, Van Slycke S. Long-term outcome of surgical techniques for sporadic primary hyperparathyroidism in a tertiary referral center in Belgium. *Langenbecks Arch Surg* 2022; **407**: 3045-3055 [PMID: 36048245 DOI: 10.1007/s00423-022-02660-z]

22 **Cheung K**, Wang TS, Farrokhyar F, Roman SA, Sosa JA. A meta-analysis of preoperative localization techniques for patients with primary hyperparathyroidism. *Ann Surg Oncol* 2012; **19**: 577-583 [PMID: 21710322 DOI: 10.1245/s10434-011-1870-5]

23 **Ruda JM**, Hollenbeak CS, Stack BC Jr. A systematic review of the diagnosis and treatment of primary hyperparathyroidism from 1995 to 2003. *Otolaryngol Head Neck Surg* 2005; **132**: 359-372 [PMID: 15746845 DOI: 10.1016/j.otohns.2004.10.005]

24 **Carlier T**, Oudoux A, Mirallιt E, Seret A, Daumy I, Leux C, Bodet-Milin C, Kraeber-Bodιt F, Ansquer C. 99mTc-MIBI pinhole SPECT in primary hyperparathyroidism: comparison with conventional SPECT, planar scintigraphy and ultrasonography. *Eur J Nucl Med Mol Imaging* 2008; **35**: 637-643 [PMID: 17960377 DOI: 10.1007/s00259-007-0625-9]

25 **Wang TS**, Cheung K, Farrokhyar F, Roman SA, Sosa JA. Would scan, but which scan? *Surgery* 2011; **150**: 1286-1294 [PMID: 22136852 DOI: 10.1016/j.surg.2011.09.016]

26 **Neumann DR**, Obuchowski NA, Difilippo FP. Preoperative 123I/99mTc-sestamibi subtraction SPECT and SPECT/CT in primary hyperparathyroidism. *J Nucl Med* 2008; **49**: 2012-2017 [PMID: 18997051 DOI: 10.2967/jnumed.108.054858]

27 **Jones JM**, Russell CF, Ferguson WR, Laird JD. Pre-operative sestamibi-technetium subtraction scintigraphy in primary hyperparathyroidism: experience with 156 consecutive patients. *Clin Radiol* 2001; **56**: 556-559 [PMID: 11446753 DOI: 10.1053/crad.2001.0701]

28 **Rodgers SE**, Hunter GJ, Hamberg LM, Schellingerhout D, Doherty DB, Ayers GD, Shapiro SE, Edeiken BS, Truong MT, Evans DB, Lee JE, Perrier ND. Improved preoperative planning for directed parathyroidectomy with 4-dimensional computed tomography. *Surgery* 2006; **140**: 932-40; discussion 940 [PMID: 17188140 DOI: 10.1016/j.surg.2006.07.028]

29 **Hessman O**, Stɛlberg P, Sundin A, Garske U, Rudberg C, Eriksson LG, Hellman P, Akerstrφm G. High success rate of parathyroid reoperation may be achieved with improved localization diagnosis. *World J Surg* 2008; **32**: 774-81; discussion 782 [PMID: 18335276 DOI: 10.1007/s00268-008-9537-5]

30 **Mortenson MM**, Evans DB, Lee JE, Hunter GJ, Shellingerhout D, Vu T, Edeiken BS, Feng L, Perrier ND. Parathyroid exploration in the reoperative neck: improved preoperative localization with 4D-computed tomography. *J Am Coll Surg* 2008; **206**: 888-95; discussion 895 [PMID: 18471717 DOI: 10.1016/j.jamcollsurg.2007.12.044]

31 **Cham S**, Sepahdari AR, Hall KE, Yeh MW, Harari A. Dynamic Parathyroid Computed Tomography (4DCT) Facilitates Reoperative Parathyroidectomy and Enables Cure of Missed Hyperplasia. *Ann Surg Oncol* 2015; **22**: 3537-3542 [PMID: 25691276 DOI: 10.1245/s10434-014-4331-0]

32 **Ramalho D**, Rocha G, Oliveira JM, Oliveira MJ. Fluorine-18 Fluorocholine Positron Emission Tomography/Computed Tomography in Primary Hyperparathyroidism: A Case Report and Review of Literature. *Cureus* 2022; **14**: e21958 [PMID: 35282562 DOI: 10.7759/cureus.21958]

33 **Latge A**, Riehm S, Vix M, Bani J, Ignat M, Pretet V, Helali M, Treglia G, Imperiale A. (18)F-Fluorocholine PET and 4D-CT in Patients with Persistent and Recurrent Primary Hyperparathyroidism. *Diagnostics (Basel)* 2021; **11** [PMID: 34943620 DOI: 10.3390/diagnostics11122384]

34 **Christakis I**, Khan S, Sadler GP, Gleeson FV, Bradley KM, Mihai R. (18)Fluorocholine PET/CT scanning with arterial phase-enhanced CT is useful for persistent/recurrent primary hyperparathyroidism: first UK case series results. *Ann R Coll Surg Engl* 2019; **101**: 501-507 [PMID: 31305126 DOI: 10.1308/rcsann.2019.0059]

35 **Kawai Y**, Iima M, Yamamoto H, Kawai M, Kishimoto AO, Koyasu S, Yamamoto A, Omori K, Kishimoto Y. The added value of non-contrast 3-Tesla MRI for the pre-operative localization of hyperparathyroidism. *Braz J Otorhinolaryngol* 2022; **88** Suppl 4: S58-S64 [PMID: 34716111 DOI: 10.1016/j.bjorl.2021.07.010]

36 **Dombrowsky A**, Weiss D, Bushman N, Chen H, Balentine CJ. Can imaging studies be omitted in patients with sporadic primary hyperparathyroidism? *J Surg Res* 2018; **231**: 257-262 [PMID: 30278938 DOI: 10.1016/j.jss.2018.05.046]

37 **Tang AL**, Aunins B, Chang K, Wang JC, Hagen M, Jiang L, Lee CY, Randle RW, Houlton JJ, Sloan D, Steward DL. A multi-institutional study evaluating and describing atypical parathyroid tumors discovered after parathyroidectomy. *Laryngoscope Investig Otolaryngol* 2022; **7**: 901-905 [PMID: 35734061 DOI: 10.1002/lio2.814]

38 **Saponaro F**, Pardi E, Mazoni L, Borsari S, Torregrossa L, Apicella M, Frustaci G, Materazzi G, Miccoli P, Basolo F, Marcocci C, Cetani F. Do Patients With Atypical Parathyroid Adenoma Need Close Follow-up? *J Clin Endocrinol Metab* 2021; **106**: e4565-e4579 [PMID: 34157106 DOI: 10.1210/clinem/dgab452]

39 **Ying W**, Zhen-Long Z, Xiao-Jing C, Li-Li P, Yan L, Ming-An Y. A study on the causes of operative failures after microwave ablation for primary hyperparathyroidism. *Eur Radiol* 2021; **31**: 6522-6530 [PMID: 33651201 DOI: 10.1007/s00330-021-07761-9]

40 **Gawrychowska A**, Kowalski G, Nabrdalik M, Bu³a G, Lackowska B, Bednarczyk A, Werbowski M, Polczyk J, Gawrychowski J. Flow cytometric DNA analysis of parathyroid benign lesions. *Endokrynol Pol* 2021; **72**: 44-50 [PMID: 33125694 DOI: 10.5603/EP.a2020.0076]

41 **Gorbacheva AM**, Eremkina AK, Mokrysheva NG. [Hereditary syndromal and nonsyndromal forms of primary hyperparathyroidism]. *Probl Endokrinol (Mosk)* 2020; **66**: 23-34 [PMID: 33351310 DOI: 10.14341/probl10357]

42 **Tao X**, Xu T, Lin X, Xu S, Fan Y, Guo B, Deng X, Jiao Q, Chen L, Wei Z, Chen C, Yang W, Zhang Z, Yu X, Yue H. Genomic profiling reveals the variant landscape of sporadic parathyroid adenomas in Chinese population. *J Clin Endocrinol Metab* 2023 [PMID: 36611251 DOI: 10.1210/clinem/dgad002]

43 **Mazarico-Altisent I**, Capel I, Baena N, Bella-Cueto MR, Barcons S, Guirao X, Albert L, Cano A, Pareja R, Caixῶs A, Rigla M. Novel germline variants of CDKN1B and CDKN2C identified during screening for familial primary hyperparathyroidism. *J Endocrinol Invest* 2022 [PMID: 36334246 DOI: 10.1007/s40618-022-01948-7]

44 **McCoy KL**, Yip L, Dhir M, Langenborg K, Seethala RR, Carty SE. Histologic hypercellularity in a biopsied normal parathyroid gland does not correlate with hyperfunction in primary hyperparathyroidism. *Surgery* 2021; **169**: 524-527 [PMID: 32807505 DOI: 10.1016/j.surg.2020.06.039]

45 **Krupinova JA**, Elfimova AR, Rebrova OY, Voronkova IA, Eremkina AK, Kovaleva EV, Maganeva IS, Gorbacheva AM, Bibik EE, Deviatkin AA, Melnichenko GA, Mokrysheva NG. Mathematical model for preoperative differential diagnosis for the parathyroid neoplasms. *J Pathol Inform* 2022; **13**: 100134 [PMID: 36268079 DOI: 10.1016/j.jpi.2022.100134]

46 **Donatini G**, Marciniak C, Lenne X, Clıment G, Bruandet A, Sebag F, Mirallıı E, Mathonnet M, Brunaud L, Lifante JC, Tresallet C, Mınıgaux F, Theis D, Pattou F, Caiazzo R; on the behalf of AFCE Study Group. Risk Factors of Redo Surgery After Unilateral Focused Parathyroidectomy: Conclusions From a Comprehensive Nationwide Database of 13,247 Interventions Over 6 Years. *Ann Surg* 2020; **272**: 801-806 [PMID: 32833757 DOI: 10.1097/SLA.0000000000004269]

47 **Shirali AS**, Wu SY, Chiang YJ, Graham PH, Grubbs EG, Lee JE, Perrier ND, Fisher SB. Recurrence after successful parathyroidectomy-Who should we worry about? *Surgery* 2022; **171**: 40-46 [PMID: 34340820 DOI: 10.1016/j.surg.2021.06.035]

48 **Jinih M**, O'Connell E, O'Leary DP, Liew A, Redmond HP. Focused Versus Bilateral Parathyroid Exploration for Primary Hyperparathyroidism: A Systematic Review and Meta-analysis. *Ann Surg Oncol* 2017; **24**: 1924-1934 [PMID: 27896505 DOI: 10.1245/s10434-016-5694-1]

49 **Norlın O**, Wang KC, Tay YK, Johnson WR, Grodski S, Yeung M, Serpell J, Sidhu S, Sywak M, Delbridge L. No need to abandon focused parathyroidectomy: a multicenter study of long-term outcome after surgery for primary hyperparathyroidism. *Ann Surg* 2015; **261**: 991-996 [PMID: 25565223 DOI: 10.1097/SLA.0000000000000715]

50 **Patel N**, Mihai R. Long-term Cure of Primary Hyperparathyroidism After Scan-Directed Parathyroidectomy: Outcomes From A UK Endocrine Surgery Unit. *World J Surg* 2022; **46**: 2189-2194 [PMID: 35412058 DOI: 10.1007/s00268-022-06556-3]

51 **Lou I**, Balentine C, Clarkson S, Schneider DF, Sippel RS, Chen H. How long should we follow patients after apparently curative parathyroidectomy? *Surgery* 2017; **161**: 54-61 [PMID: 27863779 DOI: 10.1016/j.surg.2016.05.049]

52 **Singh Ospina NM**, Rodriguez-Gutierrez R, Maraka S, Espinosa de Ycaza AE, Jasim S, Castaneda-Guarderas A, Gionfriddo MR, Al Nofal A, Brito JP, Erwin P, Richards M, Wermers R, Montori VM. Outcomes of Parathyroidectomy in Patients with Primary Hyperparathyroidism: A Systematic Review and Meta-analysis. *World J Surg* 2016; **40**: 2359-2377 [PMID: 27094563 DOI: 10.1007/s00268-016-3514-1]

53 **Krawitz R**, Glover A, Koneru S, Jiang J, Di Marco A, Gill AJ, Aniss A, Sywak M, Delbridge L, Sidhu S. The Significance of Histologically "Large Normal" Parathyroid Glands in Primary Hyperparathyroidism. *World J Surg* 2020; **44**: 1149-1155 [PMID: 31773224 DOI: 10.1007/s00268-019-05302-6]

54 **Rubio-Manzanares Dorado M**, Pino-Diaz V, Padillo-Ruvz J, Martos-Martvnez JM. Prevertebral cervical approach to posterior mediastinum parathyroid adenomas. *Surg Endosc* 2022; **36**: 6319-6325 [PMID: 35608699 DOI: 10.1007/s00464-022-09279-7]

55 **Xie LD**, Wang N, Zhang JP, Wang X, Chen XP, Zhang B, Bu S. [Normocalcemic with elevated post-operative parathormone in primary hyperpara-thyroidism: 9 case reports and literature review]. *Beijing Da Xue Xue Bao Yi Xue Ban* 2021; **53**: 573-579 [PMID: 34145863 DOI: 10.19723/j.issn.1671-167X.2021.03.022]

56 **Abdel-Aziz TE**, Gleeson F, Sadler G, Mihai R. Dwarfs and Giants of Parathyroid Adenomas-No Difference in Outcome After Parathyroidectomy. *J Surg Res* 2019; **237**: 56-60 [PMID: 30694792 DOI: 10.1016/j.jss.2018.12.021]

57 **Yang PS**, Liu CL, Liu TP, Chen HH, Wu CJ, Cheng SP. Parathyroidectomy decreases neutrophil-to-lymphocyte and platelet-to-lymphocyte ratios. *J Surg Res* 2018; **224**: 169-175 [PMID: 29506836 DOI: 10.1016/j.jss.2017.12.016]

58 **Thier M**, Daudi S, Bergenfelz A, Almquist M. Predictors of multiglandular disease in primary hyperparathyroidism. *Langenbecks Arch Surg* 2018; **403**: 103-109 [PMID: 29294178 DOI: 10.1007/s00423-017-1647-9]

59 **Anamaterou C**, Lang M, Schimmack S, Rudofsky G, Bóchler MW, Schmitz-Winnenthal H. Autotransplantation of parathyroid grafts into the tibialis anterior muscle after parathyroidectomy: a novel autotransplantation site. *BMC Surg* 2015; **15**: 113 [PMID: 26467771 DOI: 10.1186/s12893-015-0098-x]

60 **Walker MD**, Shane E. Hypercalcemia: A Review. *JAMA* 2022; **328**: 1624-1636 [PMID: 36282253 DOI: 10.1001/jama.2022.18331]

61 **Wei Y**, Zhao ZL, Cao XJ, Peng LL, Li Y, Wu J, Yu MA. Microwave ablation *versus* parathyroidectomy for the treatment of primary hyperparathyroidism: a cohort study. *Eur Radiol* 2022; **32**: 5821-5830 [PMID: 35381852 DOI: 10.1007/s00330-022-08759-7]

62 **Peng CZ**, Chai HH, Zhang ZX, Hu QH, Zeng Z, Cui AL, Pang HS, Ruan LT. Radiofrequency ablation for primary hyperparathyroidism and risk factors for postablative eucalcemic parathyroid hormone elevation. *Int J Hyperthermia* 2022; **39**: 490-496 [PMID: 35285391 DOI: 10.1080/02656736.2022.2047231]

63 **Wang TS**, Pasieka JL, Carty SE. Techniques of parathyroid exploration at North American endocrine surgery fellowship programs: what the next generation is being taught. *Am J Surg* 2014; **207**: 527-532 [PMID: 24495320 DOI: 10.1016/j.amjsurg.2013.05.012]

64 **Irvin GL 3rd**, Carneiro DM, Solorzano CC. Progress in the operative management of sporadic primary hyperparathyroidism over 34 years. *Ann Surg* 2004; **239**: 704-8; discussion 708 [PMID: 15082975 DOI: 10.1097/01.sla.0000124448.49794.74]

65 **Claflin J**, Dhir A, Espinosa NM, Antunez AG, Cohen MS, Gauger PG, Miller BS, Hughes DT. Intraoperative parathyroid hormone levels ≤40 pg/mL are associated with the lowest persistence rates after parathyroidectomy for primary hyperparathyroidism. *Surgery* 2019; **166**: 50-54 [PMID: 30975497 DOI: 10.1016/j.surg.2019.01.024]

66 **Prescott JD**, Udelsman R. Remedial operation for primary hyperparathyroidism. *World J Surg* 2009; **33**: 2324-2334 [PMID: 19290572 DOI: 10.1007/s00268-009-9962-0]

67 **Medas F**, Cappellacci F, Canu GL, Noordzij JP, Erdas E, Calç PG. The role of Rapid Intraoperative Parathyroid Hormone (ioPTH) assay in determining outcome of parathyroidectomy in primary hyperparathyroidism: A systematic review and meta-analysis. *Int J Surg* 2021; **92**: 106042 [PMID: 34339883 DOI: 10.1016/j.ijsu.2021.106042]

68 **Akgón IE**, άnló MT, Aygun N, Kostek M, Uludag M. Contribution of intraoperative parathyroid hormone monitoring to the surgical success in minimal invasive parathyroidectomy. *Front Surg* 2022; **9**: 1024350 [PMID: 36211265 DOI: 10.3389/fsurg.2022.1024350]

69 **Lerchenberger M**, Al Arabi N, Gallwas JKS, Stepp H, Hallfeldt KKJ, Ladurner R. Intraoperative Near-Infrared Autofluorescence and Indocyanine Green Imaging to Identify Parathyroid Glands: A Comparison. *Int J Endocrinol* 2019; **2019**: 4687951 [PMID: 31662746 DOI: 10.1155/2019/4687951]

70 **Liang TJ**, Wang KC, Wang NY, Chen IS, Liu SI. Indocyanine Green Angiography for Parathyroid Gland Evaluation during Transoral Endoscopic Thyroidectomy. *J Pers Med* 2021; **11** [PMID: 34575620 DOI: 10.3390/jpm11090843]

71 **Spartalis E**, Ntokos G, Georgiou K, Zografos G, Tsourouflis G, Dimitroulis D, Nikiteas NI. Intraoperative Indocyanine Green (ICG) Angiography for the Identification of the Parathyroid Glands: Current Evidence and Future Perspectives. *In Vivo* 2020; **34**: 23-32 [PMID: 31882459 DOI: 10.21873/invivo.11741]

72 **Papavramidis TS**, Anagnostis P, Chorti A, Pliakos I, Panidis S, Koutsoumparis D, Michalopoulos A. Do Near-Infrared Intra-Operative Findings Obtained Using Indocyanine Green Correlate with Post-Thyroidectomy Parathyroid Function? *Endocr Pract* 2020; **26**: 967-973 [PMID: 33471701 DOI: 10.4158/EP-2020-0119]

73 **Aygón N**, Uludaπ M. Intraoperative Adjunct Methods for Localization in Primary Hyperparathyroidism. *Sisli Etfal Hastan Tip Bul* 2019; **53**: 84-95 [PMID: 32377064 DOI: 10.14744/SEMB.2019.37542]

74 **Huang K**, Luo D, Huang M, Long M, Peng X, Li H. Protection of parathyroid function using carbon nanoparticles during

thyroid surgery. *Otolaryngol Head Neck Surg* 2013; **149**: 845-850 [PMID: 24163324 DOI: 10.1177/0194599813509779]

75 **Bononi M**, Viviana F, De Feo MS, Sollaku S, Pani A, Falconi R, Pani R, Cavallaro G, Brozzetti S, De Vincentis G. Gonioprobe, an Innovative Gamma-probe to Guide Parathyroid Radioguided Surgery: First Clinical Experiences with Navigator and Lock-ontarget Functions. *Curr Radiopharm* 2021; **14**: 161-169 [PMID: 32693772 DOI: 10.2174/1874471013666200721013903]

76 **Ghani U**, Assad S. Role of Intraoperative Nerve Monitoring During Parathyroidectomy to Prevent Recurrent Laryngeal Nerve Injury. *Cureus* 2016; **8**: e880 [PMID: 28003944 DOI: 10.7759/cureus.880]

77 **Zhu Y**, Gao DS, Lin J, Wang Y, Yu L. Intraoperative Neuromonitoring in Thyroid and Parathyroid Surgery. *J Laparoendosc Adv Surg Tech A* 2021; **31**: 18-23 [PMID: 32614658 DOI: 10.1089/lap.2020.0293]

78 **Aiti A**, Rossi M, Alviano F, Morara B, Burgio L, Cioccoloni E, Cavicchi O, Pasquinelli G, Bonsi L, Buzzi M. Parathyroid Tissue Cryopreservation: Does the Storage Time Affect Viability and Functionality? *Biopreserv Biobank* 2019; **17**: 418-424 [PMID: 31025874 DOI: 10.1089/bio.2018.0140]

World Journal of Clinical Cases

Submit a Manuscript: https://www.f6publishing.com

World J Clin Cases 2023 April 6; 11(10): 2226-2236

DOI: 10.12998/wjcc.v11.i10.2226

ISSN 2307-8960 (online)

ORIGINAL ARTICLE

Retrospective Study

Hepatobiliary system and intestinal injury in new coronavirus infection (COVID-19): A retrospective study

Konstantin V Kozlov, Konstantin V Zhdanov, Anna K Ratnikova, Vyacheslav A Ratnikov, Artem V Tishkov, Vladimir Grinevich, Yuriy A Kravchuk, Panteley I Miklush, Polina O Nikiforova, Vera V Gordienko, Alexander F Popov, Boris G Andryukov

Specialty type: Medicine, research and experimental

Provenance and peer review: Unsolicited article; Externally peer reviewed.

Peer-review model: Single blind

Peer-review report's scientific quality classification

Grade A (Excellent): 0
Grade B (Very good): B
Grade C (Good): 0
Grade D (Fair): D
Grade E (Poor): 0

P-Reviewer: Tenreiro N, Portugal; Wani I, India

Received: September 29, 2022
Peer-review started: September 29, 2022
First decision: January 3, 2023
Revised: January 22, 2023
Accepted: March 6, 2023
Article in press: March 6, 2023
Published online: April 6, 2023

Konstantin V Kozlov, Konstantin V Zhdanov, Yuriy A Kravchuk, Panteley I Miklush, Polina O Nikiforova, Vera V Gordienko, Department of Infectious Disease, Military Medical Academy Named After SM. Kirov, Saint-Petersburg 194044, Russia

Anna K Ratnikova, Department of Admission, Federal State Budgetary Institution "North-West District Scientific and Clinical Center Named After LG. Sokolov Federal Medical and Biological Agency", Saint-Petersburg 194291, Russia

Vyacheslav A Ratnikov, Department of Roentgenology, Federal State Budgetary Institution "North-West District Scientific and Clinical Center Named After LG. Sokolov Federal Medical and Biological Agency", Saint-Petersburg 194291, Russia

Artem V Tishkov, Department of Physics, Mathematics and Informatics, FSBEI HE IP. Pavlov SPbSMU MOH Russia, Saint-Petersburg 197022, Russia

Vladimir Grinevich, 2nd Department of Therapy (Advanced Medical Education), Military Medical Academy Named After SM. Kirov, Saint-Petersburg 194044, Russia

Alexander F Popov, Boris G Andryukov, School of Medicine, Far Eastern Federal University, Vladivostok 690922, Russia

Corresponding author: Vera V Gordienko, MD, Doctor, Teacher, Department of Infectious Disease, Military Medical Academy named after S.M. Kirov, No. 6 Lebedeva Street, Saint-Petersburg 194044, Russia. ivanovavmeda@gmail.com

Abstract

BACKGROUND

An important area of effective control of the coronavirus disease 19 (COVID-19) pandemic is the study of the pathogenic features of severe acute respiratory syndrome coronavirus 2 infection, including those based on assessing the state of the intestinal microbiota and permeability.

AIM

To study the clinical features of the new COVID-19 in patients with mild and moderate severity at the stage of hospitalization, to determine the role of hepato-biliary injury, intestinal permeability disorders, and changes in the qualitative and

quantitative composition of the microbiota in the development of systemic inflammation in patients with COVID-19.

METHODS

The study was performed in 80 patients with COVID-19, with an average age of 45 years, 19 of whom had mild disease, and 61 had moderate disease severity. The scope of the examination included traditional clinical, laboratory, biochemical, instrumental, and radiation studies, as well as original methods for studying microbiota and intestinal permeability.

RESULTS

The clinical course of COVID-19 was studied, and the clinical and biochemical features, manifestations of systemic inflammation, and intestinal microbiome changes in patients with mild and moderate severity were identified. Intestinal permeability characteristics against the background of COVID-19 were evaluated by measuring levels of proinflammatory cytokines, insulin, faecal calprotectin, and zonulin.

CONCLUSION

This study highlights the role of intestinal permeability and microbiota as the main drivers of gastroenterological manifestations and increased COVID-19 severity.

Key Words: Novel coronavirus infection; COVID-19; SARS-CoV-2; Zonulin; Faecal calprotectin; Microbiota

Core Tip: The clinical course of coronavirus disease 19 (COVID-19) was studied, and the clinical and biochemical features, manifestations of systemic inflammation, and intestinal microbiome changes in patients with mild and moderate severity were identified. Intestinal permeability characteristics against the background of COVID-19 were evaluated by measuring levels of proinflammatory cytokines, insulin, faecal calprotectin, and zonulin. This study highlights the role of intestinal permeability and microbiota as the main drivers of gastroenterological manifestations and increased COVID-19 severity.

Citation: Kozlov KV, Zhdanov KV, Ratnikova AK, Ratnikov VA, Tishkov AV, Grinevich V, Kravchuk YA, Miklush PI, Nikiforova PO, Gordienko VV, Popov AF, Andryukov BG. Hepatobiliary system and intestinal injury in new coronavirus infection (COVID-19): A retrospective study. *World J Clin Cases* 2023; 11(10): 2226-2236
URL: https://www.wjgnet.com/2307-8960/full/v11/i10/2226.htm
DOI: https://dx.doi.org/10.12998/wjcc.v11.i10.2226

INTRODUCTION

While gaining experience in the diagnosis and treatment of the new coronavirus disease (COVID-19), an increasing number of researchers are focusing on the extremely high prevalence of extrapulmonary symptoms, including gastroenterological manifestations in patients with COVID-19[1]. The frequency of gastrointestinal (GI) symptoms in patients with COVID-19 is variable and depends on the severity of the disease and, probably, the viral strain that causes the disease[2]. The severe form of COVID-19, as a rule, is associated with polysegmental lung damage and liver injury and a steep increase in the intestinal epithelium's permeability with the subsequent transfer of bacterial and fungal products into the blood and the development of systemic inflammation. Bidirectional communication impairment in the intestinal-lung axis is considered a risk factor for the development of severe respiratory disease. It follows the principle of positive feedback and develops due to dysbiotic changes in the intestinal microbiota on the one hand and cytokine storm on the other[3,4].

Zonulin is a modulator and serum marker of intestinal permeability, which, when connected to the receptors of intercellular tight junctions, causes contraction of the cytoskeleton of epithelial cells and, therefore, facilitates the transport of macromolecules[5-7]. High serum zonulin levels have been associated with severe COVID-19 in several studies[7]. Thus, one of the possible therapeutic goals in treating severe COVID-19 may be to prevent the pathological increase in zonulin-mediated intestinal permeability[8,9]. The combination of low-grade endotoxemia (an increase in the concentration of lipopolysaccharide secreted by the microbiota) with an increased level of zonulin may indicate an increase in intestinal permeability, which is one of the mechanisms underlying the pathogenesis of COVID-19 and its gastroenterological manifestations[10]. It is also known that intestinal dysfunction

and microbial translocation strongly correlate with increased systemic inflammation and complement activation decreased metabolic function of the intestine, and higher mortality rate[11].

According to research data dedicated to the study of cytokine levels in patients with severe and sometimes fatal forms of COVID-19, it was found that plasma concentrations of interleukin (IL) -1-beta, 6, 7, 8, 9, and 10, and tumor necrosis factor-alpha (TNF-α) were increased[12].

The intestinal microbiome of patients with COVID-19 is characterized by the enrichment of opportunistic microorganisms and depletion of normal intestinal microflora with immunomodulatory potential, such as Faecalibacterium prausnitzii, Eubacterium rectale, and bifidobacteria[13]. At the same time, the disturbed composition of the microbiota correlated with the severity of the disease, corresponding to increased concentrations of inflammatory cytokines and markers of inflammation in the blood (including C-reactive protein and lactate dehydrogenase), which was most likely due to the modulation of the immune response[14].

MATERIALS AND METHODS

The study was carried out at the North-Western District Scientific and Clinical Center named after LG Sokolov FMBA of Russia (SZONKTS named after LG Sokolov) between July 2020 to March 2021. It included 80 hospitalized patients with COVID-19, whose median age was 45 years (range: 39–56 years). All patients provided informed consent to participate in the study; 19 (23.8%) of them had mild, and 61 (76.2%) had moderate severity of COVID-19. The diagnosis of the disease in all the patients was verified by detecting severe acute respiratory syndrome-related etoronavirus 2(SARS-CoV-2) RNA using nucleic acid amplification. Patients were hospitalized on the 7th day of illness (range: 5.0–9.0), which corresponded to the peak period of the infectious process. As a control, a group of 17 healthy individuals, with an average age of 41 years (range: 22.0–59.5 years), who underwent examination at the outpatient dispensary of SZONKTS (named after LG Sokolov), were included. The patient groups did not differ in terms of their demographic and clinical characteristics. The study did not include patients with chronic viral hepatitis (B and C), anemia of any etiology, or patients whose treatment required transfer to the intensive care unit.

On admission, all patients with COVID-19 underwent standard examination and treatment protocol, and the severity of the disease was determined in accordance with the current versions of the Temporary Guidelines of the Ministry of Health of the Russian Federation on the prevention, diagnosis, and treatment of new coronavirus infections[15]. Computed tomography (CT) of the chest was supplemented with post-processing and assessment of qualitative and quantitative criteria for defining the state of the parenchymal and hollow organs of the GI tract, which were visualized during the chest CT scan, was done.

To assess the complaints related to the GI tract, a questionnaire was developed that included a detailed assessment of abdominal pain syndrome according to a visual analogue scale, an assessment of the presence of symptoms of dyspepsia, and the presence and duration of concomitant gastroenterological pathology. All patients completed the questionnaire based on the main questionnaire and 36-Item Short Form Survey quality of life questionnaire.

To assess the state of the intestinal barrier, qualitatively and quantitatively assess the state of the microbiota and hepatobiliary system, as well as evaluate systemic inflammation indicators that develop during COVID-19, the scope of the survey was supplemented with an analysis of a biomarker complex: Alanine aminotransferase (ALT), aspartate aminotransferase (AST), total bilirubin, zonulin in feces and blood, and calprotectin in feces. TNF and IL1-beta, 6, 8, 10, and insulin levels were also examined in the blood. To assess insulin resistance, the homeostasis model assessment of insulin resistance (HOMA-IR) index was used. The index was calculated using the formula: HOMA-IR = fasting insulin (μU/mL) × fasting glucose (mmol/L)/22.5. Indirect determination of the composition of the intestinal microbiota was performed using an Agilent 7890 gas chromatograph with mass selective and flame ionization detectors (Agilent Technologies, United State of America). The proposed method of gas chromatography combined with mass spectrometry makes it possible to detect in blood and then, to the contents of the intestine, extrapolate components of cells of a wide range of microorganisms of normal and pathogenic human microbiota.

Blood and stool samples were collected on day 8 (range: 5–11.5 d) of the COVID-19 illness. The healthy individuals in the control group underwent similar examinations.

The entire spectrum of the obtained data was transformed into an information base, represented by 720 parameters for assessing the condition of each patient, adapted for subsequent mathematical and statistical processing. The statistical analysis was carried out using the IBM SPSS 20.0 program using parametric and nonparametric statistical methods. Descriptive statistics for the samples that fit the normal distribution are represented by the arithmetic mean and standard deviation. Descriptive statistics for non-Gaussian distributions included the median and upper bounds for the 1st and 3rd quartiles. The differences between the two numerical samples were determined using Student's t-test in the case of a normal distribution and the Mann-Whitney test in the case of a non-Gaussian distribution. To compare related samples, the paired Student's t-test was used if the samples were normally

distributed, and the Wilcoxon test was used for non-Gaussian samples. The normality of the samples was checked using the Kolmogorov-Smirnov test with Lilliefors correction.

Descriptive statistics for non-numeric data are represented by the number of objects with corresponding values as well as the proportion (percentage) of representation of each value in the sample. To find differences in the counting data, Fisher's exact test and Pearson's χ^2 test were used.

In all cases of hypothesis testing, the critical significance level was considered to be equal to or less than 0.05.

RESULTS

Patients with mild COVID-19 showed no evidence of lung damage on CT in addition to the clinical, virological, and clinical laboratory manifestations of the disease; however, all of these patients exhibited symptoms of mild general infectious intoxication (low-grade fever in 13 (68.4%) patients), anosmia was detected in 6 (31.6%) patients and hyposmia in 1 (6%) patient. With an average disease severity, the most frequent clinical manifestation of COVID-19 was low-grade fever, which was observed in 57 (93.4%) patients; anosmia was observed in 29 (48%) patients and hyposmia in 6 (9.8%) patients. A respiratory rate of > 22 *per* minute, shortness of breath during physical exertion, a decrease in hemoglobin oxygen saturation to 95% -93%, and characteristic signs of viral lung damage on CT involving more than 25% of lung tissue were observed in 49 (80%) patients.

Abdominal CT analysis showed localized or diffuse low liver density (signs of steatosis) and adipose tissue accumulation around the gallbladder.

According to survey data, the frequency and severity of most GI symptoms during the peak of the infectious process caused by SARS-CoV-2 did not vary with disease severity. Dyspeptic syndrome was found in 67 (83.8%) patients with mild to moderate severity, with flatulence and stool instability being the most common (51.25%, 41 patients). A decreased appetite was observed in 41 patients (51.25%). Abdominal pain syndrome was detected in 36 (45%) patients. However, patients with COVID-19 do not typically experience localized pain. The most distinctive pains were in the epigastrium: 6.0 points (4.5-6.5), in the lower abdomen: 6.0 points (5.0-7.0) and night pains: 5.5 points (3.0-7.0). At the same time, the duration of the manifestations of dyspepsia in patients with moderate severity was significantly longer: 15.0 d (range: 10.5–21.0 d) than that in patients with mild severity: 13.5 d (range: 9.0-15.0 d, $P = 0.041$). The study of the anamnesis of the disease showed that patients with moderate severity at the pre-hospital stage more often took azithromycin ($P = 0.003$) and non-steroidal anti-inflammatory drugs ($P = 0.004$) than patients with mild severity, which could have also contributed to the appearance of GI symptoms.

As shown in Table 1, Compared with control group, patients with COVID-19 had increased level of ALT (35; 43.7%), AST (45; 56.2%) and total bilirubin (32; 39.4%).

As shown in Table 2, after first CT, the lower of liver density < 45 hounsfield unit (HU) was noted in 28 (34.7%). Patients with moderate severity had significantly lower liver density 42.6 HU (39.2-47.8), compare with patients with mild COVID-19 48.5 HU (43.7-52.1) ($P < 0.05$). The liver/spleen density ratio was also lower in moderate severity group, 0.87 (0.69-0.98) and 1.02 (0.92-1.09) ($P < 0.05$) suggest.

One of the most characteristic changes in patients with mild and moderate COVID-19 compared with the control group was a statistically significant increase in insulin content up to 19.10 mIU/L (8.90-34.575) [(control group: 6.90 mIU/L (4.325-15.4)], $P = 0.0026$, as well as an insignificant trend towards an increase in the insulin resistance index to 1.70 (1.08-2.97), $P = 0.88$. At the same time, in patients with COVID-19 with moderate severity, the level of insulin was 1.8 times higher than in patients with mild severity of the disease ($P = 0.0026$). The analysis of indicators of systemic inflammation in patients with COVID-19 on the first day of hospitalization showed that the average level of TNF, as well as IL 1-beta, 6, 8, and 10, did not differ statistically significantly from those in the control group. However, upon further study, it was found that by the 7th day of hospitalization with moderate severity of COVID-19, the TNF content was significantly higher: 1.00 pg/mL (range: 1.00–3.00 pg/mL), IL6: 13.0 (range: 1.0-18.0, $P < 0.001$)- and there was also a tendency for an increase in the content of IL 1-beta, 8, and 10.

A set of indicators reflecting intestinal permeability and inflammatory activity in patients with mild to moderate COVID-19 compared to the control group at the initial examination is presented in Table 3.

As shown in Table 3, the faecal calprotectin content in the control group and patients with COVID-19 did not differ significantly. The concentration of zonulin in the feces of patients with COVID-19 was significantly higher than that in the control group ($P = 0.003$). Simultaneously, the zonulin content in the blood of patients with COVID-19 was lower than that in the control group ($P = 0.046$).

In the next stage of the study, the levels of these indicators were assessed depending on the severity of the infection caused by SARS-CoV-2.

As shown in Table 3, with an average severity of COVID-19, a statistically significant increase in faecal calprotectin content was observed, as well as a tendency toward an increase in zonulin content in the feces.

In accordance with the purpose of this study, a comparative analysis of some indicators characterizing the qualitative and quantitative composition of the intestinal microbiota and the functional state

Table 1 Changes of alanine aminotransferase, aspartate aminotransferase and serum bilirubin in patients with coronavirus disease 19 compared with the control group, depending on the severity of the disease

Indication	COVID-19 patients (*n* = 80)	Control Group (*n* = 17)	*P* value	COVID-19-patients, mild severity (*n* = 19)	COVID-19-patients, moderate severity (*n* = 61)	*P* value
ALT, IU/L	75 (21-96)	21 (5-30)	< 0.05	57 (16-65)	89 (79-96)	< 0.05
AST, IU/L	81 (26-112)	26 (8-35)	< 0.05	60 (20-69)	102 (90;112)	< 0.05
Total bilirubin, μmol /L	63.2 (13.8-70.2)	22.1 (5.4-25.3)	< 0.05	41.3 (22.8-62.1)	72.4 (35.2-89.2)	< 0.05

Compared with control group, patients with COVID-19 had increased level of ALT (35; 43.7%), AST (45; 56.2%) and total bilirubin (32; 39.4%). COVID-19: Coronavirus disease 19; AST: Aspartate aminotransferase; ALT: Alanine aminotransferase.

Table 2 Changes of liver/spleen density in patients with coronavirus disease 19, depending on the severity of the disease

Indication	Density, HU		*P* value
	COVID-19 patients, mild severity (*n* = 19)	COVID-19 patients, moderate severity (*n* = 61)	
Liver	48.52 (43.7-52.1)	42.63 (39.2-47.8)	< 0.05
Spleen	47.41 (42.1-51.5)	48.78 (43.4-52.8)	0.47
Liver/spleen ratio	1.02 (0.92-1.09)	0.87 (0.69-0.98)	< 0.05

After first CT, the lower of liver density < 45 HU was noted in 28 (34.7%). Patients with moderate severity had significantly lower liver density 42.6 HU (39.2-47.8), compare with patients with mild COVID-19 48.5 HU (43.7-52.1) ($P < 0.05$). The liver/spleen density ratio was also lower in moderate severity group, 0.87 (0.69-0.98) and 1.02 (0.92-1.09) ($P < 0.05$) suggest. COVID-19: Coronavirus disease 19; HU: Hounsfield unit; CT: Computed tomography.

Table 3 Factors characterizing intestinal permeability in patients with coronavirus disease 19 compared with the control group, depending on the severity of the disease Me (UQ; LQ)

Indication	COVID-19 patients (*n* = 80)	Control Group (*n* = 17)	*P* value	COVID-19 patients, mild severity (*n* = 19)	COVID-19 patients, moderate severity (*n* = 61)	*P* value
Fecal calprotectin (mg/g)	87.5 (53.525-227.75)	109.65 (23.275-213.75)	0.97	53.1 (21.0-153.0)	105.0 (58.2-236.0)	0.018
Zonulin, feces (ng/mL)	141 (110-180)	64.4 (32.1-74.8)	0.003	134.9 (78.8-167.5)	143 (119-155.9)	0.74
Zonulin, blood (ng/mL)	67.9 (20.3-77.8)	85.7 (23.0-98.1)	0.039	67.9 (20.3-76.1)	71.1 (20.0-81.7)	0.55

The content of fecal calprotectin in the control group and in patients with COVID-19 did not differ statistically significantly. At the same time, the concentration of zonulin in feces in patients with COVID-19 was statistically significantly higher than in the control group ($P = 0.003$). At the same time, the content of zonulin in the blood in patients with COVID-19 was lower than in the control group ($P = 0.046$). COVID-19: Coronavirus disease 19.

of the intestine in patients with COVID-19 was carried out (Table 4).

As shown in Table 4, Propionibacterium/Cl. Subterminale, content of fungi, and lactobacilli ratios significantly changed among patients with mild and moderately severe COVID-19 compared with the control group. It is extremely important to note a significant (more than three times) and statistically significant ($P = 0.0000779$) increase in the endotoxin content. At the same time, the endotoxin content in the feces of patients with mild to moderate severity of the new coronavirus infection did not differ significantly.

To study the interdependence of the indicators of the intestinal microbiota and the most commonly used indicators in clinical and biochemical studies, a correlation matrix was built (Figure 1).

Table 4 Intestinal microbiota indications in coronavirus disease 19 patients compared with the control group Me (UQ; LQ)

Symptom	Patients with COVID-19 (*n* = 80)	Control group (*n* = 17)	*P* value
Eubacterium/Cl. Coccoides, amt. × 10^5/r	6849 (3380-7987)	8211 (2996-10987)	0.17
Herpes, amt. × 10^5/r	0.00 (0.00-1808.25)	3610 (1914-5316)	0.001
Propionibacterium/Cl. Subterminale, amt. × 10^5/r	2706 (1614-3476)	1992 (704-2118)	0.0016
Bifidobacteria, amt. × 10^5/r	3768 (2000-4678)	4614 (1653-6123)	0.13
Fungus, amt. × 10^5/r	1200 (423-1851)	540 (384-774)	0.0406
Lactobacillus, amt. × 10^5/r	7488 (4221-8790)	4309 (2521-5198)	0.0016
The ratio of anaerobic to aerobic flora	1.801 (0.718-3.01)	1.983 (0.637-3.09)	0.39
The ratio of beneficial flora to opportunistic	1.009 (0.359-2.110)	0.992 (0.300-1.990)	0.86
Beneficial flora, amt. × 10^5/r	20953 (5508-36018)	19126 (3930-35764)	0.18
Sum, amt. × 10^5/r	44651 (8152-97098)	42566 (6297-89016)	0.33
Large intestine (anaerobes), amt. × 10^5/r	26171 (7088-44099)	24964 (4423-43871)	0.44
Small intestine (aerobes), amt. × 10^5/r	15944 (4620-19087)	13570 (3692-20114)	0.06
Opportunistic flora, amt. × 10^5/r	21927 (5493-25900)	19849 (3690-23983)	0.11
Cytomegalovirus, amt. × 10^5/r	0.00 (0.00-40.00)	0.00 (0.00-0.00)	0.12
Endotoxin (sum), amt. × 10^5/r	2.44 (1.21-6.11)	0.689 (0.490-1.11)	0.0000779

Propionibacterium /Cl. Subterminale, content of fungi, lactobacill ratios significantly changed among mild and moderate COVID-19 patients compared with the control group. It is extremely important to note a significant (more than 3 times) and statistically significant (P = 0.0000779) increase in endotoxin content. At the same time, the content of endotoxin in feces in patients with mild to moderate severity of new coronavirus infection did not differ significantly. COVID-19: Coronavirus disease 19.

DISCUSSION

According to the study results, it was found that the majority of GI symptoms during the peak of the infectious process did not differ depending on the severity of the infection caused by SARS-CoV-2. The data obtained regarding the symptoms of GI tract damage among patients with COVID-19 are generally consistent with the results of previous studies, which confirms the relevance of improving approaches to the early diagnosis of gastroenterological manifestations of the disease, identifying the pathogenetic mechanisms of their development, and finding effective treatment[16,17].

In the course of this work, new data were also obtained that supplement the opinion of several researchers regarding the duration of manifestations of dyspepsia during the inpatient treatment of patients with COVID-19. Therefore, among patients with moderate severity, dyspepsia lasted significantly longer than in those with mild severity, which could be linked, among other things, to the administration of nonsteroidal anti-inflammatory drugs and antibiotics at the pre-hospital stage.

One of the most characteristic changes in patients with COVID-19 of mild and moderate severity compared with the control group was a statistically significant increase in liver aminotransferases, bilirubin, and insulin levels, as well as a trend towards an increase in the insulin resistance index. At the same time, it is important to note that in patients with COVID-19 with moderate severity, the insulin level was 1.8 times higher than that in patients with mild disease severity. The data obtained can provide evidence for the need to monitor insulin resistance during treatment.

According to many authors, indicators of systemic inflammation play a fundamental role in patients with COVID-19. Several studies have shown that the severity of COVID-19 positively correlates with the level of inflammatory cytokines, and in patients with severe disease, there is also a significant decrease in the number of lymphocytes[18,19]. However, data pertaining to patients with mild to moderate COVID-19, especially during hospitalization, is limited. In this regard, the obtained data seem important, as they complement the clinical picture of SARS-CoV-2 infection.

In the professional literature, there is an active discussion of the role of the functional intestinal-lung axis as a bidirectional communication network. Many respiratory infections are often accompanied by symptoms of GI tract pathology or intestinal dysfunction[20]. It is also known that acute lung injury disrupts the microbiota of the respiratory tract, causing transient translocation of bacteria into the bloodstream and increased bacterial load in the caecum. In addition, normal microbiota maintains tolerogenic immunomodulatory effects in the intestine and protects against systemic inflammatory diseases[21]. Moreover, among several scientists, there is an opinion that the state of the intestinal

	msEuClCocc	msHerpes	msPropClSubterm	msBifido	msMyco	msLacto	msAnaeroAero	msUsefulPatho	msUseful	msSum	msAnaero	msAero	msPatho	msCytomeg	msEndotox
glu1	0.109	-0.011	-0.124	0.057	-0.140	0.054	-0.029	-0.111	0.101	0.193	0.144	0.178	0.238	-0.155	-0.099
alt1	0.066	0.064	0.036	0.013	-0.087	0.042	-0.040	0.083	0.051	0.016	0.004	0.027	-0.012	-0.069	-0.260
ast1	-0.026	-0.012	-0.012	0.090	-0.092	0.105	-0.058	0.058	0.057	-0.009	-0.020	0.105	0.000	-0.110	-0.187
dercf1	-0.177	-0.108	-0.049	-0.025	0.068	0.030	-0.022	-0.151	-0.112	-0.085	-0.080	0.044	0.023	0.065	0.220
bil1	-0.041	0.060	0.121	-0.056	-0.032	-0.023	0.143	0.058	0.047	-0.005	0.075	-0.139	-0.064	0.209	0.145
bilp1	-0.102	0.093	0.054	-0.082	-0.016	0.067	0.009	0.017	0.027	-0.001	0.008	-0.011	-0.045	0.233	0.071
crea1	-0.131	0.065	0.070	0.138	-0.044	0.196	-0.073	0.176	0.145	-0.030	-0.055	0.102	-0.134	-0.055	0.149
ckdepi1	-0.071	0.184	-0.048	-0.285	-0.092	-0.168	-0.033	-0.159	-0.261	-0.220	-0.207	-0.130	-0.127	0.037	-0.233
urea1	0.055	-0.059	0.120	0.094	0.082	0.060	0.167	0.157	0.135	0.042	0.088	-0.057	-0.072	0.111	0.129
crp1	0.131	-0.060	-0.058	0.033	-0.045	0.135	0.000	0.089	0.180	0.185	0.142	0.132	0.128	-0.146	0.015
fer1	-0.027	-0.126	0.070	0.048	0.055	0.176	-0.053	-0.021	0.126	0.161	0.106	0.178	0.164	0.135	0.070
ldg1	-0.042	0.027	0.006	0.003	-0.153	0.122	-0.114	0.124	0.102	0.034	-0.016	0.136	-0.028	-0.106	-0.084
sodium1	-0.005	-0.088	0.083	-0.072	0.176	0.038	-0.020	-0.037	0.038	0.047	-0.020	0.037	0.007	-0.025	-0.145
potasium1	-0.074	-0.087	-0.047	-0.027	0.145	-0.041	-0.021	-0.033	-0.050	-0.074	-0.097	0.006	-0.073	0.168	0.071
chlor1	0.053	-0.170	0.064	-0.090	0.294	-0.090	0.139	0.070	-0.082	-0.116	-0.068	-0.229	-0.189	0.139	-0.095
hemog1	-0.017	0.169	0.054	-0.084	-0.086	0.027	-0.070	-0.157	0.048	0.141	0.088	0.239	0.189	0.061	-0.017
erythr1	0.034	0.123	0.135	0.043	-0.133	-0.052	0.044	-0.138	0.106	0.193	0.223	0.166	0.230	-0.061	0.027
hematoc1	0.065	0.056	0.099	0.051	-0.063	0.016	0.015	-0.099	0.144	0.223	0.215	0.219	0.242	-0.018	0.045
mch1	-0.118	0.050	-0.180	-0.256	0.004	0.182	-0.253	-0.010	-0.110	-0.172	-0.310	0.109	-0.149	0.146	-0.090
rdw1	0.089	0.075	-0.102	0.085	-0.018	-0.123	0.044	-0.048	-0.096	-0.002	0.012	-0.104	-0.009	-0.081	-0.162
mcv1	0.044	-0.153	-0.069	-0.123	0.090	0.127	-0.062	0.055	0.016	-0.021	-0.071	0.039	-0.026	-0.011	0.073
plt1	0.107	0.034	-0.226	-0.284	0.026	-0.021	0.003	0.105	-0.074	-0.207	-0.187	-0.145	-0.250	-0.058	-0.195
leu1	-0.026	-0.025	-0.177	-0.069	-0.143	-0.074	0.022	-0.068	-0.040	-0.085	-0.031	0.009	-0.006	-0.016	0.032
segmne1	0.034	-0.128	-0.188	0.001	-0.081	-0.099	0.091	-0.061	-0.021	-0.056	0.037	-0.045	0.035	-0.019	0.115
segmnePerc1	0.084	-0.186	-0.109	0.028	-0.002	-0.053	0.101	-0.024	0.028	0.025	0.102	-0.034	0.096	-0.092	0.119
stabne1	-0.089	0.092	-0.106	-0.075	-0.173	0.011	-0.084	-0.143	-0.186	-0.049	-0.060	0.024	0.074	-0.035	-0.099
stabnePerc1	-0.123	0.087	-0.102	0.001	-0.176	0.075	-0.129	-0.117	-0.154	-0.022	-0.066	0.073	0.072	-0.079	-0.113
eo1	0.089	0.152	-0.104	-0.170	0.063	-0.202	0.082	-0.057	-0.161	-0.176	-0.098	-0.182	-0.103	0.133	-0.107
eoPerc1	0.004	0.081	-0.009	-0.183	0.127	-0.096	0.020	-0.026	-0.119	-0.146	-0.129	-0.133	-0.112	0.180	-0.123
baso1	0.070	-0.173	0.089	0.037	0.047	-0.093	0.223	0.053	0.058	-0.103	0.092	-0.179	-0.120	-0.093	0.125
basoPerc1	0.036	-0.002	0.034	-0.180	0.064	0.015	-0.045	-0.019	-0.053	-0.117	-0.135	-0.083	-0.114	-0.024	-0.239
lym1	0.014	0.178	-0.088	0.008	-0.039	-0.084	0.021	-0.010	-0.015	-0.082	-0.067	-0.048	-0.129	0.018	-0.036
lymPerc1	-0.034	0.200	0.074	0.008	0.125	-0.019	-0.048	-0.003	-0.022	-0.002	-0.074	0.000	-0.084	0.093	-0.093
mono1	0.109	0.101	-0.032	-0.046	-0.219	-0.069	0.069	0.068	-0.027	-0.140	-0.021	-0.122	-0.138	0.025	-0.121
monoPerc1	0.013	0.053	0.097	-0.014	-0.090	0.090	-0.068	0.141	0.006	-0.074	-0.089	-0.014	-0.133	0.061	-0.087
soe1	0.130	-0.018	-0.152	0.171	-0.068	0.081	0.076	0.099	0.140	0.152	0.154	0.017	0.097	-0.112	-0.029
aptt1	-0.052	0.052	-0.106	-0.160	-0.074	0.146	-0.193	-0.013	-0.057	-0.091	-0.196	0.136	-0.035	-0.109	-0.218
protro1	-0.034	0.037	-0.167	-0.049	0.117	-0.062	-0.138	-0.134	-0.090	0.045	-0.097	0.096	0.120	-0.073	-0.274
inr1	-0.038	0.034	0.133	0.079	-0.088	0.164	0.029	0.081	0.141	0.023	0.061	0.066	-0.037	0.105	0.229
fibr1	0.398	0.022	0.197	0.220	0.170	-0.116	0.296	0.088	0.224	0.319	0.403	-0.062	0.215	-0.059	0.035
trotime1	-0.241	-0.050	-0.451	-0.164	0.282	0.077	-0.473	-0.419	-0.282	0.073	-0.264	0.333	0.387	0.153	-0.314
antitro1	-0.201	0.344	0.092	0.243	-0.611	-0.569	0.555	-0.159	-0.477	-0.469	-0.059	-0.569	-0.444	-0.298	0.059
dd1	0.090	0.115	-0.044	0.122	-0.155	0.243	-0.104	0.179	0.236	0.178	0.079	0.140	0.039	-0.096	-0.088

DOI: 10.12998/wjcc.v11.i10.2226

Figure 1 Correlation matrix of interdependence of a number of indicators of the intestinal microbiota (presented horizontally, in columns from B to P) and the most frequently used clinical and biochemical indicators (in rows from 2 to 44). Correlation values are presented as absolute values, their strength is determined by both the value of the indicated values and the color intensity. In this case, direct correlation has shades of red, inverse correlation has shades of blue and a negative value. The main indicators of the intestinal microbiota were in a rather weak direct (from 0.023 to 0.229) and inverse (from -0.012 to -0.274) interdependence. However, as shown by a detailed analysis of the results presented in the table, in particular, lines No. 41-43, a significant dependence of a number of microbiota indicators was discovered on the content of fibrinogen (line 41), thrombin time (line 42), the content of antithrombin-III (line 43). It was found that the most significant inverse correlation was observed between the content of antithrombin-III and the number of fungi (-0.611), the number of lactobacilli (-0.569), the number of aerobes in the small intestine (-0.569). Moreover, a direct correlation was established (0.555) between the content of antithrombin-III and the ratio of anaerobic flora to aerobic.

microbiota and intestinal permeability are the driving factors of pathogenic processes that can determine the features of the course of COVID-19[22]. With these data in mind, the key indicators of intestinal permeability were analyzed in this study. Thus, the faecal calprotectin content in the control group and in patients with COVID-19 did not differ, and zonulin in feces was significantly higher in patients with COVID-19. At the same time, zonulin content in the blood of patients with COVID-19 was significantly lower than that in the control group. In addition, in patients with moderately severe COVID-19, a statistically significant increase in faecal calprotectin content and a tendency towards an increase in faecal zonulin content were observed. The data obtained generally agree with the opinion of Fasano (2012) on the role of zonulin in the pathogenesis of intestinal permeability disorders[6]; however, they contradict the opinion of many researchers who believe that the level of zonulin in the blood and feces, both synergistically increase in all patients with COVID-19[10]. It is likely that an increase in the level of zonulin in feces during the peak period is a more subtle marker of changes in intestinal permeability and requires further study.

Undoubtedly, the state of the intestinal target organ functional axis plays a special role in the pathogenesis of COVID-19[23]. The understanding that the human intestine is an ecological niche for a large population of intestinal microbiota is based on the idea that it is dominated by Bacteroidetes and Firmicutes[24], which produce several metabolites to maintain intestinal homeostasis[25]. The gut microbiota plays an important role in defense against pathogens as well as in the differentiation and proliferation of the intestinal epithelium[26]. In this regard, any deviation from the normal microbial composition of the intestine is defined as "microbial dysbiosis", which is characterized by a change in the role of pathobionts and instability or reduction in populations of "key" taxon such as Bacteroidetes and Firmicutes[27].

Modern literature data on the possible relationship between changes in intestinal microbiota and the severity of COVID-19 manifestations[28] served as an incentive for this study. Significant differences were found in the parameters of the intestinal microbiota in patients with COVID-19 compared to the control group in terms of the Propionibacterium/Cl. Subterminale ratio and the content of fungi and lactobacilli. It is important to note a statistically significant (more than 3 times) increase in the total endotoxin content in the blood of patients with COVID-19, which certainly enhances the body's general inflammatory response to SARS-CoV-2.

To study the interdependence of the indicators of the intestinal microbiota and the most commonly used indicators of clinical and biochemical studies, a correlation matrix was built, which showed that the main parameters of the microbiota are interrelated with many clinical and biochemical indicators, including the fibrinogen content, thrombin time, and antithrombin III content. The most significant inverse correlation was found between the antithrombin-III content and the number of fungi, lactobacilli, and aerobes in the small intestine. A direct correlation was also established between the antithrombin III content and the ratio of anaerobic flora to aerobic flora.

The data obtained in the course of this work are relatively contradictory. They may indicate not only the important role of the pathogen in the genesis of GI lesions but also the importance of drugs used in treating patients with COVID-19 and affecting inflammation, microcirculation, and blood clotting[17]. Nevertheless, the issues raised in this study require further study.

CONCLUSION

Currently, success in the fight against COVID-19 is associated with a complex of anti-epidemic measures and an increase in the rate of immunization of the population, as well as with a deep systemic study of the pathogenetic mechanisms of the development of the disease, the search for effective therapies, and methods of preventing complications[29].

The mechanisms of various gastroenterological manifestations of COVID-19 are largely mediated by impaired intestinal permeability and homeostasis of the human microbiome. The search for new criteria for the early detection of changes in the intestinal microflora, as well as intestinal permeability, requires the study of this problem at all stages of medical care, including hospitalization.

The approaches proposed in this study to assess the clinical and laboratory manifestations of COVID-19, microbiota, and intestinal permeability indicators are of scientific and practical interest not only in the context of determining the pathogenic mechanisms of the new coronavirus infection and polymorphism of its clinical manifestations, but also for developing predictive models for the course of COVID-19, the introduction of new methods of treatment, and the prevention of complications, including post-COVID syndrome.

ARTICLE HIGHLIGHTS

Research background

An important area of effective control of the coronavirus disease 2019 (COVID-19) pandemic is the

study of the pathogenic features of severe acute respiratory syndrome-related coronavirus 2 (SARS-CoV-2) infection, including those based on assessing the state of the intestinal microbiota and permeability.

Research motivation

To study the clinical features of the COVID-19 in patients with mild and moderate severity at the stage of hospitalization.

Research objectives

The objective of this clinical study was to determine the role of hepatobiliary injury, intestinal permeability disorders, and changes in composition of the microbiota in the development of systemic inflammation in patients with SARS-CoV-2 infection.

Research methods

The study was performed in 80 patients with mild and moderate severity of COVID-19. The scope of the examination included traditional clinical, laboratory, biochemical, instrumental, and radiation studies, as well as original methods for studying microbiota and intestinal permeability.

Research results

The clinical and biochemical features, manifestations of systemic inflammation, and intestinal microbiome changes in patients with mild and moderate severity were identified.

Research conclusions

This study highlights the role of intestinal permeability and microbiota as the main drivers of gastroenterological manifestations and increased COVID-19 severity.

Research perspectives

Our study showed that there is a change in the composition of the intestinal microflora, an increase in zonulin in feces, and intestinal dysfunction, which might be connected to COVID-19. We believe that additional studies should give more promising results. We also suggest that the use of probiotics, prebiotics, short chain fatty acids might show the success in treating intestinal dysbiosis caused by SARS-CoV-2 infection. If the effectiveness of these drugs is confirmed, the results can be used to complement the algorithms for COVID-19 treatment.

FOOTNOTES

Author contributions: Kozlov KV, Zhdanov KV, Ratnikova AK, Ratnikov VA, Tishkov AV, Grinevich V, Kravchuk YA, Miklush PI, Nikiforova PO, Gordienko VV, Popov AF, Andryukov BG wrote the manuscript, reviewed and agreed to the final version of the manuscript.

Institutional review board statement: The present study was reviewed and approved by the independent ethics committee of the Military Medical Academy named after SM. Kirov, protocol (Approval No. 246).

Informed consent statement: Informed written consent was obtained from the patient and her family for publication of this report and any accompanying images.

Conflict-of-interest statement: All the authors report no relevant conflicts of interest for this article.

Data sharing statement: The datasets used and/or analyzed during the current study are available from the corresponding author on reasonable request.

Country/Territory of origin: Russia

ORCID number: Konstantin V Kozlov 0000-0002-4398-7525; Konstantin V Zhdanov 0000-0002-3679-1874; Anna K Ratnikova 0000-0003-3279-6448; Vyacheslav A Ratnikov 0000-0002-9645-8408; Artem V Tishkov 0000-0002-4282-8717; Panteley I Miklush 0000-0002-5668-462X; Vera V Gordienko 0000-0003-2078-2196; Boris G Andryukov 0000-0003-4456-808X.

S-Editor: Liu GL

L-Editor: A
P-Editor: Liu GL

REFERENCES

1 **Yakovenko EP**, Yakovenko AV, Ivanov AN. Pathology of the digestive tract and liver in COVID-19. *Experimental and Clinical Gastroenterology* 2020 [DOI: 10.31146/1682-8658-ecg-176-4-19-23]
2 **Huang C**, Wang Y, Li X, Ren L, Zhao J, Hu Y, Zhang L, Fan G, Xu J, Gu X, Cheng Z, Yu T, Xia J, Wei Y, Wu W, Xie X, Yin W, Li H, Liu M, Xiao Y, Gao H, Guo L, Xie J, Wang G, Jiang R, Gao Z, Jin Q, Wang J, Cao B. Clinical features of patients infected with 2019 novel coronavirus in Wuhan, China. *Lancet* 2020; **395**: 497-506 [PMID: 31986264 DOI: 10.1016/S0140-6736(20)30183-5]
3 **Giron LB**, Dweep H, Yin X, Wang H, Damra M, Goldman AR, Gorman N, Palmer CS, Tang HY, Shaikh MW, Forsyth CB, Balk RA, Zilberstein NF, Liu Q, Kossenkov A, Keshavarzian A, Landay A, Abdel-Mohsen M. Plasma Markers of Disrupted Gut Permeability in Severe COVID-19 Patients. *Front Immunol* 2021; **12**: 686240 [PMID: 34177935 DOI: 10.3389/fimmu.2021.686240]
4 **Ahlawat S**, Asha, Sharma KK. Immunological co-ordination between gut and lungs in SARS-CoV-2 infection. *Virus Res* 2020; **286**: 198103 [PMID: 32717345 DOI: 10.1016/j.virusres.2020.198103]
5 **Troisi J**, Venutolo G, Pujolassos Tanyà M, Delli Carri M, Landolfi A, Fasano A. COVID-19 and the gastrointestinal tract: Source of infection or merely a target of the inflammatory process following SARS-CoV-2 infection? *World J Gastroenterol* 2021; **27**: 1406-1418 [PMID: 33911464 DOI: 10.3748/wjg.v27.i14.1406]
6 **Fasano A**. Intestinal permeability and its regulation by zonulin: diagnostic and therapeutic implications. *Clin Gastroenterol Hepatol* 2012; **10**: 1096-1100 [PMID: 22902773 DOI: 10.1016/j.cgh.2012.08.012]
7 **Llorens S**, Nava E, Muñoz-López M, Sánchez-Larsen Á, Segura T. Neurological Symptoms of COVID-19: The Zonulin Hypothesis. *Front Immunol* 2021; **12**: 665300 [PMID: 33981312 DOI: 10.3389/fimmu.2021.665300]
8 **Di Micco S**, Musella S, Sala M, Scala MC, Andrei G, Snoeck R, Bifulco G, Campiglia P, Fasano A. Peptide Derivatives of the Zonulin Inhibitor Larazotide (AT1001) as Potential Anti SARS-CoV-2: Molecular Modelling, Synthesis and Bioactivity Evaluation. *Int J Mol Sci* 2021; **22** [PMID: 34502335 DOI: 10.3390/ijms22179427]
9 **Leffler DA**, Kelly CP, Green PH, Fedorak RN, DiMarino A, Perrow W, Rasmussen H, Wang C, Bercik P, Bachir NM, Murray JA. Larazotide acetate for persistent symptoms of celiac disease despite a gluten-free diet: a randomized controlled trial. *Gastroenterology* 2015; **148**: 1311-9.e6 [PMID: 25683116 DOI: 10.1053/j.gastro.2015.02.008]
10 **Oliva A**, Cammisotto V, Cangemi R, Ferro D, Miele MC, De Angelis M, Cancelli F, Pignatelli P, Venditti M, Pugliese F, Mastroianni CM, Violi F. Low-Grade Endotoxemia and Thrombosis in COVID-19. *Clin Transl Gastroenterol* 2021; **12**: e00348 [PMID: 34092777 DOI: 10.14309/ctg.0000000000000348]
11 **Öztürk C**, Keskin B H, Ince N, Kayabaşı E, Kaya S, Cangür Ş, Yıldız Gülhan P, Demir M C. Investigation of the Effect of Leaky Gut on COVID-19 Clinic. *Sağlık Bilimlerinde Değer* 2022; **12**: 440-444 [DOI: 10.33631/sabd.1082004]
12 **Guan WJ**, Ni ZY, Hu Y, Liang WH, Ou CQ, He JX, Liu L, Shan H, Lei CL, Hui DSC, Du B, Li LJ, Zeng G, Yuen KY, Chen RC, Tang CL, Wang T, Chen PY, Xiang J, Li SY, Wang JL, Liang ZJ, Peng YX, Wei L, Liu Y, Hu YH, Peng P, Wang JM, Liu JY, Chen Z, Li G, Zheng ZJ, Qiu SQ, Luo J, Ye CJ, Zhu SY, Zhong NS; China Medical Treatment Expert Group for Covid-19. Clinical Characteristics of Coronavirus Disease 2019 in China. *N Engl J Med* 2020; **382**: 1708-1720 [PMID: 32109013 DOI: 10.1056/NEJMoa2002032]
13 **Zuo T**, Zhang F, Lui GCY, Yeoh YK, Li AYL, Zhan H, Wan Y, Chung ACK, Cheung CP, Chen N, Lai CKC, Chen Z, Tso EYK, Fung KSC, Chan V, Ling L, Joynt G, Hui DSC, Chan FKL, Chan PKS, Ng SC. Alterations in Gut Microbiota of Patients With COVID-19 During Time of Hospitalization. *Gastroenterology* 2020; **159**: 944-955.e8 [PMID: 32442562 DOI: 10.1053/j.gastro.2020.05.048]
14 **Yeoh YK**, Zuo T, Lui GC, Zhang F, Liu Q, Li AY, Chung AC, Cheung CP, Tso EY, Fung KS, Chan V, Ling L, Joynt G, Hui DS, Chow KM, Ng SSS, Li TC, Ng RW, Yip TC, Wong GL, Chan FK, Wong CK, Chan PK, Ng SC. Gut microbiota composition reflects disease severity and dysfunctional immune responses in patients with COVID-19. *Gut* 2021; **70**: 698-706 [PMID: 33431578 DOI: 10.1136/gutjnl-2020-323020]
15 **Temporary guidelines**. Prevention, diagnosis and treatment of new coronavirus infection (COVID-19). [Internet] [cited 03 June 2020]. Available from: https://journal.pulmonology.ru/pulm/article/view/1249
16 **Kordzadeh-Kermani E**, Khalili H, Karimzadeh I. Pathogenesis, clinical manifestations and complications of coronavirus disease 2019 (COVID-19). *Future Microbiol* 2020; **15**: 1287-1305 [PMID: 32851877 DOI: 10.2217/fmb-2020-0110]
17 **Zhou Z**, Zhao N, Shu Y, Han S, Chen B, Shu X. Effect of Gastrointestinal Symptoms in Patients With COVID-19. *Gastroenterology* 2020; **158**: 2294-2297 [PMID: 32199880 DOI: 10.1053/j.gastro.2020.03.020]
18 **Zheng M**, Gao Y, Wang G, Song G, Liu S, Sun D, Xu Y, Tian Z. Functional exhaustion of antiviral lymphocytes in COVID-19 patients. *Cell Mol Immunol* 2020; **17**: 533-535 [PMID: 32203188 DOI: 10.1038/s41423-020-0402-2]
19 **Wang J**, Jiang M, Chen X, Montaner LJ. Cytokine storm and leukocyte changes in mild *vs* severe SARS-CoV-2 infection: Review of 3939 COVID-19 patients in China and emerging pathogenesis and therapy concepts. *J Leukoc Biol* 2020; **108**: 17-41 [PMID: 32534467 DOI: 10.1002/JLB.3COVR0520-272R]
20 **Gao QY**, Chen YX, Fang JY. 2019 Novel coronavirus infection and gastrointestinal tract. *J Dig Dis* 2020; **21**: 125-126 [PMID: 32096611 DOI: 10.1111/1751-2980.12851]
21 **He Y**, Wen Q, Yao F, Xu D, Huang Y, Wang J. Gut-lung axis: The microbial contributions and clinical implications. *Crit Rev Microbiol* 2017; **43**: 81-95 [PMID: 27781554 DOI: 10.1080/1040841X.2016.1176988]
22 **Immanence VI**, Maev IV, Tkacheva ON, Alekseenko SA, Andreev DN, Bordin DS, Vlasov TD, Vorobyeva NM, Grinevich V, Gubonina IV, Drobizhev MYu, Efremov NS, Karateev AE, Kotovskaya YuV, Kravchuk IA, Krivoborodov GG, Kulchavenya EV, Lila AM, Mayevskaya MV, Poluektova EA, Popkova TV, Sablin OA, Solovyeva OI, Suvorov AN,

Tarasova GN, Trukhan DI, Fedotova AV. Syndrome of increased epithelial permeability in clinical practice Multidisciplinary national Consensus. *Cardiovascular Therapy and Prevention* 2021; **20**: 2758 [DOI: 10.15829/1728-8800-2021-2758]

23 **Ahlawat S**, Asha, Sharma KK. Gut-organ axis: a microbial outreach and networking. *Lett Appl Microbiol* 2021; **72**: 636-668 [PMID: 32472555 DOI: 10.1111/lam.13333]

24 **Foster JA**, McVey Neufeld KA. Gut-brain axis: how the microbiome influences anxiety and depression. *Trends Neurosci* 2013; **36**: 305-312 [PMID: 23384445 DOI: 10.1016/j.tins.2013.01.005]

25 **Carabotti M**, Scirocco A, Maselli MA, Severi C. The gut-brain axis: interactions between enteric microbiota, central and enteric nervous systems. *Ann Gastroenterol* 2015; **28**: 203-209 [PMID: 25830558]

26 **Hillman ET**, Lu H, Yao T, Nakatsu CH. Microbial Ecology along the Gastrointestinal Tract. *Microbes Environ* 2017; **32**: 300-313 [PMID: 29129876 DOI: 10.1264/jsme2.ME17017]

27 **Duboc H**, Rajca S, Rainteau D, Benarous D, Maubert MA, Quervain E, Thomas G, Barbu V, Humbert L, Despras G, Bridonneau C, Dumetz F, Grill JP, Masliah J, Beaugerie L, Cosnes J, Chazouillères O, Poupon R, Wolf C, Mallet JM, Langella P, Trugnan G, Sokol H, Seksik P. Connecting dysbiosis, bile-acid dysmetabolism and gut inflammation in inflammatory bowel diseases. *Gut* 2013; **62**: 531-539 [PMID: 22993202 DOI: 10.1136/gutjnl-2012-302578]

28 **Dhar D**, Mohanty A. Gut microbiota and Covid-19- possible link and implications. *Virus Res* 2020; **285**: 198018 [PMID: 32430279 DOI: 10.1016/j.virusres.2020.198018]

29 **Savushkina OI**, Cherniak AV, Kryukov EV, Kulagina IT, Samsonova MV, Kalmanova EN, Zykov KA. Pulmonary function after COVID-19 in early convalescence phase. *Medical Alphabet* 2020; 7-12 [DOI: 10.33667/2078-5631-2020-25-7-12]

World Journal of Clinical Cases

Submit a Manuscript: https://www.f6publishing.com

World J Clin Cases 2023 April 6; 11(10): 2237-2245

DOI: 10.12998/wjcc.v11.i10.2237

ISSN 2307-8960 (online)

ORIGINAL ARTICLE

Retrospective Study

Impact of lockdown policies during the COVID-19 outbreak on a trauma center of a tertiary hospital in China

Bi-Sheng Shen, Wei-Yin Cheng, Zhang-Rong Liang, Qi Tang, Kuang-Yi Li

Specialty type: Medicine, research and experimental

Provenance and peer review: Unsolicited article; Externally peer reviewed.

Peer-review model: Single blind

Peer-review report's scientific quality classification

Grade A (Excellent): 0
Grade B (Very good): B, B
Grade C (Good): C
Grade D (Fair): 0
Grade E (Poor): 0

P-Reviewer: Aseni P, Italy; Pantelis AG, Greece; Taghizadeh-Hesary F, Iran

Received: October 20, 2022
Peer-review started: October 20, 2022
First decision: December 26, 2022
Revised: January 3, 2023
Accepted: March 15, 2023
Article in press: March 15, 2023
Published online: April 6, 2023

Bi-Sheng Shen, Zhang-Rong Liang, Qi Tang, Kuang-Yi Li, Department of Emergency Medicine, Foshan Hospital of Traditional Chinese Medicine, Foshan 528000, Guangdong Province, China

Wei-Yin Cheng, Department of Clinical Nutrition, Foshan Hospital of Traditional Chinese Medicine, Foshan 528000, Guangdong Province, China

Corresponding author: Bi-Sheng Shen, MMeD, Doctor, Department of Emergency Medicine, Foshan Hospital of Traditional Chinese Medicine, No. 6 Qinren Road, Chancheng District, Foshan 528000, Guangdong Province, China. 736366461@qq.com

Abstract

BACKGROUND

Coronavirus disease 2019 (COVID-19) is a major and costly public health emergency.

AIM

To investigate the impact of China's lockdown policies during the COVID-19 outbreak on the level I trauma center of a tertiary comprehensive hospital of Traditional Chinese Medicine.

METHODS

All patients admitted to our trauma center during a lockdown in 2020 and the same period in 2019 were enrolled. We collected data on demographics, daily visits, injury type, injury mechanism, injury severity score, and patient management for comparative analysis.

RESULTS

The total number of patients in the trauma center of our hospital decreased by 50.38% during the COVID-19 Lockdown in 2020 compared to the same period in 2019. The average number of trauma visits per day in 2019 was 47.94, compared to 23.79 in 2020. Comparing the patients' demographic data, loss of employment was the most predominate characteristic in 2020 compared to 2019, while there was no significant difference in gender, age, and marital status between both periods. During the lockdown period, the proportion of traffic accident-related injuries, injuries due to falls greater than 1.5 m, and mechanical injuries decreased significantly, whereas the proportion of injuries caused by falls less than 1.5 m, cuts, assault, bites, and suicidal tendencies and other injuries increased relatively. In addition, the proportion of patients with minor injuries increased and serious

injuries decreased during the lockdown. The hospitalization rate increased significantly, and there was no significant difference in emergency surgery and death rates.

CONCLUSION

The lockdown policies during the COVID-19 outbreak significantly altered the number and mechanism of traumatic events in our hospital, which can be monitored regularly. Our results suggest that mandatory public health prevention and control measures by the government can reduce the incidence of traumatic events and the severity of traumatic injuries. Emergency surgery and mortality rates remain high, increased because of factors such as family injury and penetrating injury, and hospitalization rates have increased significantly. Therefore, our trauma center still needs to be fully staffed. Finally, from the perspective of the injury mechanism, indoor trauma is a major risk during a lockdown, and it is particularly important to develop prevention strategies for such trauma to reduce the medical burden of the next catastrophic epidemic.

Key Words: COVID-19 outbreak; Lockdown; Trauma; Mechanisms; Injury severity score; Retrospective study

Core Tip: First of all, during the coronavirus disease 2019 pandemic, the incidence of traumatic events in our city has been greatly reduced thanks to effective government control. In addition, from the perspective of injury mechanism, indoor trauma is a major risk during lockdown periods; therefore, it is particularly important to develop prevention strategies for such trauma to reduce the medical burden of the next catastrophic epidemic.

Citation: Shen BS, Cheng WY, Liang ZR, Tang Q, Li KY. Impact of lockdown policies during the COVID-19 outbreak on a trauma center of a tertiary hospital in China. *World J Clin Cases* 2023; 11(10): 2237-2245
URL: https://www.wjgnet.com/2307-8960/full/v11/i10/2237.htm
DOI: https://dx.doi.org/10.12998/wjcc.v11.i10.2237

INTRODUCTION

Coronavirus disease 2019 (COVID-19) was first detected in Wuhan, China[1], which spread rapidly worldwide and emerged as a pandemic[2-3], posing a major threat to the health of all populations[4]. The Chinese government adopted a series of unprecedented restrictions to contain the COVID-19 pandemic, including community lockdown, transportation restrictions, work cessation, school closures, home quarantine, and bans on all types of social activities. Guangdong province initiated a level I special major public health emergency response from January 23 to February 24, 2020, which marked the official start of a total lockdown. During this period, many major hospitals globally showed an overall decrease in the number of patients admitted and the admission rates for unrelated COVID-19 infections[5-6], as well as corresponding changes in trauma patterns and mechanisms[7-10]. It is unknown whether these lockdown policies reduced the demand on the health care system and the occurrence of trauma injuries. As a result, we conducted a study to investigate the impact of the lockdown policies on the level I trauma center of a tertiary comprehensive hospital of traditional Chinese medicine (TCM).

It should be noted that our hospital did not admit any COVID-19 patients during this period. Therefore, we believe that this study objectively presents accurate evidence of traumatic conditions unrelated to COVID-19, as the impact of visits attrition due to COVID-19 patients was excluded.

MATERIALS AND METHODS

Data collection

We conducted a retrospective study of all trauma patients admitted to the trauma center of a tertiary comprehensive Hospital of TCM. This is a comprehensive tertiary hospital located in the center of Foshan City, Guangdong Province, and it is famous for its orthopedics department. Its comprehensive strength has been ranked first among TCM hospitals in prefecture-level cities for many years in China, and the trauma center of the emergency department is particularly prominent. This study enrolled all patients who visited the emergency trauma center from January 23 to February 24 in 2019 and 2020. All

data were obtained from the Electronic Registration Database of Trauma Institutions in the emergency department of our hospital. There were 1582 cases in 2019 and only 785 cases in 2020. The study was approved by the Institutional Review Board of our hospital, and the need for informed consent was waived.

We collected data on demographics, daily visits, injury type, injury mechanism, injury severity score (ISS), and patient management. Demographic characteristics included gender, age, occupation, and marital status. The injury type was defined to include blunt, penetrating, burns, and others. The injury mechanisms were divided into the following categories: (1) Traffic accident-related, including motor vehicle collisions, motorcycle collisions, and other pedestrian accidents; (2) falls greater than or less than 1.5 m; (3) machine-related; (4) cuts; (5) assault; (6) bites, including bee stings and animal and snake bites; (7) suicidal tendencies; and (8) reasons other than those mentioned above. The severity of the injury was set according to the international ISS scoring standard. Patient management included emergency surgery, hospitalization, leave granted, death, and others. We obtained complete data for all patients, and no one was excluded from the analysis.

Statistical method

Categorical data were described as number (percentage) and compared using Chi-squared and Fisher's Exact test, as appropriate. Continuous variables were expressed as mean (standard deviation, SD) and compared using the two-sample *t*-test. $p < 0.05$ was considered statistically significant. Statistical Package for the Social Sciences version 22.0 was used for statistical analysis.

RESULTS

As shown in Table 1, our hospital enrolled a total of 2367 trauma patients in both phases, none of whom had been diagnosed with COVID-19. There were 1582 trauma cases in 2019 and only 785 in 2020, indicating a 50.38% overall decline in trauma cases in 2020 compared to the same period in 2019. Besides the significant difference in employment status in the occupational classification between 2020 and 2019 (21.81% and 18.22%, $p = 0.042$), there was no significant difference in the remaining demographic characteristics ($p > 0.05$).

As shown in Figure 1, the data were combined into the total number of cases over 3 d. The daily intake of trauma patients in our hospital during the lockdown phase in 2020 was less than that in 2019, with an average of 47.94 trauma patient visits per day in 2019 compared to 23.79 in 2020.

As shown in Figure 2, there was not significant difference in injury type, including blunt injury (74.02% *vs* 72.10%, $p = 0.320$), penetrating injury (21.18% *vs* 23.31%, $p = 0.237$), burns (1.52% *vs* 1.66%, $p = 0.797$), and others (3.29% *vs* 2.93%, $p = 0.641$), between the 2020 and 2019 periods, and there was no association between injury type and the government blockade policy in 2020 (all $p > 0.05$).

As shown in Table 2, the number of all injury mechanisms decreased in 2020 compared with 2019, but their proportions varied in the same period. The proportion of traffic accident-related injury (20.51% *vs* 24.72%, $p = 0.023$), fall (> 1.5 m) injury (6.75% *vs* 9.73%, $p = 0.016$), and mechanical injury (18.09% *vs* 22.06%, $p = 0.025$) showed a significant decreasing trend from 2019 to 2020. However, the proportion of fall (< 1.5 m) (18.34% *vs* 15.04%, $p = 0.040$), cut (14.90% *vs* 10.81%, $p = 0.004$), assault (3.69% *vs* 2.28%, $p = 0.047$), bites (3.18% *vs* 2.28%, $p = 0.189$), suicidal tendencies (1.66% *vs* 1.52%, $p = 0.797$), and other injury mechanisms (12.87% *vs* 11.57%, $p = 0.360$) all increased. Among them, there was a significant difference in fall (< 1.5 m), cut, and assault ($p < 0.05$), but there was no significant difference in the other three injury mechanisms ($p > 0.05$).

Regarding the assessment of trauma severity (shown in Table 3), the overall mean ISS level in 2020 was lower than that in 2019, and the difference was statistically significant ($p < 0.05$). Further division of ISS according into degrees showed that the proportion of patients with ISS score < 15 (81.91% *vs* 78.13%, $p = 0.032$) in 2020 was significantly higher than that in 2019, while the proportion of patients with ISS score > 25 (1.40% *vs* 2.72%, $p = 0.043$) was significantly higher in 2019 compared with 2020. There was no difference in the proportion of patients with ISS score between 15 and 25 ($p > 0.05$).

In terms of disposal methods (shown in Table 4), the rates of emergency surgery (37.07% *vs* 33.63%, $p = 0.098$) and hospitalization (18.47% *vs* 12.20%, $p < 0.01$) in 2020 were both higher than those in 2019, but with no statistical difference in the former ($p > 0.05$). However, there was a decrease in the proportion of leave granted (41.27% *vs* 50.63%, $p < 0.01$), death (0.25% *vs* 0.38%, $p = 0.908$), and others (2.93% *vs* 3.16%, $p = 0.760$) in 2020 compared with 2019, with a significant difference only in the rate of leave granted ($p < 0.05$).

DISCUSSION

It is well known that trauma places a heavy burden on global healthcare systems[11]. The COVID-19 pandemic poses an even more serious challenge to trauma centers, similar to a relentless mass casualty

Table 1 Demographic comparison of patients, *n* (%)

		2019, *n* = 1582	2020, *n* = 785	*P* value
Age, mean (SD)		34.01 (22.13)	32.84 (23.57)	0.236
Age groups	< 18	396 (25.03)	195 (24.84)	0.92
	18–45	712 (45.01)	348 (44.33)	0.756
	46–60	237 (14.98)	107 (13.63)	0.38
	> 60	237 (14.98)	135 (17.20)	0.163
Gender	Male	1052 (66.50)	505 (64.33)	0.296
	Female	530 (33.50)	280 (35.67)	
Occupation	Employed	345 (21.81)	143 (18.22)	0.042[a]
	Unemployed	759 (47.98)	377 (48.02)	0.982
	Not recorded	478 (30.21)	265 (33.76)	0.08
Marital status	Married	554 (35.02)	282 (35.92)	0.665
	Unmarried	727 (45.95)	368 (46.88)	0.671
	Minor	301 (19.03)	135 (17.20)	0.28

[a]*P* < 0.05, indicating the statistical difference.

Table 2 Comparison of injury mechanisms, *n* (%)

	2019, *n* = 1582	2020, *n* = 785	*P* value
Traffic accident-related	391 (24.72)	161 (20.51)	0.023[a]
Fall-greater than 1.5 m	154 (9.73)	53 (6.75)	0.016[a]
Fall-less than 1.5 m	238 (15.04)	144 (18.34)	0.040[a]
Machine-related	349 (22.06)	142 (18.09)	0.025[a]
Cut	171 (10.81)	117 (14.90)	0.004[a]
Assault	36 (2.28)	29 (3.69)	0.047[a]
Bites	36 (2.28)	25 (3.18)	0.189
Suicidal tendencies	24 (1.52)	13 (1.66)	0.797
Other	183 (11.57)	101 (12.87)	0.36

[a]*P* < 0.05, indicating the statistical difference.

event[12]. In addition, the morbidity and mortality caused by COVID-19 prompted the government to institute an unprecedented and severe lockdown policy to control the spread of the virus[13]. Some scholars reported that the COVID-19 outbreak has increased the pressure of medical care, and that many facilities have exceeded their original resource capacity load and will be exhausted[14]. Another study suggested that the burden of trauma during COVID-19 can be reduced by social distancing and the advice to stay at home[15]. Based on the above findings, it is unclear how these lockdown policies have affected our trauma center.

Our study showed an overall decline of 50.38% in the number of trauma patients treated in the trauma center of our hospital during the lockdown period from January 23 to February 24, 2020, compared to the same period in 2019. Both daily and total visits decreased, which is similar to the results in most countries[16-20]. Young and middle-aged individuals accounted for the highest proportion of the trauma patients, and the injuries were observed mainly among males. In addition, we found that the number of employed patients declined significantly during the COVID-19 outbreak. This may be due to the disproportionate combined influence of various socioeconomic factors. For instance, most high-income individuals have transitioned to working at home, while most unemployed persons may continue to work outside due to economic pressure[21]. Such employees include taxi drivers, construction workers, teachers, technicians, and civil servants. However, our study did not make this

Table 3 Comparison of patient's injury severity score, *n* (%)

ISS	2019, *n* = 1582	2020, *n* = 785	*P* value
Mean (SD)	9.87 (8.31)	9.15 (7.11)	0.038[a]
< 15	1236 (78.13)	643 (81.91)	0.032[a]
15–25	303 (19.15)	131 (16.69)	0.145
> 25	43 (2.72)	11 (1.40)	0.043[a]

[a]*P* < 0.05, indicating the statistical difference.
ISS: Injury severity score.

Table 4 Comparison of patient's management, *n* (%)

Management	2019, *n* = 1582	2020, *n* = 785	*P* value
Emergency surgery	532 (33.63)	291 (37.07)	0.098
Hospitalization	193 (12.20)	145 (18.47)	< 0.001[a]
Leave granted	801 (50.63)	324 (41.27)	< 0.001[a]
Death	6 (0.38)	2 (0.25)	0.908
Other	50 (3.16)	23 (2.93)	0.76

[a]*P* < 0.05, indicating the statistical difference.
Death, it refers to deaths that occur in-hospital on arrival at the emergency room.

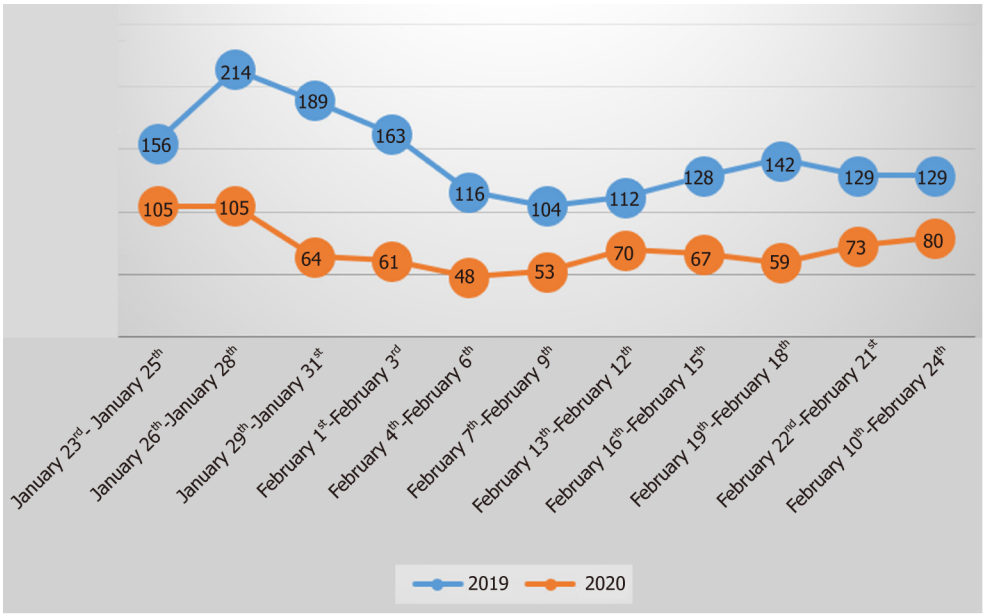

DOI: 10.12998/wjcc.v11.i10.2237

Figure 1 Line chart of the daily number of patients.

comparison.

Although the injury types in these two periods were similar to those in other studies[22], there was no significant difference after analysis of the results. However, there are certain rules in the mechanism of injury. We found that the lockdown period significantly reduced injuries due to traffic accident, falls greater than 1.5 m, and machine-related injuries, whereas other injury mechanisms such as falls less than 1.5 m, cuts, and assault increased. The Chinese government's lockdown policy reduced travel, construction works, and manufacturing operations, while home quarantine measures were implemented to limit the spread of the virus. As a result, traffic accidents, high fall injury, mechanical injury, and other types of injury were greatly reduced. Global studies have similarly shown a significant

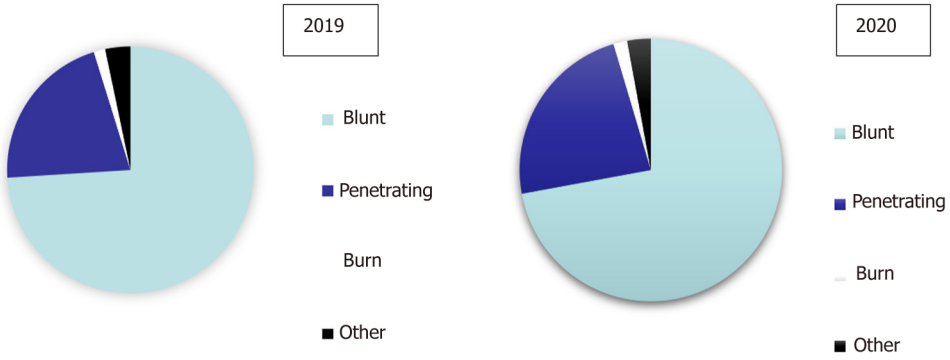

DOI: 10.12998/wjcc.v11.i10.2237

Figure 2 Comparison of injury types.

decrease in the number of transportation-related traumas during the COVID-19 pandemic[23-24]. However, the risk of indoor injury did not decrease[8]. For instance, some studies[25-26] showed that injuries caused by falling from a height and using tools at home increased during the lockdown period. The incidence of domestic violence caused by economic pressure, loneliness, and psychological pressure was also much higher during the COVID-19 pandemic than before[27-29]. Regarding trauma severity, we observed that the mean ISS score during the lockdown period was lower than that of the same period in 2019, with the main significant difference being an increase in the proportion of low scores (< 15) and a decrease in the proportion of high scores (> 25). This is consistent with the studies of Andreozzi *et al*[30] and Qasim *et al*[12], considering that factors such as family injury and penetrating injury increase the proportion of emergency surgery, but the risk of death is also small due to the low severity of this type of injuries[12,30]. The proportions of emergency surgery and mortality in the two periods were not significantly different. However, the hospital's demand for emergency surgery and inpatient wards remained unchanged[31]. This indicates that a lockdown period can indeed reduce the overall severity of injuries, and that mainly minor injuries occur during such periods[32,33]. Moreover, our study found that hospitalization rates increased significantly during lockdown periods. Trauma is still an important cause of many hospitalizations[11].

Limitations and prospects

Our study has some limitations. First, the data were only from the trauma center of one hospital, and the sample size was small, which did not satisfy the needs of other regions in China. Second, results of retrospective studies based on electronic medical records have a certain degree of subjectivity, which may increase the information error. However, we believe that COVID-19 Lockdown regularly has a negative impact on humans, and this study certainly adds to existing evidence. It is hoped that we can conduct a national multi-center study to confirm similar findings and further evaluate the impact of the Chinese government's lockdown policy on hospital trauma centers to provide information and allocate trauma medical resources for the prevention of the next catastrophic infectious disease.

CONCLUSION

The lockdown policy during the COVID-19 outbreak significantly changed the number and mechanism of traumatic events in our hospital, which can be monitored regularly. Mandatory prevention and control measures by the government can reduce the occurrence and severity of traumatic events and significantly reduce the incidence of traffic accidents, falling injuries, and machine injuries. However, high rates of emergency surgery, mortality, and hospitalizations have led to the need for better staffing of health care personnel. Finally, there is a need to focus on indoor trauma, which is particularly important in terms of prevention strategies, to reduce the medical burden of the next catastrophic epidemic.

ARTICLE HIGHLIGHTS

Research background

Coronavirus disease 2019 (COVID-19) was spread rapidly worldwide and emerged as a pandemic, posing a major threat to the health of all populations.

Research motivation

It is unknown whether these lockdown policies reduced the demand on the health care system and the occurrence of trauma injuries. As a result, we conducted a study to investigate the impact of the lockdown policies on the level I trauma center of a tertiary comprehensive hospital of traditional Chinese medicine (TCM).

Research objectives

This study aimed to investigate the impact of China's lockdown policies during the COVID-19 outbreak on the level I trauma center of a tertiary comprehensive hospital of TCM.

Research methods

All patients admitted to our trauma center during a lockdown in 2020 and the same period in 2019 were enrolled. We collected data on demographics, daily visits, injury type, injury mechanism, injury severity score, and patient management for comparative analysis.

Research results

The total number of patients in the trauma center of our hospital decreased by 50.38% during the COVID-19 Lockdown in 2020 compared to the same period in 2019. The average number of trauma visits per day in 2019 was 47.94, compared to 23.79 in 2020. Comparing the patients' demographic data, loss of employment was the most predominate characteristic in 2020 compared to 2019, while there was no significant difference in gender, age, and marital status between both periods. During the lockdown period, the proportion of traffic accident-related injuries, injuries due to falls greater than 1.5 m, and mechanical injuries decreased significantly, whereas the proportion of injuries caused by falls less than 1.5 m, cuts, assault, bites, and suicidal tendencies and other injuries increased relatively. In addition, the proportion of patients with minor injuries increased and serious injuries decreased during the lockdown. The hospitalization rate increased significantly, and there was no significant difference in emergency surgery and death rates.

Research conclusions

The lockdown policies during the COVID-19 outbreak significantly altered the number and mechanism of traumatic events in our hospital, which can be monitored regularly. Our results suggest that mandatory public health prevention and control measures by the government can reduce the incidence of traumatic events and the severity of traumatic injuries. Increased due to factors such as family injury and penetrating injury, emergency surgery and death rates remain high, and hospitalization rates have increased significantly.

Research perspectives

Therefore, our trauma center still needs to be fully staffed. Finally, from the perspective of the injury mechanism, indoor trauma is a major risk during a lockdown, and it is particularly important to develop prevention strategies for such trauma to reduce the medical burden of the next catastrophic epidemic.

FOOTNOTES

Author contributions: Shen BS and Li KY designed topics, programs and drafted writing, as the main contributor and share the first authorship; Cheng WY participated in data statistics and analysis; Liang ZR and Tang Q produced metadata for initial use and later reuse.

Institutional review board statement: The study was reviewed and approved by the Foshan Hospital of TCM Institutional Review Board, No. KY[2023]024.

Conflict-of-interest statement: All the authors report no relevant conflicts of interest for this article.

Data sharing statement: This manuscript has not been submitted elsewhere for publication, in whole or in part, and all authors have contributed to read, and approved the enclosed manuscript. No additional data are available.

Country/Territory of origin: China

ORCID number: Bi-Sheng Shen 0000-0001-9061-4396; Kuang-Yi Li 0000-0002-3434-160X.

S-Editor: Li L
L-Editor: A
P-Editor: Li L

REFERENCES

1 **Huang H**, Zhang M, Chen C, Zhang H, Wei Y, Tian J, Shang J, Deng Y, Du A, Dai H. Clinical characteristics of COVID-19 in patients with preexisting ILD: A retrospective study in a single center in Wuhan, China. *J Med Virol* 2020; **92**: 2742-2750 [PMID: 32533777 DOI: 10.1002/jmv.26174]
2 **World Health Organization**. WHO Director-General's opening remarks at the media briefing on COVID-19. Mar 11, 2020. [cited April 24, 2020]. Available from: https://www.who.int/director-general/speeches/detail/who-director-general-s-opening-remarks-at-the-media-briefing-on-covid-19---11-may-2020
3 **Chu DK**, Akl EA, Duda S, Solo K, Yaacoub S, Schünemann HJ; COVID-19 Systematic Urgent Review Group Effort (SURGE) study authors. Physical distancing, face masks, and eye protection to prevent person-to-person transmission of SARS-CoV-2 and COVID-19: a systematic review and meta-analysis. *Lancet* 2020; **395**: 1973-1987 [PMID: 32497510 DOI: 10.1016/S0140-6736(20)31142-9]
4 **Rakhsha A**, Azghandi S, Taghizadeh-Hesary F. Decision on Chemotherapy Amidst COVID-19 Pandemic: a Review and a Practical Approach from Iran. *Infect Chemother* 2020; **52**: 496-502 [PMID: 33263246 DOI: 10.3947/ic.2020.52.4.496]
5 **Williams CH**, Scott EM, Dorfman JD, Simon BJ. Traumatic Injury Under COVID-19 Stay-at-Home Advisory: Experience of a New England Trauma Center. *J Surg Res* 2022; **269**: 165-170 [PMID: 34563843 DOI: 10.1016/j.jss.2021.08.005]
6 **Meara JG**, Leather AJ, Hagander L, Alkire BC, Alonso N, Ameh EA, Bickler SW, Conteh L, Dare AJ, Davies J, Mérisier ED, El-Halabi S, Farmer PE, Gawande A, Gillies R, Greenberg SL, Grimes CE, Gruen RL, Ismail EA, Kamara TB, Lavy C, Lundeg G, Mkandawire NC, Raykar NP, Riesel JN, Rodas E, Rose J, Roy N, Shrime MG, Sullivan R, Verguet S, Watters D, Weiser TG, Wilson IH, Yamey G, Yip W. Global Surgery 2030: evidence and solutions for achieving health, welfare, and economic development. *Int J Obstet Anesth* 2016; **25**: 75-78 [PMID: 26597405 DOI: 10.1016/j.ijoa.2015.09.006]
7 **Rhodes HX**, Petersen K, Biswas S. Trauma Trends During the Initial Peak of the COVID-19 Pandemic in the Midst of Lockdown: Experiences From a Rural Trauma Center. *Cureus* 2020; **12**: e9811 [PMID: 32953322 DOI: 10.7759/cureus.9811]
8 **Hakeem FF**, Alshahrani SM, Ghobain MA, Albabtain I, Aldibasi O, Alghnam S. The Impact of COVID-19 Lockdown on Injuries in Saudi Arabia: Results From a Level-I Trauma Center. *Front Public Health* 2021; **9**: 704294 [PMID: 34327189 DOI: 10.3389/fpubh.2021.704294]
9 **Kreis CA**, Ortmann B, Freistuehler M, Hartensuer R, Van Aken H, Raschke MJ, Schliemann B. Impact of the first COVID-19 shutdown on patient volumes and surgical procedures of a Level I trauma center. *Eur J Trauma Emerg Surg* 2021; **47**: 665-675 [PMID: 33881555 DOI: 10.1007/s00068-021-01654-8]
10 **Nia A**, Popp D, Diendorfer C, Apprich S, Munteanu A, Hajdu S, Widhalm HK. Impact of lockdown during the COVID-19 pandemic on number of patients and patterns of injuries at a level I trauma center. *Wien Klin Wochenschr* 2021; **133**: 336-343 [PMID: 33656596 DOI: 10.1007/s00508-021-01824-z]
11 **Aljuboori Z**, Sieg E. The early effects of social distancing resultant from COVID-19 on admissions to a Level I trauma center. *Injury* 2020; **51**: 2332 [PMID: 32605787 DOI: 10.1016/j.injury.2020.06.036]
12 **Qasim Z**, Sjoholm LO, Volgraf J, Sailes S, Nance ML, Perks DH, Grewal H, Meyer LK, Walker J, Koenig GJ, Donnelly J, Gallagher J, Kaufman E, Kaplan MJ, Cannon JW. Trauma center activity and surge response during the early phase of the COVID-19 pandemic-the Philadelphia story. *J Trauma Acute Care Surg* 2020; **89**: 821-828 [PMID: 32618967 DOI: 10.1097/TA.0000000000002859]
13 **Xie J**, Tong Z, Guan X, Du B, Qiu H, Slutsky AS. Critical care crisis and some recommendations during the COVID-19 epidemic in China. *Intensive Care Med* 2020; **46**: 837-840 [PMID: 32123994 DOI: 10.1007/s00134-020-05979-7]
14 **Jackson SE**, Garnett C, Shahab L, Oldham M, Brown J. Association of the COVID-19 lockdown with smoking, drinking and attempts to quit in England: an analysis of 2019-20 data. *Addiction* 2021; **116**: 1233-1244 [PMID: 33089562 DOI: 10.1111/add.15295]
15 **Stinner DJ**, Lebrun C, Hsu JR, Jahangir AA, Mir HR. The Orthopaedic Trauma Service and COVID-19: Practice Considerations to Optimize Outcomes and Limit Exposure. *J Orthop Trauma* 2020; **34**: 333-340 [PMID: 32301767 DOI: 10.1097/BOT.0000000000001782]
16 **McGuinness MJ**, Harmston C; Northern Region Trauma Network. Association between COVID-19 public health interventions and major trauma presentation in the northern region of New Zealand. *ANZ J Surg* 2021; **91**: 633-638 [PMID: 33656252 DOI: 10.1111/ans.16711]
17 **Morris D**, Rogers M, Kissmer N, Du Preez A, Dufourq N. Impact of lockdown measures implemented during the Covid-19 pandemic on the burden of trauma presentations to a regional emergency department in Kwa-Zulu Natal, South Africa. *Afr J Emerg Med* 2020; **10**: 193-196 [PMID: 32837876 DOI: 10.1016/j.afjem.2020.06.005]
18 **van Aert GJJ**, van der Laan L, Boonman-de Winter LJM, Berende CAS, de Groot HGW, Boele van Hensbroek P, Schormans PMJ, Winkes MB, Vos DI. Effect of the COVID-19 pandemic during the first lockdown in the Netherlands on the number of trauma-related admissions, trauma severity and treatment: the results of a retrospective cohort study in a level 2 trauma centre. *BMJ Open* 2021; **11**: e045015 [PMID: 33608406 DOI: 10.1136/bmjopen-2020-045015]
19 **Venter A**, Lewis CM, Saffy P, Chadinha LP. Locked down: Impact of COVID-19 restrictions on trauma presentations to the emergency department. *S Afr Med J* 2020; **111**: 52-56 [PMID: 33404006 DOI: 10.7196/SAMJ.2021.v111i1.15289]

20 **Harris D**, Ellis DY, Gorman D, Foo N, Haustead D. Impact of COVID-19 social restrictions on trauma presentations in South Australia. *Emerg Med Australas* 2021; **33**: 152-154 [PMID: 33124718 DOI: 10.1111/1742-6723.13680]

21 **Talev M**. Axios-Ipsos Coronavirus Index: rich sheltered, poor shafted amid virus. 2020. [cited May 2020]. Available from: https://www.i-com.org/news-articles/axios-ipsos-coronavirus-index-rich-sheltered-poor-shafted-amid-virus

22 **Devarakonda AK**, Wehrle CJ, Chibane FL, Drevets PD, Fox ED, Lawson AG. The Effects of the COVID-19 Pandemic on Trauma Presentations in a Level One Trauma Center. *Am Surg* 2021; **87**: 686-689 [PMID: 33231483 DOI: 10.1177/0003134820973715]

23 **Poggetti A**, Del Chiaro A, Nucci AM, Suardi C, Pfanner S. How hand and wrist trauma has changed during covid-19 emergency in Italy: Incidence and distribution of acute injuries. What to learn? *J Clin Orthop Trauma* 2021; **12**: 22-26 [PMID: 32921952 DOI: 10.1016/j.jcot.2020.08.008]

24 **Keays G**, Friedman D, Gagnon I. Injuries in the time of COVID-19. *Health Promot Chronic Dis Prev Can* 2020; **40**: 336-341 [PMID: 32924925 DOI: 10.24095/hpcdp.40.11/12.02]

25 **Ruiz-Medina PE**, Ramos-Meléndez EO, Cruz-De La Rosa KX, Arrieta-Alicea A, Guerrios-Rivera L, Nieves-Plaza M, Rodríguez-Ortiz P. The effect of the lockdown executive order during the COVID-19 pandemic in recent trauma admissions in Puerto Rico. *Inj Epidemiol* 2021; **8**: 22 [PMID: 33752760 DOI: 10.1186/s40621-021-00324-y]

26 **Garude K**, Natalwala I, Hughes B, West C, Bhat W. Patterns of Adult and Paediatric Hand Trauma During the COVID-19 Lockdown. *J Plast Reconstr Aesthet Surg* 2020; **73**: 1575-1592 [PMID: 32527666 DOI: 10.1016/j.bjps.2020.05.087]

27 **Mackolil J**, Mackolil J. Addressing psychosocial problems associated with the COVID-19 lockdown. *Asian J Psychiatr* 2020; **51**: 102156 [PMID: 32413617 DOI: 10.1016/j.ajp.2020.102156]

28 **Boserup B**, McKenney M, Elkbuli A. Alarming trends in US domestic violence during the COVID-19 pandemic. *Am J Emerg Med* 2020; **38**: 2753-2755 [PMID: 32402499 DOI: 10.1016/j.ajem.2020.04.077]

29 **Bradbury-Jones C**, Isham L. The pandemic paradox: The consequences of COVID-19 on domestic violence. *J Clin Nurs* 2020; **29**: 2047-2049 [PMID: 32281158 DOI: 10.1111/jocn.15296]

30 **Andreozzi V**, Marzilli F, Muselli M, Previ L, Cantagalli MR, Princi G, Ferretti A. The impact of COVID-19 on orthopaedic trauma: A retrospective comparative study from a single university hospital in Italy. *Orthop Rev (Pavia)* 2020; **12**: 8941 [PMID: 33585026 DOI: 10.4081/or.2020.8941]

31 **İlhan B**, Bozdereli Berikol G, Aydın H, Arslan Erduhan M, Doğan H. COVID-19 outbreak impact on emergency trauma visits and trauma surgery in a level 3 trauma center. *Ir J Med Sci* 2022; **191**: 2319-2324 [PMID: 34618300 DOI: 10.1007/s11845-021-02793-y]

32 **Christey G**, Amey J, Campbell A, Smith A. Variation in volumes and characteristics of trauma patients admitted to a level one trauma centre during national level 4 lockdown for COVID-19 in New Zealand. *N Z Med J* 2020; **133**: 81-88 [PMID: 32325471]

33 **Trier F**, Fjølner J, Raaber N, Sørensen AH, Kirkegaard H. Effect of the COVID-19 pandemic at a major Danish trauma center in 2020 compared with 2018-2019: A retrospective cohort study. *Acta Anaesthesiol Scand* 2022; **66**: 265-272 [PMID: 34748218 DOI: 10.1111/aas.13997]

World Journal of Clinical Cases

Submit a Manuscript: https://www.f6publishing.com

World J Clin Cases 2023 April 6; 11(10): 2246-2253

DOI: 10.12998/wjcc.v11.i10.2246

ISSN 2307-8960 (online)

ORIGINAL ARTICLE

Observational Study

Interaction between the left ventricular ejection fraction and left ventricular strain and its relationship with coronary stenosis

Hai-Yan Gui, Shu-Wen Liu, Dong-Fang Zhu

Specialty type: Radiology, nuclear medicine and medical imaging

Provenance and peer review: Unsolicited article; Externally peer reviewed.

Peer-review model: Single blind

Peer-review report's scientific quality classification

Grade A (Excellent): 0
Grade B (Very good): 0
Grade C (Good): C, C
Grade D (Fair): 0
Grade E (Poor): 0

P-Reviewer: Jeon Y, South Korea; Kaneko T, Japan

Received: January 20, 2023
Peer-review started: January 20, 2023
First decision: February 10, 2023
Revised: February 28, 2023
Accepted: March 3, 2023
Article in press: March 3, 2023
Published online: April 6, 2023

Hai-Yan Gui, MRI Room, Harbin No. 4 Hospital, Harbin 150026, Heilongjiang Province, China

Shu-Wen Liu, Dong-Fang Zhu, Department of Cardiology, Harbin No. 4 Hospital, Harbin 150026, Heilongjiang Province, China

Corresponding author: Shu-Wen Liu, MM, Associate Chief Physician, Department of Cardiology, Harbin No. 4 Hospital, No. 119 Jingyu Street, Daowai District, Harbin 150026, Heilongjiang Province, China. shuwenl007@yeah.net

Abstract

BACKGROUND

Coronary artery stenosis (CAS) is the most common type of heart disease and the leading cause of death in both men and women globally. CAS occurs when the arteries that supply blood to the heart muscle harden and become narrower due to plaque buildup - cholesterol and other material - on their inner walls. As a result, the heart muscle cannot receive the blood or oxygen it needs. Most heart attacks happen when a blood clot suddenly cuts off the hearts' blood supply, causing permanent heart damage.

AIM

To analyze the relationship between the left ventricular ejection fraction (LVEF), left ventricular strain (LVS), and coronary stenosis.

METHODS

A total of 190 participants were enrolled in this trail. The control group comprised 93 healthy individuals, and observation group comprised 97 patients with coronary heart disease who were hospitalized between July 2020 and September 2021. Coronary lesions were assessed using the Gensini score, and the LVEF and LVS were measured using magnetic resonance imaging (MRI). The interaction between the LVEF and LVS was examined using a linear regression model. The relationship between LVEF and coronary stenosis was examined using Spearman's correlation.

RESULTS

The LVEF of the observation group was lower than that of the control group. The left ventricular end-systolic volume (LVESV) and left ventricular end-diastolic volume (LVEDV) of the observation group were significantly higher than those of the control group ($P < 0.05$). The longitudinal and circumferential strains (LS, CS)

of the observation group were significantly higher than those of the control group; however, the radial strain (RS) of the observation group was significantly lower than that of the control group ($P < 0.05$). LVS, LS, and CS were significantly negatively correlated with the LVEF, and RS was positively correlated with the LVEF. There were significant differences in the LVEF, LVESV, and LVEDV of patients with different Gensini scores; the LVEF significantly decreased and the LVESV and LVEDV increased with increasing Gensini scores ($P < 0.05$). In the observation group, the LVEF was negatively correlated and the LVESV and LVEDV were positively correlated with coronary stenosis ($P < 0.05$).

CONCLUSION

The LVEF measured using MRI is significantly linearly correlated with LVS and negatively correlated with coronary stenosis.

Key Words: Magnetic resonance imaging; Left ventricular ejection fraction; Left ventricular strain; Coronary stenosis; Left ventricular end-diastolic volume; Left ventricular end-systolic volume

Core Tip: This study aimed to analyze the relationship between the left ventricular ejection fraction (LVEF), left ventricular strain (LVS), and coronary artery stenosis (CAS), 93 healthy individuals were selected as the control group, while 97 patients with coronary heart disease were selected as the observation group. Through the analysis of the Gensini score, magnetic resonance imaging, a linear regression model, and Spearman's correlation, we found that LVEF is significantly linearly correlated with LVS and negatively correlated with CAS.

Citation: Gui HY, Liu SW, Zhu DF. Interaction between the left ventricular ejection fraction and left ventricular strain and its relationship with coronary stenosis. *World J Clin Cases* 2023; 11(10): 2246-2253
URL: https://www.wjgnet.com/2307-8960/full/v11/i10/2246.htm
DOI: https://dx.doi.org/10.12998/wjcc.v11.i10.2246

INTRODUCTION

Coronary artery stenosis (CAS) is a common clinical disease. As the condition worsens, myocardial cells are damaged to varying degrees, resulting in abnormal myocardial blood perfusion and changes in ventricular function and structure[1]. Therefore, a timely and effective clinical evaluation of the left ventricular function is necessary to assess the risk of coronary heart disease[2]. Currently, magnetic resonance imaging (MRI) is widely used in clinical practice as a non-invasive examination method because it can effectively assess the function and structure of the left ventricle and coronary arteries[3]; thus, MRI has gradually become the gold standard for this purpose[4]. However, there are few clinical studies on the correlation between left ventricular ejection fraction (LVEF) and other cardiac function indicators. Therefore, this study included patients with coronary heart disease admitted to our hospital and analyzed the relationship between the LVEF measured using MRI, left ventricular strain (LVS), and coronary stenosis.

MATERIALS AND METHODS

General materials

This study was approved by the ethics committee of Harbin No. 4 Hospital. The observation group comprised 97 patients with coronary heart disease who were hospitalized between July 2020 and September 2021, while the control group comprised 93 healthy individuals. The observation group included 52 men and 45 women (age, 56.21 ± 7.32 years; heart rate, 64.93 ± 6.33 beats/min), while the control group included 51 men and 42 women (age, 55.91 ± 8.13 years; heart rate, 64.56 ± 7.43 beats/min). The clinical data of the groups were comparable, with no discernible differences ($P > 0.05$). The inclusion criteria were as follows: (1) Fulfilled the coronary computed tomography angiography diagnostic criteria for coronary heart disease; (2) available imaging results with satisfactory image quality; (3) no history of coronary intervention; and (4) provided a signed informed consent form. The exclusion criteria were as follows: (1) Congenital heart disease or valvular heart disease; (2) severe arrhythmia; (3) cardiomyopathy; (4) liver and kidney insufficiency; (5) history of hypertension (grade 3

or higher); and (6) pregnancy or breastfeeding.

Methods

All participants were examined using a Philips Ingenia 3.0 T MRI machine with a 12-channel phased-array coil while in the supine decubitus position. Sagittal, coronal, and axial scans were performed. The four-chamber long-axis view, two-chamber view, short-axis view, and the entrance and exit of the left ventricle were obtained; the heart axis was centered during imaging. The images of each slice were collected at the end of expiration, and the steady-state free precession (SSFP) scanning parameters were as follows: Left ventricular short-axis slice thickness, 8 mm; echo time (TE), 1.7 ms; repetition time (TR), 51.5 ms; field of view (FOV), 340 mm × 360 mm; matrix, 256 × 192; flip angle, 70°; and total number of plies, 8 to 10. Delayed enhanced images were obtained using Gd-DTPA as the contrast agent, which was injected *via* the peripheral vein with a high-pressure syringe at a rate of 4 mL/s; the contrast agent dose was 0.2 mmol/kg. An equal volume of physiological saline was also injected at the same rate. At 7 min after the injection, phase-sensitive inversion recovery (left ventricular short-axis thickness, 8 mm; TE, 2.6 ms; TR, 750 ms; FOV, 340 mm × 360 mm; matrix, 256 × 192) was performed. The inversion time (TI) was determined in real time according to the darkest layer of the myocardium. A total of 8 to 10 Layers were collected, and the slices were the same as those used for SSFP.

Image processing

All images were transmitted to the supporting workstation. Two radiologists with more than 3 years of experience judged the results and post-processed the images. Using the post-processing standards published by the American Cardiovascular Magnetic Resonance Committee, the epicardium and endocardium were delineated using the SSFP images to determine the LVEF, left ventricular end-systolic volume (LVESV), and left ventricular end-diastolic volume (LVEDV). Patients with coronary artery lesions were evaluated using the Gensini score and CAS scoring standards [5]. Scores based on the degree of stenosis were as follows: 1%–25%, 1 point; > 25%–50%, 2 points; > 50%–75%, 4 points; > 75%–90%, 8 points; > 90%–< 100%, 16 points; and 100%, 32 points. Scores based on the lesion site were scored as follows: left main artery, 5 points; left anterior descending branch or proximal circumflex branch, 2.5 points; intermediate section of the left anterior descending artery, 1.5 points; distal segment of the left anterior descending artery, 1 point; intermediate and distal segments of the left circumflex artery, 1 point; right coronary artery, 1 point; and small branches, 0.5 points. The total score was the sum of the stenosis degree and lesion site scores, and patients were categorized as follows: score ≤ 30, mild disease group; score > 30–60, moderate disease group; and score > 60, severe disease group. Supporting software of Philips Ingenia 3.0T magnetic resonance instrument was used to detect myocardial strain parameters, and the epicardial and endocardial displacements were automatically tracked to quantify the left ventricular myocardial motion and analyze three-dimensional longitudinal strain (LS), circumferential strain (CS), and radial strain (RS).

Statistical analysis

Statistical analysis was performed using SPSS version 20.0 (Armonk, NY: IBM Corp). The enumeration data were expressed as percentages, and χ^2 test for comparisons. The measurement data of the two groups were expressed as the mean ± SD, and a *t*-test was used for comparisons. Differences in measurement data among multiple groups were evaluated using an analysis of variance. The linear regression model was used to analyze the interaction between the LVEF and LVS. Spearman's correlation was used to analyze the relationship between LVEF and coronary stenosis. $P < 0.05$ indicated a statistically significant difference.

RESULTS

MRI results of the left ventricular function

The LVESV and LVEDV of the observation group were substantially greater than those of the control group; however, the LVEF of the observation group was lower than that of the control group ($P < 0.05$; Table 1). The typical case diagram is shown in Figure 1.

Left ventricular stress test results

The LS and CS of the observation group were much greater than those of the control group; however, the RS of the observation group was lower than that of the control group ($P < 0.05$; Table 2).

Interaction between the left ventricular ejection fraction and left ventricular strain

The LVS, LS, and CS were significantly negatively correlated with the LVEF, and the RS was significantly positively correlated with the LVEF (Table 3, Figure 2).

Table 1 Magnetic resonance imaging results of the left ventricular function

Group	Participants	LVEF, %	LVESV, mL	LVEDV, mL
Observation	97	44.19 ± 9.71	88.51 ± 17.52	147.32 ± 18.32
Control	93	66.92 ± 10.23	33.64 ± 10.23	100.03 ± 23.19
t value		15.713	26.215	15.613
P value		0.000	0.000	0.000

LVEDV: Left ventricular end-diastolic volume; LVEF: Left ventricular ejection fraction; LVESV: Left ventricular end-systolic volume.

Table 2 Left ventricular stress test results

Groups	Participants	LS, %	CS, %	RS, %
Observation	97	-11.21 ± 3.87	-14.85 ± 5.96	31.44 ± 10.45
Control	93	-15.43 ± 2.42	-19.83 ± 4.09	45.43 ± 6.12
t value		8.969	6.684	11.194
P value		0.000	0.000	0.000

CS: Circumferential strain; LS: Longitudinal strain; RS: Radial strain.

Table 3 Interaction between the left ventricular ejection fraction and left ventricular strain

Independent variable	Model	R^2
LS	y = -2.5269x + 17.285	0.9805
CS	y = -1.6514x + 21.462	0.9836
RS	y = 0.9325x + 16.356	0.9848

CS: Circumferential strain; LS: Longitudinal strain; RS: Radial strain.

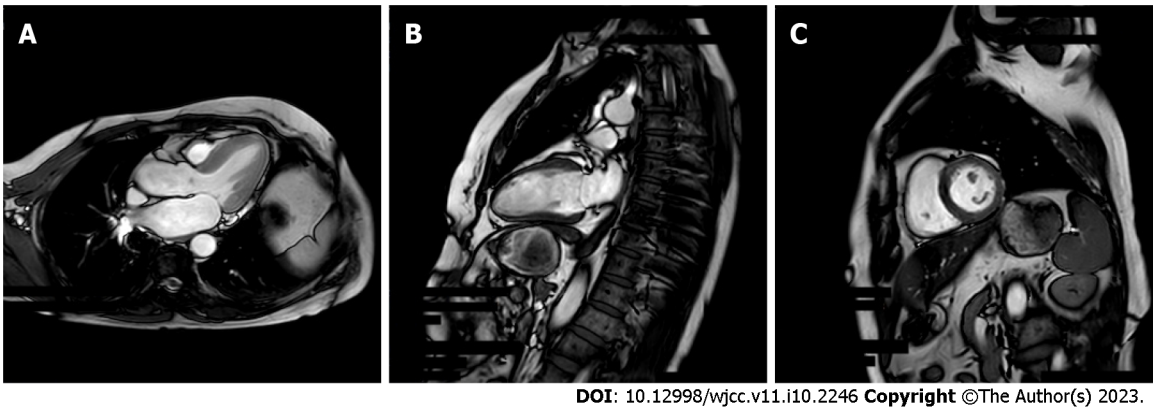

DOI: 10.12998/wjcc.v11.i10.2246

Figure 1 Magnetic resonance imaging results of a 56-year-old woman with hypertension, diabetes, chest tightness, and shortness of breath. A: Functional imaging shows decreased left ventricular end-diastolic systole; B: The perfusion scan shows extensive subendocardial ischemia; C: The delayed scan shows partial myocardial fibrosis. Extensive myocardial ischemia was considered. Partial myocardial infarction causes abnormal cardiac function.

Left ventricular function of participants with different degrees of coronary stenosis

There were significant differences in the LVEF, LVESV, and LVEDV of patients with different Gensini scores. The LVEF significantly decreased and the LVESV and LVEDV significantly increased with increasing Gensini scores ($P < 0.05$; Table 4).

Table 4 Left ventricular function of participants with different degrees of coronary stenosis

Gensini score	Participants	LVEF, %	LVESV, mL	LVEDV, mL
< 5	12	54.93 ± 8.12	70.94 ± 15.34	125.49 ± 17.43
5–< 25	41	45.67 ± 7.92	85.21 ± 17.83	142.85 ± 12.93
≥ 25–< 60	36	40.88 ± 8.87	95.09 ± 13.21	155.93 ± 16.54
≥ 60	8	35.39 ± 9.05	102.17 ± 11.09	164.23 ± 13.82
F value		11.755	10.027	17.025
P value		0.000	0.000	0.000

LVEDV: Left ventricular end-diastolic volume; LVEF: Left ventricular ejection fraction; LVESV: Left ventricular end-systolic volume.

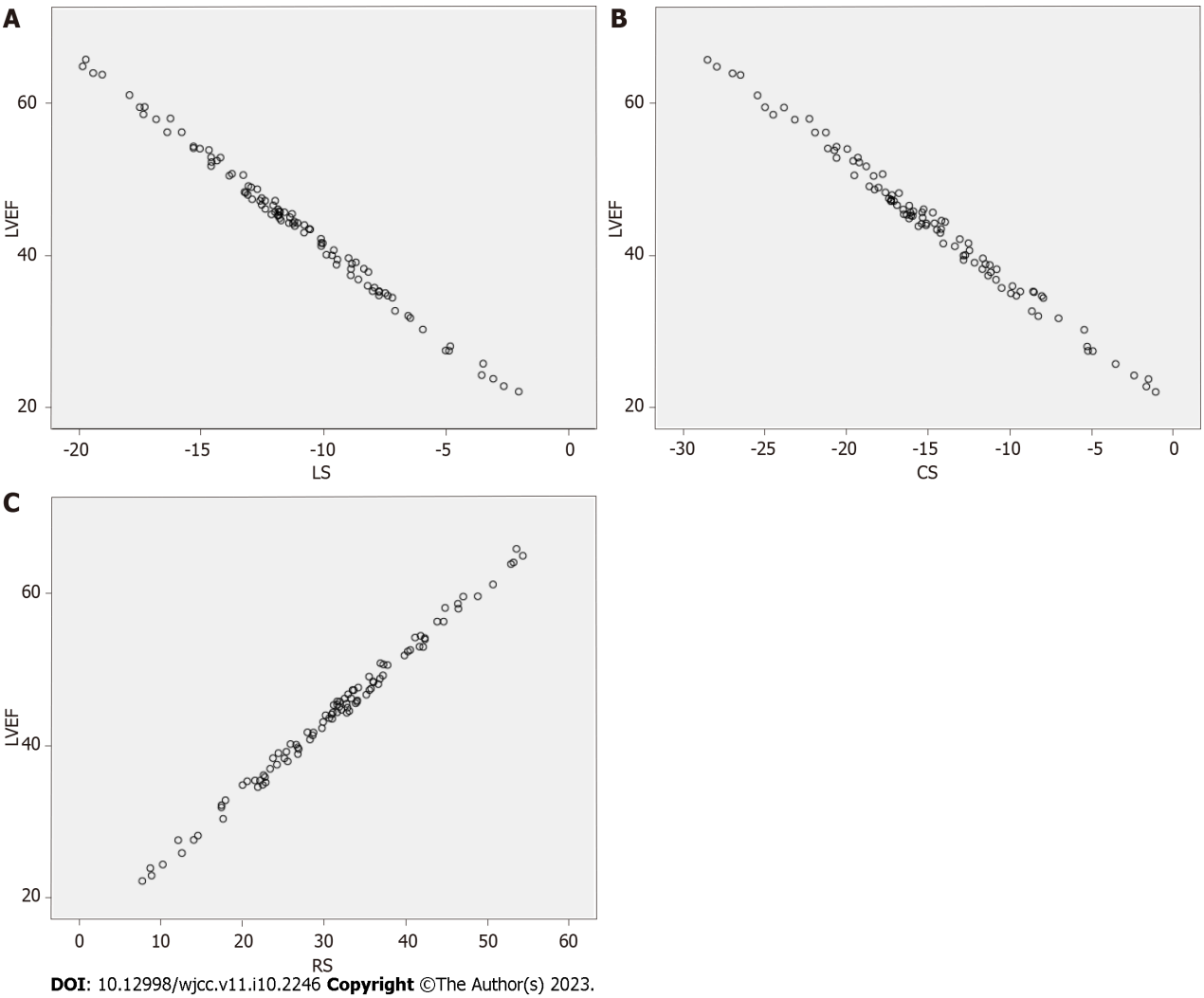

DOI: 10.12998/wjcc.v11.i10.2246

Figure 2 Interaction between the left ventricular ejection fraction and left ventricular strain. A: Longitudinal strains; B: Circumferential strain; C: Radial strain. LVEF: Left ventricular ejection fraction; LS: Longitudinal strain; CS: Circumferential strain; RS: Radial strain.

Relationship between left ventricular function and coronary stenosis

In the observation group, the LVEF (r = -0.754) was significantly negatively correlated with and the LVESV (r = -0.682) and LVEDV (r = 0.701) were significantly positively correlated with coronary stenosis (P < 0.05).

DISCUSSION

Coronary heart disease is a prevalent clinical illness and major cause of disability and death[6]. Patients with coronary heart disease often have coronary obstruction or stenosis, which can lead to angina pectoris and myocardial infarction, reduce cardiac compliance, and cause heart failure and cardiac enlargement[7,8]. Moreover, when CAS exceeds 40%, the blood flow reserve function is significantly reduced; furthermore, when the degree of vascular stenosis exceeds 75%, the coronary resting blood flow decreases significantly because of increased vascular stenosis, resulting in impaired myocardial contractility[9]. Although coronary angiography has been used as the gold standard for evaluating and analyzing coronary heart disease, clinical use and patient acceptance rates are low because of its invasiveness[10,11]. Furthermore, the rapid development of medical science has resulted in the development of additional methods of evaluating left ventricular function. For example, MRI is a non-invasive method that is widely used in clinical practice, and it is one of the most accurate methods of evaluating the left ventricular volume[12].

The LVEF, LVEDV, and LVESV are the main indicators of the ability of the heart to pump blood; furthermore, they are important for evaluating coronary heart disease and predicting the survival rate of such patients[13,14]. The LVEF is the ratio of the left ventricular stroke volume to the end-diastolic volume, and it is one of the core values used for the basic evaluation of cardiac function in clinical practice[15]. MRI is the gold standard for assessing the LVEF and left ventricular function in clinical practice[16]. Myocardial strain, which has received much attention, is a quantitative measurement used to analyze myocardial deformation and to evaluate changes in the myocardial segment length[7]: positive myocardial strain indicates prolonged myocardial thickening, while negative myocardial strain indicates that the myocardium is thinning and shortening. Myocardial strain is expressed as a percentage[17]. Tissue tracking technology can be used to calculate myocardial strain during cardiac MRI and echocardiography; these results have good reproducibility and high clinical value[18]. The LS and CS of the observation group were higher than those of the control group; however, the RS of the observation group was lower than that of the control group. The results of the linear regression model analysis showed that LVS, LS, and CS were significantly inversely correlated with the LVEF; however, the RS was positively correlated with the LVEF. Further analysis demonstrated that the LVEF of the observation group was lower than that of the control group; however, the LVESV and LVEDV of the observation group were higher than those of the control group. Patients with different degrees of coronary stenosis had significantly different LVEF, LVESV, LVEDV, and Gensini scores. The LVEF significantly decreased and the LVESV and LVEDV increased with increasing Gensini scores. In the observation group, the LVEF was significantly negatively correlated with and the LVESV and LVEDV were positively correlated with coronary stenosis. This research suggested that the degree of coronary artery disease can be systematically estimated by using MRI to detect the LVEF. Myocardial ischemia and hypoxia in patients with CAS induce degeneration and necrosis of myocardial cells and lead to impaired myocardial contractility[19]. With weakened myocardial contractility of the left atrium, the ejection capacity decreases, which causes blood to remain in the left atrium and left ventricle, resulting in increased end-systolic and end-diastolic volumes, left ventricular remodeling, and reduced cardiac systolic function. Therefore, the LVEF decreased significantly with increasing Gensini scores.

CONCLUSION

The LVEF, when measured using MRI, showed a significant linear correlation with LVS and a negative correlation with coronary stenosis. This study did not conduct a long-term follow-up of the patients, and did not include patients from other institutions. Therefore, further exploration and research are necessary in this regard.

ARTICLE HIGHLIGHTS

Research background

Coronary artery stenosis (CAS) is a common term for the buildup of plaque in the heart's arteries that could lead to a heart attack. However, the relationship between various cardiac function indicators and CAS is rarely studied.

Research motivation

CAS is one of the major cardiovascular diseases affecting humans worldwide. This disease has been shown to be the leading cause of death in both developed and developing countries. Exploring the correlation between cardiac function indicators and CAS will benefit the patients.

Research objectives

The purpose of our study was to analyze the correlation between the left ventricular ejection fraction (LVEF), left ventricular strain (LVS), and coronary stenosis.

Research methods

The control group comprised 93 healthy individuals, while the observation group comprised 97 patients with coronary artery disease who were hospitalized between July 2020 and September 2021. Coronary artery disease was assessed using the Gensini score, and LVEF and LVS were measured using magnetic resonance imaging. The interaction between LVEF and LVS was investigated using a linear regression model, while the relationship between LVEF and CAS was examined using Spearman's correlation.

Research results

The LVEF of the observation group was lower than that of the control group. The left ventricular end-systolic volume (LVESV) and left ventricular end-diastolic volume (LVEDV) of the observation group were significantly higher than those of the control group. The longitudinal strain (LS) and circumferential strain (CS) of the observation group were significantly higher than those of the control group; however, the radial strain (RS) of the observation group was lower than that of the control group. LVS, LS, and CS were significantly negatively correlated with the LVEF, while RS was positively correlated with the LVEF. There were significant differences in the LVEF, LVESV, and LVEDV of patients with different Gensini scores. The LVEF significantly decreased and the LVESV and LVEDV increased with increasing Gensini scores. In the observation group, the LVEF was negatively correlated and the LVESV and LVEDV were positively correlated with coronary stenosis.

Research conclusions

The LVEF showed a significant linear correlation with LVS and negative correlation with coronary stenosis.

Research perspectives

This study did not follow patients over time and did not include patients from other institutions. Therefore, further exploration and research are necessary.

FOOTNOTES

Author contributions: Gui HY designed and performed the research and wrote the manuscript; Liu SW contributed to the analysis and revised the manuscript; Zhu DF supervised the research.

Institutional review board statement: This study was approved by the ethics committee of Harbin No. 4 Hospital.

Informed consent statement: Written informed consent was obtained from all study participants or their legal guardian prior to study enrollment.

Conflict-of-interest statement: The authors have no conflicts of interest to reported.

Data sharing statement: All datasets are available from the corresponding author.

STROBE statement: The authors have read the STROBE Statement - checklist of items, and the manuscript was prepared and revised according to the STROBE Statement - checklist of items.

Country/Territory of origin: China

ORCID number: Hai-Yan Gui 0000-0002-5290-5018; Shu-Wen Liu 0000-0001-6461-0041; Dong-Fang Zhu 0000-0002-1415-1753.

S-Editor: Wang JL
L-Editor: A
P-Editor: Wang JL

REFERENCES

1 **Pewowaruk RJ**, Barton GP, Johnson C, Ralphe JC, Francois CJ, Lamers L, Roldán-Alzate A. Stent interventions for pulmonary artery stenosis improve bi-ventricular flow efficiency in a swine model. *J Cardiovasc Magn Reson* 2021; **23**: 13 [PMID: 33627121 DOI: 10.1186/s12968-021-00709-4]

2 **Calin A**, Mateescu AD, Popescu AC, Bing R, Dweck MR, Popescu BA. Role of advanced left ventricular imaging in adults with aortic stenosis. *Heart* 2020; **106**: 962-969 [PMID: 32179586 DOI: 10.1136/heartjnl-2019-315211]

3 **Marques-Alves P**, Marinho AV, Teixeira R, Baptista R, Castro G, Martins R, Gonçalves L. Going beyond classic echo in aortic stenosis: left atrial mechanics, a new marker of severity. *BMC Cardiovasc Disord* 2019; **19**: 215 [PMID: 31601185 DOI: 10.1186/s12872-019-1204-2]

4 **Ando K**, Nagao M, Watanabe E, Sakai A, Suzuki A, Nakao R, Ishizaki U, Sakai S, Hagiwara N. Association between myocardial hypoxia and fibrosis in hypertrophic cardiomyopathy: analysis by T2* BOLD and T1 mapping MRI. *Eur Radiol* 2020; **30**: 4327-4336 [PMID: 32211964 DOI: 10.1007/s00330-020-06779-9]

5 **Wang BL**, Li HJ, Wu YA, Dai WR, Li YH, Guo W, Pan BS. [Correlation between serum biochemical parameters and the degree of coronary artery stenosis in patients with coronary heart disease]. *Jianyan Yixue* 2020; **35**: 12-16 [DOI: 10.3969/j.issn.1673-8640.2020.01.002]

6 **Isaza N**, Desai MY, Kapadia SR, Krishnaswamy A, Rodriguez LL, Grimm RA, Conic JZ, Saijo Y, Roselli EE, Gillinov AM, Johnston DR, Svensson LG, Griffin BP, Popović ZB. Long-Term Outcomes in Patients With Mixed Aortic Valve Disease and Preserved Left Ventricular Ejection Fraction. *J Am Heart Assoc* 2020; **9**: e014591 [PMID: 32204665 DOI: 10.1161/JAHA.119.014591]

7 **Zhang LJ**, Tian JF, Yang XY, Xu L, He Y, Song XT. [Clinical value of left ventricular strain analysis by cardiovascular magnetic resonance in patients with coronary chronic total occlusion]. *Zhonghua Xin Xue Guan Bing Za Zhi* 2021; **49**: 601-609 [PMID: 34126728 DOI: 10.3760/cma.j.cn112148-20201217-00992]

8 **Roumeliotis AG**, Power D, Reisman AM, Sartori S, Cao D, Zhang Z, Chiarito M, Chandiramani R, Nicolas J, Goel R, Claessen B. E, Sweeny J, Dangas GD, Mehran R, Kini AS, Sharma SK. TCT CONNECT-307 Long-Term Outcomes After Coronary Intervention With Drug Eluting Stents for Unprotected Left Main Coronary Artery Stenosis According to Diabetes Mellitus Status. *J Am Coll Cardiol* 2020; **76**: B132 [DOI: 10.1016/j.jacc.2020.09.327]

9 **Zuo WJ**, Yang MM, Chen YF, Xie AM, Chen LJ, Ma GS. [Analysis of factors related to functional ischemia based on FFR and its diagnostic value]. *Linchuang Xinxueguanbing Zazhi* 2019; **35**: 55-59 [DOI: 10.13201/j.issn.1001-1439.2019.04.013]

10 **Dhillon AS**, Narayanan MR, Tun H, Hindoyan A, Matthews R, Mehra A, Shavelle DM, Clavijo LC. In-Hospital Outcomes of Rotational Atherectomy in High-Risk Patients With Severely Calcified Left Main Coronary Artery Disease: A Single-Center Experience. *J Invasive Cardiol* 2019; **31**: 101-106 [PMID: 30643039]

11 **Jerzy S**, Krawczyk K, Gierlotka M. Fully percutaneous insertion and removal of the Impella CP *via* a subclavian approach. *Postepy Kardiol Interwencyjnej* 2020; **16**: 343-346 [PMID: 33598002 DOI: 10.5114/aic.2020.99273]

12 **Yuan JH**, Yang J. [The value of MRI and ultrasound in evaluating left ventricular function in patients with hypertension and ventricular hypertrophy]. *Zhongguo CT he MRI Zazhi* 2019; **17**: 40-43 [DOI: 10.3969/j.issn.1672-5131.2019.03.013]

13 **Wang J**, Shi K, Xu HY, Zhao Q, Liu X, Gao Y, Yu H, Guo YK, Yang ZG. Left Ventricular Deformation in Patients with Connective Tissue Disease: Evaluated by 3.0T Cardiac Magnetic Resonance Tissue Tracking. *Sci Rep* 2019; **9**: 17913 [PMID: 31784546 DOI: 10.1038/s41598-019-54094-1]

14 **Kitano T**, Nabeshima Y, Otsuji Y, Negishi K, Takeuchi M. Accuracy of Left Ventricular Volumes and Ejection Fraction Measurements by Contemporary Three-Dimensional Echocardiography with Semi- and Fully Automated Software: Systematic Review and Meta-Analysis of 1,881 Subjects. *J Am Soc Echocardiogr* 2019; **32**: 1105-1115.e5 [PMID: 31230780 DOI: 10.1016/j.echo.2019.04.417]

15 **Le TT**, Ang BWY, Bryant JA, Chin CY, Yeo KK, Wong PEH, Ho KW, Tan JWC, Lee PT, Chin CWL, Cook SA. Multiparametric exercise stress cardiovascular magnetic resonance in the diagnosis of coronary artery disease: the EMPIRE trial. *J Cardiovasc Magn Reson* 2021; **23**: 17 [PMID: 33658056 DOI: 10.1186/s12968-021-00705-8]

16 **Chang MC**, Wu MT, Weng KP, Chien KJ, Lin CC, Su MY, Lin KL, Chang MH, Peng HH. Biventricular myocardial adaptation in patients with repaired tetralogy of Fallot: Mechanistic insights from magnetic resonance imaging tissue phase mapping. *PLoS One* 2020; **15**: e0237193 [PMID: 32780780 DOI: 10.1371/journal.pone.0237193]

17 **Schwaiger JP**, Reinstadler SJ, Tiller C, Holzknecht M, Reindl M, Mayr A, Graziadei I, Müller S, Metzler B, Klug G. Baseline LV ejection fraction by cardiac magnetic resonance and 2D echocardiography after ST-elevation myocardial infarction - influence of infarct location and prognostic impact. *Eur Radiol* 2020; **30**: 663-671 [PMID: 31428825 DOI: 10.1007/s00330-019-06316-3]

18 **Kordalis AA**, Gatzoulis KA, Arsenos PP, Tsiachris DL, Tsioufis CP. Magnetic Resonance for Risk Stratification of Coronary Artery Disease Patients: Toward an Electrophysiology-Guided Approach? *J Am Coll Cardiol* 2021; **77**: 2157 [PMID: 33888257 DOI: 10.1016/j.jacc.2021.02.052]

19 **Brown J**, Coulthard A, Dixon AK, Dixon JM, Easton DF, Eeles RA, Evans DG, Gilbert FG, Hayes C, Jenkins JP, Leach MO, Moss SM, Padhani AP, Pointon LJ, Ponder BA, Sloane JP, Turnbull LW, Walker LG, Warren RM, Watson W; UK MRI Breast Screening Study Advisory Group. Rationale for a national multi-centre study of magnetic resonance imaging screening in women at genetic risk of breast cancer. *Breast* 2000; **9**: 72-77 [PMID: 14731702 DOI: 10.1054/brst.2000.0135]

World Journal of Clinical Cases

Submit a Manuscript: https://www.f6publishing.com

World J Clin Cases 2023 April 6; 11(10): 2254-2259

DOI: 10.12998/wjcc.v11.i10.2254

ISSN 2307-8960 (online)

CASE REPORT

Neonatal hyperinsulinism with an *ABCC8* mutation: A case report

Meng-Tong Liu, Hui-Xia Yang

Specialty type: Obstetrics and gynecology

Provenance and peer review: Unsolicited article; Externally peer reviewed.

Peer-review model: Single blind

Peer-review report's scientific quality classification

Grade A (Excellent): A
Grade B (Very good): 0
Grade C (Good): C
Grade D (Fair): D
Grade E (Poor): 0

P-Reviewer: Lang FC, United States; Redkar RG, India

Received: October 13, 2022
Peer-review started: October 13, 2022
First decision: December 13, 2022
Revised: January 16, 2023
Accepted: February 15, 2023
Article in press: February 15, 2023
Published online: April 6, 2023

Meng-Tong Liu, Hui-Xia Yang, Department of Gynecology and Obstetrics, Peking University First Hospital, Beijing 100034, China

Corresponding author: Hui-Xia Yang, PhD, Professor, Department of Gynecology and Obstetrics, Peking University First Hospital, No. 1 Xi'anmen Street, Beijing 100034, China. yanghuixia@bjmu.edu.cn

Abstract

BACKGROUND

Neonatal hyperinsulinism can result from perinatal stress, genetic disorders, or syndromes, which can lead to persistent or intractable hypoglycemia in newborns. Mutations in the *ABCC8* gene result in abnormal functioning of potassium channel proteins in pancreatic β-cells, leading to an overproduction of insulin and congenital hyperinsulinemia.

CASE SUMMARY

We report a case of a high-birth-weight infant with postnatal hypoglycemia and hyperinsulinemia, whose mother had pregestational diabetes mellitus with poor glycemic control and whose sister had a similar history at birth. Whole-exome sequencing revealed a new mutation in the *ABCC8* gene in exon 8 (c.1257T>G), which also occurred in his sister and mother; thus, the patient was diagnosed with neonatal hyperinsulinism with an *ABCC8* mutation. With oral diazoxide treatment, the child's blood glucose returned to normal, and the pediatrician gradually discontinued treatment because of the child's good growth and development.

CONCLUSION

We report a new mutation locus in the *ABCC8* gene. This mutation locus warrants attention for genetic disorders and long-term prognoses of hypoglycemic children.

Key Words: Newborn; Hypoglycemia; Congenital hyperinsulinism; *ABCC8*; Hyperglycemia in pregnancy; Case report

Core Tip: Neonatal hyperinsulinemia can have multiple causes. Persistent hypoglycemia caused by a genetic mutation is difficult to correct by conventional glucose and hydrocortisone infusion treatments, which may lead to adverse outcomes. In this case, the newborn had a family history of hypoglycemia and hyperinsulinism, was exposed to perinatal stress, and exhibited a mutation locus in the *ABCC8* gene in exon 8 (c.1257T>G), which has not been previously reported. With diazoxide treatment, the child recovered well, and family genetic examinations showed a good prognosis.

Citation: Liu MT, Yang HX. Neonatal hyperinsulinism with an *ABCC8* mutation: A case report. *World J Clin Cases* 2023; 11(10): 2254-2259
URL: https://www.wjgnet.com/2307-8960/full/v11/i10/2254.htm
DOI: https://dx.doi.org/10.12998/wjcc.v11.i10.2254

INTRODUCTION

Neonatal hyperinsulinemia occurs in three types: Perinatal-stress-related, monogenic, and syndromic (*e.g.*, Beckwith-Wiedemann syndrome). Primarily resulting from single gene defects, congenital hyperinsulinism (CHI) can cause infants to be large for their gestational age and can lead to persistent or intractable hypoglycemia, seizures, and potentially hypoglycemic encephalopathy. This condition can arise from mutations in common genes such as *ABCC8* and KCN1, which can be autosomal recessive or dominant[1]. In the general population, the prevalence of CHI is approximately 1/50000-1/28000, reaching up to 1/2700 in consanguineous couples[2].

The *ABCC8* gene, located on chromosome 11p15,1, encodes the sulfonylurea receptor 1 subunit of the pancreatic β-cell ATP-sensitive potassium channel protein (KATP), which regulates the flux of K+ ions and binds glucose *via* membrane electrical activity and insulin release. Mutations in the *ABCC8* gene result in abnormal functioning of the potassium channel protein, such as the deletion of membrane surface proteins and closure of potassium channels, causing pancreatic β-cells to overproduce insulin[3, 4], which results in CHI. Prognoses vary widely, ranging from adverse neurodevelopment and the need for lifelong medication to situations requiring no intervention[5].

Consequently, a better understanding of neonatal hypoglycemia and hyperinsulinism is needed. Quickly identifying the underlying genetic abnormalities in patients and improving genetic testing may be helpful for future treatments and prognoses. However, many reported genetic abnormalities remain undetected, and their genetic characteristics are unclear. Herein, we report a case of neonatal hyperinsulinism in a macrosomia male newborn with an *ABCC8* mutation located in exon 8 (c.1257T>G), which has not been previously reported. The effects of this mutation require further elucidation, but we propose that this genetic mutation combined with perinatal stress caused severe hyperinsulinism and hypoglycemia in this patient. We also present a review of previous studies, summarize clinical features and treatment methods, and identify potential prognostic factors for this mutation.

CASE PRESENTATION

Chief complaints

A large-for-gestational-age male newborn was brought to the neonatal intensive care unit because of mild asphyxia, with an APGAR score of 7/10/10. After two hours, the infant presented intractable hypoglycemia and hyperinsulinism.

History of present illness

This term male infant was born to nonconsanguineous parents on February 22, 2021, with a birth weight of 5020 g. This baby represented his mother's second gestation. The mother was 38 years old and was diagnosed with pregestational diabetes mellitus at 25 wk of gestation, with an oral glucose tolerance test value of 6.28-12.63-14.11 mmol/L, which was unsatisfactorily controlled by diet and treated by insulin. Her glycosylated hemoglobin changed from 6.10% (2020-12-16) to 6.40% (2021-1-20) and 6.10% (2021-2-18), and her glycosylated albumin changed from 17.52% (2020-12-16) to 15.19% (2020-12-28), 14.88% (2021-1-20), and 13.70% (2021-2-18).

History of past illness

The patient's mother had previously developed gestational diabetes (controlled with diet) during her first gestation, which occurred eight years ago.

Personal and family history

The patient's older sister was also large for her gestational age, with a birth weight of 4000 g. She presented severe hypoglycemia with brain damage after birth, but is currently in good condition.

Physical examination

The child showed an appearance of macrosomia with a ruddy complexion and good crying but a poor mental response. The oxygen saturation level was 70%-89%. The patient's breath sounds were mildly rough in both lungs. A pair of ears was visible on the right. The remainder of the physical examination showed no obvious abnormalities.

Laboratory examinations

The child had a minimum postnatal terminal glucose level of 2.70 mmol/L, minimum intravenous glucose level of 2.66 mmol/L, maximum insulin level of 122.60 μIU/mL, and C-peptide level of 17.08 ng/mL during this period. His blood and urine amino acid and organic acid metabolic screening showed no abnormalities.

The persistent hypoglycemia and hyperinsulinemia state of the child could not be explained by perinatal stress alone; thus, whole-exome sequencing was performed and identified a missense heterozygous mutation in the *ABCC8* gene in exon 8 (c.1257T>G), resulting in amino acid p.N419K (p.Asn419Lys). Unsurprisingly, genetic examinations of the family revealed similar mutations in the mother and sister but no variation in the father (Figure 1).

Imaging examinations

On day 1, the patient's postnatal electrocardiogram showed mild abnormalities: Multifocal spike and spike-wave issuance during sleep QS. Postnatal re-examinations on days 4 and 12 showed normal neonatal electroencephalography findings. A cranial ultrasound showed mild enhancement of cerebral white matter echogenicity; the ultrasound was later repeated and showed a reduction compared with the previous ultrasound. The ultrasound showed mild enhancement of bilateral paraventricular white matter echogenicity 11 d after birth. Cranial MRI did not show any significant abnormalities (Table 1).

FINAL DIAGNOSIS

The child was diagnosed with neonatal hyperinsulinism with an *ABCC8* mutation.

TREATMENT

The child was given endotracheal intubation and mechanical ventilation and was withdrawn from ventilator assistance 23 h after birth. He was initially treated with glucose and hydrocortisone infusion, but his blood glucose was still not well controlled. Next, he was treated with octreotide and glucagon, which did not provide satisfactory results; thus, he was treated with diazoxide, which was effective. The patient's condition was stable 25 d after birth, and he was discharged from the hospital and continued to take diazoxide orally.

OUTCOME AND FOLLOW-UP

After discharge, the patient was treated at a local hospital, and the medication was tapered off. Currently, his blood glucose level is average, and his growth and development are acceptable. His mother's fasting glucose level is impaired.

DISCUSSION

A variety of CHI cases caused by mutations in the *ABCC8* gene have been previously reported in multiple countries. Snider *et al*[6] reviewed genetic variants in 417 children with CHI and reported 160 mutations in the *ABCC8* gene, 91 of which resulted in single-amino-acid changes. The mode of inheritance of CHI due to mutations in the *ABCC8* gene is primarily autosomal recessive. However, cases of paternal gene mutation with maternal chromosome deletion in the tissue of the pancreatic lesion often respond poorly to diazoxide treatment and require surgical resection treatment. The features of dominant KATP hyperinsulinemia differ substantially from those of recessive inheritance, including a retention of normal subunit transport and impaired channel activity. This mild hypoglycemic phenotype can usually be effectively treated by diazoxide and may even go undetected in

Table 1 Timeline

Time	Incidents
8 yr ago	The patient's mother was diagnosed gestational diabetes (controlled with diet) during her first gestation, and deliver a girl with a birth weight of 4000 g, who presented severe hypoglycemia with brain damage after birth
At the mother's 25th wk of gestation	The mother was diagnosed with pregestational diabetes mellitus and was treated by insulin
20 min after birth	The patient was diagnosed mild asphyxia, with an APGAR score of 7/10/10, and was brought to the neonatal intensive care unit
2 h after birth	The infant presented intractable hypoglycemia and hyperinsulinism
During hospitalization	He was initially treated with glucose and hydrocortisone infusion. Next, he was treated with octreotide and glucagon. whole-exome sequencing was performed because the upper treatments are ineffective. Thus, he was treated with diazoxide, which was effective
25 d after birth	The patient was discharged from the hospital and continued to take diazoxide orally, and the medication was tapered off
30 d after birth	The whole-exome sequencing identified a missense heterozygous mutation in the *ABCC8*
Now	The patient's blood glucose level is average, and his growth and development are acceptable. His mother's fasting glucose level is impaired

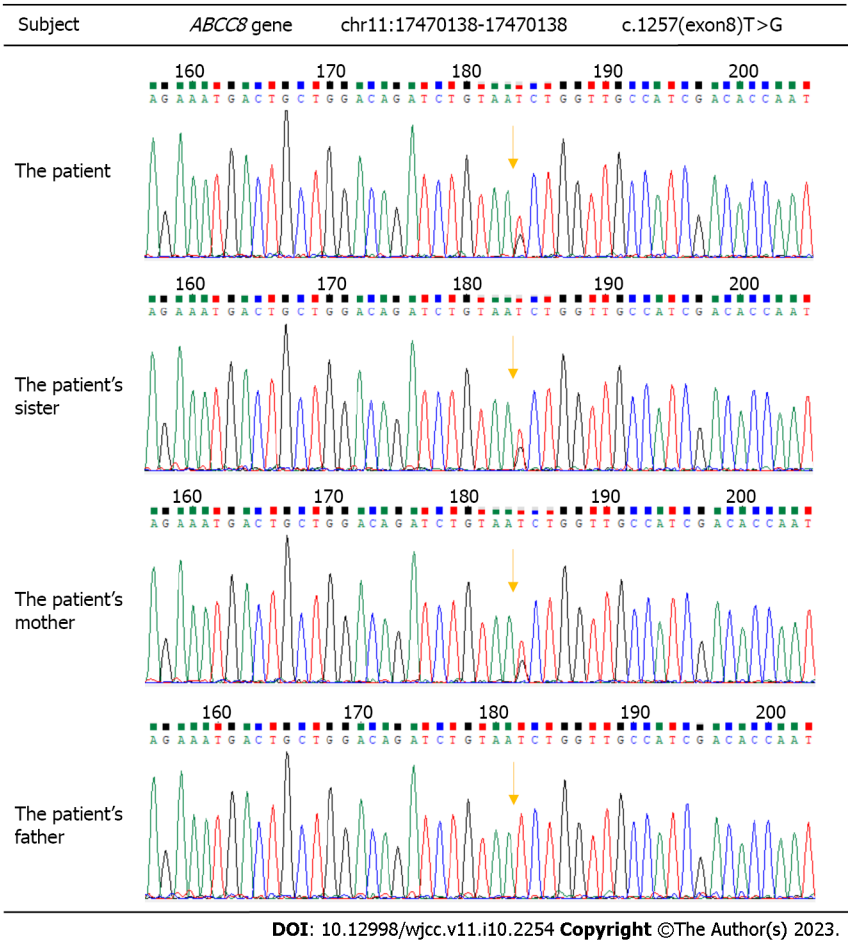

DOI: 10.12998/wjcc.v11.i10.2254

Figure 1 Sanger sequencing results of the *ABCC8* gene in the child, his sister, and his parents. A c.1257 mutation (thymine displacement in coding region no. 1257) occurred in the *ABCC8* gene in the child and his sister. The mutation derived from the patient's mother.

the absence of clinical symptoms. This phenotype also has a better prognosis, with the hypoglycemic component resolving spontaneously, and in some cases, treatment can be stopped altogether[7]. From a histopathological viewpoint, CHI is roughly divided into diffuse and focal types, with surgical lesion resection being the treatment of choice for the latter. For diffuse CHI, which appears to predominantly arise from paternally inherited mutations[8], a pharmacological approach is considered as the first line of treatment[5].

In this case, the child's mother had gestational diabetes mellitus with poor glycemic control and macrosomia. The intrauterine fetus was exposed to high glucose levels during development, which led to an excessive activation of pancreatic islet cells and overproduction of insulin. Research has shown that these conditions result in a significantly higher incidence of hypoglycemia among newborns; thus, it was considered that the child was born with hypoglycemia and high insulin due to perinatal stress and his mother's poor glycemic control during pregnancy. However, theoretically, the mother's blood glucose did not reach a sufficiently high level to cause the degree of hyperinsulinemia observed in the child. Moreover, the child's sister showed similar symptoms at birth, despite her mother having reasonable glycemic control during her pregnancy; therefore, familial CHI could not be excluded. The child was found to have an *ABCC8* missense heterozygous mutation [c.1257(exon8)T>G]. Both his mother and sister had similar mutations, and diazoxide was effective in treating the child's hypoglycemia with a good follow-up prognosis. Hence, it was considered that maternal autosomal dominant inheritance may have led to CHI.

Similar cases of macrosomia combined with transient CHI have been attributed to dominant mutations in *ABCC8*[9,10]. A mild form of CHI channel activity with a reduced KATP pathway in infancy can be effectively treated with the potassium channel opener diazoxide, with a good prognosis; however, by the time these patients reach adulthood, this mutation leads to decreased insulin secretion capacity and glucose intolerance, and long-term prognoses may be associated with diabetes[10-12]. Kassem *et al*[13] studied 23 children with CHI and found that the natural disease course may lead to progressive glucose intolerance and diabetes mellitus. It has also been recently reported that multifarious *ABCC8* genetic variants cause early-onset diabetes in Chinese individuals[14]. This condition may be caused by increased β-cell apoptosis and slow progressive loss of insulin secretory function. These findings suggest that attention should be given to the long-term glycemic situation of this child and his sister, although the effects of the mutation locus in exon 8 (c.1257T>G) are not yet clear.

Upon searching the Human Gene Mutation Database, we found no previous reports related to mutations at the c.1257 Locus similar to the mutation in this child; thus, the effect of such mutations on protein expression requires further investigation. A total of approximately 180 variants of unknown significance (VUSs) have been reported for the *ABCC8* gene[3], accounting for approximately 15% of the clinically reported variants found in CHI. It has been proposed that variant-induced splicing alterations may be the primary mechanism of inheritance. Therefore, functional analysis may be required for further pathogenicity assessment to clarify VUSs or phenotype-associated *ABCC8* mutations[15].

This case report provides insights for perinatal medicine practitioners when neonatal hypoglycemia or hyperinsulinemia is not easily corrected. Apart from considering the association with maternal glycemic control, the possibility of a single gene defect should be considered to inform the long-term prognosis of the child and subsequent pregnancies of the mother.

CONCLUSION

Neonatal hyperinsulinemia can arise from multiple causes. Genetic causes such as *ABCC8* mutations should be considered when a persistent hypoglycemic state cannot be explained by perinatal stress alone. In such cases, genetic testing is recommended. Moreover, genetic testing may help in developing individual treatment plans and predicting outcomes and future impacts for these newborns and their families.

FOOTNOTES

Author contributions: Liu MT contributed to manuscript writing and editing, data collection, and data analysis; Yang HX contributed to conceptualization and supervision; all authors have read and approved the final manuscript.

Informed consent statement: Informed written consent was obtained from the patients for the publication of this report and any accompanying images.

Conflict-of-interest statement: The authors declare that they have no conflict of interest to disclose.

CARE Checklist (2016) statement: The authors have read the CARE Checklist (2016), and the manuscript was prepared and revised according to the CARE Checklist (2016).

Country/Territory of origin: China

ORCID number: Meng-Tong Liu 0000-0002-7309-607X; Hui-Xia Yang 0000-0001-8154-4007.

S-Editor: Chen YL
L-Editor: A
P-Editor: Chen YL

REFERENCES

1 **James C**, Kapoor RR, Ismail D, Hussain K. The genetic basis of congenital hyperinsulinism. *J Med Genet* 2009; **46**: 289-299 [PMID: 19254908 DOI: 10.1136/jmg.2008.064337]
2 **Yau D**, Laver TW, Dastamani A, Senniappan S, Houghton JAL, Shaikh G, Cheetham T, Mushtaq T, Kapoor RR, Randell T, Ellard S, Shah P, Banerjee I, Flanagan SE. Using referral rates for genetic testing to determine the incidence of a rare disease: The minimal incidence of congenital hyperinsulinism in the UK is 1 in 28,389. *PLoS One* 2020; **15**: e0228417 [PMID: 32027664 DOI: 10.1371/journal.pone.0228417]
3 **De Franco E**, Saint-Martin C, Brusgaard K, Knight Johnson AE, Aguilar-Bryan L, Bowman P, Arnoux JB, Larsen AR, Sanyoura M, Greeley SAW, Calzada-León R, Harman B, Houghton JAL, Nishimura-Meguro E, Laver TW, Ellard S, Del Gaudio D, Christesen HT, Bellanné-Chantelot C, Flanagan SE. Update of variants identified in the pancreatic β-cell K(ATP) channel genes KCNJ11 and *ABCC8* in individuals with congenital hyperinsulinism and diabetes. *Hum Mutat* 2020; **41**: 884-905 [PMID: 32027066 DOI: 10.1002/humu.23995]
4 **Stanley CA**. Perspective on the Genetics and Diagnosis of Congenital Hyperinsulinism Disorders. *J Clin Endocrinol Metab* 2016; **101**: 815-826 [PMID: 26908106 DOI: 10.1210/jc.2015-3651]
5 **Banerjee I**, Salomon-Estebanez M, Shah P, Nicholson J, Cosgrove KE, Dunne MJ. Therapies and outcomes of congenital hyperinsulinism-induced hypoglycaemia. *Diabet Med* 2019; **36**: 9-21 [PMID: 30246418 DOI: 10.1111/dme.13823]
6 **Snider KE**, Becker S, Boyajian L, Shyng SL, MacMullen C, Hughes N, Ganapathy K, Bhatti T, Stanley CA, Ganguly A. Genotype and phenotype correlations in 417 children with congenital hyperinsulinism. *J Clin Endocrinol Metab* 2013; **98**: E355-E363 [PMID: 23275527 DOI: 10.1210/jc.2012-2169]
7 **Pinney SE**, MacMullen C, Becker S, Lin YW, Hanna C, Thornton P, Ganguly A, Shyng SL, Stanley CA. Clinical characteristics and biochemical mechanisms of congenital hyperinsulinism associated with dominant KATP channel mutations. *J Clin Invest* 2008; **118**: 2877-2886 [PMID: 18596924 DOI: 10.1172/JCI35414]
8 **Bellanné-Chantelot C**, Saint-Martin C, Ribeiro MJ, Vaury C, Verkarre V, Arnoux JB, Valayannopoulos V, Gobrecht S, Sempoux C, Rahier J, Fournet JC, Jaubert F, Aigrain Y, Nihoul-Fékété C, de Lonlay P. *ABCC8* and KCNJ11 molecular spectrum of 109 patients with diazoxide-unresponsive congenital hyperinsulinism. *J Med Genet* 2010; **47**: 752-759 [PMID: 20685672 DOI: 10.1136/jmg.2009.075416]
9 **Kole MB**, Ayala NK, Clark MA, Has P, Esposito M, Werner EF. Factors Associated With Hypoglycemia Among Neonates Born to Mothers With Gestational Diabetes Mellitus. *Diabetes Care* 2020; **43**: e194-e195 [PMID: 33051333 DOI: 10.2337/dc20-1261]
10 **Kapoor RR**, Flanagan SE, James CT, McKiernan J, Thomas AM, Harmer SC, Shield JP, Tinker A, Ellard S, Hussain K. Hyperinsulinaemic hypoglycaemia and diabetes mellitus due to dominant *ABCC8*/KCNJ11 mutations. *Diabetologia* 2011; **54**: 2575-2583 [PMID: 21674179 DOI: 10.1007/s00125-011-2207-4]
11 **Huopio H**, Otonkoski T, Vauhkonen I, Reimann F, Ashcroft FM, Laakso M. A new subtype of autosomal dominant diabetes attributable to a mutation in the gene for sulfonylurea receptor 1. *Lancet* 2003; **361**: 301-307 [PMID: 12559865 DOI: 10.1016/S0140-6736(03)12325-2]
12 **Hussain K**, Cosgrove KE. From congenital hyperinsulinism to diabetes mellitus: the role of pancreatic beta-cell KATP channels. *Pediatr Diabetes* 2005; **6**: 103-113 [PMID: 15963039 DOI: 10.1111/j.1399-543X.2005.00109.x]
13 **Kassem SA**, Ariel I, Thornton PS, Scheimberg I, Glaser B. Beta-cell proliferation and apoptosis in the developing normal human pancreas and in hyperinsulinism of infancy. *Diabetes* 2000; **49**: 1325-1333 [PMID: 10923633 DOI: 10.2337/diabetes.49.8.1325]
14 **Li M**, Gong S, Han X, Zhang S, Ren Q, Cai X, Luo Y, Zhou L, Zhang R, Liu W, Zhu Y, Zhou X, Sun Y, Li Y, Ma Y, Ji L. Genetic variants of *ABCC8* and phenotypic features in Chinese early onset diabetes. *J Diabetes* 2021; **13**: 542-553 [PMID: 33300273 DOI: 10.1111/1753-0407.13144]
15 **Saint-Martin C**, Cauchois-Le Mière M, Rex E, Soukarieh O, Arnoux JB, Buratti J, Bouvet D, Frébourg T, Gaildrat P, Shyng SL, Bellanné-Chantelot C, Martins A. Functional characterization of *ABCC8* variants of unknown significance based on bioinformatics predictions, splicing assays, and protein analyses: Benefits for the accurate diagnosis of congenital hyperinsulinism. *Hum Mutat* 2021; **42**: 408-420 [PMID: 33410562 DOI: 10.1002/humu.24164]

World Journal of Clinical Cases

Submit a Manuscript: https://www.f6publishing.com

World J Clin Cases 2023 April 6; 11(10): 2260-2266

DOI: 10.12998/wjcc.v11.i10.2260

ISSN 2307-8960 (online)

CASE REPORT

Unilateral contrast-induced encephalopathy with contrast medium exudation: A case report

Zhi-Yuan Zhang, Hang Lv, Pei-Jian Wang, Dan-Yang Zhao, Li-Yong Zhang, Ji-Yue Wang, Ji-Heng Hao

Specialty type: Neurosciences

Provenance and peer review: Unsolicited article; Externally peer reviewed.

Peer-review model: Single blind

Peer-review report's scientific quality classification

Grade A (Excellent): 0
Grade B (Very good): B
Grade C (Good): C, C
Grade D (Fair): D
Grade E (Poor): 0

P-Reviewer: Fernandes SA, Brazil; Pitton Rissardo J, Brazil; Tavan H, Iran

Received: November 3, 2022
Peer-review started: November 3, 2022
First decision: December 26, 2022
Revised: February 8, 2023
Accepted: March 3, 2023
Article in press: March 3, 2023
Published online: April 6, 2023

Zhi-Yuan Zhang, Pei-Jian Wang, Li-Yong Zhang, Ji-Yue Wang, Ji-Heng Hao, Department of Neurosurgery, Liaocheng People's Hospital, Liaocheng 252001, Shandong Province, China

Hang Lv, School of Clinical Medicine, Weifang Medical University, Weifang 261053, Shandong Province, China

Dan-Yang Zhao, Department of Neurology, Shenyang First People's Hospital, Shenyang 110041, Liaoning Province, China

Corresponding author: Ji-Heng Hao, Doctor, Professor, Department of Neurosurgery, Liaocheng People's Hospital, No. 45 Huashan Road, Economic Development Zone, Dongchangfu District, Liaocheng 252001, Shandong Province, China. haojiheng@163.com

Abstract

BACKGROUND

Contrast-induced encephalopathy (CIE) is a rare transient, reversible abnormality in the structure or function of the nervous system caused by the intravascular use of contrast agents. CIE can present with a range of neurological manifestations, including focal neurological deficits (hemiplegia, hemianopia, cortical blindness, aphasia, and parkinsonism) and systemic symptoms (confusion, seizures, and coma). However, if not accurately diagnosed and treated in a timely manner, CIE can cause irreversible damage to patients, especially critically ill patients.

CASE SUMMARY

A male in his 50 s, 2 h after digital subtraction angiography, had a progressive disorder of consciousness, mixed aphasia, bilateral pupillary sluggish light reflex, and right limb weakness. Seven hours after the procedure, he developed unconsciousness, high fever (39.5 °C), seizures, hemiplegia, neck stiffness (+), and right Babinski signs (+). computed tomography (CT) findings 2 h postprocedure were very confusing and led us to misdiagnose the patient with subarachnoid hemorrhage. Brain CT was performed again 7 h after the procedure. Compared with the CT 2 h after the procedure, the CT 7 h after the procedure showed that the manifestations of subarachnoid hemorrhage in the left cerebral hemisphere had disappeared and were replaced by brain tissue swelling, and the cerebral sulci had disappeared. Combined with the clinical manifestations of the patient and after the exclusion of subarachnoid hemorrhage and cerebrovascular embolism, we diagnosed the patient with CIE, and intravenous fluids were given for adequate hydration, as well as mannitol, albumin dehydration, furosemide and the glucocorticoid methylprednisolone. After 17 d of active treatment, the

patient was discharged with no sequelae.

CONCLUSION
CIE should be taken seriously, but it is easily misdiagnosed, and once CIE is diagnosed, rapid, accurate diagnosis and treatment are critical steps. Whether a follow-up examination using a contrast agent can be performed should be closely evaluated, and the patient should be fully informed of the associated risks.

Key Words: Contrast agents; Diagnosis; Encephalopathy; Mechanisms; Treatment

Core Tip: Contrast-induced encephalopathy (CIE) is a rare disease induced by the injection of contrast agents. In this case, unilateral CIE was caused by a long time of internal carotid arteriogram on left side and a large amount of contrast agent. The onset was misdiagnosed as subarachnoid hemorrhage at an early stage, and he was discharged without sequelae after 18 d of diagnosis and treatment of CIE. The main treatment measures are corticosteroids, dehydration and diuresis, and adequate hydration. Rapid, accurate diagnosis and treatment are critical steps. Whether the follow-up examination using contrast agent can be done should be closely evaluated and fully informed.

Citation: Zhang ZY, Lv H, Wang PJ, Zhao DY, Zhang LY, Wang JY, Hao JH. Unilateral contrast-induced encephalopathy with contrast medium exudation: A case report. *World J Clin Cases* 2023; 11(10): 2260-2266
URL: https://www.wjgnet.com/2307-8960/full/v11/i10/2260.htm
DOI: https://dx.doi.org/10.12998/wjcc.v11.i10.2260

INTRODUCTION

Contrast-induced encephalopathy (CIE) is a rare, transient, reversible abnormality in the structure or function of the nervous system caused by the intravascular use of contrast agents. It can present with a range of neurological manifestations, including focal neurological deficits (hemiplegia, hemianopia, cortical blindness, aphasia, and parkinsonism) and systemic symptoms (confusion, seizures, and coma) [1,2]. In general, the severity of the clinical manifestations of CIE varies, ranging from mild headache symptoms to severe clinical manifestations such as coma and even death. We report a case of severe unilateral contrast-induced encephalopathy characterized by acute unilateral hemispheric neurological dysfunction. The incidence of CIE is less than 1%, and unilateral concentration of lesions is less commonly reported. Compared with bilateral lesions, unilateral lesions are more confusing and need to be distinguished from subarachnoid hemorrhage and cerebrovascular embolism or spasm. This case is special in that the lesion was concentrated on one side (left side), the symptoms lasted for a long time, and the condition was misdiagnosed during the initial course of treatment. Our report aims to improve the awareness of this condition so as to provide early diagnosis and active treatment and effectively prevent the occurrence of irreversible damage to patients.

CASE PRESENTATION

Chief complaints

A male in his 50 s was admitted to the hospital because of "headache for 1 d".

History of present illness

The patient had episodic headache 1 d before without obvious causes. At that time, he recorded his blood pressure at 178/100 mmHg, and he took "valsartan". He had no rotatory vision and no nausea or vomiting.

History of past illness

A middle-aged male with a 10-year history of hypertension who was taking "valsartan" orally for treatment. He had a 3-year history of diabetes and was treated with oral "metformin" with unknown glycemic control.

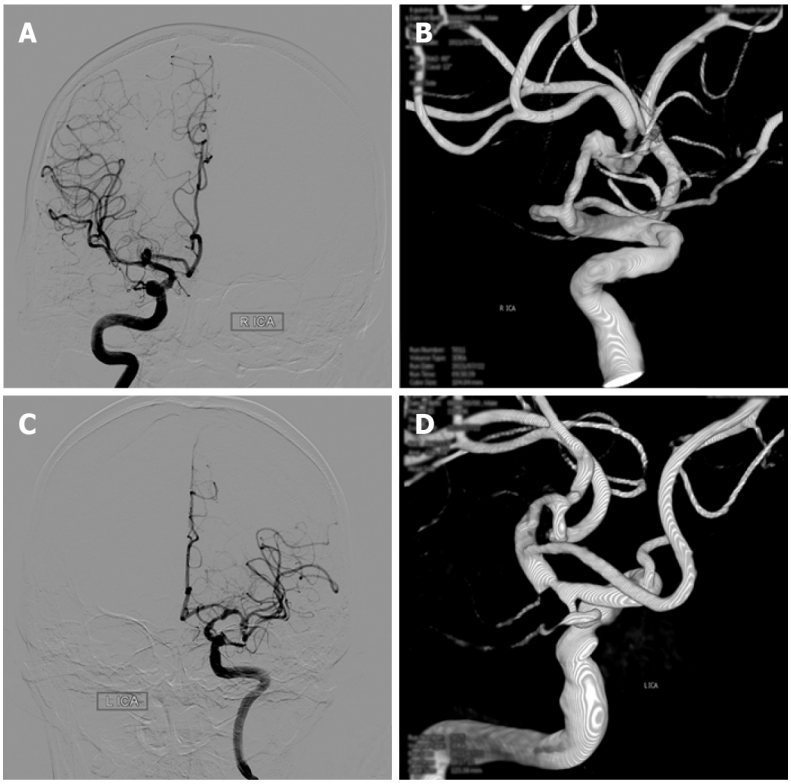

DOI: 10.12998/wjcc.v11.i10.2260 **Copyright** ©The Author(s) 2023.

Figure 1 Angiography of the intracranial aneurysm. A and B: The right middle cerebral artery aneurysm; C and D: Digital subtraction angiography showing the left internal carotid artery terminal aneurysm.

Personal and family history

The patient and his family had no relevant medical history.

Physical examination

Vital signs: R 22 times/min P 90 times/min H 170 cm T 36.2 °C W 75 kg BP 118/81 mmHg. The patient was conscious, with fluent speech and equal-sized and round pupils with a diameter of 3 mm. The presence of light reflex, flexible eye movements in all directions, bilateral nasolabial fold symmetry, and tongue protrusion to the left was noted. Other cranial nerves were normal. His limb muscle strength was grade 5 and muscle tension was acceptable, tendon reflexes (++), and bilateral pathological signs were negative. His sense of depth and lightness was normal, and motor function was normal.

Imaging examinations

Digital subtraction angiography (DSA) confirmed the diagnosis of a middle cerebral artery aneurysm (Figure 1). Two hours later, the patient suddenly had slurred speech, accompanied by right limb weakness. An emergency CT scan (within 15 min of onset) showed that the density of the interhemispheric cistern, the left fissure cistern, and the left part of the sulcus was increased (Figure 2). Subarachnoid hemorrhage was considered first and treated accordingly. Seven hours after DSA, the patient's condition significantly deteriorated, and the nervous system examination findings are shown in Table 1. A re-examination of the brain computed tomography (CT) showed significant changes: the temporal, parietal, and occipital lobes of the brain were swollen, the high-density shadows in the sulci and gyri had disappeared, and the sulci and gyri had become shallow and disappeared (Figure 2).

FINAL DIAGNOSIS

The patient was diagnosed as contrast-induced encephalopathy.

TREATMENT

CIE was considered at this time, and then the patient was given intravenous fluid for full hydration,

Table 1 Patient's nervous system physical examination during hospitalization

	Preoperative	2 h after DSA	7 h	3 d	6 d	On discharge
Vital signs	R 22 times/min; P 90 times/min; H 170 cm; T 36.2 °C; W 75 kg; BP 118/81 mmHg		High fever (39.5 °C)			
Nervous system examination findings	The patient was conscious, with fluent speech and equal-sized and round pupils with a diameter of 3 mm. The presence of light reflex, flexible eye movements in all directions, bilateral nasolabial fold symmetry, and tongue protrusion to the left was noted. Other cranial nerves were normal. His limb muscle strength was grade 5 and muscle tension was acceptable, tendon reflexes (++), and bilateral pathological signs were negative. His sense of depth and lightness was normal, and motor function was normal	He suddenly had slurred speech, accompanied by right limb weakness	He developed unconsciousness, high fever (39.5 °C), seizures, hemiplegia of the right limb, neck stiffness (+), and right Babinski signs (+)	His consciousness gradually improved, he was able to open eyes voluntarily, and he could answer simple questions even though he was not fluent in speech. His pupils were equal in size and round, with a diameter of 3 mm. His light reflex was sluggish, his eyes moved flexibly in all directions, and his bilateral nasolabial folds were symmetrical. His muscle tension of the four limbs was acceptable, the left limb movement was acceptable, the right limb muscle strength was grade 3, tendon reflexes (+), and right pathological signs (+)	The patient was clearly conscious, but his speech was still not fluent. The seizures did not recur.The muscle strength of the healthy limb recovered to grade 4	The patient was conscious and in good spirits. He had fluent speech. Both pupils were of equal size and were round, 3 mm in diameter. The presence of the light reflex, flexible eye movements in all directions, bilateral nasolabial fold symmetry, and tongue protrusion to the left (same as preprocedure) was noted. The remaining cranial nerves were not (see exception). The muscle strength of the limbs was grade 5, the muscle tension was acceptable, the tendon reflex (+), and the bilateral Babinski signs were negative

DSA: Digital subtraction angiography; R: Respiratory; P: Pulse; H: Height; W: Weight; BP: Blood pressure.

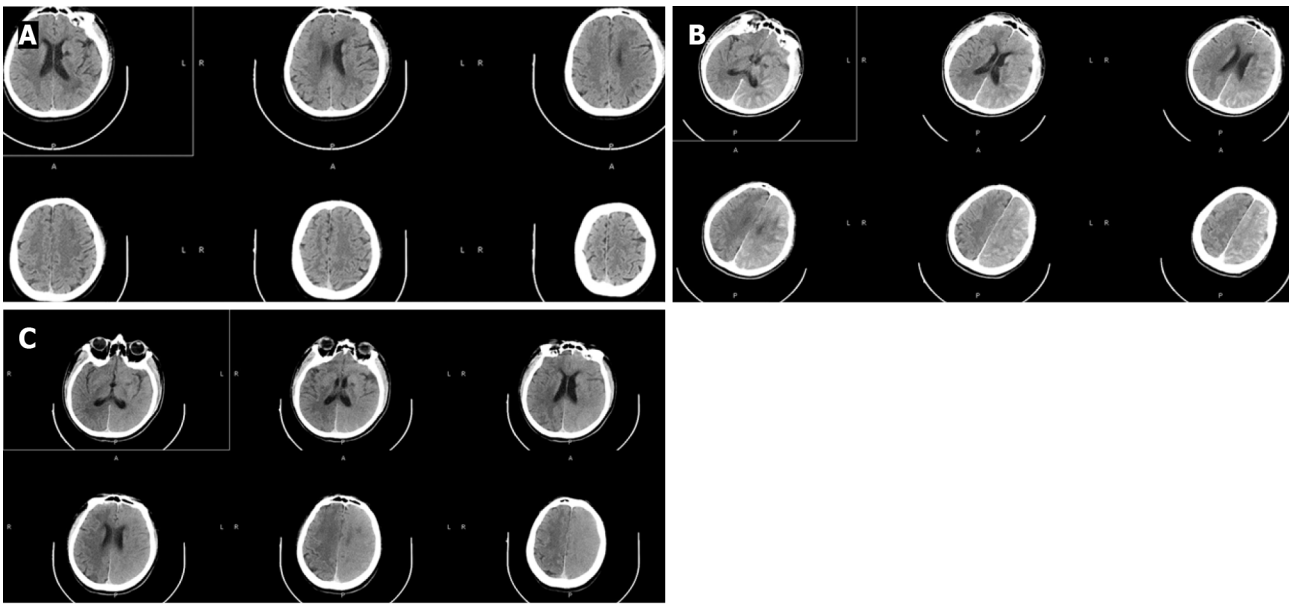

DOI: 10.12998/wjcc.v11.i10.2260

Figure 2 Computed tomography of the brain before and 2 h and 7 h after the procedure. A: The normal occipital lobe of the left cerebral hemisphere on the preprocedure computed Tomography (CT); B: The increased density of the interhemispheric cistern, left fissure cistern and part of the left sulcus on CT 2 h after digital subtraction angiography (DSA); C: Seven hours after DSA, indicating the swelling of the left frontal, temporal, parietal and occipital lobe brain tissue, the disappearance of the high-density shadow of sulci and gyri, the shallow appearance of the sulci and gyri, and the higher density of the left cerebral hemisphere than the right cerebral hemisphere.

including 20% mannitol 250 mL Q6H, albumin 10 g bid for dehydration and furosemide 20 mg bid to accelerate the excretion of contrast media and reduce cerebral edema; the glucocorticoid methylprednisolone 40 mg bid was given to protect the blood-brain barrier. However, the patient was still restless, with limb convulsions and grand mal seizures. After intravenous injection of diazepam 10 mg, the seizures stopped; continuous intravenous pump dexmedetomidine was continued, and continuous intravenous pump sodium valproate 1.2 g was added to combat epilepsy symptoms.

OUTCOME AND FOLLOW-UP

Three days after the treatment, the patient's consciousness gradually improved, and the nervous system examination findings are shown in Table 1. A repeat cranial CT showed that the swelling of brain tissue was significantly reduced, and there was no significant difference in the density of the bilateral cerebral hemispheres (Figure 3). On the 6th d, the patient was clearly conscious, but his speech was still not fluent, and his muscle strength level was 4. On the 17th d, there was no obvious abnormality in cranial magnetic resonance imaging (MRI) examination (Figure 3). When the patient was discharged on the 18th postprocedure day, there were no sequelae.

DISCUSSION

The first documented case of CIE was reported in 1970, and the patient presented with transient cortical blindness after coronary angiography[3]. According to a systematic review published in December 2020, the total number of CIE cases recorded after coronary angiography was 75[4].

It has been reported in the literature that contrast-induced encephalopathy usually occurs 2-12 h after the injection of contrast agent and disappears within 24-72 h, with a reported incidence of 0.06%[5]. Our department has conducted more than 3000 DSA procedures, and this is the first case of CIE. The pathogenesis of contrast-induced encephalopathy is still unclear, and potential mechanisms include: (1) Blood-brain barrier disruption: Normally, iodine compounds do not cross the blood-brain barrier. It is speculated that the integrity of the blood-brain barrier is destroyed during CIE, and the contrast agent penetrates into the central nervous system[6,7]; (2) neurotoxic effects: The blood-brain barrier is destroyed, and the contrast agent extravasation and direct stimulation of nerve cells caused by it led to neurotoxicity; however, the mechanism of the direct toxicity of contrast agents to neurons has not been elucidated; and (3) iodinated contrast agents can promote transient vasoconstriction. Animal studies have shown that iodinated contrast agents can increase the release of endothelin from endothelial cells and reduce the production of nitric oxide[8].

The clinical manifestations of CIE vary in severity, ranging from mild headache symptoms to severe clinical manifestations such as coma and even death. The clinical manifestations of CIE reported in the literature include transient cortical blindness and neurological symptoms such as restlessness, visual hallucinations, and deafness. Physical examination shows delirium state, increased muscle tone, tendon hyperreflexia, and positive pathological signs.

Based on the CT 2 h after DSA, we misdiagnosed the patient with subarachnoid hemorrhage (SAH). The disturbance of consciousness rapidly and progressively worsened 7 h after DSA. To exclude increased bleeding, new intracranial hemorrhage and cerebral infarction, the cranial CT was re-examined, and CIE was confirmed. Subarachnoid hemorrhage-like changes on CT in CIE have not been reported before. CIE imaging contrast enhancement, bleeding 40-60 (HU), CIE 100-300 (HU). MRI: T2, DWI and FLAIR high signal, MRI-derived apparent diffusion coefficient (ADC) in acute ischemic stroke ADC decreased, normal in CIE, can serve to differentiate from intracranial hemorrhage[9]. The diagnosis of CIE has to be based on both clinical symptoms and neurological signs: It appears within minutes to hours after the injection of an iodinated contrast agent. It usually recovers completely within 48-72 h. Other pathological processes, such as cerebral ischemia, *etc.*, should be excluded. In this case, the neurological deficit lasted for a significantly longer time, and the symptoms began to resolve on the 3rd d after DSA. On the 6th d, there was still a lack of fluency in speech and poor calculation skills, but there were no sequelae at the 3-mo follow-up.

In this case, the lesions in this patient were mainly concentrated on the left side. This patient was a male with a history of hypertension, hyperlipidemia, and diabetes. Combined with intracranial aneurysm, the patient is prone to blood-brain barrier damage and belongs to the CIE risk group. In addition to common risk factors, the surgeon considered that the procedure time of angiography on the left side was longer than that on the right side, and the amount of contrast agent used was higher than that on the right side.

The patient did not undergo further interventional therapy for the aneurysm after DSA. Regarding the risk of CIE recurrence, Law reported a patient with binocular vision impairment following a previous cardiac catheterization who was prescribed antihistamines and corticosteroids as prophylaxis before a second procedure, but seizures and hemianopia occurred after the second angiography using iodixanol; these symptoms resolved after 24 h[10]. Spina reported a 65-year-old man with transient limb weakness after angiography. After a second coronary angiography two years later, he showed complete aphasia postprocedure despite preprocedure corticosteroids[11]. However, patients with a previous history of CIE who undergo repeat cardiac catheterization without adverse reactions after limiting the amount of contrast agent used and providing adequate hydration have also been reported. Therefore, the relevant reports show inconsistent conclusions on the recurrence of CIE.

CONCLUSION

In view of the large number of procedures in which contrast agents are used every year worldwide, CIE should be taken seriously. In patients with neurological and psychiatric symptoms after angiography, the possibility of CIE needs to be considered, but CIE must be distinguished from acute cerebrovascular accidents, including subarachnoid hemorrhage. Treatment measures include mainly corticosteroids, dehydration and diuresis, and adequate hydration. Patients with a history of contrast-induced encephalopathy should be carefully evaluated before any subsequent intravascular injection of contrast media and should be fully informed of the relevant risks.

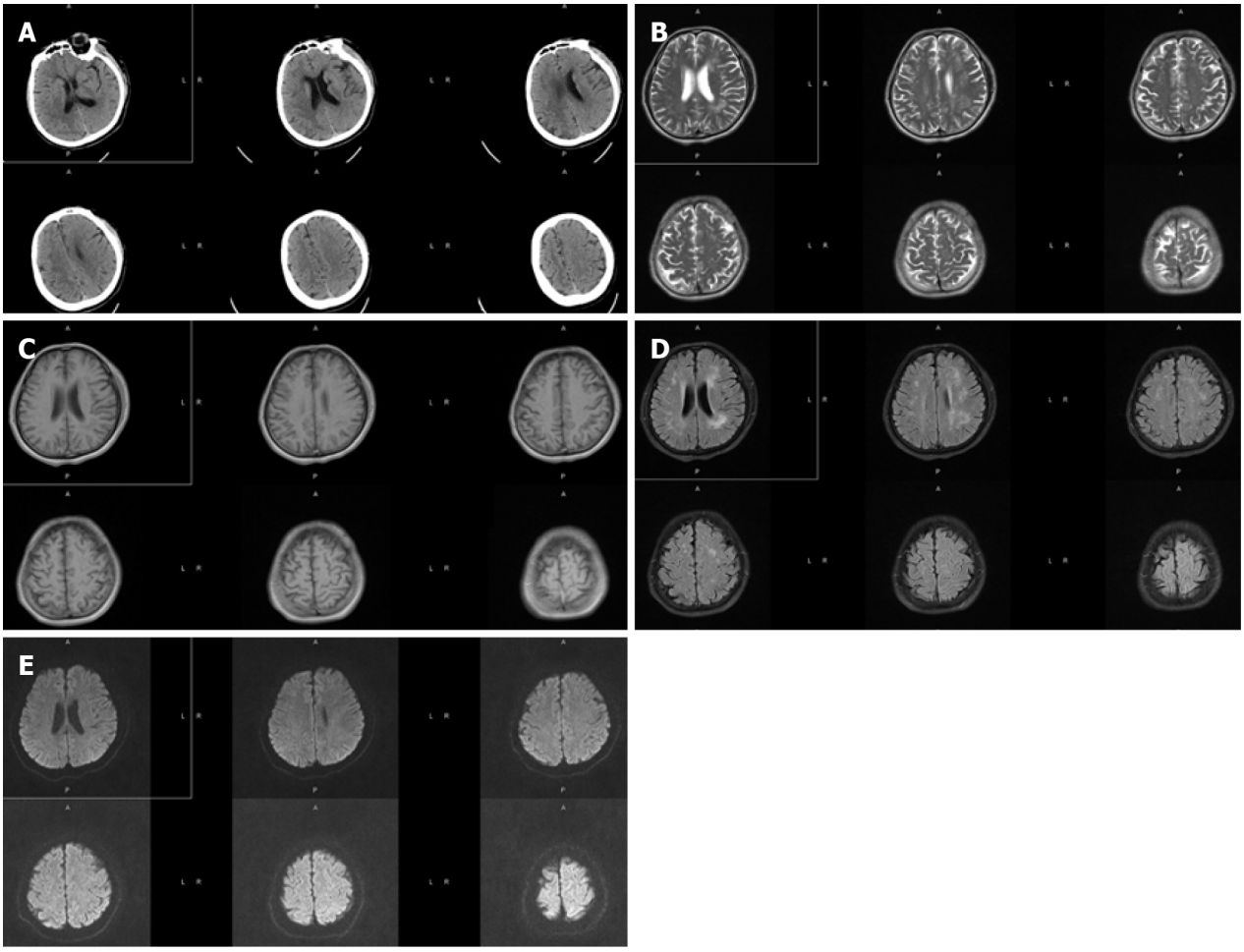

DOI: 10.12998/wjcc.v11.i10.2260

Figure 3 Computed tomography 3 d after digital subtraction angiography and magnetic resonance imaging 17 d after digital subtraction angiography. A: The brain computed tomography (CT) 3 d after digital subtraction angiography (DSA), which showed that brain tissue swelling in the left cerebral hemisphere was significantly reduced, and there was no significant difference in the density of bilateral cerebral hemispheres; B-E: Brain magnetic resonance imaging re-examination 17 d after DSA. The signals of T1, T2, and diffusion-weighted imaging in bilateral brain tissues were symmetrical without significant differences.

FOOTNOTES

Author contributions: Zhang ZY contributed to conception and design of experiments, implementation of research, collection of data, analysis/interpretation of data, and drafting articles; Lv H contributed to conduct research, analyze/interpret data, and draft articles; Wang PJ contributed to collect data and draft articles; Zhao DY contributed to analyze/interpret data, draft articles, and critical review of the intellectual content of articles; Zhang LY contributed to work support, access to research funding, guidance, and supportive contributions; Wang JY contributed to work support, access to research funding , guidance, and supportive contributions; Hao JH contributed to conception and design of experiments, guidance, and supportive contributions.

Informed consent statement: Informed written consent was obtained from the patients for the publication of this report and any accompanying images.

Conflict-of-interest statement: The authors declare that they have no conflict of interest.

CARE Checklist (2016) statement: The authors have read the CARE Checklist (2016), and the manuscript was prepared and revised according to the CARE Checklist (2016).

Country/Territory of origin: China

ORCID number: Hang Lv 0000-0001-6738-6938; Li-Yong Zhang 0000-0001-5831-6823; Ji-Heng Hao 0000-0002-0299-3830.

S-Editor: Chen YL
L-Editor: A
P-Editor: Chen YL

REFERENCES

1 **Sawaya RA**, Hammoud R, Arnaout S, Alam S. Contrast-induced encephalopathy following coronary angioplasty with iohexol. *South Med J* 2007; **100**: 1054-1055 [PMID: 17943057 DOI: 10.1097/SMJ.0b013e3181540086]
2 **Frontera JA**, Pile-Spellman J, Mohr JP. Contrast-induced neurotoxicity and selective cortical injury. *Cerebrovasc Dis* 2007; **24**: 148-151 [PMID: 17565207 DOI: 10.1159/000103621]
3 **Fischer-Williams M**, Gottschalk PG, Browell JN. Transient cortical blindness. An unusual complication of coronary angiography. *Neurology* 1970; **20**: 353-355 [PMID: 5534969 DOI: 10.1212/wnl.20.4.353]
4 **Kariyanna PT**, Aurora L, Jayarangaiah A, Das S, Gonzalez JC, Hegde S, McFarlane IM. Neurotoxicity Associated with Radiological Contrast Agents Used during Coronary Angiography: A Systematic Review. *Am J Med Case Rep* 2020; **8**: 60-66 [PMID: 32440532 DOI: 10.12691/ajmcr-8-2-6]
5 **de Bono D**. Complications of diagnostic cardiac catheterisation: results from 34,041 patients in the United Kingdom confidential enquiry into cardiac catheter complications. The Joint Audit Committee of the British Cardiac Society and Royal College of Physicians of London. *Br Heart J* 1993; **70**: 297-300 [PMID: 8398509 DOI: 10.1136/hrt.70.3.297]
6 **Sterrett PR**, Bradley IM, Kitten GT, Janssen HF, Holloway LS. Cerebrovasculature permeability changes following experimental cerebral angiography. A light- and electron-microscopic study. *J Neurol Sci* 1976; **30**: 385-403 [PMID: 1003253 DOI: 10.1016/0022-510x(76)90142-8]
7 **Lalli AF**. Contrast media reactions: data analysis and hypothesis. *Radiology* 1980; **134**: 1-12 [PMID: 6985735 DOI: 10.1148/radiology.134.1.6985735]
8 **Yanagisawa M**, Inoue A, Ishikawa T, Kasuya Y, Kimura S, Kumagaye S, Nakajima K, Watanabe TX, Sakakibara S, Goto K. Primary structure, synthesis, and biological activity of rat endothelin, an endothelium-derived vasoconstrictor peptide. *Proc Natl Acad Sci U S A* 1988; **85**: 6964-6967 [PMID: 3045827 DOI: 10.1073/pnas.85.18.6964]
9 **Yu J**, Dangas G. Commentary: New insights into the risk factors of contrast-induced encephalopathy. *J Endovasc Ther* 2011; **18**: 545-546 [PMID: 21861746 DOI: 10.1583/11-3476C.1]
10 **Law S**, Panichpisal K, Demede M, John S, Marmur JD, Nath J, Baird AE. Contrast-Induced Neurotoxicity following Cardiac Catheterization. *Case Rep Med* 2012; **2012**: 267860 [PMID: 23251169 DOI: 10.1155/2012/267860]
11 **Spina R**, Simon N, Markus R, Muller DW, Kathir K. Recurrent contrast-induced encephalopathy following coronary angiography. *Intern Med J* 2017; **47**: 221-224 [PMID: 28201864 DOI: 10.1111/imj.13321]

World Journal of Clinical Cases

Submit a Manuscript: https://www.f6publishing.com

World J Clin Cases 2023 April 6; 11(10): 2267-2275

DOI: 10.12998/wjcc.v11.i10.2267

ISSN 2307-8960 (online)

CASE REPORT

Diagnosis and treatment of primary seminoma of the prostate: A case report and review of literature

Zhi-Lie Cao, Bi-Jun Lian, Wei-Ying Chen, Xu-Dong Fang, Hang-Yang Jin, Ke Zhang, Xiao-Ping Qi

Specialty type: Medicine, research and experimental

Provenance and peer review: Unsolicited article; Externally peer reviewed.

Peer-review model: Single blind

Peer-review report's scientific quality classification

Grade A (Excellent): 0
Grade B (Very good): 0
Grade C (Good): C, C, C, C
Grade D (Fair): D
Grade E (Poor): 0

P-Reviewer: Boopathy Vijayaraghavan KM, India; Faraji N, Iran; Marickar F, India

Received: November 17, 2022
Peer-review started: November 17, 2022
First decision: January 12, 2023
Revised: February 1, 2023
Accepted: March 6, 2023
Article in press: March 6, 2023
Published online: April 6, 2023

Zhi-Lie Cao, Bi-Jun Lian, Xu-Dong Fang, Hang-Yang Jin, Xiao-Ping Qi, Department of Urology, The 903rd PLA Hospital, Hangzhou Medical College, Hangzhou 310004, Zhejiang Province, China

Wei-Ying Chen, Department of Urology, Taizhou Hospital of Zhejiang Province Affiliated to Wenzhou Medical University, Enze Hospital, Taizhou Enze Medical Center (Group), Taizhou 318050, Zhejiang Province, China

Ke Zhang, Center for Radiation Oncology, Affiliated Hangzhou Cancer Hospital, Zhejiang University School of Medicine, Hangzhou 310002, Zhejiang Province, China

Corresponding author: Xiao-Ping Qi, MM, Professor, Department of Urology, The 903rd PLA Hospital, Hangzhou Medical College, No. 40 Jichang Road, Hangzhou 310004, Zhejiang Province, China. qxplmd@163.com

Abstract

BACKGROUND

Primary seminoma of the prostate (PSP) is a rare type of extragonadal germ cell tumour that is easily misdiagnosed, owing to the lack of specific clinical features. It is therefore necessary for clinicians to work toward improving the accuracy of PSP diagnosis.

CASE SUMMARY

A 59-year-old male patient presenting with acute urinary retention was admitted to a local hospital. A misdiagnosis of benign prostatic hyperplasia led to an improper prostatectomy. Histopathology revealed PSP invading the bladder neck and bilateral seminal vesicles. Further radiotherapy treatment for the local lesion was performed, and the patient had a disease-free survival period of 96 mo. This case was analysed along with 13 other cases of PSP identified from the literature. Only four of the cases (28.6%) were initially confirmed by prostate biopsy. In these cases, imaging examinations showed an enlarged prostate (range 6-11 cm) involving the bladder neck (13/14). Of the 14 total cases, 11 (78.6%) presented typical pure seminoma cell features, staining strongly positive for placental alkaline phosphatase, CD117, and OCT4. The median age at diagnosis was 51 (range 27-59) years, and patients had a median progression-free survival time of 48 (range 6-156) mo after treatment by cisplatin-based chemotherapy combined with surgery or radiotherapy. The remaining three were cases of mixed embryonal tumours with focal seminoma, which had clinical features similar to those of pure PSP, in addition that they also had elevated serum alpha-

fetoprotein, beta-human chorionic gonadotropin, and lactose dehydrogenase.

CONCLUSION
PSP should be considered in patients younger than 60 years with an enlarged prostate invading the bladder neck. Further prostate biopsies may aid in proper PSP diagnosis. Cisplatin-based chemotherapy is still the main primary therapy for PSP.

Key Words: Prostatic neoplasms; Seminoma; Germ cell and embryonic neoplasms; Diagnosis; Case report

Core Tip: Primary seminoma of the prostate (PSP) is a rare type of extragonadal germ cell tumour that is easily misdiagnosed, owing to the lack of specific clinical features. To the best of our knowledge, there have been only 13 cases of PSP reported in the literature, and there is a lack of systemic research on the condition. Through this case report and literature review, we suggested that PSP should be considered in patients younger than 60 years with an enlarged prostate invading the bladder neck. This symptom occurs in 92.9% of PSP patients, and has a high sensitivity but low specificity for diagnosis. However, additional prostate biopsies may aid diagnosis, and histopathological studies are the most effective diagnostic technique. The prognoses of PSP patients are often good. While cisplatin-based chemotherapy remains to be the first-line treatment, surgery or radiotherapy may also be important options, depending on each patient's response to chemotherapy and the location of the residual tumour.

Citation: Cao ZL, Lian BJ, Chen WY, Fang XD, Jin HY, Zhang K, Qi XP. Diagnosis and treatment of primary seminoma of the prostate: A case report and review of literature. *World J Clin Cases* 2023; 11(10): 2267-2275
URL: https://www.wjgnet.com/2307-8960/full/v11/i10/2267.htm
DOI: https://dx.doi.org/10.12998/wjcc.v11.i10.2267

INTRODUCTION

Germ cell tumours (GCTs) are growths of cells that form from reproductive cells. Most GCTs occur in the testicles or ovaries; however, some GCTs, named extragonadal germ cell tumours (EGCTs), occur in other areas of the body *via* mechanisms that remain unclear[1]. EGCTs are rare, and most of them occur in the midline of the body, such as mediastinal tumours, thymus tumours, retroperitoneal tumours, and pineal tumours[1]. Seminoma is the most common form of GCT, and one of the rare malignant tumours that can be cured by chemotherapy[2]. Primary seminoma of the prostate (PSP) without any primary testicular lesions is extremely rare. To the best of our knowledge, only 13 cases have been previously reported in the literature. The clinical symptoms of EGCTs are non-specific and vary according to tumour location. In the prostate, EGCTs may cause urinary symptoms. The clinical manifestations of PSP may include progressive dysuria, haematuria, and an enlarged prostate invading the bladder[3-7]. The diagnosis of PSP is difficult based on these non-specific clinical features alone, and the standard of treatment remains controversial[8-12]. We herein report the case of a patient with primary seminoma arising from the prostate. We also systematically review the previous literature on PSP and summarize potential optimal diagnostic and clinical management options for this tumor.

CASE PRESENTATION

Chief complaints

A 59-year-old man presenting with acute urinary retention was admitted to a local hospital in August 2014.

History of present illness

The patient had been diagnosed with benign prostatic hyperplasia (BPH) for the preceding three years, with a chief symptom of progressive obstructive voiding.

History of past illness

The patient's past medical history was unremarkable.

Personal and family history
The patient denied any family history of related conditions.

Physical examination
Physical examination showed that the patient's prostate was enlarged to more than twice the normal size, and was slightly hard without any palpable nodule on a digital rectal examination.

Laboratory examinations
Microscopic haematuria was evident, but the patient's serum prostate specific antigen (PSA) level was within normal limits (1.412 ng/mL).

Imaging examinations
Ultrasound and computed tomography (CT) revealed an enlarged prostate (7.0 cm × 6.5 cm × 5.5 cm) involving the bladder neck (Figure 1A).

Initial diagnosis and treatment
Due to the progression of the patient's urinary symptoms despite medical treatment and lack of necessary equipment for transurethral resection of the prostate at the local hospital, the patient was initially submitted to traditional suprapubic prostatectomy. During the operation, it was confirmed that the lesion was more than just BPH, with a neoplasm that involved the prostate capsule, seminal vesicles, and bladder neck as well. Subsequently, the patient underwent prostatectomy, excision of the seminal vesicles, and rectal surgical repair (due to intraoperative rectal injury).

Histopathology revealed seminoma of the prostate, invading the bladder neck and bilateral seminal vesicles with a positive margin, but no involvement of the rectal wall. Postoperatively, careful examination of the scrotum, mediastinum, and retroperitoneum by ultrasound, and CT/magnetic resonance imaging (MRI) scanning revealed no neoplastic lesion. Serum GCT markers including alpha-fetoprotein (AFP), beta-human chorionic gonadotropin (β-hCG), and lactose dehydrogenase (LDH) had no abnormality.

All prostatectomy specimens were fixed in 10% neutral buffered formalin, embedded in paraffin, and routinely processed. After referral to a tertiary hospital, histology sections were cut at 4 μm intervals and stained with haematoxylin and eosin. Immunohistochemical stains were prepared using the MaxVision™ method (MaxVision TM HRP-Polymer anti-Mouse IHC Kit, Maixin Biotech. Co. Ltd, Fuzhou, China). Immunostains were performed for the following antibodies: AFP (polyclonal, Abnova, Taipei, Taiwan), β-hCG (clone ZSH17), pan-cytokeratin (clone AE1/AE3), high molecular weight cytokeratin (clone 34βE12), CD45RB/leukocyte common antigen (LCA) (clone PD7/26+2B11), vimentin (clone V9), S100 protein (clone 4c4.9), epithelial membrane antigen (EMA) (clone E29), Bcl-2 (clone 8C8), PSA (clone ER-PR8), prostatic serum acid phosphatase (PSAP) (clone PASE/4LJ), placental alkaline phosphatase (PLAP) (clone 8A9), CD117, and c-Kit (clone YR145) (β-hCG-CD117, c-Kit, all provided by Maixin Biotech. Co. Ltd., Fuzhou, China). Periodic acid-Schiff staining (ab-150680, Abcam, Cambridge, United Kingdom) was also performed. Microscopically, the prostatectomy specimen revealed a poorly circumscribed infiltrative tumour with poorly-defined margins invading the prostate capsule, bladder neck, and bilateral seminal vesicles. The neoplastic cells were arranged in ill-defined solid nests, had no glandular structure, abundant clear cytoplasm, distinct cell membranes, and large hyperchromatic and prominent nucleoli. Many lymphocytes and plasma cells infiltrated into the interstitial tissue (Figure 2). Compared to common prostate adenocarcinomas, the atypical nests of the patient's poorly-differentiated tumour cells were more prominent, with various abnormal areas of necrosis. Immunohistochemical studies demonstrated that the tumour cells were diffuse and showed strong expression of PLAP (Figure 3) and CD117 as well as positive periodic acid-Schiff staining, but were negative for cytokeratin AE1/AE3, 34βE12, PSA, PSAP, AFP, LCA, Bcl-2, vimentin, S100 protein, and EMA.

In addition, clustered data were also identified from other patients with seminoma involving the prostate through PubMed (http://www.ncbi.nlm.nih.gov/pubmed/) and ISI Web of Knowledge (http://apps.isiknowledge.com/) with a cutoff date of August 2022, using the terms seminoma and prostate (or "extragonadal") (limitations "primary" and "English"). In addition to the current case, another 13 cases of PSP previously reported in the literature are summarized in Table 1 for comparative purposes. Of these, only four cases were initially confirmed by prostate biopsy (28.6%), and ten were initially misdiagnosed (71.4%) as carcinoma/tumour, sarcoma, BPH, or abscess. The common clinical manifestations were dysuria (10/14), haematuria (6/14), frequent urination (3/14), and lumbago (3/14). Imaging examinations showed an enlarged prostate (range 6-11 cm) involving the bladder neck (13/14, 92.8%). Of these, 11 (78.6%) presented with pure PSP, with a median age at diagnosis of 51 (range 27-59) years. Immunohistochemical examination showed that the typical seminoma cell components were all strongly positive for PLAP, CD117, OCT4, and negative for epithelial markers. All 11 patients had complete remission. Among the eight who received chemotherapy, three were treated just by chemotherapy, three by chemotherapy combined with surgery, and two with chemotherapy followed by further radiotherapy for the iliac lymph node. Of the remaining three, one received surgery and radiotherapy, one received just radiotherapy, and the third lacked detailed treatment information. The

Table 1 Clinical data of patients with primary seminoma of the prostate

No.	Age	Symptoms	Finding (max size of the prostate)	Initial diagnosis	Treatment	Final diagnosis	Follow-up (mo)	Ref.
1	51	Lumbago, fatigue	Large prostate (6 cm) retroperitoneal mass	Adenocarcinoma	CBC 4 cycles	Prostate seminoma involving BN[1]	6 (alive)	Arai *et al*[3], 1988
2	58	Hematuria, urgency	LPIBN (NA)	Bladder neck and prostate urethra tumor	CBC 3 cycles	Prostate seminoma involving BN[2]	10 (alive)	Khandekar *et al*[4], 1993
3	31	Hematuria, dysuria, hematospermia	Large prostate (NA); lymph node mass (NA)	Prostate abscess	CBC 4 cycles + radiotherapy 40 Gy	Prostate seminoma involving BN, seminal vesicles[2]	156 (alive)	Hayman *et al* [5], 1995
4	27	Hematuria, dysuria, lumbago	LPIBN (10 cm)	Rhabdomyosarcoma[3]	Total pelvic exenteration + CBC 3 cycles	Prostate seminoma invading BN, seminal vesicles and rectal wall[1]	72 (alive)	Kimura *et al* [6], 1995
5	54	Dysuria	LPIBN (NA)	Prostate seminoma[3]	CBC 3 cycles	Prostate seminoma involving BN[2]	28 (alive)	Hashimoto *et al*[7], 2009
6	54	Dysuria, nocturia	LPIBN (9.5 cm)	Prostate cancer[3]	Total pelvic exenteration + CTX 9 cycles	Prostate seminoma invading BN, seminal vesicles[1]	132 (alive)	Zheng *et al* [8], 2015
7	47	Dysuria, nocturia frequency, urgency	Large prostate (NA)	BPH	Transurethral resection of prostate + CBC 4 cycles	Prostate seminoma[1]	48 (alive)	Kazmi *et al* [9], 2019
8	46	Dysuria, frequency	LPIBN (7.5 cm)	Prostate seminoma[3]	CBC 2 cycles + radiotherapy 36 Gy	Prostate seminoma involving BN, seminal vesicles[1]	NA	Gundavda *et al*[10], 2020
9	56	Scrotal pain, frequency, urgency	LPIBN (10.2 cm)	Prostate seminoma[3]	Radiotherapy 50 Gy	Prostate seminoma involving BN, seminal vesicles[1]	24 (alive)	Akingbade *et al*[11], 2021
10	35	Dysuria	Large prostate mass (NA)	Prostate seminoma[3]	NA	Prostate seminoma involving BN[2]	NA	Hayasaka *et al*[12], 2011
11	59	Hematuria, dysuria	LPIBN (7 cm)	BPH	Suprapubic prostatectomy + radiotherapy 36 Gy	Prostate seminoma invading BN and seminal vesicles[1]	96 (alive)	Current case
12[4]	24	Microhematuria, lumbago	LPIBN (6 cm)	Prostatic tumor	Total prostatectomy + CBC 4 cycles	EST with seminoma in the prostate invading BN[1]	8 (dead)	Han *et al*[13], 2003
13[4]	47	Dysuria, hematuria	LPIBN (11 cm)	Adenocarcinoma[3]	Radical prostatectomy + CBC 4 cycles	Immature teratoma, seminoma, EST invading BN[1]	16 (alive)	Liu *et al*[14], 2014
14[4]	47	Dysuria	LPIBN (11 cm)	BPH	Bleomycin, etoposide and cisplatin 4 cycles	Prostate with yolk sac tumor and seminoma invading BN[1]	12 (alive)	Antunes *et al* [15], 2018

[1]Final diagnosis by imaging examination and histopathological examination.
[2]Diagnosis by imaging examination.
[3]Initial diagnosis by biopsy.
[4]Mixed extragonadal germ cell tumor with focal seminoma.
CBC: Cisplatin-based chemotherapy; BN: Bladder neck; NA: Not available; CTX: Cyclophosphamide; BPH: Benign prostatic hyperplasia; LPIBN: Large prostate invading the bladder neck; EST: Endodermal sinus tumor.

available follow-up for the 11 patients with pure PSP indicated a good prognosis with a median progression free survival of 48 (range 6-156) mo (Table 1). The remaining three all had mixed endodermal sinus tumours with focal seminoma of the prostate. Their ages at diagnosis were 24, 47, and 47 years, and their chief clinical findings were severe low urinary tract symptoms (dysuria, haematuria, and lumbago) and signs of prostatic enlargement, with elevated serum AFP, β-hCG, and LDH. Cisplatin-based chemotherapy was the main chemotherapy used for treatment. One patient died after 8 mo of chemotherapy, whereas the other two were still living after 16 and 12 mo, respectively.

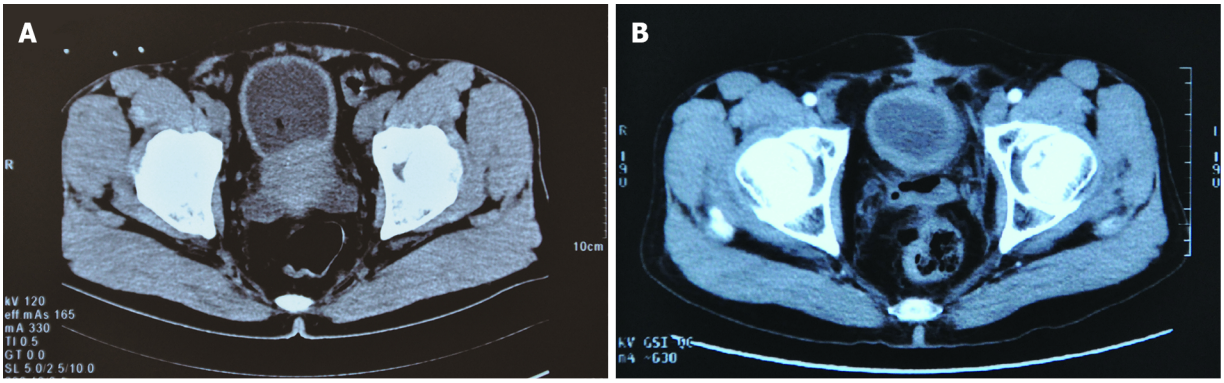

DOI: 10.12998/wjcc.v11.i10.2267 **Copyright** ©The Author(s) 2023.

Figure 1 Computed tomography images of the patient before and after treatment. A: Pelvic computed tomography (CT) image reveals an irregularly heterogeneity enlarged prostate with a rough surface involving the bladder neck and thickening of the bladder wall; B: Pelvic CT image shows no residue or recurrence of the tumor (10 mo after postoperative radiotherapy).

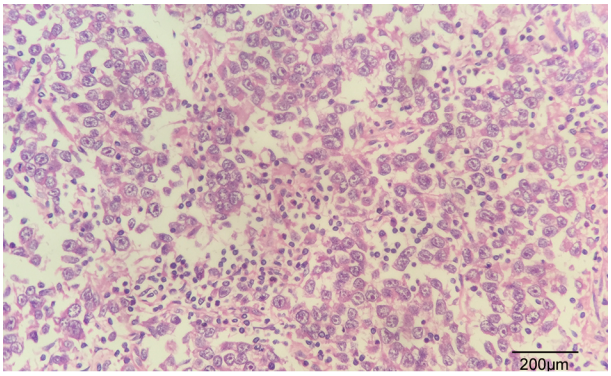

DOI: 10.12998/wjcc.v11.i10.2267 **Copyright** ©The Author(s) 2023.

Figure 2 Histological image showing diffuse distribution of plasmacytoid/clear cytoplasm tumor cells with round to polygonal nuclei with prominent nucleoli; note admixed lymphocytes (hematoxylin-eosin staining, scale bar represents 200 μm).

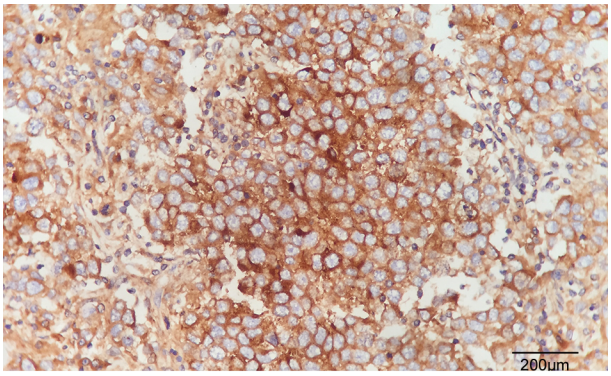

DOI: 10.12998/wjcc.v11.i10.2267 **Copyright** ©The Author(s) 2023.

Figure 3 Immunohistochemical image showing strong membranous and cytoplasmic reactiveity for placental alkaline phosphatase in seminoma tumor cells (scale bar represents 200 μm).

FINAL DIAGNOSIS

A diagnosis of PSP was made, which satisfied the diagnostic criteria of the absence of any demonstrable tumour in either testis, and a tumour confined to the prostate and bladder neck, without regional lymph node/distant metastasis involvement.

TREATMENT

Due to the positive margin and an apprehension over chemotherapy, image guided radiation therapy was performed with a total prostate regional dose of 36 Gy over 18 fractions in a regional hospital, 2 mo after the patient's surgical operation.

OUTCOME AND FOLLOW-UP

Complete remission of the patient's dysuria symptom was achieved, but frequency and urgency of urination persisted. In July 2015, the patient was referred to our hospital (a tertiary hospital). CT/MRI scanning showed no obvious mass at the surgical site (Figure 1B), and no evidence of para-aortic lymphadenopathy or distant metastasis. Cystoscopy showed a slightly coarse urothelium, especially at the posterior bladder neck and trigone. Histopathology by cystoscopy and biopsy revealed that the bladder neck had inflammatory reactants, but there was no evidence of tumour recurrence. The patient has been followed every 6 to 12 mo since that time, and has had a PSP disease-free survival for 96 mo so far, at the time of writing this report.

DISCUSSION

EGCTs are very rare but well-known neoplasms, arising principally from the mediastinum, retroperitoneum, thymus, or pineal gland, of which seminoma accounts for more than 60%[1]. Based on the current study, there have been a total of 14 cases of prostatic seminoma without testicular involvement, including 13 reported previously, of which 11 had primary pure seminoma and 3 had malignant embryonal tumour mixed with seminoma[13-15].

All PSPs in the patients had no specific symptoms, with progressive difficulty in urination being the most common symptom[4-8]. Seminoma grows slowly and manifests concealed, slow, progressive symptoms, so most tumours were bulky by the time when they were discovered, in late presentation. An enlarged prostate (range 6-11 cm) that is tender/slightly hard and extends into the bladder neck, may represent a significant clinical characteristic of PSP, especially for patients younger than 60 years. Of the 11 cases of pure seminoma, the median age at diagnosis was 51 (range 27-59) years, whereas patients with mediastinal or retroperitoneal primary seminoma were diagnosed at a median age of 33 (range 18-65) or 41 (range 23-70) years, respectively[16]. An initial misdiagnosis of PSP occurred in 71.4% of patients. This study highlights the notion that a prostate biopsy is crucial for an accurate diagnosis and proper management strategy for PSP, with positive immunohistochemical staining for PLAP, OCT4, and CD117, or negative biochemical tests such as PSA, AFP, β-hCG, and LDH, similar to the case for testicular seminoma[16-18]. In the case that we described, a lack of prostate biopsy before prostatectomy in the local hospital was a significant shortcoming. Operative morbidity including rectal injury could have been avoided if a biopsy had been done, considering the patient's CT findings.

Cytogenetically, most EGCTs are similar to their testicular counterparts[18]. The diagnosis of primary extragonadal seminoma requires careful examination of the entire body, particularly in males, and the condition should be considered as being primary in that area until the testes have been thoroughly examined and excluded as a possible source[18]. It has been documented that metastases from occult testicular tumours may masquerade as primary EGCTs if the original tumour site has already regressed, leaving only a scar, referred to in the literature as a "burned-out" primary[13,16,19-21]. Approximately 1/3 of patients with EGCTs present with metachronous testicular carcinoma *in situ*[22]. As in the current case, examination data often suggest normal testes, which implies that testicular biopsies should not be recommended[23]. Clinical gonadal ultrasound examination and biochemical marker (AFP, β-hCG, and LDH) tests should be routinely performed, however, and urinary cytology examination should be considered[20-24].

Seminomas have been noted to be sensitive to both chemotherapy and radiotherapy. The relapse-free rates in patients with stage 1 testicular seminoma managed with surveillance, radiotherapy, 1 × carboplatin, and 2 × carboplatin were 91.8%, 97.6%, 95%, and 98.5%, respectively, after a 30-mo follow-up, in one report[25]. Based on current data, the optimal treatment for PSP remains controversial due to the limited number of cases. All 11 of the pure PSP cases that we described here, including our case, achieved complete remission after treatment, with a specific progression free survival rate of 100%. Two other cases with iliac lymph node metastases had a specific progression free survival rate of over 10 years. Of these two cases, one received cisplatin-based chemotherapy followed by radiotherapy[5], while the other received nine cycles of cyclophosphamide after total pelvic exenteration[8]. Three other cases received only cisplatin-based chemotherapy and had no relapses[3,4,7]. These results suggest that cisplatin-based chemotherapy as a primary therapy for PSP has a good curative effect, consistent with the efficacy of primary chemotherapy for patients with extragonadal seminoma (an objective remission rate of 92% and a 5-year overall survival rate of 88%). Chemotherapy should therefore be considered as the first-line therapy for these cases. In this case, radiotherapy was performed after prostatectomy,

which found no evidence of distant metastasis and a positive tumour margin. This course of therapy resulted in a complete remission lasting over 6 years. Another case with a suspicious iliac lymph node was also treated with radiotherapy alone, and achieved complete remission for at least 2 years[11]. However, it should be noted that recurrence rates approach 50% in patients with mediastinal or bulky retroperitoneal seminoma who are treated only by radiotherapy[16,24]. Because there are few cases reported of patients treated only by radiotherapy, the use of radiotherapy alone in patients with PSP should be considered carefully, and the most appropriate option still seems to be chemotherapy for cases of PSP with extraprostatic invasion[16,24].

Regarding the issue of Klinefelter syndrome (KS), there are more than 50 cases of KS in patients with EGCTs of the nonseminomatous subtype reported[26-30]. In the present study, one-tenth of the cases with prostate pure seminoma also presented with KS. Bokemeyer *et al*[16,24] reported that all 103 patients who presented with extragonadal seminomas in their study (51 mediastinal and 52 retroperitoneal seminomas), however, had no KS[31-33]. Further studies are needed to clarify the role of KS in this rare tumour type.

CONCLUSION

The clinical presence of an enlarged prostate invading the bladder neck, and laboratory examination of prostate biopsies, may help in the diagnosis of the extremely rare pure PSP form of cancer. Cisplatin-based chemotherapy seems to be the first-line treatment for this condition, and surgery or radiotherapy may also represent important treatment options, depending on each patient's response to chemotherapy and the location of the residual tumour.

FOOTNOTES

Author contributions: Cao ZL and Lian BJ wrote and revised the manuscript and they contributed equally to this work; Qi XP, Chen WY, and Zhang K conceived and designed the study and reviewed the manuscript; Fang XD and Jin HY collected the clinical data; all authors have read and approved the final version of the manuscript, and agree to publish the manuscript with the order of presentation of the authors.

Supported by National Natural Science Foundation of China, No. 81472861; The Key Project of Zhejiang Province Science and Technology Plan, China, No. 2014C03048-1; and Hangzhou Municipal Commission of Health and Family Planning Science and Technology Program, No. B20210355.

Informed consent statement: The guardian of the patient provided written informed consent to publish this case report and any accompanying images.

Conflict-of-interest statement: All the authors report no relevant conflicts of interest for this article.

CARE Checklist (2016) statement: The authors have read the CARE Checklist (2016), and the manuscript was prepared and revised according to the CARE Checklist (2016).

Country/Territory of origin: China

ORCID number: Bi-Jun Lian 0000-0001-9387-2120; Ke Zhang 0000-0001-8139-1418; Xiao-Ping Qi 0000-0003-1543-0727.

S-Editor: Fan JR
L-Editor: Wang TQ
P-Editor: Fan JR

REFERENCES

1 **Mahankali P**, Trimble L, Panciera D, Li H, Obaid T. Extragonadal Perirectal Mature Cystic Teratoma in the Adult Male. *CRSLS* 2022; **9** [PMID: 36299832 DOI: 10.4293/CRSLS.2022.00035]
2 **Lian B**, Zhang W, Wang T, Yang Q, Jia Z, Chen H, Wang L, Xu J, Wang W, Cao K, Gao X, Sun Y, Shao C, Liu Z, Li J. Clinical Benefit of Sorafenib Combined with Paclitaxel and Carboplatin to a Patient with Metastatic Chemotherapy-

Refractory Testicular Tumors. *Oncologist* 2019; **24**: e1437-e1442 [PMID: 31492770 DOI: 10.1634/theoncologist.2019-0295]
3 **Arai Y**, Watanabe J, Kounami T, Tomoyoshi T. Retroperitoneal seminoma with simultaneous occurrence in the prostate. *J Urol* 1988; **139**: 382-383 [PMID: 3339752 DOI: 10.1016/s0022-5347(17)42426-8]
4 **Khandekar JD**, Holland JM, Rochester D, Christ ML. Extragonadal seminoma involving urinary bladder and arising in the prostate. *Cancer* 1993; **71**: 3972-3974 [PMID: 8508362 DOI: 10.1002/1097-0142(19930615)71:12<3972::aid-cncr2820711228>3.0.co;2-p]
5 **Hayman R**, Patel A, Fisher C, Hendry WF. Primary seminoma of the prostate. *Br J Urol* 1995; **76**: 273-274 [PMID: 7545065 DOI: 10.1111/j.1464-410x.1995.tb07698.x]
6 **Kimura F**, Watanabe S, Shimizu S, Nakajima F, Hayakawa M, Nakamura H. [Primary seminoma of the prostate and embryonal cell carcinoma of the left testis in one patient: a case report]. *Nihon Hinyokika Gakkai Zasshi* 1995; **86**: 1497-1500 [PMID: 7474641 DOI: 10.5980/jpnjurol1989.86.1497]
7 **Hashimoto T**, Ohori M, Sakamoto N, Matsubayashi J, Izumi M, Tachibana M. Primary seminoma of the prostate. *Int J Urol* 2009; **16**: 967-970 [PMID: 20002841 DOI: 10.1111/j.1442-2042.2009.02403.x]
8 **Zheng W**, Wang L, Yang D, Fang K, Chen X, Wang X, Li X, Li Z, Song X, Wang J. Primary extragonadal germ cell tumor: A case report on prostate seminoma. *Oncol Lett* 2015; **10**: 2323-2326 [PMID: 26622843 DOI: 10.3892/ol.2015.3592]
9 **Kazmi Z**, Sulaiman N, Shaukat M, Rafi A, Ahmed Z, Ather MH. Atypical Presentation of Seminoma in the Prostate - Case Report. *Urology* 2019; **132**: 33-36 [PMID: 31136770 DOI: 10.1016/j.urology.2019.05.011]
10 **Gundavda K**, Bakshi G, Prakash G, Menon S, Pal M. The Curious Case of Primary Prostatic Seminoma. *Urology* 2020; **144**: e6-e9 [PMID: 32758494 DOI: 10.1016/j.urology.2020.07.035]
11 **Akingbade A**, Gopaul D, Brastianos HC, Hubay S. Radiotherapy as a Single Modality in Primary Seminoma of the Prostate. *Cureus* 2021; **13**: e14264 [PMID: 33959446 DOI: 10.7759/cureus.14264]
12 **Hayasaka K**, Koyama M, Fukui I. FDG PET imaging in a patient with primary seminoma of the prostate. *Clin Nucl Med* 2011; **36**: 593-594 [PMID: 21637070 DOI: 10.1097/RLU.0b013e3182177350]
13 **Han G**, Miura K, Takayama T, Tsutsui Y. Primary prostatic endodermal sinus tumor (yolk sac tumor) combined with a small focal seminoma. *Am J Surg Pathol* 2003; **27**: 554-559 [PMID: 12657943 DOI: 10.1097/00000478-200304000-00018]
14 **Liu SG**, Lei B, Li XN, Chen XD, Wang S, Zheng L, Zhu HL, Lin PX, Shen H. Mixed extragonadal germ cell tumor arising from the prostate: a rare combination. *Asian J Androl* 2014; **16**: 645-646 [PMID: 24589456 DOI: 10.4103/1008-682X.122871]
15 **Antunes HP**, Almeida R, Sousa V, Figueiredo A. Mixed extragonadal germ cell tumour of the prostate. *BMJ Case Rep* 2018; **2018** [PMID: 29991542 DOI: 10.1136/bcr-2017-223603]
16 **Bokemeyer C**, Nichols CR, Droz JP, Schmoll HJ, Horwich A, Gerl A, Fossa SD, Beyer J, Pont J, Kanz L, Einhorn L, Hartmann JT. Extragonadal germ cell tumors of the mediastinum and retroperitoneum: results from an international analysis. *J Clin Oncol* 2002; **20**: 1864-1873 [PMID: 11919246 DOI: 10.1200/JCO.2002.07.062]
17 **Alsharif M**, Aslan DL, Jessurun J, Gulbahce HE, Pambuccian SE. Cytologic diagnosis of metastatic seminoma to the prostate and urinary bladder: a case report. *Diagn Cytopathol* 2008; **36**: 734-738 [PMID: 18773441 DOI: 10.1002/dc.20881]
18 **Gîngu CV**, Mihai M, Baston C, Crăsneanu MA, Dick AV, Olaru V, Sinescu I. Primary retroperitoneal seminoma - embryology, histopathology and treatment particularities. *Rom J Morphol Embryol* 2016; **57**: 1045-1050 [PMID: 28002522]
19 **Plummer ER**, Greene DR, Roberts JT. Seminoma metastatic to the prostate resulting in a rectovesical fistula. *Clin Oncol (R Coll Radiol)* 2000; **12**: 229-230 [PMID: 11005688 DOI: 10.1053/clon.2000.9159]
20 **Farnham SB**, Mason SE, Smith JA Jr. Metastatic testicular seminoma to the prostate. *Urology* 2005; **66**: 195 [PMID: 16009406 DOI: 10.1016/j.urology.2005.01.058]
21 **Torelli T**, Lughezzani G, Catanzaro M, Nicolai N, Colecchia M, Biasoni D, Piva L, Maffezzini M, Stagni S, Necchi A, Giannatempo P, Farè E, Salvioni R. Prostatic metastases from testicular nonseminomatous germ cell cancer: two case reports and a review of the literature. *Tumori* 2013; **99**: e203-e207 [PMID: 24362870 DOI: 10.1177/030089161309900513]
22 **Fosså SD**, Aass N, Heilo A, Daugaard G, E Skakkebaek N, Stenwig AE, Nesland JM, Looijenga LH, Oosterhuis JW. Testicular carcinoma in situ in patients with extragonadal germ-cell tumours: the clinical role of pretreatment biopsy. *Ann Oncol* 2003; **14**: 1412-1418 [PMID: 12954581 DOI: 10.1093/annonc/mdg373]
23 **Comiter CV**, Renshaw AA, Benson CB, Loughlin KR. Burned-out primary testicular cancer: sonographic and pathological characteristics. *J Urol* 1996; **156**: 85-88 [PMID: 8648846]
24 **Bokemeyer C**, Droz JP, Horwich A, Gerl A, Fossa SD, Beyer J, Pont J, Schmoll HJ, Kanz L, Einhorn L, Nichols CR, Hartmann JT. Extragonadal seminoma: an international multicenter analysis of prognostic factors and long term treatment outcome. *Cancer* 2001; **91**: 1394-1401 [PMID: 11283942]
25 **Chung P**, Daugaard G, Tyldesley S, Atenafu EG, Panzarella T, Kollmannsberger C, Warde P. Evaluation of a prognostic model for risk of relapse in stage I seminoma surveillance. *Cancer Med* 2015; **4**: 155-160 [PMID: 25236854 DOI: 10.1002/cam4.324]
26 **Nichols CR**, Heerema NA, Palmer C, Loehrer PJ Sr, Williams SD, Einhorn LH. Klinefelter's syndrome associated with mediastinal germ cell neoplasms. *J Clin Oncol* 1987; **5**: 1290-1294 [PMID: 3040921 DOI: 10.1200/JCO.1987.5.8.1290]
27 **Tay HP**, Bidair M, Shabaik A, Gilbaugh JH 3rd, Schmidt JD. Primary yolk sac tumor of the prostate in a patient with Klinefelter's syndrome. *J Urol* 1995; **153**: 1066-1069 [PMID: 7853565]
28 **Namiki K**, Tsuchiya A, Noda K, Oyama H, Ishibashi K, Kusama H, Furusato M. Extragonadal germ cell tumor of the prostate associated with Klinefelter's syndrome. *Int J Urol* 1999; **6**: 158-161 [PMID: 10226829 DOI: 10.1046/j.1442-2042.1999.06314.x]
29 **Aguirre D**, Nieto K, Lazos M, Peña YR, Palma I, Kofman-Alfaro S, Queipo G. Extragonadal germ cell tumors are often associated with Klinefelter syndrome. *Hum Pathol* 2006; **37**: 477-480 [PMID: 16564924 DOI: 10.1016/j.humpath.2006.01.029]

30 **Konheim JA**, Israel JA, Delacroix SE. Klinefelter Syndrome with Poor Risk Extragonadal Germ Cell Tumor. *Urol Case Rep* 2017; **10**: 1-3 [PMID: 27800296 DOI: 10.1016/j.eucr.2016.09.006]

31 **Shi D**, Chen C, Huang H, Tian J, Zhou J, Jin S. Primary seminoma of prostate in a patient with Klinefelter syndrome: A case report. *Medicine (Baltimore)* 2022; **101**: e29117 [PMID: 35512069 DOI: 10.1097/MD.0000000000029117]

32 **Inai H**, Kawai K, Morishita Y, Nagata M, Noguchi M, Akaza H. Retroperitoneal extragonadal germ cell tumor in a patient with Klinefelter's syndrome. *Int J Urol* 2005; **12**: 765-767 [PMID: 16174054 DOI: 10.1111/j.1442-2042.2005.01151.x]

33 **Kurabayashi A**, Furihata M, Matsumoto M, Sonobe H, Ohtsuki Y, Aki M, Kuwahara M. Primary intrapelvic seminoma in Klinefelter's syndrome. *Pathol Int* 2001; **51**: 624-628 [PMID: 11564217 DOI: 10.1046/j.1440-1827.2001.01246.x]

World Journal of Clinical Cases

Submit a Manuscript: https://www.f6publishing.com

World J Clin Cases 2023 April 6; 11(10): 2276-2281

DOI: 10.12998/wjcc.v11.i10.2276

ISSN 2307-8960 (online)

CASE REPORT

Primary intra-abdominal paraganglioma: A case report

Wei Guo, Wei-Wei Li, Min-Jie Chen, Ling-Yu Hu, Xiao-Guang Wang

Specialty type: Surgery

Provenance and peer review: Unsolicited article; Externally peer reviewed.

Peer-review model: Single blind

Peer-review report's scientific quality classification

Grade A (Excellent): 0
Grade B (Very good): B, B
Grade C (Good): 0
Grade D (Fair): 0
Grade E (Poor): 0

P-Reviewer: Lucke-Wold B, United States; Maurea S, Italy

Received: December 26, 2022
Peer-review started: December 26, 2022
First decision: January 20, 2023
Revised: January 29, 2023
Accepted: March 3, 2023
Article in press: March 3, 2023
Published online: April 6, 2023

Wei Guo, Graduate School, Zhejiang Chinese Medicine University, Hangzhou 310053, Zhejiang Province, China

Wei Guo, Department of General Surgery, Jiaxing The Second Hospital, Jiaxing 314000, Zhejiang Province, China

Wei-Wei Li, Min-Jie Chen, Ling-Yu Hu, Xiao-Guang Wang, Department of Hepatobiliary Surgery, Jiaxing The Second Hospital, Jiaxing 314000, Zhejiang Province, China

Corresponding author: Xiao-Guang Wang, Doctor, Academic Editor, Doctor, Department of Hepatobiliary Surgery, Jiaxing The Second Hospital, No. 1518 Huancheng North Road, Nanhu District, Jiaxing 314000, Zhejiang Province, China. xiaoguangwangs@163.com

Abstract

BACKGROUND

Paragangliomas are rare neuroendocrine tumors. We hereby report a case of a localized paraganglioma found in the abdominal cavity, and review the relevant literature to improve the understanding of this disease.

CASE SUMMARY

A 29-year-old Chinese female patient was referred to our hospital due to an abdominal mass found on physical examination. Imaging revealed a mass in the left upper abdomen, suggestive of either a benign stromal tumor or an ectopic accessory spleen. Laparoscopic radical resection was subsequently performed, and histopathological analysis confirmed the diagnosis of a paraganglioma. The patient was followed up 3 months post-operation, and reported good recovery with no metastasis.

CONCLUSION

Radical resection can effectively treat intra-abdominal paragangliomas, with few side effects and low recurrence risk. In addition, early and accurate diagnosis and timely intervention are essential for the prognosis of this disease.

Key Words: Abdominal cavity; Paraganglioma; Surgical treatment; Case report

Core Tip: Intraperitoneal paraganglioma is clinically rare without characteristic imaging findings, and many clinicians may never encounter it. However, clinicians must remain vigilant to suspect, identify, locate, and remove the tumor, as the associated symptoms and hypertension can be cured by surgical resection. If the tumor is not diagnosed and removed, there is a risk of death and heart disease. Therefore, due to the small number of cases, the lack of understanding of its clinical features and imaging signs, especially easy to miss diagnosis.

Citation: Guo W, Li WW, Chen MJ, Hu LY, Wang XG. Primary intra-abdominal paraganglioma: A case report. *World J Clin Cases* 2023; 11(10): 2276-2281
URL: https://www.wjgnet.com/2307-8960/full/v11/i10/2276.htm
DOI: https://dx.doi.org/10.12998/wjcc.v11.i10.2276

INTRODUCTION

Paragangliomas are rare neuroendocrine tumors that can occur at any age. It represents an important cause of secretory hypertension as it is often characterized by the excessive production of catecholamines. This study aimed to report a case of an intra-abdominal paraganglioma, and improve the understanding of this disease by elucidating the clinical features of the patient, while reviewing the relevant literature.

CASE PRESENTATION

Chief complaints

A 29-year-old woman was referred to the Department of General Surgery of the Second Hospital of Jiaxing on July 20, 2022 following findings of an abdominal mass 5 d ago.

History of present illness

Initial abdominal computed tomography (CT) revealed soft tissue nodules with central calcification in the left upper abdomen, which warranted further imaging with contrast-enhanced CT.

History of past illness

The patient had no surgical or tumor history. Besides a 2-year history of Hashimoto's thyroiditis and hyperthyroidism, no other underlying diseases such as hypertension and diabetes were reported.

Personal and family history

The patient denied any family history of cancer.

Physical examination

Physical examination was grossly unremarkable. No gastrointestinal symptoms such as abdominal pain, distension, nausea and vomiting, jaundice, abnormal bowel movements, or abnormal stool forms were noted. Urinary symptoms such as gross hematuria, frequency, urgency, and dysuria were not noted as well. The patient was not pyrexic, and denied any chest tightness or shortness of breath.

Laboratory examinations

Laboratory results were as follows: Thyroid stimulating hormone, 0.003 μIU/mL; anti-thyroglobulin, 282.92 IU/mL, anti-thyroid peroxidase antibody, 149.91 IU/mL (reference range, 0–34 IU/mL); and CA19-9, 2.0 U/mL (reference range 0–37 U/m). The remaining laboratory test results were otherwise unremarkable.

Pathological examination of the lesion suggested a paraganglioma (Figure 1). Immunohistochemical staining was subsequently performed, which demonstrated the following: Syn (-), CgA (-), CD56 (-), Ki-67 (+ 5%), CD10 (-), S-100 (+), NES (+), AE1/AE3 (-), SOX10 (-), and P53 (wild type). A diagnosis of an intra-abdominal paraganglioma was thus confirmed.

Imaging examinations

Contrast-enhanced CT confirmed a mass in the left upper abdomen. At this stage, a benign stromal tumor of mesenchymal origin or an ectopic accessory spleen was considered (Figure 2).

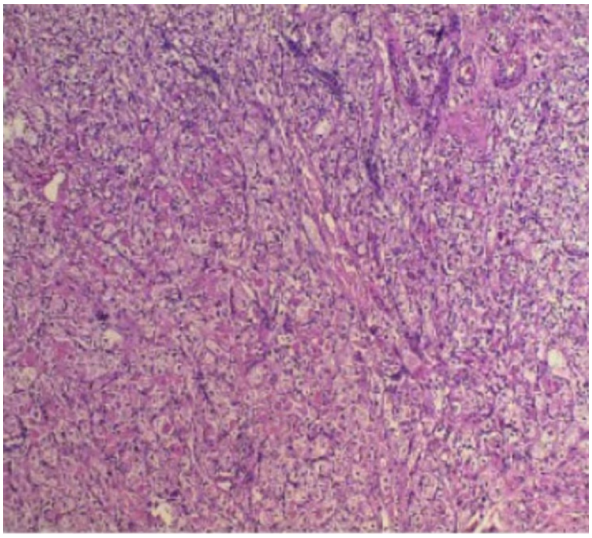

DOI: 10.12998/wjcc.v11.i10.2276 **Copyright** ©The Author(s) 2023.

Figure 1 Pathological result suggestive of a paraganglioma (HE × 400).

DOI: 10.12998/wjcc.v11.i10.2276 **Copyright** ©The Author(s) 2023.

Figure 2 Contrast-enhanced computed tomography showing a mass in the left upper abdomen, indicating either a benign mesenchymal tumor or an ectopic accessory spleen.

FINAL DIAGNOSIS

The patient was diagnosed with a primary intra-abdominal paraganglioma.

TREATMENT

Laparoscopic radical resection of the abdominal mass was indicated. During the operation, the mass was found adhered to the surrounding omentum in the left upper abdominal region, in close proximity to the spleen, stomach, small intestine, and colon. The lesion was approximately 22 mm × 26 mm in size. Postoperative chemotherapy was not indicated.

OUTCOME AND FOLLOW-UP

The patient recovered well without any discomfort. At 3 mo follow-up, no complications such as recurrence or metastasis were observed.

DISCUSSION

Paragangliomas are rare neuroendocrine tumors originating from either the adrenal medulla, or the extra-adrenal sympathetic and parasympathetic ganglia. Symptoms involve the classic triad of headache, palpitation, and sweating. Adrenal and extra-adrenal sympathetic paragangliomas are often characterized by the excessive production of catecholamines, which can not only result in hypertension, but also associate with the risk of acute cardiovascular complications. Diagnosis is often based on plasma or urinary metanephrine measurements and nuclear imaging. Moreover, normal catecholamine levels have been reported to virtually exclude the presence of a sympathetic paraganglioma[1]. Intra-abdominal paragangliomas are particularly rare, with incidence of approximately 1 in 500000.

Parasympathetic paragangliomas are usually located in the head and neck, while sympathetic paragangliomas are more commonly located in the abdomen, followed by the chest and pelvis[2]. And the tumer that may present with cranial neuropathies when located along the skull base[3]. Head and neck paragangliomas are usually painless and slow growing, and are thus often an incidental clinical finding. They mainly manifest as carotid body tumors and vagal paragangliomas. As parasympathetic paragangliomas are non-secretory, symptoms are usually secondary to mass effects. These may include neck pain and dysphagia, conductive hearing loss and pulsatile tinnitus in cervical tympanic paragangliomas, as well as lower cranial nerve defects in advanced tumors[4]. Paragangliomas located outside of the head and neck may also be non-secretory, and are often accompanied by mild symptoms[5].

Due to the catecholamine-secreting nature of abdominal paragangliomas, the common clinical symptoms may include malignant hypertension, palpitation, headache, dizziness, anxiety, metabolic disorder syndrome, orthopnea, oliguria, anuria, and hepatic encephalopathy, among others. In rare cases, patients may experience paraganglioma crises, an endocrine emergency resulting in life-threatening hemodynamic instability and end-organ damage[6]. This can often be misdiagnosed as septic shock, heart failure, thyroid storm, and malignant hyperthermia[7,8]. Given its mortality rate of approximately 15%, early recognition of the signs and symptoms of paragangliomas is thereby critical[7, 9]. It was found that in patients with paraganglioma, the metaiodobenzylguanidine (MIBG) uptake intensity ratio was significantly higher in malignant lesions than in benign lesions. Therefore, iodine-131 MIBG uptake was able to distinguish between benign and malignant diseases, which was not helped by magnetic resonance imaging[10]. Furthermore, one study used radio-labeled MIBG and somatostatin analogues for scintillation imaging for correct localization. The results showed that MIBG was more accurate in imaging pheochromocytoma than somatostatin analogues. But somatostatin analogues are more accurate than MIBGs in detecting neuroendocrine tumors[11]. While symptoms are often paroxysmal, the clinical manifestations of paragangliomas can vary based on catecholamine subtypes, and may range from asymptomatic to life-threatening[12]. As exemplified in our case, the lack of obvious clinical abnormalities such as abdominal pain, abdominal distension, hypertension, and dizziness could have led to misdiagnosis or missed diagnosis.

Paragangliomas are mostly benign in nature, with surgical resection being the main treatment of choice. In contrast, malignant paragangliomas often warrant a multidisciplinary approach, involving endocrinology, oncology, surgery, nuclear medicine, radiotherapy, interventional radiology, and histology. So far, there are no standardized treatment regimens for metastatic diseases. Current treatment measures mainly involve beta-blockers and catecholamine synthesis inhibitors (A-methyl-p-tyrosine) to prevent tumor progression and minimize catecholamine-induced symptoms[13].

The diagnosis of paraganglioma in our case was mainly based on pathology, and was confirmed upon findings of Syn (-) and S-100 (+) on immunohistochemical staining. While morphologically similar to malignant perivascular epithelioid cell and stromal tumors, S-100 played a role as a differentiating factor. As a neurogenic index, the positive expression of S-100 observed in our patient was in keeping with the origin of paragangliomas from chromaffin cells of the neural crest. In contrast, perivascular epithelioid cell tumors are mostly malignant in nature, and are characterized by positive HMB45, SMA, and Desmin, the latter 2 of which are myogenic indices. Stromal tumors are also commonly malignant, and are distinguished by the expression of CD117. In our case, the low expression of Ki-67 indicated a benign tumor.

CONCLUSION

In conclusion, intra-abdominal paragangliomas are clinically rare with no characteristic imaging findings, and are, as such, easily missed. However, surgical resection can associate with good clinical prognosis.

ACKNOWLEDGEMENTS

We thank the patient for his contribution to this case report. We also thank the Department of General Surgery of the Second Affiliated Hospital of Jiaxing University for their support with the treatment of

this case.

FOOTNOTES

Author contributions: Li WW and Chen MJ contributed to the treatment of case and data collection; Guo W, Hu LY, and Wang XG contributed to the writing and revising the manuscript; All authors have read and approve the final version of manuscript.

Supported by Jiaxing Science and Technology Planning Project, No. 2020AY30017.

Informed consent statement: Informed written consent was obtained from the patient for publication of this report and any accompanying images.

Conflict-of-interest statement: All the authors declare that they have no conflict of interest.

CARE Checklist (2016) statement: The authors have read the CARE Checklist (2016), and the manuscript was prepared and revised according to the CARE Checklist (2016).

Country/Territory of origin: China

ORCID number: Wei Guo 0000-0003-4479-4124; Ling-Yu Hu 0000-0002-5698-7700; Xiao-Guang Wang 0000-0002-5698-8800.

S-Editor: Liu JH
L-Editor: A
P-Editor: Liu JH

REFERENCES

1 **Cornu E**, Belmihoub I, Burnichon N, Grataloup C, Zinzindohoué F, Baron S, Billaud E, Azizi M, Gimenez-Roqueplo AP, Amar L. [Phaeochromocytoma and paraganglioma]. *Rev Med Interne* 2019; **40**: 733-741 [PMID: 31493938 DOI: 10.1016/j.revmed.2019.07.008]
2 **Lenders JW**, Duh QY, Eisenhofer G, Gimenez-Roqueplo AP, Grebe SK, Murad MH, Naruse M, Pacak K, Young WF Jr; Endocrine Society. Pheochromocytoma and paraganglioma: an endocrine society clinical practice guideline. *J Clin Endocrinol Metab* 2014; **99**: 1915-1942 [PMID: 24893135 DOI: 10.1210/jc.2014-1498]
3 **Moor R**, Goutnik M, Lucke-Wold B, Laurent D, Chen S, Friedman W, Rahman M, Allen N, Rivera-Zengotita M, Koch M. Clival Paraganglioma, Case Report and Literature Review. *OBM Neurobiol* 2022; **6** [PMID: 35844205 DOI: 10.21926/obm.neurobiol.2203128]
4 **Smith JD**, Harvey RN, Darr OA, Prince ME, Bradford CR, Wolf GT, Else T, Basura GJ. Head and neck paragangliomas: A two-decade institutional experience and algorithm for management. *Laryngoscope Investig Otolaryngol* 2017; **2**: 380-389 [PMID: 29299512 DOI: 10.1002/lio2.122]
5 **Fishbein L**. Pheochromocytoma/Paraganglioma: Is This a Genetic Disorder? *Curr Cardiol Rep* 2019; **21**: 104 [PMID: 31367972 DOI: 10.1007/s11886-019-1184-y]
6 **Meijs AC**, Snel M, Corssmit EPM. Pheochromocytoma/paraganglioma crisis: case series from a tertiary referral center for pheochromocytomas and paragangliomas. *Hormones (Athens)* 2021; **20**: 395-403 [PMID: 33575936 DOI: 10.1007/s42000-021-00274-6]
7 **Whitelaw BC**, Prague JK, Mustafa OG, Schulte KM, Hopkins PA, Gilbert JA, McGregor AM, Aylwin SJ. Phaeochromocytoma [corrected] crisis. *Clin Endocrinol (Oxf)* 2014; **80**: 13-22 [PMID: 24102156 DOI: 10.1111/cen.12324]
8 **Juszczak K**, Drewa T. Adrenergic crisis due to pheochromocytoma - practical aspects. A short review. *Cent European J Urol* 2014; **67**: 153-155 [DOI: 10.5173/ceju.2014.02.art7]
9 **Martucci VL**, Pacak K. Pheochromocytoma and paraganglioma: diagnosis, genetics, management, and treatment. *Curr Probl Cancer* 2014; **38**: 7-41 [PMID: 24636754 DOI: 10.1016/j.currproblcancer.2014.01.001]
10 **Maurea S**, Cuocolo A, Imbriaco M, Pellegrino T, Fusari M, Cuocolo R, Liuzzi R, Salvatore M. Imaging characterization of benign and malignant pheochromocytoma or paraganglioma: comparison between MIBG uptake and MR signal intensity ratio. *Ann Nucl Med* 2012; **26**: 670-675 [PMID: 22752959 DOI: 10.1007/s12149-012-0624-1]
11 **Lastoria S**, Maurea S, Vergara E, Acampa W, Varrella P, Klain M, Muto P, Bernardy JD, Salvatore M. Comparison of labeled MIBG and somatostatin analogs in imaging neuroendocrine tumors. *Q J Nucl Med* 1995; **39**: 145-149 [PMID: 9002775]
12 **Petrák O**, Rosa J, Holaj R, Štrauch B, Krátká Z, Kvasnička J, Klímová J, Waldauf P, Hamplová B, Markvartová A, Novák

K, Michalský D, Widimský J, Zelinka T. Blood Pressure Profile, Catecholamine Phenotype, and Target Organ Damage in Pheochromocytoma/Paraganglioma. *J Clin Endocrinol Metab* 2019; **104**: 5170-5180 [PMID: 31009053 DOI: 10.1210/jc.2018-02644]

13 **Corssmit EPM**, Snel M, Kapiteijn E. Malignant pheochromocytoma and paraganglioma: management options. *Curr Opin Oncol* 2020; **32**: 20-26 [PMID: 31599769 DOI: 10.1097/CCO.0000000000000589]

World Journal of Clinical Cases

Submit a Manuscript: https://www.f6publishing.com

World J Clin Cases 2023 April 6; 11(10): 2282-2289

DOI: 10.12998/wjcc.v11.i10.2282

ISSN 2307-8960 (online)

CASE REPORT

Successful surgical treatment of bronchopleural fistula caused by severe pulmonary tuberculosis: A case report and review of literature

Lei Shen, Yu-Hui Jiang, Xi-Yong Dai

Specialty type: Surgery

Provenance and peer review: Unsolicited article; Externally peer reviewed.

Peer-review model: Single blind

Peer-review report's scientific quality classification

Grade A (Excellent): 0
Grade B (Very good): B
Grade C (Good): C
Grade D (Fair): 0
Grade E (Poor): 0

P-Reviewer: Keikha M, Iran; Skrzypczak PJ, Poland

Received: December 22, 2022
Peer-review started: December 22, 2022
First decision: January 20, 2023
Revised: February 1, 2023
Accepted: March 9, 2023
Article in press: March 9, 2023
Published online: April 6, 2023

Lei Shen, Yu-Hui Jiang, Xi-Yong Dai, Department of Thoracic Surgery, Wuhan Pulmonary Hospital, Wuhan 430030, Hubei Province, China

Corresponding author: Xi-Yong Dai, MD, Surgeon, Department of Thoracic Surgery, Wuhan Pulmonary Hospital, No. 28 Baofeng Road, Wuhan 430030, Hubei Province, China. xiyongdai71@163.com

Abstract

BACKGROUND

Bronchopleural fistula (BPF) is a relatively rare, but severe complication of pulmonary tuberculosis. It is associated with significant mortality; however, its management remains a major therapeutic challenge.

CASE SUMMARY

We present a 24-year-old man with BPF resulting from severe pulmonary tuberculosis combined with mixed infections. The damaged right upper lobe and concomitant empyema were demonstrated *via* computed tomography. After undergoing open-window thoracostomy and tuberculosis treatment for 4 mo, decortication and right upper lobectomy were subsequently performed, leading to the resolution of tuberculosis and other concurrent pulmonary infections. Follow-up, 6 mo after surgery, failed to reveal any evidence of infection recurrence resulting in a good prognosis.

CONCLUSION

The disease course of tuberculous BPF is particularly challenging. Surgical intervention serves as an effective and safe therapeutic strategy for BPF.

Key Words: Bronchopleural fistula; Tuberculosis; Surgery; Case report

Core Tip: Bronchopleural fistula (BPF) is a relatively rare but severe complication of pulmonary tuberculosis. However, no consensus has been reached on the ideal treatment modality. This article presents a patient with a BPF resulting from severe pulmonary tuberculosis accompanied by mixed infections. Strict preoperative evaluation of surgical indications, including standard preoperative anti-tuberculosis treatment and controlling the infection through an open-window thoracostomy during surgery, can achieve a satisfactory long-term prognosis for the treatment of BPF through this three-pronged approach.

Citation: Shen L, Jiang YH, Dai XY. Successful surgical treatment of bronchopleural fistula caused by severe pulmonary tuberculosis: A case report and review of literature. *World J Clin Cases* 2023; 11(10): 2282-2289
URL: https://www.wjgnet.com/2307-8960/full/v11/i10/2282.htm
DOI: https://dx.doi.org/10.12998/wjcc.v11.i10.2282

INTRODUCTION

Tuberculosis is ranked as the second leading infectious killer after coronavirus disease 2019. In 2021, 10.6 million people were diagnosed with active tuberculosis, out of which 1.6 million cases resulted in death[1]. Bronchopleural fistula (BPF) is a relatively rare but life-threatening complication of tuberculosis, with a mortality rate varying between 18% to 67%[2]. BPF most commonly manifests as a postoperative complication of pulmonary resection, particularly pneumonectomy[3]. Other common causes of BPF include lung necrosis complicating infection, persistent spontaneous pneumothorax, chemoradiotherapy, and tuberculosis[4]. The treatment of BPF involves various surgical methods, drug therapy, or bronchoscopic procedures. However, due to limited studies on the condition, there is a lack of consensus concerning its optimal treatment. The purpose of this article is to describe an effective treatment strategy for BPF caused by serious pulmonary tuberculosis.

CASE PRESENTATION

Chief complaints

A 24-year-old man was referred to our hospital with a productive cough accompanied by expectoration of purulent sputum, weight loss, and exertional polypnea. The patient was treated for tuberculosis but he subsequently developed fever and chest pain, 2 mo after being discharged from our hospital.

History of present illness

When the severity of the clinical symptoms increasingly progressed, the patient was readmitted to our hospital for further evaluation and treatment.

History of past illness

The patient had no significant medical history.

Personal and family history

The patient denied smoking previously and had no past history of lung disease. His family history was unremarkable.

Physical examination

On physical examination, the patient was in poor general condition. The patient's body mass index was around 20. Lung auscultation indicated decreased breath sounds in the right lower lung. Chest wall collapse was evident upon visual inspection.

Laboratory examinations

Laboratory analysis evidenced that sputum smears for acid-fast bacilli, sputum culture, GeneXpert Mtuberculosis/RIF, and polymerase chain reaction were all positive for tuberculosis. Furthermore, multidrug-resistant Klebsiella pneumoniae and Aspergillus fumigatus were isolated in the bacterial culture of the effusion and sputum. The blood markers were as follows: White blood count: 13.67 × 10^9/L (81.1% neutrophils and 5.6% lymphocytes); C-reactive protein: 89.54 mg/L; ESR: 34 mm/h; procalcitonin: 0.22 ng/mL. The patient's liver and kidney functions, electrolytes, myocardial enzymes, and coagulation were normal.

Imaging examinations

The chest computed tomography (CT) scan showed bilateral pulmonary infection with cavitary lesions (Figure 1A). The right lung was completely compressed and atelectatic with severe air leakage; pleural thickening of the right upper lung indicated right lung damage (Figure 1B). The coarctation of the right intercostal space is noted on the chest CT (Figure 1D). Bronchoscopy at admission (Figure 2A) and 1 mo after the anti-tuberculosis treatment showed a 5 mm fistula of the right upper bronchus (Figure 2B), along with erythema, erosion, and hyperplasia of the apical bronchus, and a small amount of necrotic material.

FINAL DIAGNOSIS

This patient was diagnosed with BPF, endobronchial tuberculosis, pulmonary tuberculosis, tuberculosis lung damage, and pleural empyema.

TREATMENT

The timeline of management is shown in Figure 3. Closed thoracic drainage and anti-tuberculosis therapy were conducted after the patient's hospital admission. The patient's anti-tuberculosis treatment program included the following medications taken once daily: Isoniazid 300 mg qd; rifampicin 450 mg qd; ethambutol 750 mg qd; levofloxacin 600 mg qd; amikacin 600 mg qd and linezolid 200 mg qd. The patient was subsequently discharged to continue treatment at home. Despite anti-tuberculosis treatment for 2 mo, the disease progressed leading to readmission. A previously installed chest tube from the initial hospitalization was removed due to a complicated pleural infection. Due to difficulty finding an appropriate location for closed drainage, the patient underwent a right open-window thoracostomy to improve fluid drainage. The 7th and 8th partial ribs were removed to construct a window, 10 cm in diameter. Surgery confirmed the presence of a thick pleural membrane surrounding the right lung and a 5 mm fistula with air leakage from the right upper lung. In addition, mold was found on the pleural surface (Figure 4A). To address the pleural empyema, gauzes soaked in iodine were packed into the pleural space through the window, once or twice a day after surgery. Voriconazole and intrapleural irrigation of amphotericin B were administered for antifungal treatment. Amphotericin B (10 mg) was diluted with 5% glucose solution to form a total volume of approximately 50 mL. Subsequently, the aspergillosis-infected pleura was irrigated with this solution by packing amphotericin-soaked gauze into the emphysematous space. Irrigation was performed once daily for 1 mo.

Infection was controlled remarkably after surgery, through continuous treatment with antibiotics and antifungal agents over 4 mo. The patient underwent right upper lobectomy accordingly. Intraoperatively, thick, fibrotic pleural membranes were found and decortication was conducted. Bronchial stump reinforcement was performed through the mediastinal pleura. Finally, the thoracic window was closed. In order to prevent recurrence, postoperative antifungal treatment was continued for 3 mo, and anti-tuberculosis treatment for 6 months.

OUTCOME AND FOLLOW-UP

Improvement of symptoms and postoperative examination demonstrated the positive effects of the therapeutic strategy. Repeat cultures of sputum and bronchoalveolar lavage fluid were negative. Chest CT at 6 mo after the treatment revealed diminished lung lesions. (Figure 1B). Repeat bronchoscopy also demonstrated improvement of the right upper bronchial tuberculosis and the absence of any abnormality in the middle and lower bronchus (Figure 2C). The pleural effusion were resolved and no lesions were found on the pleural surface (Figure 4B). The patient's physical strength returned after dietary intervention. The right lung expanded well and the chest wall deformity resolved 6 mo after the operation (Figure 1C). The patient showed a favorable long-term prognosis and no evidence of recurrence at follow-up.

DISCUSSION

Many therapeutic strategies have been implemented in the treatment of BPF[5-11], but a consensus on the best treatment modality has yet to be reached. The current therapeutic options can be complementary, and the treatment needs to be individualized[12]. Herein, we described the successful treatment of tuberculous BPF through surgery. Favorable surgical outcomes for BPF depend on the selection and timing of the operation, standard preoperative anti-tuberculosis treatment, full thoracic

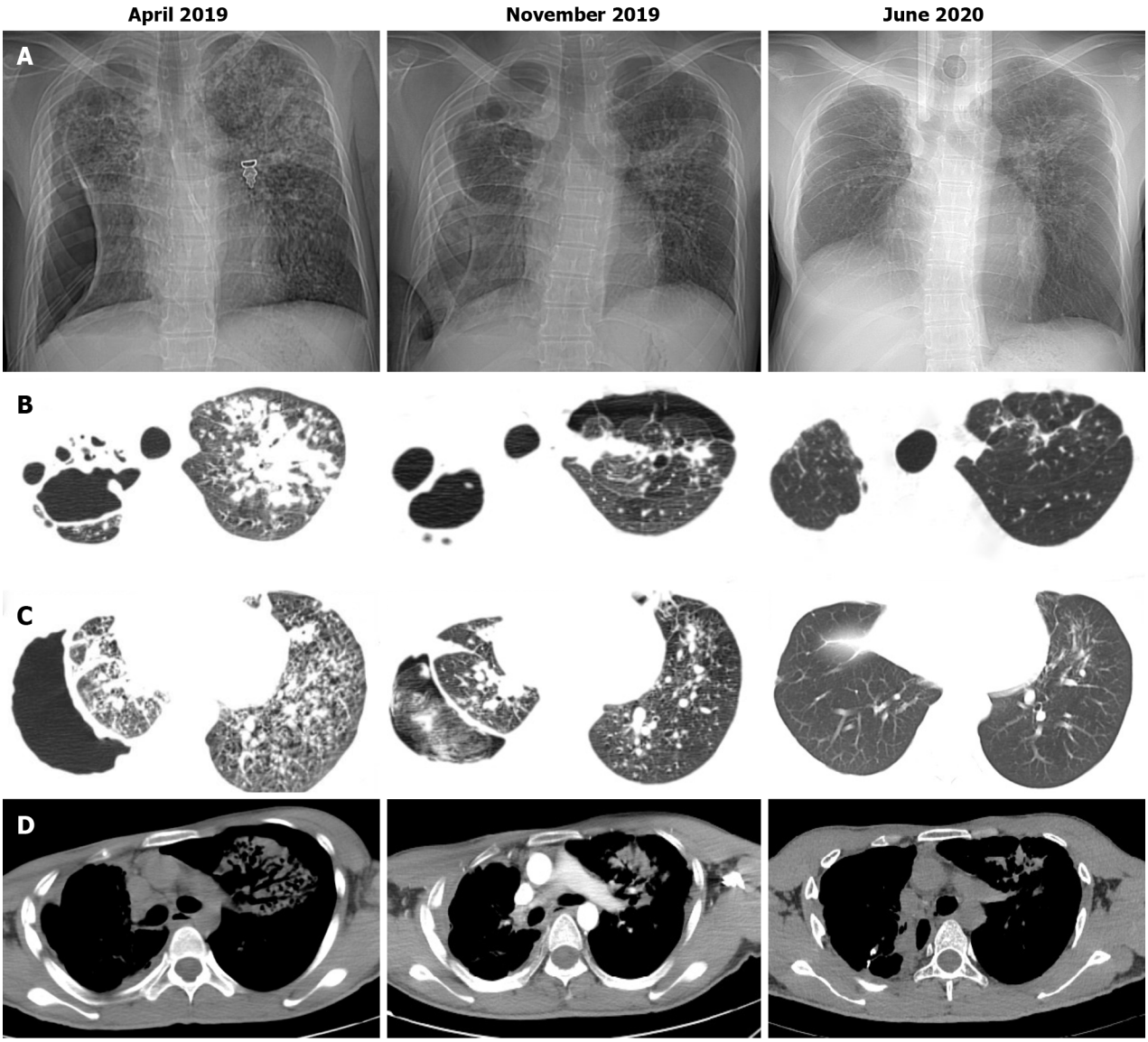

DOI: 10.12998/wjcc.v11.i10.2282

Figure 1 Chest computed tomography scans of patient. A: At admission and before surgery show bilateral pulmonary infection and complete compression and atelectasis of the right lung. Postoperative chest computed tomography (CT) demonstrates right lung expansion; B: Chest CT scan showing the destruction of the right upper lung; C: Both the presence of pus in the pleural cavity and iodine gauze in the emphysematous pleural space are observed. The residual cavity is eliminated after surgery; D: The coarctation of the right intercostal space is noted on chest CT. The patient's right chest wall deformity has almost resolved, 6 months after the operation.

drainage, and infection control.

Clinical treatment of tuberculous BPF complicated with multiple infections is a huge challenge. We believe that preoperative standard anti-tuberculosis treatment combined with full thoracic drainage is crucial[13,14]. For patients with Mycobacterium tuberculosis-positive sputum before surgery, a drug-resistant tuberculosis test is needed to choose effective anti-tuberculosis drugs. In our case, however, drug therapy for inflammation caused by *Klebsiella pneumoniae spp.* and *Aspergillus fumigatus* was not effective. Full drainage of the thoracic cavity was eventually achieved through open-window thoracostomy, which led to the significant improvement of chronic inflammation. Open-window thoracostomy is a simple, certain, and last resort drainage procedure for thoracic empyema[15,16]. It is the best means to drain purulent effusion caused by empyema from the pleural space and is an excellent interim treatment for BPF[17,18]. Furthermore, intrapleural irrigations of amphotericin B have been proven effective in preventing the recurrence of lung aspergillomas[19,20]. As prolonged air leaks caused by BPF create ventilatory abnormalities through the ineffective gas exchange, packing iodine-soaked gauzes into the empyema-affected pleural space through an open window can add positive intrapleural pressure during inspiration. This procedure could decrease the air leaks caused by BPF. *Klebsiella pneumoniae spp.* and *Aspergillus fumigatus* are opportunistic infections associated with immunodeficiency. Accordingly, nutritional supplementation also plays a very important role in recuperation from these infections.

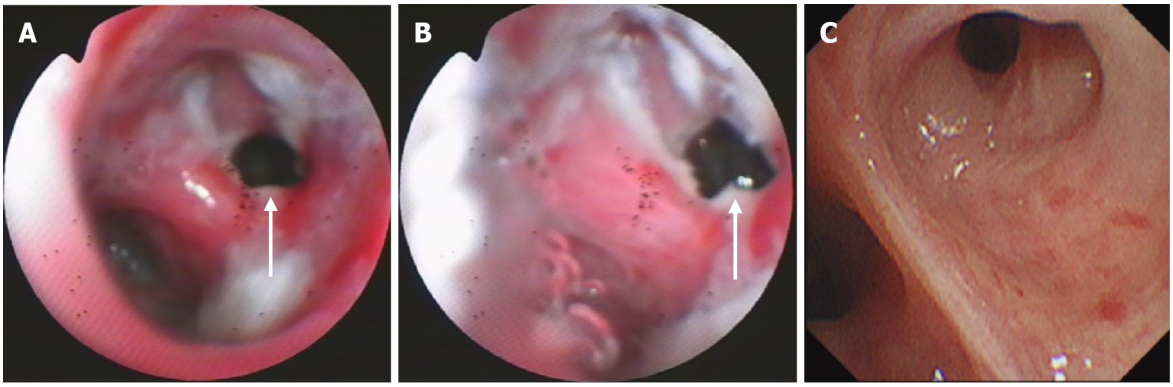

DOI: 10.12998/wjcc.v11.i10.2282 **Copyright** ©The Author(s) 2023.

Figure 2 Bronchoscopic view of the right upper bronchus. A: Bronchoscopy at admission shows a 5 mm fistula (white arrows) of the right upper bronchus, along with erythema, erosion, and hyperplasia of the apical bronchus, and a small amount of necrotic material; B: Bronchoscopy is performed 1 mo after the anti-tuberculosis treatment; C: Bronchoscopy is performed 6 mo after the anti-tuberculosis treatment.

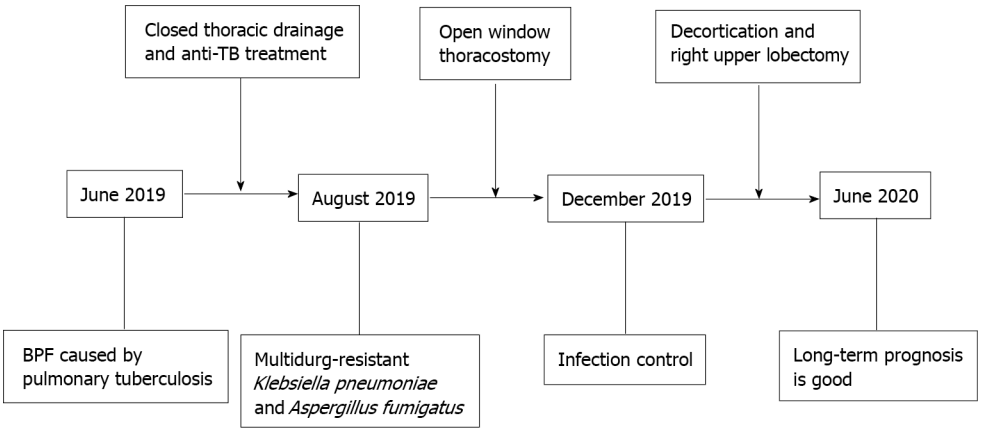

DOI: 10.12998/wjcc.v11.i10.2282 **Copyright** ©The Author(s) 2023.

Figure 3 The timeline of treatment and procedures. TB: Tuberculosis; BPF: Bronchopleural fistula.

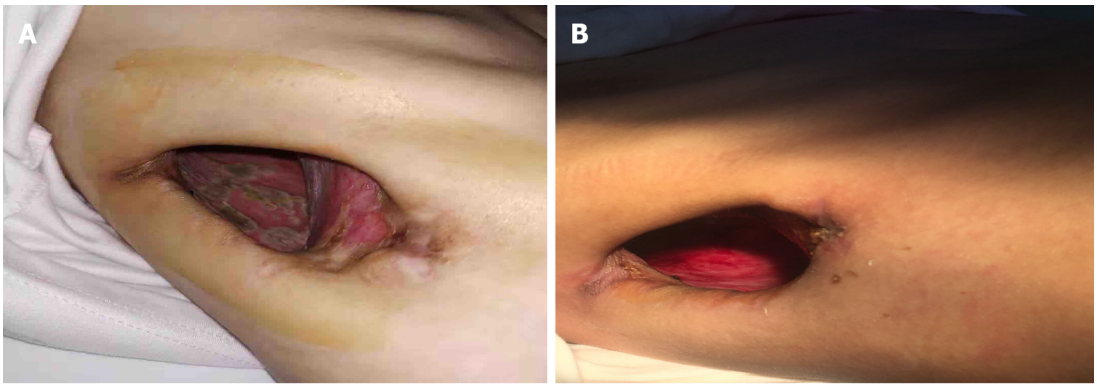

DOI: 10.12998/wjcc.v11.i10.2282 **Copyright** ©The Author(s) 2023.

Figure 4 Intraoperative and postoperative findings. A: Open-window thoracostomy was performed on the patient; intraoperatively, mold was noted on the pleural surface; B: No effusions were noted in the pleural cavity and no lesions were seen on the pleural surface.

The main challenge in BPF lies in closing the fistula and eliminating the cavitation. A variety of surgical and bronchoscopic strategies for treating BPF have been described, although none of these approaches has been successful or suitable for all patients. According to Li *et al*[10], the scope of bronchoscopy makes it difficult to treat peripheral BPF. The size of BPF > 8 mm is generally unsuitable for bronchoscopic treatment[12,21]. The degree of infection, timing of diagnosis, underlying disease, localization and the size of the fistula may be the critical factors in choosing between surgical and

bronchoscopic procedures for treatment[8,22,23]. In our case, as the bronchial stump was affected by tuberculosis and the right upper lung was damaged, we did not select the minimally invasive bronchoscopic method as a treatment strategy. In a patient with lobar lung damage combined with empyema, especially in patients with BPF, aggressive radical therapy with lobectomy or thoracoplasty is necessitated[24,25]. However, the effectiveness of surgery in the treatment of drug-resistant tuberculosis remains unclear[26]. The advantages of bronchial stump reinforcement in preventing BPF are also still controversial, and no consensus has been reached on the ideal buttressing tissue to use[27-29]. Patients with empyema and bronchial tuberculosis undergoing lung resections are at increased risk for BPF recurrence. Besides, preoperative bronchoscopy is used to exclude endobronchial tuberculosis. Hence, we used the mediastinal pleura to cover the bronchial stump. However, as these procedures carries a high risk of mortality and recurrence[30], it is not universally recommended and its indications should be carefully considered. In our patient, chest CT and bronchoscopic images were reviewed regularly to assess the progression of pulmonary and bronchial lesions, preoperatively. The disease course is even more complicated for patients with tuberculous BPF. The key to the treatment of pulmonary tuberculosis complicated with BPF is to have a continual and effective anti-tuberculosis treatment. The preoperative anti-tuberculosis treatment regimen is complex. Clinicians should be ready to adjust the regimen at any time according to its therapeutic effects and adverse reactions.

CONCLUSION

In summary, the treatment of tuberculous BPF has been a challenging issue in thoracic surgery. Surgery is the modality of choice for tuberculous BPF, but it has many complications. Strict preoperative evaluation of surgical indications is required, including standard preoperative anti-tuberculosis treatment with medical therapy and full thoracic drainage to control the infection. The proper selection of patients for surgical intervention can achieve a satisfactory long-term prognosis, and the procedures are safe and efficient. Further research is required to obtain more definitive evidence.

FOOTNOTES

Author contributions: Shen L was responsible for patient care and wrote the first draft of the manuscript; Jiang YH contributed to the diagnosis and treatment of the patient and to the revision of the manuscript; Dai XY supervised the patients' care, conceptualized the study, and revised the manuscript; all authors read and approved the final manuscript.

Supported by grants of Wuhan Municipal Health Commission, No. WX20Z30.

Informed consent statement: Informed written consent was obtained from the patient for publication of this report and any accompanying images.

Conflict-of-interest statement: The authors declare that they have no conflict of interest to disclose.

CARE Checklist (2016) statement: The authors have read the CARE Checklist (2016), and the manuscript was prepared and revised according to the CARE Checklist (2016).

Country/Territory of origin: China

ORCID number: Xi-Yong Dai 0000-0002-8938-2978.

S-Editor: Yan JP
L-Editor: A
P-Editor: Yan JP

REFERENCES

1 **World Health Organization**. Global Tuberculosis Report 2022. Geneva: World Health Organization 2022. [cited December 10, 2022]. Available from: https://www.who.int/teams/global-tuberculosis-programme/tb-reports/global-

tuberculosis-report-2022
2 **Hollaus PH**, Lax F, el-Nashef BB, Hauck HH, Lucciarini P, Pridun NS. Natural history of bronchopleural fistula after pneumonectomy: a review of 96 cases. *Ann Thorac Surg* 1997; **63**: 1391-6; discussion 1396 [PMID: 9146332 DOI: 10.1016/s0003-4975(97)00409-8]
3 **Okuda M**, Go T, Yokomise H. Risk factor of bronchopleural fistula after general thoracic surgery: review article. *Gen Thorac Cardiovasc Surg* 2017; **65**: 679-685 [PMID: 29027099 DOI: 10.1007/s11748-017-0846-1]
4 **Sato M**, Saito Y, Fujimura S, Usuda K, Takahashi S, Kanma K, Imai S, Suda H, Nakada T, Hashimoto K. [Study of postoperative bronchopleural fistulas--analysis of factors related to bronchopleural fistulas]. *Nihon Kyobu Geka Gakkai Zasshi* 1989; **37**: 498-503 [PMID: 2768924]
5 **Giller DB**, Kesaev OS, Koroev VV, Enilenis II, Shcherbakova GV, Romenko MA, Ratobylsky GV, Pekhtusov VA, Martel II. [Surgical treatment of bronchopleural complications after lung resection and pleurectomy in patients with tuberculosis]. *Khirurgiia (Mosk)* 2021; 39-46 [PMID: 34786915 DOI: 10.17116/hirurgia202111139]
6 **Misaki N**, Yokomise H. [Surgical Approach for Treatment of Postoperative Bronchopleural Fistula and Pyothorax]. *Kyobu Geka* 2021; **74**: 856-861 [PMID: 34548459]
7 **Bai Y**, Li Y, Chi J, Guo S. Endobronchial closure of the bronchopleural fistula with the ventricular septal defect occluder: a case series. *BMC Pulm Med* 2021; **21**: 313 [PMID: 34620149 DOI: 10.1186/s12890-021-01676-3]
8 **Song X**, Gu Y, Wang H, Zhang L. The efficacy of endobronchial valves for the treatment of bronchopleural fistula: a single-arm clinical trial. *J Thorac Dis* 2022; **14**: 712-720 [PMID: 35399250 DOI: 10.21037/jtd-22-258]
9 **Siddique A**, Sabbah BN, Arabi T, Shakir IM, Abdulqawi R, AlKattan K, Ahmed MH. Treatment of bronchial anastomotic fistula using autologous platelet-rich plasma post lung transplantation. *J Cardiothorac Surg* 2022; **17**: 204 [PMID: 36002865 DOI: 10.1186/s13019-022-01965-w]
10 **Li X**, Wang S, Yin M, Li X, Qi Y, Ma Y, Li C, Wu G. Treatment of peripheral bronchopleural fistula with interventional negative pressure drainage. *Ther Adv Respir Dis* 2022; **16**: 17534666221111877 [PMID: 35848793 DOI: 10.1177/17534666221111877]
11 **Fruchter O**, Kramer MR, Dagan T, Raviv Y, Abdel-Rahman N, Saute M, Bruckheimer E. Endobronchial closure of bronchopleural fistulae using amplatzer devices: our experience and literature review. *Chest* 2011; **139**: 682-687 [PMID: 21362655 DOI: 10.1378/chest.10-1528]
12 **Lois M**, Noppen M. Bronchopleural fistulas: an overview of the problem with special focus on endoscopic management. *Chest* 2005; **128**: 3955-3965 [PMID: 16354867 DOI: 10.1378/chest.128.6.3955]
13 **Sikander N**, Ahmad T, Mazcuri M, Ali N, Thapaliya P, Nasreen S, Abid A. Role of Anti-Tuberculous Treatment in the Outcome of Decortication for Chronic Tuberculous Empyema. *Cureus* 2021; **13**: e12583 [PMID: 33575146 DOI: 10.7759/cureus.12583]
14 **Piccolo F**, Popowicz N, Wong D, Lee YC. Intrapleural tissue plasminogen activator and deoxyribonuclease therapy for pleural infection. *J Thorac Dis* 2015; **7**: 999-1008 [PMID: 26150913 DOI: 10.3978/j.issn.2072-1439.2015.01.30]
15 **Hiramatsu M**, Atsumi J, Shiraishi Y. Surgical Management of Mycobacterial Infections and Related Complex Pleural Space Problems: From History to Modern Day. *Thorac Surg Clin* 2022; **32**: 337-348 [PMID: 35961742 DOI: 10.1016/j.thorsurg.2022.04.009]
16 **Fukui T**, Matsukura T, Wakatsuki Y, Yamawaki S. Simple chest closure of open window thoracostomy for postpneumonectomy empyema: a case report. *Surg Case Rep* 2019; **5**: 53 [PMID: 30953209 DOI: 10.1186/s40792-019-0612-y]
17 **Dantis K**, Kumar Dewan R. Surgical outcomes and the factors affecting lung expansion following open window thoracostomy in chronic tuberculous empyema with destroyed lung. *Asian Cardiovasc Thorac Ann* 2022; **30**: 696-705 [PMID: 35635131 DOI: 10.1177/02184923221104431]
18 **Massera F**, Robustellini M, Della Pona C, Rossi G, Rizzi A, Rocco G. Open window thoracostomy for pleural empyema complicating partial lung resection. *Ann Thorac Surg* 2009; **87**: 869-873 [PMID: 19231408 DOI: 10.1016/j.athoracsur.2008.12.003]
19 **Chen QK**, Jiang GN, Ding JA. Surgical treatment for pulmonary aspergilloma: a 35-year experience in the Chinese population. *Interact Cardiovasc Thorac Surg* 2012; **15**: 77-80 [PMID: 22499801 DOI: 10.1093/icvts/ivs130]
20 **Denning DW**, Cadranel J, Beigelman-Aubry C, Ader F, Chakrabarti A, Blot S, Ullmann AJ, Dimopoulos G, Lange C; European Society for Clinical Microbiology and Infectious Diseases and European Respiratory Society. Chronic pulmonary aspergillosis: rationale and clinical guidelines for diagnosis and management. *Eur Respir J* 2016; **47**: 45-68 [PMID: 26699723 DOI: 10.1183/13993003.00583-2015]
21 **Shekar K**, Foot C, Fraser J, Ziegenfuss M, Hopkins P, Windsor M. Bronchopleural fistula: an update for intensivists. *J Crit Care* 2010; **25**: 47-55 [PMID: 19592205 DOI: 10.1016/j.jcrc.2009.05.007]
22 **Salik I**, Vashisht R, Abramowicz AE. Bronchopleural Fistula. 2022 May 8. In: StatPearls [Internet]. Treasure Island (FL): StatPearls Publishing; 2022 Jan- [PMID: 30521186]
23 **Brennan PG**, Hsu DS, Banks KC, Maxim CL, Hornik B, Velotta JB. Vertical rectus abdominis myocutaneous free flap repair of post-pneumonectomy bronchopleural fistula: a case report. *AME Case Rep* 2022; **6**: 33 [PMID: 36339911 DOI: 10.21037/acr-22-20]
24 **Okabayashi K**, Yamazaki K, Hamatake D, Yoshida Y, Shirakusa T. [Pleuropneumonectomy for pulmonary tuberculosis and chronic tuberculous empyema]. *Kyobu Geka* 2004; **57**: 1033-1037 [PMID: 15510817]
25 **Bai L**, Hong Z, Gong C, Yan D, Liang Z. Surgical treatment efficacy in 172 cases of tuberculosis-destroyed lungs. *Eur J Cardiothorac Surg* 2012; **41**: 335-340 [PMID: 21684172 DOI: 10.1016/j.ejcts.2011.05.028]
26 **Ghazvini K**, Keikha M. The elimination of drug-resistant tuberculosis from a pulmonary resection surgery perspective. *Int J Surg* 2022; **104**: 106790 [PMID: 35918001 DOI: 10.1016/j.ijsu.2022.106790]
27 **Ceylan KC**, Batıhan G, Kaya ŞÖ. Novel method for bronchial stump coverage for prevents postpneumonectomy bronchopleural fistula: pedicled thymopericardial fat flap. *J Cardiothorac Surg* 2022; **17**: 286 [PMID: 36369041 DOI: 10.1186/s13019-022-02032-0]
28 **Sfyridis PG**, Kapetanakis EI, Baltayiannis NE, Bolanos NV, Anagnostopoulos DS, Markogiannakis A, Chatzimichalis A.

Bronchial stump buttressing with an intercostal muscle flap in diabetic patients. *Ann Thorac Surg* 2007; **84**: 967-971 [PMID: 17720409 DOI: 10.1016/j.athoracsur.2007.02.088]

29 **Skrzypczak P**, Roszak M, Kasprzyk M, Dyszkiewicz W, Kamiński M, Gabryel P, Piwkowski C. The technique of stump closure has no impact on post-pneumonectomy bronchopleural fistula in the non-small cell lung cancer-a cross-sectional study. *J Thorac Dis* 2022; **14**: 3343-3351 [PMID: 36245618 DOI: 10.21037/jtd-22-240]

30 **Bribriesco A**, Patterson GA. Management of Postpneumonectomy Bronchopleural Fistula: From Thoracoplasty to Transsternal Closure. *Thorac Surg Clin* 2018; **28**: 323-335 [PMID: 30054070 DOI: 10.1016/j.thorsurg.2018.05.008]

World Journal of Clinical Cases

Submit a Manuscript: https://www.f6publishing.com

World J Clin Cases 2023 April 6; 11(10): 2290-2300

DOI: 10.12998/wjcc.v11.i10.2290

ISSN 2307-8960 (online)

CASE REPORT

Clinical and genetic features of Kenny-Caffey syndrome type 2 with multiple electrolyte disturbances: A case report

Ning Yuan, Lin Lu, Xiao-Ping Xing, Ou Wang, Yue Jiang, Ji Wu, Ming-Hai He, Xiao-Juan Wang, Le-Wei Cao

Specialty type: Medicine, research and experimental

Provenance and peer review: Unsolicited article; Externally peer reviewed.

Peer-review model: Single blind

Peer-review report's scientific quality classification

Grade A (Excellent): 0
Grade B (Very good): B
Grade C (Good): 0
Grade D (Fair): D
Grade E (Poor): 0

P-Reviewer: Thongon N, Thailand; Tica I, Romania

Received: December 2, 2022
Peer-review started: December 2, 2022
First decision: January 17, 2023
Revised: January 30, 2023
Accepted: March 15, 2023
Article in press: March 15, 2023
Published online: April 6, 2023

Ning Yuan, Ming-Hai He, Xiao-Juan Wang, Le-Wei Cao, Department of Endocrinology, Nanchong Central Hospital, The Second Clinical College, North Sichuan Medical College, Nanchong 637000, Sichuan Province, China

Lin Lu, Xiao-Ping Xing, Ou Wang, Yue Jiang, Department of Endocrinology, Key Laboratory of National health commission, Peking Union Medical College Hospital, Peking Union Medical College, Chinese Academy of Medical Science, Beijing 100730, China

Ji Wu, Department of Urology, Nanchong Central Hospital, The Second Clinical College, North Sichuan Medical College, Nanchong 637000, Sichuan Province, China

Corresponding author: Lin Lu, MD, Professor, Department of Endocrinology, Key Laboratory of National health commission, Peking Union Medical College Hospital, Peking Union Medical College, Chinese Academy of Medical Science, No. 1 Shuaifuyuan, Wangfujing, Dongcheng District, Beijing 100730, China. lulin88@sina.com

Abstract

BACKGROUND

Hypoparathyroidism, which can be sporadic or a component of an inherited syndrome, is the most common cause of hypocalcemia. If hypocalcemia is accompanied by other electrolyte disturbances, such as hypokalemia and hypomagnesemia, then the cause, such as renal tubular disease, should be carefully identified.

CASE SUMMARY

An 18-year-old female visited our clinic because of short stature and facial deformities, including typical phenotypes, such as low ear position, depression of the nasal bridge, small hands and feet, and loss of dentition. The lab results suggested normal parathyroid hormone but hypocalcemia. In addition, multiple electrolyte disturbances were found, including hypokalemia, hypocalcemia and hypomagnesemia. The physical signs showed a short fourth metatarsal bone of both feet. The X-ray images showed cortical thickening of long bones and narrowing of the medulla of the lumen. Cranial computed tomography indicated calcification in the bilateral basal ganglia. Finally, the genetic investigation showed a *de novo* heterogenous mutation of "FAM111A" (c. G1706A:p.R569H). Through a review of previously reported cases, the mutation was found to be the most common mutation site in Kenny-Caffey syndrome type 2 (KCS2) cases reported thus far (16/23, 69.6%). The mutation was slightly more prevalent in females than in males (11/16, 68.8%). Except for hypocalcemia, other clinical

manifestations are heterogeneous.

CONCLUSION

As a rare autosomal dominant genetic disease of hypoparathyroidism, the clinical manifestations of KCS2 are atypical and diverse. This girl presented with short stature, facial deformities and skeletal deformities. The laboratory results revealed hypocalcemia as the main electrolyte disturbance. Even though her family members showed normal phenotypes, gene detection was performed to find the mutation of the *FAM111A* gene and confirmed the diagnosis of KCS2.

Key Words: Hypocalcemia; Hypomagnesemia; Hypoparathyroidism; Kenny-Caffey syndrome type 2; *FAM111A* gene; Case report

Core Tip: The *FAM111A* mutation was more likely to be a *de novo* mutation. Since the patient was an adult at the time of consultation, long-term follow-up treatment and observation of electrolyte status is necessary. Moreover, the fertility of the patient and the genetics of her offspring should be determined.

Citation: Yuan N, Lu L, Xing XP, Wang O, Jiang Y, Wu J, He MH, Wang XJ, Cao LW. Clinical and genetic features of Kenny-Caffey syndrome type 2 with multiple electrolyte disturbances: A case report. *World J Clin Cases* 2023; 11(10): 2290-2300

URL: https://www.wjgnet.com/2307-8960/full/v11/i10/2290.htm

DOI: https://dx.doi.org/10.12998/wjcc.v11.i10.2290

INTRODUCTION

Calcium ions (Ca^{2+}) are essential to life, participating in many pathophysiological processes, such as the synthesis and release of neurotransmitters, the synthesis and secretion of hormones, blood coagulation, muscle contraction, nerve activity and bone mineralization. Under normal circumstances, parathyroid hormone and vitamin D maintain normal serum calcium concentrations. One of the most common causes of hypocalcemia is hypoparathyroidism, which can be transient or persistent. There are also various causes, of which the most common cause of chronic hypoparathyroidism is thyroid surgery, accounting for approximately 75% of cases[1]. Nonoperative causes include (1) autoimmunity: Autoimmune polyendocrine syndrome type 1; and (2) genetic disorders: Familial isolated hypoparathyroidism, autosomal dominant hypocalcemia, and complex disorders, which include hypothyroidism and abnormal magnesium metabolism. Hypothyroidism can be part of the following complex disorders: DiGeorge syndrome, hypoparathyroidism, sensorineural deafness, renal dysplasia (HDR) syndrome, Kenny-Caffey syndrome (KCS), Kearns-Sayre syndrome, mitochondrial encephalomyopathy with lactic acidosis and stroke-like attack syndrome, mitochondrial trifunctional protein deficiency syndrome, and Sanjad-Sakati syndrome (SSS). Hypoparathyroidism is often difficult to diagnose because of its complicated and heterogeneous manifestations, which require careful differential diagnosis depending on clinical manifestations, laboratory examinations and imaging features. DiGeorge syndrome type 1, or 22q11.2 deletion syndrome, is an autosomal dominant genetic disease caused by heterozygous microdeletions on chromosome 22; it can lead to immunodeficiency, abnormal cardiac outflow tracts and hypoparathyroidism. Deletion of the transcription factor TBX1 is necessary for parathyroid development and is considered to be a cause of hypoparathyroidism[2]. HDR syndrome is an autosomal dominant genetic disease caused by *GATA3* gene deletion mutations. *GATA3* is a transcription factor that plays an important role in parathyroid organogenesis[3]. KCS is a rare disease characterized by short stature, osteosclerotic bone dysplasia and hypoparathyroidism. The autosomal recessive form (type 1) is caused by the mutation of tubulin-specific chaperone protein E (TBCE)[4], whereas the autosomal dominant form (type 2) is caused by a *FAM111A* gene mutation[5]. This study presents a rare case of Kenny-Caffey syndrome type 2 (KCS2) with short stature, skeletal deformities and multiple electrolyte disturbances confirmed by genetic analysis. This study was approved by the Ethics Committee of Nanchong Central Hospital, The Second Clinical College, North Sichuan Medical College, and written informed consent was obtained from the patient.

CASE PRESENTATION

Chief complaints

The proband was an 18-year-old female who was hospitalized with abnormal behavior for 3 d beginning October 19, 2021.

History of present illness

Three days before she visited the local psychiatric hospital, she suddenly refused to eat, accompanied by glazed eyes and with no definitive causes.

History of past illness

She was born by cesarean section at the 33rd week of her mother's second pregnancy. Her weight was 3.8 kg [+1 standard deviation (SD)], and her height was 48 cm (-1 SD) at birth. Fontanel closure was delayed until she was 5 years old. During her childhood, she was always shorter than other children of the same age, but her body weight was overweight. She had occasional muscle tetany and limb numbness. Her studying ability in school was slightly poorer than that of her classmates. Menarche started at the age of 13 years, followed by irregular periods (cycle of 28-90 d).

Personal and family history

Her parents were not consanguineous and were in good health. The growth and development of her two sisters were normal, and there was no family history of hereditary diseases.

Physical examination

The patient's blood pressure was 104/78 mmHg; her height was 132 cm (-5 SD), weight was 40 kg (-2 SD), waist circumference was 80 cm, and head circumference was 48 cm; and some peculiar clinical characteristics were observed, including cheek freckles, high anterior hairline, sparse scalp hair, prominent forehead, depressed nasal bridge, low-set ears, partially absent dentition, small mandible, slightly higher mandibular arch, increased quilt hair, stubby limbs, small hands and feet and short bilateral 4th toes (Figure 1). She had no cubitus valgus, no nail thickening or roughness and no scoliosis. Gynecological examination showed breast development at Tanner stage 4 and pubic hair at Tanner stage 4. Her Mini-Mental State Examination (MMSE) score was 28 points after her symptoms improved.

Laboratory examinations

The patient had low calcium, low potassium, low magnesium, and high phosphorus levels. Her serum aspartate aminotransferase (AST) level was 94 U/L (reference range: 0 to 40), and her serum alanine transaminase (ALT) level was 70 U/L (reference range: 7 to 40). Serum potassium was 2.57 mmol/L (reference range: 3.5 to 5.3), chlorine was 96.4 mmol/L (reference range: 99.0 to 110.0), corrected calcium level was 1.06 mmol/L (reference range: 2.11 to 2.52), magnesium was 0.45 mmol/L (reference range: 0.75-1.02), and phosphorus was 1.86 mmol/L (reference range: 0.85 to 1.51). Details of laboratory findings are listed in Table 1. Therefore, she was referred to our hospital for further diagnosis and treatment.

Imaging examinations

Ophthalmological examination revealed hyperopia. Visual acuity was 0.15 in the left eye and 0.8 in the right eye. No evidence of cataract or papilledema was observed. Her hearing test results were normal. Cranial computed tomography showed sporadic symmetrical calcifications in the cerebellar hemisphere, frontotemporal parietal lobe, basal ganglia, and thalamus. Thyroid ultrasonography showed a cystic-solid mixed nodule measuring approximately 2.3 mm × 1.2 mm in the right lobe, with a Thyroid Imaging Reporting and Data System grade of 2. X-rays of the left knee, anteroposterior pelvis, left hand, and both feet showed a smaller right ilium compared to the contralateral side, shallow acetabular fossa on both sides, and no obvious abnormalities in the bone structure of the remaining pelvis or the structures of the sacroiliac and hip joints on either side (Figure 2). No abnormal density was observed in the pelvis. The phalanges of the left little finger were short, with thickening of the cortex of the tubular bone and narrowing of the medulla. The 4th and 5th metatarsal bones and the corresponding phalanges of both feet were short and small. Ultrasonography of the pelvic cavity showed an anteverted uterus measuring approximately 2.7 cm × 1.9 cm × 3.0 cm. Uniform endometrial echogenicity was observed with no obvious tumor-like structures. The endometrial thickness was approximately 0.4 cm. The bilateral ovaries were normal in size, with no obvious space-occupying lesions in the bilateral adnexal areas.

FINAL DIAGNOSIS

Peripheral blood samples of the patient as well as her parents (who had no abnormal manifestations)

Table 1 Examination value and reference range of laboratory tests

Tests	Measured value	Reference range
Serum potassium (mmol/L)	2.56	3.5-5.3
24-h urinary potassium (mmol)	46.82	25-100
PH	7.40	7.35-7.45
Blood HCO_3^- (mmol/L)	25	22-27
ALD (pg/mL)[1]	355.586	40-310
Renin (pg/mL)[1]	300.452	4-38
Angiotensin II (pg/mL)[1]	329.740	49-310
Serum cortisol (μg/dL)[2]	18.33	6.02-18.4
Serum ACTH (pg/mL)[2]	13.72	7.2-63.3
PTH (pg/mL)	10	15-65
25-hydroxyvitamin D (ng/mL)	17.61	30-100
Corrected serum calcium (mmol/L)	1.12	2.11-2.52
Serum P (mmol/L)	1.86	0.85-1.51
Serum Mg (mmol/L)	0.69	0.75-1.02
24-h urinary calcium (mmol/L)	3.66	< 6.75
FT_4 (pmol/L)	16.2	12-22
FT_3 (pmol/L)	4.43	3.1-6.8
TSH (uIU/mL)	0.8	0.27-4.2
LH (uIU/mL)	4.08	2.4-12.6
FSH (uIU/mL)	3.57	3.5-12.5
PRL (uIU/mL)	644.2	102-496
E_2 (pg/mL)	52.93	12.4-233
P (nmol/L)	0.72	0.181-2.84
T (nmol/L)	1.76	0.29-1.67

[1]In sitting position.
[2]8 am.
PH: Potential of hydrogen; ALD: Aldosterone; ACTH: Adrenocorticotropic hormone; PTH: Parathyroid hormone; P: Phosphorus; Mg: Magnesium; FT_4: Serum free thyroxine; FT_3: Serum free triiodothyronine; TSH: Thyroid-stimulating hormone; LH: Luteinizing hormone; FSH: Follicle-stimulating hormone; PRL: Prolactin; E_2: Estrogen; P: Progesterone; T: Total testosterone.

were collected, and DNA analysis was performed after obtaining informed consent. This study was conducted according to the principles of the Declaration of Helsinki with the approval of the ethics committee of Nanchong Central Hospital. The samples were subjected to Sanger sequencing by polymerase chain reaction (PCR) and whole-exome sequencing.

First, DNA was extracted from the blood samples. Libraries were then constructed, and sequencing was performed on the Illumina platform. After obtaining the original sequencing results, analysis was performed with the given reference sequence or genome (GRCh37/hg19). The analysis included the following three steps: (1) Quality assessment of the sequencing data; (2) variation detection; and (3) variation screening and prediction of disease associations. Burrows–Wheeler Aligner was used to align the sequenced fragments to the reference genome, and Picard software was used to remove sequences generated by PCR duplication. After analyzing the patient gene sequencing results for single-nucleotide variants (SNVs) and insertions-deletions with reference to the hg19 genome, somatic mutation predictions were made on paired samples using MuTect, followed by annotation of the SNVs using the ANNOVAR program combined with the refGene annotation in the UCSC Genome Browser. Finally, the effects of SNV mutation sites in the exonic region on protein translation were annotated using SIFT and PolyPhen.

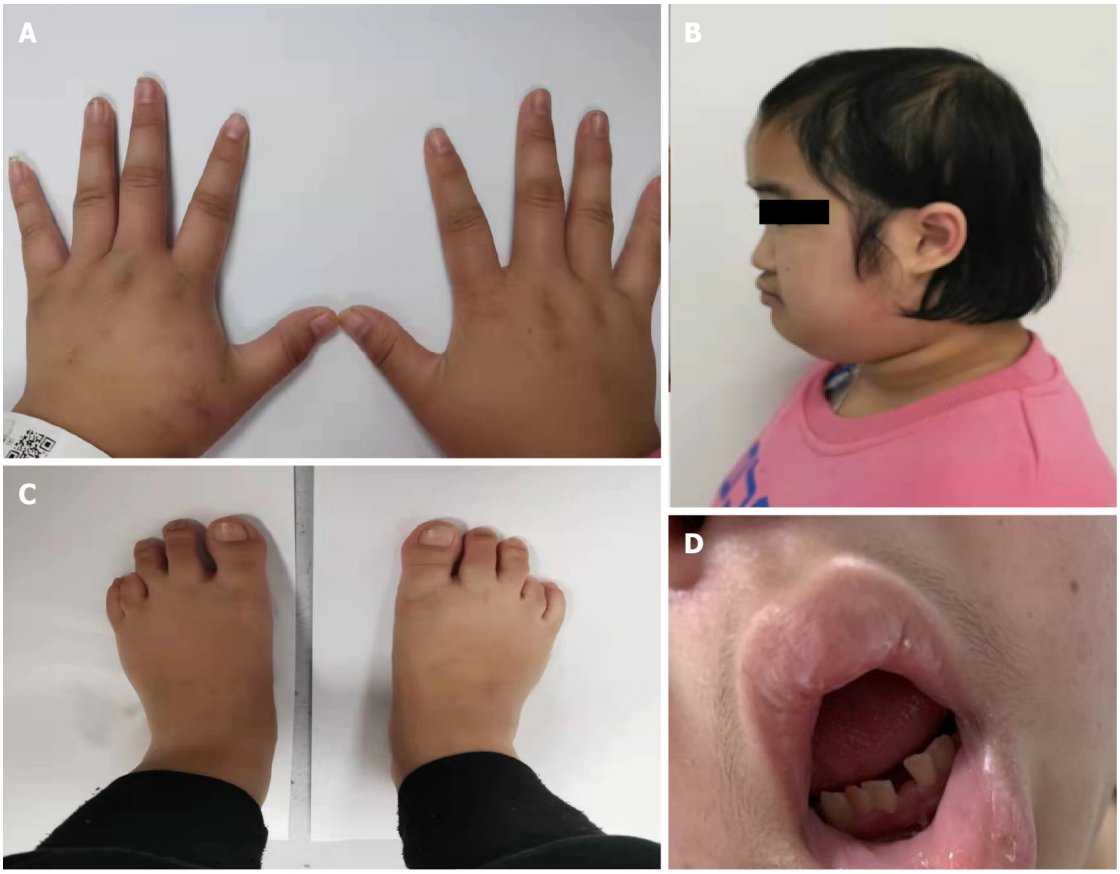

DOI: 10.12998/wjcc.v11.i10.2290

Figure 1 Special phenotypes of this 18-year-old female patient with Kenny-Caffey syndrome type 2. A: Small hands; B: Cheek freckles, high anterior hairline, sparse scalp hair, prominent forehead, depressed nasal bridge, low-set ears, small mandible, slightly higher mandibular arch, increased quilt hair; C: Feet and short in bilateral 4th toes; D: Partially absent dentition.

Operating procedures

Sample collection: Peripheral venous blood was collected from the patient and her family members, anticoagulated with sodium citrate, and stored at -20 °C for subsequent use.

Genomic DNA extraction: Genomic DNA was extracted using a blood DNA extraction kit (QIAamp DNA Blood Mini Kit) per the manufacturer's instructions.

PCR amplification: Exon 5 of *FAM111A* was amplified by PCR (Applied Biosystems Veriti® 96-Well Thermal Cycler, Applied Biosystems, United States; ABI3130XL genetic analyzer, Applied Biosystems, United States), and sequencing was performed. The primers were as follows: Forward, TGCTTGTGCT-GTGATCCCTC; reverse, ATGCCTATGAAATAACAACTCC. The total volume of the PCR was 30 μL, including 3 μL of template DNA, 1.5 μL each of the forward and reverse primers, 15 μL of 2 × HieffTM PCR Master Mix (With Dye, Yeasen, China), and 9 μL of ddH_2O.

Sequencing of the PCR products and analysis of DNA mutations: All sequencing results were compared against the known sequencing results of the genomic DNA of FAM111A in the NCBI Blast database.

PCR results

First, whole-exome sequencing showed a missense mutation in exon 5 (c.1706G>A) of FAM111A (NM_001142519) of the patient (Figure 3), which resulted in an amino acid substitution (R569H). The American College of Medical Genetics and Genomics rating of the variant was a variant of uncertain significance. No mutation in TBCE was observed. Neither of her parents, who showed no clinical manifestations, carried this gene mutation, indicating that this was a *de novo* mutation of a novel nonsynonymous coding variant, consistent with three cases of novel KCS2 mutations reported in Japan [6].

DOI: 10.12998/wjcc.v11.i10.2290 **Copyright** ©The Author(s) 2023.

Figure 2 The head computed tomography and skeletal X-ray features of the patient are indicated by arrows A–E, respectively. A: Head computed tomography (noncontrast) showing symmetrical calcifications in the cerebellar hemisphere, frontotemporal parietal lobe, basal ganglia, and thalamus; B: Digital radiography (DR) of the anteroposterior pelvis showing that the right ilium is smaller compared to the left side, as well as shallow acetabular fossa on both sides; C: DR of the left foot showing short and small 4th and 5th metatarsal bones and corresponding phalanges in both feet; D: The phalanges of the left little finger are short, with thickening of the cortex of the tubular bone and narrowing of the medulla; E: DR of the left lower limb showing thickening of the cortex of the tubular bone and narrowing of the medulla.

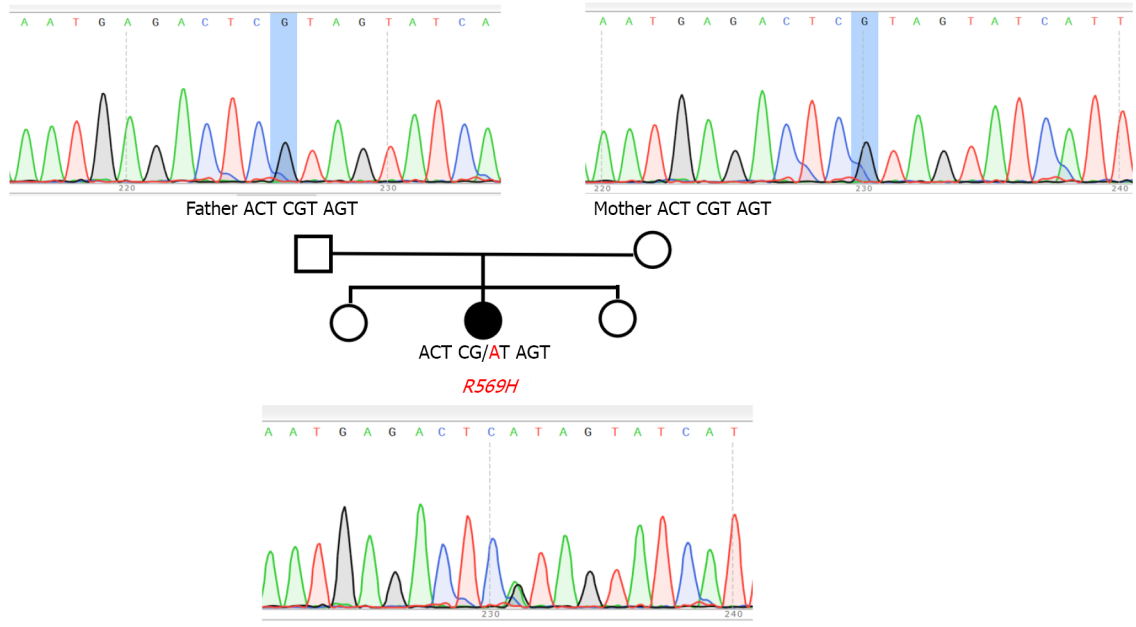

DOI: 10.12998/wjcc.v11.i10.2290 **Copyright** ©The Author(s) 2023.

Figure 3 Genetic pedigree of the patient showing the chromatograms of Sanger sequencing results of the *FAM111A* mutation for the patient and her parents. Data were obtained by Sanger sequencing during the confirmation of the diagnosis. Forward sequencing was performed for the mutation. In the pedigree, the black symbols represent probands. Squares and circles represent males and females, respectively. In the chromatogram, the black letters indicate the nucleotide sequence of the wild-type, while the nucleotides in red indicate mutations. *R569H* was identified in all probands but not in the parents who received the sequencing tests. The younger and older sisters were phenotypically normal and did not agree to undergo Sanger sequencing.

TREATMENT

The patient was treated with calcium carbonate D3 (600 mg qd) and calcitriol (0.25 μg qd) after the diagnosis of primary hypoparathyroidism.

OUTCOME AND FOLLOW-UP

After intravenous treatment with magnesium sulfate improved the hypomagnesemia, the regimen was changed to potassium magnesium aspartate (2 tablets tid for continued magnesium supplementation). Follow-up after 2 mo of treatment showed a 24 h urinary calcium concentration of 1.69 mmoL (urine volume: 1300 mL), ALT concentration of 51 U/L, AST concentration of 47.2 U/L, blood potassium concentration of 3.41 mmol/L, blood calcium concentration of 2.10 mmol/L, blood phosphorus concentration of 2.0 mmol/L, and blood magnesium concentration of 0.57 mmol/L. The patient was generally in good condition, with no numbness of the extremities or muscle twitching.

Literature review

In addition to previously reported cases, the clinical features and gene mutation sites of the patient with KCS2 are summarized in Table 2[5-17]. The 23 patients included 10 males and 13 females. The main clinical manifestations were as follows: (1) Signs such as short stature, polydactyly, developmental delay, abnormal liver function, eye abnormalities (hyperopia and pseudopapilledema), and normal intelligence; (2) hypocalcemia, hypomagnesemia, hyperphosphatemia, and low parathyroid hormone (PTH) level, with some patients showing abnormal liver function and hypothyroidism; and (3) calcification in the basal ganglia, with thickening of the cortex and medullary stenosis. Abnormal head circumference was also observed, combined with delayed closure of the anterior fontanelle. Sanger sequencing analysis of FAM111A showed that c.1706G>A (p.R569H) is the hotspot in most reported cases (16/23, 69.6%) and is more common in women (11/16, 68.8%). However, only three female patients were followed up after the age of 18 years (22, 25, 40 and 56 years of age), two of whom carried *de novo* mutations (the other was unknown).

DISCUSSION

In 1966, Kenny and Linarelli[18] reported a mother and child with severely short stature and hypocalcemia combined with hypomagnesemia, while Caffey[19] reported detailed imaging features of the skeletal deformities of this mother and child, namely, long and thin bones and narrowing of the marrow cavity. This rare teratogenic disorder was later referred to collectively as KCS, which is characterized by severely short stature, thickening of the tubular cortex and medullary stenosis, delayed closure of the anterior fontanelle, eye abnormalities (hyperopia, amblyopia, cataracts, pseudo papilledema, etc), and hypocalcemia due to hypoparathyroidism. According to the inheritance mode, clinical manifestations, and mutated genes, KCS is divided into two types: (1) KCS type 1 (OMIM #244460) is an autosomal recessive disorder that manifests as intrauterine growth retardation and mental retardation in addition to KCS symptoms. The pathogenic gene has mutations in TBCE; and (2) KCS2 (OMIM #127000) is an autosomal dominant or *de novo* mutation disorder that usually manifests as postnatal growth retardation without intellectual abnormalities. KCS2 is rarer than KCS1, with < 30 cases reported worldwide up to date. The pathogenetic gene is a mutation (NM_001142519.1) in the *FAM111A* gene proposed by Unger *et al*[5] in 2013, which is located on the long arm of chromosome 11 (11q12.1) and encodes an unknown protein consisting of 611 amino acids. The C-terminal region of this protein is homologous to a trypsin-like peptidase, and the catalytic triad specific for this peptidase is conserved [20,21]. However, the specific role of *FAM111A* has not been determined, and observational findings suggest that *FAM111A* regulates and interacts with the C-terminal region of the large T antigen in a cell-dependent manner[20]. *FAM111A* appears to be critical for pathways that control parathyroid hormone production, calcium homeostasis, and bone development and growth[5]. Here, we describe a case of KCS2 caused by a *de novo* pathogenic variant of *FAM111A*. This patient fit the characteristic phenotypes described for KCS2: Short stature; facial deformities, including low-set ears and depressed nose bridge; short hands and feet; missing dentition; delayed anterior fontanelle closure; hypoparathyroidism; hypocalcemia; hyperphosphatemia; hypokalemia; and hypomagnesemia. However, the patient had no previously reported pseudo papilledema, hearing abnormalities, anemia, or spinal curvature.

Patients with KCS2 may also have different clinical manifestations due to different mutation sites in *FAM111A*. Even for mutations at the same site, the described phenotypes may differ. This report describes a case of a young woman who presented with a 3-d history of psychosis, in addition to severely short stature, thickening of the tubular cortex and medullary stenosis, delayed anterior fontanelle closure, hyperopia, missing dentition, hypokalemia, hypochloremia, uneven hip bone size, and overweight on top of hypocalcemia as a result of hypothyroidism. The patient did not have scoliosis. She also showed normal intelligence, with no familial genetic background. Whole-exome sequencing was performed on the proband based on the high suspicion given her clinical manifestations and laboratory imaging results. The relevant loci were also sequenced in samples from her parents. The results showed that the patient had a missense point mutation (c.1706G>A, p.R569H) in *FAM111A*, with no abnormal mutations in her parents. Therefore, the patient was considered to have a *de novo* mutation, which was consistent with previous reports[6].

Table 2 Summary of the clinical manifestations and genetic loci of previously reported patients with Kenny-Caffey syndrome type 2

	Year	Country	Fellow-up age	Sex	Inheritance patterns	Nucleotide change	Amino acid alteration	Ref.
1	2013	Switzerland	40 yr	F	De novo	c.1706G>A	p.R569H	[5]
2		India	17 yr	M	NA	c.1706G>A	p.R569H	[5]
3		Germany	10 yr	M	NA	c.1706G>A	p.R569H	[5]
4		Italy	6 mo	F	De novo	c.1706G>A	p.R569H	[5]
5		India	7 yr	M	NA	c.1531T>C	p.Y511H	[5]
6	2014	Japan	10 yr	F	De novo	c.1706G>A	p.R569H	[6]
7		Japan	16 yr	M	De novo	c.1706G>A	p.R569H	[6]
8		Japan	22 yr	F	De novo	c.1706G>A	p.R569H	[6]
9		Japan	38 yr	M	NA	c.1706G>A	p.R569H	[6]
10	2014	Canada	3 yr	F	AD	c.1706G>A	p.R569H	[7]
11		Canada	25 yr	F	NA	c.1706G>A	p.R569H	[7]
12	2014	America	NA	F	De novo	c.1706G>A	p.R569H	[8]
13	2017	Australia	6 yr	F	NA	c.1622C> A	p.S541Y	[9]
14	2019	China	10 yr	F	NA	c.1706G>A	p.R569H	[10]
15	2020	Brazil	18 yr	M	De novo	c.1706G>A	p.R569H	[11]
16	2020	China	23 yr	M	De novo	c.1621T>C	p.S541P	[12]
17		China	23 yr	M	De novo	c.1621T>C	p.S541P	[12]
18	2020	America	20 mo	M	De novo	c.968G>A	p.G323E	[13]
19	2020	Brazil	10 yr	F	De novo	c.1706G>A	p.R569H	[14]
20	2021	India	9 yr	F	NA	g.58920847G>A	p.R569H	[15]
21	2021	Turkey	NA	M	AR	c.976T>A	NA	[16]
						c.1714_1716del		
22	2021	China	18 yr	F	De novo	c.1706G>A	p.R569H	Our patient
23	2023	Japan	56 yr	F	NA	c.1706G>A	p.R569H	[17]

F: Female; M: Male; NA: Not applicable; AR: Autosomal recessive; AD: Autosomal dominant.

The patient also showed microcephaly. Cavole *et al*[11] reported a case in Brazil of an 18-year-old male with a head circumference of 33 cm (ninth percentile) and suggested that microcephaly may be due to a biological spectral overlap between FAM111A and the TBCE locus in SSS. However, no TBCE mutation was detected in the present case. Moreover, when the patient's electrolyte levels improved, her language expression was clear, and she showed no intellectual impairment according to the MMSE. Therefore, there was no evidence for SSS, which was consistent with the description of patients with KCS2 showing no intellectual abnormalities. A report of a pair of adult twin males in China described macrocephaly, ankylosing spondylitis, and scoliosis among the clinical manifestations of KCS2[12]. However, these characteristics were not observed in the present case. Inconsistent reports regarding the head circumference of the upper third of the cephalofacial deformity of patients with KCS2 have been noted, suggesting that imaging findings of calvarial thinning, sclerosis, or hypoplasia are more useful for the confirmation of the diagnosis than measurements of head circumference[13].

Few studies have reported reproductive function in adult female patients with KCS2, with two previous cases mentioning fertility. The mother reported by Kenny had normal intelligence and had menarche at 12 years of age, followed by regular menstruation[18]. She had three pregnancies. The first pregnancy led to the delivery of a normal boy without any skeletal abnormalities *via* cesarean section due to her small pelvis. The second pregnancy with a baby girl was terminated at 7 mo, while the third pregnancy, a son who had the same phenotype as his mother, was delivered by cesarean section at 37 wk. Although the woman had not received genetic testing, KCS2 was highly likely based on her intelligence. Menstruation was not described for the Canadian mother with KCS2 reported with her daughter[7]. Based on previous reports, KCS2 may have little effect on the gonadal axis. However, since most of the previous patients were minors, additional reports on the effect of KCS2 on menstruation and

pregnancy are required for analysis and summary. In the present case, the age of menarche was 13 years, with no obvious abnormalities compared to other young women of the same age and race. However, the menstruation cycle of the patient was extremely irregular. Her testosterone level was slightly increased, which indicated possible polycystic ovary syndrome (PCOS). Pelvic ultrasound did not find features of polycystic ovarian changes. Further assessments, including basal body temperature and oral glucose tolerance tests, have been recommended to determine the etiology of hyperandrogenism during follow-up. Previous studies have suggested that, despite the equivalent prevalence of KCS2 between male and female patients, male patients have microorchidism and infertility, resulting in no father-to-son cases reported to date[11,12]. For patients with KCS2, in addition to hypocalcemia, which requires long-term calcium supplementation, and biochemical disorders as a result of hypoparathyroidism, genetic counseling is required before pregnancy[12]. Previous case reports rarely mentioned the presence of menstrual irregularity in female patients. According to the current literature, it is unclear whether KCS2 is related to female hyperandrogenemia.

The differences between this patient and previous reports include the following: (1) Sudden onset of psychiatric disorder. The patient was admitted to the hospital with hypokalemia, hypomagnesemia, hypocalcemia, and hyperphosphatemia. However, her urinary calcium level was not low. Her hypocalcemia, hypokalemia, and hypomagnesemia were corrected after treatment, suggesting the presence of electrolyte abnormalities, especially the possible presence of a syndrome including hypoparathyroidism, which has been reported in patients with severe hypocalcemia accompanied by hypomagnesemia. The fourth KCS2 patient mentioned in a report by Isojima *et al*[6] from Japan had hypoparathyroidism secondary to hypomagnesemia, as confirmed by magnesium load and calcium restriction tests. The serum calcium levels of the patient were corrected when the calcium supplementation regimen was changed from vitamin D and calcium lactate to magnesium supplementation with magnesium sulfate. Support therapy for KSC2 may be associated with complex electrolyte disorders, and the correction of low magnesium levels may be a critical step in the treatment of this condition; and (2) this patient was more obese than patients in previous reports based on the patient's appearance, waist circumference, and body mass index. These values were inconsistent with the normal or lean body shapes in previous reports[6,9,12,14,15], suggesting that some patients with KSC2 may be obese or overweight. The patient had no acanthosis nigricans, insulin resistance, or polycystic findings on color Doppler ultrasound of the uterine appendage. PCOS was not supported despite the patient's menstrual disorders.

Exome sequencing of the four patients with KCS2 from Japan reported by Isojima *et al*[6] identified *FAM111A* as the pathogenic gene of KCS2. One of the patients showed a heterozygous *de novo* mutation of *FAM111A* (R569H), which was the same mutation observed in the present case. The mRNA expression levels of the individual with this mutation were comparable to those of the normal controls. Thus, the *FAM111A* mutation may have caused atypical features of phenylalanine by altering the intermolecular protein interactions. Five patients with clinical diagnoses of KCS2 in five different countries reported by Unger *et al*[5] also showed *de novo* mutations in *FAM111A*, with four of them having the c.1706G>A (p.Arg569His) mutation. Pathogenic mutations of *FAM111A* were also identified in subsequently reported cases of KCS2 in different populations, with the R569H mutation being the most common. There were no genetic relationships among these sporadic cases (Table 1). FAM111A is located on the long arm of chromosome 11 (11q12.1) and encodes a protein whose C-terminal region is homologous to trypsin-like peptidase[14]. The C-terminus is an evolutionarily conserved region of proteins and appears to be a hotspot for mutations[9,11,22]. The cellular function of *FAM111A* remains unclear. Previous studies have speculated that *FAM111A* may be involved in transcriptional regulation owing to its cell cycle-dependent expression and nuclear localization. One plausible model to explain these findings is that FAM111A is active when unbound but inactive when bound to an as-yet unidentified chaperone[5]. A recent study suggested that alterations in peptidase activity and the acquisition of functional mechanisms are the pathophysiological mechanisms of *FAM111A*-related diseases. Pathogenic mutations increase the proteolytic activity of proteins, resulting in decreased DNA replication and transcription, ultimately leading to programmed cell death[22]. Furthermore, molecular simulations showed that the reported variants were not located at the putative active site but rather at or near the protein surface. Different mutation sites in *FAM111A* may lead to different phenotypes. For example, Müller *et al*[23] reported a case in the United States of a fetus whose prenatal ultrasound showed skeletal dysplasia with edema, spleen dysplasia, and cerebellum deletion, as well as C.1685A>C and p.Tyr562Ser/Y562S. *FAM111A* has also been proposed to lead to a phenotypic overlap with osteocraniostenosis, which is associated with more severe perinatal mortality, cerebellar hypoplasia or hypomineralization, wider metaphysis, and hypoplastic or absent spleen. *FAM111A* is expressed in the bone and parathyroid glands and may play a key role in regulating intracellular pathways involved in skeletal development, height growth, parathyroid development and regulation, and calcium homeostasis[12]. However, the exact mechanism remains unclear. KCS2 is an extremely rare condition. Among 173 patients with childhood-onset hypoparathyroidism reported in a 2019 single-center study by the Peking Union Medical College, samples from 23 patients were subjected to next-generation sequencing and multiplex ligation-dependent probe amplification analysis[20]. Only one patient (0.6%) was diagnosed with KCS2[15]. Most of the reported patients were children with short-term follow-up. Therefore, a detailed description of the phenotype and natural course of KCS2 in adults is lacking. In

this case, due to the absence of obvious symptoms of hypocalcemia, the patient did not visit a doctor for a definite diagnosis for a long time, resulting in a delay in the treatment of her conditions. It was not until she developed a severe electrolyte disorder (hypocalcemia, hypomagnesemia, hypokalemia, and hyperphosphatemia) requiring hospital admission that the patient first saw a doctor and was diagnosed with KCS2 based on the results of genetic sequencing.

CONCLUSION

In conclusion, we detected a missense variant of *FAM111A* in a patient with an acute onset of psychiatric symptoms combined with short stature, electrolyte disorders including hypocalcemia and hypomagnesemia, and abnormal skeletal manifestations consistent with KCS2. The clinical features in this patient were consistent with those previously reported. Moreover, the R569H variant was similar to other reported pathogenic variants and was consistent with the proposed pathophysiological mechanisms. However, the patient showed different manifestations, including overweight, severe electrolyte disorder, and psychiatric disorders. In addition, microcephaly was a relatively rare manifestation, suggesting an overlap with SSS. This was a sporadic case, which suggested that the *FAM111A* mutation was more likely to be a *de novo* mutation. Since the patient was an adult at the time of consultation, long-term follow-up treatment and observation of electrolyte status are necessary. Moreover, the fertility of the patient and the genetics of her offspring should be determined.

ACKNOWLEDGEMENTS

The authors thank our families for their support, as well as the patient and her family, who inspired us during the clinical and genetic research.

FOOTNOTES

Author contributions: Yuan N and Lu L designed the study; Yuan N wrote the manuscript; Xing XP, Wang O, Jiang Y, Wu J, He MH, Wang XJ and Cao LW collected, analyzed and interpreted the data; Lu L critically reviewed, edited and approved the manuscript; All authors read and approved the final manuscript.

Supported by National Natural Science Foundation of China, No. 82070817.

Informed consent statement: Written informed consent has been obtained from all patients.

Conflict-of-interest statement: All the authors report no relevant conflicts of interest for this article.

CARE Checklist (2016) statement: The authors have read the CARE Checklist (2016), and the manuscript was prepared and revised according to the CARE Checklist (2016).

Country/Territory of origin: China

ORCID number: Ning Yuan 0000-0002-6627-1554; Lin Lu 0000-0003-3379-8277; Xiao-Ping Xing 0000-0002-2759-5177; Yue Jiang 0000-0003-0547-2595.

S-Editor: Fan JR
L-Editor: A
P-Editor: Fan JR

REFERENCES

1 **Clarke BL**, Brown EM, Collins MT, Jüppner H, Lakatos P, Levine MA, Mannstadt MM, Bilezikian JP, Romanischen AF, Thakker RV. Epidemiology and Diagnosis of Hypoparathyroidism. *J Clin Endocrinol Metab* 2016; **101**: 2284-2299 [PMID: 26943720 DOI: 10.1210/jc.2015-3908]

2 **Yagi H**, Furutani Y, Hamada H, Sasaki T, Asakawa S, Minoshima S, Ichida F, Joo K, Kimura M, Imamura S, Kamatani N,

Momma K, Takao A, Nakazawa M, Shimizu N, Matsuoka R. Role of TBX1 in human del22q11.2 syndrome. *Lancet* 2003; **362**: 1366-1373 [PMID: 14585638 DOI: 10.1016/s0140-6736(03)14632-6]

3 **Van Esch H**, Groenen P, Nesbit MA, Schuffenhauer S, Lichtner P, Vanderlinden G, Harding B, Beetz R, Bilous RW, Holdaway I, Shaw NJ, Fryns JP, Van de Ven W, Thakker RV, Devriendt K. GATA3 haplo-insufficiency causes human HDR syndrome. *Nature* 2000; **406**: 419-422 [PMID: 10935639 DOI: 10.1038/35019088]

4 **Parvari R**, Hershkovitz E, Grossman N, Gorodischer R, Loeys B, Zecic A, Mortier G, Gregory S, Sharony R, Kambouris M, Sakati N, Meyer BF, Al Aqeel AI, Al Humaidan AK, Al Zanhrani F, Al Swaid A, Al Othman J, Diaz GA, Weiner R, Khan KT, Gordon R, Gelb BD; HRD/Autosomal Recessive Kenny-Caffey Syndrome Consortium. Mutation of TBCE causes hypoparathyroidism-retardation-dysmorphism and autosomal recessive Kenny-Caffey syndrome. *Nat Genet* 2002; **32**: 448-452 [PMID: 12389028 DOI: 10.1038/ng1012]

5 **Unger S**, Górna MW, Le Béchec A, Do Vale-Pereira S, Bedeschi MF, Geiberger S, Grigelioniene G, Horemuzova E, Lalatta F, Lausch E, Magnani C, Nampoothiri S, Nishimura G, Petrella D, Rojas-Ringeling F, Utsunomiya A, Zabel B, Pradervand S, Harshman K, Campos-Xavier B, Bonafé L, Superti-Furga G, Stevenson B, Superti-Furga A. FAM111A mutations result in hypoparathyroidism and impaired skeletal development. *Am J Hum Genet* 2013; **92**: 990-995 [PMID: 23684011 DOI: 10.1016/j.ajhg.2013.04.020]

6 **Isojima T**, Doi K, Mitsui J, Oda Y, Tokuhiro E, Yasoda A, Yorifuji T, Horikawa R, Yoshimura J, Ishiura H, Morishita S, Tsuji S, Kitanaka S. A recurrent de novo FAM111A mutation causes Kenny-Caffey syndrome type 2. *J Bone Miner Res* 2014; **29**: 992-998 [PMID: 23996431 DOI: 10.1002/jbmr.2091]

7 **Nikkel SM**, Ahmed A, Smith A, Marcadier J, Bulman DE, Boycott KM. Mother-to-daughter transmission of Kenny-Caffey syndrome associated with the recurrent, dominant FAM111A mutation p.Arg569His. *Clin Genet* 2014; **86**: 394-395 [PMID: 24635597 DOI: 10.1111/cge.12290]

8 **Guo MH**, Shen Y, Walvoord EC, Miller TC, Moon JE, Hirschhorn JN, Dauber A. Whole exome sequencing to identify genetic causes of short stature. *Horm Res Paediatr* 2014; **82**: 44-52 [PMID: 24970356 DOI: 10.1159/000360857]

9 **Abraham MB**, Li D, Tang D, O'Connell SM, McKenzie F, Lim EM, Hakonarson H, Levine MA, Choong CS. Short stature and hypoparathyroidism in a child with Kenny-Caffey syndrome type 2 due to a novel mutation in FAM111A gene. *Int J Pediatr Endocrinol* 2017; **2017**: 1 [PMID: 28138333 DOI: 10.1186/s13633-016-0041-7]

10 **Wang Y**, Nie M, Wang O, Li Y, Jiang Y, Li M, Xia W, Xing X. Genetic Screening in a Large Chinese Cohort of Childhood Onset Hypoparathyroidism by Next-Generation Sequencing Combined with TBX1-MLPA. *J Bone Miner Res* 2019; **34**: 2254-2263 [PMID: 31433868 DOI: 10.1002/jbmr.3854]

11 **Cavole TR**, Perrone E, de Faria Soares MF, Dias da Silva MR, Maeda SS, Lazaretti-Castro M, Alvarez Perez AB. Overlapping phenotype comprising Kenny-Caffey type 2 and Sanjad-Sakati syndromes: The first case report. *Am J Med Genet A* 2020; **182**: 3029-3034 [PMID: 33010201 DOI: 10.1002/ajmg.a.61896]

12 **Cheng SSW**, Chan PKJ, Luk HM, Mok MT, Lo IFM. Adult Chinese twins with Kenny-Caffey syndrome type 2: A potential age-dependent phenotype and review of literature. *Am J Med Genet A* 2021; **185**: 636-646 [PMID: 33263187 DOI: 10.1002/ajmg.a.61991]

13 **Turner AE**, Abu-Ghname A, Davis MJ, Shih L, Volk AS, Streff H, Buchanan EP. Kenny-Caffey Syndrome Type 2: A Unique Presentation and Craniofacial Analysis. *J Craniofac Surg* 2020; **31**: e471-e475 [PMID: 32310878 DOI: 10.1097/SCS.0000000000006439]

14 **Deconte D**, Kreusch TC, Salvaro BP, Perin WF, Ferreira MAT, Kopacek C, da Rosa EB, Heringer JI, Ligabue-Braun R, Zen PRG, Rosa RFM, Fiegenbaum M. Ophthalmologic Impairment and Intellectual Disability in a Girl Presenting Kenny-Caffey Syndrome Type 2. *J Pediatr Genet* 2020; **9**: 263-269 [PMID: 32765931 DOI: 10.1055/s-0039-3401831]

15 **Yerawar C**, Kabde A, Deokar P. Kenny-Caffey syndrome type 2. *QJM* 2021; **114**: 267-269 [PMID: 32428224 DOI: 10.1093/qjmed/hcaa175]

16 **Eren E**, Tezcan Ünlü H, Ceylaner S, Tarım Ö. Compound Heterozygous Variants in FAM111A Cause Autosomal Recessive Kenny-Caffey Syndrome Type 2. *J Clin Res Pediatr Endocrinol* 2023; **15**: 97-102 [PMID: 34382758 DOI: 10.4274/jcrpe.galenos.2021.2020.0315]

17 **Ohmachi Y**, Urai S, Bando H, Yokoi J, Yamamoto M, Kanie K, Motomura Y, Tsujimoto Y, Sasaki Y, Oi Y, Yamamoto N, Suzuki M, Shichi H, Iguchi G, Uehara N, Fukuoka H, Ogawa W. Case report: Late middle-aged features of FAM111A variant, Kenny-Caffey syndrome type 2-suggestive symptoms during a long follow-up. *Front Endocrinol (Lausanne)* 2022; **13**: 1073173 [PMID: 36686468 DOI: 10.3389/fendo.2022.1073173]

18 **Kenny FM**, Linarelli L. Dwarfism and cortical thickening of tubular bones. Transient hypocalcemia in a mother and son. *Am J Dis Child* 1966; **111**: 201-207 [PMID: 5322798 DOI: 10.1001/archpedi.1966.02090050133013]

19 **Caffey J**. Congenital stenosis of medullary spaces in tubular bones and calvaria in two proportionate dwarfs--mother and son; coupled with transitory hypocalcemic tetany. *Am J Roentgenol Radium Ther Nucl Med* 1967; **100**: 1-11 [PMID: 6023894 DOI: 10.2214/ajr.100.1.1]

20 **Fine DA**, Rozenblatt-Rosen O, Padi M, Korkhin A, James RL, Adelmant G, Yoon R, Guo L, Berrios C, Zhang Y, Calderwood MA, Velmurgan S, Cheng J, Marto JA, Hill DE, Cusick ME, Vidal M, Florens L, Washburn MP, Litovchick L, DeCaprio JA. Identification of FAM111A as an SV40 host range restriction and adenovirus helper factor. *PLoS Pathog* 2012; **8**: e1002949 [PMID: 23093934 DOI: 10.1371/journal.ppat.1002949]

21 **Rawlings ND**, Barrett AJ, Bateman A. MEROPS: the peptidase database. *Nucleic Acids Res* 2010; **38**: D227-D233 [PMID: 19892822 DOI: 10.1093/nar/gkp971]

22 **Hoffmann S**, Pentakota S, Mund A, Haahr P, Coscia F, Gallo M, Mann M, Taylor NM, Mailand N. FAM111 protease activity undermines cellular fitness and is amplified by gain-of-function mutations in human disease. *EMBO Rep* 2020; **21**: e50662 [PMID: 32776417 DOI: 10.15252/embr.202050662]

23 **Müller R**, Steffensen T, Krstić N, Cain MA. Report of a novel variant in the FAM111A gene in a fetus with multiple anomalies including gracile bones, hypoplastic spleen, and hypomineralized skull. *Am J Med Genet A* 2021; **185**: 1903-1907 [PMID: 33750016 DOI: 10.1002/ajmg.a.62182]

World Journal of Clinical Cases

Submit a Manuscript: https://www.f6publishing.com

World J Clin Cases 2023 April 6; 11(10): 2301-2307

DOI: 10.12998/wjcc.v11.i10.2301

ISSN 2307-8960 (online)

CASE REPORT

Dupilumab for treatment of severe atopic dermatitis accompanied by lichenoid amyloidosis in adults: Two case reports

Xue-Qi Zhao, Wen-Jing Zhu, Yan Mou, Meng Xu, Jian-Xin Xia

Specialty type: Medicine, research and experimental

Provenance and peer review: Unsolicited article; Externally peer reviewed.

Peer-review model: Single blind

Peer-review report's scientific quality classification

Grade A (Excellent): 0
Grade B (Very good): B
Grade C (Good): C
Grade D (Fair): 0
Grade E (Poor): 0

P-Reviewer: Rolla G, Italy; Teragawa H, Japan

Received: December 4, 2022
Peer-review started: December 4, 2022
First decision: February 7, 2023
Revised: February 18, 2023
Accepted: March 14, 2023
Article in press: March 14, 2023
Published online: April 6, 2023

Xue-Qi Zhao, Wen-Jing Zhu, Yan Mou, Meng Xu, Jian-Xin Xia, Department of Dermatology, The Second Hospital of Jilin University, Changchun 130041, Jilin Province, China

Corresponding author: Jian-Xin Xia, MD, PhD, Professor, Department of Dermatology, The Second Hospital of Jilin University, No. 218 Ziqiang Street, Nanguan District, Changchun 130041, Jilin Province, China. 911469806@qq.com

Abstract

BACKGROUND

Lichenoid amyloidosis (LA) is a subtype of primary cutaneous amyloidosis characterized by persistent multiple groups of hyperkeratotic papules, usually on the lower leg, back, forearm, or thigh. LA may be associated with several skin diseases, including atopic dermatitis (AD). The treatment of LA is considered to be difficult. However, as there is some overlap in the etiopathogenesis of LA and AD, AD treatment may also be effective for LA.

CASE SUMMARY

Case 1: A 70-year-old man was diagnosed with severe AD with LA based on large dark erythema and papules on the trunk and buttocks and dense hemispherical millet-shaped papules with pruritus on the extensor side of the lower limbs. He had a long history of the disease (8 years), with repeated and polymorphic skin lesions. Given the poor efficacy of traditional treatments, this patient was recommended to receive dupilumab treatment. At the initial stage, 300 mg was injected subcutaneously every 2 wk. After 28 wk, the drug interval was extended to 1 mo due to the pandemic. Follow-up observations revealed that the patient reached an Eczema Area Severity Index of 90 (skin lesions improved by 90% compared with the baseline) by the end of the study. Moreover, Investigator's Global Assessment score was 1, and scoring atopic dermatitis index and numeric rating scale improved by 97.7% and 87.5% compared with the baseline, respectively, with LA skin lesions having largely subsided. Case 2: A 30-year-old woman was diagnosed with severe AD with LA, due to dense and substantial papules on the dorsal hands similar to changes in cutaneous amyloidosis, and erythema and papules scattered on limbs and trunk with pruritus, present for 25 years. After 16 wk of dupilumab treatment, she stopped, and skin lesions completely subsided, without recurrence since the last follow-up.

CONCLUSION

Dupilumab shows rational efficacy and safety in the treatment of severe AD with

LA, in addition to benefits in the quality of life of the patients.

Key Words: Atopic dermatitis; Lichenoid amyloidosis; Dupilumab; Treatment; Case report

Core Tip: Although cases of atopic dermatitis (AD) with lichenoid amyloidosis (LA) are not uncommon, there are few reports on the use of AD treatment for LA. In this paper, two adult patients with severe AD and LA are described. Treatment with dupilumab significantly improved the AD and LA skin lesions with no adverse reactions, confirming the efficacy and safety of dupilumab in the treatment of AD with LA, and providing a reference for clinically similar diseases.

Citation: Zhao XQ, Zhu WJ, Mou Y, Xu M, Xia JX. Dupilumab for treatment of severe atopic dermatitis accompanied by lichenoid amyloidosis in adults: Two case reports. *World J Clin Cases* 2023; 11(10): 2301-2307
URL: https://www.wjgnet.com/2307-8960/full/v11/i10/2301.htm
DOI: https://dx.doi.org/10.12998/wjcc.v11.i10.2301

INTRODUCTION

Atopic dermatitis (AD), a chronic recurrent disease driven by type-2 inflammation, is clinically characterized as chronic eczematoid manifestations[1]. Lichenoid amyloidosis (LA) is a subtype of primary cutaneous amyloidosis, which is characterized by persistent multiple groups of hyperkeratotic papules, usually in the lower leg, back, forearm, or thigh[2]. It has been demonstrated that primary cutaneous amyloidosis is associated with AD, with an elusive mechanism[3-5]. Dupilumab, a human monoclonal antibody targeting for interleukin (IL)-4/13 receptor α chain, can inhibit the development of type-2 inflammation, and has shown promising efficacy and safety in the treatment of medium and severe AD [6,7]. Currently, there are cases reported that dupilumab may hold promise in the treatment of AD-related LA, but with minor cases, and few studies focused on the changes of skin lesions after drug withdrawal and the efficacy and safety of the long-term application. This paper reports two cases of severe AD with LA in adults. The patients were treated with subcutaneous dupilumab injection after ineffective traditional treatment. In case 1, the skin lesions of AD and LA virtually disappeared after long-term application of dupilumab, with promising efficacy and safety. In case 2, the skin lesions of AD and LA skin lesions disappeared after dupilumab treatment, without recurrence after discontinuation.

CASE PRESENTATION

Chief complaints

Case 1: On August 12, 2021, a 70-year-old man was admitted to our department due to the appearance of large dark erythematous papules on his trunk and buttocks, together with dense hemispherical millet granular miliary papules with itching on the extensor sides of his lower limbs.

Case 2: On December 21, 2020, a 30-year-old woman was admitted to our department due to substantial dense papules on the back of her hands and scattered erythema, papules, and itching on her limbs and torso.

History of present illness

Case 1: A 70-year-old man developed erythema and papules on his lower limbs 8 years ago, and pruritus. He was diagnosed with chronic eczema at a local hospital and treated with a Chinese medicine decoction. He stopped taking this medicine after most skin lesions subsided. The patient subsequently complained of mildly symptomatic recurrent skin lesions following the cessation of treatment. The patient did not seek further treatment at this time. Three years ago, he was diagnosed with AD at the Dermatology Department of the Second Hospital of Jilin University. Treatment with a topical glucocorticoid and oral levocetirizine controlled the skin lesions and prevented recurrence. However, two years ago, the skin lesions became aggravated without obvious inducement and spread to the entire body. Dense, hemispherical, millet-shaped papules appeared on the extensor surfaces of both lower limbs. The patient's condition did not improve despite self-medication with traditional Chinese medicine and a topical glucocorticoid and the patient experienced expanded skin lesions and sleep severely affected by

pruritus. In August 2021, he visited our department for further treatment.

Case 2: A 30-year-old woman developed several coin-sized erythema lesions and papules on her hips and both lower limbs along with pruritus without obvious inducement 25 years ago. She was diagnosed with chronic eczema at a local hospital and was treated with a topical glucocorticoid and oral loratadine. Following treatment, the skin lesions partially subsided, with occasional recurrence. Two years ago, the patient developed dense erythema and papules covered by small scales, keratosis, and chapped skin on the dorsal side of both hands. After self-medication with antihistamines and a topical glucocorticoid, the skin lesions showed no improvement and gradually progressed to the elbows and trunk. Concomitantly, her pruritus severely affected her sleep. In December 2020, she visited our department for further treatment.

History of past illness

Case 1: The patient's past history was unremarkable.

Case 2: The patient had a history of allergic rhinitis for 5 years, which aggravated in autumn every year. Oral loratadine or levocetirizine was required to relieve the allergic rhinitis.

Personal and family history

Case 1: There was no family history of similar disease.

Case 2: The patient's grandfather and aunt suffered from allergic rhinitis.

Physical examination

Case 1: Systemic examination revealed no obvious abnormalities. The dermatological conditions included dryness of the skin over the whole body, while the trunk and buttocks showed extensive dark erythema and papules. The skin lesions were thickened, lichenized, and pruritic. Similarly, dense hemispherical millet-shaped papules were observed on the lateral sides of both lower legs, with scattered erythema and papules on both feet (Figure 1A and B). The scoring atopic dermatitis index (SCORAD), Eczema Area Severity Index (EASI), numeric rating scale (NRS), and Investigator's Global Assessment (IGA) scores were 60.8, 13.5, 8, and 4, respectively.

Case 2: Systemic examination revealed no obvious abnormalities. Dermatological conditions included dry skin affecting the entire body, chapping erythema covered by a few scales affecting the palms of both hands, densely filled millet grain-to-sorghum grain-sized papules on the dorsal surface of both hands with keratinized surfaces reminiscent of cutaneous amyloidosis, thick and lichenized lesions on both elbows and feet, erythema and papules scattered on the trunk, and scratches and blood scabs on the buttocks (Figure 2A and B). SCORAD, EASI, NRS, and IGA scores were 53.1, 13.1, 7, and 4, respectively.

Laboratory examinations

Case 1: Routine blood analysis showed an eosinophil count of 1.96×10^9/L.

Case 2: Allergen-specific immunoglobulin E: Artemisia > 100 IU/mL, positive value: 6.0; ragweed: 9.4 IU/mL, positive value: 3.4.

Imaging examinations

Case 1: Histopathology of dense papules on the extensor surface of the lower leg showed amorphous amyloid lump deposition with mild eosinophilic staining in the dermal papillary layer, which was consistent with amyloidosis (Figure 3).

Case 2: No histological examination was performed because the patient refused invasive examination.

FINAL DIAGNOSIS

Severe AD accompanied by LA.

TREATMENT

A designated staff assigned to cases 1 and 2 independently collected the basic information, clinical features, medical history, drug allergy history, and family history of the patients and established personal AD files. Both patients received an initial subcutaneous injection of 600 mg dupilumab followed by 300 mg every 2 wk. During the treatment period, the patients were followed regularly,

DOI: 10.12998/wjcc.v11.i10.2301 **Copyright** ©The Author(s) 2023.

Figure 1 Skin lesions at various follow-up time points of patient 1 after the application of dupilumab to the lesions. A: Skin lesions on the back before the treatment of dupilumab; B: Skin lesions on both lower limbs before the treatment of dupilumab; C: Posterior trunk at 16-wk follow-up; D: Back at 55-wk follow-up; E: Skin lesions on both lower limbs at 55-wk follow-up.

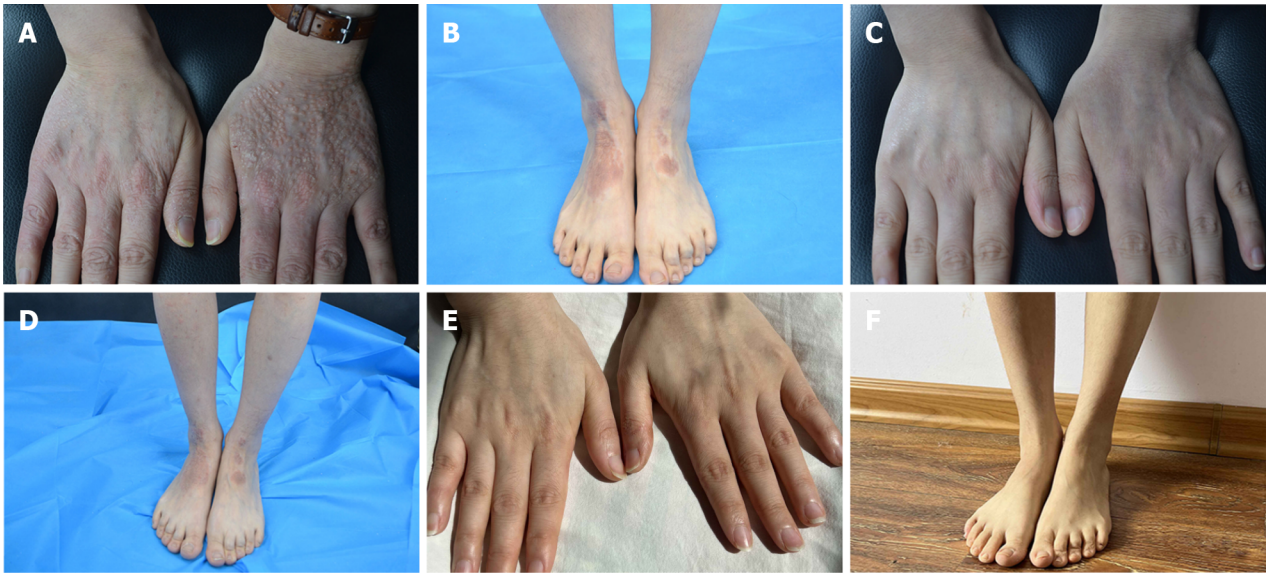

DOI: 10.12998/wjcc.v11.i10.2301 **Copyright** ©The Author(s) 2023.

Figure 2 Skin lesions at various follow-up time points of patient 2 after application of dupilumab to the lesions. A: Skin lesions of hands before the treatment of dupilumab; B: Skin lesions of both lower limbs before the treatment of dupilumab; C: 16-wk follow-up; D: 16-wk follow-up; E: Hands 1.5 year post-treatment follow-up; F: Lower limbs 1.5 years post-treatment follow-up.

during which the skin lesions were photographed, SCORAD, EASI, NRS, and IGA were recorded, and the incidence of any adverse reactions was noted.

OUTCOME AND FOLLOW-UP

Case 1: The patient was first treated with dupilumab on August 21, 2021. The pruritus was relieved after 1 wk and the skin lesions improved after 4 wk. During the treatment, all scores continued to decline, without adverse reactions. After 16 wk of treatment, most skin lesions had improved, and papules on both legs had partially flattened. In the 28th week (February 8, 2022), most of the skin lesions had subsided with some pigmentation remaining on the trunk and buttocks, without recurrence. The skin over the entire body was still dry, and the patient was advised to use external moisturizing emollients regularly. SCORAD, EASI, NRS, and IGA scores were 7.1, 2.3, 2, and 1, respectively (Figure 1C). Due to the access limitations associated with the COVID-19 pandemic, the subcutaneous injection of dupilumab was adjusted to 300 mg every month. The patient was treated with dupilumab for a total of 55 wk, after which the skin lesions of the whole body had largely subsided, without adverse reactions during the

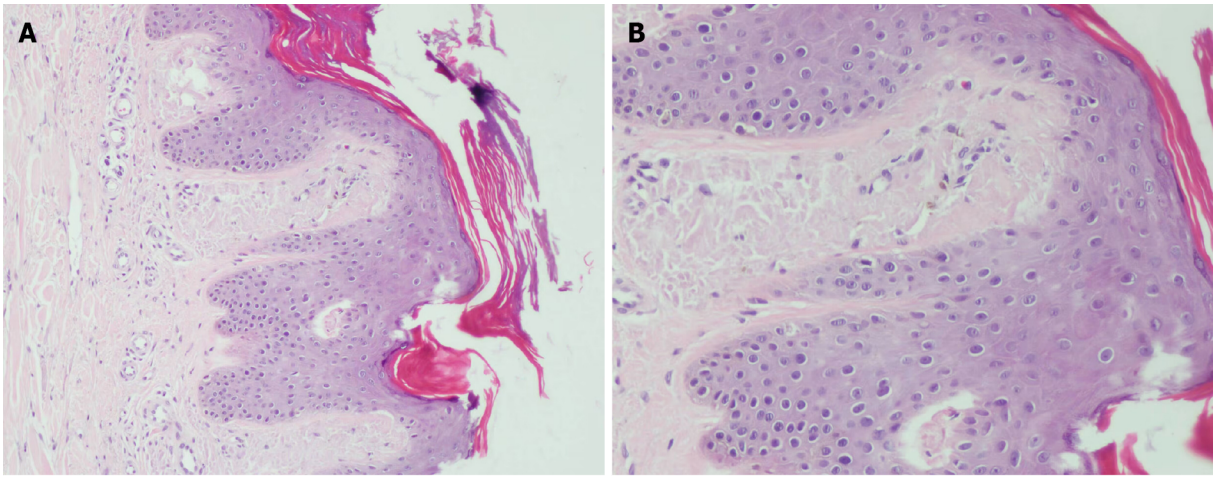

DOI: 10.12998/wjcc.v11.i10.2301

Figure 3 Skin histopathology. A: Amorphous amyloid lump deposition with mild eosinophilic staining in the dermal papillary layer, consistent with amyloidosis (hematoxylin-eosin staining, 100 ×); B: Amorphous amyloid lump deposition with mild eosinophilic staining in the dermal papillary layer, consistent with amyloidosis (hematoxylin-eosin staining, 400 ×).

treatment (Figure 1D and E). SCORAD, EASI, NRS, and IGA scores were 1.4, 1.2, 1, and 1, respectively, reaching EASI90 (skin lesions improved by 90% from baseline). Notably, SCORAD and NRS scores improved by 97.7% and 87.5% from baseline, respectively.

Case 2: The patient was first treated with dupilumab on December 21, 2020. The pruritus was relieved after 1 wk, and the skin lesions improved after 2 wk of treatment. During the treatment, all scores continued to decline, without adverse reactions. The final injection was administered on April 9, 2021, by which the patient had received a total of eight dupilumab injections. At this point, the skin lesions had completely subsided and with each score reaching 0 (Figure 2C and D). The last follow-up was done 1.5 years since the termination of drug treatment, and no recurrence of skin lesions was observed. The symptoms of allergic rhinitis were also significantly improved, and no further medical treatment was deemed necessary (Figure 2E and F).

DISCUSSION

AD, a chronic recurrent disease driven by type-2 inflammation, is clinically characterized by chronic eczematoid manifestations with pruritus, which can be diagnosed according to the previously reported clinical criteria[1,8]. In addition to eczematoid manifestations, the skin lesions of the two patients in this study exhibited lichen amyloidosis, a subtype of primary cutaneous amyloidosis which manifested as numerous persistent groups of hyperkeratotic papules, usually on the lower leg, back, forearm or thigh [2]. It was first proposed by Shanon *et al*[9] in 1970 that cutaneous amyloidosis was related to atopic disease. Currently, studies have found that AD is related to primary cutaneous amyloidosis; however, the exact mechanism remains elusive[3-5]. Primary cutaneous amyloidosis can be caused by the deposition of skin amyloid protein through the "itching-scratching" cycle. Since AD patients generally have pruritus, it is currently believed that the destruction of the skin barrier in AD through chronic scratching and friction can lead to the damage and death of keratinocytes and the subsequent deposition of amyloid protein, resulting in amyloidosis[10,11]. The treatment of AD is typically individualized and different treatment methods are selected according to the severity of the disease. Moderate and severe AD patients can be treated with topical drugs, systemic drugs, and immunosuppressants[12]. In our study, two patients with a long history of repeated dermatological illness were selected and treated with dupilumab based on the inefficacies of the traditional medicines that had been trialed in these patients previously. Dupilumab is a human monoclonal antibody that targets the receptor for Th2 cytokines IL-4/13 (IL-4 receptor α chain), thereby inhibiting type-2 inflammation by blocking the pro-inflammatory effects of IL-4/13[6]. It has been demonstrated that dupilumab effectively inhibits type-2 pathway genes as early as the 4th week of treatment, and significantly improves the clinical efficacy indexes of AD in the 16th week of treatment[13].

Currently, several treatments exist for primary cutaneous amyloidosis associated with AD, including oral antihistamines, CO_2 laser, cyclosporine, and acitretin. However, it is proven difficult to achieve complete skin lesion regression through these methods[14-17]. Primary cutaneous amyloidosis is related to pruritus, and IL-4 and IL-13 have been shown to promote pruritus *via* their role in the type-2 inflammation pathway. Thus, dupilumab may relieve pruritus and inhibit the development of amyloidosis by

blocking the effects of IL-4 and IL-13[18]. However, the specific mechanism of dupilumab in the treatment of primary cutaneous amyloidosis has not been clarified. Previous studies have detected increased expression of IL-31 in the skin lesions of patients with familial primary cutaneous amyloidosis. IL-31 is also one of the pro-pruritus factors secreted by Th2 cells. Dupilumab can indirectly inhibit the secretion of IL-31 by Th2 cells by inhibiting type-2 inflammation, and therefore may exert beneficial effects in primary cutaneous amyloidosis through this mechanism[19,20]. To date, there is one case where remission of AD-related lichen amyloidosis skin lesions was achieved after treatment with dupilumab, indicating that dupilumab can have a therapeutic benefit in AD-related amyloidosis[11]. In this study, case 1 experienced reduced pruritus after one week of dupilumab. To date, the skin lesions of lichen amyloidosis have largely subsided in this patient, without adverse reactions, demonstrating that dupilumab has a rational efficacy against AD-related lichen amyloidosis, and long-term treatment can achieve skin lesion control with high safety. In case 2, the skin lesions of lichen amyloidosis completely subsided 16 wk after dupilumab was applied, and have not recurred since the termination of treatment, indicating that dupilumab may inhibit the recurrence of AD-related lichen amyloidosis on the basis of its therapeutic effect.

CONCLUSION

In this study, the treatment of AD with dupilumab substantially reduced the appearance of skin lesions in two patients with lichen amyloidosis. Long-term treatment of dupilumab for AD and lichen amyloidosis in case 1 was deemed effective and safe. In case 2, there was no recurrence of skin lesions of AD and lichen amyloidosis following termination of treatment. Moreover, compared to the previous traditional treatments, dupilumab was more effective and deemed safe in the treatment of AD and its associated amyloidosis. The above two cases further indicate that the treatments indicated for AD may also have rational efficacy against AD-related lichen amyloidosis.

ACKNOWLEDGEMENTS

We thank the patients and their family members for their support.

FOOTNOTES

Author contributions: Zhao XQ and Xia JX contributed to study conception and design, and data collection and analysis; Zhu WJ contributed to study conception and design, and data collection; Mou Y and Xu M contributed to data collection and analysis; all authors issued final approval for the version to be submitted.

Supported by National Natural Science Foundation of China, No. 81803160; and Scientific Development Program of Jilin Province, No. 20200801078GH.

Informed consent statement: Informed consent was obtained from the patients for publication of this report and any accompanying images.

Conflict-of-interest statement: All the authors report no relevant conflicts of interest for this article.

CARE Checklist (2016) statement: The authors have read the CARE Checklist (2016), and the manuscript was prepared and revised according to the CARE Checklist (2016).

Country/Territory of origin: China

ORCID number: Xue-Qi Zhao 0000-0003-2174-5936; Wen-Jing Zhu 0000-0003-1253-0503; Yan Mou 0000-0002-9152-6301; Meng Xu 0000-0001-7131-4320; Jian-Xin Xia 0000-0002-0067-2910.

Corresponding Author's Membership in Professional Societies: Dermatopathology Group, Pathology Branch of Chinese Medical Association.

S-Editor: Fan JR

L-Editor: Wang TQ
P-Editor: Fan JR

REFERENCES

1 **Ständer S**. Atopic Dermatitis. *N Engl J Med* 2021; **384**: 1136-1143 [PMID: 33761208 DOI: 10.1056/NEJMra2023911]
2 **Hamie L**, Haddad I, Nasser N, Kurban M, Abbas O. Primary Localized Cutaneous Amyloidosis of Keratinocyte Origin: An Update with Emphasis on Atypical Clinical Variants. *Am J Clin Dermatol* 2021; **22**: 667-680 [PMID: 34286474 DOI: 10.1007/s40257-021-00620-9]
3 **Lee DD**, Huang CK, Ko PC, Chang YT, Sun WZ, Oyang YJ. Association of primary cutaneous amyloidosis with atopic dermatitis: a nationwide population-based study in Taiwan. *Br J Dermatol* 2011; **164**: 148-153 [PMID: 21070198 DOI: 10.1111/j.1365-2133.2010.10024.x]
4 **Chia B**, Tan A, Tey HL. Primary localized cutaneous amyloidosis: association with atopic dermatitis. *J Eur Acad Dermatol Venereol* 2014; **28**: 810-813 [PMID: 23489336 DOI: 10.1111/jdv.12144]
5 **Akar A**, Taştan HB, Demiriz M, Erbil H. Lack of effect of cyclosporine in lichen amyloidosis associated with atopic dermatitis. *Eur J Dermatol* 2002; **12**: 612-614 [PMID: 12459544]
6 **Gooderham MJ**, Hong HC, Eshtiaghi P, Papp KA. Dupilumab: A review of its use in the treatment of atopic dermatitis. *J Am Acad Dermatol* 2018; **78**: S28-S36 [PMID: 29471919 DOI: 10.1016/j.jaad.2017.12.022]
7 **Halling AS**, Loft N, Silverberg JI, Guttman-Yassky E, Thyssen JP. Real-world evidence of dupilumab efficacy and risk of adverse events: A systematic review and meta-analysis. *J Am Acad Dermatol* 2021; **84**: 139-147 [PMID: 32822798 DOI: 10.1016/j.jaad.2020.08.051]
8 **Liu P**, Zhao Y, Mu ZL, Lu QJ, Zhang L, Yao X, Zheng M, Tang YW, Lu XX, Xia XJ, Lin YK, Li YZ, Tu CX, Yao ZR, Xu JH, Li W, Lai W, Yang HM, Xie HF, Han XP, Xie ZQ, Nong X, Guo ZP, Deng DQ, Shi TX, Zhang JZ. Clinical Features of Adult/Adolescent Atopic Dermatitis and Chinese Criteria for Atopic Dermatitis. *Chin Med J (Engl)* 2016; **129**: 757-762 [PMID: 26996468 DOI: 10.4103/0366-6999.178960]
9 **Shanon J**. Cutaneous amyloidosis associated with atopic disorders. *Dermatologica* 1970; **141**: 297-302 [PMID: 5487488 DOI: 10.1159/000252484]
10 **Fujisawa T**, Shu E, Ikeda T, Seishima M. Primary localized cutaneous nodular amyloidosis that appeared in a patient with severe atopic dermatitis. *J Dermatol* 2012; **39**: 312-313 [PMID: 21767295 DOI: 10.1111/j.1346-8138.2011.01247.x]
11 **Aoki K**, Ohyama M, Mizukawa Y. A case of lichen amyloidosis associated with atopic dermatitis successfully treated with dupilumab: A case report and literature review. *Dermatol Ther* 2021; **34**: e15005 [PMID: 34037298 DOI: 10.1111/dth.15005]
12 **Goh MS**, Yun JS, Su JC. Management of atopic dermatitis: a narrative review. *Med J Aust* 2022; **216**: 587-593 [PMID: 35644531 DOI: 10.5694/mja2.51560]
13 **Guttman-Yassky E**, Bissonnette R, Ungar B, Suárez-Fariñas M, Ardeleanu M, Esaki H, Suprun M, Estrada Y, Xu H, Peng X, Silverberg JI, Menter A, Krueger JG, Zhang R, Chaudhry U, Swanson B, Graham NMH, Pirozzi G, Yancopoulos GD, D Hamilton JD. Dupilumab progressively improves systemic and cutaneous abnormalities in patients with atopic dermatitis. *J Allergy Clin Immunol* 2019; **143**: 155-172 [PMID: 30194992 DOI: 10.1016/j.jaci.2018.08.022]
14 **Kang MJ**, Kim HS, Kim HO, Park YM. A case of atopic dermatitis-associated lichen amyloidosis successfully treated with oral cyclosporine and narrow band UVB therapy in succession. *J Dermatolog Treat* 2009; **20**: 368-370 [PMID: 19954395 DOI: 10.3109/09546630802691325]
15 **Koh WS**, Oh EH, Kim JE, Ro YS. Alitretinoin treatment of lichen amyloidosis. *Dermatol Ther* 2017; **30** [PMID: 28906049 DOI: 10.1111/dth.12537]
16 **Chu H**, Shin JU, Lee J, Park CO, Lee KH. Successful treatment of lichen amyloidosis accompanied by atopic dermatitis by fractional CO(2) laser. *J Cosmet Laser Ther* 2017; **19**: 345-346 [PMID: 28535110 DOI: 10.1080/14764172.2017.1326612]
17 **Oiso N**, Yudate T, Kawara S, Kawada A. Successful treatment of lichen amyloidosus associated with atopic dermatitis using a combination of narrowband ultraviolet B phototherapy, topical corticosteroids and an antihistamine. *Clin Exp Dermatol* 2009; **34**: e833-e836 [PMID: 20055846 DOI: 10.1111/j.1365-2230.2009.03574.x]
18 **Moniaga CS**, Tominaga M, Takamori K. The Pathology of Type 2 Inflammation-Associated Itch in Atopic Dermatitis. *Diagnostics (Basel)* 2021; **11** [PMID: 34829437 DOI: 10.3390/diagnostics11112090]
19 **Schreml S**. Is targeting interleukin-31 a cure for the itch? *Br J Dermatol* 2016; **174**: 1192-1193 [PMID: 27317285 DOI: 10.1111/bjd.14491]
20 **Garcovich S**, Maurelli M, Gisondi P, Peris K, Yosipovitch G, Girolomoni G. Pruritus as a Distinctive Feature of Type 2 Inflammation. *Vaccines (Basel)* 2021; **9** [PMID: 33807098 DOI: 10.3390/vaccines9030303]

World Journal of Clinical Cases

Submit a Manuscript: https://www.f6publishing.com

World J Clin Cases 2023 April 6; 11(10): 2308-2314

DOI: 10.12998/wjcc.v11.i10.2308

ISSN 2307-8960 (online)

CASE REPORT

Reabsorption of intervertebral disc prolapse after conservative treatment with traditional Chinese medicine: A case report

Cong-An Wang, Hong-Fei Zhao, Jing Ju, Li Kong, Cheng-Jiao Sun, Yue-Kun Zheng, Feng Zhang, Guang-Jian Hou, Chen-Chen Guo, Sheng-Nan Cao, Dan-Dan Wang, Bin Shi

Specialty type: Medicine, research and experimental

Provenance and peer review: Unsolicited article; Externally peer reviewed.

Peer-review model: Single blind

Peer-review report's scientific quality classification

Grade A (Excellent): 0
Grade B (Very good): 0
Grade C (Good): C, C
Grade D (Fair): 0
Grade E (Poor): 0

P-Reviewer: Cheng TH, Taiwan; Li J, China

Received: December 16, 2022
Peer-review started: December 16, 2022
First decision: January 31, 2023
Revised: February 16, 2023
Accepted: March 9, 2023
Article in press: March 9, 2023
Published online: April 6, 2023

Cong-An Wang, Postdoctoral Mobile Station of Shandong University of Traditional Chinese Medicine, Shandong University of Traditional Chinese Medicine, Jinan 250014, Shandong Province, China

Cong-An Wang, Yue-Kun Zheng, Feng Zhang, Chen-Chen Guo, Sheng-Nan Cao, Bone Biomechanics Engineering Laboratory of Shandong Province, Neck-Shoulder and Lumbocrural Pain Hospital of Shandong First Medical University, Shandong First Medical University and Shandong Academy of Medical Sciences, Jinan 250014, Shandong Province, China

Hong-Fei Zhao, School of Acupuncture-Tuina, Shandong University of Traditional Chinese Medicine, Shandong University of Traditional Chinese Medicine, Jinan 250014, Shandong Province, China

Jing Ju, Weihai Hospital of Traditional Chinese Medicine, Weihai 264200, Shandong Province, China

Li Kong, Department of Intensive Care Medicine, The Affiliated Hospital of Shandong University of Traditional Chinese Medicine, Jinan 250011, Shandong Province, China

Cheng-Jiao Sun, Huantai County Hospital of Traditional Chinese Medicine, Zibo 256400, Shandong Province, China

Guang-Jian Hou, Shandong University of Traditional Chinese Medicine, School of Acupuncture-Tuina, Jinan 250014, Shandong Province, China

Dan-Dan Wang, Bin Shi, Shandong First Medical University and Shandong Academy of Medical Sciences, Neck-Shoulder and Lumbocrural Pain Hospital, Shandong Medicinal Biotechnology Center, Jinan 250062, Shandong Province, China

Corresponding author: Bin Shi, MD, Full Professor, Shandong First Medical University and Shandong Academy of Medical Sciences, Neck-Shoulder and Lumbocrural Pain Hospital, Shandong Medicinal Biotechnology Center, No. 18877 Jingshi Road, Jinan 250062, Shandong Province, China. sdyky-shibin@163.com

Abstract

BACKGROUND

Conservative treatments have been reported to diminish or resolve clinical symptoms of lumbar intervertebral disc herniation (LIDH) within a few weeks.

CASE SUMMARY
Computed tomography and magnetic resonance imaging (MRI) of the lumbar region of a 25-year-old male diagnosed with LIDH showed prolapse of the L5/S2 disc. The disc extended 1.0 cm beyond the vertebral edge and hung along the posterior vertebral edge. The patient elected a conservative treatment regimen that included traditional Chinese medicine (TCM), acupuncture, and massage. During a follow-up period of more than 12 mo, good improvement in pain was reported without complications. MRI of the lumbar region after 12 mo showed obvious reabsorption of the herniation.

CONCLUSION
A conservative treatment regimen of TCM, acupuncture, and massage promoted reabsorption of a prolapsed disc.

Key Words: Intervertebral disc degeneration; Traditional Chinese medicine; Reabsorption; Acupuncture; Massage; Case report

Core Tip: Lumbar intervertebral disc herniation is diagnosed worldwide. Generally, non-surgical treatments are recommended and may consist of physical therapy, complementary and alternative medicine options (*e.g.*, acupuncture, acupotomy, Chinese massage, and Chinese herbal medicine), and pharmacotherapy. The latter can include muscle relaxants, systemic steroids, and steroid injections. We report a case of reabsorption of lumbar disc herniation following a conservative treatment regimen involving traditional Chinese medicine, acupuncture, and massage.

Citation: Wang CA, Zhao HF, Ju J, Kong L, Sun CJ, Zheng YK, Zhang F, Hou GJ, Guo CC, Cao SN, Wang DD, Shi B. Reabsorption of intervertebral disc prolapse after conservative treatment with traditional Chinese medicine: A case report. *World J Clin Cases* 2023; 11(10): 2308-2314
URL: https://www.wjgnet.com/2307-8960/full/v11/i10/2308.htm
DOI: https://dx.doi.org/10.12998/wjcc.v11.i10.2308

INTRODUCTION

Lumbar intervertebral disc herniation (LIDH) affects approximately 9% of the population worldwide, with 30%–40% of asymptomatic individuals diagnosed with LIDH upon imaging examination[1]. For the majority of affected patients, non-surgical treatment can achieve varying degrees of pain relief, as well as relief or cure of other symptoms[2]. Since Guinto *et al*[3] reported reabsorption of disc herniation in 1984[3], cases involving reabsorption of the nucleus pulposus have been reported more frequently[4]. In contrast, reports of reabsorption of seriously prolapsed discs following conservative traditional Chinese medicine (TCM) treatment have been rarer. The present case report describes a patient manifesting obvious disc nucleus pulposus reabsorption. Conservative treatment with TCM, including acupuncture, massage, and Chinese medicine, was elected and the results are described.

CASE PRESENTATION

Chief complaints
A 25-year-old man had low back pain with right lower limb pain for 15 d.

History of present illness
The patient presented with low back pain with right lower limb pain 15 d ago.

History of past illness
Past health denied any other medical history.

Personal and family history
The patient denied any history of genetic disease or infection.

Physical examination

Vital signs for the patient upon admittance were: body temperature, 36.5 °C; blood pressure, 112/70 mmHg; heart rate, 84 beats per min; respiratory rate, 18 breaths per min. The patient presented in a forced position, was limping, and exhibited slight straightening of lumbar curvature. Obvious limited mobility of the lumbar region was noted, with marked tenderness present between the L4 and S1 spinous process and the right side of the spine. Radiating numbness in the right lower limb and negative knocking pain were further reported. A neurological examination revealed no abnormalities. Various physical tests were performed. Positive results were obtained for the right straight leg raising test (Lasegue) to 30°, strengthening test, right piriformis muscle tension test, cervical flexion test (Linder), and lying on the back with a straight stomach test. In contrast, the cross leg lifts test, right femoral nerve stretching test, and Patrick test were negative. Patellar tendon reflex, Achilles tendon reflex, and double lower limb muscle strength and tension were normal. There were no obvious abnormalities in depth sensation. Grade five bilateral hallux dorsalis extension muscle strength was observed and the bilateral Babinski sign was negative.

Laboratory examinations

Routine blood work was performed: Neutrophilic granulocyte percentage, 75.54%; percentage of eosinophils, 0.24%; lymphocyte percentage, 17.92%; hypersensitive C-reactive protein, 11.89 mg/L. Routine examination of urine and stool showed no abnormalities. Liver function, erythrocyte sedimentation rate, and biochemical examinations were also within normal ranges.

Imaging examinations

A computed tomography (CT) scan of the lumbar region was conducted in October 2017 and revealed a L5/S1 disc prolapse, nucleus pulposus detachment into the spinal canal, and compression of the right nerve root (Figure 1). The scan indicated a serious condition where protrusion could potentially cause damage to the spinal cord. To determine the extent of bone marrow compression, magnetic resonance imaging (MRI) was also performed of the lumbar region. Stenosis of the right lateral recess and compression of the right nerve root were found to be caused by a L5/S1 intervertebral disc prolapse (Figure 1). The disc was 1.0 cm beyond the vertebral edge and hung along the posterior vertebral edge. The effective sagittal diameter of the spinal canal was 0.7–0.8 cm (Figure 1). The patient was diagnosed with LIDH and surgical resection was recommended. However, the patient elected to undergo conservative treatment involving TCM.

FINAL DIAGNOSIS

The combination of symptoms and signs allowed the patient to be finally diagnosed as having LIDH.

TREATMENT

Intravenous medication

The patient received an injection of 4 mg Lornoxicam (Hangzhou Aoya Biotechnology Company Limited; catalog No. H20043685) diluted in 250 mL 0.9% sodium chloride once daily for a total of six days.

Massage manipulation

Multiple procedures were applied to the patient's lumbar vertebra for a total of 10 d. (1) A palm rubbing method was applied to the patient's waist, buttocks, and right lower limb repeatedly in that order for approximately 5 min; (2) Pressure was applied to vertical pressure acupoints for 1 min with both hands applied to Sanjiaoshu (BL22), Shenshu (BL23), Qihaishu (BL24), Dachangshu (BL25), Guanyuanshu (BL26), Huantiao (GB30), and Weizhong (BL40), respectively (Figure 2); (3) A pulling and shaking method was applied while the patient had both hands extended outwards and upwards to hold the edge of the bed. The physician held the patient's ankles for 2 min to apply continuous traction. The patient's lower limbs were then lifted slightly and shaken gently five times to apply force to the waist; (4) A Pull waist method was applied with the doctor pressing on the lumbar area with both hands. The pressing maintained a rhythm consistent with the breathing pattern of the patient for 1 min, with pressing applied upon expiration and pressing relieved upon inspiration. The effect was to achieve a vibration in the lumbar region. When pressing and fixing the affected waist, the lower limbs were pulled backward (either one side was pulled back at a time, and then the same motion applied to the other side, or both sides could be pulled back at the same time). This manipulation was performed three times in succession; and (5) With the patient lying on their back, flexion and hip compression was performed two to three times. This induced the spine to flex forward and leave the vertebral back margin relatively open.

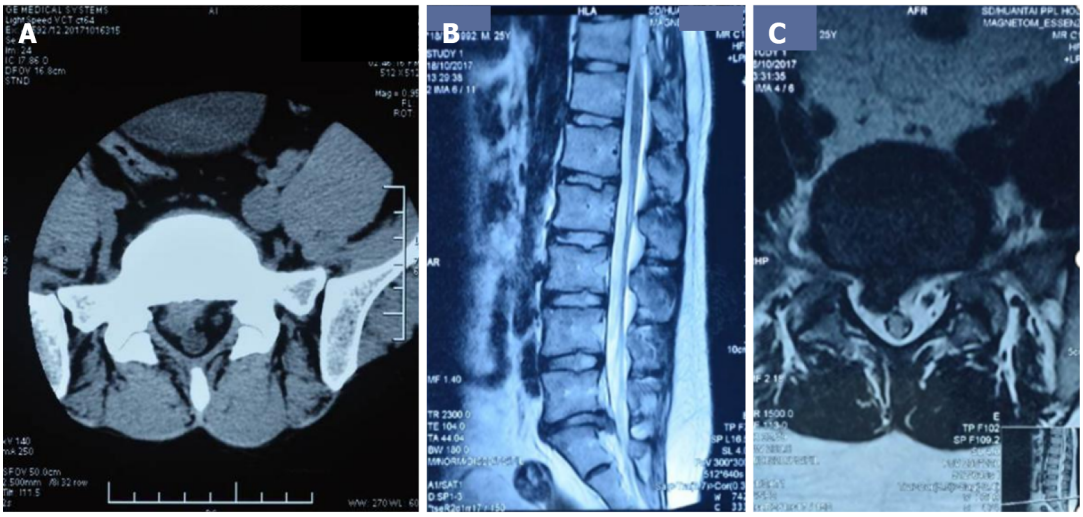

DOI: 10.12998/wjcc.v11.i10.2308 **Copyright** ©The Author(s) 2023.

Figure 1 Computed tomography scan of lumbar prolapsed intraforaminal right-sided L5/S1 disc obtained in 2017. A: Transverse position: L5/S1 disc herniation; B: Sagittal position: L5/S1 disc herniation; C: Nucleus pulposus detached into spinal canal, right nerve root compression.

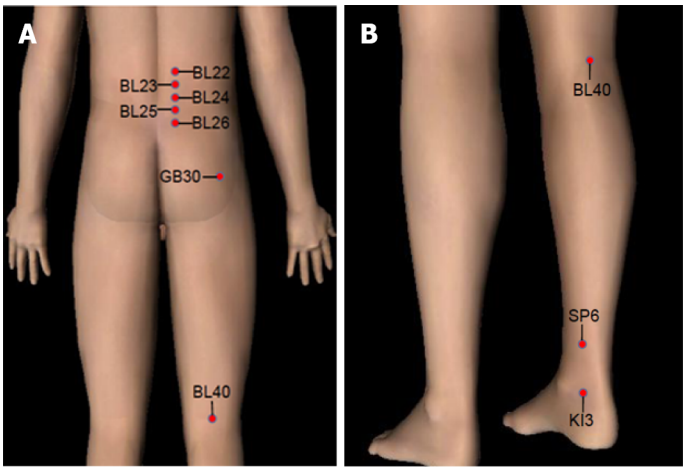

DOI: 10.12998/wjcc.v11.i10.2308 **Copyright** ©The Author(s) 2023.

Figure 2 Acupoint diagram for massage and acupuncture treatments performed. A: The points selected at the waist and back and the posterior side of the lower limbs are indicated by red dots: Sanjiaoshu (BL22), Shenshu (BL23), Qihaishu (BL24), Dachangshu (BL25), Guanyuanshu (BL26), Huantiao (GB30), Weizhong (BL40); B: The points selected at the back of the lower extremities are indicated by red dots: Weizhong (BL40), Sanyinjiao (SP6), and Taixi (KI3). BL22: Sanjiaoshu; BL23: Shenshu; BL24: Qihaishu; BL25: Dachangshu; BL26: Guanyuanshu; GB30: Huantiao; BL40: Weizhong; SP6: Sanyinjiao; KI3: Taixi.

Acupuncture treatment

The acupuncture points used in this study were: Sanjiaoshu (BL22), Shenshu (BL23), Qihaishu (BL24), Dachangshu (BL25), Guanyuanshu (BL26), Huantiao (GB30), Weizhong (BL40), Sanyinjiao (SP6), and Taixi (KI3) (Figure 2). Briefly, the patient was placed in a prone position on the treatment bed and the acupoints were disinfected with iodine. A total of 18 bilateral punctures were made using sterile disposable acupuncture needles (34G, 0.25 mm × 40 mm, Hua Tuo, Suzhou Medical Supplies Factory Co. LTD., Jiangsu, China). Each needle was kept in the acupuncture point for 30 min. In addition, the waist and right hip were irradiated using a specific electromagnetic spectrum (TDP) magic lamp (Hengming Medical LTD., Sichuan, China).

OUTCOME AND FOLLOW-UP

After the treatment period, the patient's lower back pain and numbness of the right lower limb were alleviated. Discharge instructions indicated that the patient was to keep warm and rested. Instructions for frequently exercising muscles in the lower back were also provided. For more than 12 mo, the patient demonstrated good improvement in pain without any complications. A second lumbar MRI was

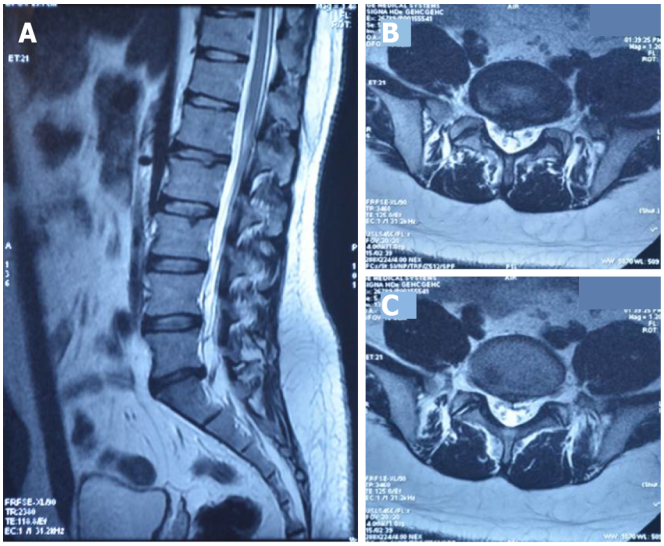

DOI: 10.12998/wjcc.v11.i10.2308

Figure 3 Lumbar magnetic resonance imaging obtained in 2018 showing prolapsed intraforaminal right-sided L5/S1 disc. A: Sagittal position: Reabsorption of herniated intervertebral disc L5/S1; B and C: Transverse position: Reabsorption of nucleus pulposus previously protruding into spinal canal, relief of right nerve root compression achieved.

performed in November 2018. Significant reabsorption of the herniation was observed (Figure 3).

DISCUSSION

Both genetic and environmental factors can accelerate loss of nutrition and induce a mechanical imbalance of an intervertebral disc. As a result, the structure of the intervertebral disc can be compromised and lumbar disc herniation can occur[5]. Non-surgical treatment is primarily recommended for lumbar disc herniation[6,7], and this can include drug treatment, physiotherapy, acupuncture, and massage[6]. With advances in intervertebral disc imaging, an increasing number of cases have demonstrated absorption of herniated lumbar discs[7]. Furthermore, it has been demonstrated that the size of a herniation positively correlates with the symptoms of LIDH[7].

Disc prolapse can cause lumbar and leg pain. For prolapsed lumbar discs, surgery is a common treatment[8]. However, negative effects can accompany the treatment effects achieved with surgery[9, 10]. Consequently, non-surgical treatment options have been more frequently considered. Hong and Ball[7] reported a 29-year-old female patient with a prolapsed lumbar 4/5 intervertebral disc who underwent physical therapy and epidural injections of glucocorticoids for treatment[7]. After five months, the protruding nucleus pulposus was gradually absorbed[7]. Herniated nucleus pulposus reabsorption has become an active and engaging topic in both clinical and basic research. It also represents a new direction in conservative treatment. In the present case, the patient exhibited a much more serious prolapse than previously reported cases, with the lumbar disc extending 1.0 cm beyond the vertebral edge and hanging along the posterior vertebral edge. Nevertheless, the prolapsed lumbar disc was reabsorbed after applying a treatment regimen that included TCM, acupuncture, and massage.

Massage is widely used in China and can have a significant effect. Massage as used in TCM involves an acupoint massage manipulation that is based on the meridian theory. Briefly, massage mediates a dredging of the meridians, thereby promoting blood circulation, invigorating qi, removing cold, and relieving pain[11,12]. Modern medicine has ascribed three functions to massage of the waist area. First, it can reduce pressure in an intervertebral disc, concomitantly it increases the pressure outside the disc, and it promotes reinstatement of the protrusion and creates favorable conditions for repair of the fibrous ring. Second, massage changes the position of the protrusion to release adhesions between the protrusion and the nerve root, relieves or reduces compression, stimulates the nerve root affected by the protrusion, and relieves symptoms[13]. Third, massage relaxes muscles in the waist and buttocks[14], strengthens circulation of local qi and blood, and facilitates recovery of normal function in diseased nerve roots[12]. However, the biological mechanisms mediating the effects of massage treatment of LIDH and reabsorption of prolapsed intervertebral discs remain unclear and require further investigation.

The present case demonstrates that it is possible for a prolapsed disc to be reabsorbed with application of acupuncture and massage therapy in combination with TCM. Generally, prolapse is an indication for surgical treatment. However, the present case expands the scope of non-surgical

treatment and provides an example of successful conservative treatment of LIDH with TCM. It remains for the possibility and probability of prolapsed intervertebral disc absorption to be evaluated in order to ensure the effectiveness and safety of this type of conservative treatment. Further study is also needed to provide a theoretical basis for this type of non-surgical treatment of a prolapsed lumbar disc. A large sample epidemiological investigation could demonstrate the likelihood of disc reabsorption, while a randomized controlled clinical trial could evaluate the effectiveness and safety of acupuncture and massage as a conservative therapy.

CONCLUSION

In the present case report, conservative treatment including TCM, acupuncture and massage were able to relieve a patient's LIDH symptoms of waist and leg pain and numbness. The TCM regimen applied also promoted significant reabsorption of the prolapsed intervertebral disc to its normal position. Thus, TCM may represent an alternative non-surgical treatment for ruptured giant prolapse of an intervertebral disc that patients should consider.

FOOTNOTES

Author contributions: Wang DD and Shi B conceived and designed the conservative therapy of TCM; Wang CA, Zhao HF, and Kong L contributed to the clinical treatment of the patient; Ju J, Sun CJ, Zheng YK, Zhang F, Hou GJ, Cao SN, and Guo CC analyzed the case materials; Wang CA, Zhao HF, and Kong L wrote the paper; All authors have read and approved the final manuscript.

Supported by National Nature Science Foundation of China, No. 82004495; Natural Science Foundation of Shandong Province, China, No. ZR2020QH318; The 69th batch of a grant from China Postdoctoral Foundation, No. 2021M691985; and Taishan Scholars Young Experts Program, China, No. tsqn202211349.

Informed consent statement: Informed written consent was obtained from the patient for publication of this report and any accompanying images.

Conflict-of-interest statement: All the authors report no relevant conflicts of interest for this article.

CARE Checklist (2016) statement: The authors have read the CARE Checklist (2016), and the manuscript was prepared and revised according to the CARE Checklist (2016).

Country/Territory of origin: China

ORCID number: Cong-An Wang 0000-0002-2483-9260; Hong-Fei Zhao 0000-0003-0437-9321; Jing Ju 0000-0002-1964-6763; Li Kong 0000-0002-0988-1022; Cheng-Jiao Sun 0000-0001-5343-7503; Yue-Kun Zheng 0000-0002-4030-2340; Feng Zhang 0000-0002-3577-161X; Guang-Jian Hou 0000-0001-7591-0488; Chen-Chen Guo 0000-0002-6076-194X; Sheng-Nan Cao 0000-0002-7341-5608; Dan-Dan Wang 0000-0001-5774-2871; Bin Shi 0000-0001-9305-5438.

S-Editor: Fan JR
L-Editor: A
P-Editor: Fan JR

REFERENCES

1 **Ropper AH**, Zafonte RD. Sciatica. *N Engl J Med* 2015; **372**: 1240-1248 [PMID: 25806916 DOI: 10.1056/NEJMra1410151]
2 **Abou-Elroos DA**, El-Toukhy MAE, Nageeb GS, Dawood EA, Abouhashem S. Prolonged Physiotherapy versus Early Surgical Intervention in Patients with Lumbar Disk Herniation: Short-term Outcomes of Clinical Randomized Trial. *Asian Spine J* 2017; **11**: 531-537 [PMID: 28874970 DOI: 10.4184/asj.2017.11.4.531]
3 **Guinto FC Jr**, Hashim H, Stumer M. CT demonstration of disk regression after conservative therapy. *AJNR Am J Neuroradiol* 1984; **5**: 632-633 [PMID: 6435432]
4 **Zhong M**, Liu JT, Jiang H, Mo W, Yu PF, Li XC, Xue RR. Incidence of Spontaneous Resorption of Lumbar Disc

Herniation: A Meta-Analysis. *Pain Physician* 2017; **20**: E45-E52 [PMID: 28072796]

5 **Tsarouhas A**, Soufla G, Tsarouhas K, Katonis P, Pasku D, Vakis A, Tsatsakis AM, Spandidos DA. Molecular profile of major growth factors in lumbar intervertebral disc herniation: Correlation with patient clinical and epidemiological characteristics. *Mol Med Rep* 2017; **15**: 2195-2203 [PMID: 28260009 DOI: 10.3892/mmr.2017.6221]

6 **Zhang B**, Xu H, Wang J, Liu B, Sun G. A narrative review of non-operative treatment, especially traditional Chinese medicine therapy, for lumbar intervertebral disc herniation. *Biosci Trends* 2017; **11**: 406-417 [PMID: 28904328 DOI: 10.5582/bst.2017.01199]

7 **Hong J**, Ball PA. IMAGES IN CLINICAL MEDICINE. Resolution of Lumbar Disk Herniation without Surgery. *N Engl J Med* 2016; **374**: 1564 [PMID: 27096582 DOI: 10.1056/NEJMicm1511194]

8 **Kapoor S**, Amarouche M, Al-Obeidi F, U-King-Im JM, Thomas N, Bell D. Giant thoracic discs: treatment, outcome, and follow-up of 33 patients in a single centre. *Eur Spine J* 2018; **27**: 1555-1566 [PMID: 28688062 DOI: 10.1007/s00586-017-5192-6]

9 **Wilson CA**, Roffey DM, Chow D, Alkherayf F, Wai EK. A systematic review of preoperative predictors for postoperative clinical outcomes following lumbar discectomy. *Spine J* 2016; **16**: 1413-1422 [PMID: 27497886 DOI: 10.1016/j.spinee.2016.08.003]

10 **Dorow M**, Löbner M, Stein J, Pabst A, Konnopka A, Meisel HJ, Günther L, Meixensberger J, Stengler K, König HH, Riedel-Heller SG. The Course of Pain Intensity in Patients Undergoing Herniated Disc Surgery: A 5-Year Longitudinal Observational Study. *PLoS One* 2016; **11**: e0156647 [PMID: 27243810 DOI: 10.1371/journal.pone.0156647]

11 **Niu JF**, Zhao XF, Hu HT, Wang JJ, Liu YL, Lu DH. Should acupuncture, biofeedback, massage, Qi gong, relaxation therapy, device-guided breathing, yoga and tai chi be used to reduce blood pressure? *Complement Ther Med* 2019; **42**: 322-331 [PMID: 30670261 DOI: 10.1016/j.ctim.2018.10.017]

12 **Mei L**, Miao X, Chen H, Huang X, Zheng G. Effectiveness of Chinese Hand Massage on Anxiety Among Patients Awaiting Coronary Angiography: A Randomized Controlled Trial. *J Cardiovasc Nurs* 2017; **32**: 196-203 [PMID: 26646596 DOI: 10.1097/JCN.0000000000000309]

13 **Kukimoto Y**, Ooe N, Ideguchi N. The Effects of Massage Therapy on Pain and Anxiety after Surgery: A Systematic Review and Meta-Analysis. *Pain Manag Nurs* 2017; **18**: 378-390 [PMID: 29173797 DOI: 10.1016/j.pmn.2017.09.001]

14 **Weerapong P**, Hume PA, Kolt GS. The mechanisms of massage and effects on performance, muscle recovery and injury prevention. *Sports Med* 2005; **35**: 235-256 [PMID: 15730338 DOI: 10.2165/00007256-200535030-00004]

World Journal of Clinical Cases

Submit a Manuscript: https://www.f6publishing.com

World J Clin Cases 2023 April 6; 11(10): 2315-2320

DOI: 10.12998/wjcc.v11.i10.2315

ISSN 2307-8960 (online)

CASE REPORT

Development of subdural empyema from subdural effusion after suppurative encephalitis: A case report

Rui-Xi Yang, Bei Chen, Yun Zhang, Yao Yang, Shu Xie, Lin He, Jian Shi

Specialty type: Medicine, research and experimental

Provenance and peer review: Unsolicited article; Externally peer reviewed.

Peer-review model: Single blind

Peer-review report's scientific quality classification

Grade A (Excellent): A
Grade B (Very good): B
Grade C (Good): C
Grade D (Fair): 0
Grade E (Poor): 0

P-Reviewer: Kung WM, Taiwan; Shen CC, Taiwan

Received: December 13, 2022
Peer-review started: December 13, 2022
First decision: February 8, 2023
Revised: February 18, 2023
Accepted: March 10, 2023
Article in press: March 10, 2023
Published online: April 6, 2023

Rui-Xi Yang, Department of Infectious Diseases, Mianyang Central Hospital, Mianyang 621000, Sichuan Province, China

Bei Chen, Yun Zhang, Yao Yang, Shu Xie, Lin He, Department of Psychosomatic Medicine, Mianyang Central Hospital, Mianyang 621000, Sichuan Province, China

Jian Shi, Department of Psychosomatic Medicine, Mianyang Central Hospital, School of Medicine, University of Electronic Science and Technology of China, Mianyang 621000, Sichuan Province, China

Corresponding author: Jian Shi, MM, Doctor, Department of Psychosomatic Medicine, Mianyang Central Hospital, School of Medicine, University of Electronic Science and Technology of China, No. 12 Changjia Lane, Fucheng District, Mianyang 621000, Sichuan Province, China. psychome@foxmail.com

Abstract

BACKGROUND

Chronic subdural effusion is very common in the cranial imaging of middle-aged and older people. Herein, we report a patient misdiagnosed with subdural effusion, who was eventually diagnosed with chronic subdural empyema (SDE) caused by Streptococcus pneumoniae.

CASE SUMMARY

A 63-year-old man was brought to our emergency room with a headache, vomiting, and disturbed consciousness. Computed tomography (CT) revealed a bilateral subdural effusion at the top left side of the frontal lobe. Cerebrospinal fluid examination after lumbar puncture indicated suppurative meningitis, which improved after anti-infective therapy. However, the patient then presented with acute cognitive dysfunction and right limb paralysis. Repeat CT showed an increase in left frontoparietal subdural effusion, disappearance of the left lateral ventricle, and a shift of the midline to the right. Urgent burr hole drainage showed SDE that was culture-positive for Streptococcus pneumoniae. His condition improved after adequate drainage and antibiotic treatment.

CONCLUSION

Patients with unexplained subdural effusion, especially asymmetric subdural effusion with intracranial infection, should be assessed for chronic SDE. Early surgical treatment may be beneficial.

Key Words: Subdural effusion; Subdural empyema; Streptococcus pneumoniae; Meningoencephalitis; Drainage; Case report

Core Tip: Detection of chronic subdural effusion is very common in the cranial imaging of middle-aged and older people. Herein, we report a patient misdiagnosed with subdural effusion, who was eventually diagnosed with chronic subdural empyema (SDE) caused by Streptococcus pneumoniae. Patients with unexplained subdural effusion, especially asymmetric subdural effusion with intracranial infection, should be assessed for chronic SDE. Early surgical treatment may be beneficial.

Citation: Yang RX, Chen B, Zhang Y, Yang Y, Xie S, He L, Shi J. Development of subdural empyema from subdural effusion after suppurative encephalitis: A case report. *World J Clin Cases* 2023; 11(10): 2315-2320
URL: https://www.wjgnet.com/2307-8960/full/v11/i10/2315.htm
DOI: https://dx.doi.org/10.12998/wjcc.v11.i10.2315

INTRODUCTION

Subdural empyema (SDE) is a rare but potentially fatal infection that involves collection of pus in the subdural space between the dura and the arachnoid. This condition was previously termed a subdural abscess, cortical abscess, purulent dura mater, mucoid meningitis, and subdural suppuration. Most commonly, SDE is caused by sinusitis, otitis media, or upper respiratory tract infections. The infection can spread directly from adjacent sources (most commonly meningitis)[1] or from distant blood sources [2]. Because the subdural space is continuous and has no anatomical barrier, SDE can spread between both cerebral hemispheres. Specific symptoms may include disturbed consciousness and/or other focal neurological deficits, in addition to generalized underlying symptoms such as fever, headaches, seizures, and altered consciousness[3]. Because the skull is a closed cavity, intracranial SDE can also lead to severe symptoms and even death from direct compression and brain damage[4]. After reviewing the current literature, only five cases of Streptococcus pneumoniae SDE have been reported worldwide since 2006 (Table 1). Herein, we report a case initially diagnosed with meningoencephalitis caused by streptococcus pneumoniae, but who was eventually found to have an SDE. The patient was treated with burr hole drainage and intravenous antibiotics, and his condition improved.

CASE PRESENTATION

Chief complaints

A 63-year-old Chinese man presented with cognitive impairment, paralysis, and epilepsy for 1 h.

History of present illness

His symptoms started at 1 h before presentation, which included acute cognitive impairment, right limb paralysis, and recurrent generalized epilepsy.

History of past illness

At 1 mo before visiting our hospital, he developed cold symptoms, including a cough and headache, for which he received no treatment. He was brought to our emergency room with a headache, vomiting, and confusion. Physical examination revealed confusion, a Glasgow coma score of 9, and fever (maximum body temperature of 39.5 °C). Lung computed tomography (CT) showed scattered inflammatory lesions in both lungs, while head CT showed a bilateral frontal top subdural effusion that was most obvious on the left side (Figure 1A). Cerebrospinal fluid (CSF) examination after SDE showed a white blood cell count of 8157 × 10^6 cells/L, CSF protein of 3.78 g/L, and glucose < 0.2 mmol/L (blood glucose of 8.91 mmol/L). Three blood cultures and sputum cultures were unremarkable, while two CSF cultures suggested Streptococcus pneumoniae. The patient improved after intravenous anti-infective treatment [vancomycin hydrochloride injection (1 g, q12h) + meropenem injection (2 g, q8h) for 12 d, followed by levofloxacin hydrochloride injection (0.5 g, qd) + ceftriaxone sodium injection (2 g, q12h) for 10 d). CSF examination showed leukocytes of 10´10^6 cells/L, CSF protein of 0.61 g/L, and glucose of 1.68 mmol/L (blood glucose of 7.47 mmol/L). The patient was discharged from the hospital after 1 wk.

Table 1 Summary of reported cases of subdural empyema infected by streptococcus pneumonia

Ref.	Publication	Age (years)/gender	Risk factor	Symptoms	Causative organism	Surgery
Hicdonmez *et al*[17], 2006	1	1.5/Female	Young age	Fever, lethargy, and inability to walk	Streptococcus pneumoniae	Craniotomy
Hoshina *et al* [18], 2008	2	1/Male	Young age	Fever, convulsions	Streptococcus pneumoniae	Burr holedrainage
Jorgensen *et al* [19], 2010	3	1.1/Male	Young age, choroid plexus carcinoma	Diarrhoea, vomiting, coryzal symptoms, and persistent pyrexia	Streptococcus pneumoniae serotype 6A	Craniotomy
Kagami *et al* [20], 2011	4	68/Female	Acute subdural hematoma	Fever, headache, coma	Streptococcus pneumoniae	Burr hole drainage
Greve *et al*[21], 2011	5	11/Female	Sinusitis	Headache, fever, vomiting, change of personality, paresis of the left foot and classical signs of infection of the right upper palpebra	Streptococci intermedius	Burr hole drainage

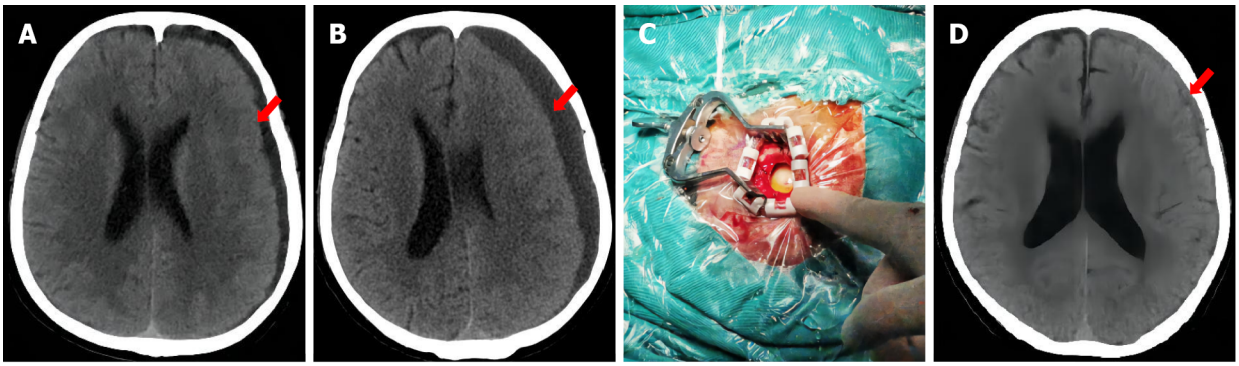

DOI: 10.12998/wjcc.v11.i10.2315 **Copyright** ©The Author(s) 2023.

Figure 1 Clinical pictures of the patient. At his first hospital visit (February 3, 2022), the patient was diagnosed with suppurative meningitis and bilateral subdural effusion (predominantly on the left side). A: At his second hospital visit (March 9, 2022), the left subdural lesion was significantly enlarged, the left lateral ventricle had disappeared, and the midline had shifted to the right; B: He was diagnosed with subdural empyema; C: The dura mater was exposed during the operation, and was colored yellow-green with high tension; D: Head computed tomography after left burr hole drainage (April 7, 2022) revealed a significant reduction in the left subdural lesions, and recovery of the left lateral ventricle and the midline shift.

Personal and family history

The patient denied any family history of genetic disease or tumors.

Physical examination

On physical examination, his vital signs were body temperature of 36.4 °C, blood pressure of 180/103 mmHg, heart rate of 130 beats per min, and respiratory rate of 20 breaths per min. Acute cognitive impairment, right limb paralysis, and recurrent generalized epilepsy were also observed.

Laboratory examinations

Drainage fluid examination showed a white blood cell count of 3487 × 10^6 cells/L, CSF protein of 10.27 g/L, CSF glucose of 0.1 mmol/L (blood glucose of 6.88 mmol/L), and culture-positive for Streptococcus pneumoniae.

Imaging examinations

Head CT revealed that the left frontal top subdural effusion had increased in size, the left lateral ventricle had disappeared, and the midline was shifted to the right (Figure 1B).

FINAL DIAGNOSIS

Combined with the patient's medical history, the final diagnosis was SDE.

TREATMENT

After consultation between neurology, neurosurgery, and the infection departments, emergency burr hole drainage was performed and the dura mater was exposed. The dura mater was yellow-green with high tension (Figure 1C), a pus coating, extremely high pressure, and slow drainage of approximately 60 mL of green liquid. Numerous purulent floccules were seen under the dura, and there was obvious brain tissue edema. The drainage tube provided adequate drainage for 3 d, and his condition improved after antibiotic treatment [vancomycin hydrochloride injection (0.5 g, q8h) for 21 d].

OUTCOME AND FOLLOW-UP

Follow-up CSF testing showed a white blood cell count of 5×10^6 cells/L, CSF protein of 0.35 g/L, and a CSF glucose of 3.3 mmol/L (blood glucose of 9 mmol/L). Head CT showed that the SDE was significantly improved (Figure 1D), the left lateral ventricle was clearly visible, and the midline had returned to the center. The patient's condition improved and he was discharged home.

DISCUSSION

SDE is a rare and potentially life-threatening condition if not managed properly. SDE is characterized by collection of purulent fluid between the dura mater and the arachnoid, which can be secondary to meningitis in childhood, especially in infants. Sinusitis, mastoiditis, or otitis media can also cause SDE in older children[5]. Meningitis caused by external infectious factors can cause local inflammation and damage to the blood–brain barrier, which allows bacteria to enter the subdural space between the dura and the arachnoid tissue. Inflammatory products and necrotic tissues can form subdural abscesses.

The most common pathogens in community-acquired bacterial meningitis were reported to be Streptococcus pneumoniae, Neisseria meningitidis, and Haemophilus influenzae[6]-Streptococcus pneumoniae was detected in the present case. An elevated CSF protein/glucose ratio > 4.65 was also suggested to be an indicator of aggravation of meningitis or transformation into SDE[7]. The protein/glucose ratio in the present case was 18.9, which was significantly higher than the reference estimate. Thus, on the basis of our CSF results, we should have considered the potential for SDE.

SDE is often accompanied by signs and symptoms of infection. However, it can also be asymptomatic in the early stages. Notable symptoms include fever, headache, nausea, vomiting, focal neurological deficits, and altered mental status. Some patients also experience seizures. Physical examination can detect fever, tachycardia, and respiratory failure, while neurological examination can detect meningeal irritation, contralateral hemiplegia, cranial nerve palsy, pupillary disparity, and papilledema. Typically, these symptoms are progressive and may worsen if left untreated. In severe cases, patients can enter a coma or even die[8]. Our patient initially presented with headache, vomiting, and confusion, along with fever and meningeal irritation, which can be easily confused with meningitis. SDE should be suspected if treatment fails or local neurological findings are found during bacterial meningitis treatment.

On CT, SDE appears as a hypodense area at the edge of the hemisphere or at the edge of the falx cerebri. Additional CT scans can improve delineation of the SDE margins. CT can also determine the extent and size of the empyema, and visualize any mass effects associated with displacement of midline structures. Magnetic resonance imaging may have advantages over CT because diffusion-weighted imaging sequences have a high sensitivity for these lesions. SDE can also metastasize into the spinal subdural space, requiring more precise imaging studies[9-11].

Laboratory tests are very important for detecting SDE. Blood analysis can detect leukocytosis, and inflammatory infection can cause a left shift with associated neutropenia. An elevated erythrocyte sedimentation rate, C-reactive protein, and procalcitonin are also potential indicators of SDE. However, blood tests are only indirect indicators compared with biochemical CSF tests. Etiological examination is also very important, especially blood culture and empyema stock solution culture, because sensitive antibiotic treatment can markedly improve patient prognosis.

In our case, the first head CT revealed only a small amount of subdural fluid. However, CSF examination suggested a severe intracranial infection. The second head CT showed significant enlargement of the left subdural lesion, disappearance of the left lateral ventricle, and right midline displacement. SDE was diagnosed by combining biochemical examination and the subdural lesion cultures. SDE is easily missed or misdiagnosed, especially when the symptoms are atypical in the early disease stage. With disease evolution, diagnosis can only be confirmed by combining imaging and laboratory examinations[12].

Treatment of a subdural abscess requires multimodal monitoring and multidisciplinary participation, including liaison and consultation with brain surgery, infectious diseases, neurology, rehabilitation, and psychiatry departments[13]. The use of antibiotic treatments alone is rare in SDE. Generally, powerful broad-spectrum antibiotics are used in combination, and the types and doses of antibiotics are then adjusted on the basis of pathogenic microorganism cultures and drug susceptibility tests. Particular

attention should be paid to bacterial resistance and the antibiotic treatment time, which generally takes 3–6 wk[14]. Surgical treatment consists of multiple drill holes or craniotomy for drainage and debridement. Craniotomy usually provides better outcomes and fewer recurrences, but requires patient and family consent[15]. Patient outcomes depend on the preoperative status, intervention duration, and treatment aggressiveness. Most patients who are awake and alert have a good prognosis, while coma and comatose patients have a high mortality rate[16]. Although our patient received a sufficient length of antibiotic treatment, SDE gradually developed and aggravated his condition. Fortunately, a craniotomy and drainage was performed in time (the patient's family did not agree with the craniotomy), and further antibiotics were administered. The patient's condition improved after the treatment course.

CONCLUSION

SDE is a neurosurgical emergency. For patients with unexplained subdural effusion, early identification and management are required, especially when asymmetric subdural effusion is accompanied by intracranial infection. Clinicians should consider the potential for chronic SDE, and early surgical treatment may be beneficial.

FOOTNOTES

Author contributions: Yang RX and Chen B are contributed equally; Zhang Y, Yang Y, Xie S and He L performed the clinical investigation and cared for the patient; Yang RX and Chen B drafted the manuscripts; Shi J reviewed and revised the manuscripts; All authors have read and approved the final manuscript.

Supported by Sichuan Provincial Health and Family Planning Commission, China, No. 17PJ088.

Informed consent statement: The patient gave written consent for their personal or clinical details along with any identifying images to be published in this study.

Conflict-of-interest statement: All the authors report no relevant conflicts of interest for this article.

CARE Checklist (2016) statement: The authors have read the CARE Checklist (2016), and the manuscript was prepared and revised according to the CARE Checklist (2016).

Country/Territory of origin: China

ORCID number: Jian Shi 0000-0002-2645-3142.

S-Editor: Fan JR
L-Editor: A
P-Editor: Fan JR

REFERENCES

1 **Thigpen MC**, Whitney CG, Messonnier NE, Zell ER, Lynfield R, Hadler JL, Harrison LH, Farley MM, Reingold A, Bennett NM, Craig AS, Schaffner W, Thomas A, Lewis MM, Scallan E, Schuchat A; Emerging Infections Programs Network. Bacterial meningitis in the United States, 1998-2007. *N Engl J Med* 2011; **364**: 2016-2025 [PMID: 21612470 DOI: 10.1056/NEJMoa1005384]
2 **Wang T**, Uddin A, Mobarakai N, Gilad R, Raden M, Motivala S. Secondary encephalocele in an adult leading to subdural empyema. *IDCases* 2020; **21**: e00916 [PMID: 32775205 DOI: 10.1016/j.idcr.2020.e00916]
3 **Lu HF**, Yue CT, Kung WM. Salmonella Group D1 Subdural Empyema Mimicking Subdural Hematoma: A Case Report. *Infect Drug Resist* 2022; **15**: 6357-6363 [PMID: 36337934 DOI: 10.2147/IDR.S388101]
4 **Fernández-de Thomas RJ**, De Jesus O. Subdural Empyema. 2022 May 8. In: StatPearls [Internet]. Treasure Island (FL): StatPearls Publishing; 2022 Jan- [PMID: 32491761]
5 **Osborn MK**, Steinberg JP. Subdural empyema and other suppurative complications of paranasal sinusitis. *Lancet Infect Dis* 2007; **7**: 62-67 [PMID: 17182345 DOI: 10.1016/S1473-3099(06)70688-0]

6 **van de Beek D**, Brouwer MC, Koedel U, Wall EC. Community-acquired bacterial meningitis. *Lancet* 2021; **398**: 1171-1183 [PMID: 34303412 DOI: 10.1016/S0140-6736(21)00883-7]

7 **Yalçinkaya R**, Tanir G, Kaman A, Öz FN, Aydin Teke T, Yaşar Durmuş S, Ekşioğlu AS, Aycan AE, Ceyhan M. Pediatric subdural empyema as a complication of meningitis: could CSF protein/CSF glucose ratio be used to screen for subdural empyema? *Eur J Pediatr* 2021; **180**: 415-423 [PMID: 32875444 DOI: 10.1007/s00431-020-03791-5]

8 **Widdrington JD**, Bond H, Schwab U, Price DA, Schmid ML, McCarron B, Chadwick DR, Narayanan M, Williams J, Ong E. Pyogenic brain abscess and subdural empyema: presentation, management, and factors predicting outcome. *Infection* 2018; **46**: 785-792 [PMID: 30054798 DOI: 10.1007/s15010-018-1182-9]

9 **Viola S**, Montoya G, Arnold J. Streptococcus pyogenes subdural empyema not detected by computed tomography. *Int J Infect Dis* 2009; **13**: e15-e17 [PMID: 18635385 DOI: 10.1016/j.ijid.2008.02.014]

10 **Smibert OC**, Vujovic O, Hoy J. Neisseria meningitidis subdural empyema causing acute cauda equina syndrome. *Lancet Infect Dis* 2017; **17**: 780 [PMID: 28653638 DOI: 10.1016/S1473-3099(17)30343-2]

11 **Mortazavi MM**, Quadri SA, Suriya SS, Fard SA, Hadidchi S, Adl FH, Armstrong I, Goldman R, Tubbs RS. Rare Concurrent Retroclival and Pan-Spinal Subdural Empyema: Review of Literature with an Uncommon Illustrative Case. *World Neurosurg* 2018; **110**: 326-335 [PMID: 29174228 DOI: 10.1016/j.wneu.2017.11.082]

12 **Adriani KS**, van de Beek D, Troost D, Brouwer MC. The diagnostic pitfall of infratentorial subdural empyema. *Arch Neurol* 2012; **69**: 1076-1077 [PMID: 22507887 DOI: 10.1001/archneurol.2012.151]

13 **Guan J**, Spivak ES, Wilkerson C, Park MS. Subdural Empyema in the Setting of Multimodal Intracranial Monitoring. *World Neurosurg* 2017; **97**: 749.e1-749.e6 [PMID: 27826090 DOI: 10.1016/j.wneu.2016.10.133]

14 **Antimicrobial Resistance Collaborators**. Global burden of bacterial antimicrobial resistance in 2019: a systematic analysis. *Lancet* 2022; **399**: 629-655 [PMID: 35065702 DOI: 10.1016/S0140-6736(21)02724-0]

15 **Jim KK**, Brouwer MC, van der Ende A, van de Beek D. Subdural empyema in bacterial meningitis. *Neurology* 2012; **79**: 2133-2139 [PMID: 23136260 DOI: 10.1212/WNL.0b013e3182752d0e]

16 **Konar S**, Gohil D, Shukla D, Sadashiva N, Uppar A, Bhat DI, Srinivas D, Arimappamagan A, Devi BI. Predictors of outcome of subdural empyema in children. *Neurosurg Focus* 2019; **47**: E17 [PMID: 31370020 DOI: 10.3171/2019.5.FOCUS19268]

17 **Hicdonmez T**, Cakir B, Hamamcioglu MK, Kilincer C, Cobanoglu S. Giant subdural empyema in a child: a case report. *Surg Neurol* 2006; **66**: 632-3; discussion 633 [PMID: 17145333 DOI: 10.1016/j.surneu.2006.02.036]

18 **Hoshina T**, Kusuhara K, Saito M, Mizoguchi M, Morioka T, Mizuno Y, Aoki T, Hara T. Infected subdural hematoma in an infant. *Jpn J Infect Dis* 2008; **61**: 412-414 [PMID: 18806357]

19 **Jorgensen M**, Bate J, Gatscher S, Chisholm JC. Invasive pneumococcal disease following treatment for choroid plexus carcinoma. *Support Care Cancer* 2010; **18**: 647-650 [PMID: 20076974 DOI: 10.1007/s00520-009-0804-2]

20 **Kagami H**, Muto J, Nakatukasa M, Inamasu J. Infected acute subdural hematoma associated with invasive pneumococcal disease. *Neurol Med Chir (Tokyo)* 2011; **51**: 368-370 [PMID: 21613763 DOI: 10.2176/nmc.51.368]

21 **Greve T**, Clemmensen D, Ridderberg W, Pedersen LN, Møller JK. Polymicrobial subdural empyema: involvement of Streptococcus pneumoniae revealed by lytA PCR and antigen detection. *BMJ Case Rep* 2011; **2011** [PMID: 22707602 DOI: 10.1136/bcr.09.2010.3344]

World Journal of Clinical Cases

Submit a Manuscript: https://www.f6publishing.com

World J Clin Cases 2023 April 6; 11(10): 2321-2328

DOI: 10.12998/wjcc.v11.i10.2321

ISSN 2307-8960 (online)

CASE REPORT

Treatment of periprosthetic knee infection and coexistent periprosthetic fracture: A case report and literature review

Lin-Jie Hao, Peng-Fei Wen, Yu-Min Zhang, Wei Song, Juan Chen, Tao Ma

Specialty type: Surgery

Provenance and peer review: Unsolicited article; Externally peer reviewed.

Peer-review model: Single blind

Peer-review report's scientific quality classification

Grade A (Excellent): 0
Grade B (Very good): 0
Grade C (Good): C
Grade D (Fair): D
Grade E (Poor): 0

P-Reviewer: Oommen AT, India; Primadhi RA, Indonesia

Received: December 15, 2022
Peer-review started: December 15, 2022
First decision: January 20, 2023
Revised: February 8, 2023
Accepted: March 6, 2023
Article in press: March 6, 2023
Published online: April 6, 2023

Lin-Jie Hao, Peng-Fei Wen, Yu-Min Zhang, Wei Song, Juan Chen, Tao Ma, Department of Joint Surgery, Honghui Hospital, Xi'an Jiaotong University, Xi'an 710000, Shaanxi Province, China

Corresponding author: Tao Ma, MD, Chief Doctor, Surgeon, Department of Joint Surgery, Honghui Hospital, Xi'an Jiaotong University, No. 555 Youyi East Road, Xi'an 710000, Shaanxi Province, China. 171303186@qq.com

Abstract

BACKGROUND

Periprosthetic joint infection (PJI) and periprosthetic fracture (PPF) are among the most serious complications following total knee arthroplasty. Herein, we present one patient with these two complications with details on the characteristics, treatment strategy, and outcome.

CASE SUMMARY

A 69-year-old female patient who suffered from PJI and PPF following total knee arthroplasty was treated by a two-stage revision surgery. After thorough foreign material removal and debridement, we used a plate that was covered with antibiotic-loaded bone cement to link with a hand-made cement spacer to occupy the joint space and fix the fracture. Although the infection was cured, the fracture did not heal and caused bone defect due to the long interval between debridement and revision. In the revision surgery, a cemented stem and cortical allogenic splints were used to reconstruct the fracture and bone defect. At the final follow-up 27 mo after revision, the patient was satisfied with postoperative knee functions with satisfactory range of motion (104°) and Hospital for Special Surgery knee score (82 points). The radiographs showed no loosening of the prosthesis and that the bone grafts healed well with the femur.

CONCLUSION

Our two-stage revision surgery has proved to be successful and may be considered in other patients with PJI and PPF.

Key Words: Knee arthroplasty; Periprosthetic joint infection; Periprosthetic fractures; Complications; Surgical revision; Case report

Core Tip: Periprosthetic joint infection (PJI) and periprosthetic fracture (PPF) are among the most serious complications of knee arthroplasty. A two-stage revision surgery should be progressively performed in the treatment of PJI and coexistent PPF with bone loss. In the first-stage operation, a T-shaped cement spacer made from a rectangular vancomycin laden cement block and a cement coated plate was used after debridement. In the second-stage operation, the combination of cemented prosthesis and freeze-dried cortical allogenic splints were used for knee revision and fixation of PPF. Our approach offers an option for successful treatment of PJI and PPF.

Citation: Hao LJ, Wen PF, Zhang YM, Song W, Chen J, Ma T. Treatment of periprosthetic knee infection and coexistent periprosthetic fracture: A case report and literature review. *World J Clin Cases* 2023; 11(10): 2321-2328
URL: https://www.wjgnet.com/2307-8960/full/v11/i10/2321.htm
DOI: https://dx.doi.org/10.12998/wjcc.v11.i10.2321

INTRODUCTION

For patients with posttraumatic osteoarthritis, the presence of periarticular hardware complicates total knee arthroplasty (TKA) and increases the incidence of periprosthetic joint infection (PJI)[1-3]. Meanwhile, PJI may significantly prolong the treatment period, resulting in longer hospitalization, more complications, higher medical costs, and lower quality of life[4-6]. Periprosthetic fracture (PPF) is also one of the most serious complications after TKA and usually results in joint dysfunctions or even disabilities[7]. Patients may suffer from both PJI and PPF simultaneously, which makes a therapeutic approach difficult to formulate because of different or contradicting treatment concepts. Once an infection occurs, all foreign materials including prosthesis and internal fixation need to be removed; however, PPF needs to be stabilized by internal fixation. Therefore, the most crucial question is how to deal with both fracture fixation and infection treatment appropriately.

In this case report, we describe a patient with concomitant PJI and PPF who was successfully treated and followed for 2 years.

CASE PRESENTATION

Chief complaints

A 69-year-old Chinese woman was admitted to our joint clinic with a complaint of right thigh pain and swelling for 3 d.

History of present illness

Symptoms started 3 d before presentation with severe thigh pain and swelling (July 2019).

History of past illness

The patient fell and fractured her right distal femur in November 2017. She underwent an open reduction and internal fixation (ORIF) at a local hospital. In December 2018, the patient was diagnosed with posttraumatic osteoarthritis of the right knee, for which the removal of original internal fixation implants and TKA were simultaneously performed (Figure 1A and B). In April 2019, the patient suffered PJI of the right knee with a sinus formation and was treated with antibiotic suppression; however, the infection did not improve.

Personal and family history

The patient had no personal or family history.

Physical examination

The right thigh was swollen and deformed. The right knee had a sinus tract and limited range of motion.

Laboratory examinations

The serum erythrocyte sedimentation rate (ESR), C-reactive protein (CRP), white blood cell (WBC) count, and neutrophil percentage were elevated (97 mm/h, 126.19 mg/L, 12.18 × 10^9/L, and 75.2%, respectively). The synovial fluid WBC count and synovial fluid polymorphonuclear neutrophil percentage were 12045/uL and 94%, respectively. Methicillin-resistant *Staphylococcus aureus* (MRSA) was detected on the synovial fluid culture.

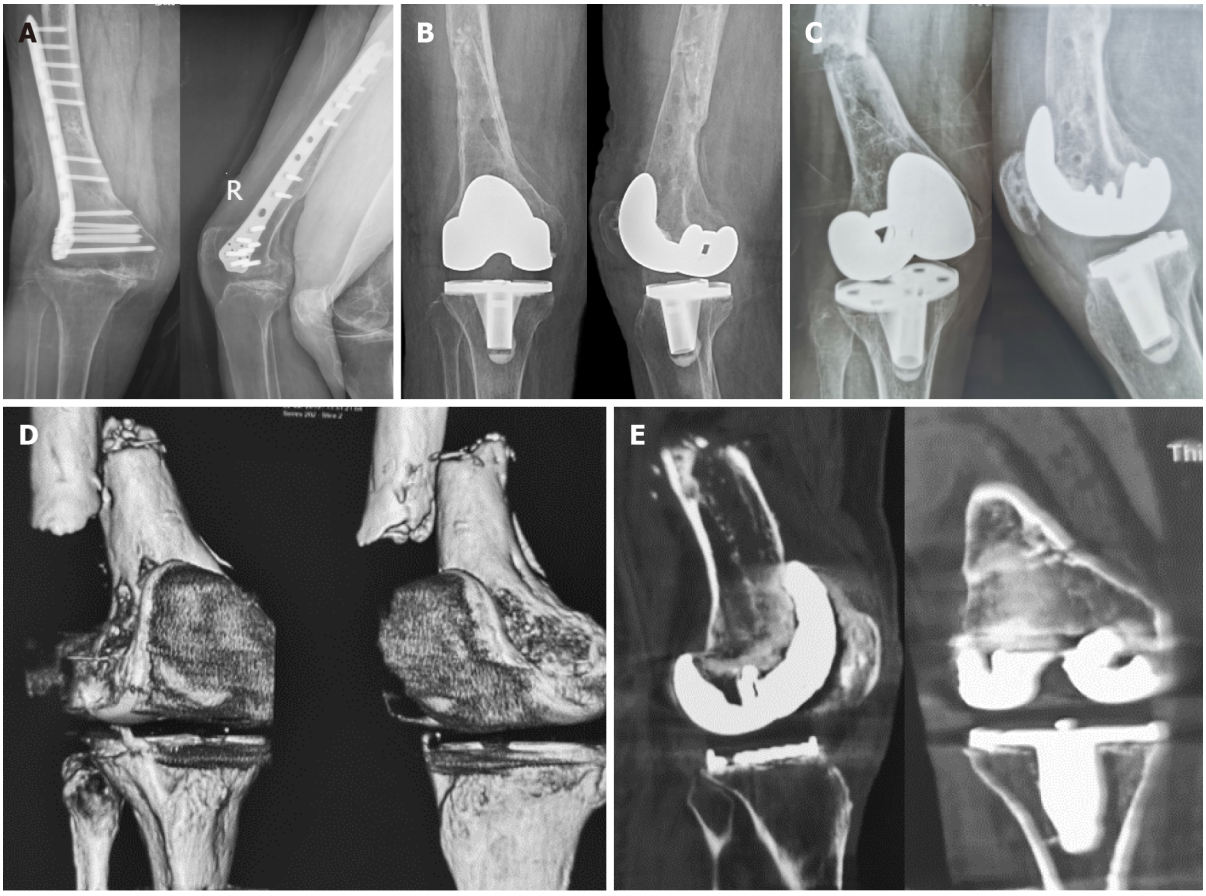

DOI: 10.12998/wjcc.v11.i10.2321 **Copyright** ©The Author(s) 2023.

Figure 1 X-ray and computed tomography images. A: Anterior–posterior and lateral X-ray images of the right knee before primary total knee arthroplasty showing an end-stage osteoarthritis of the right knee with valgus deformity and a hardware fixed on right femur without signs of fracture (December 2018); B: Anterior–posterior and lateral X-ray images of the right knee after the primary total knee arthroplasty showing satisfactory position of the knee prosthesis and that the original hardware was completely removed without fracture (December 2018); C: Anterior–posterior and lateral X-ray images of the right knee after fall showing the distal femur fracture with significant displacement and that the knee prosthesis was seemingly stable (July 2019); D: Three-dimensional computed tomography (CT) images showing fractures of the right distal femur with severe displacement (July 2019); E: Coronal and sagittal CT images showing radiolucent lines around the femoral and tibial prosthesis (July 2019).

Imaging examinations

The X-ray and computed tomography (CT) scan revealed a fracture of the right femur and loosening of the knee prosthesis (Figure 1C-E).

FINAL DIAGNOSIS

The patient was diagnosed with PJI and PPF (Rorabeck and Taylor[8] type II) of the right knee.

TREATMENT

A two-stage revision surgery was planned with an interval of about 3 mo. The first-stage operation (Figure 2) was performed in two steps. The first step was resection of the prosthesis and debridement. The second step was the placement of an antibiotic cement spacer and fixation of PPF. We used a rectangular vancomycin laden cement (Palacos R+G, Heraeus Medical GmbH) block linking with a cement-coated plate (Limited contact dynamic compression plate, Synthes GmbH) to make a T-shaped spacer. A longer plate was not selected to avoid the spread of infection. Five different specimens around the prosthesis were sent for culture, and the detected pathogen was still MRSA. An infectious disease specialist prescribed a regimen of anti-MRSA drugs, consisting of intravenous drip of vancomycin and oral rifampicin at dosages of 1000 and 600 mg/d, respectively. After 2 wk, the regimen was changed to 300 mg/d of oral rifampicin and 500 mg/d of oral ciprofloxacin for 6 wk. After the operation, the patient was instructed to walk without weight-bearing. However, the patient was lost to follow-up and

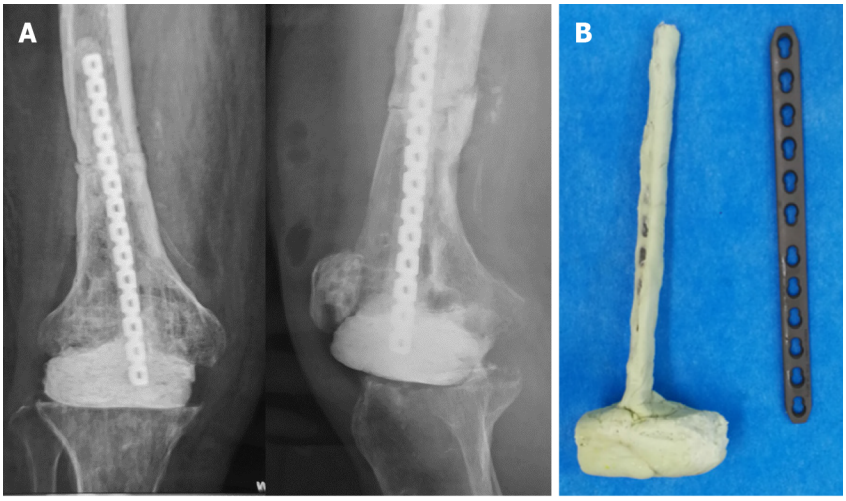

DOI: 10.12998/wjcc.v11.i10.2321

Figure 2 X-ray and intraoperative images. A: Anterior–posterior and lateral X-ray images of the right knee after the first stage operation showing favorable position of the cement spacer and satisfactory reduction and fixation of the femoral fracture (July 2019); B: A hand-made T-shaped antibiotic-laden cement spacer for knee gap occupation and femoral fracture fixation.

did not undergo the second-stage operation (Figure 3) in October 2019 as planned. In May 2020, she revisited our outpatient clinic. By this time, she had suffered severe functional impairment with a Hospital for Special Surgery (HSS) knee score of only 23 points. She was admitted into the hospital. After infection was ruled out through a series of blood tests and synovial fluid culture, the second-stage operation consisting of ORIF of PPF and revision TKA was performed in three steps. First, we performed debridement and removed any foreign material and sequestrum. Second, the fixation of periprosthetic femoral fracture was done. Two pieces of freeze-dried cortical allogenic splint (Shanxi Aorui Biomaterials Co. LTD) of approximately 10 centimeter in length were used for auxiliary fixation of the femur. Then, cables (Synthes Cable System) and wires were used to bundle bone splits, and autologous bone graft was applied to the bone defect. Finally, knee revision prosthesis (NexGen LCCK, Zimmer Inc.) was installed. A 150-millimeter-long stem with a diameter of 14 millimeters was used on the femoral side. A 100-millimeter-long stem with a diameter of 14 millimeters was used on the tibial side. A 5-millimeter-thick metal pad was added to both medial and lateral sides of the distal femoral prosthesis, and a 10-millimeter-thick metal pad was added to the posterior condyle of the femoral prosthesis. X-rays were taken at 3 d postoperatively. Postoperative rehabilitation exercise consisted of partial weight bearing of the right lower limb for 6 wk. The antibiotic therapy was continued according to the instructions of the infectious disease specialist. A timeline of the clinical course and management is provided in Table 1.

OUTCOME AND FOLLOW-UP

The patient was followed periodically (6, 12, and 24 wk and annually thereafter) after revision TKA. The wound healed well without redness or swelling. The serum CRP and ESR decreased continuously and returned to normal at 3 mo post-revision. The HSS score was 59, 69, and 85 points at 6, 12, and 24 wk after revision, respectively. At the final follow-up 27 mo after revision (Figure 4), the range of motion was 104°, the HSS score was 82 points, and the Western Ontario MacMaster Universities Osteoarthritis Index score was 36 points. The patient was satisfied with the course of treatment and postoperative knee function. There was no sign of infection recurrence or loosening of the prosthesis.

DISCUSSION

PJI and PPF are among the most serious complications following TKA and usually raise concern for both patients and surgeons[9-11]. The incidence of PJI after primary TKA is 0.7%-2%[12,13], while that after revision is 5.6%-35%[14-16]. Meanwhile, the incidence of PPF ranges from 0.3% to 2.5% after primary TKA and 1.6% to 38% after revision TKA[17-19]. Each complication needs precise assessment and specific care to prevent further serious issues. If PJI is simultaneous with PPF for one patient, it is going to be a very tricky situation. There is no optimal management strategy regarding this issue due to lack of standards and controversy over treatment effectiveness. The treatment of this patient for

Table 1 Overview of the timeline of the clinical history, diagnosis, and treatment

Date	Diagnosis	Treatment
November 17	Right femoral fracture	ORIF
December 18	Posttraumatic osteoarthritis of right knee	Removal of internal fixation and TKA
April 19	PJI	Antibiotic suppression
July 19	PJI and PPF	Resection of prosthesis with placement of antibiotic spacer and fixation of fracture
May 20	Post-operation of prosthesis removal	Revision knee arthroplasty and fixation of right PPF

ORIF: Open reduction and internal fixation; TKA: Total knee arthroplasty; PJI: Periprosthetic joint infection; PPF: Periprosthetic fracture.

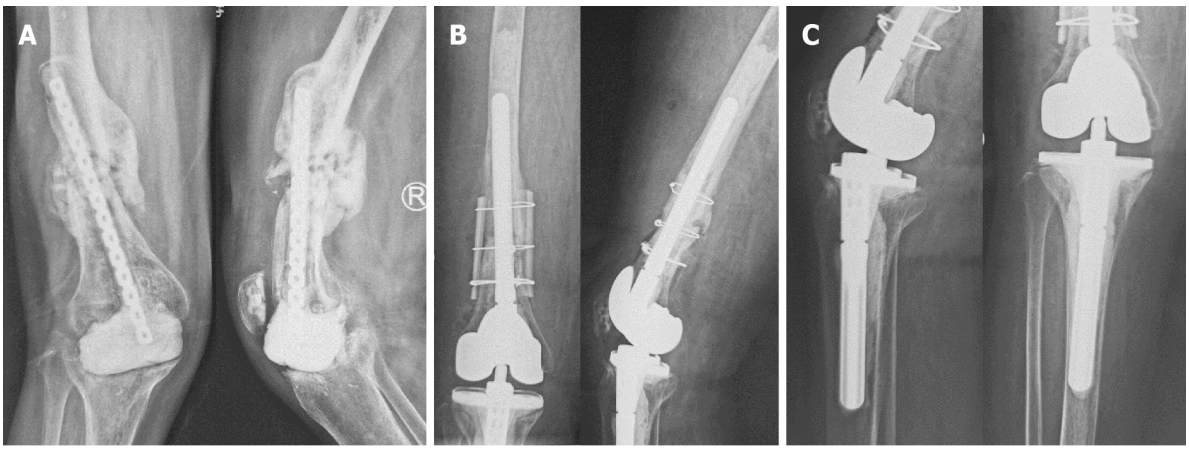

DOI: 10.12998/wjcc.v11.i10.2321 **Copyright** ©The Author(s) 2023.

Figure 3 X-ray images. A: Anterior–posterior and lateral X-ray images of the right knee before the second stage operation showing that the cement spacer slightly displaced to the medial side, the proximal end of internal fixator came out through the middle femoral shaft, callus formed at the previous fracture of the femur but not healing yet, and bone defects existed in the distal femur and proximal tibia, which resulted in valgus deformity of the right knee (May 2020); B and C: Anterior–posterior and lateral X-ray images of the right knee after the second stage operation showing no loosening of cemented revision knee prosthesis and that the femoral fracture was fixed with intramedullary stem and extramedullary cortical splints (May 2020).

infection and fracture after TKA with periarticular internal fixators offers possible strategies for this condition.

The incidence of PJI in patients with a history of ORIF who underwent TKA is similar to that after revision[20]. Suzuki *et al*[21] reported that previous ORIF and remnants of previous internal fixation materials showed significant correlation with postoperative infections. A prospective matched cohort study conducted by Lizaur-Utrilla *et al*[22] found that the incidence of surgical site infection was higher in the posttraumatic group and recommended removal of hardware prior to TKA. In contrast, Klatte *et al*[23] found that the risk of developing periprosthetic knee infection was not significantly increased with pre-existing orthopaedic implants. In general, more and more studies identified previous fracture history and remnants of pre-existing fixation-devices as major risk factors for PJI after TKA[21,22,24] and suggested that complete removal of the fixators 4 to 6 mo before TKA could reduce the incidence of PJI[22,25]. For clinical implication, surgeons should be conscious of the infection potential when performing knee arthroplasty on patients with these risk factors.

From our point of view, fixing the fracture is the main difficulty for patients with both PJI and PPF and also is an important factor to ensure fracture union and prevent postoperative infection. In this study, the combination of antibiotic-laden cement spacer and cement-coated plate, which was used as an intramedullary nail, provided a solution. Bonacker *et al*[26] presented a two-stage surgical strategy conducted in a 69-year-old male patient with a periprosthetic tibia fracture, infectious nonunion, and loosening of the TKA due to ascending infection. After removing all implants, a deep debridement was performed, and a tibial nail connected with a hand-formed bone cement knee spacer including antibiotics and two additional antibiotic-impregnated chains was implanted. In the revision surgery, the tibial fracture site was stabilized with a long uncemented stem. Sanz-Ruiz *et al*[27] presented a biarticular cement spacer, made from a cephalomedullary nail, to treat infected hip arthroplasty with massive bone loss. They covered the nail with antibiotic-laden cement and obtained satisfactory results of infection control and functional retention. In this case, a cement-coated plate which can slowly release antibiotics, preventing bacterial adhesion and proliferation and biofilm formation, was also used to

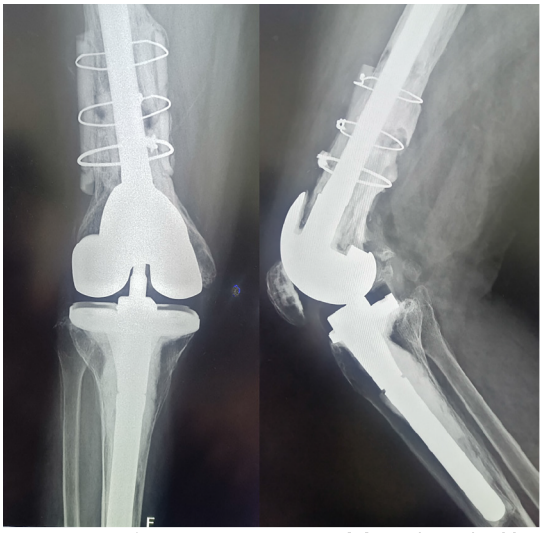

DOI: 10.12998/wjcc.v11.i10.2321

Figure 4 X-ray images. Anterior–posterior and lateral X-ray images showing a large amount of new bone formed between the cortical splits and femoral shaft with no loosening of the knee prosthesis (August 2022).

substitute a metal-exposed plate as intramedullary nail for fracture immobilization. In addition, a cemented femoral stem was used instead of cementless one during the revision, because a fully long cementless stem could not be implanted due to the anterior femoral curvature and large defect of the previous fracture. Meanwhile, the cemented one could stabilize the proximal and distal parts of femoral fracture. What needs illustration is that cement smeared at the fracture was strictly prohibited and measure of heat control was indispensable when the cement generate heat during solidification to avoid affecting the union of fracture.

Müller *et al*[28] reported a two-stage revision for the treatment of 8 patients with PPF and infection. The fractures were fixed by three strategies: 2 patients by plate, 3 by intramedullary rod/pin, and 3 by plate and rod/pin. At the final follow-up, one infection recurred, and three individuals developed nonunion of fracture, getting a high nonunion rate. A systematic review conducted by Ebraheim *et al*[29] concluded that the complication rate of PPF after TKA separately treated with intramedullary nail/rod or locking plate is as high as 53% and 35%, respectively, and the most common complication is non/delayed union. Therefore, to ensure fracture healing, it is necessary not only to cure infection, but also to obtain the fixation stability of the fracture. In such revision surgery, extramedullary auxiliary fixation is often required if intramedullary stem cannot guarantee the fixation stability of fracture. Except for plates, bone splints are commonly used. Carta *et al*[30] reported that cortical allogenic splints should be considered the use instead of metal plates for the treatment of periprosthetic femoral fracture, which usually has bone loss and/or a potential mechanical instability. In a cadaveric study, Peters *et al*[31] concluded that allograft cortical splints offer biomechanical advantages as an alternative to metal plates for the fixation of femur fracture below a well-fixed femoral component. In this study, we used titanium cable and wires to fix the two splints which were placed on the medial and lateral aspects of the femur. Then, bone graft was also performed. Comparing with using single metal plates, we could get potential benefits from the use of cortical allogenic splints, which can increase bone quantity and quality, decrease stress shielding, stabilize the entirety, so as to reduce fracture nonunion occurrence and other complications, and improve the patients' quality of life by accelerating function recovery. However, the potential disadvantages of the customized transplant, such as transmission of infectious diseases, risks of infections, longer surgical time, and more complex surgical procedures, must be taken into consideration.

Another aspect that we have learned from this case is the importance of strengthening patients' management and guidance to avoid similar incidents. In the future, we should establish a more diversified and convenient follow-up system, strengthen the patient education on the post-discharge process, urge patients who need special care to attend follow-up visits regularly, and involve family members in the patient care.

The main limitation of this study is that it is a report of a single case, which is due to the low incidence of the coexistence of PJI and PPF.

CONCLUSION

PJI, PPF, and nonunion with bone defect individually pose a challenge in orthopedics and trauma

surgery. We present a highly complex case on account of the consecutive occurrence of these complications. The lack of standards resulted in the requirement of an individualized strategy under this circumstance, and the key to success was synergistic execution of simultaneous fracture stabilization and infection eradication. Our approach offers an option for successful treatment, upon which future strategies can be developed. Highly specialized interdisciplinary centers are needed for desirable therapeutic outcomes.

FOOTNOTES

Author contributions: Ma T and Zhang YM conceived and performed the surgery; Hao LJ assembled previous reported records and drafted the manuscript; Wen PF, Song W, and Chen J helped perform the surgery and revised the manuscript for important intellectual content; all authors have read and approved the final manuscript.

Supported by the General Cultivation Project of Xi'an Health Commission, No. 2021ms08.

Informed consent statement: Informed written consent was obtained from the patient for the publication of this case report.

Conflict-of-interest statement: All the authors declare that they have no conflict of interest to disclose.

CARE Checklist (2016) statement: The authors have read the CARE Checklist (2016), and the manuscript was prepared and revised according to the CARE Checklist (2016).

Country/Territory of origin: China

ORCID number: Lin-Jie Hao 0000-0001-6081-8427; Yu-Min Zhang 0000-0003-4932-1369; Tao Ma 0000-0001-5971-1964.

S-Editor: Liu JH
L-Editor: Wang TQ
P-Editor: Liu JH

REFERENCES

1 **Best MJ**, Amin RM, Raad M, Kreulen RT, Musharbash F, Valaik D, Wilckens JH. Total Knee Arthroplasty after Anterior Cruciate Ligament Reconstruction. *J Knee Surg* 2022; **35**: 844-848 [PMID: 33242906 DOI: 10.1055/s-0040-1721423]
2 **Farfalli LA**, Farfalli GL, Aponte-Tinao LA. Complications in total knee arthroplasty after high tibial osteotomy. *Orthopedics* 2012; **35**: e464-e468 [PMID: 22495843 DOI: 10.3928/01477447-20120327-21]
3 **El-Galaly A**, Haldrup S, Pedersen AB, Kappel A, Jensen MU, Nielsen PT. Increased risk of early and medium-term revision after post-fracture total knee arthroplasty. *Acta Orthop* 2017; **88**: 263-268 [PMID: 28464756 DOI: 10.1080/17453674.2017.1290479]
4 **Parvizi J**, Zmistowski B, Berbari EF, Bauer TW, Springer BD, Della Valle CJ, Garvin KL, Mont MA, Wongworawat MD, Zalavras CG. New definition for periprosthetic joint infection: from the Workgroup of the Musculoskeletal Infection Society. *Clin Orthop Relat Res* 2011; **469**: 2992-2994 [PMID: 21938532 DOI: 10.1007/s11999-011-2102-9]
5 **Kurtz SM**, Lau E, Watson H, Schmier JK, Parvizi J. Economic burden of periprosthetic joint infection in the United States. *J Arthroplasty* 2012; **27**: 61-5.e1 [PMID: 22554729 DOI: 10.1016/j.arth.2012.02.022]
6 **Zingg M**, Kheir MM, Ziemba-Davis M, Meneghini RM. Reduced Infection Rate After Aseptic Revision Total Knee Arthroplasty With Extended Oral Antibiotic Protocol. *J Arthroplasty* 2022; **37**: 905-909 [PMID: 35077819 DOI: 10.1016/j.arth.2022.01.040]
7 **Kurtz SM**, Lau EC, Ong KL, Adler EM, Kolisek FR, Manley MT. Which Clinical and Patient Factors Influence the National Economic Burden of Hospital Readmissions After Total Joint Arthroplasty? *Clin Orthop Relat Res* 2017; **475**: 2926-2937 [PMID: 28108823 DOI: 10.1007/s11999-017-5244-6]
8 **Rorabeck CH**, Taylor JW. Classification of periprosthetic fractures complicating total knee arthroplasty. *Orthop Clin North Am* 1999; **30**: 209-214 [PMID: 10196422 DOI: 10.1016/s0030-5898(05)70075-4]
9 **Postler A**, Lützner C, Beyer F, Tille E, Lützner J. Analysis of Total Knee Arthroplasty revision causes. *BMC Musculoskelet Disord* 2018; **19**: 55 [PMID: 29444666 DOI: 10.1186/s12891-018-1977-y]
10 **Sukhonthamarn K**, Strony JT, Patel UJ, Brown SA, Nazarian DG, Parvizi J, Klein GR. Distal Femoral Replacement and Periprosthetic Joint Infection After Non-Oncological Reconstruction: A Retrospective Analysis. *J Arthroplasty* 2021; **36**: 3959-3965 [PMID: 34518056 DOI: 10.1016/j.arth.2021.08.013]

11 **Meyer JA**, Zhu M, Cavadino A, Coleman B, Munro JT, Young SW. Infection and periprosthetic fracture are the leading causes of failure after aseptic revision total knee arthroplasty. *Arch Orthop Trauma Surg* 2021; **141**: 1373-1383 [PMID: 33515323 DOI: 10.1007/s00402-020-03698-8]

12 **Pulido L**, Ghanem E, Joshi A, Purtill JJ, Parvizi J. Periprosthetic joint infection: the incidence, timing, and predisposing factors. *Clin Orthop Relat Res* 2008; **466**: 1710-1715 [PMID: 18421542 DOI: 10.1007/s11999-008-0209-4]

13 **Cram P**, Lu X, Kates SL, Singh JA, Li Y, Wolf BR. Total knee arthroplasty volume, utilization, and outcomes among Medicare beneficiaries, 1991-2010. *JAMA* 2012; **308**: 1227-1236 [PMID: 23011713 DOI: 10.1001/2012.jama.11153]

14 **Schroer WC**, Berend KR, Lombardi AV, Barnes CL, Bolognesi MP, Berend ME, Ritter MA, Nunley RM. Why are total knees failing today? *J Arthroplasty* 2013; **28**: 116-119 [PMID: 23954423 DOI: 10.1016/j.arth.2013.04.056]

15 **Srivastava K**, Bozic KJ, Silverton C, Nelson AJ, Makhni EC, Davis JJ. Reconsidering Strategies for Managing Chronic Periprosthetic Joint Infection in Total Knee Arthroplasty: Using Decision Analytics to Find the Optimal Strategy Between One-Stage and Two-Stage Total Knee Revision. *J Bone Joint Surg Am* 2019; **101**: 14-24 [PMID: 30601412 DOI: 10.2106/JBJS.17.00874]

16 **Di Benedetto P**, Di Benedetto ED, Salviato D, Beltrame A, Gissoni R, Cainero V, Causero A. Acute periprosthetic knee infection: is there still a role for DAIR? *Acta Biomed* 2017; **88**: 84-91 [PMID: 28657569 DOI: 10.23750/abm.v88i2-S.6518]

17 **Mortazavi SM**, Kurd MF, Bender B, Post Z, Parvizi J, Purtill JJ. Distal femoral arthroplasty for the treatment of periprosthetic fractures after total knee arthroplasty. *J Arthroplasty* 2010; **25**: 775-780 [PMID: 20171053 DOI: 10.1016/j.arth.2009.05.024]

18 **Agarwal S**, Sharma RK, Jain JK. Periprosthetic fractures after total knee arthroplasty. *J Orthop Surg (Hong Kong)* 2014; **22**: 24-29 [PMID: 24781608 DOI: 10.1177/230949901402200108]

19 **Dyrhovden GS**, Lygre SHL, Badawy M, Gøthesen Ø, Furnes O. Have the Causes of Revision for Total and Unicompartmental Knee Arthroplasties Changed During the Past Two Decades? *Clin Orthop Relat Res* 2017; **475**: 1874-1886 [PMID: 28299718 DOI: 10.1007/s11999-017-5316-7]

20 **Schwarz EM**, Parvizi J, Gehrke T, Aiyer A, Battenberg A, Brown SA, Callaghan JJ, Citak M, Egol K, Garrigues GE, Ghert M, Goswami K, Green A, Hammound S, Kates SL, McLaren AC, Mont MA, Namdari S, Obremskey WT, O'Toole R, Raikin S, Restrepo C, Ricciardi B, Saeed K, Sanchez-Sotelo J, Shohat N, Tan T, Thirukumaran CP, Winters B. 2018 International Consensus Meeting on Musculoskeletal Infection: Research Priorities from the General Assembly Questions. *J Orthop Res* 2019; **37**: 997-1006 [PMID: 30977537 DOI: 10.1002/jor.24293]

21 **Suzuki G**, Saito S, Ishii T, Motojima S, Tokuhashi Y, Ryu J. Previous fracture surgery is a major risk factor of infection after total knee arthroplasty. *Knee Surg Sports Traumatol Arthrosc* 2011; **19**: 2040-2044 [PMID: 21541707 DOI: 10.1007/s00167-011-1525-x]

22 **Lizaur-Utrilla A**, Collados-Maestre I, Miralles-Muñoz FA, Lopez-Prats FA. Total Knee Arthroplasty for Osteoarthritis Secondary to Fracture of the Tibial Plateau. A Prospective Matched Cohort Study. *J Arthroplasty* 2015; **30**: 1328-1332 [PMID: 25795233 DOI: 10.1016/j.arth.2015.02.032]

23 **Klatte TO**, Schneider MM, Citak M, Oloughlin P, Gebauer M, Rueger M, Gehrke T, Kendoff D. Infection rates in patients undergoing primary knee arthroplasty with pre-existing orthopaedic fixation-devices. *Knee* 2013; **20**: 177-180 [PMID: 23540939 DOI: 10.1016/j.knee.2013.02.004]

24 **Ge DH**, Anoushiravani AA, Kester BS, Vigdorchik JM, Schwarzkopf R. Preoperative Diagnosis Can Predict Conversion Total Knee Arthroplasty Outcomes. *J Arthroplasty* 2018; **33**: 124-129.e1 [PMID: 28939032 DOI: 10.1016/j.arth.2017.08.019]

25 **Ehlinger M**, D'Ambrosio A, Vie P, Leclerc S, Bonnomet F, Bonnevialle P, Lustig S, Parratte S, Colmar M, Argenson JN; French Society of Orthopedic Surgery, Traumatology (SoFCOT). Total knee arthroplasty after opening- versus closing-wedge high tibial osteotomy. A 135-case series with minimum 5-year follow-up. *Orthop Traumatol Surg Res* 2017; **103**: 1035-1039 [PMID: 28888524 DOI: 10.1016/j.otsr.2017.07.011]

26 **Bonacker J**, Darowski M, Haar P, Westphal T, Bergschmidt P. Periprosthetic Tibial Fracture with Nonunion and Ascending Prosthetic Joint Infection: A Case Report of an Individual Treatment Strategy. *J Orthop Case Rep* 2018; **8**: 3-8 [PMID: 30915283 DOI: 10.13107/jocr.2250-0685.1232]

27 **Sanz-Ruiz P**, Matas-Diez JA, Villanueva-Martinez M, Carbo-Laso E, Lopez-Torres II, Vaquero-Martín J. A new biarticular cement spacer technique for infected total hip and knee arthroplasty with massive bone loss. *Hip Int* 2021; **31**: 242-249 [PMID: 31746228 DOI: 10.1177/1120700019884557]

28 **Müller M**, Winkler T, Märdian S, Trampuz A, Renz N, Perka C, Karczewski D. The worst-case scenario: treatment of periprosthetic femoral fracture with coexistent periprosthetic infection-a prospective and consecutive clinical study. *Arch Orthop Trauma Surg* 2019; **139**: 1461-1470 [PMID: 31432205 DOI: 10.1007/s00402-019-03263-y]

29 **Ebraheim NA**, Kelley LH, Liu X, Thomas IS, Steiner RB, Liu J. Periprosthetic Distal Femur Fracture after Total Knee Arthroplasty: A Systematic Review. *Orthop Surg* 2015; **7**: 297-305 [PMID: 26790831 DOI: 10.1111/os.12199]

30 **Carta S**, Fortina M, Riva A, Meccariello L, Manzi E, Di Giovanni A, Ferrata P. The Biological Metallic versus Metallic Solution in Treating Periprosthetic Femoral Fractures: Outcome Assessment. *Adv Med* 2016; **2016**: 2918735 [PMID: 27990462 DOI: 10.1155/2016/2918735]

31 **Peters CL**, Bachus KN, Davitt JS. Fixation of periprosthetic femur fractures: a biomechanical analysis comparing cortical strut allograft plates and conventional metal plates. *Orthopedics* 2003; **26**: 695-699 [PMID: 12875564 DOI: 10.3928/0147-7447-20030701-13]

World Journal of Clinical Cases

Submit a Manuscript: https://www.f6publishing.com

World J Clin Cases 2023 April 6; 11(10): 2329-2335

DOI: 10.12998/wjcc.v11.i10.2329

ISSN 2307-8960 (online)

CASE REPORT

Formation of a rare curve-shaped thoracolith documented on serial chest computed tomography images: A case report

Fu-Chieh Hsu, Tsai-Wang Huang, Ta-Wei Pu

Specialty type: Surgery

Provenance and peer review: Unsolicited article; Externally peer reviewed.

Peer-review model: Single blind

Peer-review report's scientific quality classification

Grade A (Excellent): A
Grade B (Very good): 0
Grade C (Good): C
Grade D (Fair): D
Grade E (Poor): 0

P-Reviewer: Jian X, China; Liu S, China; Zhao JW, China

Received: December 26, 2022
Peer-review started: December 26, 2022
First decision: January 5, 2023
Revised: January 11, 2023
Accepted: March 6, 2023
Article in press: March 6, 2023
Published online: April 6, 2023

Fu-Chieh Hsu, Department of Surgery, Tri-Service General Hospital, Taipei 114, Taiwan

Tsai-Wang Huang, Division of Thoracic Surgery, Department of Surgery, Tri-Service General Hospital, Taipei 114, Taiwan

Ta-Wei Pu, Division of Colon and Rectal Surgery, Department of Surgery, Tri-Service General Hospital, Taipei 114, Taiwan

Corresponding author: Tsai-Wang Huang, MD, PhD, Professor, Division of Thoracic Surgery, Department of Surgery, Tri-Service General Hospital, No. 325 Section 2, Chenggong Rd, Neihu District, Taipei 114, Taiwan. chi-wang@yahoo.com.tw

Abstract

BACKGROUND

Thoracolithiasis is a rare benign condition that manifests with one or more small nodules in the pleural cavity. In most cases, it is asymptomatic and found incidentally on chest imaging or during thoracic surgery. The thoracolithiasis formation process is rarely documented. Herein, we present a case of a rare, large, curve-shaped thoracolith, the formation of which was documented on serial computed tomography (CT) images.

CASE SUMMARY

A 46-year-old male patient who denied any prior systemic disease was evaluated due to intermittent right-sided lateral chest pain lasting for a year. Chest radiography and CT revealed a circumscribed calcified nodule measuring 3.5 mm in the right lower lung lobe. Nodule biopsy revealed fungal infection, which was treated with antifungal medication. After 2 years of follow-up, the patient developed intermittent chest discomfort caused by pleural adhesions, and underwent video-assisted thoracic surgery with pneumolysis. Postoperatively, he developed empyema, which fully resolved with antibiotic therapy. Thereafter, he was followed up at the outpatient clinic and underwent chest CT twice per year. Over time, we observed thickening of the right distal pleura near the lower posterior mediastinum, and several sporadic calcified nodules with gradually increasing intensity, which eventually merged into a single calcified curve-shaped thoracolith measuring approximately 9 cm in length during the 5-year follow-up.

CONCLUSION

This study documented the formation of a rare thoracolith shape observed for the first time.

Key Words: Thoracolithiasis; Thoracolith; Pleural stone; Intrathoracic calculus; Pleurolith; Case report

Core Tip: Thoracolithiasis, a rare benign condition manifesting with one or more small nodules in the pleural cavity, is usually asymptomatic and discovered incidentally on imaging or during surgery. We present the case of a 46-year-old man who was treated for lung fungal infection and subsequently underwent video-assisted thoracic surgery with pneumolysis due to pleural adhesions. The serial chest computed tomography images obtained during the 5-year follow-up showed right pleural thickening near the lower posterior mediastinum with formation of a large curve-shaped thoracolith from sporadic calcified nodules. Thoracolithiasis formation is rarely observed, and this is the first case of such thoracolith shape.

Citation: Hsu FC, Huang TW, Pu TW. Formation of a rare curve-shaped thoracolith documented on serial chest computed tomography images: A case report. *World J Clin Cases* 2023; 11(10): 2329-2335
URL: https://www.wjgnet.com/2307-8960/full/v11/i10/2329.htm
DOI: https://dx.doi.org/10.12998/wjcc.v11.i10.2329

INTRODUCTION

Thoracolithiasis, also known as pleurolithiasis, intrathoracic calculosis, or pleural stones, is a rare benign condition manifesting with one or more small nodules in the pleural cavity[1]. In most cases, it is asymptomatic and is usually found incidentally on chest imaging or during thoracic surgery. To the best of our knowledge, there have been no reported cases of symptomatic thoracolithiasis[2]. In addition, its formation process has rarely been documented.

Herein, we report the formation of a curve-shaped thoracolith in a 46-year-old male patient over a 5-year period, documented on serial computed tomography (CT) images.

CASE PRESENTATION

Chief complaints

A 46-year-old male patient presented with a complaint of intermittent right-sided lateral chest pain.

History of present illness

His symptoms started approximately 1 year previously and occurred intermittently. The patient experienced mild dull pain that occurred occasionally with exertion or forced expiration over the right lateral chest, but he was unable to point its exact location. The chest had no skin lesions and expanded symmetrically. The discomfort increased in frequency within a month, which bothered his exercise habit. No history of trauma was mentioned.

History of past illness

The patient denied any prior systemic diseases.

Personal and family history

The patient had smoked for a year but had quit for 30 years and denied using alcohol or medications. The family history revealed nothing noteworthy.

Physical examination

The patient had clear breathing sounds with symmetrical chest wall expansion.

Laboratory examinations

A serum test revealed leukocytosis with elevated white blood cell and C-reactive protein levels of 15.73 (10^3/uL) and 10 mg/dL, respectively, during the course of the emphysema. All lab results were found to be normal during the follow-up interval.

Imaging examinations

Chest radiography showed increased lung markings with peribronchial wall thickening in the bilateral lower lung fields (Figure 1), while chest CT revealed a circumscribed calcified nodule measuring 3.5 mm in the right lower lung lobe (Figure 2). Since an infection with an unknown pathogen or malignancy was suspected, a CT-guided biopsy was performed. The histopathological examination of the biopsy specimen revealed a fungal infection.

FINAL DIAGNOSIS

Based on the clinical, imaging, and histopathological findings, the patient was diagnosed with fungal infection of the lungs.

TREATMENT

The patient was prescribed an antifungal medicine, fluconazole 50 mg per day for 6 mo.

OUTCOME AND FOLLOW-UP

Following the completion of therapy, the patient regularly followed-up at the outpatient clinic every month for the next two years. A follow-up chest CT was performed every 6 mo for 2 years due to complaints of occasional chest discomfort with a mild pricking pain after the last discharge, which revealed a thickening of the right pleura with focal atelectasis in the right middle lung lobe (Figure 3). We suspected that the chest pain was caused by pleural adhesions and performed video-assisted thoracic surgery with pneumolysis. Postoperatively, turbid pleural fluid was discharged from the chest tube inserted into the right chest cavity. The culture test revealed methicillin-resistant *Staphylococcus aureus*. The patient was administered antibiotic therapy, which resulted in resolution of the empyema. He was discharged from the hospital and followed up at the outpatient clinic.

During the follow-up, the patient continued to experience intermittent chest discomfort, and occasionally, a cough, which could be relieved with medicines. The follow-up chest radiographs showed calcified shadows in the right lower lung field (Figure 4). Follow-up chest CT was performed twice per year, with loss to follow-up from 2019 to 2021. In reviewing the serial CT images obtained during the 5-year follow-up, we observed gradual thickening of the right pleura near the lower posterior mediastinum, and several sporadic calcified nodules in the same region with increasing intensity, which became intensive and curved calcified lesions, and eventually formed a large curve-shaped thoracolith measuring approximately 9 cm in length (Figure 5). Despite the progression of thoracolithiasis on CT images, the patient only reported intermittent chest discomfort and denied symptoms such as dyspnea, dysphagia, or hemoptysis. Therefore, no further treatment was prescribed and the patient continued to be followed up on outpatient basis.

DISCUSSION

Thoracolithiasis is a rare benign condition with a very low incidence in the general population of 0.086% [3]. It was first reported in 1968 by Dias *et al*[4]. Since then, approximately 70 cases have been reported in the literature, and in many of these the pleural nodules were surgically resected to rule out neoplasia [3,5,6]. No age or sex preference has been reported, although a slight female advantage was observed in a previous report by Kinoshita *et al*[3]. In most cases, thoracolithiasis is asymptomatic and discovered incidentally on chest imaging or during surgery. Pleural stones are most commonly found in the pendent portion of the pleural cavity, possibly as a result of gravity, particularly on the surface of the diaphragm, along the chest wall near the lower lung fields, next to the left heart border, or near the paravertebral spaces[8].

In a recent major series, all nodules with calcification were reported on CT images[3]. However, although they can be calcified, in some cases, thoracoliths can be indistinguishable from intrapulmonary nodules on CT images[9]. In fact, in one-third of cases, immobile nodules were preoperatively diagnosed as peripheral pulmonary tumors[10]. In some cases, the nodules contained areas of calcification with spotty, central, peripheral, or diffuse patterns[3]. Furthermore, some thoracoliths can be difficult to distinguish from malignant lesions because they enlarge over time[4,11]. Less calcified or immobile thoracoliths are often misdiagnosed, resulting in unnecessary surgical treatment; therefore, accurate diagnosis is important[12].

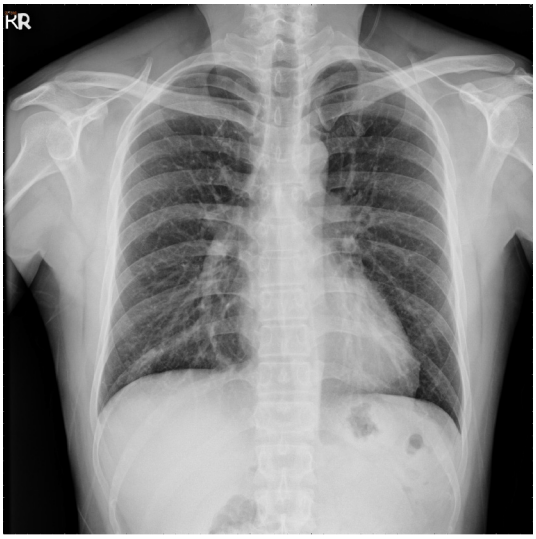

DOI: 10.12998/wjcc.v11.i10.2329 **Copyright** ©The Author(s) 2023.

Figure 1 Chest radiograph obtained after the initial examination. The image shows increased lung markings with peribronchial wall thickening in the bilateral lower lung fields.

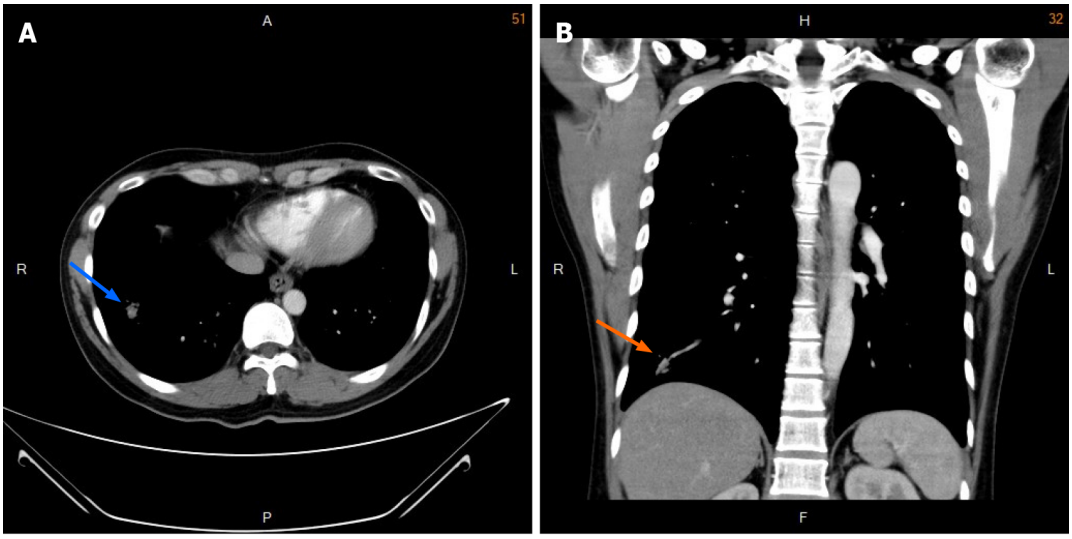

DOI: 10.12998/wjcc.v11.i10.2329 **Copyright** ©The Author(s) 2023.

Figure 2 Chest computed tomography images obtained after the initial examination. A: Axial and B: Coronal images obtained in a soft tissue setting showing a circumscribed calcified nodule measuring 3.5 mm in the right lower lung lobe (blue and orange arrows).

When thoracolithiasis is suspected, it is difficult to obtain a diagnosis by transthoracic or endobronchial biopsy due to the firm consistency of thoracolith lesions and their loose fixation in the pleural cavity[13]. Based on the unique radiological findings, major surgery is usually not required and not recommended[14]. If they are not calcified or enlarged on follow-up images or the lesion nature is indeterminate, surgical resection should be considered to confirm the diagnosis[4,11,15]. Thoracoscopy, which has the advantage of a minimally invasive procedure that can be performed under local anesthesia, can be used to confirm the diagnosis[16]. The differential diagnosis of thoracoliths includes foreign body granulomas and, rarely, extravasated gallstones after laparoscopic cholecystectomy that have migrated into the pleural cavity[17-19].

Although the etiology of thoracolithiasis is unknown, several hypotheses have been proposed regarding the pathological processes underlying their formation: pericardial fat necrosis and shedding in the pleural cavity, old tuberculosis lesions, or clusters of macrophages phagocytizing dust, which over time form calcified lesions shaped under the impact of long-term breathing movements[10,11,15]. Thoracolithiasis may also develop from inflammation, which facilitates fibrosis[10].

In previously reported cases, thoracoliths ranged in size from 5 to 15 mm (mean size, 8 mm)[3], and in most cases, presented as multiple small ovoid nodules located in the left pleura[3,4,11,20]. In our case, the thoracolith measured approximately 9 cm in length. In addition, this case demonstrated the 5-year

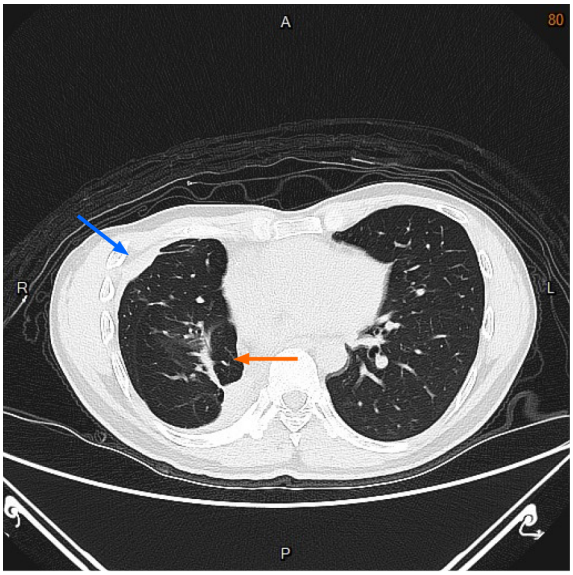

DOI: 10.12998/wjcc.v11.i10.2329 **Copyright** ©The Author(s) 2023.

Figure 3 Follow-up chest computed tomography image obtained two years after the initial therapy. Axial image showing thickening of the right pleura (blue arrow) and focal atelectasis (orange arrow) in the right middle lung lobe.

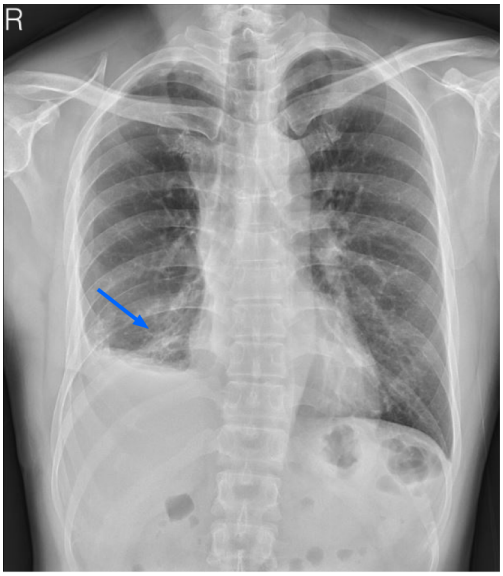

DOI: 10.12998/wjcc.v11.i10.2329 **Copyright** ©The Author(s) 2023.

Figure 4 Follow-up chest radiograph obtained two years postoperatively. The image shows calcified shadows over the right lower lung field (blue arrow).

formation process of the large curve-shaped thoracolith. Multiple sporadic calcified nodules accumulated in the pleura over time, abutting each other, and eventually assembled into a large thoracolith. The sporadic calcified nodules increased in size on follow-up CT images and were seen in the pendant portion of the pleural cavity, possibly secondary to gravity. Based on their growth pattern and imaging characteristics, the lesions were not consistent with tumor lesions. In our patient, thoracolithiasis may have resulted from pericardial or right mediastinal fat necrosis, reflecting the prior episodes of fungal infection and empyema. The exact etiology of thoracolithiasis is unknown; we hypothesize that a previous pleural infection, fungal or bacterial, could facilitate inflammation and fibrosis, which would further lead to the formation of calcified masses.

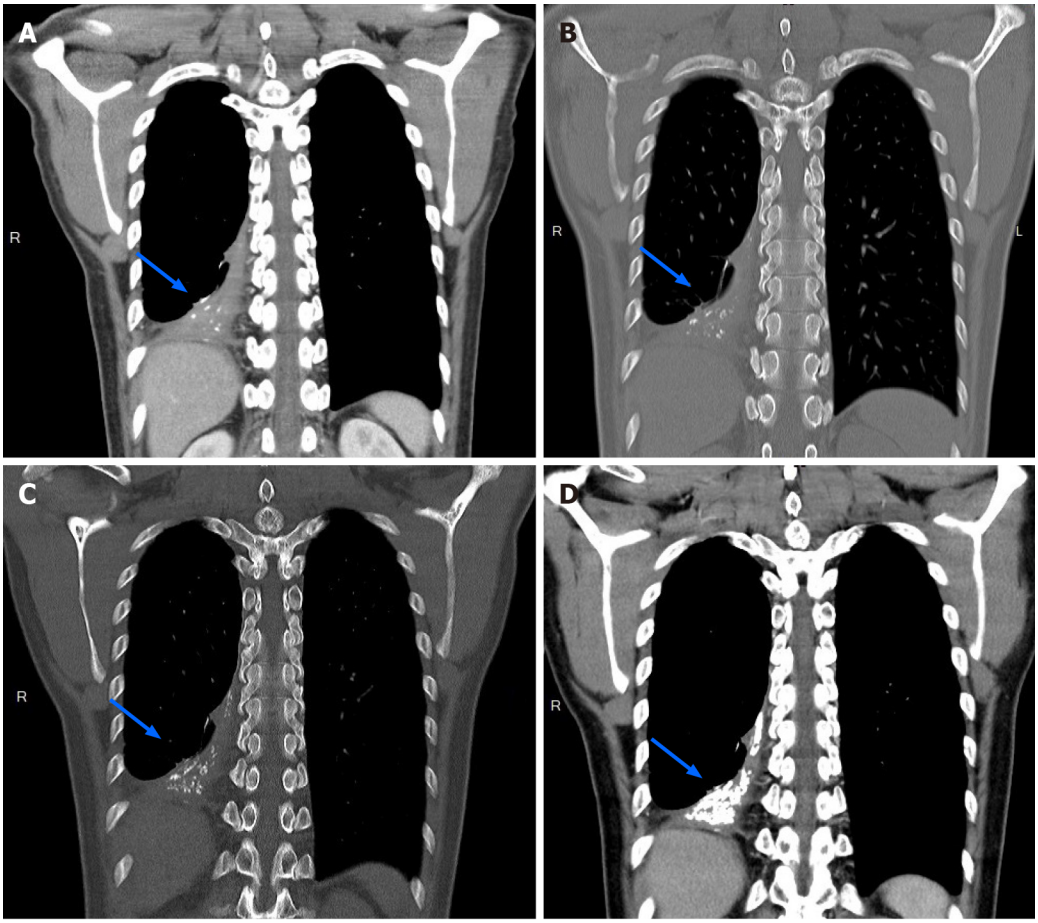

DOI: 10.12998/wjcc.v11.i10.2329

Figure 5 Serial computed tomography images obtained during a 5-year follow-up. Coronal images showing gradual thickening of the right pleura near the lower posterior mediastinum and several sporadic calcified nodules (blue arrow) in the same region with increasing intensity over time, which eventually formed a large curve-shaped calcified thoracolith measuring approximately 9 cm in length. A: 5-year follow-up in 2017; B: 5-year follow-up in 2018; C: 5-year follow-up in 2019; D: 5-year follow-up in 2022.

CONCLUSION

The present case provided a rare opportunity to observe the formation process of a large curve-shaped thoracolith. This thoracolith shape was observed for the first time as opposed to the commonly encountered multiple small ovoid thoracoliths. Pericardial or right mediastinal fat necrosis may have resulted in its formation.

ACKNOWLEDGEMENTS

The authors would like to express their gratitude to Fu-Chieh Hsu, MD, for his contributions in drafting the article as well as the conception and design of the study; Ta-Wei Pu, MD, for his role in critically reviewing the manuscript for keu intellectual content; and Tsai-Wang Huang, MD, PhD, for overseeing the study and endorsing the data.

FOOTNOTES

Author contributions: Hsu FC contributed to data collection and manuscript writing; Huang TW and Pu DW contributed to manuscript revision and study supervision; All authors have read and approved the final manuscript.

Informed consent statement: Informed written consent was obtained from the patient for the publication of this report and any accompanying images.

Conflict-of-interest statement: All the authors declare that they have no conflicts of interest to disclose.

CARE Checklist (2016) statement: The authors have read the CARE Checklist (2016), and the manuscript was prepared and revised according to the CARE Checklist (2016).

Country/Territory of origin: Taiwan

ORCID number: Fu-Chieh Hsu 0000-0001-8071-1635; Tsai-Wang Huang 0000-0001-8741-9223; Ta-Wei Pu 0000-0002-0538-407X.

S-Editor: Liu JH
L-Editor: A
P-Editor: Liu JH

REFERENCES

1 **Peungjesada S**, Gupta P, Mottershaw AM. Thoracolithiasis: a case report. *Clin Imaging* 2012; **36**: 228-230 [PMID: 22542384 DOI: 10.1016/j.clinimag.2011.08.023]
2 **Kang N**, Choi Y, Im Y, Choe J, Kim J, Han J, Kim TJ, Kim H. A rare case of numerous thoracolithiasis with chest discomfort. *Respir Med Case Rep* 2018; **25**: 264-266 [PMID: 30338224 DOI: 10.1016/j.rmcr.2018.10.002]
3 **Kinoshita F**, Saida Y, Okajima Y, Honda S, Sato T, Hayashibe A, Hiramatsu S. Thoracolithiasis: 11 cases with a calcified intrapleural loose body. *J Thorac Imaging* 2010; **25**: 64-67 [PMID: 20160605 DOI: 10.1097/RTI.0b013e3181a4ba03]
4 **Dias AR**, Zerbini EJ, Curi N. Pleural stone. A case report. *J Thorac Cardiovasc Surg* 1968; **56**: 120-122 [PMID: 5663123 DOI: 10.1016/S0022-5223(19)42882-1]
5 **Tsuchiya T**, Ashizawa K, Tagawa T, Tsutsui S, Yamasaki N, Miyazaki T, Hayashi T, Nagayasu T. A case of migrated thoracolithiasis. *J Thorac Imaging* 2009; **24**: 325-327 [PMID: 19935229 DOI: 10.1097/RTI.0b013e3181c2f25d]
6 **Strzelczyk J**, Holloway BJ, Pernicano PG, Kelly AM. Rolling stones in the pleural space: thoracoliths on CT, and a review of the literature. *Clin Radiol* 2009; **64**: 100-104 [PMID: 19070704 DOI: 10.1016/j.crad.2008.09.001]
7 **Kim Y**, Shim SS, Chun EM, Won TH, Park S. A Pleural Loose Body Mimicking a Pleural Tumor: A Case Report. *Korean J Radiol* 2015; **16**: 1163-1165 [PMID: 26355378 DOI: 10.3348/kjr.2015.16.5.1163]
8 **Hamanaka R**, Masuda R, Iwazaki M. A Case of Thoracolithiasis Extracted with a Thoracoscope. *Tokai J Exp Clin Med* 2021; **46**: 162-165 [PMID: 34859414]
9 **Cornellas L**, Soler-Perromat JC, Vollmer I. Thoracolithiasis: A Rare Cause of Migratory Thoracic Mass. *Arch Bronconeumol (Engl Ed)* 2019; **55**: 534 [PMID: 30851982 DOI: 10.1016/j.arbres.2019.01.020]
10 **Iwasaki T**, Nakagawa K, Katsura H, Ohse N, Nagano T, Kawahara K. Surgically removed thoracolithiasis: report of two cases. *Ann Thorac Cardiovasc Surg* 2006; **12**: 279-282 [PMID: 16977300]
11 **Kosaka S**, Kondo N, Sakaguchi H, Kitano T, Harada T, Nakayama K. Thoracolithiasis. *Jpn J Thorac Cardiovasc Surg* 2000; **48**: 318-321 [PMID: 10860288 DOI: 10.1007/BF03218148]
12 **Gayer G**. Thoracolithiasis-Computed Tomography Findings of Intrapleural Loose Bodies. *Semin Ultrasound CT MR* 2017; **38**: 634-640 [PMID: 29179903 DOI: 10.1053/j.sult.2017.08.004]
13 **Komatsu T**, Sowa T, Fujinaga T. A case of thoracolithiasis diagnosed thoracoscopically. *Int J Surg Case Rep* 2012; **3**: 415-416 [PMID: 22705577 DOI: 10.1016/j.ijscr.2012.05.006]
14 **Motamedi P**, Palacio D, Campion J. Mobile Thoracolithiasis. *Am J Med* 2018; **131**: e251-e252 [PMID: 29453942 DOI: 10.1016/j.amjmed.2018.01.025]
15 **Hochhegger B**, Camargo SM, Nascimento D, Zanetti G, Marchiori E. Thoracolithiasis: A Rare Cause of Multiple Nodules. *Am J Respir Crit Care Med* 2018; **197**: 1212-1213 [PMID: 29490153 DOI: 10.1164/rccm.201710-2067IM]
16 **Nakagawa H**, Ohuchi M, Fujita T, Ozaki Y, Nakano Y, Inoue S. Thoracolithiasis diagnosed by thoracoscopy under local anesthesia. *Respirol Case Rep* 2015; **3**: 102-104 [PMID: 26392857 DOI: 10.1002/rcr2.114]
17 **Oestmann JW**, Bridenbaugh S, Eggeling I. Gallstone migration into the pleural space. *Am J Gastroenterol* 2000; **95**: 836-837 [PMID: 10710103 DOI: 10.1111/j.1572-0241.2000.01868.x]
18 **Brazinsky SA**, Colt HG. Thoracoscopic diagnosis of pleurolithiasis after laparoscopic cholecystectomy. *Chest* 1993; **104**: 1273-1274 [PMID: 8404206 DOI: 10.1378/chest.104.4.1273]
19 **Quail JF**, Soballe PW, Gramins DL. Thoracic gallstones: a delayed complication of laparoscopic cholecystectomy. *Surg Infect (Larchmt)* 2014; **15**: 69-71 [PMID: 24116737 DOI: 10.1089/sur.2012.218]
20 **Tanaka D**, Niwatsukino H, Fujiyoshi F, Nakajo M. Thoracolithiasis--a mobile calcified nodule in the intrathoracic space: radiographic, CT, and MRI findings. *Radiat Med* 2002; **20**: 131-133 [PMID: 12126085]

World Journal of Clinical Cases

Submit a Manuscript: https://www.f6publishing.com

World J Clin Cases 2023 April 6; 11(10): 2336-2342

DOI: 10.12998/wjcc.v11.i10.2336

ISSN 2307-8960 (online)

CASE REPORT

Neurofibromatosis type 1 with multiple gastrointestinal stromal tumors: A case report

Min-Quan Yao, Yu-Peng Jiang, Bing-Hong Yi, Yong Yang, Da-Zhuang Sun, Jin-Xing Fan

Specialty type: Medicine, research and experimental

Provenance and peer review: Unsolicited article; Externally peer reviewed.

Peer-review model: Single blind

Peer-review report's scientific quality classification

Grade A (Excellent): 0
Grade B (Very good): B
Grade C (Good): C
Grade D (Fair): 0
Grade E (Poor): E

P-Reviewer: Almousa M, Syria; Otani K, Japan; Wani I, India

Received: December 21, 2022
Peer-review started: December 21, 2022
First decision: January 20, 2023
Revised: February 1, 2023
Accepted: March 14, 2023
Article in press: March 14, 2023
Published online: April 6, 2023

Min-Quan Yao, Yu-Peng Jiang, Bing-Hong Yi, Yong Yang, Da-Zhuang Sun, Department of Gastrointestinal Surgery, Tongxiang First People's Hospital, Jiaxing 314500, Zhejiang Province, China

Jin-Xing Fan, Endoscopy Center, Tongxiang First People's Hospital, Jiaxing 314500, Zhejiang Province, China

Corresponding author: Jin-Xing Fan, BSc, Nurse, Endoscopy Center, Tongxiang First People's Hospital, No. 1918 Jiaochang East Road, Jiaxing 314500, Zhejiang Province, China.
116304728@qq.com

Abstract

BACKGROUND

Neurofibromatosis type 1 (NF1) is characterized by café-au-lait patches on the skin and the presence of neurofibromas. Gastrointestinal stromal tumor (GIST) is the most common non-neurological tumor in NF1 patients. In NF1-associated GIST, *KIT* and *PDGFRA* mutations are frequently absent and imatinib is ineffective. Surgical resection is first-line treatment.

CASE SUMMARY

A 56-year-old woman with NF1 was hospitalized because of an incidental pelvic mass. Physical examination was notable for multiple café-au-lait patches and numerous subcutaneous soft nodular masses of the skin of the head, face, trunk, and limbs. Her abdomen was soft and nontender. No masses were palpated. Digital rectal examination was unremarkable. Abdominal computed tomography was suspicious for GIST or solitary fibrous tumor. Laparoscopy was performed, which identified eight well-demarcated masses in the jejunum. All were resected and pathologically diagnosed as GISTs. The patient was discharged on day 7 after surgery without complications. No tumor recurrence was evident at the 6-mo follow-up.

CONCLUSION

Laparoscopy is effective for both diagnosis and treatment of NF1-associated GIST.

Key Words: Neurofibromatosis type 1; Gastrointestinal stromal tumors; *KIT*; *PDGFRA*; Laparoscopy; Case report

Core Tip: A thorough medical history and physical examination are imperative in patients with neurofibromatosis type 1 and gastrointestinal symptoms. Such symptoms may indicate the presence of one or more gastrointestinal stromal tumors. Abdominal computed tomography, capsule endoscopy, or small bowel endoscopy should be performed. Laparoscopy may also be performed for both diagnosis and treatment.

Citation: Yao MQ, Jiang YP, Yi BH, Yang Y, Sun DZ, Fan JX. Neurofibromatosis type 1 with multiple gastrointestinal stromal tumors: A case report. *World J Clin Cases* 2023; 11(10): 2336-2342
URL: https://www.wjgnet.com/2307-8960/full/v11/i10/2336.htm
DOI: https://dx.doi.org/10.12998/wjcc.v11.i10.2336

INTRODUCTION

Neurofibromatosis type 1 (NF1), also known as von Recklinghausen's disease, is an autosomal dominant disorder with an incidence of 1/3000 to 1/4000[1]. Clinical diagnosis of NF1 is based on the presence of at least two of the following criteria: (1) Six or more café-au-lait patches over 5 mm in diameter in prepubertal children and over 15 mm in diameter in postpubertal individuals and adults; (2) two or more neurofibromas or one plexiform neurofibroma; (3) freckles in the axilla or inguinal region; (4) optic glioma; (5) two or more Lisch nodes; (6) osseous lesion; and (7) first-degree relative with NF1[2]. Gastrointestinal stromal tumor (GIST) is a tumor of mesenchymal origin that usually arises in the stomach (60%–70%) or small intestine (20%–30%). Multiple GISTs are uncommon[3]. We report an NF1 patient with a pelvic mass who underwent laparoscopic examination of the abdomen and pelvis and was diagnosed with multiple GISTs.

CASE PRESENTATION

Chief complaints

A 56-year-old woman with NF1 was hospitalized because of an incidental pelvic mass.

History of present illness

Ultrasonography of the pelvis performed at another hospital showed a mixed echoic mass approximately 4.5 cm × 4.5 cm × 4.0 cm in size in the left lower abdomen. Boundaries were clear and shape was irregular. No internal fluid echoes were visualized. Color Doppler flow imaging showed abundant blood flow signals within the mass. Clinically, the patient denied any gastrointestinal symptoms.

History of past illness

The patient had multiple café-au-lait patches and cutaneous nodular masses on the head, face, trunk, and limbs which had been increasing in number and size for more than 30 years. She had no symptoms of itchy skin. Biopsy of a nodular upper limb mass 10 years previously was consistent with neurofibroma. She had undergone laparoscopic cholecystectomy for a gallbladder stone 10 years previously and partial ileal resection for a strangulated bowel obstruction associated with adhesions 8 years previously. She had no history of hypertension, diabetes mellitus, or heart disease.

Personal and family history

The patient had no history of smoking or drinking. One sister and one brother had NF1.

Physical examination

The patient exhibited soft cutaneous nodular masses of 0.2 to 3 cm in diameter on the head, face, trunk, and limbs as well as multiple café-au-lait patches (Figure 1). Examinations of the eyes, lungs, and heart were normal. Hearing testing was normal. Freckles were seen in the axilla and inguinal region. No lymphadenopathy was detected in the neck, axilla, or inguinal region. The abdomen was soft and without tenderness or palpable masses. Bowel sounds were normal. Digital rectal exam was unremarkable.

Laboratory examinations

White blood cell count was 7.2 × 10^9/L. Red blood cell count was 4.45 × 10^{12}/L. Hemoglobin concentration was 136 g/L. Platelet count was 260.0 × 10^9/L. C-reactive protein concentration was 3.65 mg/L. Fecal occult blood testing was negative. Concentrations of carcinoembryonic antigen, cancer antigen

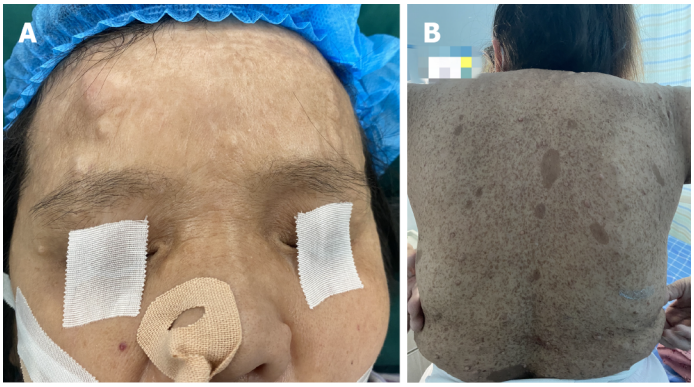

DOI: 10.12998/wjcc.v11.i10.2336

Figure 1 Café-au-lait patches and cutaneous nodular masses. A: Multiple cutaneous nodular masses on the head and face; B: Multiple café-au-lait patches and cutaneous nodular masses on the back.

125, and carbohydrate antigen 19-9 were all within normal range.

Imaging examinations

Contrast-enhanced computed tomography (CT) of the abdomen showed an irregular cystic mass with an oblique diameter of approximately 44 mm in the left pelvis. Its solid component exhibited contrast enhancement (Figure 2) and had no clear border with the adjacent intestinal wall. GIST of the small intestine or solitary fibrous tumor was suspected.

FINAL DIAGNOSIS

NF1 with GISTs.

TREATMENT

After multidisciplinary team consultation, laparoscopy was performed. Eight well-demarcated encapsulated masses were found in the jejunum between 20 and 120 cm from the Trietz ligament. The remainder of the small intestine was free of masses. The largest mass was approximately 4.5 cm in diameter and located 20 cm from the Trietz ligament. The others were 0.3 to 0.8 cm in diameter. The small intestine was approximately 200 cm in length and the original small intestine anastomosis from her previous surgery was open. Because resecting 100 cm of the intestine could cause short bowel syndrome, we elected to perform resection of the jejunal masses. A 6 cm median upper abdominal incision was made to raise the small intestine into the abdominal cavity. Partial jejunostomy was performed 20 cm from the Trietz ligament and the masses were resected (Figure 3). Histopathology of the 4.5 cm jejunal mass was consistent with GIST with hemorrhagic infarction. Mitosis count was < 5 in 50 high-power fields. Based on the modified National Institutes of Health criteria, the tumor was classified as low risk. The other masses were also diagnosed as GISTs. None exhibited invasive growth. CD34, CD117, and DOG-1 staining was positive (Figure 4). S-100 staining was negative. Ki-67 index was less than 5%. Genetic testing demonstrated wild type *KIT* and *PDGFRA* genes. The final diagnosis was multiple NF1-associated GISTs.

OUTCOME AND FOLLOW-UP

The patient was discharged on day 7 after surgery. No complications occurred. No sign of tumor recurrence or metastasis was present at the 6-mo follow-up. Annual follow-up by contrast-enhanced abdominal CT or magnetic resonance imaging is planned. Any small recurrent tumors in the small intestine will be removed enteroscopically.

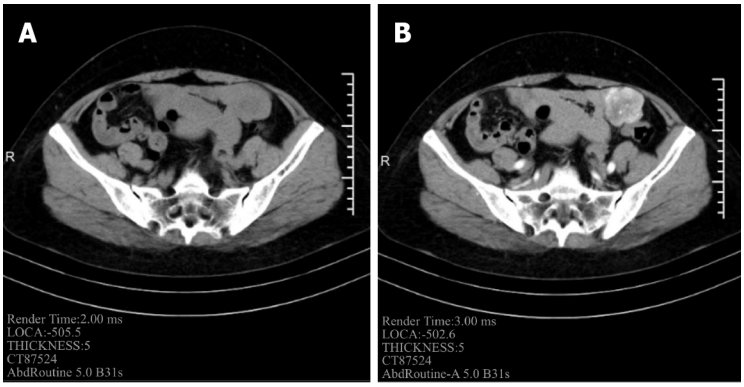

DOI: 10.12998/wjcc.v11.i10.2336 **Copyright** ©The Author(s) 2023.

Figure 2 Abdominal computed tomography. A: A cystic solid mass with an oblique diameter of approximately 44 mm is seen in the left pelvis; B: The solid component exhibits arterial enhancement.

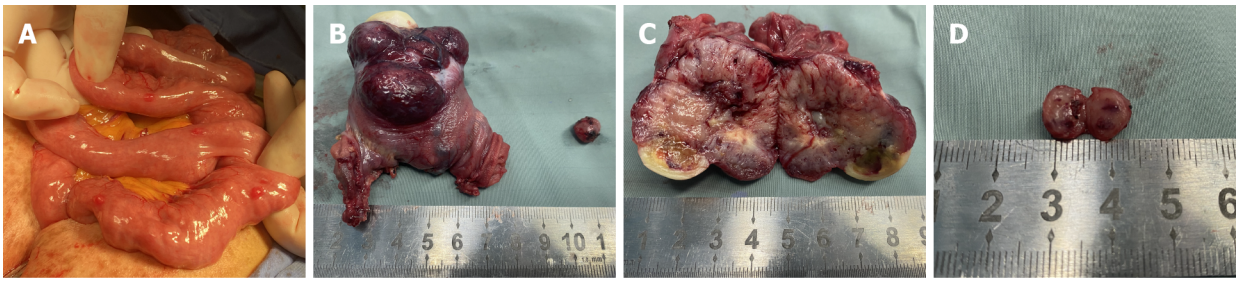

DOI: 10.12998/wjcc.v11.i10.2336 **Copyright** ©The Author(s) 2023.

Figure 3 Intraoperative view. A: Multiple masses in the jejunal wall demonstrated clear borders; B: A 4.5 cm diameter tumor in the jejunum 20 cm from the Trietz ligament; C: Large tumor with a grayish white, nodular, cystic surface; D: Small tumor with an oval shape and solid nodules.

DISCUSSION

The gene responsible for NF1 is located at chromosome 17q11.2. Mutations can result in inability to produce the corresponding neurofibromin protein. Deletion leads to abnormal activation of the RAS/RAF/MAP signaling pathway, which results in loss of neurofibromin's tumor suppressor function and increases susceptibility to development of tumors such as neurofibroma, optic glioma, malignant peripheral nerve sheath tumor, neuroblastoma, pheochromocytoma, and breast cancer[1]. GIST is rare and develops in approximately 7% of all NF1 patients[4]. It originates from mesenchymal tissue of the gastrointestinal tract, usually in the stomach and small intestine, and pathology mainly shows spindle cells and epithelioid cells. *KIT* mutations are detected in approximately 90% of GISTs, while *PDGFRA* mutations are found in approximately 5%[5]. Mutations of these two genes are the main cause of GIST, although *BRAF* mutations are present in some cases. GISTs are multiple in less than 5% of cases. Multiple GISTs are frequently associated with NF1 and familial GIST. GIST is the most common non-neurological tumor in NF1 patients. Incidence of GIST is 45 times higher in NF1 patients than in the general population. Unlike sporadic GIST, NF1-associated GIST develops at a younger age and is more common in women[6]; moreover, most tumors are multiple and located in the small intestine (90%)[7]. Pathologically, NF1-associated GIST consists predominantly of spindle cells and behaves as a low-grade malignancy with slow progression. *KIT* and *PDGFRA* mutations are frequently not present, suggesting a different pathogenesis from the sporadic form. Prognosis is better for NF1-associated GIST than the sporadic form (Table 1). GIST may present with abdominal pain, nausea and vomiting, gastrointestinal bleeding, anemia, abdominal mass, intestinal obstruction. However, it may be asymptomatic and found incidentally. Since NF1-associated GIST is usually located in the small intestine, gastroscopy is often negative. Therefore, middle-aged and elderly NF1 patients with gastrointestinal symptoms should undergo abdominal CT or magnetic resonance imaging[8]. Abdominal CT can reveal tumor size, location, border, and relationship with surrounding tissues, as well as metastases. Capsule endoscopy and small bowel endoscopy are also commonly used for diagnosis, which is confirmed *via* pathologic examination and immunohistochemical and genetic testing of a tumor specimen. CD117 and CD34 are positive in most cases of NF1-associated GIST, which facilitates diagnosis[9]. Tumor location, size, and mitotic activity are GIST prognostic factors. Ki-67 index is associated with recurrence and survival[10]. Imatinib is ineffective in most NF1-associated GISTs because of their lack of *KIT* and *PDGFRA*

Table 1 Comparison of neurofibromatosis 1-associated and sporadic gastrointestinal intestinal stromal tumor

	NF1 with GIST	Sporadic GIST
Age of onset	Young	Older
Most common sites	Small intestine (90%)	Stomach (60%-70%)
Number of tumors	Often multiple	Often solitary
Nuclear fission rate	Low	High
KIT and *PDGFRA* gene mutation	Rare	Common
Imatinib treatment	Ineffective	Effective
Disease progression	Slow	Quick
Postoperative recurrence rate	Low	High
Prognosis	Good	Common

NF1: Neurofibromatosis 1; GIST: Gastrointestinal stromal tumor.

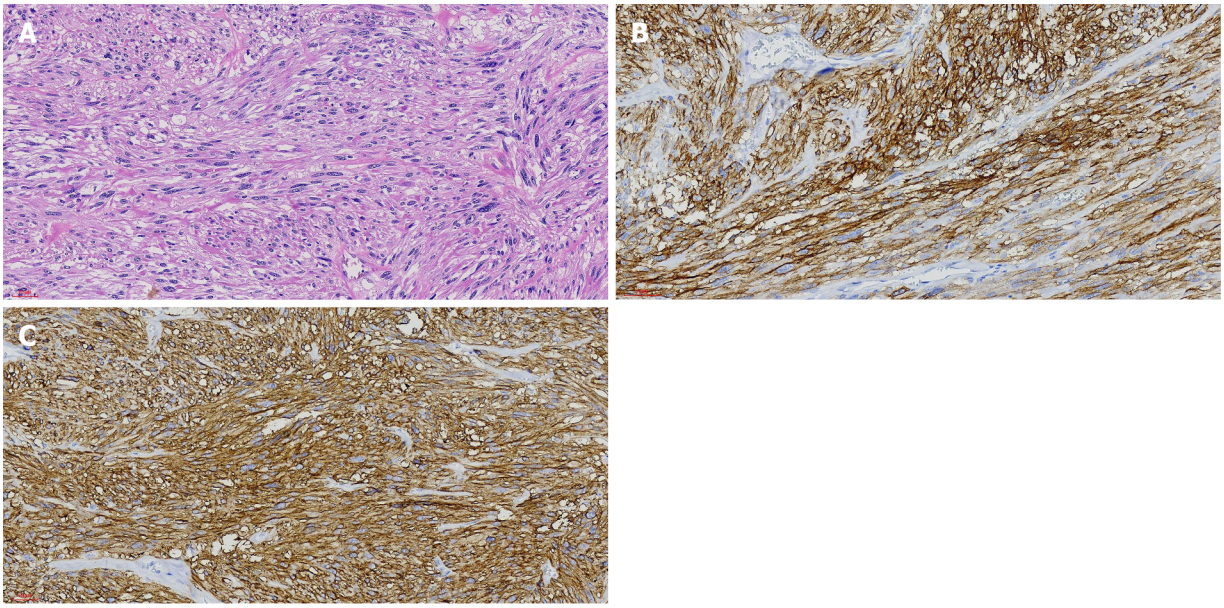

DOI: 10.12998/wjcc.v11.i10.2336

Figure 4 Postoperative pathology and immunohistochemical results. A: Diffuse spindle cells with rod-shaped nuclei (hematoxylin–eosin, × 200); B: Diffusely strong expression of CD117 (× 200); C: Diffusely strong expression of DOG-1 (× 200).

mutations[11]. Surgical resection of tumor or bowel segment is the first choice of treatment, depending on tumor size. Usually a resection margin of 1 cm is sufficient[12]. Complete removal without lymph node dissection is recommended[13]. Even after radical surgical treatment, approximately 50% of patients experience relapse[14]. The recurrence rate in patients with NF1 is similar to that in patients with sporadic GIST. Laparoscopic surgery is as effective as open surgery and associated with a similar rate of recurrence; however, procedure-related pain is less, recovery is faster, and length of hospital stay is shorter.

CONCLUSION

GIST should be suspected in NF1 patients with gastrointestinal symptoms. NF1 should be considered in patients with multiple GISTs located outside the stomach. A thorough medical history and physical examination are imperative, and abdominal CT, capsule endoscopy, or small bowel endoscopy should be performed. Laparoscopy may also be performed for both diagnosis and treatment.

FOOTNOTES

Author contributions: Yao MQ and Jiang YP wrote the manuscript; Yang Y and Sun DZ collected the information and images; Yi BH and Fan JX reviewed the manuscript; all authors were involved in drafting the manuscript and revising it critically for important intellectual content, read and approved the final manuscript, and take public responsibility for appropriate portions of the content and have agreed to be accountable for all aspects of the work.

Supported by Clinical Research Fund Project of Zhejiang Medical Association, China, No. 2021ZYC-A173.

Informed consent statement: Informed consent was obtained from the patient for publication of this report.

Conflict-of-interest statement: All the authors report no relevant conflicts of interest for this article.

CARE Checklist (2016) statement: The authors have read the CARE Checklist (2016), and the manuscript was prepared and revised according to the CARE Checklist (2016).

Country/Territory of origin: China

ORCID number: Min-Quan Yao 0000-0001-8567-9021; Yu-Peng Jiang 0000-0001-9250-3606; Bing-Hong Yi 0000-0003-0498-7204; Yong Yang 0000-0002-7785-8182; Da-Zhuang Sun 0000-0001-7527-7379; Jin-Xing Fan 0000-0003-2003-7858.

S-Editor: Fan JR
L-Editor: Wang TQ
P-Editor: Fan JR

REFERENCES

1 **Brems H**, Beert E, de Ravel T, Legius E. Mechanisms in the pathogenesis of malignant tumours in neurofibromatosis type 1. *Lancet Oncol* 2009; **10**: 508-515 [PMID: 19410195 DOI: 10.1016/S1470-2045(09)70033-6]
2 **Neurofibromatosis**. Conference statement. National Institutes of Health Consensus Development Conference. *Arch Neurol* 1988; **45**: 575-578 [PMID: 3128965]
3 **Joensuu H**, Hohenberger P, Corless CL. Gastrointestinal stromal tumour. *Lancet* 2013; **382**: 973-983 [PMID: 23623056 DOI: 10.1016/S0140-6736(13)60106-3]
4 **Nishida T**, Tsujimoto M, Takahashi T, Hirota S, Blay JY, Wataya-Kaneda M. Gastrointestinal stromal tumors in Japanese patients with neurofibromatosis type I. *J Gastroenterol* 2016; **51**: 571-578 [PMID: 26511941 DOI: 10.1007/s00535-015-1132-6]
5 **Takazawa Y**, Sakurai S, Sakuma Y, Ikeda T, Yamaguchi J, Hashizume Y, Yokoyama S, Motegi A, Fukayama M. Gastrointestinal stromal tumors of neurofibromatosis type I (von Recklinghausen's disease). *Am J Surg Pathol* 2005; **29**: 755-763 [PMID: 15897742 DOI: 10.1097/01.pas.0000163359.32734.f9]
6 **Miettinen M**, Fetsch JF, Sobin LH, Lasota J. Gastrointestinal stromal tumors in patients with neurofibromatosis 1: a clinicopathologic and molecular genetic study of 45 cases. *Am J Surg Pathol* 2006; **30**: 90-96 [PMID: 16330947 DOI: 10.1097/01.pas.0000176433.81079.bd]
7 **Salvi PF**, Lorenzon L, Caterino S, Antolino L, Antonelli MS, Balducci G. Gastrointestinal stromal tumors associated with neurofibromatosis 1: a single centre experience and systematic review of the literature including 252 cases. *Int J Surg Oncol* 2013; **2013**: 398570 [PMID: 24386562 DOI: 10.1155/2013/398570]
8 **Ylä-Outinen H**, Loponen N, Kallionpää RA, Peltonen S, Peltonen J. Intestinal tumors in neurofibromatosis 1 with special reference to fatal gastrointestinal stromal tumors (GIST). *Mol Genet Genomic Med* 2019; **7**: e927 [PMID: 31397088 DOI: 10.1002/mgg3.927]
9 **Pan D**, Liang P, Xiao H. Neurofibromatosis type 1 associated with pheochromocytoma and gastrointestinal stromal tumors: A case report and literature review. *Oncol Lett* 2016; **12**: 637-643 [PMID: 27347193 DOI: 10.3892/ol.2016.4670]
10 **Mandalà S**, Lupo M, Guccione M, La Barbera C, Iadicola D, Mirabella A. Small bowel gastrointestinal stromal tumor presenting with gastrointestinal bleeding in patient with type 1 Neurofibromatosis: Management and laparoscopic treatment. Case report and review of the literature. *Int J Surg Case Rep* 2021; **79**: 84-90 [PMID: 33444965 DOI: 10.1016/j.ijscr.2020.12.095]
11 **von Mehren M**, Joensuu H. Gastrointestinal Stromal Tumors. *J Clin Oncol* 2018; **36**: 136-143 [PMID: 29220298 DOI: 10.1200/JCO.2017.74.9705]
12 **Tian H**, Wu XD, Ma Y, Jin SZ, Song SW. [Multiple gastrointestinal stromal tumors of the small intestine with gastrointestinal bleeding: a case report]. *Zhonghua Putongwaike Zazhi* 2019; **34**: 639 [DOI: 10.3760/cma.j.issn.1007-631X.2019.07.029]
13 **Kim JJ**, Lim JY, Nguyen SQ. Laparoscopic resection of gastrointestinal stromal tumors: Does laparoscopic surgery provide an adequate oncologic resection? *World J Gastrointest Endosc* 2017; **9**: 448-455 [PMID: 28979709 DOI:

10.4253/wjge.v9.i9.448]
14 **Xu MM**, Angeles A, Kahaleh M. Endoscopic full-thickness resection of gastric stromal tumor: one and done. *Endoscopy* 2018; **50**: E42-E43 [PMID: 29136673 DOI: 10.1055/s-0043-121566]

World Journal of Clinical Cases

Submit a Manuscript: https://www.f6publishing.com

World J Clin Cases 2023 April 6; 11(10): 2343-2348

DOI: 10.12998/wjcc.v11.i10.2343

ISSN 2307-8960 (online)

CASE REPORT

Coexisting cytomegalovirus colitis in an immunocompetent patient with *Clostridioides difficile* colitis: A case report

Jun Hyoung Kim, Hee-Sung Kim, Hye Won Jeong

Specialty type: Medicine, research and experimental

Provenance and peer review: Unsolicited article; Externally peer reviewed.

Peer-review model: Single blind

Peer-review report's scientific quality classification

Grade A (Excellent): 0
Grade B (Very good): 0
Grade C (Good): C, C, C
Grade D (Fair): 0
Grade E (Poor): 0

P-Reviewer: Faraji N, Iran; Gao C, China

Received: December 21, 2022
Peer-review started: December 21, 2022
First decision: January 5, 2023
Revised: January 12, 2023
Accepted: March 6, 2023
Article in press: March 6, 2023
Published online: April 6, 2023

Jun Hyoung Kim, Hee-Sung Kim, Hye Won Jeong, Department of Internal Medicine, Chungbuk National University Hospital, Cheongju 28644, Chungbuk, South Korea

Hee-Sung Kim, Hye Won Jeong, Department of Internal Medicine, Chungbuk National University College of Medicine, Cheongju 28644, Chungbuk, South Korea

Corresponding author: Hye Won Jeong, MD, PhD, Professor, Department of Internal Medicine, Chungbuk National University College of Medicine, No. 1 Chungdae-ro, Seowon-gu, Cheongju 28644, Chungbuk, South Korea. hwjeong@chungbuk.ac.kr

Abstract

BACKGROUND

Clostridioides difficile (*C. difficile*) colitis is one of the most common infections in hospitalized patients, characterized by fever and diarrhea. It usually improves after appropriate antibiotic treatment; if not, comorbidities should be considered. Cytomegalovirus (CMV) colitis is a possible co-existing diagnosis in patients with *C. difficile* infection with poor treatment response. However, compared with immunocompromised patients, CMV colitis in immunocompetent patients is not well studied.

CASE SUMMARY

We present an unusual case of co-existing CMV colitis in an immunocompetent patient with *C. difficile* infection. An 80-year-old female patient was referred to the infectious disease department due to diarrhea, abdominal discomfort, and fever for 1 wk during her hospitalization for surgery. *C. difficile* toxin B polymerase chain reaction on stool samples was positive. After *C. difficile* infection was diagnosed, oral vancomycin treatment was administered. Her symptoms including diarrhea, fever and abdominal discomfort improved for ten days. Unfortunately, the symptoms worsened again with bloody diarrhea and fever. Therefore, a sigmoidoscopy was performed for evaluation, showing a longitudinal ulcer on the sigmoid colon. Endoscopic biopsy confirmed CMV colitis, and the clinical symptoms improved after using ganciclovir.

CONCLUSION

Co-existing CMV colitis should be considered in patients with aggravated *C. difficile* infection on appropriate treatment, even in immunocompetent hosts.

Key Words: Cytomegalovirus; *Clostridioides difficile*; Coinfection; Colitis;

Immunocompetent; Case report

Core Tip: Cytomegalovirus (CMV) colitis is rare in immunocompetent patients, but colitis is the main clinical manifestation. The *Clostridioides difficile* (*C. difficile*) infection and CMV colitis symptoms might be indistinguishable clinically. Therefore, it is difficult to consider their co-existence in patients suspected of *C. difficile* infection. If a patient treated with *C. difficile* infection does not show clinical improvement, the possibility of co-existing CMV colitis should be considered as one of the differential diagnoses. Sigmoidoscopy with biopsy is crucial in diagnosing co-existing CMV and *C. difficile* infection colitis.

Citation: Kim JH, Kim HS, Jeong HW. Coexisting cytomegalovirus colitis in an immunocompetent patient with *Clostridioides difficile* colitis: A case report. *World J Clin Cases* 2023; 11(10): 2343-2348
URL: https://www.wjgnet.com/2307-8960/full/v11/i10/2343.htm
DOI: https://dx.doi.org/10.12998/wjcc.v11.i10.2343

INTRODUCTION

Cytomegalovirus (CMV) is a member of the herpesvirus family and forms latent infection after the resolution of the primary infection[1]. CMV primary infection can cause mononucleosis-like symptoms in immunocompetent adults[1]. After the primary CMV infection, CMV remains in host cells and CMV replication is controlled by the immune system in immunocompetent patients[1]. Immunodeficiency is the leading risk factor for invasive CMV diseases[2]. Invasive CMV diseases can occur in immunocompromised patients, including transplant recipients or patients with HIV, by primary infection or reactivation and could have significant morbidity and mortality[3]. This mostly affects the gastrointestinal tract, comprising 30% of tissue-invasive CMV diseases in immunocompromised patients [4]. Clinical manifestation of CMV colitis in immunocompromised patients varies and depends on the site of involvement which could cause odynophagia, abdominal pain, hematochezia, and fever[4].

CMV colitis in immunocompetent patients was previously considered very rare. However, there has been an increasing number of case reports in immunocompetent patients[5,6]. The symptoms of CMV colitis in immunocompetent patients also present odynophagia, abdominal pain, hematochezia, and fever[5,6]. However, its epidemiology, clinical features, and outcomes in immunocompetent patients are not completely understood[4-8].

Clostridioides difficile (*C. difficile*) colitis is a cause of diarrhea in hospitalized patients and is one of the most common causes of nosocomial infections[9]. *C. difficile* infection is usually suspected when hospitalized patients develop diarrhea and fever[9]. CMV colitis symptoms are clinically indistinguishable from those of *C. difficile* infection. Therefore, if the immunocompromised status of patients who develop *C. difficile* infection does not improve even with appropriate treatment, accompanying CMV colitis should be considered. However, this may not be considered in immunocompromised patients because cases of co-existing *C. difficile* infection and CMV colitis are rare in immunocompetent patients. We report an unusual case of CMV colitis in an immunocompetent *C. difficile* infection patient with literature review.

CASE PRESENTATION

Chief complaints

An 80-year-old female patient was referred for an infectious disease (ID) consult due to diarrhea, abdominal discomfort, and fever for 1 wk during her rehabilitation treatment after spinal stenosis surgery.

History of present illness

She underwent spinal stenosis surgery three weeks ago for back pain. She took methylprednisolone 250 mg per day for a week from the time of surgery due to paralysis of the lower extremities associated with spinal stenosis. She was treated with piperacillin/tazobactam for 7 d and cefixime for 4 d for a urinary tract infection before ID consultation. She had diarrhea, abdominal discomfort, and fever for 1 wk. *C. difficile* toxin A, B polymerase chain reaction (PCR) tests were performed on stool samples. *C. difficile* toxin B PCR was positive. Computed tomography (CT) of the abdomen/pelvis showed diffuse wall thickening in the rectum with mild perirectal infiltration in the upstream colon. The patient was treated

with oral vancomycin 250 mg every 6 h for 10 d, after which fever and diarrhea improved for ten days. However, the symptoms worsened again with bloody diarrhea and fever.

History of past illness

She had a medical history of hypertension and diabetes.

Personal and family history

The patient had no family history.

Physical examination

Vital signs were a temperature of 37.8 °C, blood pressure of 110/60 mmHg, pulse rate of 84 beats/min, respiratory rate of 18 breaths/min on the consultation day. The patient's Glasgow Coma Scale score was 15. She had hyperactive bowel sounds, no tenderness or rebound tenderness, no abdominal distension.

Laboratory examinations

On the consultation day, laboratory evaluation revealed anemia (Hb = 9.5 g/dL), an increased level of C-reactive protein (7.3 mg/dL), and an increased erythrocyte sedimentation rate (61 mm/h) with a normal white blood cell counts of 9730 cell/mm^3 (neutrophils = 80%, lymphocyte = 15%). Stool culture for *Salmonella* spp., *Shigella* spp., *Campylobacter* spp., and *Escherichia coli* O-157:H7 was negative. In routine stool examination, there is no helminth or protozoa, and stool white blood cell counts are 1-5 cell/high power field.

Imaging examinations

Flexible sigmoidoscopy showed a longitudinal ulcer from the anal verge (AV) to 12 cm above the AV (Figure 1). The biopsy was performed on the ulcer site. Cells with basophilic intranuclear inclusion body surrounded by a clear halo on hematoxylin and eosin stain and positive immunohistochemistry for CMV (Figure 2).

FINAL DIAGNOSIS

Co-existing CMV colitis with *C. difficile* colitis.

TREATMENT

Antiviral treatment with intravenous ganciclovir (10 mg/kg/day) was initiated. Fever and bloody diarrhea improved after 5 d of using ganciclovir, and the treatment was continued for 3 wk.

OUTCOME AND FOLLOW-UP

A sigmoidoscopy performed after the treatment showed an improvement in the ulcer lesion, and a biopsy performed 1 mo after the treatment showed negative findings. The patient was discharged to a nursing home after successful treatment with improved symptoms.

DISCUSSION

Although CMV infection in immunocompetent hosts has been considered rare, one review article retrieved 89 articles reporting on severe CMV infection in immunocompetent adults from 1950 to 2007 [10]. They were mainly gastrointestinal and central nervous system diseases. Symptoms of CMV infection in immunocompetent patients are not well documented; however, severe life-threatening CMV infections in immunocompetent hosts might not be such a rare condition as was previously thought [10]. Currently, a rapidly rising number of literature cases worldwide indicate that CMV infections can also be observed in immunocompetent patients with altered immune status such as steroid use[8,11]. A total of 51 immunocompetent patients were diagnosed with CMV colitis between January 1995 and February 2014 at a tertiary care university hospital in South Korea, with 36 cases diagnosed after 2008, suggesting the growing number of immunocompetent CMV patients[8]. Similarly, 42 immunocompetent patients were diagnosed between April 2002 and December 2016 at a hospital in Taiwan[11]. Ko *et al*[8] reported that risk factors of CMV colitis in immunocompetent patients were steroid use and RBC transfusion within 1 mo. Our patient also received steroid treatment, and this could be the risk factor of CMV colitis. Wetwittayakhlang *et al*[5] compared clinical features and endoscopic findings of

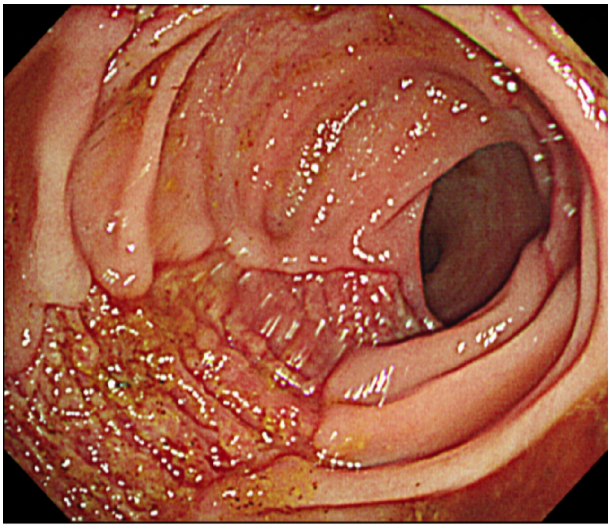

DOI: 10.12998/wjcc.v11.i10.2343 **Copyright** ©The Author(s) 2023.

Figure 1 Sigmoidoscopy image. Sigmoidoscopy image shows presenting a longitudinal ulcer from the anal verge (AV) to 12 cm above the AV.

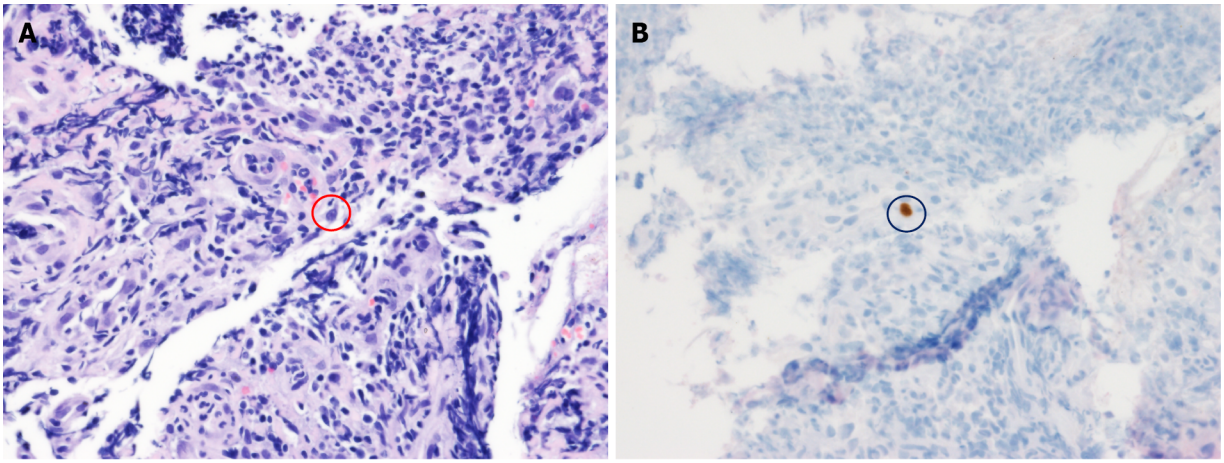

DOI: 10.12998/wjcc.v11.i10.2343 **Copyright** ©The Author(s) 2023.

Figure 2 Pathology findings. A: Red circle shows a cell with a basophilic intranuclear inclusion body surrounded by a clear halo (hematoxylin and eosin stain, 400 ×); B: Black circle shows positive immunohistochemistry for cytomegalovirus (immunohistochemical stain, 400 ×).

gastrointestinal CMV diseases between immunocompetent and immunocompromised patients and found that immunocompetent patients were older and had more GI bleeding and shorter symptom period than immunocompromised patients[5]. Small bowel involvement was more frequent in the immunocompetent group[5]. Chaemsupaphan *et al*[6] also reported that most immunocompetent patients presented with gastrointestinal bleeding compared to immunocompromised patients[6]. In another study by Yoon *et al*[7], CMV gastroenterocolitis of immunocompetent patients occurred in older patients with comorbidities and had various endoscopic features such as discrete ulcer type and diffuse edematous type with no association with clinical outcomes[7].

C. difficile infection is a common cause of colitis in hospitalized patients. Although there are variations according to region and year by year, *C. difficile* infection occurs in approximately 10 cases per 1000 hospitalization days[12]. Clinical manifestations of *C. difficile* infection vary from mild diarrhea to life-threatening conditions such as toxic megacolon and bowel perforation[12]. Patients with mild *C. difficile* infection often recovered 5 to 10 d after stopping antibiotics[13]. However, fulminant *C. difficile* infection could occur in approximately 1% to 3% of patients[13]. Generally, patients with *C. difficile* infection are known to recover after 10-14 d of treatment[13,14]. Currently, the diagnosis of *C. difficile* infection is based on detection of *C. difficile* toxins and glutamate dehydrogenase with enzyme immunoassay or nucleic acid amplification test[13]. Endoscopy is not recommended in patients with typical *C. difficile* infection confirmed by laboratory tests and clinical features[13]. However, endoscopic evaluation is recommended if diagnostic problems occur such as clinically suspected *C. difficile* infection with negative laboratory test, if there was no response to treatment, or when an alternative diagnosis is

suspected[13]. Our patient underwent endoscopy because of worsening symptoms gained after the *C. difficile* infection treatment for 10 d. As *C. difficile* infection and CMV colitis have similar symptoms, it is difficult to differentiate them simply based on the symptoms. However, severe watery diarrhea is more characteristic of *C. difficile* infection and bloody diarrhea or sometimes massive bleeding in CMV colitis [15]. In our case, the patient developed worsening bloody diarrhea with fever; we performed endoscopy and the biopsy confirmed CMV colitis.

CONCLUSION

Clinicians should be aware of the possibility of co-existing CMV colitis in patients with *C. difficile* infection, even in those with immunocompetent status, especially if patients do not respond to the *C. difficile* infection treatment. Early endoscopy could help diagnose the possible co-existing CMV colitis in patients with refractory *C. difficile* infection.

FOOTNOTES

Author contributions: Kim JH contributed to manuscript writing and editing; Kim HS and Jeong HW supervised the study; Jeong HW conceived the study; all authors have read and approved the final manuscript.

Informed consent statement: Informed written consent was obtained from the patient and her family for publication of this report and any accompanying images.

Conflict-of-interest statement: All the authors report no relevant conflicts of interest for this article.

CARE Checklist (2016) statement: The authors have read the CARE Checklist (2016), and the manuscript was prepared and revised according to the CARE Checklist (2016).

Country/Territory of origin: South Korea

ORCID number: Jun Hyoung Kim 0000-0002-0595-2110; Hee-Sung Kim 0000-0001-7559-4438; Hye Won Jeong 0000-0002-1063-8476.

S-Editor: Fan JR
L-Editor: A
P-Editor: Fan JR

REFERENCES

1 **Picarda G**, Benedict CA. Cytomegalovirus: Shape-Shifting the Immune System. *J Immunol* 2018; **200**: 3881-3889 [PMID: 29866770 DOI: 10.4049/jimmunol.1800171]
2 **Yerushalmy-Feler A**, Padlipsky J, Cohen S. Diagnosis and Management of CMV Colitis. *Curr Infect Dis Rep* 2019; **21**: 5 [PMID: 30771028 DOI: 10.1007/s11908-019-0664-y]
3 **Griffiths P**, Reeves M. Pathogenesis of human cytomegalovirus in the immunocompromised host. *Nat Rev Microbiol* 2021; **19**: 759-773 [PMID: 34168328 DOI: 10.1038/s41579-021-00582-z]
4 **Fakhreddine AY**, Frenette CT, Konijeti GG. A Practical Review of Cytomegalovirus in Gastroenterology and Hepatology. *Gastroenterol Res Pract* 2019; **2019**: 6156581 [PMID: 30984257 DOI: 10.1155/2019/6156581]
5 **Wetwittayakhlang P**, Rujeerapaiboon N, Wetwittayakhlung P, Sripongpun P, Pruphetkaew N, Jandee S, Chamroonkul N, Piratvisuth T. Clinical Features, Endoscopic Findings, and Predictive Factors for Mortality in Tissue-Invasive Gastrointestinal Cytomegalovirus Disease between Immunocompetent and Immunocompromised Patients. *Gastroenterol Res Pract* 2021; **2021**: 8886525 [PMID: 33897776 DOI: 10.1155/2021/8886525]
6 **Chaemsupaphan T**, Limsrivilai J, Thongdee C, Sudcharoen A, Pongpaibul A, Pausawasdi N, Charatcharoenwitthaya P. Patient characteristics, clinical manifestations, prognosis, and factors associated with gastrointestinal cytomegalovirus infection in immunocompetent patients. *BMC Gastroenterol* 2020; **20**: 22 [PMID: 32000707 DOI: 10.1186/s12876-020-1174-y]
7 **Yoon J**, Lee J, Kim DS, Lee JW, Hong SW, Hwang HW, Hwang SW, Park SH, Yang DH, Ye BD, Myung SJ, Jung HY, Yang SK, Byeon JS. Endoscopic features and clinical outcomes of cytomegalovirus gastroenterocolitis in

immunocompetent patients. *Sci Rep* 2021; **11**: 6284 [PMID: 33737711 DOI: 10.1038/s41598-021-85845-8]

8 **Ko JH**, Peck KR, Lee WJ, Lee JY, Cho SY, Ha YE, Kang CI, Chung DR, Kim YH, Lee NY, Kim KM, Song JH. Clinical presentation and risk factors for cytomegalovirus colitis in immunocompetent adult patients. *Clin Infect Dis* 2015; **60**: e20-e26 [PMID: 25452594 DOI: 10.1093/cid/ciu969]

9 **Balsells E**, Shi T, Leese C, Lyell I, Burrows J, Wiuff C, Campbell H, Kyaw MH, Nair H. Global burden of Clostridium difficile infections: a systematic review and meta-analysis. *J Glob Health* 2019; **9**: 010407 [PMID: 30603078 DOI: 10.7189/jogh.09.010407]

10 **Rafailidis PI**, Mourtzoukou EG, Varbobitis IC, Falagas ME. Severe cytomegalovirus infection in apparently immunocompetent patients: a systematic review. *Virol J* 2008; **5**: 47 [PMID: 18371229 DOI: 10.1186/1743-422X-5-47]

11 **Chan KS**, Yang CC, Chen CM, Yang HH, Lee CC, Chuang YC, Yu WL. Cytomegalovirus colitis in intensive care unit patients: difficulties in clinical diagnosis. *J Crit Care* 2014; **29**: 474.e1-474.e6 [PMID: 24556151 DOI: 10.1016/j.jcrc.2014.01.003]

12 **Turner NA**, Grambow SC, Woods CW, Fowler VG Jr, Moehring RW, Anderson DJ, Lewis SS. Epidemiologic Trends in Clostridioides difficile Infections in a Regional Community Hospital Network. *JAMA Netw Open* 2019; **2**: e1914149 [PMID: 31664443 DOI: 10.1001/jamanetworkopen.2019.14149]

13 **Czepiel J**, Dróżdż M, Pituch H, Kuijper EJ, Perucki W, Mielimonka A, Goldman S, Wultańska D, Garlicki A, Biesiada G. Clostridium difficile infection: review. *Eur J Clin Microbiol Infect Dis* 2019; **38**: 1211-1221 [PMID: 30945014 DOI: 10.1007/s10096-019-03539-6]

14 **Guery B**, Galperine T, Barbut F. Clostridioides difficile: diagnosis and treatments. *BMJ* 2019; **366**: l4609 [PMID: 31431428 DOI: 10.1136/bmj.l4609]

15 **Chan KS**, Lee WY, Yu WL. Coexisting cytomegalovirus infection in immunocompetent patients with Clostridium difficile colitis. *J Microbiol Immunol Infect* 2016; **49**: 829-836 [PMID: 26850320 DOI: 10.1016/j.jmii.2015.12.007]

World Journal of Clinical Cases

Submit a Manuscript: https://www.f6publishing.com

World J Clin Cases 2023 April 6; 11(10): 2349-2354

DOI: 10.12998/wjcc.v11.i10.2349

ISSN 2307-8960 (online)

CASE REPORT

Paradoxical vocal fold motion masquerading as post-anesthetic respiratory distress: A case report

Jongyoon Baek, Dae-Lim Jee, Yoon Seok Choi, Sang Woo Kim, Eun Kyung Choi

Specialty type: Anesthesiology

Provenance and peer review: Unsolicited article; Externally peer reviewed.

Peer-review model: Single blind

Peer-review report's scientific quality classification
Grade A (Excellent): 0
Grade B (Very good): B
Grade C (Good): C
Grade D (Fair): 0
Grade E (Poor): 0

P-Reviewer: Roy S, United States; Zhang YN, China

Received: December 22, 2022
Peer-review started: December 22, 2022
First decision: January 9, 2023
Revised: January 18, 2023
Accepted: March 15, 2023
Article in press: March 15, 2023
Published online: April 6, 2023

Jongyoon Baek, Dae-Lim Jee, Eun Kyung Choi, Department of Anesthesiology and Pain Medicine, Yeungnam University College of Medicine, Daegu 42415, South Korea

Yoon Seok Choi, Department of Otorhinolaryngology-Head and Neck Surgery, Yeungnam University College of Medicine, Daegu 42415, South Korea

Sang Woo Kim, Department of Neurosurgery, Yeungnam University College of Medicine, Daegu 42415, South Korea

Corresponding author: Eun Kyung Choi, MD, PhD, Assistant Professor, Department of Anesthesiology and Pain Medicine, Yeungnam University College of Medicine, 170, Hyeonchung-ro, Nam-gu, Daegu 42415, South Korea. zzini0527@naver.com

Abstract

BACKGROUND

Functional vocal cord disorders can be a differential diagnosis for postoperative upper airway obstruction requiring urgent intervention. However, this may be unfamiliar to anesthesiologists who would favor inappropriate airway intervention and increased morbidity.

CASE SUMMARY

A 61-year-old woman underwent cervical laminectomy, followed by laparoscopic cholecystectomy 10 mo later. Despite adequate reversal of neuromuscular blockade, the patient experienced repetitive respiratory difficulty with inspiratory stridor after extubation. After the second operation, the patient was diagnosed with paradoxical vocal fold motion (PVFM) by an otolaryngologist based on the clinical features and fiberoptic bronchoscopy results, and the patient was successfully treated.

CONCLUSION

PVFM should be considered a differential diagnosis if a patient presents with stridor after general anesthesia.

Key Words: Anesthesiology; Vocal fold; Paradoxical motion; Postoperative respiratory distress; Case report

Core Tip: Postoperative upper airway obstruction after general anesthesia requires urgent airway intervention. Postoperative stridor is a common cause of laryngeal spasm, but functional vocal cord disorders may also be a cause. However, anesthesiologists may be unfamiliar with functional vocal cord disorders, and this may lead to inappropriate interventions. We present the case of a patient with post-extubation repetitive stridor who was postoperatively diagnosed with paradoxical vocal fold motion (PVFM) by an otolaryngologist and discuss the diagnosis and treatment of PVFM. Our case presentation showed that PVFM should be considered in the differential diagnosis of postoperative stridor.

Citation: Baek J, Jee DL, Choi YS, Kim SW, Choi EK. Paradoxical vocal fold motion masquerading as post-anesthetic respiratory distress: A case report. *World J Clin Cases* 2023; 11(10): 2349-2354
URL: https://www.wjgnet.com/2307-8960/full/v11/i10/2349.htm
DOI: https://dx.doi.org/10.12998/wjcc.v11.i10.2349

INTRODUCTION

Postoperative upper airway obstruction after general anesthesia is a significant problem that can cause severe complications that require urgent airway intervention. In addition to common causes, such as laryngeal spasm induced by residual muscle relaxants, a functional vocal cord disorder can also be a differential diagnosis of postoperative stridor[1,2]. However, as this cause may be unfamiliar to those in anesthesiology, it could lead to inappropriate airway interventions and increased morbidity.

Here, we present the case of a patient with repetitive stridor after extubation who was postoperatively diagnosed with paradoxical vocal fold motion (PVFM) by an otolaryngologist.

CASE PRESENTATION

Chief complaints

A 61-year-old woman (weight, 70 kg; height, 155 cm; body mass index, 29.14) developed respiratory difficulties with inspiratory stridor after extubation for each of her surgeries.

History of present illness

First surgery: The patient underwent a cervical laminectomy to resect an extradural tumor at the C2 to C3 vertebral level. No premedication was administered, and standard anesthetic monitoring, including electrocardiogram, non-invasive blood pressure, and pulse oximetry, was conducted after arriving at the operating room. Anesthesia was induced with propofol and rocuronium, and a 7.5 mm armored endotracheal tube was used, without difficulty, during intubation. The Cormack-Lehane grade observed on laryngoscopy during intubation was grade 1. Anesthesia was maintained with desflurane and 50% oxygen for 3 h and 30 min. There were no notable intraoperative events. Pyridostigmine and glycopyrrolate were injected to reverse the neuromuscular blockade, and the patient was extubated without difficulty. Spontaneous breathing was maintained immediately after extubation, and no abnormal respiratory signs were observed. However, 5 min after arriving at the post-anesthesia care unit (PACU), breathing difficulties and tachypnea were observed. The patient developed respiratory difficulty with inspiratory stridor.

Second surgery: Ten months after the first surgery, the patient was scheduled to undergo laparoscopic cholecystectomy for gallstones and polyps. Preoperative evaluations conducted by an otolaryngologist revealed normal structure and movement of the vocal cords. Intravenous propofol and rocuronium were administered to induce anesthesia. Before intubation with the endotracheal tube, intravenous lidocaine was administered to attenuate airway reflexes and hemodynamic fluctuations. As a vocal cord disorder developed after the previous operation, a 6.5 mm cuffed endotracheal tube was used with special caution, and dexamethasone 5 mg was administered 30 min before extubation. Anesthesia was maintained with desflurane, 50% oxygen, and an infusion of 0.5-1.5 μg/kg/min of remifentanil for 50 min. There were no special intraoperative events. After clinical confirmation of adequate neuromuscular blockade reversal using train-of-four (TOF), the endotracheal tube was removed. Shortly after extubation, the patient developed respiratory difficulty, and stridor was heard again. An O_2 mask was applied with 100% oxygen, and breathing was assisted with a bag-valve mask. Despite these efforts, the respiratory distress and inspiratory stridor did not improve.

History of past illness

There were no abnormal findings in the preoperative evaluation, including physical examination,

laboratory tests, electrocardiogram, and chest X-ray. The patient had an average-sized neck, and the preoperative Mallampati score was grade 1.

Personal and family history

Three years before the present admission, the patient was diagnosed with thyroid cancer and had undergone total thyroidectomy. No perioperative complications related to anesthesia were observed at that time. The patient's medical history was unremarkable. The patient did not smoke or drink alcohol and had no history of allergies.

Physical examination

First surgery: Immediately after extubation, the patient's oxygen saturation (SpO_2) in the operating room was 99%. After arriving at the PACU, 100% oxygen was administered at 2 L/min *via* a nasal cannula; SpO_2 was 99%. Complete clinical reversal was confirmed by observing a TOF (peripheral nerve stimulator) after the development of inspiratory stridor.

Second surgery: Adequate reversal of neuromuscular blockade was clinically confirmed by TOF immediately before extubation. Oxygen saturation was maintained above 98% by providing 100% oxygen immediately after the stridor started.

Laboratory examinations

The preoperative laboratory test results were within normal limits. However, mild hyperventilation (pH, 7.48; $PaCO_2$, 31.6 mmHg; PaO_2, 106 mmHg) was observed in arterial blood gas analysis when reintubation was performed due to postoperative stridor.

Imaging examinations

After the second surgery, an otolaryngologist performed a nasal fiberoptic bronchoscopy to resolve these repetitive episodes. No laryngeal trauma, edema, or vocal cord paralysis was observed. However, the vocal cords moved paradoxically during inspiration (Figure 1).

FINAL DIAGNOSIS

The patient was finally diagnosed with PVFM by the otolaryngologist.

TREATMENT

First surgery

Although complete clinical reversal was confirmed, reversal agents for neuromuscular blockade were additionally administered for suspected laryngeal spasm. Intravenous lidocaine, dexamethasone, and intraoral salbutamol spray were administered to relieve respiratory distress, and the patient's head was elevated. Her vital signs, including SpO_2 remained stable, but the inspiratory stridor lasted for approximately 10 min. No other lung parenchymal sounds were noted on auscultation except for stridor. The decision to perform re-intubation was made, and intravenous propofol was given. After intubation, the patient's breathing patterns improved, and arterial blood sampling showed mild hyperventilation (pH, 7.48; $PaCO_2$, 31.6 mmHg; PaO_2, 106 mmHg). The SpO_2 remained at > 98% without oxygen support. After discussion with the neurosurgery department, the patient was transferred to the intensive care unit for close observation. The otolaryngologist suspected that her symptoms were due to underlying asymptomatic vocal cord paralysis after total thyroidectomy, which was not recognized before the operation, or vocal cord irritation caused by intubation. A few hours later, the patient was extubated under close observation. She developed mild hoarseness; however, her breath sounds were normal, and her SpO_2 was 99% with no stridor. The patient was discharged without further evaluation based on her wishes.

Second surgery

After fiberoptic bronchoscopy, 2 mg of midazolam was administered with reassurance for suspected PVFM. The stridor intensity was reduced, and the patient was moved to the PACU. The patient did not develop respiratory distress, and her oxygen saturation was maintained at 98%-100% on 2 L/min of oxygen *via* a nasal cannula.

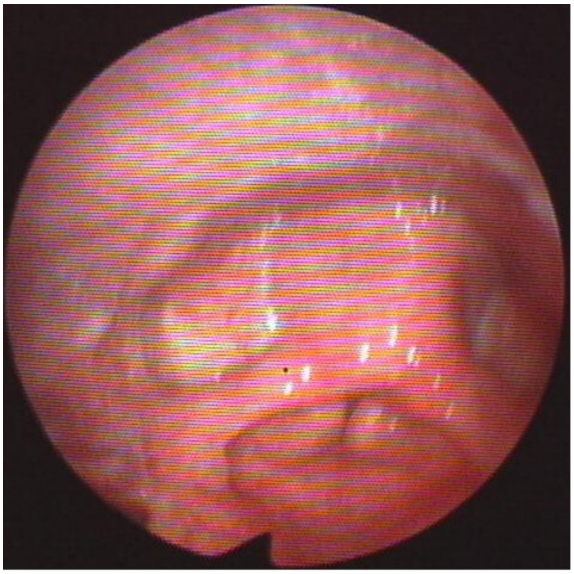

DOI: 10.12998/wjcc.v11.i10.2349

Figure 1 Nasal fiberoptic bronchoscopy image of paradoxical vocal cord motion during inspiration.

OUTCOME AND FOLLOW-UP

The patient was discharged three days after the second surgery without complications. One month later, the patient revisited the otorhinolaryngology department because of laryngeal symptoms, including chronic cough, the sensation of a lump in her throat, and repeated throat clearing. Furthermore, the patient experienced three episodes of dyspnea with stridor lasting for several minutes, similar to the events that occurred after the two surgeries while sleeping or eating. The otolaryngologist suspected PVFM clinically and prescribed a proton pump inhibitor and laryngeal control therapy. After two months of treatment, all symptoms improved, and the patient was finally diagnosed with PVFM by the otolaryngologist.

DISCUSSION

After the first surgery, the patient did not receive a timely and proper diagnosis and treatment. Because the patient had no previous respiratory or psychiatric history, and there was no increased awareness of the functional causes of upper airway obstruction, PVFM was not recognized as a cause of sustained stridor and dyspnea. Consequently, the patient was reintubated in the PACU without additional fiberoptic bronchoscopic examinations to diagnose this disorder.

Postoperative upper airway obstruction presenting with inspiratory stridor is a common phenomenon in anesthesiology. Depressed laryngeal muscle activity due to residual effects of anesthetics and muscle relaxants, laryngeal edema caused by the prolonged placement of the endotracheal tube, and laryngeal stimulation by secretions such as blood and mucus can precipitate laryngospasm in partially awake or, rarely, fully awake patients[3]. In addition to the aforementioned causes, vocal cord paralysis and laryngomalacia can be considered identifiable organic etiologies of postoperative upper airway obstruction[3]. Although some cases of post-extubation stridor do not require urgent intervention, others can result in disastrous clinical symptoms requiring resuscitation, which increases patient morbidity and mortality. Therefore, accurate diagnosis and adequate treatment are necessary.

Stridor management should be directed toward the underlying cause. Stridor is usually inspiratory and is a sign of upper airway obstruction. However, not all stridor has organic cause. Typically, PVFM is a functional stridor. This condition shows paradoxical adduction of vocal cords during inspiration and occasionally during early expiration[4]. Other names for PVFM include functional inspiratory stridor, factitious asthma, and emotional laryngismus[5]. Owing to clinical presentations that mimic serious upper airway obstruction, PVFM is often misdiagnosed as several pathological states, including croup, subglottic stenosis, traumatic airway edema, laryngomalacia, and asthma[3], leading to inappropriate treatment, extensive investigation, and considerable delay in making a proper diagnosis. According to one case series, 28% of 95 patients with PVFM were intubated, and some underwent tracheostomy[6]. In this case, the patient presented with sustained respiratory difficulties with inspiratory stridor, although oxygen saturation remained within the normal range. After excluding the residual effects of muscle relaxants and anesthetics, the patient was initially treated conservatively

without improvement. After the first surgery, we had not yet considered PVFM as a differential diagnosis related to postoperative airway obstruction, and the patient was eventually reintubated to resolve severe respiratory distress. If there was an awareness of functional vocal cord disorders, fiberoptic bronchoscopy could have been performed to determine the cause of inspiratory stridor, and other treatment options such as sedation and reassurance would have been performed instead of reintubation.

PVFM can occur at any age but is more common in adult females[7]. A history of recent respiratory tract infection and stress-related psychiatric disorder is often present in PVFM. Moreover, upper airway obstruction features such as dysphonia, accessory muscle use, and stridor can be present, often resulting in a misdiagnosis of asthma[8]. The most important consideration for anesthesiologists is that PVFM can occur after general anesthesia. PVFM is a rare condition in anesthesiology and has only partly been reported in the respiratory and otorhinolaryngology fields. Therefore, clinicians should suspect PVFM in patients presenting with postoperative stridor. In other words, the differential diagnosis of postoperative stridor should include PVFM, laryngeal spasm, laryngeal edema, and vocal cord paralysis. Some case reports have discussed functional stridor after anesthesia[9,10]. A confirmative diagnosis of PVFM can be obtained by fiberoptic laryngoscopy, which reveals abnormal adduction of the vocal cords on inspiration and normal vocal cord motion during expiration[11]. However, organic disorders related to upper airway obstruction should be excluded first. Once diagnosed, short-term sedation and reassurance may help control symptoms in the acute phase, and definitive treatment includes psychotherapy, speech therapy, and patient education.

CONCLUSION

PVFM should be considered a differential diagnosis if a patient presents with an episode of upper airway obstruction after general endotracheal anesthesia without organic airway disorders. An increased awareness of functional vocal cord disorders will help make timely diagnoses and avoid potentially harmful treatments.

FOOTNOTES

Author contributions: Baek J and Choi EK contributed to the investigation, original draft writing, and manuscript reviewing and editing; Jee DL contributed to supervision and manuscript reviewing and editing; Choi YS and Kim SW contributed to manuscript reviewing and editing; all authors have read and approved the final manuscript.

Informed consent statement: Informed written consent was obtained from the patient for publication of this report.

Conflict-of-interest statement: The authors declare that they have no conflict of interest to disclose.

CARE Checklist (2016) statement: The authors have read the CARE Checklist (2016), and the manuscript was prepared and revised according to the CARE Checklist (2016).

Country/Territory of origin: South Korea

ORCID number: Jongyoon Baek 0000-0003-4007-770X; Dae-Lim Jee 0000-0003-1102-5214; Yoon Seok Choi 0000-0002-0616-7122; Sang Woo Kim 0000-0002-1439-7964; Eun Kyung Choi 0000-0001-5758-6741.

S-Editor: Yan JP
L-Editor: A
P-Editor: Yan JP

REFERENCES

1 **Larsen B**, Caruso LJ, Villariet DB. Paradoxical vocal cord motion: an often misdiagnosed cause of postoperative stridor. *J Clin Anesth* 2004; **16**: 230-234 [PMID: 15217668 DOI: 10.1016/j.jclinane.2003.08.010]
2 **Kenn K**, Balkissoon R. Vocal cord dysfunction: what do we know? *Eur Respir J* 2011; **37**: 194-200 [PMID: 21205712 DOI: 10.1183/09031936.00192809]

3 **Dunn NM**, Katial RK, Hoyte FCL. Vocal cord dysfunction: a review. *Asthma Res Pract* 2015; **1**: 9 [PMID: 27965763 DOI: 10.1186/s40733-015-0009-z]

4 **Hoyte FC**. Vocal cord dysfunction. *Immunol Allergy Clin North Am* 2013; **33**: 1-22 [PMID: 23337061 DOI: 10.1016/j.iac.2012.10.010]

5 **Imam AP**, Halpern GM. Pseudoasthma in a case of asthma. *Allergol Immunopathol (Madr)* 1995; **23**: 96-100 [PMID: 8526175]

6 **Newman KB**, Mason UG 3rd, Schmaling KB. Clinical features of vocal cord dysfunction. *Am J Respir Crit Care Med* 1995; **152**: 1382-1386 [PMID: 7551399 DOI: 10.1164/ajrccm.152.4.7551399]

7 B**rugman S**. The many faces of vocal cord dysfunction: what 36 years of literature tell us. *Am J Respir Crit Care Med* 2003; **167**: A588 [DOI: 10.1055/s-2007-1006358]

8 **Falco DA**, Hammer GB, Conrad C, Messner AH. Paradoxical vocal cord motion in a child presenting with cyanosis and respiratory failure. *Pediatr Crit Care Med* 2002; **3**: 185-186 [PMID: 12780992 DOI: 10.1097/00130478-200204000-00018]

9 **Kleiman S**, Tousignant G. Paradoxical vocal cord motion. *Can J Anaesth* 1997; **44**: 785-786 [PMID: 9232315 DOI: 10.1007/BF03013399]

10 **Harbison J**, Dodd J, McNicholas WT. Paradoxical vocal cord motion causing stridor after thyroidectomy. *Thorax* 2000; **55**: 533-534 [PMID: 10817803 DOI: 10.1136/thorax.55.6.533]

11 **Morris MJ**, Allan PF, Perkins PJ. Vocal cord dysfunction: etiologies and treatment. *Clin Pulmonary Med* 2006; **13**: 73-86 [DOI: 10.1097/01.cpm.0000203745.50250.3b]

World Journal of Clinical Cases

Submit a Manuscript: https://www.f6publishing.com

World J Clin Cases 2023 April 6; 11(10): 2355-2362

DOI: 10.12998/wjcc.v11.i10.2355

ISSN 2307-8960 (online)

CASE REPORT

Full neurological recovery from severe nonexertional heat stroke with multiple organ dysfunction: A case report

Fang Du, Jun-Wei Zheng, Yan-Bo Zhao, Kai Yang, Hu-Nian Li

Specialty type: Critical care medicine

Provenance and peer review: Unsolicited article; Externally peer reviewed.

Peer-review model: Single blind

Peer-review report's scientific quality classification

Grade A (Excellent): 0
Grade B (Very good): B
Grade C (Good): C
Grade D (Fair): 0
Grade E (Poor): 0

P-Reviewer: Pantelis AG, Greece; Tangsuwanaruk T, Thailand

Received: December 26, 2022
Peer-review started: December 26, 2022
First decision: January 30, 2023
Revised: February 5, 2023
Accepted: March 9, 2023
Article in press: March 9, 2023
Published online: April 6, 2023

Fang Du, Yan-Bo Zhao, Kai Yang, Hu-Nian Li, Emergency and Critical Care Center, Hubei University of Medicine, Renmin Hospital, Shiyan 442000, Hubei Province, China

Jun-Wei Zheng, Department of Anesthesiology, Hubei University of Medicine, Renmin Hospital, Shiyan 442000, Hubei Province, China

Corresponding author: Hu-Nian Li, MM, Associate Chief Physician, Associate Professor, Emergency and Critical Care Center, Hubei University of Medicine, Renmin Hospital, No. 39 Chaoyang Middle Road, Shiyan 442000, Hubei Province, China. 1217209787@qq.com

Abstract

BACKGROUND

We report a rare case of full neurological recovery from severe nonexertional heat stroke in a 67-year-old woman with an initial Glasgow Coma Scale of 3. This report raises awareness among doctors that when heatstroke is diagnosed, comprehensive treatment should be implemented as soon as possible. Moreover, targeted temperature management, combination therapy with hemodialysis and hemoperfusion, and hyperbaric oxygen therapy may alleviate multiorgan failure and prevent neurological sequelae caused by heatstroke.

CASE SUMMARY

A previously healthy 67-year-old woman with an initial Glasgow Coma Scale of 3 was found lying prone on the road at noon on a summer day. Laboratory tests revealed multiorgan failure. As soon as heatstroke was diagnosed, comprehensive treatment was implemented. On hospital Day 3, the patient was extubated. Her initial Sequential Organ Failure Assessment score at hospitalization was 14 and decreased to 2 on hospital Day 4. On the seventh day following hospital admission, as the patient's general condition improved, the levels of laboratory test findings decreased rapidly. Finally, the patient gradually recovered with no other neurological symptoms (the Glasgow Coma Scale at discharge was 15, and her ability to walk independently was restored).

CONCLUSION

This case demonstrated that targeted temperature management, combination therapy with hemodialysis and hemoperfusion, and hyperbaric oxygen therapy may alleviate multiorgan failure and prevent neurological sequelae caused by heatstroke.

Key Words: Heat stroke; Multiple organ failure; Neurological; Recovery; Case report

Core Tip: We report a rare case of full neurological recovery from severe nonexertional heat stroke in a 67-year-old woman. As soon as heatstroke was diagnosed, comprehensive treatment was implemented. Laboratory tests revealed multiorgan failure. However, the patient gradually recovered consciousness with no other neurological symptoms. This case demonstrated that targeted temperature management, combination therapy with hemodialysis and hemoperfusion, and hyperbaric oxygen therapy may alleviate multiorgan failure and prevent neurological sequelae caused by heatstroke.

Citation: Du F, Zheng JW, Zhao YB, Yang K, Li HN. Full neurological recovery from severe nonexertional heat stroke with multiple organ dysfunction: A case report. *World J Clin Cases* 2023; 11(10): 2355-2362
URL: https://www.wjgnet.com/2307-8960/full/v11/i10/2355.htm
DOI: https://dx.doi.org/10.12998/wjcc.v11.i10.2355

INTRODUCTION

Among all heat-related illnesses, heatstroke is the most severe and is defined by a condition in which the core body temperature exceeds 40°C following a tremendous environmental heat load that overrides the body's heat dissipation efforts[1]. It is accompanied by clinical central nervous system dysfunction (such as delirium, convulsions, or coma) and/or multiorgan failure[2]. With delayed therapy, the mortality rate can be as high as 70%, especially among elderly patients. Early diagnosis and management with immediate cooling can reduce the mortality rate to 10%[3].

There are no therapeutic strategies to prevent further injury after the rapid cooling of the core body temperature to 39°C following heat stroke. Studies have demonstrated that early initiation of the targeted temperature management (TTM) technique can reduce free radicals that are produced during the cerebral hypoxia ischemia and reperfusion process, as well as the energy expenditure and metabolic rate of the brain[4,5]. Most researchers believe that the target temperature should be set at 32 to 34°C, and the duration of TTM is usually < 72 h[6]. However, there are no standard guidelines or unified management methods for TTM. Thus, the previous cooling method of just falling below 39°C may not be adequate to treat heatstroke, and more aggressive cooling measures, similar to the TTM (< 36°C for 24 h) that is routinely administered to patients in postcardiac arrest, are recommended. Continuous renal replacement therapy can effectively lower body temperature, inhibit the inflammatory cascade reaction, and reduce the concentration of toxic metabolites in serum[7]. Hyperbaric oxygen therapy utilizes high-pressure oxygen to create a therapeutic effect for ischemia reperfusion injury in cells. Through hyperbaric oxygen therapy, the oxygen content and diffusing capacity of brain tissue are increased[8]. Consequently, for the management of heatstroke patients, we propose a method that includes inducing TTM (34°C) for 24 h, hemodialysis in combination with hemoperfusion, and hyperbaric oxygen therapy to prevent neurological sequelae and alleviate multiorgan failure caused by heatstroke. It is possible that patients who suffer from heatstroke would have a better prognosis by implementing this approach.

CASE PRESENTATION

Chief complaints

Unconsciousness, accompanied by high fever and convulsions for more than 5 h.

History of present illness

The patient denied a history of present illness.

History of past illness

The patient denied a history of medical illness.

Personal and family history

The patient had no relevant personal or family history.

Physical examination

Upon arrival of the emergency physician, the patient suffered from convulsions and dyspnea; at that time, the axillary temperature was measured at 42°C. She was immediately transferred to our emergency department (ED) by an ambulance. Physical examination revealed a deep coma with a Glasgow Coma Scale of 3, blood pressure of 91/55 mmHg, heart rate of 120 beats/min, respiratory rate of 28 breaths per minute, and her rectal core temperature was as high as 41°C.

Laboratory examinations

The initial laboratory test findings are shown in Table 1 and Figure 1. Abnormal findings included elevated white blood cell count 22.82 × 10^9/L, serum creatine kinase (CK) 4379 IU/L, as well as elevated creatine-kinase-MB (CK-MB), procalcitonin (PCT), blood urea nitrogen (BUN), and positive troponin-T. Her initial Sequential Organ Failure Assessment score at hospitalization was 14 and decreased to 2 on hospital Day 4.

Imaging examinations

Head computed tomography (CT) and magnetic resonance imaging (MRI) scans did not reveal any abnormal findings (Figure 2A and B).

MULTIDISCIPLINARY EXPERT CONSULTATION

The patient did not undergo a multidisciplinary consultation.

FINAL DIAGNOSIS

Heat stroke, multiorgan failure.

TREATMENT

She was immediately transferred to our ED by an ambulance. Endotracheal intubation and ventilator-assisted breathing were immediately performed. To decrease body temperature, intravenous cold saline was administered, as well as external cooling by ice packs and water spray. After fluid and norepinephrine administration, her cardiovascular status stabilized.

Based on these findings, the patient was admitted to the Emergency Intensive Care Unit (EICU). Initial treatment in the EICU included intravenous fluid, cooling and antibiotic administration. Consciousness disturbance and a Glasgow Coma Scale level of 3 were reported upon clinical evaluation. Her rectal core temperature was 37.8°C. The laboratory test findings, shown in Table 1, suggested acute hepatic injury, myocardial injury, and rhabdomyolysis, and the patient met the criteria for multiple organ dysfunction syndrome[9,10].

On the first day in the EICU, immediate treatment included intravenous fluid administration, cooling, combination therapy with hemodialysis and hemoperfusion, broad-spectrum antibiotics, tracheal intubation and mechanical ventilation. The TTM protocol for the initial 24 h included monitoring of continuous core temperature with a rectal probe, and cooling measures continued until the target temperature of 34°C was reached. Therapeutic cooling methods included the use of cooling blankets, cooling caps, ice packs, and bladder irrigation with ice-cold saline. In addition, the patient underwent continuous renal replacement therapy because she showed rhabdomyolysis (hypercreatine kinase emia 18168 IU/L). Simultaneously, continuous renal replacement therapy can effectively lower body temperature. We combined therapy with hemodialysis and hemoperfusion; this involved connecting a perfusion device in series before the dialyzer.

On hospital Day 2, the patient was no longer receiving sedation with midazolam. Despite discontinuation, she remained unconscious for the subsequent 24 h, and re-examination of the head MRI and magnetic resonance angiography showed no obvious lesions (Figure 2C and D). At that point, enteral nutrition was administered with nasal feeding of 300 mL short-peptide enteral nutrition and alanyl glutamine and probiotics were added to promote the recovery of gastrointestinal function.

On hospital Day 3, the patient's consciousness improved; however, she showed poor responses to verbal stimuli. Re-examination of the head CT showed no cerebral hemorrhage or brain swelling, and the condition of the lungs was acceptable. The patient was extubated and administered high-flow oxygen. She was lying awake but unresponsive, except for head movements and eye blinking. Cranial nerve examination was normal, with normal limb muscle strength and muscle tone but a positive Babinski sign bilaterally. Sensation was unimpaired. Cerebellar examination was grossly abnormal, with severe dysarthria and ataxic gait, requiring two people to assist wirh ambulation. Next, she was

Table 1 Laboratory tests and results

Laboratory finding	Day 1	Day 2	Day 3	Day 4	Day 6	Day 7	Day 10	Day 15	Day 30
WBC count (10^9 /L)	**22.82**	**12.52**	**13.23**	**15.74**	**13.69**	**11.65**	12.83	6.14	7.34
Hemoglobin (g/dL)	10.5	11.2	10.4	10.4	10.0	9.6	9.4	9.6	10.0
Platelet count (10^9/L)	169	115	79	80	96	106	252	305	280
PCT (ng/mL)	**1.77**	**2.32**	**1.84**	**0.73**	0.13	0.25	0.06	0.03	0.02
PT (s)	17.2	22.1	16.7	12.1	–	11.1	12.1	10.9	11.1
APTT (s)	26.5	44.3	30.7	27.7	–	26.6	25.6	28.6	26.0
Fibrinogen (g/L)	3.02	2.91	3.07	4.83	–	4.35	3.85	2.95	3.08
D-dimer level (mg/L)	3.23	1.71	2.23	1.25	1.45	1.10	1.15	1.85	1.02
BUN (mmol/L)	4.95	1.54	3.73	4.07	4.09	–	3.67	3.67	4.34
Creatinine (umol/L)	**129.6**	47.0	69.2	57.4	46.7	–	36.0	36.0	61.7
AST (U/L)	48.0	**314.0**	**588.0**	**781.0**	**506.0**	349.0	74.2	41.0	39.0
ALT (U/L)	23.0	**90.0**	**161.0**	**252.0**	**240.0**	230.0	145.0	127.0	46.0
TBil (umol/L)	35.1	43.7	25.6	27.1	27.1	22.8	14.0	11.0	15.0
LDH (IU/L)	453.0	792.0	671.0	**1311.0**	773.0	637.0	464.0	366.0	185.0
CK (IU/L)	**4379**	**18168**	**13563**	**16520**	12171	9384	2139	434	120
CK-MB (U/L)	63	**268**	**314**	**482**	197	157	41	17	10
cTnI (ng/mL)	**0.58**	**0.21**	**0.29**	**0.14**	0.10	0.07	0.02	0.11	0.08
SOFA score	**14**	**9**	**5**	**2**	0	-	-	-	-

AST: Aspartate aminotransferase; ALT: Alanine aminotransferase; APTT: Activated partial thromboplastin time; BUN: Blood urea nitrogen; CK: Creatine kinase; CK-MB: Creatine kinase-MB; cTnI: Cardiac troponin I; LDH: Lactate dehydrogenase; PCT: Procalcitonin; PT: Prothrombin time; SOFA: Sequential Organ Failure Assessment; WBC: White blood cell.

scheduled to undergo hyperbaric oxygen therapy once a day.

On hospital Day 8, the elderly patient complained of abdominal pain, and physical examination revealed abdominal distention, abdominal softness, abdominal tenderness, negative shifting dullness, and weak bowel sounds. Whole abdominal CT showed pneumatosis and effusion in the small intestine. She was given a 120 mL glycerin enema (bid), and mosapride (5 mg per tablet, one tablet each time, tid) was administered to promote intestinal peristalsis.

OUTCOME AND FOLLOW-UP

After 15 d, the patient was discharged and was able to complete activities of daily living and walk independently. She was scheduled for outpatient follow-up at one month following the acute event. At the follow-up assessment, the patient's laboratory parameters were normalized, and the patient was clinically stable.

DISCUSSION

Heat stroke (HS) is a life-threatening condition characterized by hyperthermia and multiple organ failure. It can result from exposure to high environmental temperatures (classic HS), especially for elderly or chronically ill patients, or from strenuous physical activity (exertional HS). While the mechanisms underlying heatstroke remain largely unknown, a study has shown that high temperatures can directly cause cytotoxicity and trigger sepsis-like inflammatory cascades that lead to systemic complications and neurological sequelae in heatstroke[11]. Here, we report a case of an elderly patient with severe heatstroke with multiple organ dysfunction.

To maximize the chances of survival after heatstroke, it is critical to rapidly lower the core body temperature, support the central nervous system as well as the pulmonary, cardiovascular, and renal systems, and effectively manage late or postcooling complications[12-14]. Prompt cooling is the

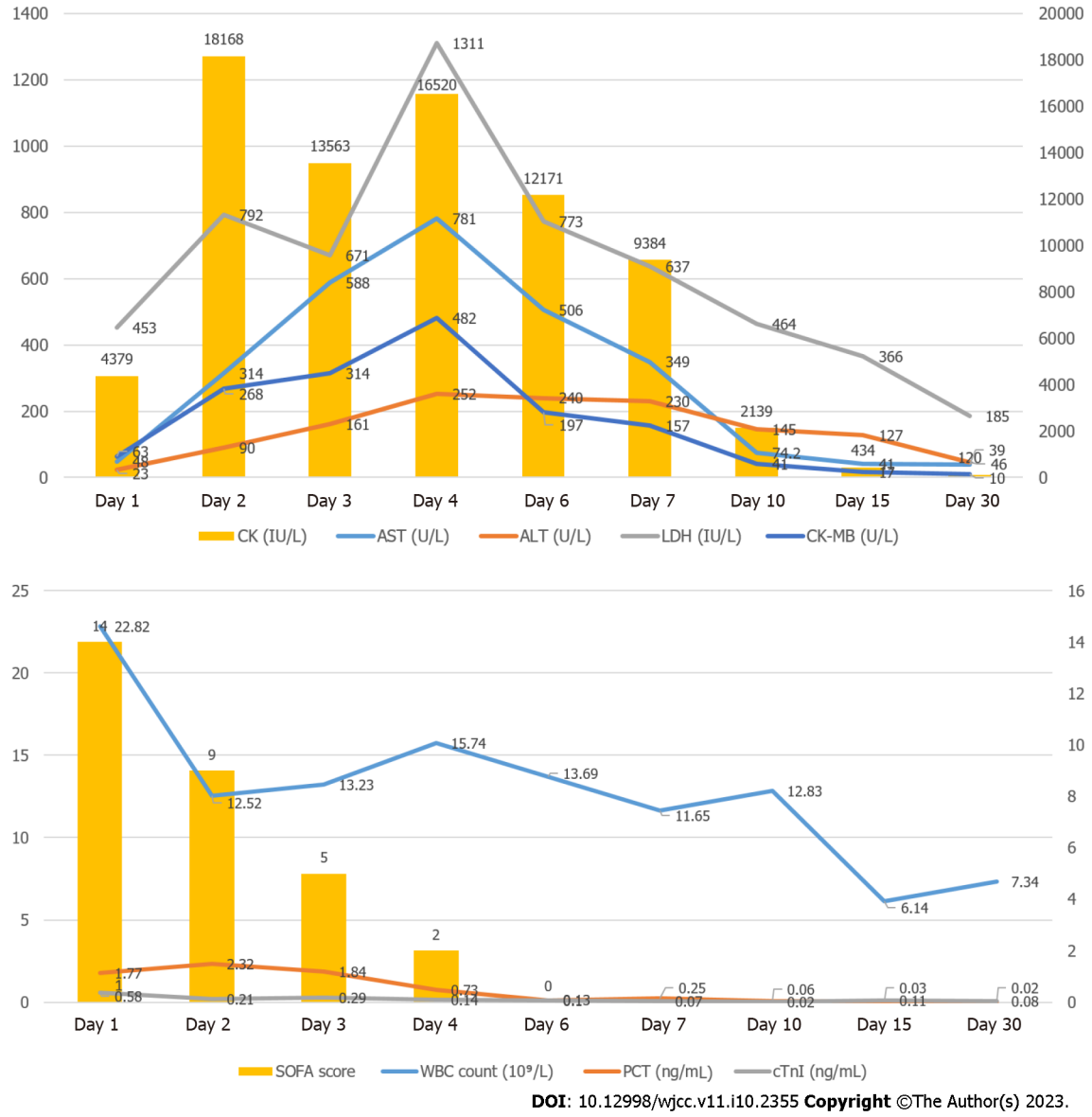

DOI: 10.12998/wjcc.v11.i10.2355

Figure 1 Clinical course. Her initial Sequential Organ Failure Assessment score at hospitalization was 14 and decreased to 2 on hospital Day 4.

cornerstone of treatment and seems to be the most important prognostic measure[15-17]. The patient's body temperature dropped to approximately 38°C 60 min after she was admitted to our ED. Our TTM protocol involves administering cooling measures until the target core temperature of 34°C is achieved for the subsequent 24 h. Upon completion of this maintenance phase, patients are rewarmed at a rate of 0.25°C/h with adequate sedation and analgesia for seizure prevention and shivering control.

Other mechanisms of heat stroke include heat stress, endotoxemia caused by heat exposure, systemic inflammatory response syndrome, and immune dysfunction. This pathological process is defined as the heat stroke "sepsis-like response". In this case study, abnormal findings included an elevated white blood cell count of 22.82 × 10^9/L, a CK level of 4379 IU/L, elevated CK-MB, BUN, PCT, and positive troponin-T. Laboratory investigations showed persistent metabolic acidosis with an increase in CK levels (18168 IU/L). Thus, we administered a combination therapy of hemodialysis and hemoperfusion with a perfusion device connected in series before the dialyzer. Hemodialysis removes small molecular toxins, and the perfusion device removes medium and large molecular toxins, simulating the working principle of the kidney. This approach to therapy can effectively lower body temperature, inhibit the inflammatory cascade reaction, and reduce the concentration of toxic metabolites in serum. On the seventh day following hospital admission, as the patient's general condition improved, the levels of creatine kinase, aspartate aminotransferase, alanine aminotransferase, lactate dehydrogenase, and white blood cells decreased rapidly.

Heat adversely affects almost all organ systems; the central nervous system is particularly vulnerable, and the cerebellum is most susceptible, followed by the cerebral cortex, spinal cord and brainstem[18]. It was reported that patients with marked cerebellar dysfunction may be radiologically normal with cerebellar atrophy appearing months or years later on CT or MRI scans[19]. In the current case, the

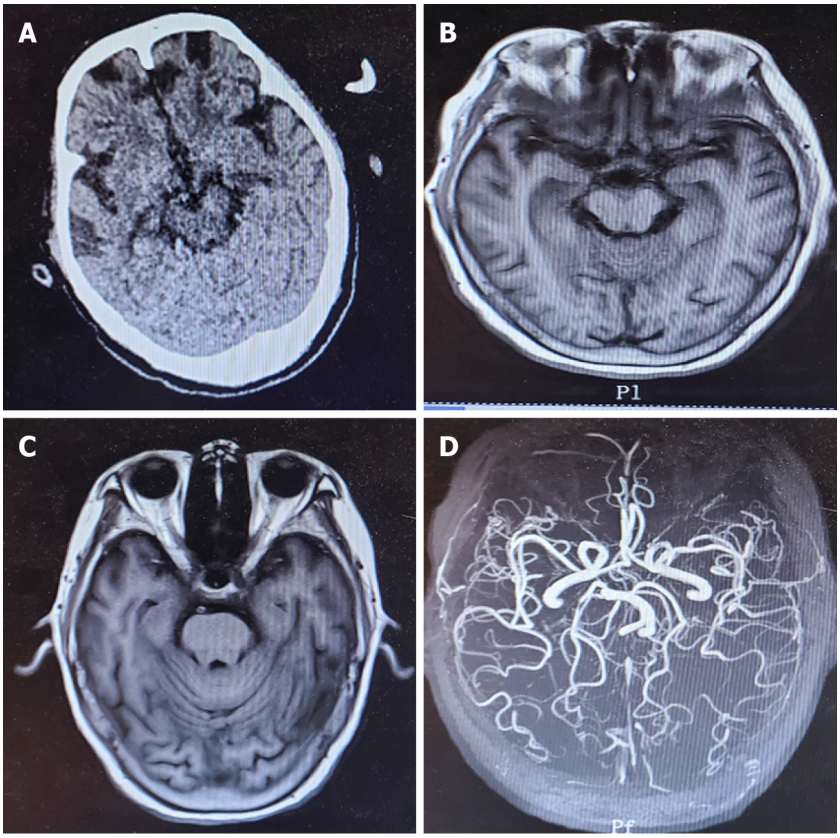

DOI: 10.12998/wjcc.v11.i10.2355 **Copyright** ©The Author(s) 2023.

Figure 2 Imaging examinations. A and B: Head computed tomography and magnetic resonance imaging (MRI) scans did not reveal any abnormal findings; C and D: Despite discontinuation, she remained unconscious for the subsequent 24 h, and re-examination of the head MRI and magnetic resonance angiography showed no obvious lesions.

duration of exposure to hyperthermia in a 67-year-old woman was not well established, but was characterized by gross cerebellar dysfunction with no acute radiographic changes. After early-stage targeted temperature management and a period of hyperbaric oxygen and nutritional nerve therapy, the patient had normal clinical and laboratory results and was clinically stable at discharge on Day 15, and throughout the remainder of the month following the acute event; this outcome is suggestive of nonprogressive cerebellar damage.

Myocardial damage caused by heatstroke has been well documented in the literature[3]. In our case, laboratory data showed elevated serum CK, CK-MB, and positive troponin-T (Table 1). Electrocardiogram (ECG) results revealed tachycardia (sinus rhythm). ECG did not reveal significant subthemes (ST) -T wave changes, and the echocardiogram showed normal left ventricular function without obvious structural heart disease. After treatment, CK, CK-MB, and troponin-T levels gradually declined. It was reported that ST elevation and positive troponin-T in heatstroke patients may not necessarily be the result of atherosclerotic heart disease[20]. However, since most heatstroke patients do not undergo coronary angiography, it is possible that some such patients complicated with atherosclerotic heart disease are not assessed.

Mild to moderate liver injury is relatively familiar and reversible in heat stroke, and liver function usually returns to normal in 2-16 d, but serious acute lung injury and acute liver failure are rare[21]. Hepatocellular injury may be delayed, as observed in some patients who presented with nonsuspicious liver function tests on admission[22], similar to our case. During heatstroke, when blood is transferred vigorously from core to peripheral circulation, reduction of splanchnic blood flow causes hypoxic/ischemic injuries in the hepatocellular and gastrointestinal system[23]. On hospital Day 8, our patient complained of abdominal pain and abdominal distension, and whole abdominal CT results showed pneumatosis and effusion in the small intestine. Considering the possibility of gastrointestinal function impairment, poor peristalsis, and intestinal obstruction caused by indigestion, the patient was given a 120-mL glycerin enema, and mosapride was administered to promote intestinal peristalsis.

Similar cases have been reported in the literature. Sagisaka *et al*[24] demonstrated that the prognosis of patients with heatstroke may be unrelated to poor EEG findings, laboratory data, unknown causes of sympathetic hyperactivity, or poor state of consciousness. Prompt cooling is the cornerstone of treatment and seems to be the most important prognostic measure[16], as it has been shown that the major determinant of outcome in heatstroke is the degree and duration of hyperthermia[2]. Sagisaka *et*

al[24] initiated immediate cooling and intensive care after detailed examination. In the present case, although the duration of exposure to hyperthermia in the elderly woman was not established, she underwent rapid cooling. In the EICU, her rectal core temperature was 37.8℃. Therefore, the patient recovered under our comprehensive management.

We recognize the limitations of our study. The primary limitation was whether our TTM process could be improved (maintenance phase longer than 24 h and goal temperature lower than 34℃). This requires more clinical research.

CONCLUSION

In conclusion, we report our first experience of full recovery of a nonexertional heatstroke case with gross cerebellar dysfunction complicated by multiple organ dysfunction. For the management of heatstroke patients, we propose the adoption of our novel method of inducing TTM (34℃) for 24 h, in combination with hemodialysis and hemoperfusion, and hyperbaric oxygen therapy to prevent neurological sequelae and alleviate multiorgan failure caused by heatstroke. Further clinical research is needed to reduce complications and mortality caused by heatstroke.

ACKNOWLEDGEMENTS

We would like to thank our colleagues in Emergency and Critical Care Center for collecting the case data and analysis.

FOOTNOTES

Author contributions: Du F was a major contributor in writing the original manuscript; Zheng JW, Zhao YB and Yang K provided clinical data, consulted literature, editing, and review; Li HN contributed to project design and operation, data interpretation, supervision, review, and revision of manuscripts; All authors read and approved the final manuscript.

Informed consent statement: Informed written consent was obtained from the patient for publication of this report and any case data.

Conflict-of-interest statement: All the authors declare no conflict of interest.

CARE Checklist (2016) statement: The authors have read the CARE Checklist (2016), and the manuscript was prepared and revised according to the CARE Checklist (2016).

Country/Territory of origin: China

ORCID number: Fang Du 0000-0003-4567-6111; Jun-Wei Zheng 0000-0003-3304-7510; Yan-Bo Zhao 0000-0002-6603-6618; Kai Yang 0000-0002-7068-1863; Hu-Nian Li 0000-0001-5896-533X.

S-Editor: Liu JH
L-Editor: A
P-Editor: Liu JH

REFERENCES

1 **Lian P**, Braber S, Garssen J, Wichers HJ, Folkerts G, Fink-Gremmels J, Varasteh S. Beyond Heat Stress: Intestinal Integrity Disruption and Mechanism-Based Intervention Strategies. *Nutrients* 2020; **12** [PMID: 32168808 DOI: 10.3390/nu12030734]

2 **People's Liberation Army Professional Committee of Critical Care Medicine**. Expert consensus on standardized diagnosis and treatment for heat stroke. *Mil Med Res* 2016; **3**: 1 [PMID: 26744628 DOI: 10.1186/s40779-015-0056-z]

3 **Yeo TP**. Heat stroke: a comprehensive review. *AACN Clin Issues* 2004; **15**: 280-293 [PMID: 15461044 DOI: 10.1097/00044067-200404000-00013]

4 **Chen X**, Li L, Hu J, Zhang C, Pan Y, Tian D, Tang Z. Anti-inflammatory effect of dexmedetomidine combined with hypothermia on acute respiratory distress syndrome in rats. *J Surg Res* 2017; **216**: 179-184 [PMID: 28807204 DOI: 10.1016/j.jss.2017.05.014]

5 **Feng RY**, Chen Q, Yang WJ, Tong XG, Sun ZM, Yan H. Immune Tolerance Therapy: A New Method for Treatment of Traumatic Brain Injury. *Chin Med J (Engl)* 2018; **131**: 1990-1998 [PMID: 30082532 DOI: 10.4103/0366-6999.238147]

6 **Sadaka F**, Veremakis C. Therapeutic hypothermia for the management of intracranial hypertension in severe traumatic brain injury: a systematic review. *Brain Inj* 2012; **26**: 899-908 [PMID: 22448655 DOI: 10.3109/02699052.2012.661120]

7 **Rimmelé T**, Kellum JA. High-volume hemofiltration in the intensive care unit: a blood purification therapy. *Anesthesiology* 2012; **116**: 1377-1387 [PMID: 22534247 DOI: 10.1097/ALN.0b013e318256f0c0]

8 **Yang L**, Li D, Chen S. Hydrogen water reduces NSE, IL-6, and TNF-α levels in hypoxic-ischemic encephalopathy. *Open Med (Wars)* 2016; **11**: 399-406 [PMID: 28352827 DOI: 10.1515/med-2016-0072]

9 **Singer M**, Deutschman CS, Seymour CW, Shankar-Hari M, Annane D, Bauer M, Bellomo R, Bernard GR, Chiche JD, Coopersmith CM, Hotchkiss RS, Levy MM, Marshall JC, Martin GS, Opal SM, Rubenfeld GD, van der Poll T, Vincent JL, Angus DC. The Third International Consensus Definitions for Sepsis and Septic Shock (Sepsis-3). *JAMA* 2016; **315**: 801-810 [PMID: 26903338 DOI: 10.1001/jama.2016.0287]

10 **Fry DE**. Sepsis, systemic inflammatory response, and multiple organ dysfunction: the mystery continues. *Am Surg* 2012; **78**: 1-8 [PMID: 22273282]

11 **Epstein Y**, Roberts WO. The pathopysiology of heat stroke: an integrative view of the final common pathway. *Scand J Med Sci Sports* 2011; **21**: 742-748 [PMID: 21635561 DOI: 10.1111/j.1600-0838.2011.01333.x]

12 **Bouchama A**, Dehbi M, Chaves-Carballo E. Cooling and hemodynamic management in heatstroke: practical recommendations. *Crit Care* 2007; **11**: R54 [PMID: 17498312 DOI: 10.1186/cc5910]

13 **Lee BC**, Kim JY, Choi SH, Yoon YH. Use of an external-cooling device for the treatment of heat stroke. *Clin Exp Emerg Med* 2014; **1**: 62-64 [PMID: 27752554 DOI: 10.15441/ceem.14.004]

14 **Pryor RR**, Roth RN, Suyama J, Hostler D. Exertional heat illness: emerging concepts and advances in prehospital care. *Prehosp Disaster Med* 2015; **30**: 297-305 [PMID: 25860637 DOI: 10.1017/S1049023X15004628]

15 **Epstein Y**, Yanovich R. Heatstroke. *N Engl J Med* 2019; **380**: 2449-2459 [PMID: 31216400 DOI: 10.1056/NEJMra1810762]

16 **Casa DJ**, Armstrong LE, Kenny GP, O'Connor FG, Huggins RA. Exertional heat stroke: new concepts regarding cause and care. *Curr Sports Med Rep* 2012; **11**: 115-123 [PMID: 22580488 DOI: 10.1249/JSR.0b013e31825615cc]

17 **Glazer JL**. Management of heatstroke and heat exhaustion. *Am Fam Physician* 2005; **71**: 2133-2140 [PMID: 15952443 DOI: 10.1056/NEJM200506023522220]

18 **Mahajan S**, Schucany WG. Symmetric bilateral caudate, hippocampal, cerebellar, and subcortical white matter MRI abnormalities in an adult patient with heat stroke. *Proc (Bayl Univ Med Cent)* 2008; **21**: 433-436 [PMID: 18982090 DOI: 10.1080/08998280.2008.11928446]

19 **Koller WC**, Glatt SL, Perlik S, Huckman MS, Fox JH. Cerebellar atrophy demonstrated by computed tomography. *Neurology* 1981; **31**: 405-412 [PMID: 6971416 DOI: 10.1212/wnl.31.4.405]

20 **Chen WT**, Lin CH, Hsieh MH, Huang CY, Yeh JS. Stress-induced cardiomyopathy caused by heat stroke. *Ann Emerg Med* 2012; **60**: 63-66 [PMID: 22153997 DOI: 10.1016/j.annemergmed.2011.11.005]

21 **Ward MD**, King MA, Gabrial C, Kenefick RW, Leon LR. Biochemical recovery from exertional heat stroke follows a 16-day time course. *PLoS One* 2020; **15**: e0229616 [PMID: 32130237 DOI: 10.1371/journal.pone.0229616]

22 **Davis BC**, Tillman H, Chung RT, Stravitz RT, Reddy R, Fontana RJ, McGuire B, Davern T, Lee WM; Acute Liver Failure Study Group. Heat stroke leading to acute liver injury & failure: A case series from the Acute Liver Failure Study Group. *Liver Int* 2017; **37**: 509-513 [PMID: 28128878 DOI: 10.1111/liv.13373]

23 **Lambert GP**. Role of gastrointestinal permeability in exertional heatstroke. *Exerc Sport Sci Rev* 2004; **32**: 185-190 [PMID: 15604939 DOI: 10.1097/00003677-200410000-00011]

24 **Sagisaka S**, Tamune H, Shimizu K, Kashiyama T. A rare case of full neurological recovery from severe nonexertional heatstroke during a bedrock bath. *J Gen Fam Med* 2018; **19**: 136-138 [PMID: 29998044 DOI: 10.1002/jgf2.178]

Published by **Baishideng Publishing Group Inc**
7041 Koll Center Parkway, Suite 160, Pleasanton, CA 94566, USA
Telephone: +1-925-3991568
E-mail: bpgoffice@wjgnet.com
Help Desk: https://www.f6publishing.com/helpdesk
https://www.wjgnet.com